Universitat d'Alacant
Universidad de Alicante

NUEVOS PRECURSORES DE ILUROS DE AZOMETINO PARA CICLOADICIONES 1,3-DIPOLARES

Juan Mancebo Aracil

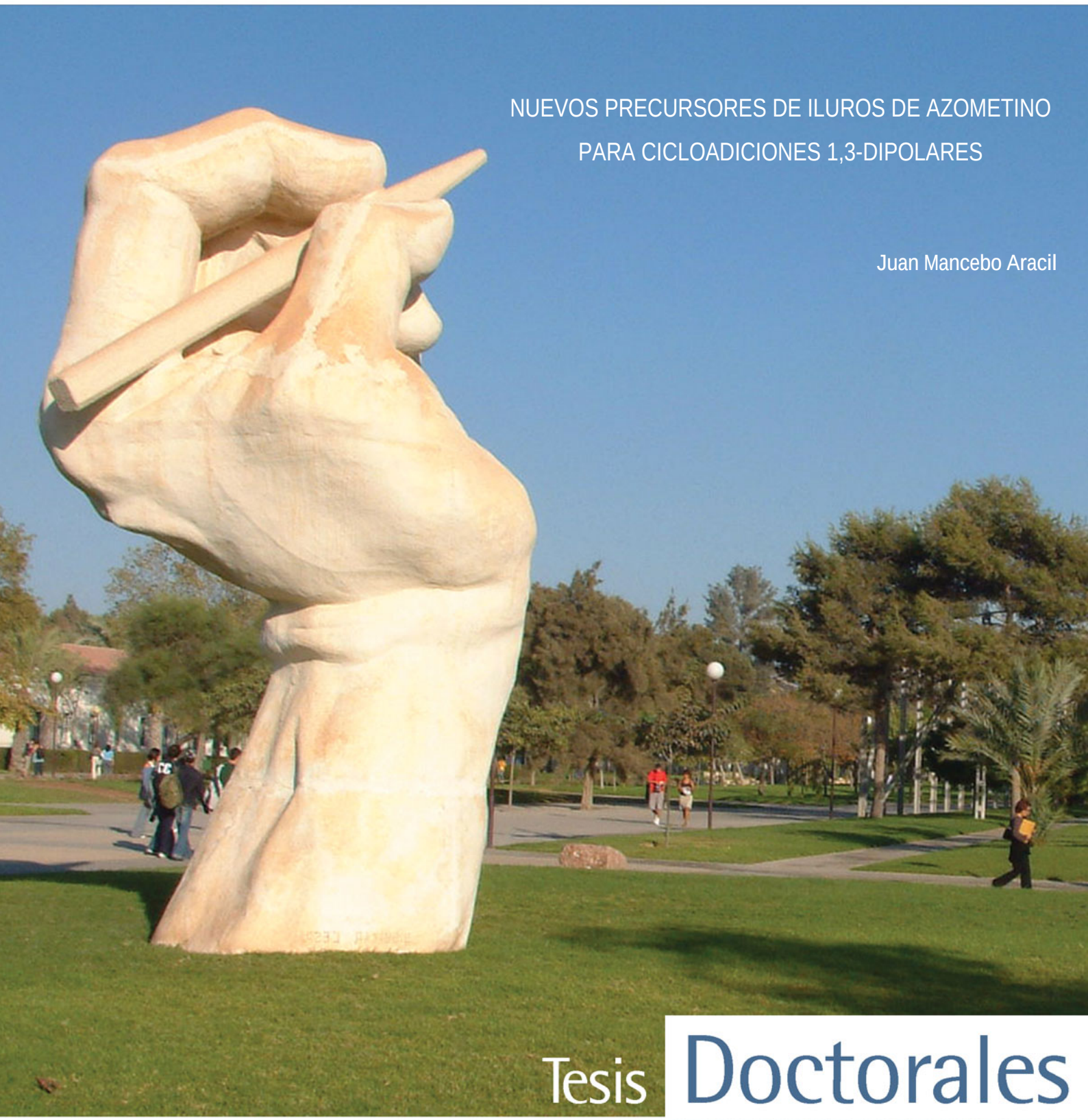

Tesis Doctorales

www.eltallerdigital.com

UNIVERSIDAD de ALICANTE

Universitat d'Alacant
Universidad de Alicante

Instituto de Síntesis Orgánica (ISO)

NUEVOS PRECURSORES DE ILUROS DE AZOMETINO PARA CICLOADICIONES 1,3-DIPOLARES

Memoria para optar al Título de Doctor por la Universidad de Alicante presentada por el licenciado:

JUAN MANCEBO ARACIL

Alicante, marzo de 2014

V.º B.º de los Directores

Fdo.: Carmen Nájera Domingo
Catedrática de Química Orgánica

Fdo.: José Miguel Sansano Gil
Catedrático de Química Orgánica

Instituto de Síntesis Orgánica (ISO), Facultad de Ciencias, Fase I, Universidad de Alicante
Campus de Sant Vicent del Raspeig, Apdo. 99, E-03080 Alicante, España
Tel. +34 965903400, ext. 2121; +34 965903549; Fax +34 965903549
Web: http://iso.ua.es; E-mail: iso@ua.es

ÍNDICE

PRÓLOGO

I.- PRÓLOGO

La cicloadición 1,3-dipolar es una reacción de gran importancia en síntesis orgánica, ya que permite la obtención de cicloaductos complejos en un solo paso de reacción controlando la regio-y la estereoselectividad del proceso. Por otro lado, las reacciones muticomponente (MCRs) se describen como una herramienta versátil y eficaz que optimiza el proceso de síntesis simplificando el gasto de reactivos y disolventes, y por tanto la generación de residuos en el laboratorio, así como permitiendo la obtención de interesantes productos de manera elegante y en general con buenos resultados.

Además de todo esto, las técnicas calorimétricas se describen como herramientas rápidas y relativamente de fácil uso, que permiten obtener parámetros termodinámicos y cinéticos que ayuden a dilucidar el proceso mecanístico de cualquier reacción.

Es por ello, que en la presente memoria se describe la cicloadición 1,3-dipolar multicomponente de iluros de azometino de forma diastereo- y enantioselectiva, usando nuevos precursores de iluros de azometino, así como el estudio cinético de dicha reacción via dos componentes, dividiéndose en consecuencia de la siguiente manera:

La mayor parte de los resultados descritos en esta memoria han sido objeto de las publicaciones que se muestran a continuación:

"Kinetic Study of Thermal 1,3-Dipolar Cycloaddition of Azomethine Ylides using Differential Scanning Calorimetry as Monitoring Window" Juan Mancebo-Aracil, María J. Muñoz-Guillena, Ion Such-Basáñez, José M. Sansano-Gil; *Chempluschem* **2012**, *77*, 770.

"Binap-silver salts as chiral catalysts for the enantioselective 1,3-dipolar cycloaddition of azomethine ylides and alkenes" Juan Mancebo-Aracil, María Martín-Rodríguez, Carmen Nájera, José M. Sansano, Paulo R. R. Costa, Evanoel Crizanto de Lima, Ayres G. Dias; *Tetrahedron: Asymmetry* **2012**, *23*, 1596.

"Silver-catalyzed azomethine ylides cycloaddition" Juan Mancebo-Aracil, María Martín-Rodríguez, Carmen Nájera, José M. Sansano, Paulo R. R. Costa, Evanoel Crizanto de Lima, Ayres G. Dias; *Synfacts* **2013**, *9(2)*, 0172.

"Microwave-assisted multicomponent diastereoselective 1,3-dipolar cycloaddition of ethyl glyoxylate derived azomethine ylides" Juan Mancebo-Aracil, Carmen Nájera, José M. Sansano; *Org. Biomol. Chem.* **2013**, *11*, 662.

"Multicomponent synthesis of unnatural pyrrolizidines using 1,3-dipolar cycloaddition of proline esters" Juan Mancebo-Aracil, Carmen Nájera, José M. Sansano; *Chem. Commun.* **2013**, *49*, 11218.

"Multicomponent Diastereoselective Silver-Catalyzed 1,3-Dipolar Cycloadditions using Ethyl Glyoxylate and 2,2-Dimethoxyacetaldehyde derived Azomethine Ylides" Juan Mancebo-Aracil, Carmen Nájera, José M. Sansano; *Org. Chem. Front.* enviado.

"Simple and diastereoselective multicomponent 1,3-dipolar cycloaddition combining cyclic α-amino esters-aldehydes-dipolarophiles for the synthesis of pyrrolizidines and indolizidines" J. Mancebo-Aracil, C. Nájera, J. M. Sansano; *Org. Biomol. Chem.* enviado .

RESUMEN

II.- RESUMEN

En la presente memoria se describe la síntesis de derivados de pirrolidina, pirrolizidina e indolizidina mediante diferentes metodologías que involicruan una cicloadición 1,3-dipolar multicomponente a través de iluros de azometino generados in situ, así como el estudio cinético de esta reacción via dos componentes.

En el **Capítulo I**, se describen diferentes métodos de estudio cinético para la interpretación y obtención de parámetros mecanísticos de dicha reacción a partir de la información obtenida mediante Analisis Térmico y más concretamente calorimetría diferencial de barrido.

En el **Capítulo II**, dividido en tres partes, se describe la síntesis de pirrolidinas mediante cicloadición 1,3-dipolar multicomponente (a partir de iluros de azometino) térmica y por irradiación por microondas (Parte 1), catalizada por plata(I) (Parte II) y asimétrica mediante catálisis por plata(I) y un ligando quiral (Parte III); así como la posible aplicabilidad en la síntesis de productos naturales o que presenten actividad biológica.

En el **Capítulo III**, se describe la síntesis de pirrolizidinas mediante la cicloadición 1,3-dipolar multicomponente con iluros de azometino con y sin uso de sales de plata(I), así como un ejemplo en la construcción de un esqueleto de indolizidina siguiendo la misma metodología.

Finalmente se incluyen las conclusiones junto con otro tipo de anexos como son las referencias, abreviaciones y la biografía.

II.1.- SUMMARY

In this work the synthesis of derivatives of pyrrolidine, indolizidine and pyrrolizidine from multicomponent 1,3-dipolar cycloaddition of azomethine ylides generated in situ are described, and the kinetic study of this reaction via two components.

The Thermal Analysis and the kinetic study of this reaction after analyze the differencial scanning calorimetry data are described in **Chapter I**.

In **Chapter II** , divided into three parts , the synthesis of pyrrolidines is described by multicomponent 1,3-dipolar cycloaddition (from azomethine ylides)

through a thermal or microwave irradiation (Part 1) , catalyzed by silver(I) (Part 2) and asymmetric catalysis using silver(I) and a chiral ligand (Part 3), as well as the potential applicability in the synthesis of natural products or which have biological activity.

In **Chapter III**, the pyrrolizidines synthesis by multicomponent 1,3-dipolar cycloaddition of azomethine ylides, with and without use of silver(I) salts are described, as well as the indolizidine structure synthesis from the same methodology

Finally, conclusions are included along with other attachments such as references , abbreviations and biography.

II.2.- RESUMEN GRÁFICO

CAPÍTULO I

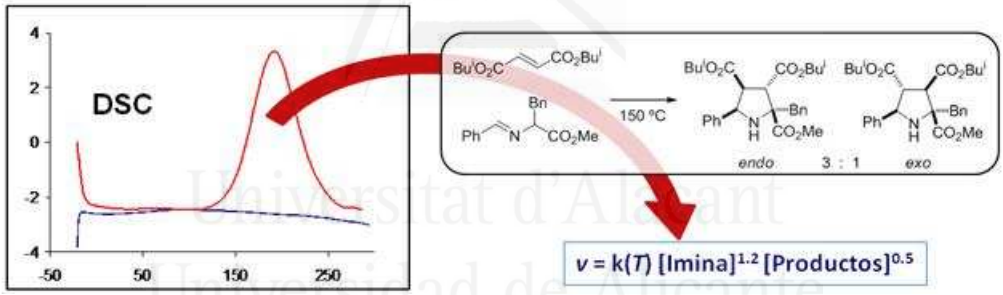

CAPÍTULO II

Capítulo II-1

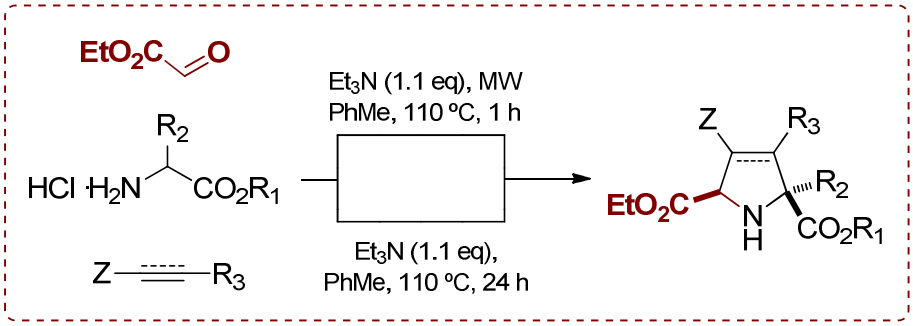

Capítulo II-2

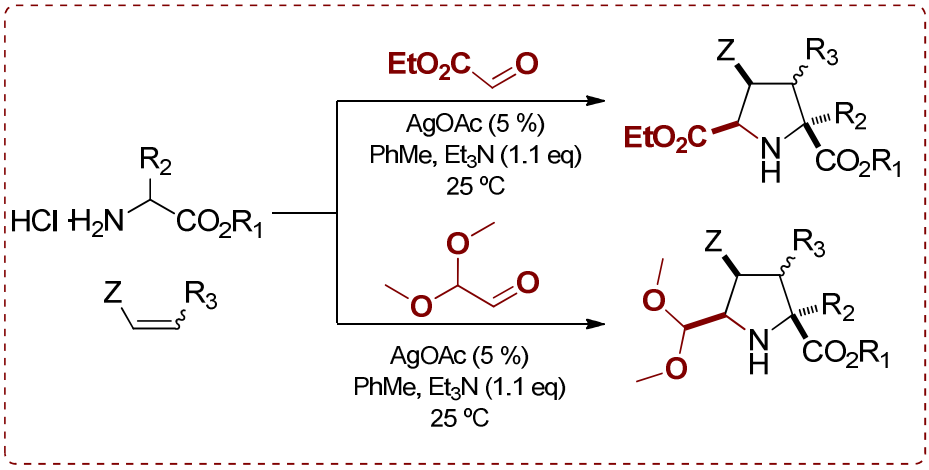

Capítulo II-3

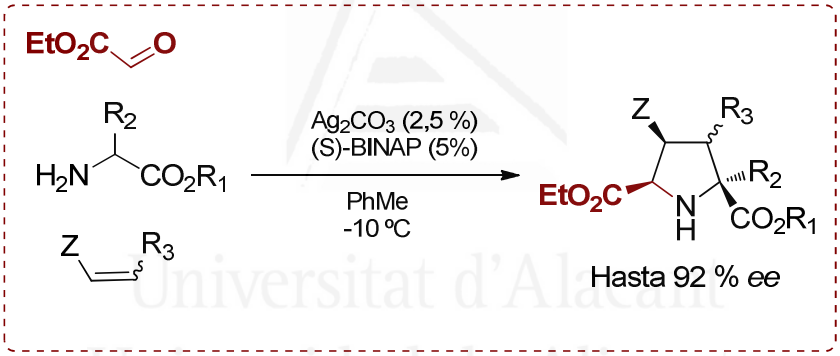

CAPÍTULO III

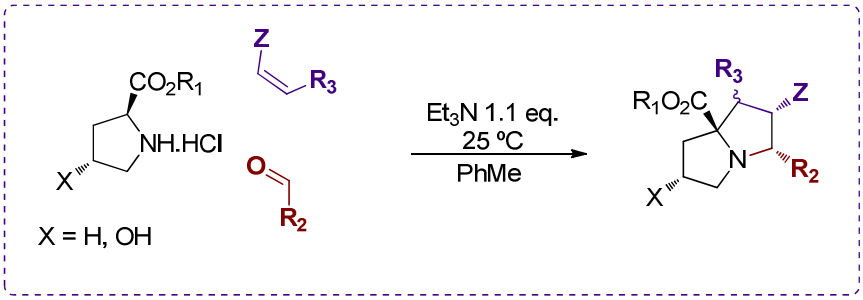

INTRODUCCIÓN GENERAL

III.- INTRODUCCIÓN GENERAL

III.1.- CICLOADICIONES 1,3-DIPOLARES

Fue en 1963 cuando Huisgen[1] publicó la clasificación de los 1,3-dipolos así como de las reacciones de cicloadición 1,3-dipolares, sin embargo no fue hasta 1976 cuando tuvo lugar la primera cicloadición 1,3-dipolar intramolecular con iluros de azometino. Existen, desde entonces, diferentes metodologías para la formación de iluros de azometino, habiéndose extendido rápidamente su uso en la síntesis de pirrolidinas y productos naturales.

Las reacciones 1,3-dipolares tienen lugar entre un dipolo, y un dipolarófilo, tal y como se verá más adelante. Atendiendo a los dipolos, estos pueden dividirse en dos grupos: dipolo del tipo anión alílico (cuya estructura es angular y con un único doble enlace) como, por ejemplo las nitronas, iluros de azometino, iluros de amina, iluros de carbonilo; y dipolos del tipo anión propargilo-alenilo (cuya estructura es lineal y se presentan en las dos formas resonantes tipo propargilo y tipo cumuleno) tales como óxidos de nitrilo, iluros de nitrilo, iminas de nitrilo, diazoalquenos y azidas (**Esquema 1**).

[1] Huisgen, R; *Angew. Chem., Int. Ed. Engl.* **1963**, *2*, 565.

Esquema 1

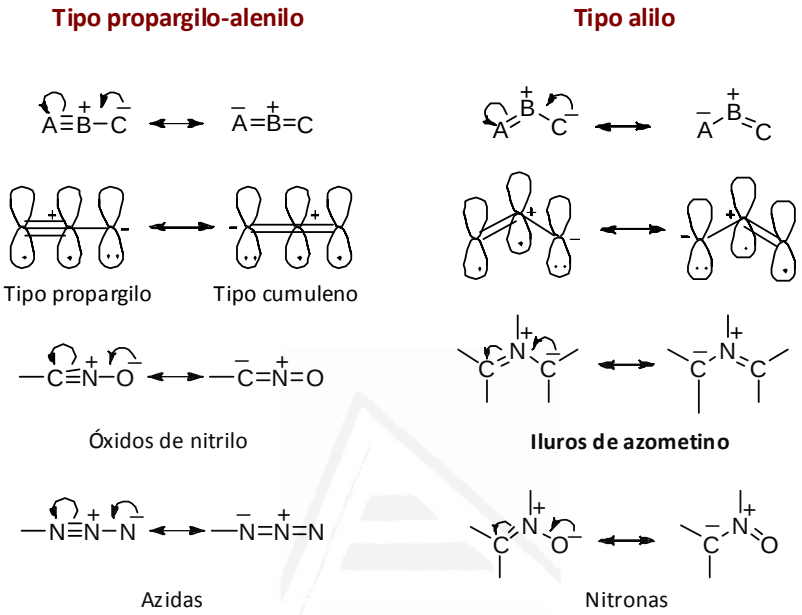

Las reacciones de cicloadición 1,3-dipolar entre 1,3-dipolos y alquenos o alquinos son muy versátiles pues permiten la presencia de muchos grupos funcionales en ambos componentes.[2] La reacción entre el dipolo **1** y el dipolarófilo **2** permite la obtención de heterociclos del tipo **3** (**Esquema 2**).

[2] **a)** Nájera, C.; Sansano, J.M.; *Angew. Chem. Int. Ed.* **2005**, *44*, 6272. **b)** Husinec, S.; Savic, V.; *Tetrahedron: Asymmetry* **2005**, *16,* 2047. **c)** Coldham, I.; Hufton, R.; *Chem. Rev.* **2005**, *105*, 2765 **d)** Nájera, C.; Sansano, J.M.; *Curr. Org. Chem.* **2003**, *7*, 1105 **e)** *Synthetic Applications of 1,3-Dipolar Cycloaddition Chemistry Toward Heterocycles and Natural Products*, Eds: Padwa, A., Wiley: Nueva York, **2003 f)** Kanemasa, S.; *Synlett* **2002**, 1371. **g)** Gothelf, K.; *Cycloaddition Reactions in Organic Synthesis*, Eds: Kobayasi, S.; Jørgensen, K. A.; Wiley-VCH, Weinheim **2002**, 211 **h)** *Cycloaddition Reactions in Organic Synthesis*, Eds: Carruthers, W., Pergamon Press: Oxford **1990**, 269 **i)** Bonin, M; Chauveau, A.; Micouin, L.; *Synlett* **2006**, *15*, 2349 **j)** Pellissier, H.; *Tetrahedron* **2007**, *63*, 3235 **k)** Padwa, A.; Bur, S.; *Tetrahedron* **2007**, *63*, 5341 **l)** Nair, V.; Suja, T.; *Tetrahedron* **2007**, *63,* 12247 **m)** Nájera, C.; Sansano, J.M.; *Heterocycl. Chem.* **2008**, *12*, 117. **n)** Pellisier, H.; *Tetrahedron* **2007**, *63*, 3235. **ñ)** Pandey, G.; Banerjee, P.; Gadre, S. R.; *Chem. Rev.* **2006,** *106,* 4484 **o)** Pinho, T. M.; Melo, V. D. *Eur. J. Org. Chem.* **2006**, 2873. **p)** Nájera, C. ; Sansano, J.M.; Yus, M.; *J. Braz. Chem. Soc*. **2010**, *21*, 377.

Esquema 2

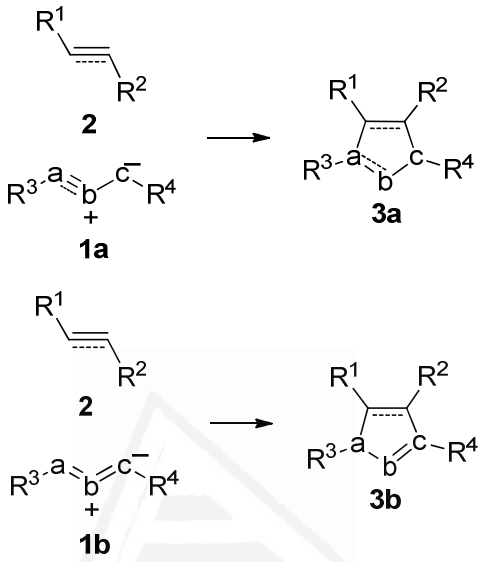

Unos de los dipolos más utilizados son los iluros de azometino, que presentan 4 electrones π distribuidos sobre tres átomos C-N-C (**Esquema 3**), siendo más común la estructura resonante que posee la carga positiva sobre el nitrógeno y la carga negativa sobre uno de los átomos de carbono, dependiendo de la naturaleza de la molécula. Los aspectos y características más generales de esta reacción se describen a continuación.

Esquema 3

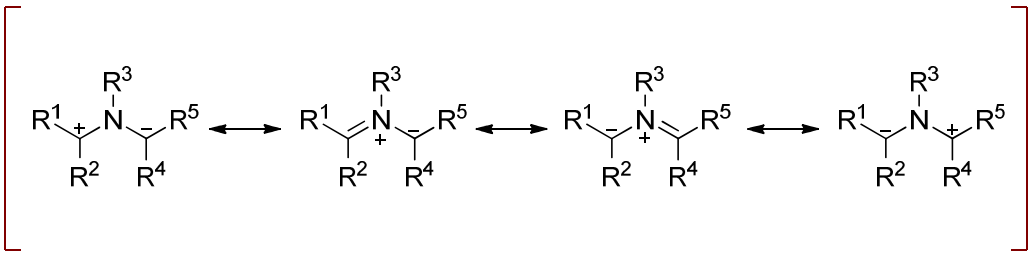

Existen estudios recientes en los que se advierte de la existencia de especies pseudoradicalarias frente a las especies zwitteriónicas descritas en el Esquema anterior.[3]

III.1.1.- Reacciones 1,3-dipolares de iluros de azometino estabilizados

III.1.1.1.- Aspectos generales

La cicloadición de un iluro de azometino con un sistema π involucra un total de 6 π electrones (π4s + π2s) y tiene lugar por vía térmica en un proceso suprafacial según las reglas de Woodward y Hoffmann. Esta cicloadición es un proceso concertado y gracias a esto se obtiene una elevada esteroespecificidad, en la que la esteroquímica relativa del alqueno (dipolarófilo) se mantiene en la pirrolidina final.[4]

La teoría de los orbitales moleculares frontera (**TOF**)[5] es una herramienta que ayuda a explicar la elevada regioquímica y esteroselectividad de la reacción. En este caso, las interacciones dominantes son las que involucran el HOMO del iluro de azometino con el LUMO del sistema-π cuando se utilizan alquenos pobres en electrones. Sin embargo, otros alquenos con LUMOs de energía superior reaccionan mal o no lo hacen, como sucede con el estireno o el metil vinil éter. Un ejemplo detallado se muestra en el **Esquema 4**, indicándose en él, diferencias de energías entre niveles HOMO-LUMO, valores calculados de coeficientes y cómo afecta todo ello a la relación de productos final.

[3] Domingo, L.R.; Emamian, S. R.; *Tetrahedron* **2014** DOI 10.1016/j.tet.2013.12.059

[4] **a)** Grigg, R.; Sridharan, V.; *Advances in Cycloaddition*, JAI Press Inc.: Greenwich, **1993**, *3*, 161 **b)** Grigg, R.*; Chem. Soc. Rev*. **1987**, *16*, 89. **c)** Grigg, R.; Kemp, J.; Malone, J.; Tangthongkum, A.; *J. Chem. Soc., Chem. Commun.* **1980**, 648 **d)** Tatsukawa, A.; Kawatake, K.; Kanemasa, S.; Rudzinski, J.; *J. Chem. Soc. Perkin Trans. 2* **1994**, 2525 **e)** Annunziata, R.; Benaglia, M.; Cinquini, M.; Raimondi, L.; *Tetrahedron* **1993**, *49*, 8629 **f)** Ayerbe, M.; Arrieta, A.; Cossío, F.; Linden, A.; *J. Org. Chem.* **1998**, *63*, 1795 **e)** Vivanco, S.; Lecea, B.; Arrieta, A.; Prieto, P.; Morao, I.; Linden, A.; Cossío, F.; *J. Am. Chem. Soc.* **2000**, *122*, 6078 **f)** Vivanco, S.; Tesis doctoral, Universidad del País Vasco, San Sebastián, **2002**

[5] **a)** *Frontier Orbitals and Organic Chemical Reactions*, Eds: Fleming I., Wiley: Chichester, **1976 b)** *Pericyclic Reaction*, Eds: Fleming, I., Oxford Science Publications, Oxford, **1994**.

Esquema 4

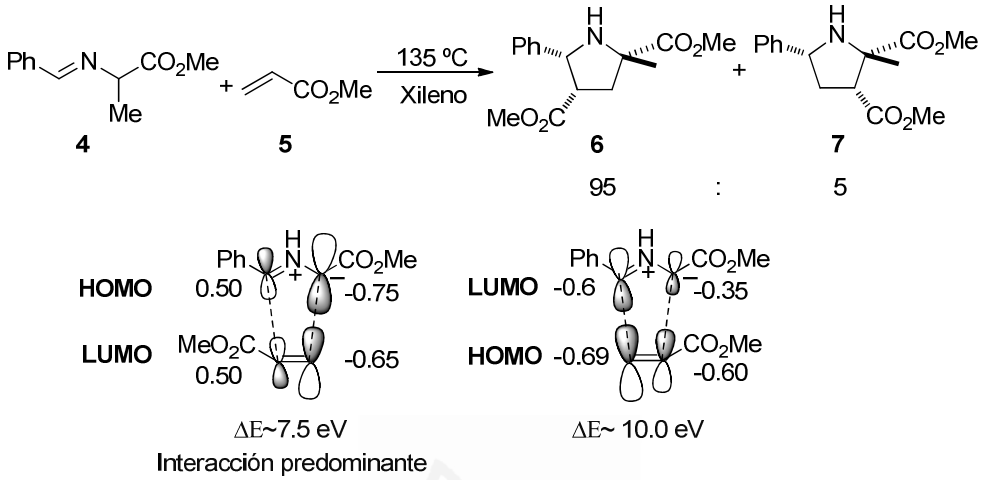

III.1.1.2.- Generación de los iluros de azometino

La generación de iluros de azometino puede llevarse a cabo de distintas maneras, siendo la 1,2-prototropía térmica de iminoésteres y la formación de iluros de metalo-azometino las dos vías más comunes. Aunque menos frecuente, otra forma de sintetizarlos es a través de las aziridinas, un ejemplo concreto de esta metodología se muestra en el **Esquema 12**.

Los α-iminoésteres **8** (**Esquema 5**), bajo condiciones térmicas, experimentan 1,2-prototropía que, controlada cinéticamente, da lugar a un dipolo con configuración *E,E*-(*sin*)-**9** o dipolo en forma de W-**9**. La reacción de cicloadición de este iluro con un dipolarófilo puede dar lugar a una mezcla de cicloaductos *endo*-**10** y *exo*-**10**, obtenidos a partir de los estados de transición *endo* y *exo*, respectivamente, con configuración relativa 2,5-*cis*. Cuando el sustituyente que retira carga del dipolarófilo (R^4 en los **Esquemas 5** y **6**) se acerca al dipolo durante la formación del estado de transición se habla de una aproximación *endo*, mientras que en una aproximación *exo* este sustituyente queda más alejado del dipolo. La formación de iluros de azometino es sensible al pK_a del átomo de hidrógeno en posición α respecto al carbonilo. La formación inicial del iluro *E,E* puede sufrir estereomutación para producir los iluros *E,Z*-**9** o *Z,E*-**9** o dipolo en

forma de S-**9**, los cuales pueden sufrir a su vez la correspondiente cicloadición para dar lugar a los cicloaductos **11** o **12** con configuración relativa 2,5-*trans* ambos. Esta progresión cinética del iluro *E,E*-**9** está controlada generalmente por diversos factores tales como: estructura de la imina, disolvente, temperatura de reacción y reactividad del dipolarófilo empleado.[6]

Esquema 5

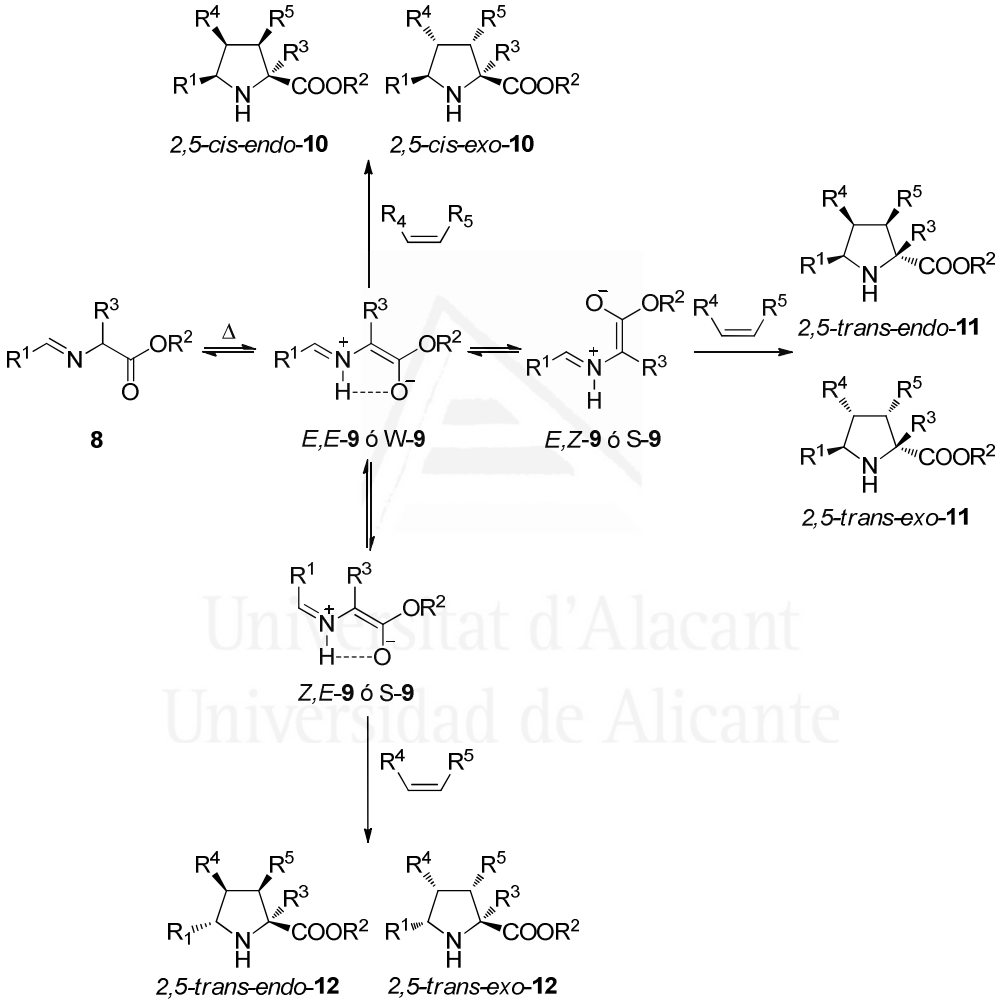

[6] **a)** Grigg, R.; Donegan, G.; Gunaratne, H.; Kennedy, D.; Malone, J.; Sridharan, V.; Thianpatanagul, S.; *Tetrahedron* **1989**, *45*, 1723 **b)** Van Es, J.; Jaarsveld, K.; van der Gen, A.; *J. Org. Chem.* **1990**, *55*, 4063 **c)** Van Es, J.; Wolde, A.; van der Gen, A.; *J. Org. Chem.* **1990**, *55*, 4069 **d)** Grigg, R.; Jordan, M.; Malone, J.; Armstrong, P.; *Tetrahedron* **1985**, *41*, 3547 **e)** Grigg, R.; Kemp, J.; *Tetrahedron Lett.* **1980**, *21*, 2461 **f)** Tsuge, O.; Ueno, K.; Kanemasa, S.; Yorozu, K.; *Bull. Chem. Soc. Jpn.* **1986**, *59*, 1809.

Relacionado con el proceso de 1,2-prototropía, existe un procedimiento para generar iluros de metalo-azometino (**Esquema 6**). Esencialmente, en estas transformaciones el átomo implicado en el proceso de formación del correspondiente iluro es un ión metálico mientras que en el caso de la 1,2-prototropía se trataba de un átomo de hidrógeno. Los primeros ejemplos que involucraban a uno de estos iluros de metalo-azometino fueron estudiados a finales de los años setenta.[7] En dichos estudios se mostraba que el complejo del metal y la imina, derivada de α-aminoácidos y cetonas con un grupo adicional coordinante, reaccionaban con alquenos activados para generar pirrolidinas. Aunque la mezcla de diasteroisómeros obtenidos sugiriese que el mecanismo de la reacción se tratara de un doble proceso, adición Michael seguida de condensación de Mannich, investigaciones posteriores demostraron que el proceso transcurría a través de un mecanismo concertado 4π+2π.[7e] Más adelante se ha confirmado que el mecanismo concertado y el mecanismo por etapas depende especialmente de la naturaleza del dipolarófilo.[8]

Todos los esfuerzos anteriores culminaron con el desarrollo de un método sencillo y eficiente para generar iluros de metalo-azometino empleando ácidos de Lewis con bases débiles (**Esquema 6**).[4a]

[7] **a)** Casella, L.; Gulloti, M.; Pasini, A.; Pasaro, R.; *Synthesis* **1979**, 150 **b)** Grigg, R.; Sridharan, V.; Thianpatanagul, S.; *J. Chem. Soc., Perkin Trans.* **1986**, *1,* 1669. **c)** Casella, L.; Gulloti, M.; Melani, E.; *J. Chem. Soc., Perkin Trans.* **1982**, *1,* 1827 **d)** Tsuge, O.; Kanemasa, S.; Yoshioka, M.; *J. Org. Chem.* **1988**, *53*, 1384 **e)** Barr, D.; Grigg, R.; Gunaratne, H.; Kemp, J.; McMeekin, P.; Sridharan, V.; *Tetrahedron* **1988**, *44*, 557

[8] de Cózar, A.; Cossío, F.; *Phys. Chem. Chem. Phys.* **2011**, *13*, 10858.

Esquema 6

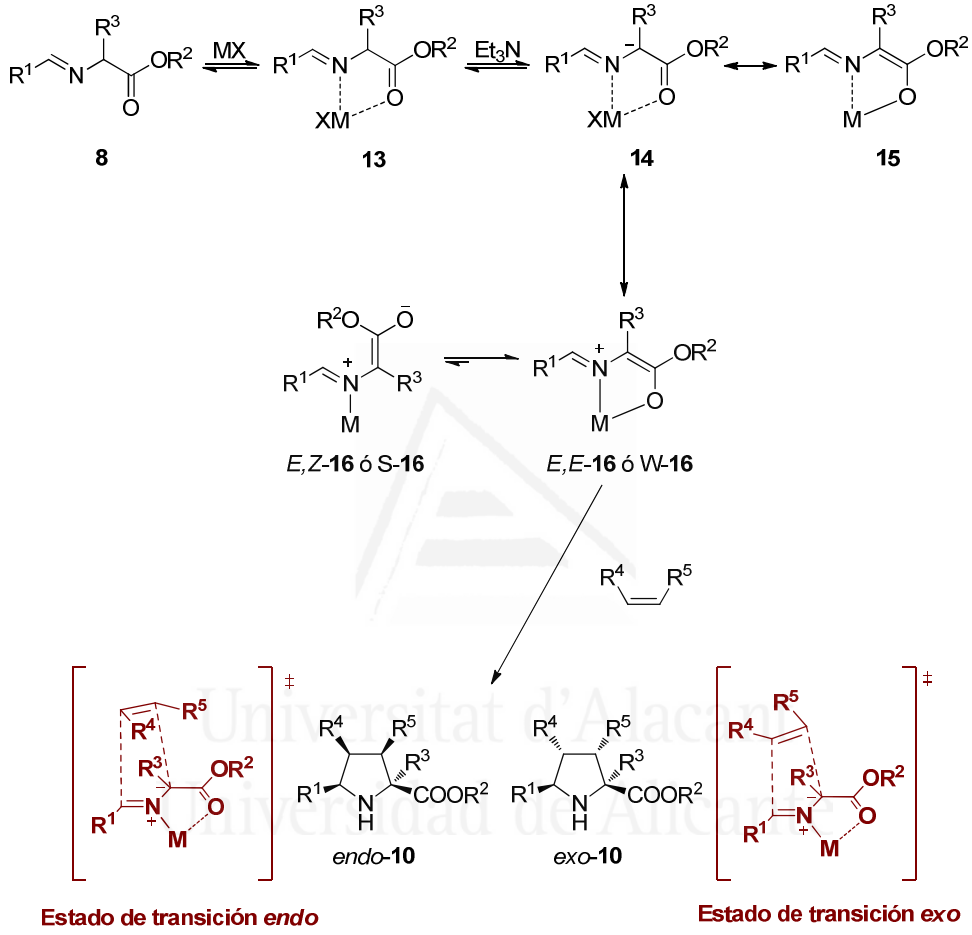

La coordinación del ión metálico, tanto por parte de la imina como por el éster, incrementa la acidez del hidrógeno en α al carbonilo y facilita la desprotonación mediante una base débil, obteniéndose mayoritariamente de forma cinética el iluro de azometino *E*,*E*-**16** llamada también conformación W-**16,** y apenas nada del iluro de azometino *E,Z*-**16** o S-**16**. De esta forma, el iluro de azometino *E*,*E*-**16** evoluciona a partir de dos estados de transición posibles, *endo* y *exo*, para dar lugar a los correspondientes cicloaductos **10** con configuración relativa 2,5-*cis*. Varios ácidos de Lewis pueden emplearse para este propósito,

tales como sales de Ag^{I}, Tl^{I}, Li^{I}, Ca^{II}, Mg^{II}, Co^{II}, Ti^{IV}, Zn^{II}, Cu^{I}, Cu^{II} y Sn^{IV}, junto con bases orgánicas como la de Hünig o diisopropiletilamina (**DIPEA**), Et_3N, 1,3-diazabiciclo[5.4.0]undecano (**DBU**), tetrametiletiléndiamina (**TMEDA**), derivados de guanidina y fosfacenos, así como con bases inorgánicas. Esta reacción también puede producirse en ausencia de base, pero de forma más lenta y siendo necesarias temperaturas superiores.

La mayor ventaja de los iluros de metalo-azometino respecto a la 1,2-prototropía es que existe un gran control de la geometría del dipolo que se traduce en la elevada estereoselectividad de las pirrolidinas que se obtienen. El iluro *E,E*-**9**, generado térmicamente por 1,2-prototropía, puede sufrir un proceso de estereomutación que, junto con las dos posibles aproximaciones (*endo* y *exo*), contribuye a la complejidad de la reacción, alcanzándose así una mezcla de productos (**Esquema 5**). Éste no es el caso cuando el proceso se produce a través de iluros de metalo-azometino, que se generan bajo condiciones de reacción más suaves, obteniéndose generalmente una única especie (iluro *E,E*-**16**, **Esquema 6**), especialmente cuando se parte de iminas formadas a partir de aldehídos aromáticos y aminoésteres. En este caso, la cicloadición es muy selectiva hacia la formación del producto *endo*, aunque puede depender de las propiedades estructurales del dipolarófilo. La estereomutación en el iluro **16** puede observarse al emplear iminas derivadas de aldehídos alifáticos.[9] Este proceso puede evitarse con la elección del ácido de Lewis y del disolvente adecuado. Además, gracias a las condiciones suaves de reacción con las que pueden generarse los iluros de metalo-azometino se pueden emplear iminas derivadas de aldehídos alifáticos; mientras que, bajo condiciones térmicas (1,2-prototropía), estas iminas sufren una isomerización imina-enamina, dando lugar a bajos rendimientos en la cicloadición.

Todo este elevado control estereoquímico y la ordenación previa de los componentes en los estados de transición hace que la síntesis asimétrica de prolinas polisustituidas a través de esta reacción dipolar sea un área de especial interés en síntesis orgánica.

[9] Grigg, R.; Montgomery, J.; Somasunderam, A.; *Tetrahedron* **1992**, *48*, 10431.

CAPÍTULO I

IV.- CAPÍTULO I: ESTUDIO CINÉTICO DE LA CICLOADICIÓN 1,3-DIPOLAR TÉRMICA

IV.1.- ANTECEDENTES BIBLIOGRÁFICOS

IV.1.1.- Introducción

La cinética química es un área generalmente vinculada a la química-física, que estudia la velocidad de las reacciones químicas, así como las condiciones y variables que le afectan. Su objetivo es por tanto medir las velocidades de las reacciones químicas y encontrar ecuaciones que relacionen la velocidad de una reacción con variables experimentales.

En este área la detección, estimación e identificación de la concentración de las especies en una reacción química constituyen los puntos clave para realizar un análisis cinético con éxito.[10] Para ello, existen numerosas técnicas, siendo la cromatografía, espectroscopía y la espectrometría de masas las tres más usadas. Actualmente, las más empleadas son las técnicas basadas en la tecnología de láser,[11] técnicas de fluorescencia, espectroscopía fotoelectrónica y rayos X, y resonancia magnética nuclear (**RMN**).

La velocidad de una reacción varía considerablemente de unos casos a otros. Por ejemplo la reacción que tiene lugar entre H_3O^+ (ac.) y OH^- (ac.) es instantánea, mientras que en otras situaciones la reacción es tan lenta, que parece no suceder, como es el caso de la conversión de $C_{diamante}$ en $C_{grafito}$. En el rango intermedio encontramos todas aquellas reacciones que pueden ser motivo de estudio. Si bien es cierto, en todos los casos, la concentración del reactivo decrece con el tiempo, y la velocidad de reacción mostrará por tanto, cómo de rápido es ese decrecimiento.

Así pues, pueden clasificarse, de forma muy general, las reacciones en lentas y rápidas como muestra la **Tabla 1** a continuación.

[10] Wright, M. R.; *An Introduction to Chemical Kinetics*, John Wiley & Sons, Chichester, **2004**.
[11] El láser abarca desde el rango de microondas hasta el infrarrojo (IR) visible, y desde el visible al ultravioleta (UV).

Tabla 1. Clasificación de las reacciones por su velocidad.

Tipo de Reacción	Duración aparente para ser completa	Vida media
Muy rápida	microsegundos o menos	10^{-12} a 10^{-6} s.
Rápida	segundos	10^{-6} a 1 s.
Moderada	minutos u horas	1 a 10^{-3} s.
Lenta	semanas	10^{3} a 10^{6} s.
Muy lenta	semanas o años	>10^{6} s.

Existen numerosos factores que afectan a la velocidad de la reacción, como por ejemplo la presencia o no de catalizadores, los disolventes y el medio en general, la presión especialmente en reacciones en fase gas o la radiación en caso de reacciones fotoquímicas. Pero si hay un efecto al que la velocidad de las reacciones sea especialmente sensible es la temperatura, y por ello el análisis térmico se convierte en un área extensa y compleja a la hora de llevar a cabo un análisis de la cinética química.

IV.1.2.- Análisis Térmico

La confederación internacional de análisis térmico y calorimetría (**ICTAC**) define el análisis térmico (**TA**) como un grupo de técnicas en las cuales una propiedad de la muestra es estudiada en función del tiempo o la temperatura, mientras que la temperatura de la muestra es controlada en un medio específico.[12]

Existen diferentes metodologías basadas en este principio, que difieren entre ellas en las propiedades a estudiar y en los programas de temperatura. Así pues, el análisis térmico está estrechamente ligado al concepto de calorimetría, que no es más, como su propio nombre indica, que la medida del calor en un medio dado.

[12] Gallagher, P. K; *Handbook of Thermal Analysis and Calorimetry*. Ed. Vol. 1-5, Elsevier Science, Amsterdam, **2003-2007**.

En el análisis térmico los cambios de peso configuran la base de la termogravimetría (**TG**), mientras que la medida de los cambios de energía constituye la base del análisis térmico diferencial (**DTA**) y de la calorimetría diferencial de barrido (**DSC**). Así por ejemplo, la termogravimetría nos dice cuando una muestra pierde o gana peso y cuanto, mientras que el **DTA** y la **DSC** nos dice si una reacción o cambio físico es endotérmico o exotérmico, y a menudo es capaz de medir la variación de calor.

Estas técnicas se pueden aplicar al estudio de casi cualquier sustancia; sin embargo, existen otra serie de propiedades que también pueden ser medidas aunque las técnicas a las que dan lugar sean de aplicación más limitada.

Dichas técnicas pueden clasificarse en función de la propiedad física o química sometida a estudio, como recoge la siguiente tabla (**Tabla 2**).

Tabla 2. Clasificación primaria de métodos calorimétricos y termoanalíticos

Método	Propiedad	Abreviación
Análisis Térmico Diferencial	Diferencia de Temperatura	DTA
Calorimetría Diferencial de Barrido	Masa	DSC
Análisis Termogravimétrico		TGA
Termogravimetría		TG
Análisis Termomecánico	Dimensión/Propiedades Mecánicas	TMA
Análisis Termomanométrico	Presión	
Análisis Termoeléctrico	Propiedades Eléctricas	TEA
Análisis Termomagnético	Propiedades Magnéticas	
Análisis Termoóptico	Propiedades Ópticas	TOA
Análisis Termoacústico	Propiedades Acústicas	TAA

Específicamente, la calorimetría diferencial de barrido es una técnica experimental dinámica que permite determinar la cantidad de calor que absorbe o libera una sustancia, cuando es mantenida a temperatura constante, durante un tiempo determinado, o cuando es calentada o enfriada a velocidad constante, en un determinado intervalo de temperaturas. Existen dos tipos de métodos para obtener datos en **DSC**:

- **DSC** de flujo de calor (*Heat Flux DSC*): Registra la diferencia de temperatura entre la muestra y la referencia, ambos situados en un

calentador, como una medida directa de la diferencia en la velocidad de flujo de calor entre ambas muestras. En la **Figura 1** se muestra un esquema de un aparato de **DSC** de flujo de calor. Ambas células que contienen la muestra (M) y la referencia (R), están herméticamente selladas para evitar cualquier intercambio de materia. La diferencia de temperatura entre ambas se mide mediante un termopar situado en la base de las células. Un segundo grupo de termopares registra la diferencia de temperatura entre el calentador y las células. Finalmente el software procesa la información generando la curva de **DSC**.

Figura 1. Esquema de un aparato de DSC de flujo de calor.

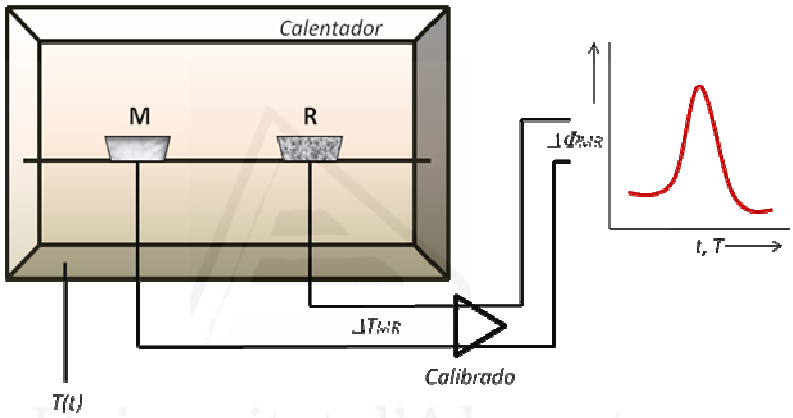

- **DSC** de potencia compensada (*Power Compensating DSC*): La muestra y la referencia se colocan en dos pequeños calentadores independientes de manera que la diferencia de temperatura entre ambos sea mínima (**Figura X**). Si conforme transcurre la medición hay una diferencia de temperatura mayor esta se asigna a una diferencia en la capacidad calorífica entre la referencia y la muestra, o bien a una transformación exotérmica/endotérmica en esta última. Esto puede ser cuantificado mediante el calor adicional suministrado o sustraído para seguir manteniendo mínima la diferencia de temperaturas.

Figura 2. Esquema de un aparato de DSC de potencia compensada.

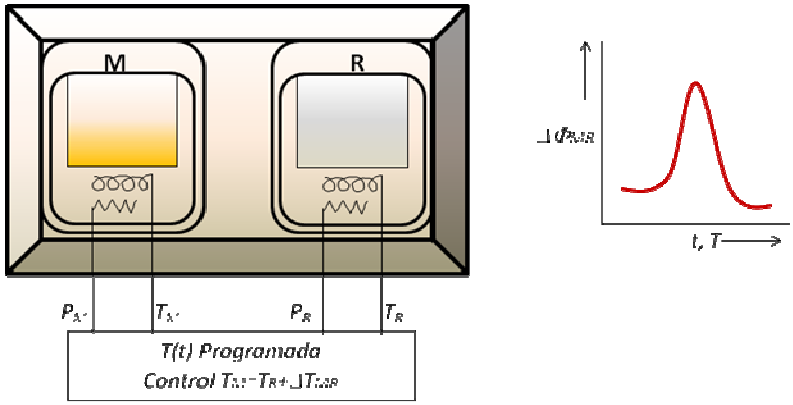

La **DSC** se establece como una técnica importante en el campo de la Ciencia de Materiales, industria alimentaria y farmacéutica debido a su elevado grado de sensibilidad y a su rápida velocidad de análisis. Por otra parte es bien sabido que el conocimiento de la estabilidad térmica de un material, así como la completa caracterización de sus transiciones es de primordial interés en los materiales con potenciales aplicaciones industriales.[13]

Como regla general, puede decirse que todas las transformaciones o reacciones donde se produce un cambio de energía, pueden medirse por **DSC**. Entre las diversas utilidades de esta técnica podemos destacar:

- Medidas de capacidad calorífica.
- Determinación de temperaturas características de transformación o de transición, tales como transición vítrea, cristalización, fusión, ebullición, sublimación, descomposición, etc.
- Estabilidad térmica de los materiales.
- Estudios cinéticos.

IV.1.3.- Estudios cinéticos por DSC

La identificación y cuantificación de la concentración de las diferentes especies presentes en una reacción química puede calcularse mediante el uso de diversas técnicas analíticas como se ha detallado anteriormente. Además de estas

[13] Suriñach, S.; Baro, M. D.; Bordas, S.; Clavaguera, N.; Clavaguera-Mora, M. T.; *Bol. Soc. Esp. Ceram. Vidr.* **1992**, *31*, 11.

técnicas, el flujo de calor obtenido a través de experimentos de **DSC**, puede utilizarse como un patrón cinético, debido a que guarda una relación proporcional con la conversión de los reactivos, y por tanto, con la velocidad de reacción. Esto es cierto para reacciones exotérmicas en las que la cinética de la reacción controla el flujo de calor. Sin embargo para el caso de reacciones endotérmicas, esta suposición puede inducir a error, debido a que el flujo de calor está condicionado por la transferencia de calor que tiene lugar entre el aparato y la propia muestra.[12]

Para llevar a cabo un estudio cinético por **DSC** existen numerosas metodologías para la interpretación de los datos obtenidos así como para el análisis de los factores cinéticos a estudiar. En la presente memoria han sido clasificados en dos categorías, en función del tipo de ensayo desarrollado, a temperatura constante (isotermo) o a velocidad de calentamiento constante (dinámico).

IV.1.3.1.- Métodos Dinámicos

Los métodos "no-isotermos" o dinámicos están basados en aquellos experimentos ejecutados con rampa de calentamiento, donde la muestra se calienta gradualmente a una velocidad de calentamiento que, generalmente, permanece constante, y que suele mantenerse entre 1 y 10 °C/min en función de la metodología.[14] Existen multitud de métodos dinámicos, pero en la presente memoria nos centraremos en sólo tres, Borchardt-Daniels (**B/D**)[15], Kissinger[16] y Ozawa-Flynn-Wall (**OFW**)[17].

IV.1.3.1.1.- Método de Kissinger

El punto de partida en los análisis cinéticos dinámicos es:

$$d\alpha/dT = (d\alpha/dt)\,(dt/dT) = (d\alpha/dt)\,(1/\beta) \qquad \textbf{(1)}$$

Donde α es la conversión de la reacción y β es la velocidad de calentamiento en °C/min. La ecuación **(1)** define la variación de la conversión

[14] ASTM E2070-00, ASTM Int., West Conshohocken, US.
[15] Borchardt, H.J.; Daniels, F.; *J. Am. Chem. Soc.* **1956**, *79*, 41.
[16] Kissinger, H. E.; *Anal. Chem.* **1957**, *29*, 1702.
[17] **a)** Ozawa, T. J.; *Therm. Anal.* **1970**, 2, 301 **b)** Flynn, J. H.; Wall, L. A.; *J. Res. Nat. Bur. Stand* **1966**, *70A*, 487.

frente a la temperatura (T) como el producto de la variación de la conversión frente al tiempo por la inversa de la variación de la temperatura frente al tiempo, o lo que es lo mismo, la inversa de β.[12]

Basándonos en la ecuación de Arrhenius[18] **(2)**:

$$k = A\exp(-E_a/RT) \qquad \textbf{(2)}$$

Y combinando ambas, la ecuación **(1)** queda como:

$$\mathrm{d}\alpha/\mathrm{d}T = (A/\beta)\exp(-E_a/RT)(1-\alpha)^{\mathrm{n}} \qquad \textbf{(3)}$$

Ya que la variación de la conversión frente al tiempo $(\mathrm{d}\alpha/\mathrm{d}t)$ puede expresarse también como la velocidad de la reacción (k).

Como se ha mencionado anteriormente, los experimentos dinámicos más comunes se llevan a cabo con una rampa de calentamiento constante, donde:

$$T = T_0 + \beta T \qquad \textbf{(4)}$$

Donde T_0 es la temperatura inicial al comenzar el experimento siendo lo suficientemente baja para realizar el ensayo correctamente.[19] Tomando el punto en el que la conversión es del 50% (punto máximo en la curva de **DSC**), y realizando la segunda derivada de la ecuación **(3)**, llegamos finalmente a la ecuación de Kissinger **(5)**. Recordemos que esta derivada debe ser igual a cero en el punto de inflexión.

$$(E_a/\mathrm{R}T_m^{\,2}) = (A/\beta)\exp(-E_a/RT) \qquad \textbf{(5)}$$

Donde T_m es la temperatura máxima del experimento. Si bien es cierto, para este ajuste, el método de Kissinger supone orden de reacción uno. Reordenando los términos y aplicando logaritmos en la ecuación de Kissinger se obtiene la ecuación **(6)**:

$$\ln(\beta/T_m^{\,2}) = \ln(AR/E_a) - (E_a/R)(1/T_m) \qquad \textbf{(6)}$$

Como puede verse, la ecuación **(6)**, que es una variación de la original obtenida por Kissinger, tiene la forma de ecuación de una recta, pudiendo

[18] Arrhenius, S.; *Z. Phys. Chem.* **1889**, *4*, 226.
[19] Roura, P.; Farjas, J.; *J. Mater. Res.* **2009**, *24*, 3095.

obtenerse de forma muy sencilla los parámetros cinéticos A y E_a, de la ordenada en el origen y la pendiente respectivamente, representando la recta entre $\ln(\beta/T_m^2)$ frente a $(1/T_m)$ a partir de los datos obtenidos por **DSC** en una serie de experimentos a diferentes velocidades de calentamiento.

La ecuación de Kissinger se ha usado ampliamente para diferentes tipos de análisis, como el estudio de la deshidrogenación de nanotubos de carbono,[20] la cristalización de vidrios,[21] o el análisis térmico de lípidos, proteínas y membranas biológicas.[22] La obtención pues de la E_a a partir de la pendiente de la recta **(6)** puede tomarse como exacta únicamente para procesos en los que sigan una cinética de primer orden. Para cinéticas con cualquier otro orden de reacción, el valor de E_a es lo bastante preciso, con un error asumible (a menudo inferior al 2%).[23] El método de Kissinger es por tanto un método versátil, que se viene utilizando desde hace más de cincuenta años, especialmente por la simplicidad y la facilidad con la que puede obtenerse diferentes parámetros cinéticos como la energía de activación. Si bien es cierto, existen métodos más exactos y precisos, pero también algo más tediosos a la hora de trabajarlos.

IV.1.3.1.2.- Método de Ozawa-Flynn-Wall (OFW)

El Profesor Ozawa mantiene el supuesto de que el orden de reacción es un valor constante independientemente de la velocidad de calentamiento la curva de **DSC** alcanza el pico máximo,[24] suponiendo también como en el método anterior, una cinética de primer orden, se obtiene la ecuación **(7)**:

$$\ln\beta = \text{cte} - (E_a/R)(1/T) \qquad \textbf{(7)}$$

De acuerdo con la ecuación **(7)**, pueden realizarse experimentos de DSC con diferentes velocidades de calentamiento, obteniendo la temperatura máxima para cada uno de las curvas de **DSC**. Representando $\ln\beta$ frente a $(1/T)$, se obtiene la recta de Ozawa. Como en el caso de la metodología propuesta por Kissinger, puede calcularse la energía de activación a partir de la pendiente de esta recta. Normalmente son necesarios tres o más experimentos que aseguren fiabilidad a

[20] Lee, J.W.; Kim, H.S.; Lee, J.Y.; Kang, J.K.; *Appl. Phys. Lett.* **2006**, *88*, 143126.

[21] **a)** Jona, E.; Simon, P.; Nemcekova, K.; Pavlik, V.; Rudinska, G.; Rudinska, E.; *J. Therm. Anal. Calorim.* **2006**, *84*, 673. **b)** Srivastava, A.P.; Srivastava, D.; Dey, G.K.; *J. Magn. Magn. Mater.* **2006**, *306*, 147.

[22] Ladbrook, B.D.; Chapman, D.; *Chem. Phys. Lipids* **1969**, *3*, 304.

[23] Budrugeac, P.; Segal, E.; *J. Therm. Anal. Calorim.* **2007**, *88*, 703.

[24] http://www.scientificsoftware-solutions.com

los resultados, con velocidades de calentamiento que oscilen entre uno a diez °C/min.

Debido a las restricciones impuestas por los métodos como el de Kissinger y Ozawa, muchos investigadores han hecho intentos por establecer una metodología de análisis libre de modelo o "Model Free Kinetics" (**MFK**). De esta forma, el profesor Flynn y el profesor Wall, reescribieron la ecuación **(3)**, con forma de integral, dónde el factor a integrar era sustituido por una función de aproximación. Así pues, la metodología seguida en este modelo es la que se conoce como método de Ozawa-Flynn-Wall (**OFW**), que no es más que el método de Ozawa optimizado.

IV.1.3.1.3.- Método de Borchardt-Daniels (B/D)

Hans J. Borchardt estudió e investigó bajo la dirección del profesor Farrington J. Daniels en la universidad de Wisconsin, donde desarrollarían juntos las bases de un nuevo método para el estudio del análisis térmico, hoy conocido como Borchardt-Daniels.

Como en los métodos anteriores, la metodología de Borchardt-Daniels también sigue un comportamiento tipo Arrhenius, y además sigue una reacción de orden n donde se cumple que:

$$\mathrm{d}\alpha/\mathrm{d}t = k(\mathrm{T})(1-\alpha)^{\mathrm{n}} \qquad \textbf{(8)}$$

Donde α es la conversión. Por tanto aplicando logaritmos queda la expresión:

$$\ln(\mathrm{d}\alpha/\mathrm{d}t) = \ln[k(\mathrm{T})] + \mathrm{n}\ln(1-\alpha) \qquad \textbf{(9)}$$

Y combinando con la ecuación de Arrhenius **(2)**, la ecuación **(9)** queda finalemente como:

$$\ln(\mathrm{d}\alpha/\mathrm{d}t) = \ln A - (E_a/\mathrm{RT}) + \mathrm{n}\ln(1-\alpha) \qquad \textbf{(10)}$$

Además de poder calcular la energía de activación y el parámetro cinético A, este método permite obtener además el orden de reacción mientras que tanto en Kissinger como en **OFW**, se suponía de primer orden. Así pues, la ecuación **(10)** puede resolverse mediante análisis de regresión multilineal o *"multiple linear*

regression" en inglés (**MLR**) siguiendo la metodología estándar.[14] Para ello, debe dividirse la curva de **DSC** en veinte segmentos uniformemente espaciados, comenzando el primer segmento en el punto que la curva alcance el 10 % del área de pico, y acabando el último segmento en un 50 % del área de pico usando la ecuación **(10)**. Después, a partir de los valores obtenidos de $\ln[k(\mathrm{T})]$, puede trazarse una recta representándolos frente a $(1/T)$ (Eq. Arrhenius), obteniendo así la energía de activación y el factor preexponencial $\ln A$.

Para que los resultados obtenidos por **B/D** sean fiables deben cumplirse dos requisitos experimentales. El primero es, como en el caso de Kissinger y **OFW**, que no debe producirse ninguna variación en la masa de la muestra durante la reacción. Para ello, las muestras deben estar herméticamente selladas como se detalla en el apartado **IV.1.2**. El segundo requisito tiene que ver con la temperatura. Es necesario eliminar cualquier efecto que produzca retrasos a la hora de registrar la temperatura. Para ello se recomienda usar velocidades de calentamiento que no superen los 10 °C/min.

Como se ha dicho anteriormente, este método es algo más tedioso a la hora de calcular diferentes factores cinéticos. Sin embargo ofrece mayor versatilidad, pudiendo ser utilizado para cinéticas más complejas cuyo orden de reacción sea fraccionario.

IV.1.3.2.- Método Isotermo

Los métodos isotermos se centran en el estudio de los parámetros cinéticos a una temperatura conocida y constante a lo largo del experimento. Los métodos dinámicos descritos anteriormente, son más rápidos y simples, pero no pueden aplicarse de manera cuantitativa para sistemas autocatalíticos.[14] Estos sistemas se caracterizan por la formación de especies intermedias o incluso el propio producto que aceleran el curso de la reacción.

Esta metodología puede ser utilizada tanto para calcular reacciones de orden n, como para reacciones exotérmicas autocatalíticas. Sin embargo este tipo de modelos no suelen usarse para reacciones endotérmicas, como para el estudio de la cinética en procesos de cristalización.

Mientras que las reacciones de orden n siguen la ecuación **(8)**, las reacciones autocatalíticas siguen la siguiente ecuación:

$$d\alpha/dt = k(T)\,\alpha^{m}\,(1-\alpha)^{n} \qquad \textbf{(11)}$$

Donde el superíndice "m" es el orden de reacción de la fracción autocatalítica, y $k(T)$ sigue un comportamiento tipo Arrhenius.

Así pues, es necesario realizar tres o más experimentos a temperatura constante, para poder obtener los diferentes valores cinéticos ($k(T)$, m, n, $\ln A$ y E_a). Además, también puede obtenerse el valor de entalpia de la reacción (ΔH), a partir de la integral de la curva **DSC** en la zona en la que se produce la transferencia de calor.

Para elegir el rango de temperaturas para realizar los experimentos, se recomienda seleccionar como temperatura más baja, aquella que se encuentre entre unos 10-20 °C por debajo de la temperatura donde empieza a tener lugar la reacción; y como temperatura más alta, aquella que dé lugar a la mitad del pico máximo de la curva de **DSC**, creada a partir de calentar la muestra con una velocidad de 5 °C/min.

Para que el análisis cinético sea preciso y reproducible, es necesario que los valores obtenidos en los diferentes experimentos, también lo sean. Si bien no existen criterios claros que determinen como llegar a un comportamiento reproducible, pueden determinarse las variaciones de conversión/tiempo entre experimentos similares. Por ejemplo variar la cantidad de alguno de los reactivos puede revelar la influencia del calentamiento o enfriamiento propio de la reacción, así como los efectos de reacciones secundarias u otro tipo de procesos físico-químicos.[12]

IV.1.4.- DSC en síntesis orgánica

Además de los numerosos campos en los que se ha usado esta técnica, ya sean industriales o más cercanos a la investigación, como los mencionados en el apartado **IV.1.2**, una de las aplicaciones más interesantes es la que involucra la síntesis orgánica por ser una herramienta de relativamente fácil uso, rápida, reproducible, versátil y que puede aportar información sobre el mecanismo de reacción que otras técnicas pasan por alto.

Sin embargo, pese a los numerosos ejemplos que pueden encontrarse en la bibliografía de análisis por **DSC** aplicado a la química orgánica, no se ha encontrado ninguno que haga un análisis profundo y detallado para reacciones de

dos o más componentes. Para el primero de los casos, puede citarse por ejemplo el trabajo de Shu y colaboradores,[25] en el que mediante por **DSC**, usando métodos dinámicos e isotermos, analizan la descomposición autocatalítica del peróxido de benzoílo. Otro ejemplo destacable es el trabajo desarrollado por el grupo de Kappe[26] en Austria, en el que mediante esta técnica aplicada a la síntesis de heterociclos, evalúan el reordenamiento y cierre intramolecular de compuestos derivados de azidas. Por otro lado Cammenga y Epple detallan las bases del TA, para polímeros y moléculas de bajo peso molecular.[27]

Para el segundo caso, es decir para reacciones más complejas, donde se involucren dos o más componentes, sólo se ha encontrado el trabajo realizado por Cammenga y colaboradores,[28] en el que en uno de los ejemplos, calculan la E_a a partir de los datos obtenidos por **DSC**, de la reacción de Diels-Alder que tiene lugar entre el hexaclorociclopentadieno y ciclopenteno, poniendo un exceso del primero y asumiendo así, una cinética de pseudo-primer orden.

[25] Liu, S.H.; Hou, H.Y.; Shu, C.M.; *Proceedings of the 6th International Conference on Process Systems Engineering (PSE ASIA)* 25 - 27 June **2013**, Kuala Lumpur.
[26] Kappe, T.; Stadlbauer, W.; *Molecules*, **1996**, *1*, 255.
[27] Cammenga, H.K.; Epple, M.; *Angew. Chem. Int. Ed. Engl,.* **1995**, *34*, 1171.
[28] Belichmeier, J.A.; Cammenga, H.K.; Schneider, P.B.; Steer,A.G.; *Thermochimica Acta*, **1998**, *310*, 147.

IV.2.- OBJETIVOS

A la vista de lo planteado en la Introducción General y de los antecedentes descritos anteriormente, se plantearon los siguientes objetivos:

- Describir las condiciones óptimas para realizar un análisis por **DSC** de una reacción bimolecular (dos componentes) como es la cicloadición 1,3-dipolar entre un iluro de azometino generado térmicamente y un dipolarófilo.
- Llevar a cabo el estudio cinético de dicha reacción, mediante el uso de diferentes metodologías de análisis que permitan obtener los parámetros cinéticos y termodinámicos como son: ΔH, E_a, $k(\mathrm{T})$, $\ln A$, así como el orden de reacción.
- Tratar de dilucidar el posible mecanismo de la cicloadición 1,3-dipolar en el ejemplo estudiado y establecer un perfil de reacción a partir de los valores obtenidos.

IV.3.- DISCUSIÓN DE RESULTADOS

De acuerdo con lo planteado en los objetivos, se llevó a cabo el estudio cinético de la cicloadición 1,3-dipolar térmica entre un iluro de azometino generado in situ a partir del iminoester correspondiente, y un dipolarófilo determinado que debía cumplir una serie de requisitos como se detalla más adelante.

Los iluros de azometino son una de las clases de 1,3-dipolos más usadas en síntesis orgánica, y existen variadas metodologías para prepararlos como se detalla en la introducción general. Una de las más empleadas es la 1,2-prototropía que puede controlarse cinéticamente dando lugar a un dipolo con configuración *E,E*-(*sin*), como puede verse en el **Esquema 7**:

Esquema 7

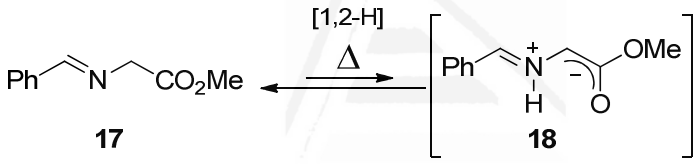

Donde el iminoester **17** es un derivado de benzaldehído y el éster derivado de glicina. Así pues, trató de llevarse a cabo un primer análisis realizando un experimento de **DSC** con la muestra **17**, con el fin de obtener evidencias que demuestren la presencia de la especie dipolar **18** en baja proporción (**Figura 3**):

Figura 3

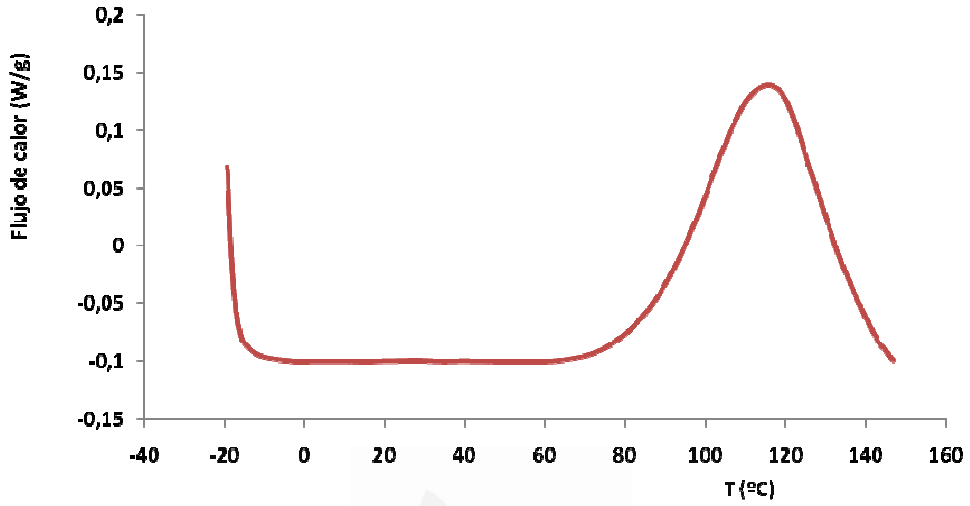

La **Figura 3** muestra una curva de **DSC** realizada a una velocidad de calentamiento de 10 °C/min. Se aprecia que a partir de 70 °C tiene lugar una reacción exotérmica, pero con una transferencia de calor demasiado elevada como para que se debiera a la formación del intermedio **18**. Además, como puede verse en el **Esquema 8**, el proceso no es reversible hacia la formación del producto de partida **X** y por tanto no puede deberse a la reacción fuertemente exotérmica que tiene lugar en la **Figura 3**.

Análisis posteriores junto con un experimento de ^{1}H-RMN realizado a la muestra después de la **DSC**, revelaron la formación de la imidazolidina **19** (**Esquema 9**), en la que la molécula **17**, tras la formación del 1,3-dipolo térmicamente, reaccionaba consigo misma través de una cicloadición 1,3-dipolar.

Esquema 9

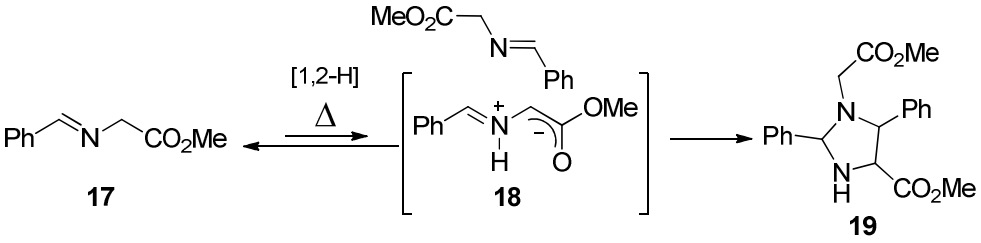

El pico que muestra una reacción exotérmica en la **Figura 3**, corresponde pues, a la reacción mostrada en el **Esquema 9**, e integrando el área total de dicha curva puede obtenerse la entalpía del proceso.[29]

Por tanto, se pensó en la posibilidad de usar como precursor del 1,3-dipolo, el derivado de fenilalanina **20** (**Esquema 10**), ya que en trabajos similares,[30] se había obtenido buenos resultados.

Por otro lado, para elegir el dipolarófilo debía tenerse en cuenta una serie de factores. Para llevar a cabo un experimento por **DSC**, la muestra debe ser lo más uniforme posible, homogénea, y que no dé lugar a problemas de reproducibilidad. Es bien conocido que para este tipo de reacciones, uno de los mejores dipolarófilos son las "maleimidas", por su rápida conversión química, y alto rendimiento y diasteroselectividad. Hay que tener en cuenta que la imina, de la cual se generará el 1,3-dipolo, a temperatura ambiente, es líquida; sin embargo, entre el catálogo de maleimidas N-sustituidas, no se encuentra ninguna que, a esta temperatura, no sea sólida. Por este motivo, se pensó primero en el fumarato de dimetilo, ya que es un dipolarófilo simétrico también que suele dar buenos resultados. Pero, como en el caso anterior, es sólido a temperatura ambiente, siendo además su punto de fusión de 102 °C, con lo que el calor asociado al cambio de estado interfiere de manera importante en el flujo de calor de la propia reacción.

Finalmente, los ensayos se llevaron a cabo con el fumarato de isobutilo, que cumple los requisitos expuestos, con un punto de fusión de 8 °C y un punto de ebullición de 249 °C.

El **Esquema 10** muestra la reacción que tiene lugar entre el fumarato de isobutilo y la imina de partida **20**, a 150 °C y sin disolvente. Se obtuvo una mezcla de diasteroisómeros (**21** Y **22**) en una proporción *endo*:*exo* de *3:1*. El flujo de calor desprendido en esta reacción, puede apreciarse en la **Figura 4** (línea roja), en un experimento de **DSC** con una velocidad de calentamientos de 10 °C/min. En un segundo experimento, se sometió a las mismas condiciones, una muestra formada únicamente por la imina **20**, sin que esta reaccionara consigo misma como sucedía en el caso de la imina **17** (línea azul de la **Figura 4**).

[29] ΔH = 262.5 J/g.
[30] Mancebo-Aracil, J.; Nájera, C.; Sansano, J.; *Org. Biomol. Chem.* **2013**, *11*, 662.

Esquema 10

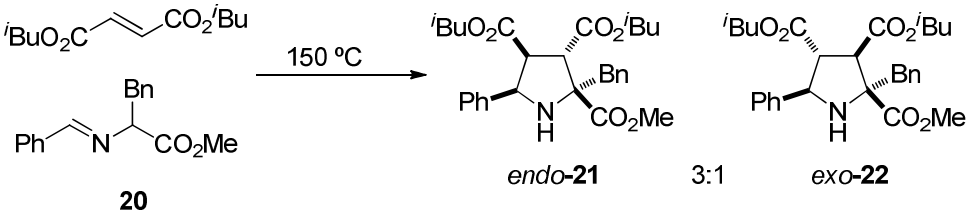

Figura 4

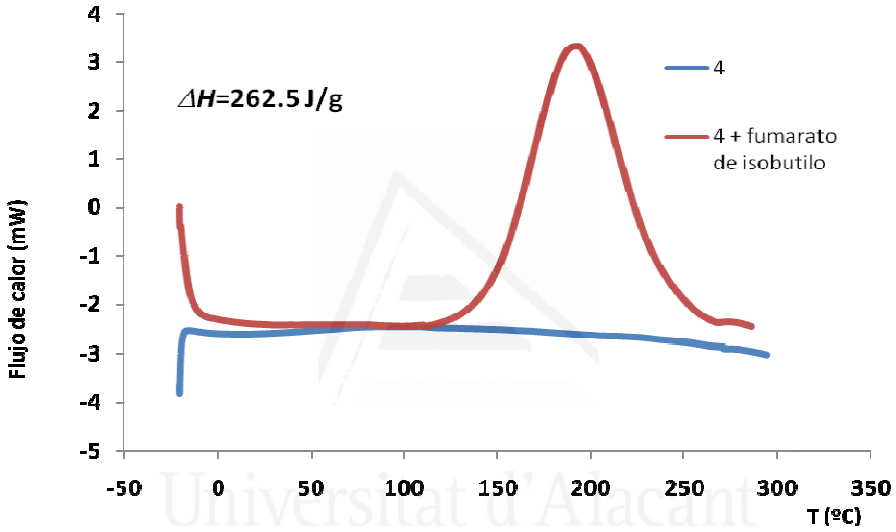

Con esta información en mano, se pasó a evaluar el rango de temperaturas óptimo para llevar a cabo este tipo de estudios cinéticos. Si observamos las curvas de **DSC** de flujo de calor frente a temperatura, se aprecia una forma de campana, que puede ser indicio de una reacción autocatalítica.[31] Además, la representación de la conversión de uno de los reactivos frente al tiempo (**Figura 5**) tiene forma de "S", comportamiento que también es indicativo de un fenómeno de autocatálisis.[32]

[31] *Handbook of Thermal Analysis*, T. Hatakeyama, Z. Liu, Eds. John Wiley & Sons, New York, **1998**, cap. 4

[32] Mata-Pérez, F.; Pérez-Benito, J.; *J. Chem. Educ.* **1987**, *64*, 925.

Figura 5

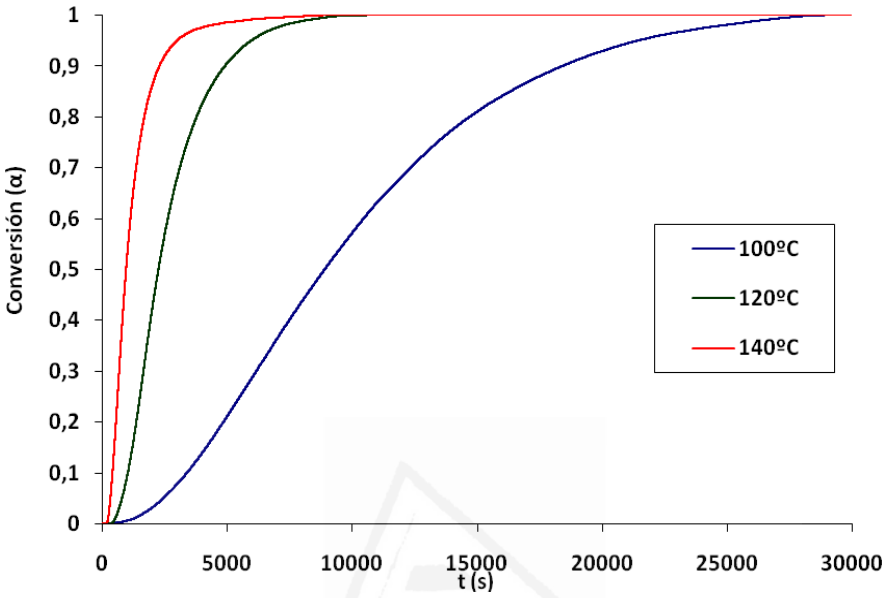

De acuerdo con lo detallado en el apartado **II.1.3**, se procedió a estudiar la cinética de la reacción (**Esquema 10**), a partir de los datos experimentales obtenidos por **DSC**, mediante el uso de diferentes modelos (ver apartado **II.1.3.1**)

Con el fin de correlacionar el proceso llevado a cabo en un calorímetro con la metodología estándar en un laboratorio de síntesis, se trato de reproducir experimentalmente en un tubo de ensayo herméticamente cerrado las condiciones que tienen lugar en el calorímetro (ver **Figura 6**). Para ello, se prepararon cantidades estequiométricas del iminoester de partida **20** y fumarato de isobutilo, haciéndolos reaccionar sin disolvente, a 130 °C con agitación magnética. Así pues se analizó la conversión de alícuotas a diferentes tiempos de reacción mediante ^{1}H-RMN (**Figura 6**, línea azul), para compararlas con los datos obtenidos a partir de la **DSC** (**Figura 6**, línea roja).

Figura 6

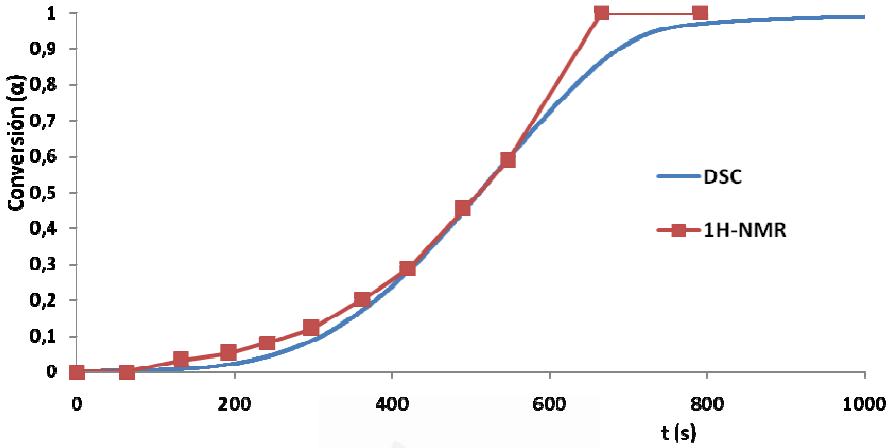

A partir de conversiones del 70 % y superiores, el experimento llevado a cabo por **DSC**, se retrasa con respecto al realizado en el laboratorio de síntesis, debido un fenómeno de difusión, que queda minimizado en el laboratorio debido a la agitación magnética. Sin embargo puede afirmarse que en conversiones entre 0-70 %, el ensayo por **DSC** es reproducible a gran escala[33] en el laboratorio, con lo que queda patente que esta técnica puede usarse junto con muchas otras en el laboratorio de síntesis, por su rapidez, precisión y reproducibilidad.

Con todos los datos obtenidos mediante el análisis térmico y cinético, puede concluirse que la reacción mostrada en el **Esquema 11**, sigue un perfil como el mostrado en la **Figura 7**, mediante un mecanismo de reacción complejo, en el que se da un fenómeno de autocatálisis, con una E_a cerca de 70 KJ/mol y un orden de reacción fraccionario cercano a 2.

[33] Apróximadamente, de unos $5 \cdot 10^{-3}$ mmol de imina **X** en el experimento de **DSC** a 2 mmol en el tubo de ensayo.

Esquema 11

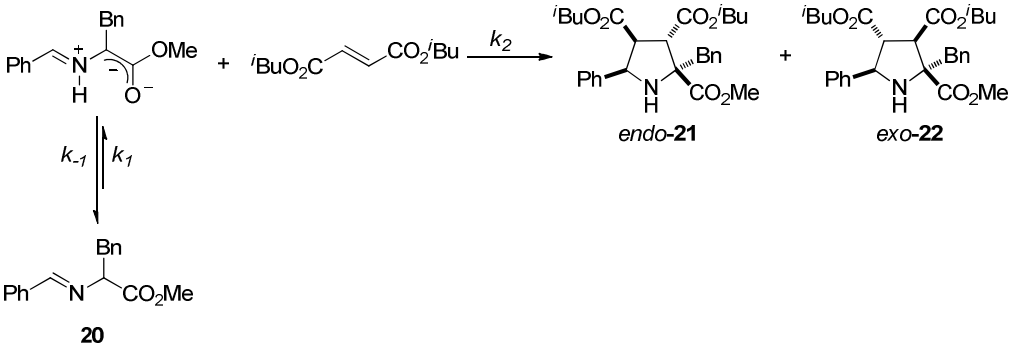

Figura 7

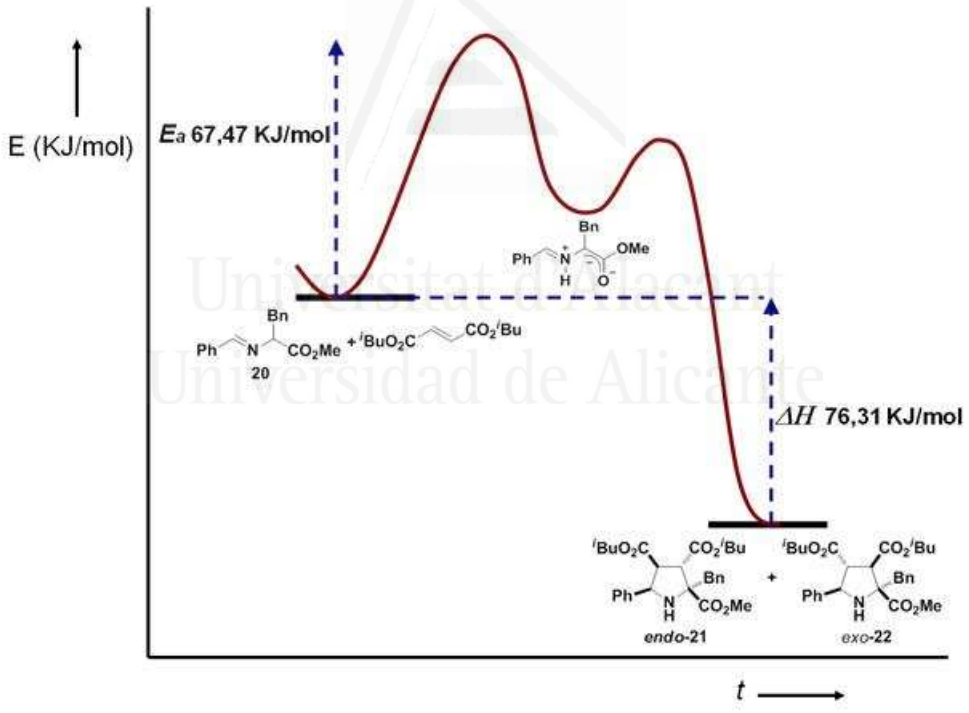

Un estudio más detallado de lo resumido anteriormente se encuentra en el siguiente apartado.

IV.4.- CHEMPLUSCHEM 2012, 77, 770

CHEMPLUSCHEM FULL PAPERS

DOI: 10.1002/cplu.201200107

Kinetic Study of Thermal 1,3-Dipolar Cycloaddition of Azomethine Ylides using Differential Scanning Calorimetry as Monitoring Window

Juan Mancebo-Aracil,[a] María J. Muñoz-Guillena,[b] Ion Such-Basáñez[b] and José M. Sansano-Gil*[a]

This paper is dedicated to Prof. Carmen Nájera on the occasion of her 60th birthday

Abstract Text. Kinetics of 1,3-dipolar cycloaddition involving azomethine ylides, generated from thermal [1,2]-prototropy of the corresponding imino ester, employing differential scanning calorimetry (DSC), is surveyed. Glycine and phenylalanine derived imino esters have different behavior. The first one prefers reacting with itself at 75 °C, rather than with the dipolarophile. However, the α-substituted imino ester gives the cycloadduct at higher temperatures. The thermal dynamic analysis by ^{1}H NMR of the neat reaction mixture of the glycine derivative reveals the presence of signals corresponding to the dipole in very small proportion. The non-isothermal and isothermal DSC curves of the cycloaddition of phenylalaninate and diisobutyl fumarate are obtained from freshly prepared samples. The application of known kinetic models and mathematical multiple non-linear regressions (NLR) allow to determine and to compare E_a, lnA, reaction orders, and reaction enthalpy. Finally a rate equation for each different temperature can be established for this particular thermal cycloaddition.

1. Introduction

The general term thermal analysis (TA) is used to describe analytical experimental techniques which investigate the behavior of a sample reaction as a function of the temperature. Differential scanning calorimetry (DSC) is frequently used to obtain a wealth of information about a material or a reaction, kinetic parameters being one of the most important data.[1] Wide-ranging applications in the field of polymer science, plastics, foods and pharmaceuticals, glasses and ceramics, proteins and life science materials, etc., have been documented. Also, valuable applications of TA in many industries have been found.[1] A DSC analyzer measures the energy changes that occur as a sample is heated, cooled or held isothermally, together with the temperature at which these changes take place. One of the major advantages of DSC is that samples are very easily encapsulated, usually with little or no preparation, ready to be placed in the DSC, so that measurements can be quickly and easily made. Additionally, due to electromechanical advances, data obtained by high performance calorimeters and thermobalances can give extremely accurate and reproducible quantitative measurements (including kinetic data) that occur in the sample.[2][3]

Concerning kinetic analysis, the detection, identification and estimation of concentrations of species present in a reaction has been accomplished by chromatographic and spectroscopic techniques, mass spectrometry, laser devices, fluorescence, photoelectron spectroscopy and NMR experiments.[4] In this study, the heat flow, obtained from DSC experiments, is used as a kinetic survey of the 1,3-dipolar cycloaddition (1,3-DC) due to its proportionality with respect to the reaction rate. This is true for exothermic reactions in which heat flow is controlled by the kinetics of the reaction, while this assumption does not hold true for endothermic reactions where the heat flow is controlled by the heat transfer between the sample and the apparatus.[5]

Many organic substances have been submitted to these types of tests but, to the best of our knowledge, no bimolecular organic reaction has been deeply analyzed[6] employing DSC techniques. Thermal 1,3-DC of imino esters and diisobutyl fumarate would be a suitable transformation to be kinetically

[a] J. Mancebo-Aracil and Dr. J. M. Sansano-Gil
Departamento de Química Orgánica e Instituto de Síntesis Orgánica (ISO), Universidad de Alicante, 03080-Alicante (Spain)
Fax: (+34-965903549)
E-mail: jmsansano@ua.es
[b] Dr. M. J. Muñoz-Guillena, and I. Such-Basáñez
Servicios Técnicos de Investigación, Universidad de Alicante, 03080-Alicante (Spain)

Supporting information for this article is available on the WWW under http://dx.doi.org/10.1002/cplu.201200107
Article first published online: 26 JUN 2012

analyzed by DSC.[7] Since the seminal Hülsgen contribution in the early 1960s,[8] 1,3-DC have been extensively studied from a theoretical point of view,[9] and experimentally applied for many purposes.[10] Despite of the efforts dedicated to survey this type of cycloadditions, several aspects are not clear, such as the presence of ionic or diradical or *pseudo*-diradical species[11] in the transition states for thermally induced generation of 1,3-dipoles, the detection of migrations able to promote the existence of them, etc.

In this work, we will determine the kinetic parameters of the above mentioned thermal 1,2-prototropy of imino esters selecting DSC as technical tool. Also, a comparison of these kinetic parameters employing different mathematical models, will be made.

2. Results and Discussion

Azomethine ylides are one of the most frequently employed 1,3-dipoles in organic synthesis[12] and, particularly, for the construction of pyrrolidines. There are many strategies for preparing them,[10b] 1,2-prototropy of α-imino ester type-**1** (Scheme 1) being widely employed as a fast strategy. The reaction can be performed from the isolated imine type-**1** plus the dipolarophile, or through a multicomponent one pot imine formation-cycloaddition. Initially, neat **1** (2.753 mg in a sealed crucible) underwent a thermal study in order to detect a small exothermic process revealing the existence of such rearrangement to yield **2** (always freshly prepared samples were used for analyses). Figure 1 showed that, under a 10 °C·min^{-1} heating rate, an exothermic process started approximately at 75 °C, however the transfer of heat seemed too high for the generation of intermediate **2**. The reversibility of the process indicated in Scheme 1 is not in agreement with such a large heat flow. Therefore, another DSC experiment consisting on iterative cycles of heating-cooling, up to a temperature in the very initial stages of the reaction (80 °C), was employed for demonstrating the described equilibrium (Figure 2). However, the repeated cycles of heating revealed that each time the sample was reheated the observed heat flow became lower so, a consumption of the starting imine **1** was bound to be occurring. The ^{1}H NMR of the thermally transformed sample revealed that the imino ester **1**, after suffering the 1,2-proton migration, reacted with itself to afford, almost quantitatively, a mixture of diastereomeric imidazolidines **3**[13] (Scheme 2). The peak observed in Figure 1 corresponds to an exothermic reaction, and the complete area of the heat flow is equivalent to the enthalpy of the whole transformation to afford them.

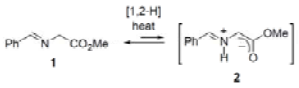

Scheme 1. Thermal generation of stabilized azomethine ylides.

With all these results derived from the fast reaction of imine **1** with itself, the addition of a dipolarophile such as diisobutyl fumarate to the dipole **2** seemed to be a difficult task. In fact, when a mixture of imine **1** and diisobutyl fumarate were allowed to undergo the analogous heating program showed in Figure 1, the resulting plot was nearly identical. Also, ^{1}H NMR experiment of the crude material indicated the presence of imidazolidine **3** and unaltered fumarate. Isobutyl fumarate was selected due to its liquid nature at ambient conditions and because a homogeneous solution was obtained by mixing it with the imino ester **1** or **4**. By contrast, dimethyl fumarate, which is a solid at room temperature, formed heterogeneous mixtures with the imino esters and the heat absorption corresponding to its melting process, at 102 °C, notably interfered with the reaction heat flow.

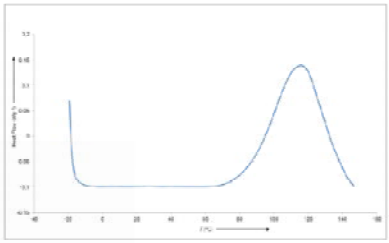

Figure 1. DSC curve at 10 °C·min^{-1} heating slope of imine **1**.

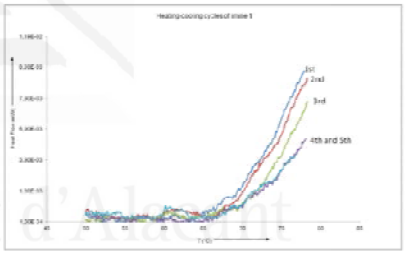

Figure 2. Several consecutive DSC heating-cooling cycles of imine **1**.

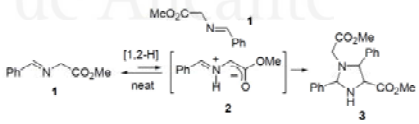

Scheme 2. Synthesis of imidazolidines **3** during thermal experiments.

Taking into account that the formation of the dipole **2** could not be demonstrated, and the reaction of **1** with itself started at around 80 °C, ^{1}H NMR and ^{13}C NMR experiments were run at

different temperatures using deuterated DMSO as solvent. The higher sensitivity of ^{1}H NMR was crucial to obtain some evidences of the 1,3-dipole. In the first attempt, the mixture formed by imine **1** and diisobutyl fumarate in DMSO-d_6 was allowed to raise 130 °C and no relevant signals of the betaine **2** were observed, but noticeable amounts of imidazolidine **3** were detected instead. The dipolarophile was not able to capture dipole **2** in this solution. ^{1}H NMR experiments were then performed reproducing the identical thermal conditions of the calorimeter. So, neat freshly prepared imino ester **1** was placed (in the absence of fumarate) in an NMR tube with a coaxial capillary tube containing DMSO-d_6 and the temperature increased 5 °C·min^{-1}. Such as it occurred in the DSC experiment at 75 °C amounts of **3** were observed. In addition, a small signal at 5.87 ppm was registered in the experiments run at 60 °C and at higher temperatures, together with a peak with identical intensity at 8.01 ppm (Figure 3). Both signals disappeared when the experiment was cooled at room temperature and immediately appeared by heating back to 60 °C. This behavior was repeatedly observed even after seven heating-cooling cycles. There are several examples of ^{1}H NMR spectra of imino ester-derived enolates in the literature but none of them is identical to dipole **2**.[14] Calculations by NMR simulators for similar systems predicted an upfield shift of the iminic hydrogen (7.9-8.0 ppm) with respect to imine **1** whether a enol-type structure was considered. However, the downfield shift of the α-proton of the dipole **2** is very notable (5.25-6.90 ppm range).[15] At 60 °C the imine **1**:dipole **2** ratio was close to 100:2, but this ratio was slightly higher (100:4 or 100:5) when the temperature was maintained above 75 °C.

The reduction of the reactivity of imino ester **1** was achieved by bonding a benzyl radical to its α-position. Thus, when 1,3-dipole precursor **4** was submitted to a heating rate of 10 °C·min^{-1} from −20 to 200 °C no exothermic peak was detected and compound **4** was recovered without any significant decomposition (Figure 4, dashed line). The solvent-free homogeneous liquid mixture of imino ester **4** and diisobutyl fumarate was next analyzed under the analogous conditions of the calorimeter. Monitoring-DSC experiment revealed that an exothermic process, corresponding to the expected 1,3-DC (Scheme 3) started at approximately 120 °C finishing at 260 °C (Figure 4, solid line). The crude product **5** was obtained (5 mg from the sealed crucible) as a 3:1 mixture of the *endo*:*exo* diastereoisomers according to NOESY experiments, and by comparison of the proton coupling constants of similar structures.

This solvent-free organic synthesis[16] ensures a fast transformation and, in consequence a fast analysis, reducing pollution, costs and raw materials.[17] Also, the stereoselectivity obtained (Scheme 3) was better than the analogous detected when the same reaction was carried out, for 24 h, in refluxing xylene as solvent (0.33*M*).[18]

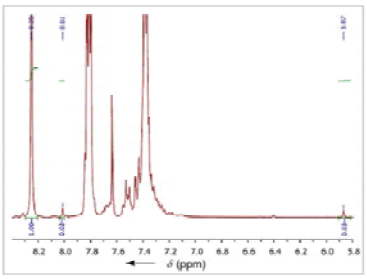

Figure 3. ^{1}H NMR spectra of the neat mixture showing two small signals corresponding to dipole **2**.

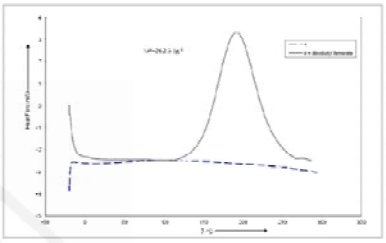

Figure 4. Dynamic DSC curve (10 °C·min^{-1}) of the reaction between imine **4** and diisobutyl fumarate (solid line) and the absence of reaction of **4** with itself (dashed line).

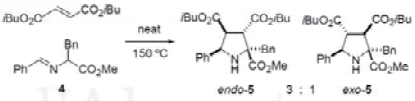

4 *endo*-**5** 3 : 1 *exo*-**5**

Scheme 3. Thermal reaction between imino ester **4** and diisobutyl fumarate to yield proline derivatives **5**.

Preliminary DSC experiments

Before studying kinetics of the 1,3-DC drawn in Scheme 3, basic isothermal DSC experiments were performed. The information obtained from Figures 5 and 6, together with the extracted from Figure 4 (above) is crucial. In order to select the best temperature to carry out the kinetic studies a set of temperatures were tested for evaluating the reaction conversion *vs* reaction time.[19] Figure 5 shows a extremely fast transformation at 150 °C. Also isothermal heat flow *vs.* time was represented at 110 °C (as an example) to show the better reaction temperature to measure the kinetic parameters (Figure 5). At that time (50 min for the reaction at 150 °C, and 150 min for the reaction at 110 °C) the conversion was judged

complete according to ^{1}H NMR. On the other hand, the bell shaped DSC heat flow *vs* time curves (e. g. 110 °C experiment in Figure 5) suggested the existence of an autocatalytic reaction mechanism.[20] Also, a reaction is considered as autocatalytic when the concentration (conversion) of one component *vs t* plot exhibits an S-shape profile[21] (Figure 6). This phenomenon is often ignored in chemistry, but it is very well known that a 1,3-DC of imino esters and alkenes is accelerated by the employment of bases and Lewis acids, so the final pyrrolidine **5** would act as autocatalyst of the model reaction (Scheme 3).[10]

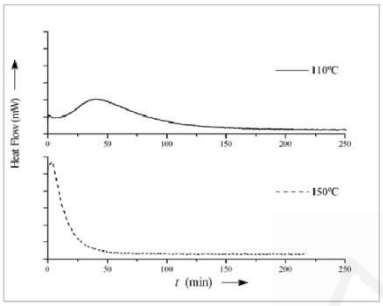

Figure 5. Isothermal plots of the reactions between **4** and diisobutyl fumarate performed at 110 °C and 150 °C

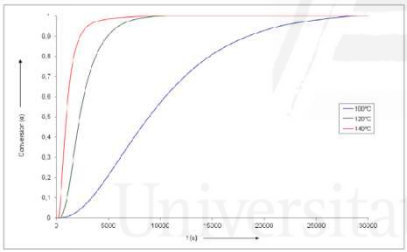

Figure 6. Conversion *vs t* plots of the reactions between **4** and diisobutyl fumarate performed at 100 °C, 120 °C and 140 °C.

Kinetic information obtained from non-isothermal (dynamic) DSC experiment.[22]

Several TA kinetic models or specific tests can be applied to investigate the kinetic parameters of this reaction. It is common the use of methods or models that rely on dynamic, non-isothermal experiments[5] such as Kissinger´s,[23] Borchardt-Daniels' (BD),[24] Ozawa's, and Ozawa-Flynn-Wall´s (OFW's)[25] methods. Although the BD method was originally developed for DTA studies of homogeneous liquid-phase reactions with no mass loss, it assumes that the reaction follows nth order kinetics, so it would be rather helpful for the calculation of reaction order and E_a and later to compare those values with the analogous ones obtained by application of the other models.[6] Non-isothermal (first order) Kissinger's and OFW´s methods were designed for homogeneous solid samples, however it has been applied to liquid ones.[26] Despite the recent development of wide advanced computational methods for the kinetic analysis of thermoanalytical experiments, the accuracy and simplicity of the Kissinger's method is still commonly used.[27] The usual starting point for kinetic analysis of non-isothermal data is:

$$d\alpha/dT = (d\alpha/dt)\,(dt/dT) = (d\alpha/dt)\,(1/\beta) \quad (1)$$

where α is the reaction conversion and β is the heating rate.

Based on an Arrhenius behavior, and working at 50% conversion (peak maximum of DSC plot), Kissinger's method[5] involves the use of the second derivative of equation (2). As this derivative must be zero at the inflexion point of a DSC curve, and considering $(1-\alpha_{max})$ is a constant for a given value of n, equation (2) can be transformed in equation (3).[28]

$$d\alpha/dT = (A/\beta)\,\exp(-E_a/RT)\,(1-\alpha)^n \quad (2)$$

$$\ln(\beta/T_{max}^2) = \text{constant} - (E_a/R)\,(1/T_{max}) \quad (3)$$

This method allows to obtain the activation energy (E_a) of the 1,3-DC between **4** and diisobutyl fumarate (Scheme 3) after plotting $\ln(\beta/T_{max}^2)$ *vs* $(1/T_{max})$ for a series of experiments at different heating rates (1 °C·min^{-1} to 20 °C·min^{-1}). It is worth to notice that T_{max} temperatures were corrected according to ASTM E698-11 to account instrumental differences due to thermal lag and sample overheating.[29] Calculations showed a good linear correlation[30] obtaining a corrected E_a value of 68.08 kJ·mol^{-1} for the Kissinger method, which also provided a good approach to the pre-exponential factor A (Table 1, entry 1).

The OFW method (refined Ozawa´s model) is applicable to the integral-type DTA curves. A group of DSC curves obtained at more than four heating rates are necessary. The DSC curves shift to higher temperature with increasing heating rates, the temperature and flow rate data being obtained at the same conversion (peak maximum, 50% conversion). Final equation (4) of the OFW approach also permitted to calculate E_a from the slope of the plot of $\ln(\beta)$ *vs* (1/T), which correlated well with a coefficient of 0.993,[30] and after further refinement of the value, a E_a value of 63.99 kJ·mol^{-1} was obtained (Table 1, entry 2).[29] The difference between the activation energies of Kissinger's and OFW's methods was 4 kJ·mol^{-1}, which encouraged us to evaluate the application of both, nth order and autocatalytic BD models to our system. nth order BD did not afford good correlation values for the experimental data, while autocatalytic BD did (Table 1, entries 3-5). So, this model was selected for further inspection of kinetic data.

$$\ln(\beta) = \text{constant} - (E_a/R)\,(1/T) \quad (4)$$

Table 1. Kinetic models applied to non-isothermal DSC curves

	Model	lnA[a]	E_a (kJ·mol^{-1})	Reaction order (n + m)
1	Kissinger	16.92	68.08	1[b]
2	OFW	15.80	63.99	1[b]
3	BD (3 ºC·min^{-1})[c]	24.16	96.43	0.38 + 0.85
4	BD (5 ºC·min^{-1})[c]	20.17	83.17	0.28 + 0.85
5	BD (10 ºC·min^{-1})[c]	18.47	78.84	0.17 + 0.79

[a] A value expressed in (s^{-1}). [b] Standard overall order reaction. [c] Data calculated by using BD model [equation (5)].

The BD kinetics approach allows the calculation of E_a, A, rate constant and reaction order. For the autocatalytic process the original formula for material transitions such as curing, crystallization, melting, decomposition, etc., is shown in equation (5).

$$\ln[d\alpha/dt] = \ln[k(T)] + n \ln[1-\alpha] + m \ln[\alpha] \quad (5)$$

This equation can be solved with a multiple linear regression (MLR) following the standard test method.[31][32] Measurements taken between approximately 3-4% (10% of peak height) and 50% conversions revealed an excellent match with the mathematical equation and a very low error. However, for each of dynamic experiment, the values of A, E_a, n and m depicted on Table 1 (entries 3-5) are averaged trough the selected data range. Experiments run at 3, 5 and 10 ºC·min^{-1} offered reasonable results of pre-exponential factors with overall 1.0 reaction order. This restriction is the main drawback of autocatalytic BD approach according to the literature (Table 1, entries 3-5).[22a][33] The ln[k(T)] *vs* 1/T plot reported higher values of E_a and lnA than the analogous ones obtained by Kissinger or OFW methods.

The initial concentration of the sample was not considered in equation (5), so a minor modification of it is detailed in equation (6). This modified expression with $[\mathbf{4}]_0$ = 2.236 M is equivalent to the general reaction rate concept [equation (7)],[34] and also equivalent to the equation (5). If we consider that BD total reaction orders are very close to 1, the difference between equations (6) and (5) is the term (m+n-1)·ln[$\mathbf{4}_0$], which is very close to zero. In this sense, equations (5) and (7) are equivalent according to BD model, and the resulting rate equation is just an approximation to the real one.

$$\ln[\mathbf{4}]_0[d\alpha/dt] = \ln[k(T)] + n \ln[\mathbf{4}]_0[1-\alpha] + m \ln[\mathbf{4}]_0[\alpha] \quad (6)$$

$$v = k(T)\,[\mathbf{4}]^n\,[\mathbf{5}]^m \quad (7)$$

A useful technique for DSC analysis is a free-kinetics model[35] based on the realization that the activation energy E_a may depend on the degree of the reaction conversion. In this method, E_a values obtained at different conversions were calculated applying Kissinger's methodology to the isoconversional DSC integral curves [slope of equation (3)·R]. Figure 7 shows the variation of the E_a *vs* conversion. At the beginning of the reaction (3% conversions) E_a reached a maximum value of 72.5 kJ·mol^{-1}. At this point, no or very little autocatalysis was taking place because the concentration of the product was very low. At higher levels of conversion (10-80%) E_a values decreased steadily giving an indication that as reaction proceeds, the autocatalytic mechanism takes advantage over the non-catalyzed processes. The higher the conversion is, the lower the activation energy is, which is in agreement with non-catalyzed and autocatalytic processes occurring at the same time but to a different extent as reaction proceeds.

A good estimation of the reaction enthalpy could be obtained from the integration of the corresponding non-isothermal DSC curves (Table 2). High heating rates (15 and 20 ºC·min^{-1}) afforded elevated ΔH values so, the average energy of the recommended tests (up to 10 ºC·min^{-1})[22] furnished 76.31 (kJ·mol^{-1}).

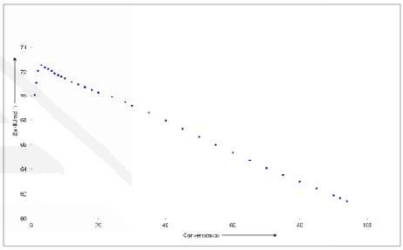

Figure 7. Variation of the E_a *vs* conversion.

Table 2. Integrated ΔH values obtained at different heating rates.

β (ºC·min^{-1})	ΔH (kJ·mol^{-1})	β (ºC·min^{-1})	ΔH (kJ·mol^{-1})
1	75.15	10	77.82
3	75.89	15	80.59
5	76.39	20	80.69

Kinetic information obtained from isothermal DSC experiments

At this point, a general overview of the process has been evaluated, but the determination of a more accurate rate equation is desirable. We wished first to assess how similar

the conversion obtained as the integral of heat flow curve *vs* time, and the conversion of the reaction in a flask *vs* time, were.

A comparison of this experiment with a higher scale reaction in the laboratory was made. For the thermal reaction in a flask, one equivalent of the imine **4** and one equivalent of diisobutyl fumarate, were mixed and the reaction was stirred rising 130 ºC as internal temperature. The data of both plots are shown in Figure 8. In the case of DSC experiment, the time taken to reach the temperature was approximately lower than 20 s with a high control of the temperature. For the conventional stirred neat reaction, using a digital thermometer immersed in the reaction mixture, the time taken to achieve 130 ºC was very close to 35 s. The plots were almost identical at the beginning and overlap in the 25-65% conversion range. Around 70% and higher conversions, the DSC lags behind the stirred reaction giving an indication that diffusion limitations are present at these conversions. So, all measurements done by DSC in the range of 0-70% conversions ensure diffusion effects free data and are similar to the laboratory solvent-free stirred conventional reaction.

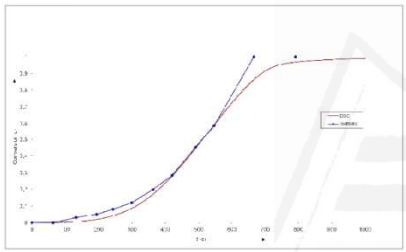

Figure 8. Comparison of isothermal plots of the reactions performed at 130 ºC in a flask and in the calorimeter.

The rate expression of this reaction was studied employing isothermal TA experiments and data obtained from the stirred mixture. With more accurate conversions determined by DSC experiments the integrated rate expressions for first, second, and even third order were properly plotted and no linear correlation was observed.[4b] The application of pseudo-order techniques offered valuable information through the displacement of the conversion *vs t* curves. Figure 9 shows conversions *vs* time plots calculated from DSC experiments run at 120 ºC with varying amounts of the different species involved in the reaction. When a double amount of diisobutyl fumarate was employed, DSC experiment indicated that the reaction rate was rather independent of the amount of dipolarophile employed (diisobutyl fumarate).[30] However, when the DSC measurement reaction was performed employing double amount of imine **1** the reaction rate was accelerated (2-3 times faster).[30] The addition of small amounts of pure pyrrolidine **5** (2%) also produced an acceleration of the reaction, which supported its autocatalytic role. In this last test the initial induction period did not exist and, in consequence, the resulting S-shape plot disappeared (Figure 9).

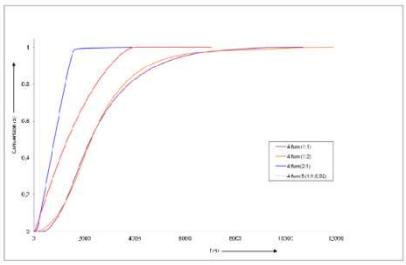

Figure 9. Pseudo-order experiments performed through DSC.

With several isothermal DSC curves in hand, we tried to adjust them to a mathematical expression analogous to equation (6), obtaining homogeneous n and m reaction orders starting from conversions closed to 3% (10% of peak height). Experimentally, when the sample is introduced to the preheated furnace an important fluctuation of the temperature occurred and it is not appropriate to take data until the thermal equilibrium is settled again. So, the following conversion ranges 3%-50% (Table 3), 3%-60%,[30] and 3-70%[30] were considered for the study, the last one being in the limit where diffusion becomes a serious inconvenient. Even when data close to diffusion limitations was considered, the kinetic parameters obtained were very similar (see Table 4). Data obtained for the analysis 3%-50% is detailed in Table 3,[30] where ln*k*(*T*), m and n reaction orders and adjustment error are shown. Regardless the range of conversion taken in the study, we observe that the values of the reaction orders are almost constant. The total reaction order can be estimated in around 1.7 as an average of the five essayed temperatures, where 0.5 partial reaction order corresponded to the concentration of cycloadduct **5** (Tables 3 and 4).This method also affords consistent both E_a (67.47 kJ·mol^{-1}) and pre-exponential term (ln*A* = 13.007, *A* = 4.46·10^5) (averaging values in Table 4), which were calculated from the linear plot of {ln*k*(*T*)} *vs* T^{-1}.[30] The most relevant aspect is that it is possible to write the rate equation for this autocatalyzed 1,3-DC under different operation temperatures (Table 5).[36]

ΔH values could also be calculated from the integration of the area involving the heat transferred by the reaction. These values are shown in Table 6 and are very close to the average value (76.31 kJ·mol^{-1}) obtained from the integration of non-isothermal DSC curves. Discrepancies among these values are due to the difficulty of the isothermal plot integration (above) using an accurate base-line.

The total process can therefore be deconvoluted in the two participating mechanisms named autocatalytic {k_2 [**4**]$_0$ [1-α] [**4**]$_0$ [α]} and non-autocatalytic {k_1 [**4**]$_0$ [1-α]}. If pseudo first order conditions are assumed the reaction rate can be expressed as

show in equation (8), which can also be written as equation (9).[21]

$$[\mathbf{4}]_0\,[d\alpha/dt] = k_1\,[\mathbf{4}]_0\,[1\text{-}\alpha] + k_2\,[\mathbf{4}]_0\,[1\text{-}\alpha]\,[\mathbf{4}]_0\,[\alpha] \quad (8)$$

$$[d\alpha/dt]\cdot[1\text{-}\alpha]^{-1} = k_1 + k_2\,[\mathbf{4}]_0\,[\alpha] \quad (9)$$

$$[d\alpha/dt]\cdot[1\text{-}\alpha]^{-1.2} = k_1 + k_2\,[\mathbf{4}]_0\,[\alpha]^{0.5} \quad (10)$$

Table 3. Kinetic parameters obtained after NLR of different isothermal DSC curves in the range of 3-50% conversion.

T (ºC)	ln*k*(*T*)	n order	m order	Σ error^{2} [a]
100	-9.0461	1.360	0.545	9.41
110	-7.8495	0.945	0.495	4.94
120	-7.4569	1.105	0.509	5.80
130	-7.1100	1.123	0.489	2.34
140	-6.7965	1.430	0.485	2.14

[a] Determined by solver mathematical NLR of the DSC plot.

Table 4. Kinetic parameters obtained from NLR followed by the linear plot of {ln*k*(*T*)} *vs* T^{-1} using different data ranges.

Conversion	E_a(kJ·mol^{-1})	lnA	R^2
3-50%	67.713	13.090	0.989
3-60%	67.298	12.958	0.974
3-70%	67.383	12.974	0.959

Table 5. Rate equations at different temperatures.

T (ºC)	Rate equation	Total order
100	$v = 1.3\cdot10^{-4}\,[\mathbf{4}]^{1.24}\,[\mathbf{5}]^{0.53}$	1.8
110	$v = 3.7\cdot10^{-4}\,[\mathbf{4}]^{1.08}\,[\mathbf{5}]^{0.51}$	1.6
120	$v = 5.0\cdot10^{-4}\,[\mathbf{4}]^{1.20}\,[\mathbf{5}]^{0.52}$	1.7
130	$v = 8.1\cdot10^{-4}\,[\mathbf{4}]^{1.12}\,[\mathbf{5}]^{0.50}$	1.6
140	$v = 1.1\cdot10^{-3}\,[\mathbf{4}]^{1.41}\,[\mathbf{5}]^{0.48}$	1.9

Table 6. Integrated ΔH values obtained at different heating rates.

β (ºC·min^{-1})	ΔH (kJ·mol^{-1})	β (ºC·min^{-1})	ΔH (kJ·mol^{-1})
100	67.13	130	75.59
110	77.97	140	63.89
120	69.89	150	—[a]

[a] Not determined because a very fast reaction occurred.

The plot of equation (9) {$[d\alpha/dt]\cdot[1\text{-}\alpha]^{-1}$} *vs* [$\alpha$] did not afford any straight line at all, but exponential curves, which demonstrates that the partial reaction orders are not equal for the same reagent/product en each term of the equation. Last tentative consisted in assuming 1.2 and 0.5 partial reaction orders for each component, but the lineal regression failed as well. So, it is very difficult to know the exact contribution of each mechanism using all this information, and the reaction order of the imine **4** seems to be different in both mechanisms.

According to all these results, the exothermic 1,3-DC would follow an approximate energetic profile similar to that represented in Figure 10 and equation (11). The rate determining step being the generation of the 1,3-dipole (intermediate) after a thermal [1,2]-prototropy, immediately after the formation of **2**, the cycloaddition occurs. This profile represents the whole process where both the catalyzed and non-catalyzed processes, coexist.

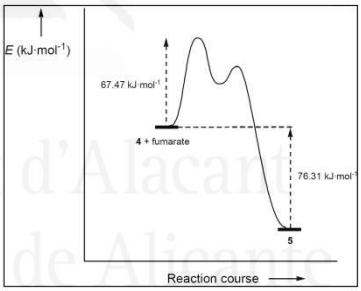

Figure 10. Energetic profile of the 1,3-DC of **4** and diisobutyl fumarate.

$$\mathbf{4} \underset{k_{-1}}{\overset{k_1}{\rightleftharpoons}} \text{dipole} + \text{fumarate} \xrightarrow{k_2} \mathbf{5} \quad (11)$$

Conclusion

In summary, DSC can be considered as a simple and fast technique (complementary with TLC, GC, HPLC, etc.) for

monitoring organic chemical processes as well as for the determination of several kinetic parameters. For the particular case of the 1,3-DC using azomethine ylides, generated by thermal [1,2]-prototropy from imine **4** are necessary 67.47 $kJ \cdot mol^{-1}$ for the reaction to occur with diisobutyl fumarate. The exothermal reaction has an enthalpy of 76.3 $kJ \cdot mol^{-1}$, which is an average of the measurements done in non-isothermal experiments up to 10 $^{o}C \cdot min^{-1}$. The total reaction order is 1.7, that means, 1.2 partial reaction order for the imine **4** and 0.5 partial reaction order for the catalyst **5**. Kissinger, and OFW models applied to dynamic experiments, reported an approximate value of E_a and lnA, even though could not provide information on reaction order as an overall first order reaction is assumed in these models. Possibly, the low impact of the real concentration in Kissinger and OFW models applied onto dynamic DSC curves, which work with second derivatives at isoconversional conditions, also helps to get a good and fast initial approach for the kinetic analysis of a reaction. In our opinion, more versatile BD model applied over dynamic experiments did not afford better results than the analogous obtained by Kissinger and OFW models in a 3-10 $^{o}C \cdot min^{-1}$ heating rate range. BD reported a total reaction order similar to 1, but with higher both E_a and lnA parameters. Dynamic tests ensure a suitable and fast calculation of the reaction enthalpy, rather than the determination employing isothermal experiments. However, NLR of isothermal data afforded very constant values of E_a, lnA and total reaction orders and allow to write the rate equation for the thermal 1,3-DC between imino ester **4** and diisobutyl fumarate. The existence of autocatalysis by the reaction product can be easily detected by studying the plot of E_a values *vs* conversions at different heating rates, and by the bell-shape form of the heat flow *vs t* or by the S-form of conversions *vs t* employing isothermal DSC curves. Due to the generation of the 1,3-dipole is rate determining step, kinetic parameters are related to the formation of the reactive species of phenylglycinate. In the same way, autocatalysis may be operating on the tautomeric equilibrium.

3. Experimental Section

Supporting Information (see footnote on the first page of this article).

Acknowledgements

This work has been supported by the Spanish Ministerio de Ciencia e Innovación (MICINN) (Consolider INGENIO 2010 CSD2007-00006, CTQ2010-20387, FEDER, Generalitat Valenciana (PROMETEO/2009/039), and by the University of Alicante.

Received: 20/March/2012
Published online: 26/June/2012

Keywords: cycloaddition / DSC / kinetics / autocatalysis / azomethine ylides

References

[1] a) *Comprehensive Handbook of Calorimetry and Thermal Analysis*, M. Sorai, Ed. John Wiley & Sons, Chichester, 2004. b) *Handbook of Thermal Analysis and Calorimetry*, P. K. Gallagher, Ed. Vol. 1-5, Elsevier Science, Amsterdam, 20032007. c) *Principles and Applications of Thermal Analysis*, P. Gabbot, Ed. Blackwell Publishing, Oxford, 2008. d) *Differential Scanning Calorimetry*, G. Höhne, W. F. Hemminger, H.-J. Flammersheim, Eds. Springer-Verlag, Heidelberg, 2010. e) *Modulated Temperature Differntial Scanning Calorimetry: Theoretical and Practical Applications in Polymer Characterization (Hot Topics in Thermal Analysis and Calorimetry)*, M. Reading, D. J. Hourston. Eds. Springer, Dordretch, 2010.

[2] T. F. J. Pijpers, V. B. F. Mathot, B. Goderis, R. L. Scherrenberg, E. W. van der Vegte, *Macromolecules* **2002**, *35*, 3601–3613.

[3] *Thermal Analysis UserCom Series*, Mettler Toledo Inc. Publishing, 1995–2012.

[4] a) K. A. Connors, in *Chemical Kinetics, The Study of Reaction Rates in Solution*, VCH Publishers, New York, 1990. b) R. I. Masel, in *Chemical Kinetics and Catalysis*, John Wiley & Sons, New York, 2001. c) M. R. Wright, in *An Introduction to Chemical Kinetics*, John Wiley & Sons, Chichester, 2004.

[5] See reference 1b, vol. 1, chp. 3, 147-224.

[6] The activation energy of the Diels-Alder reaction between hexachlorocyclopentadiene and cyclopentene was reported by using an excess of hexachlorocyclopentadiene and assuming pseudo-first order kinetics: J. A. Belichmeiera, H. K. Cammenga, P. B. Schneiderb, A. G. Steerb, *Thermochim. Acta* **1998**, *310*, 147–151.

[7] For this analysis the main features of the selected reaction must be precisely designed. For example, a small homogeneous liquid mixture of both components is required (2-5 mg) in order to promote the fast heat transfer to the sample and to avoid, as much as possible, phase changes and diffusion problems. The boiling point of the reactants must be higher than the temperature at which to the reaction occurs for avoiding undesired processes which may contribute to the total energy changes observed, thus complicating the analysis of the results.

[8] R. Hüisgen, *Angew. Chem. Int. Ed.* **1963**, *2*, 565–632.

[9] For recent computational studies concerning 1,3-DC of azomethine ylides see: a) T. K. Das, M. Banerjee, *J. Phys. Org. Chem.* **2010**, *23*, 148–155. b) L. R. Domingo, E. Chamorro, P. Pérez, *Lett. Org. Chem.* **2010**, *7*, 432–439. c) A. de Cózar, F. P. Cossío, *Phys. Chem. Chem. Phys.* **2011**, *13*, 10858–10868, and references cited therein.

[10] For general reviews displaying wide applications of 1,3-DC of azomethine ylides see: a) *Synthetic Applications of 1,3-Dipolar Cycloaddition Chemistry Towards Heterocycles and Natural Products*, A. Padwa, W. H. Pearson, Eds. John Wiley & Sons, New Jersey, 2003. b) C. Nájera, J. M. Sansano, *Curr. Org. Chem.* **2003**, *7*, 1105–1150. c) W. Eberbach, *Sci. Synth.* **2004**, *27*, chp. 11, 441–498. d) I. Coldham, R. Hufton, *Chem. Rev.* **2005**, *105*, 2765–2809; e) V. Nair, T. D. Suja, *Tetrahedron* **2007**, *63*, 12247–12275. d) A. Padwa, S. K. Bur, *Tetrahedron* **2007**, *63*, 5341–5378.

[11] A pseudo-diradical character of the three-atom components involved in this [3+2] cycloaddition has been found using electron localization function (ELF) analysis in order to explain the large reactivity of these species, see ref. 9b.

[12] The enantioselective 1,3-DC of azomethine ylides is a prolific area in organic synthesis and it is frequently being reviewed. For selected recent examples, see: a) H. Pellissier, *Tetrahedron* **2007**, *63*, 3235–3285. b) C. Nájera, J. M. Sansano in *Topics in Heterocyclic Chemistry*, A. Hassner, Ed. Springer-Verlag Berlin-Heidelberg, 2008, vol. 12, pp. 117–145; c) L. M. Stanley, M. P. Sibi, *Chem. Rev.* **2008**, *108*, 2887–2902; d) M. Álvarez-Corral, M. Muñoz-Dorado, I. Rodríguez-García, *Chem. Rev.* **2008**, *108*, 3174–3198. e) M. Naodovic, H. Yamamoto, *Chem. Rev.* **2008**, *108*, 3132–3148. f) C. Nájera, J. M. Sansano, M. Yus, *J. Braz. Chem. Soc.* **2010**, *21*, 377–412. g) M. Kissane, A. R. Maguire, *Chem. Soc., Rev.* **2010**, *39*, 845–883. h) J. Adrio, J. C. Carretero, *Chem. Commun.* **2011**, *47*, 6784–6794.

[13] The 1,3-DC of azomethine ylides with imines (including self-cycloaddition in the absence of a trapping agent) has been employed in the synthesis of α,β-dehydro-α-amino acid derivatives: a) P. W. Groundwater, T. Sharif, A. Arany, D. E. Hibbs, M. B. Hursthouse, M. Nyerges, *Tetrahedron Lett.* **1998**, *39*, 1433–1436. b) P. W. Groundwater, T. Sharif, A. Arany, D. E. Hibbs, M. B. Hursthouse, I. Garnett, M. Nyerges, *J. Chem. Soc, Perkin Trans. 1* **1998**, 2837–2846.

[14] See for instance: a) S. Jacquot-Rousseau, G. Schmitt, A. Khatyr, M. Knorr, M. M. Kubicki, E. Vigier, O. Blacque, *Eur. J. Org. Chem.* **2006**, 1555–1562. b) P. Elo, A. Pärssinen, M. Nieger, M. Leskelä, T. Repo, *J. Organometal. Chem.* **2009**, *694*, 2927–2933.

[15] Fast and accurate algorithm for the simulation of NMR spectra of large spin systems can be performed: A. M. Castillo, L. Patiny, J. Wist, *J. Magn. Reson.* **2011**, *209*, 123-133.

[16] K. Tanaka, F. Toda, *Chem. Rev.* **2000**, *100*, 1025–1074.

[17] The reaction of Scheme 2 was evaluated employing different solvents such as DMSO, triglyme, mesitylene. The generation of heterocycle **3** was slower than the corresponding transformation carried out in the absence of solvent.

[18] Under these reaction conditions a 2.4:1:1 *endo:exo*:non characterized diastereoisomer was obtained according to ^{1}H NMR experiments.

[19] There are not many examples in the literature concerning kinetics of 1,3-DC involving azomethine ylides: K. Elender, P. Riebel, A. Weber, J. Sauer, *Tetrahedron* **2000**, *56*, 4261–4265.

[20] *Handbook of Thermal Analysis*, T. Hatakeyama, Z. Liu, Eds. John Wiley & Sons, New York, 1998, chp. 4.

[21] F. Mata-Pérez, J. Pérez-Benito, *J. Chem. Educ.* **1987**, *64*, 925–927.

[22] a) TA-073, TA Instruments, http://www.tainst.com; b) TA-143A, TA Instruments, http://www.tainst.com.

[23] H. E. Kissinger, *Anal. Chem.* **1957**, *29*, 1702–1706.

[24] H.J. Borchardt, F. Daniels, *J. Am. Chem. Soc.* **1959**, *79*, 41-46.

[25] a) T. J. Ozawa, *Therm. Anal.* **1970**, *2*, 301–324. b) J. H. Flynn, L. A. Wall, *J. Res. Nat. Bur. Stand* **1966**, *70A*, 487–493.

[26] a) Z.-H. Chen, F.-Q. Zu, X.-F. Li, J. Yu, Y. Xi, R.-R. Shen, *J. Phys.: Condens. Matter* **2007**, *19*, 116106. b) S. Matecic-Musanic, I. Fiamengo-Houra, M. Suceska, *Central Eur. J. Energ. Mater.* **2010**, *7*, 233–251.

[27] J. Farjas, N. Butchosa, P. Roura, *J. Therm. Anal. Calorim.* **2010**, *102*, 615–625.

[28] P. E. Sánchez-Jiménez, J. M. Criado, A. Pérez-Maqueda, *J. Therm. Anal. Cal.* **2008**, *94*, 427–432.

[29] ASTM E698-11, ASTM Int., West Conshohocken, US.

[30] See supporting information.

[31] ASTM E2070-00, ASTM Int., West Conshohocken, US.

[32] MLR was performed using solver application tool of Microsoft Excell.

[33] J. Wang, M.-P. G. Laboire, M. P. Wolcott, *J. Appl. Polym. Sci.* **2007**, *105*, 1289–1296.

[34] The initial concentration of the fumarate was not considered in this equation because has a 0 reaction order according to the pseudo-order techniques. See isothermal tests comparing different proportions of reagents.

[35] S. V. Vyazovkin, A. I. Lesnikovich, *Thermochim. Acta* **1990**, *165*, 273–280.

[36] The elimination of the autocatalytic contribution {m ln[α]} of equation (6) represented a very poor mathematical correlation with the experimental DSC curve.

DOI: 10.1002/cplu.200((will be filled in by the editorial staff))

SUPPORTING INFORMATION

Kinetic Study of Thermal 1,3-Dipolar Cycloaddition of Azomethine Ylides using Differential Scanning Calorimetry as Monitoring Window

Juan Mancebo-Aracil,[a] María J. Muñoz-Guillena,[b] Ion Such-Basáñez[b] and José M. Sansano-Gil.[a*]

[a]Departamento de Química Orgánica e Instituto de Síntesis Orgánica (ISO), Universidad de Alicante, 03080-Alicante (Spain).
[b]Servicios Técnicos de Investigación, Universidad de Alicante, 03080-Alicante (Spain).

Correspondence should be addressed to JMS-G (jmsansano@ua.es)

Table of Contents

1. General

Aldehydes were also distilled prior to use for the elaboration of the iminoesters. Only the structurally most important peaks of the IR spectra (recorded using a Nicolet 510 P-FT and a Jasco FTIR 4100) are listed. ^{1}H NMR (300 MHz) and ^{13}C NMR (75 MHz) spectra were obtained using a Bruker AC-300 with $CDCl_3$ as solvent, at 25 ºC, and TMS as internal standard unless otherwise stated. Low-resolution electron impact (GC-EI) mass spectra were obtained at 70 eV using a Shimadzu QP-5000, and high-resolution mass spectra were obtained using a Finnigan VG Platform. HRMS (GC-EI) were recorded using a Finnigan MAT 95S instrument. Analytical TLC was performed using Schleicher & Schuell F1400/LS silica gel plates, and the spots were visualized under UV light (λ=254 nm). For flash chromatography, we employed Merck silica gel 60 (0.040–0.063 mm). CEM Discover and Explorer-Coolmate accessory were employed in the microwave-assisted reactions for the generation of iminoesters.

Mettler Toledo Microbalance MT5 was employed for the measurement of small amounts of sample placed in sealed hermetic crucibles. DSC measurements were registered in a modulated MDSC TA Instruments, model Q100 with autosampler and RCS and LNCS systems for running experiments at low temperature.

The freshly prepared mass must be kept low (<5mg) and it is preferred that the sample is placed in a hermetically sealed pan. After every experiment the mass of the sample must be in order to ensure that no mass loss has taken place during the experiment.

2. Synthesis of Iminoesters

To a suspensión of glycine methyl ester hydrochloride or phenylalanine methyl ester hydrochloride (6 mmol) in dichloromethane (5 mL) benzaldehyde (6 mmol, 636.7 mg) and Et_3N (1.1 eq, 917μL) were successively added. The sealed tube, containing this mixture, was irradiated in a microwave reactor (40 W), and 40 ºC for 1h. Then, dichloromethane was evaporated under vacuo and water (15 mL) was added. The aqueous phase was extracted with ethyl acetate (3x10 mL), the organic layer was separated dried ($MgSO_4$), and evaporated yielding very pure iminoesters A and B in 94% and 96%, respectively.

3. Thermal reactions affording cycloadducts 3 or 5

The homogeneous mixture of iminoester and dipolarophile was prepared in the corresponding proportion and submitted to the heating conditions at the selected temperature (see text) obtaining cycloadducts **3** or **5**.

(2*R,4*S**,5*S**)-Methyl 1-(methoxycarbonylmethyl)-2,5-diphenylimidazolidine-4-carboxylate** (**3** major estereoisomer): Sticky pale yellow oil; R_f 0.73 (7/3 *n*-hexane/ethyl acetate); ^{1}H NMR δ 2.70 (br. s, 1H, NH), 3.13 (s, 3H, CH_2CO_2Me), 3.22, 3.34 (2d, *J* = 18 Hz, 2H, CH_2CO), 3.54 (s, 3H, $CHCO_2$*Me*), 4.37 (d, *J* = 9Hz, 1H, *CH*CO_2Me), 4.69 (d, *J* = 9 Hz, 1H, *CH*CHCO), 5.09 (s, 1H, CHN_2), 7.31-7.81 (m, 10H, Ar*H*); ^{13}C NMR δ 47.7 (CH_2), 51.3, 51.6 (2 x OCH_3), 64.9 ($CHCO_2$), 67.4 ($CNCH_2$), 79.9 (CN_2), 128.1, 128.2, 128.7, 129.0, 129.5, 134.6, 138.6, 140.6 (Ar*C*), 171.1, 171.8, (2 x CO); IR (neat) ν_{max} 3250 (NH), 1730-1740 (3xCO) cm^{-1}; MS (EI-GC) *m/z* 354 [*M*$^+$+1, <1%], 162 (42), 75 (18), 104 (10), 91 (100) [$C_7H_7^+$] , 74 (17); HRMS calculated for $C_{20}H_{22}N_2O_4$-$C_{10}H_{12}N_2O_2$: 162.0581, found: 162.0578.

(2*R,4*S**,5*R**)-Methyl 1-(methoxycarbonylmethyl)-2,5-diphenylimidazolidine-4-carboxylate** (**3** minor stereoisomer): Sticky pale yellow oil; R_f 0.73 (7/3 *n*-hexane/ethyl acetate); ^{1}H NMR δ 2.75 (br. s, 1H, NH), 3.19, 3.17 (2d, *J* = 18 Hz, 2H, CH_2CO), 3.52 (s, 3H, CH_2CO_2*Me*), 3.78 (s, 3H, $CHCO_2$*Me*), 3.91 (d, *J* = 6 Hz, 1H, *CH*CO_2Me), 4.48 (d, *J* = 6 Hz, 1H, *CH*CHCO), 5.15 (s, 1H, CHN_2), 7.30-7.91 (m, 10H, Ar*H*); ^{13}C NMR δ 47.8 (CH_2), 52.2, 52.4 (2 x OCH_3), 67.1 ($CHCO_2$), 68.7 ($CNCH_2$), 79.8 (CN_2), 128.1, 128.2, 128.7, 129.1, 129.9, 134.6, 138.9, 140.1 (Ar*C*), 171.0, 173.4 (2 x CO); IR (neat) ν_{max} 3250 (NH), 1730-1740 (3xCO) cm^{-1}; MS (EI-GC) *m/z* 354 [*M*$^+$+1, <1%], 162 (42), 75 (18), 104 (10), 91 (100) [$C_7H_7^+$], 74 (17); HRMS calculated for $C_{20}H_{22}N_2O_4$-$C_{10}H_{12}N_2O_2$: 162.0581, found: 162.0578.

(2*S,3*S**,4*S**,5*R**)-3,4-Diisobutyl 2-methyl 2-benzyl-5-phenylpyrrolidine-2,3,4-tricarboxylate** (*endo*-**5**): Pale yellow oil; R_f 0.67 (7/3 *n*-hexane/ethyl acetate); ^{1}H NMR δ 0.67, 0.68, 0.99, 1.00 (4 x d, *J* = 6 Hz, 2 x $CHCH_3$), 1.68, 1.99 (2 x m, 2H, 2 x *CH*CH_3), 2.80 (br. s, 1H, NH), 3.25, 3.39 (2 x d, *J* = 12 Hz, CH_2Ph), 3.40 (dd, *J* = 11 and 9 Hz, 1H, C*H*CHN), 3.60 (d, *J* = 9 Hz, 1H, C*H*CBn), 3.69 (s, 3H, OCH3), 3.70-3.76 and 3.90-3.95 (2 x m, 4H, 2 x CH_2CH), 4.04 (d, *J* = 11 Hz, 1H, CHN), 7.23-7.40 (m, 10H, Ar*H*); ^{13}C NMR δ 18.8, 18.9, 19.2, 19.3 (4 x CH_3CH), 27.6, 27.7 (2 x *C*HCH$_3$), 43.2 (CH_2Ph), 52.6 (OCH_3), 55.1 (*C*HCHN), 56.0 (*C*HCBn), 65.5 (CHN), 71.0, 71.6 (2 x CH_2O), 127.1, 127.8, 128.3, 128.7, 130.1, 130.7, 136.1, 140.3 (Ar*C*), 171.1, 171.2, 174.1 (3 x CO); IR (neat) ν_{max} 3400 (NH), 1728-1737 (3xCO) cm^{-1}; MS (EI-GC) *m/z* 495 [*M*$^+$+1, <1%], 436 (6), 404 (25), 362 (12), 331 (20), 330 (100) [*M*$^+$-Bn-(CO_2Me)-Me], 228 (25), 202 (20), 170 (12), 91 (31); HRMS calculated for $C_{25}H_{37}NO_6$-$C_2H_3O_2$: 436.2458, found: 436.2460.

(2*S,3*R**,4*R**,5*R**)-3,4-Diisobutyl 2-methyl 2-benzyl-5-phenylpyrrolidine-2,3,4-tricarboxylate** (*exo*-**5**): Pale yellow oil; R_f 0.67 (7/3 *n*-hexane/ethyl acetate); 1H NMR δ 0.65, 0.69, 1.01, 1.03 (4 x d, *J* = 6 Hz, 2 x $CHCH_3$), 1.56, 2.01 (2 x m, 2H, 2 x *CH*CH3), 2.85 (br. s, 1H, NH), 2.92, 3.17 (2 x d, *J* = 12 Hz, CH_2Ph), 3.48 (dd, *J* = 9 and 7.5 Hz, 1H, CHCHN), 3.74-3.78 (m, 2H, CH_2CH), 3.77 (s, 3H, OCH_3), 3.89-4.01 (m, 3H, *CH*CBn and CH_2CH), 4.91 (d, *J* = 7.5 Hz, 1H, CHN), 7.25-7.40 (m, 10H, Ar*H*); ^{13}C NMR δ 19.0, 19.2, 19.3, 19.4 (4 x CH_3CH), 27.3, 27.8 (2 x *C*HCH$_3$), 39.7 (*C*H$_2$Ph), 53.4, 53.5 (OCH_3, *C*HCHN), 54.6 (*C*HCBn), 63.1 (CHN), 71.3, 71.5 (2 x CH_2O), 126.9, 127.7, 127.8, 128.1, 128.2, 129.7, 136.4, 140.0 (Ar*C*), 170.9, 171.0, 173.7 (3 x CO); IR (neat) ν_{max} 3400 (NH), 1728-1737 (3xCO) cm^{-1}; MS (EI-GC) *m/z* 495 [*M*$^+$+1, <1%], 436 (6), 404 (25), 362 (12), 331 (20), 330 (100) [*M*$^+$-Bn-(CO_2Me)-Me], 228 (25), 202 (20), 170 (12), 91 (31); HRMS calculated for $C_{25}H_{37}NO_6$-$C_2H_3O_2$: 436.2458, found: 436.2460.

4. ln($\beta \cdot T^{-2}$) *vs* T^{-1} for the calculation of E_a and lnA following Kissinger´s model.

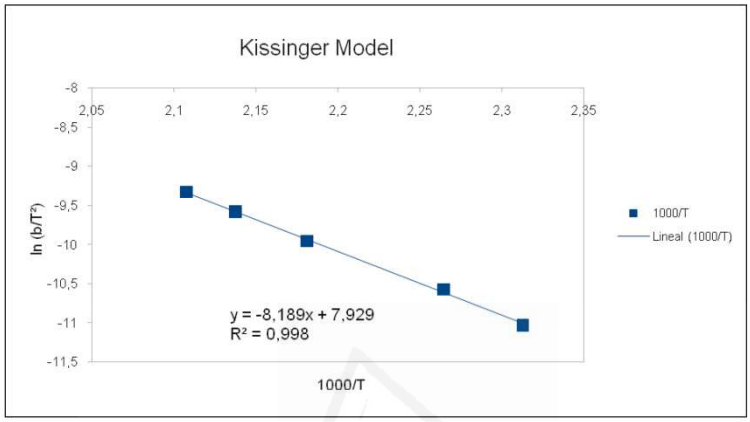

5. ln(β) *vs* T^{-1} for the calculation of E_a and lnA following Ozawa´s model.

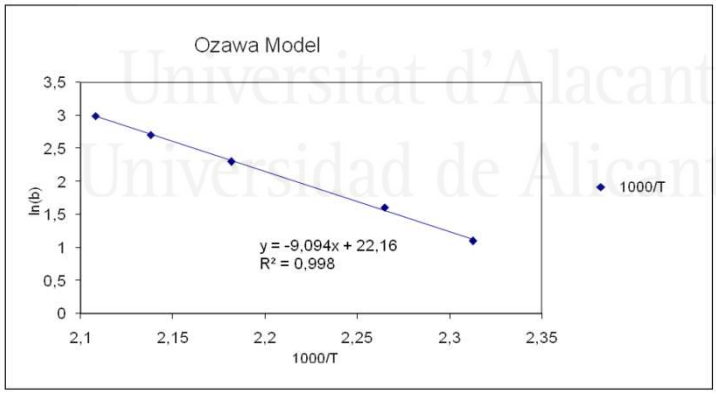

S3

6. ln(β) *vs* T^{-1} for the calculation of E_a and lnA following OFW model.

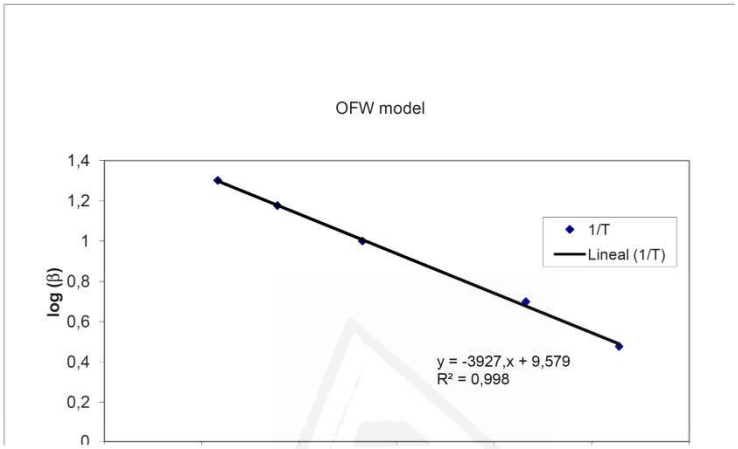

7. Dynamic DSC curves at different heating rates (β).

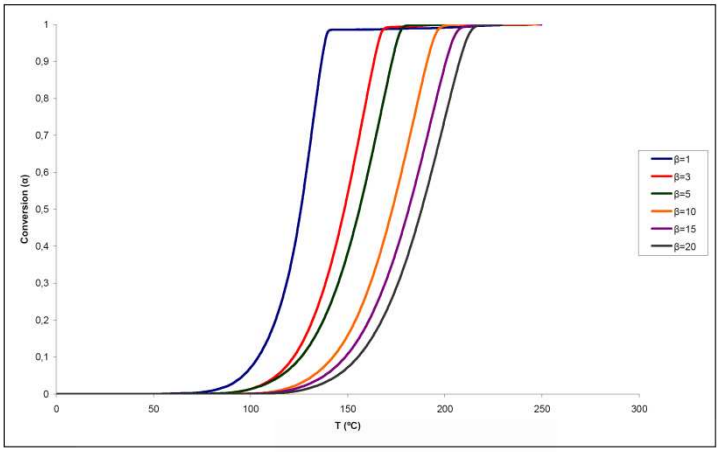

8. Table including all the kinetic parameters obtained by application of equation (6) to isothermal DSC values.

			Lnk(*T*)			m			n		
T (ºC)	*T* (K)	1/*T* (K^{-1})	α=0.5	α=0.6	α=0.7	α=0.5	α=0.6	α=0.7	α=0.5	α=0.6	α=0.7
100	373.16	2.6798	-9.0461	-8.9857	-8.9587	0.545	0.529	0.517	1.360	1.220	1.145
110	383.16	2.6099	-7.8495	-7.9187	-7.9566	0.495	0.509	0.523	0.945	1.096	1.198
120	393.16	2.5435	-7.4569	-7.5181	-7.5333	0.509	0.520	0.528	1.105	1.240	1.280
130	403.16	2.4804	-7.1100	-7.1274	-7.1290	0.489	0.498	0.499	1.123	1.212	1.190
140	413.16	2.4204	-6.7965	-6.7734	-6.7593	0.485	0.480	0.475	1.458	1.407	1.370

	α=0.5	α=0.6	α=0.7
Slope	-8144.5	-8094.5	-8104.8
Ordinate	13.091	12.95	12.974
E_a ($kJ \cdot mol^{-1}$)	67.713	67.298	67.383
A	$4.85 \cdot 10^5$	$4.21 \cdot 10^5$	$4.31 \cdot 10^5$

S5

R^2	0.92	0.95	0.95

9. ln*k*(*T*) *vs* T^{-1} linear plot for isothermal data (previous Table).

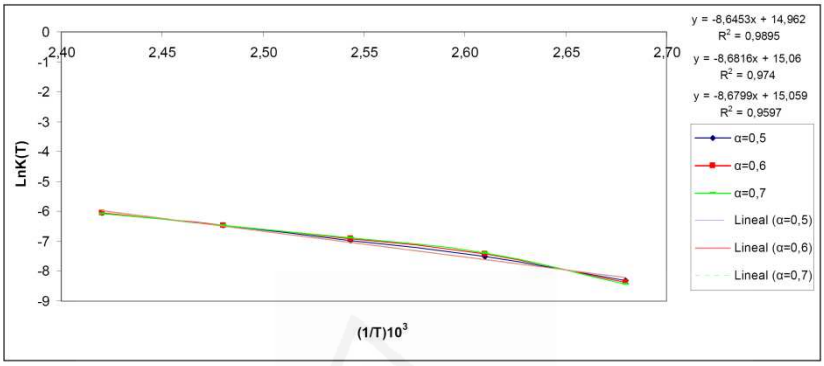

10. Tables 3b and 3c (complementary to Table 3, see main text)

Table 3b. Kinetic parameters obtained after NLR of different isothermal DSC curves in the range of 3-60% conversion.

T (ºC)	ln(*T*)	n order	m order	$\Sigma error^2$ [a]
100	-8.9857	1.220	0.529	10.24
110	-7.9817	1.096	0.509	6.25
120	-7.5181	1.240	0.520	7.22
130	-7.1274	1.212	0.498	5.55
140	-6.7965	1.407	0.480	2.26

[a] Determined by solver mathematical NLR of the DSC plot.

Table 3c. Kinetic parameters obtained after NLR of different isothermal DSC curves in the range of 3-70% conversion.

T (ºC)	ln(*T*)	n order	m order	$\Sigma error^2$ [a]
100	-8.9587	1.145	0.517	15.12
110	-7.9566	1.197	0.523	7.61
120	-7.5333	1.280	0.528	7.57

130	-7.1290	1.190	0.499	2.0
140	-6.7793	1.370	0.475	2.4

[a] Determined by solver mathematical NLR of the DSC plot.

CAPÍTULO II

V.- CAPITULO II: SÍNTESIS DE PIRROLIDINAS MEDIANTE CICLOADICIONES 1,3-DIPOLARES MULTICOMPONENTE

V.1.- INTRODUCCIÓN GENERAL

La química orgánica es un área de la química relativamente joven. El interés de los químicos por su estudio se ha incrementado exponencialmente durante la segunda mitad del siglo XX, así como su repercusión en la tecnología y la sociedad. Esto ha hecho, que en poco tiempo, se crean diferentes metodologías y procesos químicos que no siempre son fáciles de definir. Tal es el caso de todas aquellas reacciones secuenciales, en las que de forma consecutiva se rompen y crean nuevos enlaces, en procesos más o menos complejos, sin ser necesario el aislamiento de los productos intermedios.[34] Conceptos como reacción "tándem", "dominó", "multicomponente", "cascada" o "one-pot" se han usado en la bibliografía indistintamente prácticamente como sinónimos. Si bien es cierto, aproximadamente desde la última década, diferentes autores han puesto empeño en que esta nomenclatura quede mejor definida, y es a día de hoy que existe cierto consenso en las delimitaciones de cada concepto.

En cualquier caso estas reacciones se caracterizan por ser, además de un método de síntesis elegante, muy eficientes desde el punto de vista económico.[35] Generalmente, la cantidad de reactivos y disolventes disminuye notablemente si lo comparamos con otras metodologías de síntesis más convencionales por pasos, en las que debe aislarse y purificarse cada intermedio de reacción, y con ello también la formación de residuos. Además de este ahorro, estos procesos suelen generar estructuras complejas, con buena estereoselectividad y rendimiento químico. Todo esto, finalmente se traduce en un ahorro económico importante y una alta eficiencia química.

[34] Rodriguez-Ruiz, V.; Tesis Doctoral, Universidad Politécnica de Valencia, **2010**.
[35] Nicolau, K.C.; Edmonds, D.J.; Bulger, P.G.; *Angew. Chem. Int. Ed.* **2006**, *45*, 7134.

El concepto pues de reacción "multi-step" o secuencial está estrechamente ligado al de química verde o "green chemistry"[36] tan importante hoy en día.

Si seguimos el criterio del profesor Tietze,[37] las reacciones secuenciales o en cascada, se dividen en dos grandes grupos, las reacciones **dominó** y las reacciones **consecutivas**. Mientras que las primeras abarcan aquellos procesos en los que tiene lugar dos o más reacciones que guardan cierto orden, donde una reacción se da como consecuencia de la funcionalidad creada en el paso anterior; en las reacciones descritas como consecutivas, un nuevo reactivo, aditivo y/o catalizador es añadido después de una primera transformación, sin necesidad de aislar el intermedio. Hay por tanto en estos procesos one-pot, un cambio en las condiciones de reacción, ya sea en el medio, temperatura o presencia de alguno de los reactivos.

Por otro lado las reacciones **tándem** son reacciones multidireccionales, en las que pueden darse dos o más transformaciones simultáneamente en una misma molécula.

Las reacciones **multicomponente** (**MCR**) sin embargo, son reacciones en las que tres o más reacctivos se introducen a la vez para formar un nuevo producto. Son por tanto, un tipo de reacción one-pot o en cascada, en la que la diferencia reside en que el número de reactivos diferentes es mayor de dos.[38]

En la última década, el pensamiento en la industria farmacéutica ha sufrido un cambio importante, focalizándose en esta metodología por las ventajas que ofrece. Especialmente por su eficiencia, la facilidad para automatizar la síntesis, y obtener baterías enormes de compuestos con elevada complejidad estructural.

Suele situarse como primera reacción multicomponente, la síntesis de Strecker de α-aminoacidos via cianuros de α-amino compuestos publicada en 1850.[39] Sin embargo, doce años antes, Laurent y Gerhardt obtuvieron un producto muy poco soluble de la reacción entre amoniaco en agua, y aceite de almendra amarga.[40] En esta reacción, el producto crudo formado por ácido cianhídrico y

[36] **a)** Anastas, P.T.; Warner, J.C.; *Green Chemistry: Theory and Practice,* Oxford University Press, Oxford, **2000**; **b)** Matlack, A.S.; *Introduction to Green Chemistry*, Marcel Dekker, New York, **2001**.
[37] **a)** Tietze, L.F.; Brasche, G.; Gericke, K.; *Domino Reactions in Organic Synthesis*, Wiley-VCH, Weinheim, **2006**; **b)** Tietze, L.F.; Beifuss, U.; *Angew. Chem.* **1993**, *105*, 137; *Angew. Chem. Int. Ed. Engl.* **1993**, *32*, 131; **c)** Tietze, L.F.; *Chem. Rev.* **1996**, *96*, 115.
[38] Dömling, A.; Ugi, I.; *Angew. Chem. Int. Ed.* **2000**, *39*, 3168.
[39] Strecker, A.; Liebigs *Ann. Chem.* **1850**, *75*, 27.
[40] Laurent, A.; Gerhardt, C.F.; *Ann. Chimie Phys.***1838**, *66*, 181.

benzaldehído (**25** y **23**) reaccionaba con amoniaco (**24**) a través de la reacción de Strecker, generando 2-amino-2-fenilacetonitrilo (**26**), cuya base de Schiff, en presencia de benzaldehído formó la imina correspondiente (**27**) que fue llamada como "benzoyl azotide" (**Tabla 3**, entrada 1).

En mucho de los casos, las reacciones multicomponente se presentaron como una hheramienta eficaz en la síntesis de heterociclos (**Tabla 3**, entradas 2 a 5), sin embargo no fue hasta 1917 que se llevó a cabo una importante aplicación de las **MCR** en la síntesis de productos naturales, con la formación del alcaloide tropinona (**46**) a partir de aldehído succínico (**44**), metilamina (**33**) y el compuesto **45**, mediante la reacción de Robinson[41] (**Tabla 3**, entrada 7).

La **Tabla 3** muestra algunos ejemplos importantes en la síntesis de heterociclos mediante una **MCR**, ordenados cronológicamente.

[41] Robinson, R.; *J. Chem. Soc. (London)* **1917**, *111*, 876.

Tabla 3. Ejemplos de **MCR** de relevancia histórica.

Entrada	Nombre de la reacción	Año	Ejemplo
1	Síntesis de Strecker[40]	1838 (1850)	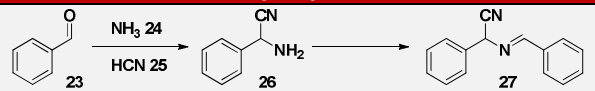
2	Síntesis de dihidropiridinas de Hantzsch[42]	1882	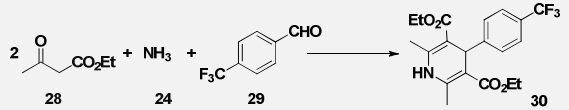
3	Síntesis de imidazoles de Radziszewski[43]	1882	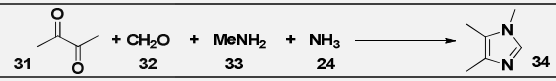
4	Síntesis de pirroles de Hantzsch[44]	1890	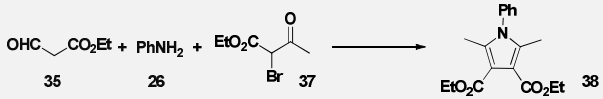
5	Reacción de Biginelli[45]	1891	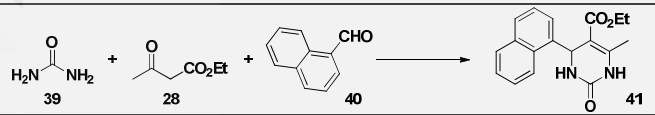
6	Reacción de Manich[46]	1912	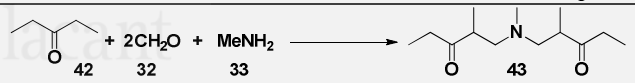
7	Reacción de Robinson[41]	1917	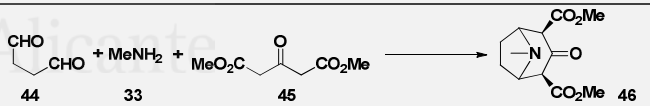

[42] Hantzsch, A.; Liebigs *Ann. Chem.* **1882**, *215*, 1.
[43] **a)** Radziszewski, B.; *Ber. Dtsch. Chem. Ges.* **1882**, *15*, 1499; **b)** Radziszewski, B.; *Ber. Dtsch. Chem. Ges.* **1882**, *15*, 2706.
[44] Hantzsch, A.; *Ber. Dtsch. Chem. Ges.* **1890**, *23*, 1474.
[45] **a)** Biginelli, P.; *Ber. Dtsch. Chem. Ges.* **1891**, *24*, 1317, 2962; **b)** Biginelli, P.; *Ber. Dtsch. Chem. Ges.* **1882**, *26*, 447.
[46] Mannich, C.; Kröschl, W.; *Arch. Pharm.* **1912**, *250*, 647.

Este proceso de síntesis se ha usado extensamente desde hace más de un siglo, aplicándolo a distintas reacciones orgánicas. Respecto a la cicloadición 1,3-dipolar, existen diversos ejemplos relativamente recientes, como el publicado por el grupo de Parsons,[47] en el que llevan a cabo la cicloadición de dipolarófilos con óxidos de nitrilo generados in situ, y el publicado por Coquerel y Rodriguez,[48] en el que sintetizan de manera diasteroselectiva, pirazolidinonas a partir de hidrazonas y cetonas.

Sin embargo no son demasiados los ejemplos de la cicloadición 1,3-dipolar multicomponente, con iluros de azometino.

En los apartados **III.2**, **III.3** y **III.4** de este capítulo, se detalla el caso concreto de esta reacción, generándose el iluro de azometino mediante 1,2-prototropía de hidrógeno (**Capítulo II-1**), o bien en presencia o no de una sal de plata (I) (**Capítulo II-2**) y la versión enantioselectiva de esta reacción (**Capítulo II-3**).

[47] Fédou, N.M.; Parsons, P.J.; Viseux, E.M.; Whittle, A.J.; *Org. Lett.* **2005**, *7*, 3179.
[48] Presset, M.; Mohanan, K.; Hamann, M.; Coquerel, Y.; Rodriguez, J.; *Org. Lett.* **2011**, *13*, 4124.

V.2.- CAPÍTULO II-1: CICLOADICIÓN 1,3-DIPOLAR MULTICOMPONENTE TÉRMICA A PARTIR DE GLIOXILATO DE ETILO COMO PRECURSOR DE ILUROS DE AZOMETINO

V.2.1.- Antecedentes Bibliográficos

Como se indica en la Introducción general, los α-iminoésteres, en condiciones térmicas pueden generar un iluro de azometino a través de una prototropía 1,2, siendo una de las maneras más habituales de generar 1,3-dipolos, capaces de sufrir la cicloadición 1,3-dipolar en presencia de dipolarófilos. Existen varios ejemplos en los que se lleva esta metodología aunque no son muy numerosos, probablemente debido a la pérdida de control en la geometría del producto final que conlleva la formación de los dipolos por una vía térmica.

Sin embargo pueden encontrarse trabajos interesantes como el publicado por van Es y col. en 1990,[49] en el que llevan a cabo la reacción entre derivados de glicina con un grupo difenilfosfinoilo y *N*-fenilmaleimida a 70 °C, y la cicloadición de iluros de azometino generados in situ a partir de ésteres de *N*-benzilidenaminoacidos publicado por Khlebnikov y col.[50]

Además de los trabajos en los que se genera el 1,3-dipolo mediante condiciones térmicas convencionales, pueden encontrarte en la bibliografía otros más recientes, que utilizan la activación por microondas. Tal es el caso del trabajo publicado por Cheng, [51] en el que a través de una cicloadición dipolar intramolecular, sintetizan heterociclos complejos con buenos rendimientos, irradiando con microondas. En esta línea, destaca también el trabajo de investigación realizado por Cossío y Díaz-Ortiz,[52] en el que estudian la cicloadición dipolar entre un iluro de azometino y nitroalquenos, desde un punto de vista tanto experimental como teórico, comparando la generación térmica del dipolo, mediante calor convencional e irradiada por microondas en ausencia de disolvente.

---

[49] van Es, J.; Jaarsveld, K.; van der Gen, A.; *J. Org. Chem.* **1990**, *55*, 4063.
[50] Khlebnikov, A.K.; Novikov, M.S.; Khlebnikov, V.A.; Kostikov, R.R.; *Russ. J. Org. Chem.* **2001**, *37*, 5073512.
[51] Cheng, Q.; Zhang, W.; Tagami, Y.; Oritani, T.; *J. Chem. Soc*., *Perkin Trans.* **2001**, *1*, 452.
[52] Cossío, F.; Díaz-Ortiz, A. y colaboradores; *J. Org. Chem.* **2007**, *72*, 4313.

Otro ejemplo interesante es el que detallan el grupo de Lopes,[53] en el que tras la formación de *N*-vinilaziridinas, seguida de apertura de ciclo térmica conrotaria para dar el iluro de azometino, sintetizan pirrolidinas *N*-substituidas con buenos rendimientos y diasteroselectividades moderadas (**Esquema 12**).

Esquema 12

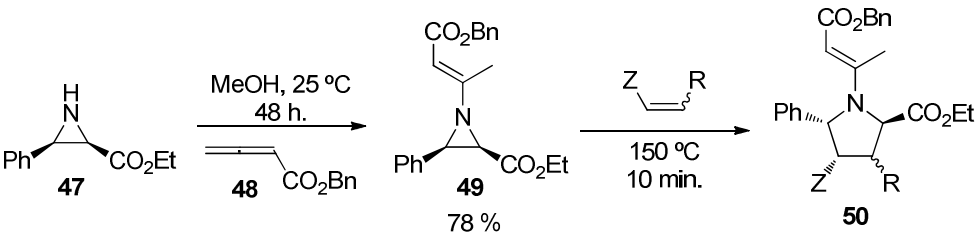

Sin embargo ninguno de estos ejemplos puede considerarse una reacción multicomponente. Tan sólo un ejemplo se ha encontrado para este caso de cicloadición con iluros de azometino, publicado por Shi y col. en 2010.[54] A partir de un aminoácido, generan el dipolo tras decarboxilación del grupo ácido, en etanol a reflujo (**Esquema 13**).

Esquema 13

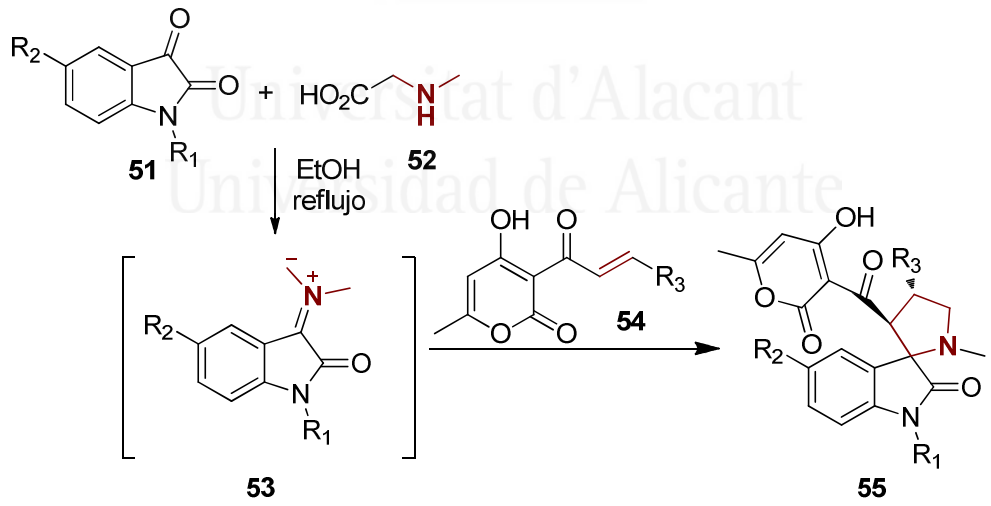

El glioxilato de etilo, es un reactivo nada habitual como precursor de iluros de azometino,ya que no pueden prepararse sus iminoésteres y por ello sólo se

[53] Lopes, S. y colaboradores; *Synthesis* **2009**, *14*, 2403.
[54] Liu, H.; Dou, G.; Shi, D.; *J. Comb. Chem.* **2010,** *12,* 633.

han descrito cuatro ejemplos de cicloadición 1,3-dipolar multicomponente con este aldehído. En todos ellos, la etapa de formación del cicloaducto se da a través de una sal de iminio cuaternaria. El más antiguo de ellos, data de 1995, en el que Harwood y col., a partir de 5-(*S*)-fenilmorfolin-2-ona **56**, glioxilato de etilo y un dipolarófilo forman el compuesto **58**, y tras hidrogenólisis catalítica preparan el aminoácido final **60** con configuración relativa 2,5-*trans*(**Esquema 14**).[55]

Esquema 14

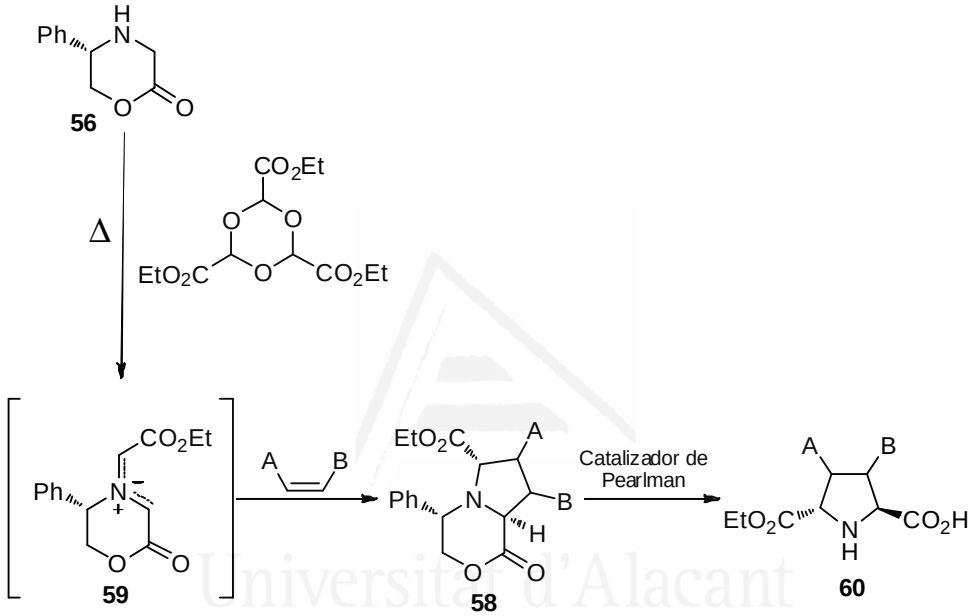

Otro ejemplo del grupo de Risch[56] consiste la cicloadición multicomponente diasteroselectiva de glioxilato de etilo, *N*-(1-feniletil)glicinato de etilo y fumarato de dimetilo para dar una mezcla diasteroselectiva de pirrolidinas *endo*/*exo* (*59*/*41)* con configuración relativa 2,5-*trans* (**Esquema 15**).

[55] Harwood, L.M.; Lilley, I.A.; *Tetrahedron: Assymetry* **1995**, *6*, 1557.
[56] Wittland, C.; Flörke, U.; Risch, N.; *Synthesis*, **1997**, 11, 1291.

Esquema 15

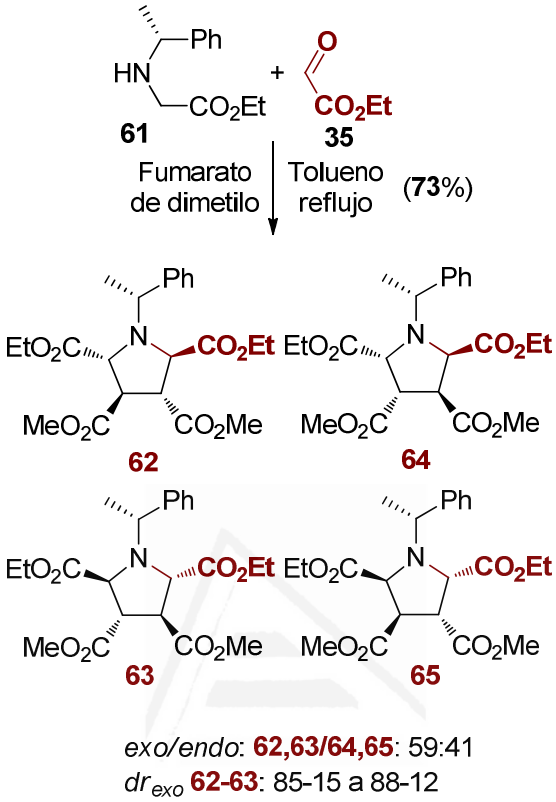

Por último, siguiendo una estrategia similar a la planteada por Harwood[55], el grupo de Bonin y Micouin llevó a cabo la cicloadición dipolar multicomponente con glioxilato de etilo a partir de una hidrazina cíclica,[57] mientras que por otro lado, Argyropoulos y colaboradores, sintetizan pirrolizidinas a partir de pirrolidinas quirales, obteniendo mezclas de productos con baja diasteroselectividad.[58]

[57]Chung, F.; Chauveau, A.; Seltki, M.; Bonin, M.; Micouin, L.; *Tetrahedron Lett.* **2004,** *45*, 3127.
[58]Argyropoulos, N.G.; Sarli, V.C.; Gdaniec, M.; *Eur. J. Org. Chem.* **2006**, 3738.

V.2.2.- Objetivos

De acuerdo con lo expuesto en relación a las cicloadiciones 1,3-dipolares térmicas con iluros de azometino se plantearon los siguientes objetivos:

- Llevar a cabo la reacción 1,3-dipolar multicomponente térmica a partir de glioxilato de etilo como precursor del iluro de azometino con el fin de obtener pirrolidinas con diferente funcionalidad en la posición cinco de dicho heterociclo.
- Estudiar y optimizar las condiciones de esta reacción, haciendo una comparativa entre el método de calentamiendo convencional por conducción y la irradiación por microondas para observar los efectos en el rendimiento y diastereoselectividad de los cicloaductos formados.
- Llevar a cabo la síntesis de un producto que presenta actividad biológica, justificando la utilización del glioxilato de etilo como precursor de la pirrolidina formada.

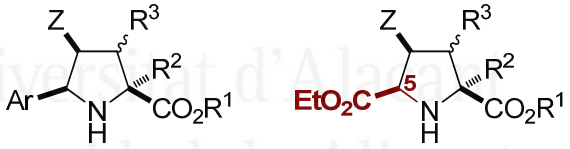

Trabajos anteriores

V.2.3.- Discusión de Resultados

Inicialmente, para llevar a cabo la optimización de la cicloadición 1,3-dipolar multicomponente se escogió el clorhidrato de 2-aminomalonato de dietilo como un buen componente fácilmente enolizable para esta reacción. Así pues se llevó a cabo la síntesis de la pirrolidina **68a**, a partir de glioxilato de etilo, el clorhidrato de 2-aminomalonato de dietilo, *N*-metilmaleimida como dipolarófilo, en presencia de 1.1 equiv. De Et_3N y tolueno como disolvente (**Esquema 16**).

Esquema 16

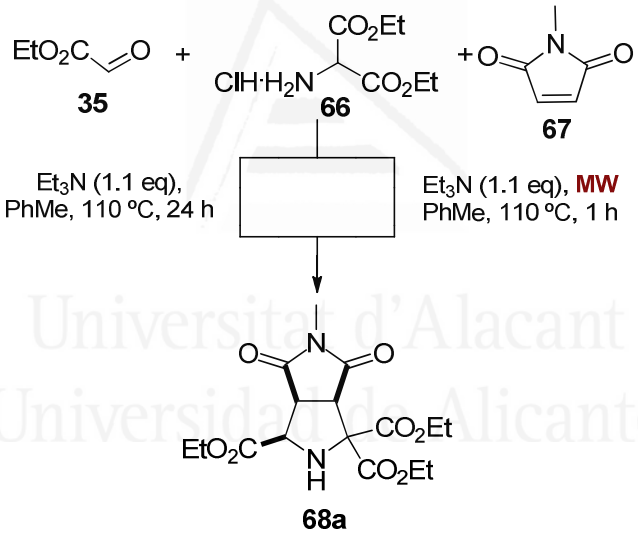

La primera reacción se llevó a cabo calentando de forma convencional, por conducción en un baño a 110 °C durante 24 horas y también mediante calentamiento por microondas, a la misma temperatura de 110 °C durante tan sólo una hora y a 60 W de potencia. Se obtuvieron buenas conversiones y diastereoselectividades en ambos casos del cicloaducto *endo*-**68a**. Sin embargo, además de ser mejor el rendimiento mediante el calentamiento por microondas, el espectro de ^{1}H-RMN del crudo de reacción indicó que el producto se obtenía prácticamente puro probablemente debido a la rapidez con la que se formaba el iluro de azometino.

Estas condiciones se estudiaron con diferentes dipolarófilos, como: *N*-bencilmaleimida, *N*-fenilmaleimida, acrilato de metilo, fumarato de dimetilo, (*E*)-1,2-bis(fenilsulfonil)etileno, propiolato de metilo y acetilendicarboxilato de dietilo (**Esquema 17**). Tanto con las maleimidas *N*-sustituidas, como con fumarato de dimetilo y (*E*)-1,2-bis(fenilsulfonil)etileno, la diastereoselectividad fue muy buena, así como el rendimiento. Sin embargo, el acrilato de metilo dio como resultado una mezcla de tres diasteroisómeros, con problemas además de regioquímica y rendimientos moderados. En todos los casos, los resultados obtenidos por microondas fueron siempre algo mejores que los obtenidos mediante calor convencional.

A la vista de los resultados obtenidos, y debido a la simplicidad de la metodología junto con la buena diasteroselectividad que presenta, se propuso llevar a cabo la síntesis de pirrolidinas a partir de derivados de aminoácidos. Se ensayaron así, las cicloadiciones 1,3-dipolares multicomponente por vía térmica, e irradiadas por microondas para los α–aminoésteres como son: clorhidrato del éster etílico de glicina, clorhidrato del éster metílico de alanina, clorhidrato del éster etílico de fenilalanina y por último el clorhidrato del éster metílico de fenilglicina (**Esquema 17**).

Esquema 17

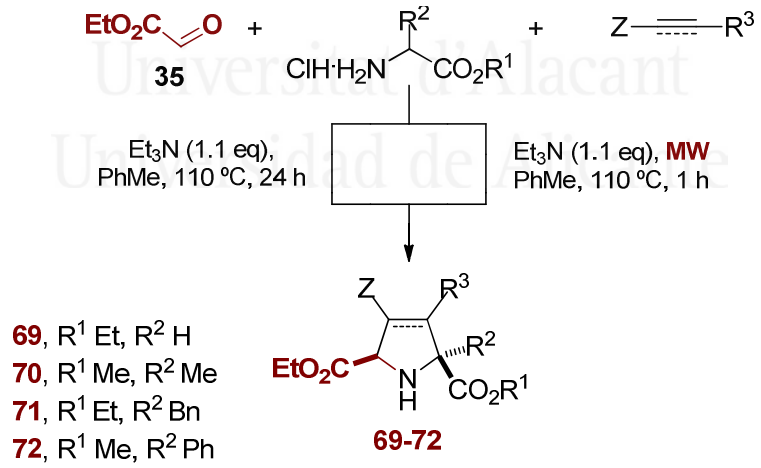

En general, la estereoquímica observada en las pirrolidinas finales, es 2,5-*cis*. Si bien es cierto que hay varias excepciones en función también del dipolarófilo empleado. Como en el caso de la reacción con el 2-aminomalonato, el acrilato de metilo fue el dipolarófilo que peores resultados ofreció independientemente del α-aminoéster empleado con una proporción importante

del otro regiosiómero. Tanto con fumarato de dimetilo como con (*E*)-1,2-bis(fenilsulfonil)etileno, se obtuvieron en general buenos rendimientos y un único diasteroisómero, salvo en el caso del derivado de fenilglicina. Éste último α-aminoéster, fue el que mostró un comportamiento más diferente respecto a los otros derivados de aminoácidos. En todos los casos salvo usando (*E*)-1,2-bis(fenilsulfonil)etileno como dipolarófilo, se obtuvieron una mezcla de diasteroisómeros en prácticamente igual proporción. Siendo además especialmente curioso el caso de la reacción de este α-aminoéster con acrilato de metilo, en el que los dos diasteroisómeros obtenidos son regioisómeros del producto esperado.

Este tipo de metodología, permite por tanto obtener con buen rendimiento y diasteroselectividad pirrolidinas que incorporen dos grupos éster en posiciones relativas 2,5-*cis*, lo cual no es fácil y supone una ventaja desde el punto de vista sintético. Como posible aplicación, se llevó a cabo la síntesis del sistema bicíclico **77** (**Esquema 19**), con potencial actividad biológica y que a su vez puede ser usado como precursor en la síntesis de otros compuestos biológicamente activos.[59] Para ello se eligió como producto de partida el cicloaducto *endo*-**73**, producto de la reacción entre glioxilato de etilo, el clorhidrato del éster etílico de *N*-fenilalanina y *N*-bencilmaleimida. En primer lugar se intentó bencilar en posición 1 de la pirrolidina, con diferentes condiciones pero no fue posible (**Esquema 18**).

Esquema 18

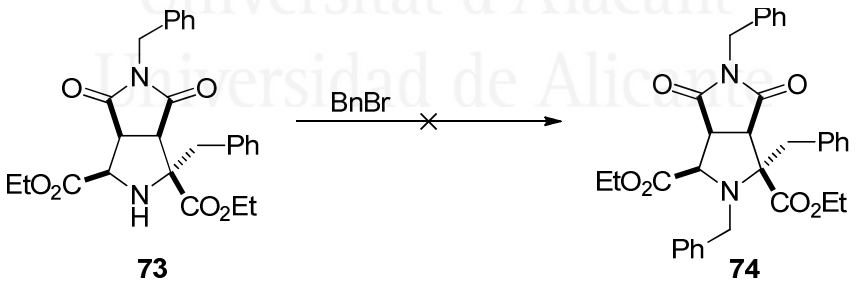

73 **74**

Por ello, se trató el producto **73** con cloruro de benzoílo, para seguidamente reducirlo con hidruro de litio y aluminio, obteniendo así una mezcla del diol deseado **75**, y el producto desbenzilado **76**. Sin embargo a este último si que fue posible alquilarlo con bromuro de bencilo, bajo reflujo de acetonitrilo, con Et_3N y K_2CO_3, consiguiendo así el diol deseado **75**. Finalmente se obtuvo el biciclo final

[59] Ver por ejemplo: Peters, D.; Redrobe, J.P.; Nielsen, E.O.; Pat., WO **2009** 109517, Apr. **2009**, CAN 2009:1107687.

77, tras doble mesilación seguida de una doble sustitución nucleofílica con bencilamina tras 19 horas de reflujo en acetonitrilo[60] (**Esquema 19**).

Esquema 19

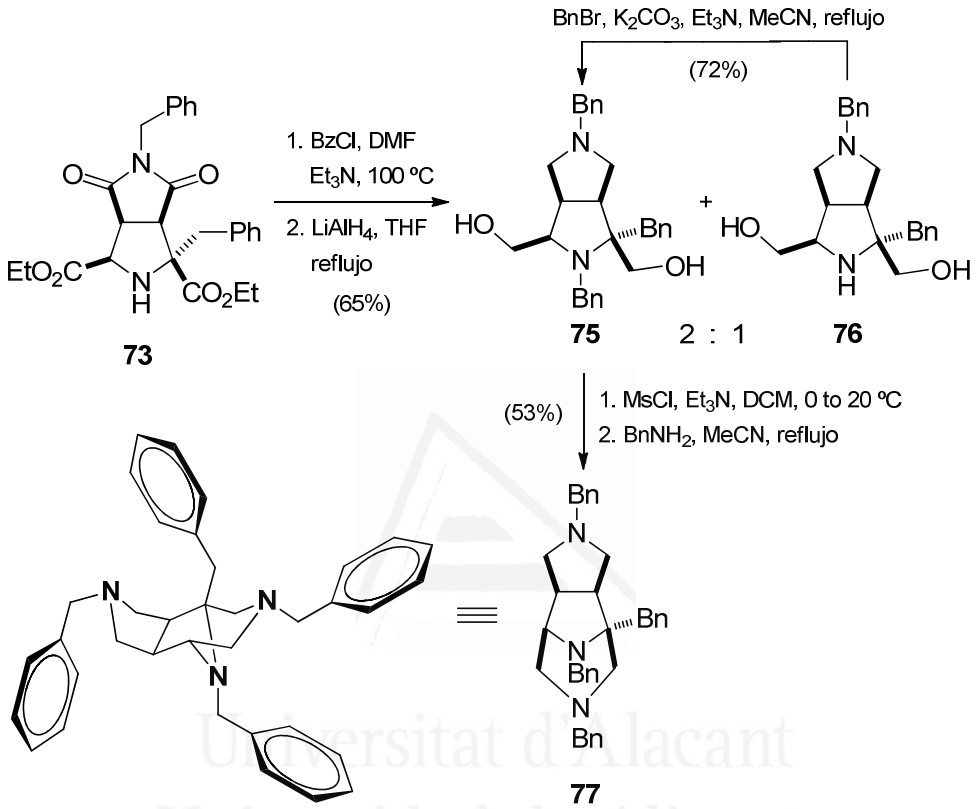

Un estudio más detallado de lo resumido anteriormente se encuentra en el siguiente apartado.

[60] Huang, L.J.; Teng, D.W.; *Chin. Chem. Lett.* **2011**, *22*, 523.

V.2.4.- Org. Biomol. Chem. 2013, 11, 662

Organic & Biomolecular Chemistry

RSC Publishing

PAPER

View Article Online
View Journal | View Issue

Microwave-assisted multicomponent diastereoselective 1,3-dipolar cycloaddition of ethyl glyoxylate derived azomethine ylides†‡

Juan Mancebo-Aracil, Carmen Nájera* and José M. Sansano*

Cite this: *Org. Biomol. Chem.*, 2013, **11**, 662

Received 24th October 2012,
Accepted 23rd November 2012

DOI: 10.1039/c2ob27072b

www.rsc.org/obc

The thermal multicomponent 1,3-dipolar cycloaddition (1,3-DC) of diethyl aminomalonate or α-amino esters (derived from glycine, alanine, phenylalanine, and phenylglycine) with ethyl glyoxylate and the corresponding dipolarophile such as maleimides, methyl acrylate, methyl fumarate, (*E*)-1,2-bis(phenylsulfonyl)ethylene, and electron deficient alkynes allows the diastereoselective synthesis of new polysubstituted pyrrolidine derivatives. Microwave-assisted heating processes give better results than conventional heating ones, affording *endo*-cycloadducts as major stereoisomers. In general, 2,5-*cis*-cycloadducts are preferentially formed according to the previous formation of the W-shaped dipole. Only in the 1,3-DC of the disulfone with phenylglycine and ethyl glyoxylate the corresponding *exo*-*trans*-cycloadduct was isolated. The compound *endo*-*cis*-**4b**, derived from phenylalanine, ethyl glyoxylate and *N*-benzylmaleimide, has been further transformed into a very complex diazabicyclo[2.2.1]octane skeleton with potential biological activity.

Introduction

The use of multicomponent reactions (MCRs)[1] in organic synthesis allows the efficient preparation of a wide range of complex molecules in an economically favourable way by using simple processes. In the case of 1,3-dipolar cycloadditions (1,3-DC)[2] of azomethine ylides and dipolarophiles, generally, the corresponding imino esters have to be prepared previously from the carbonyl compound and the α-amino acid to yield highly substituted prolines.[3–5] This core heterocyclic structure is readily involved in diversity-oriented synthesis (DOS)[6] allowing the preparation of different small structures in a reduced number of synthetic steps.

However, few examples of 1,3-DC of azomethine ylides have been described using MCR.[7] In all of these examples, aromatic carbonyl compounds and amino esters have been combined affording the corresponding prolines bearing at the 5-position an aromatic or heteroaromatic ring. Alternatively, the use of ethyl glyoxylate as the aldehyde component would allow the synthesis of 2,5-bis(alkoxycarbonyl)-substituted pyrrolidines **I** by means of 1,3-DC (Scheme 1). In this particular situation,

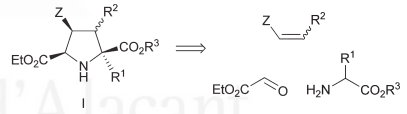

Scheme 1 Retrosynthetic analysis for the synthesis of **I**.

the preparation and isolation of imino esters is very difficult due to their instability. Therefore, in the only described contribution using ethyl glyoxylate and ethyl *N*-(1-phenylethyl)glycinate, the 1,3-DC had to be performed in a multicomponent process affording a mixture of pyrrolidines **II–V** with very low diastereoselection (Scheme 2).[8]

In this work, we describe for the first time the employment of the very reactive ethyl glyoxylate as the aldehyde component in a general domino-MCR, involving *in situ* generation of the imino esters, followed by a [1,2]-prototropy shift, and further thermal 1,3-DC with electrophilic alkenes or alkynes, for the general synthesis of prolines **I**.

Results and discussion

For initial studies, diethyl aminomalonate was chosen as an appropriate and more reactive candidate to undergo this type of multicomponent 1,3-DC.[7a–d] The model reaction between commercially available ethyl glyoxylate (50% solution in

Departamento de Química Orgánica e Instituto de Síntesis Orgánica (ISO), Facultad de Ciencias, Universidad de Alicante, 03080-Alicante, Spain. E-mail: cnajera@ua.es, jmsansano@ua.es; Fax: +34-965903549

†Dedicated to the memory of Prof. Balbino Mancheño.

‡Electronic supplementary information (ESI) available. CCDC 906384. For ESI and crystallographic data in CIF or other electronic format see DOI: 10.1039/c2ob27072b

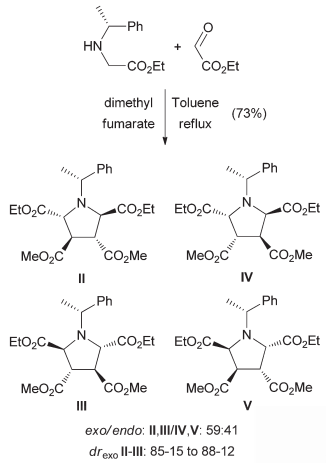

Scheme 2 Published example using ethyl glyoxylate in a multicomponent 1,3-DC.

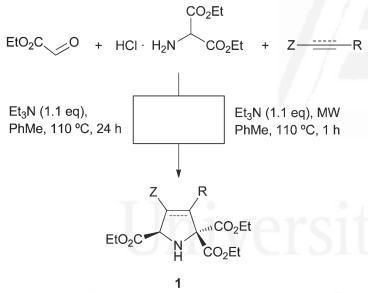

Scheme 3 1,3-DC involving diethyl aminomalonate.

toluene) diethyl aminomalonate hydrochloride and *N*-methylmaleimide, in the presence of triethylamine (1.1 equiv.), was tested using several solvents under conventional heating (CH) or through microwave (MW)-assisted heating.[9] Good conversions and stereoselections of cycloadducts **1** were achieved by using toluene as the pure solvent by heating at 110 °C for 24 h (Scheme 3). Moreover, the multicomponent microwave-assisted transformation afforded a cleaner crude reaction mixture probably due to the faster reaction (1 h) of the *in situ* generated azomethine ylide with the dipolarophile.

The scope of this 1,3-DC was studied with several dipolarophiles (Scheme 3 and Fig. 1). In the case of maleimides such as *N*-methyl, *N*-benzyl, and *N*-phenyl maleimides (NMM, NBM, and NPM, respectively) pure *endo*-cycloadducts **1a–c** were isolated in very good yields and diastereoselectivity. Dimethyl

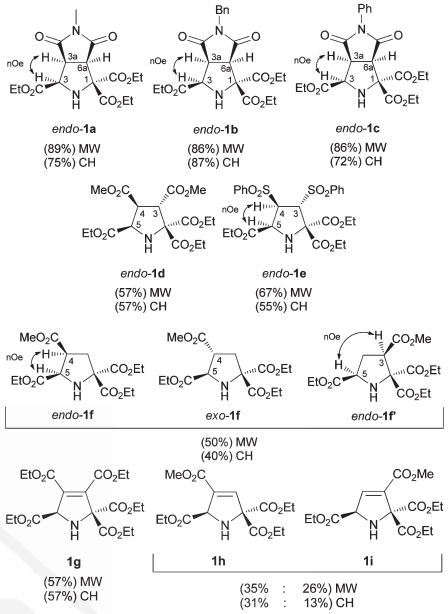

Fig. 1 1,3-DC of ethyl glyoxylate and diethyl aminomalonate in toluene.

fumarate furnished *endo*-**1d** in relatively good yield (57% regardless of the selected heating mode). (*E*)-1,2-Bis(phenylsulfonyl)ethylene, a synthetic equivalent of acetylene, was also assessed giving disulfone *endo*-**1e** in higher yield (67%) when the reaction took place under microwave irradiation. In the case of methyl acrylate an excess (10 equiv.) was required affording, under both heating conditions (MW and CH), a mixture of two *endo*-**1f**, and *exo*-**1f** stereoisomers and regioisomer *endo*-**1f'** (3 : 3 : 1) in moderate yields (Fig. 1).

Then acetylenic dipolarophiles were assayed. Symmetrical diethyl acetylenedicarboxylate afforded Δ^3-pyrroline **1g** (Fig. 1) in moderate yield (57%). An unexpected result was obtained in the thermal multicomponent reaction involving methyl propiolate. The reaction occurred in the presence of 3 equiv. of the dipolarophile in 61 and 44% overall yields under microwave-assisted and conventional heating, respectively. The corresponding products were isolated as a mixture of two regioisomers **1h** and **1i** in equal proportions (Fig. 1).

The relative configuration of products **1** was determined employing bidimensional NMR experiments (NOESY, COSY, HSMC, *etc.*) and by comparison of the experimental coupling constants with those reported in the literature for related structures.[10] For example, positive NOESY experiments and coupling constants of 8.5 Hz for the *cis*-arrangements H_3–H_{3a} and H_{3a}–H_{6a} supported the skeleton represented by *endo*-**1a**, **1b**

and **1c** structures. The higher chemical shift observed for H_{6a} (4.1–4.4 ppm, in *cis*-position with respect to an ester group) *versus* a range of 3.85–4.00 ppm for H_{6a} supported this arrangement. For the cases of *endo*-cycloadducts **1d** and **1e**, derived from 1,2-*trans*-disubstituted alkenes, both of the *cis*- and *trans*-coupling constants are very similar. NOESY experiments did not clarify the relationship of hydrogen atoms bonded at positions 3, 4 and 5 of the heterocycle of compound **1d**, but the chemical shifts of H_3 and H_5 matched with the structure represented in Fig. 1 according to the previous comment (see above). This assignment was also confirmed by the structural analysis of the molecule *endo*-**1e**, which displayed a very important positive nOe between *cis*-H_4–H_5. The observed coupling constant [$J(H_4–H_5)$ = 4.7 Hz] was slightly higher than the corresponding *trans*-H_3–H_4 (3.7 Hz), although with a lower absolute value than the analogous one observed for maleimide derivatives. Chemical shifts 4.64 ppm (H_4 in *trans*-position with respect to CO_2Et) and 5.15 ppm (H_3 in *cis*-position with respect to CO_2Et) were considered as definitive parameters to resolve the relative configuration.

The mixture of compounds **1f** was more difficult to elucidate because crucial signals appeared in very narrow ranges of ppm and also the stereoisomers could not be separated by flash chromatography. Compound *endo*-**1f** was identified according to the $J(H_4–H_5)$ = 8.2 Hz by comparison with the analogous data obtained for the *cis*-arrangement observed for cycloadduct *endo*-**1d**, and by nOe experiments. In addition, the other stereoisomer possesses a signal, with $J(H_4–H_5)$ = 6.9 Hz, which is appropriate for a *trans*-arrangement of those hydrogen atoms. Regioisomer *endo*-**1f'**, also observed in other examples of cycloaddition performed with methyl acrylate (see below), was identified in less proportion as the all-*cis* substituent pyrrolidine (confirmed by a small H_3–H_5 nOe) as a consequence of the attack of the W-shaped dipole **A** through its γ-position (Scheme 4).

In this series, the microwave-assisted reaction was much more advantageous. Surprisingly, when a freshly distilled ethyl glyoxylate was employed in this MCR the crude reaction mixture was extremely complex to analyze (^{1}H NMR). It is worth noting the importance of this multicomponent process because attempts to prepare the imine derived from diethyl aminomalonate and ethyl glyoxylate failed.

Encouraged by the good diastereoselection and simplicity of these reactions, we decided to explore the analogous transformation using α-amino esters. First, glycine ethyl ester was used for the synthesis of cycloadducts **2** under the previously described reaction conditions (Scheme 5). Microwave-assisted heating (1 h) provided similar conversions, chemical yields

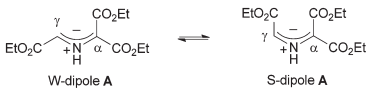

Scheme 4 Dipole conformations derived from ethyl glyoxylate and diethyl aminomalonate.

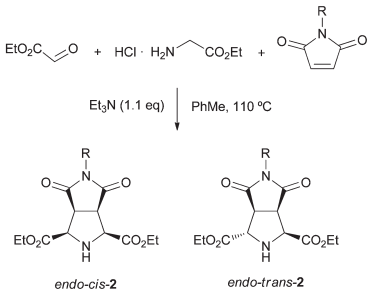

Scheme 5 1,3-DC of ethyl glycinate and ethyl glyoxylate with maleimides.

Table 1 1,3-DC between ethyl glycinate, ethyl glyoxylate, and maleimides

Entry	R	Heating[a]	Con.[b] (%)	2	Yield[c] (%)	*cis*/*trans*[b,d]
1	Me	CH	100	**2a**	75	3 : 1 (2 : 1)
2	Me	MW	100	**2a**	80	3 : 1 (2 : 1)
3	Bn	CH	100	**2b**	64	1 : 1 (2 : 1)
4	Bn	MW	85	**2b**	60	1 : 1 (2 : 1)
5	Ph	CH	100	**2c**	71[e]	>20 : 1 (4 : 1)
6	Ph	MW	96	**2c**	70[e]	>20 : 1 (4 : 1)

[a] Conventional heating (CH) takes 24 h for completion whilst microwave-assisted heating (MW) needs 1 h. [b] Determined by ^{1}H and ^{13}C NMR analysis. [c] Isolated yield after flash chromatography. [d] In brackets the diastereomeric ratio determined in the crude product. [e] Yield for compound *endo-cis*-**2c**.

and faster reactions than the analogous processes performed under conventional heating (24 h) (Table 1). Again, MW heating afforded cleanest crude reaction mixtures by ^{1}H NMR, without signals of the corresponding polymer from ethyl glyoxylate. Symmetrical dipolarophiles such as *N*-methyl, *N*-benzyl, and *N*-phenyl maleimides (NMM, NBM, and NPM, respectively) were evaluated affording cycloadducts **2** in moderate to good yields (Table 1). Nevertheless, the *cis*/*trans* ratio (referred to both CO_2Et group arrangement) of the final bicycle **2** was unexpectedly very different. Thus, NMM and NPM furnished *endo-cis*-**2a** as the major stereoisomer (Table 1, entries 1, 2, 5 and 6). However, NBM afforded equimolar amounts of both *cis*- and *trans*-isomers **2b**. The relative stereochemistry of the major *endo-cis*-**2c** was determined through NOESY experiments and by comparison of its X-ray diffraction pattern[11] with the analogous one described for a similar compound to **2c** (prepared in a fullerene-sensitized 1,3-DC between maleimides and iminodiacetic acid).[12] As was described in this last contribution the second order coupling constant did not confirm the higher value for the *cis*-arrangement. However, for the *endo-trans*-isomers a *cis*-coupling constant was observed (8.0–8.1 Hz) and smaller coupling constants in the corresponding multiplet. The imine derived from ethyl glycinate and ethyl glyoxylate could not be isolated in spite of testing several conditions and dehydrating protocols. We assume that in the case

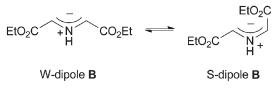

Scheme 6 Dipole conformations derived from glycine ethyl ester and ethyl glyoxylate.

of NMM and NPM the W-shaped ylide **B** reacts preferentially than the S-shaped one **B** affording mainly the 2,5-*cis* substituted pyrrolidine (Scheme 6).

The described reaction involving maleimides and glycine ethyl ester hydrochloride afforded symmetrical arrangement in structures **2**. In order to study the effect of a non-symmetrical alkene, the MW-assisted reaction was performed, in toluene as the solvent, with several dipolarophiles such as methyl acrylate, dimethyl fumarate, (*E*)-1,2-bis(phenylsulfonyl)ethylene or methyl propiolate. In all these examples, mixtures of unidentified isomers were obtained in low yields presumably due to epimerizations mainly at the 2- and/or 5-position of the pyrrolidine ring.

The microwave-assisted heating was next applied to the synthesis of more substituted pyrrolidine derivatives **3**, where methyl alaninate was selected as the dipole precursor combined with NMM and methyl acrylate as dipolarophiles (Scheme 7). In the reaction involving NMM the product *endo-cis*-**3a** was stereoselectively obtained in very good chemical yield (85%). The coupling constants of the cyclic hydrogen atoms were 8.0 Hz (*cis*-arrangement). Also, a small nOe between the methyl group and the H_3, H_{3a} or H_{6a} hydrogen atoms was observed. The reaction carried out in the presence of methyl acrylate was not so diastereoselective obtaining a

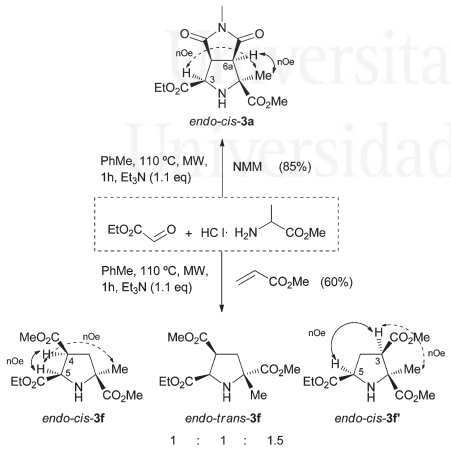

Scheme 7 1,3-DC involving ethyl alaninate, ethyl glyoxylate with NMM or methyl acrylate.

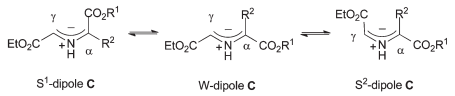

Scheme 8 Dipole conformations derived from α-substituted amino esters and ethyl glyoxylate.

mixture of *endo-cis*-regioisomers **3f** and **3f'** together with the stereomutated adduct *endo-trans*-**3f** (Scheme 7) originated by means of the S^1-dipole **C** (R^2 = Me, Scheme 8). The presence of an important amount of *endo-cis*-**3f'** implies that the isomerization of the imino ester occurred towards the formation of the thermodynamically more substituted resonance form of W-dipole **C** (R^2 = Me, Scheme 8) allowing the attack of the dipole by its γ-position. The analogous reaction with *tert*-butyl acrylate gave a very poor yield of an unidentified mixture of products. In any case involving acrylates, the reaction carried out under conventional heating afforded lower chemical yields (34–37%). The relative configuration of compound *endo-cis*-**3f** was determined according to H_4–H_5 nOe and very small nOe between the methyl group and H_5. The presence of this substituent in the ring reduced the *cis*-coupling constant to a 7.0 Hz value, which was also observed for the *endo-trans*-**3f**. For the last compound **3f'**, NOESY experiments were very helpful because intense nOe was shown between H_3–H_5 and also by the methyl group with H_3.

Lower LUMO-alkenes such as dimethyl fumarate and (*E*)-1,2-bis(phenylsulfonyl)ethylene were next examined as dipolarophiles in this multicomponent transformation (Scheme 9). In both examples, the reaction was highly diastereoselective obtaining the corresponding *endo-cis*-cycloadducts **3d** and **3e** in good yields after flash chromatography (70 and 66% yield, respectively). Apparently, other different stereoisomers were not detected either from the ^{1}H NMR reaction crude or by analysis of the purified compounds. The nature of substituents in a small-size carbocycle can alter their *cis*- and *trans*-coupling constants, thus, the reaction employing fumarate, with

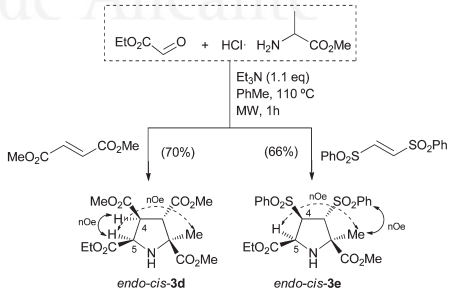

Scheme 9 1,3-DC of methyl alaninate and ethyl glyoxylate with dimethyl fumarate or (*E*)-1,2-bis(phenylsulfonyl)ethylene.

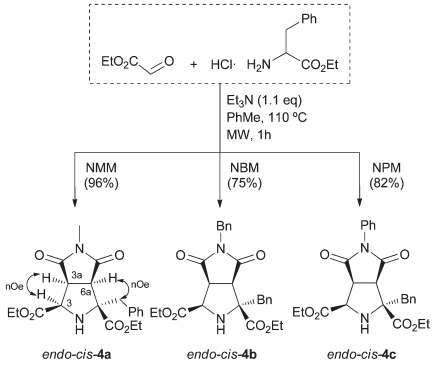

Scheme 10 1,3-DC of ethyl phenylalaninate and ethyl glyoxylate with maleimides.

$J_{cis}H_4$–H_5= 8.0 Hz, is clearly lower than the $J_{trans}H_3$–H_4= 10.0 Hz for the compound *endo-cis*-**3d** (also observed in compounds *endo-cis*-**4d** and *endo-cis*-**5d**, see below). Nevertheless, phenylsulfonyl substituents maintained the higher coupling constant for the *cis*-arrangement $J(H_4$–$H_5)$ = 6.5 Hz *versus* a 4.5 Hz value given by a *trans*-H_3–H_4 junction, such as occurred in every cycloadduct of this work derived from this disulfone. A very small nOe was detected between the methyl group and H_5 and a small one with the sulfonyl aromatic ring too (Scheme 9).

Similar behaviour was observed when the microwave-assisted heating was employed in the cycloaddition of ethyl phenylalaninate, ethyl glyoxylate and dipolarophiles. Maleimides were suitable electrophilic alkenes, for example NMM, NBM and NPM afforded exclusively, under the standard reaction conditions, products *endo-cis*-**4** in 96, 75, and 82% yield, respectively (Scheme 10). The corresponding $J_{cis}H_3$–H_{3a} coupling constants were 8.4 Hz for *endo-cis*-**4a**, and 7.8 Hz for both *endo-cis*-**4b** and **c**. The benzylic substituent is in a *cis*-position with respect to H_3–H_{3a}–H_{6a} according to NOESY experiments.

Dimethyl fumarate and phenylalaninate ethyl ester hydrochloride afforded cycloadduct *endo-cis*-**4d** in higher yield than the corresponding one obtained in the reaction using the alaninate (Scheme 11). The $J_{trans}H_3$–H_4 (10.1 Hz) and the $J_{cis}H_4$–H_5 (8.5 Hz) were similar to those observed for compound *endo-cis*-**3d**. A nOe was observed between benzylic protons and both H_4 and H_5. When disulfone (*E*)-1,2-bis(phenylsulfonyl)ethylene was allowed to react with ethyl phenylalaninate and ethyl glyoxylate, cycloadduct *exo-cis*-**4e** was obtained in 60% yield as the major diastereoisomer (*exo*/*endo* > 20 : 1, Scheme 11). Its relative configuration was determined by strong positive benzylic hydrogen atoms – H_3 nOe and a noticeable nOe between this benzylic methylene and H_5. In addition, a double J_{trans} = 5.2 Hz was observed in the H_4 signal. This opposite diastereoselectivity observed (in comparison with the diethyl aminomalonate adduct **1e** or *endo-cis*-**3e**) could be caused by steric repulsions of the benzylic substituent with the sulfonyl group.

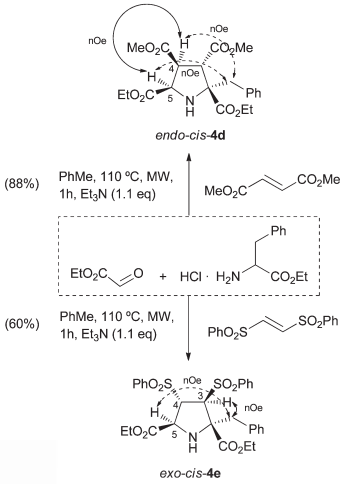

Scheme 11 1,3-DC of ethyl phenylalaninate and ethyl glyoxylate with dimethyl fumarate or (*E*)-1,2-bis(phenylsulfonyl)ethylene.

Another interesting series of α-quaternized pyrrolidine derivatives were isolated from the microwave assisted cycloaddition between methyl phenylglycinate hydrochloride, ethyl glyoxylate and different dipolarophiles (Scheme 12). Firstly, NMM afforded a 2 : 1 mixture of *endo*-cycloadducts, the

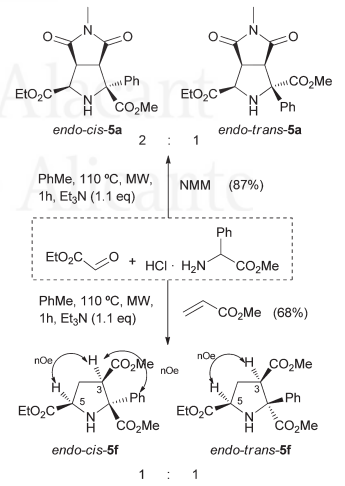

Scheme 12 1,3-DC of methyl phenylglycinate and ethyl glyoxylate with NMM or methyl acrylate.

stereomutated product being the minor isomer. The double *cis*-coupling constants for H_3–H_{3a} and H_{3a}–H_{6a} (8.5 and 7.5 Hz, respectively), and the positive nOe of H_3–H_{3a}–H_{6a} to each other supported the structure drawn for *endo-cis*-**5a** in Scheme 12. In the case of the *endo-trans*-**5a** the same positive nOe of H_3–H_{3a}–H_{6a} was detected (*cis*-coupling constants around 7.6 Hz) but the H_3 chemical shift (4.25 ppm) appeared at lower fields than the corresponding H_3 chemical shift (3.96 ppm) of the product *endo-cis*-**5a**. In the reaction performed with methyl acrylate the resulting regioselection was very high, however, the diastereoselection was similar to that described previously for NMM. The equimolar ratio of *endo-cis*-**5f**/*endo-trans*-**5f** was identified by ^{1}H NMR and the assignment of both relative configurations by NOESY experiments, specially by the nOe exhibited by H_3 with aromatic protons in cycloadduct *endo-cis*-**5f**. In both *endo-cis*-**5f** and *endo-trans*-**5f** a weak H_3–H_5 nOe was identified (Scheme 12). According to these results the S^1-dipole **C** (Scheme 8, R^1 = Me, R^2 = Ph) could be the precursor of *endo-trans*-cycloadducts. Due to steric reasons this dipole S^1-**C** reacted preferentially through its γ-position.

Dimethyl fumarate furnished an equimolecular mixture of diastereoisomers *endo-cis*-**5d** and *exo-cis*-**5d** in 87% yield (Scheme 13). For the *endo-cis*-arrangement J_{trans} was 10.1 Hz and 8.5 Hz for J_{cis}, and also H_3-CO_2Me nOe data were valuable to assign the final structure. The *exo-cis*-**5d** compound showed all-*trans* coupling constants 6.7 and 6.9 Hz, and a clear H_3-Ph nOe. From the analysis of chemical shifts of the H_3 atom in compounds **5a**, **5d** and **5f**, when this atom is in almost eclipsed conformation (*cis*-relative position) with the methyl ester group (bonded to C_2) it is deshielded by around 0.3, 0.4, and 0.5 ppm, respectively, with respect to the analogous shift appearing when H_3 and the phenyl group are in a *cis*-junction.

With all this information, it was possible to elucidate the structure of cycloadduct *exo-trans*-**5e**, which was obtained, in 68% yield, under standard reaction conditions employing (*E*)-1,2-bis(phenylsulfonyl)ethylene, ethyl glyoxylate and phenylglycine methyl ester hydrochloride (Scheme 13). Again, all-*trans* coupling constants 5.3 and 5.0 Hz, and H_3-CO_2Me nOe supported the drawn structure. However, the most relevant detail was the H_3 chemical shift (4.86 ppm), which is around 0.35 ppm higher than, for example, the chemical shift of H_3 in disulfonylated cycloadducts *exo-cis*-**4e** or *endo-cis*-**3e**.

According to very simple MM3 force field free energy calculations[13] the formation of the most energetically favoured stereoisomer *exo-trans*-**5e** was confirmed. Despite the apparent low difference in energy between the two resonance forms of S^1-dipole **C** (Scheme 8, R^1 = Me, R^2 = Ph) it seems that the bulky disulfone is better approached in an *exo*-manner due to possible hydrophobic interactions between a phenylsulfonyl ring and the phenyl group of the dipole.

Cycloadditions involving electron poor alkynes deserve a special mention. Methyl propiolate and diethyl acetylenedicarboxylate were appropriate dipolarophiles in the reaction performed with diethyl aminomalonate (Fig. 1). However, when glycinate, alaninate, phenylalaninate, and phenylglycinate were used for the 1,3-DC with methyl propiolate, the reaction mixture was extremely complex and no cycloadduct could be isolated. However, when α-substituted amino esters were allowed to react with ethyl glyoxylate and diethyl acetylenedicarboxylate, cycloadducts *cis*-**3g**, *cis*-**4g** and *cis*-**5g** were isolated after purification (flash chromatography) in moderate yields and as pure *cis*-stereoisomers (Scheme 14). In these three examples nOes between H_5 and the corresponding substituent (R^1) were observed.

This type of 1,3-DC permits the generation of pyrrolidine rings incorporating two alkoxycarbonyl groups, in many cases, with a *cis*-2,5-arrangement which is very valuable from the synthetic point of view because it is not a very easy task. As a possible application, we were interested in the synthesis of the bicyclic system **8**, which can be employed for the elaboration of large series of biologically active compounds.[14] For this

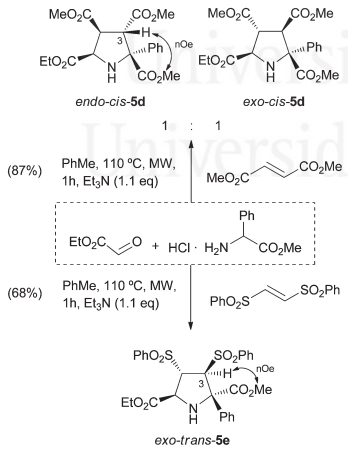

Scheme 13 1,3-DC of methyl phenylglycinate and ethyl glyoxylate with dimethyl fumarate or (*E*)-1,2-bis(phenylsulfonyl)ethylene.

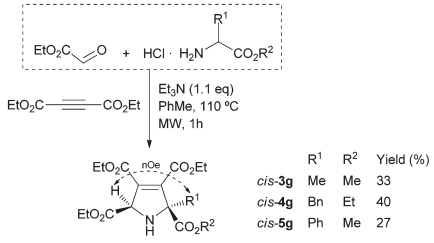

	R^1	R^2	Yield (%)
cis-**3g**	Me	Me	33
cis-**4g**	Bn	Et	40
cis-**5g**	Ph	Me	27

Scheme 14 1,3-DC of amino esters and ethyl glyoxylate with diethyl acetylenedicarboxylate.

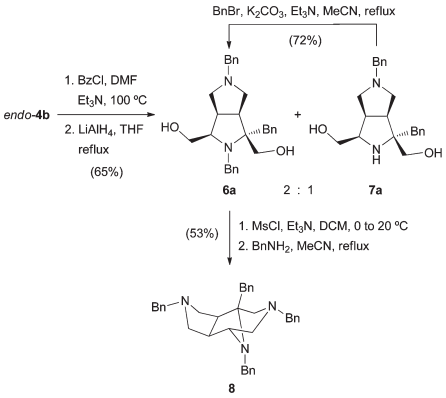

Scheme 15 Synthesis of the biologically active compound **8**.

purpose, cycloadduct *endo*-**4b** was allowed to react with benzoyl chloride[15] and the resulting amide immediately reduced in the presence of lithium aluminum hydride obtaining a 2 : 1 mixture of the desired diol **6a** and the debenzylated bicycle **7a** in 65% combined yield (Scheme 15). The latter was successfully transformed to **6a** in 78% yield by alkylation with benzyl bromide in DMF at 100 °C. The final diazabicyclo[2.2.1]-octane skeleton of **8** was achieved by a known methodology[16] employing a double mesylation followed by a ring closing nucleophilic substitution performed by benzylamine after 19 h under refluxing acetonitrile. The *all-cis*-**8** compound was isolated as a unique diastereoisomer in 53% yield, and a 34% overall yield from cycloadduct *endo*-**4b** (Scheme 15).

In conclusion, commercially available toluene solutions of reactive ethyl glyoxylate could be incorporated into the multicomponent 1,3-DC of azomethine ylides with dipolarophiles. Microwave-assisted heating was much more effective than the conventional heating affording total conversions in 1 h and cleaner reaction products in all the examples described across the text. If we analyze the effect of the 1,3-dipole nature, the normal trend of aminomalonate derived heterocycles is to react as its W-shaped type **A**, **B** or **C** 1,3-dipole (Schemes 4, 6 and 8) finding an exception when methyl acrylate was used as the dipolarophile. W-Shaped 1,3-dipole **B** (Scheme 6) is the most abundant intermediate when glycine ethyl ester was involved in the cycloaddition, although the existence of the S-shaped-**B** (Scheme 6) 1,3-dipole is noticeable. α-Substituted amino esters such as alanine methyl ester or phenylalanine ethyl ester overwhelmingly reacted through their W-shaped type **C** 1,3-dipoles. However, in the reactions dealing with the more sterically hindered phenylglycine derivative a competition of the attack through both α- and γ-positions of S^1-dipole **C** (Scheme 8) was inferred. In fact, S^1-dipole **C** precursor exclusively reacted by its γ-position when the ethylenic disulfone was employed.

According to the dipolarophiles, maleimides afforded exclusively *endo*-cycloadducts as well as dimethyl fumarate and methyl acrylate. Nevertheless, (*E*)-1,2-bis(phenylsulfonyl)ethylene reacted in a different manner depending on the amino ester. Thus, the *endo*-approach prevailed for less hindered R^2 substituents (amino malonate and alanine derivatives), meanwhile the *exo*-type interaction was favoured by phenylalanine and phenylglycine surrogates.

Finally, diethyl acetylenedicarboxylate afforded just one stereoisomer always operating under a W-shaped type **A** or **C** 1,3-dipole geometry. Methyl propiolate could only be tested in the reaction with diethyl aminomalonate affording an equimolar mixture of regioisomers as a consequence of the competition of the attack of the W-shaped type **A** dipole through its γ-position (Scheme 4).

Further studies to improve both regio- and diastereoselection by lowering the temperature of the reaction by means of an efficient catalyst are currently underway.

Experimental

General

The structurally most important peaks of the IR spectra (recorded using a Nicolet 510 P-FT and a Jasco FTIR 4100) are listed. ^{1}H NMR (300 MHz) and ^{13}C NMR (75 MHz) spectra were obtained using a Bruker AC-300 with $CDCl_3$ as the solvent and TMS as the internal standard unless otherwise stated. Low-resolution electron impact (GC-EI) mass spectra were obtained at 70 eV using a Shimadzu QP-5000, and high-resolution mass spectra were obtained using a Finnigan VG Platform. HRMS (GC-EI) were recorded using a Finnigan MAT 95S instrument. Analytical TLC was performed using Schleicher & Schuell F1400/LS silica gel plates, and the spots were visualized under UV light (λ = 254 nm). Melting points were determined with a Reichert Thermovar hot plate apparatus and are uncorrected. For flash chromatography, we employed Merck silica gel 60 (0.040–0.063 mm). CEM Discover and Explorer-Coolmate accessories were employed in the microwave-assisted reactions for the generation of imino esters.

General procedure for the microwave-assisted synthesis of cycloadducts

Ethyl glyoxylate (100 μL, 0.5 mmol, 50% in toluene), diethyl aminomalonate hydrochloride or the amino acid ethyl ester hydrochloride (0.5 mmol), the corresponding dipolarophile (0.5 mmol) and triethylamine (90 μL, 0.55 mmol) were dissolved in toluene (4 mL). The reaction vessel was sealed and irradiated in a CEM-discover microwave reactor at 110 °C and a maximum power of 60 W for 1 h. Alternatively, the reaction can be refluxed for 19 h. The solvent was evaporated under reduced pressure and the residue was dissolved in ethyl acetate, washed with brine and dried over $MgSO_4$. After evaporation the residue was purified by flash chromatography (silica gel) to afford the corresponding product.

(3*R,3a*S**,6a*R**)-Triethyl 5-methyl-4,6-dioxo hexahydropyrrolo[3,4-*c*]pyrrole-1,1,3(2*H*)-tricarboxylate *endo*-1a.** Sticky pale yellow oil; R_f 0.24 (*n*-hexane–ethyl acetate 7 : 3); IR (neat) ν_{max} 2983, 1701, 1731 cm^{-1}; ^1H NMR δ_H: 1.28–1.37 (m, 9H, 3 × $CO_2CH_2CH_3$), 2.93 (s, 3H, NCH_3), 3.42 (d, J = 10.5 Hz, 1H, N*H*), 3.60 [deform. dd, J = 8.5, 8.5 Hz, 1H, C*H*CH(CO_2Et)NH], 3.85 [dd, J = 10.5, 8.5 Hz, 1H, C*H*C(CO_2Et)NH], 4.15–4.45 [m, 7H, 3 × $CO_2CH_2CH_3$ and C*H*(CO_2Et)$_2$NH]; ^{13}C NMR δ_C: 13.8 ($CHCO_2CH_2CH_3$), 13.9 (2 × $CO_2CH_2CH_3$), 25.3 (NCH_3), 49.1 [*C*HCH(CO_2Et)NH], 51.6 [*C*HC(CO_2Et)$_2$NH], 61.2 [*C*H(CO_2Et)NH], 61.3, 61.9 (2 × $CO_2CH_2CH_3$), 62.9($CO_2CH_2CH_3$), 75.3 [*C*(CO_2Et)$_2$], 166.1, 168.5, 168.6 (3 × $CO_2CH_2CH_3$), 174.4, 174.6 (2 × CON); MS (EI-GC) *m*/*z*: 370 (M^+ + 1, <1%), 298 (15), 297 (100), 166 (56), 138 (11), 94 (15), 93 (10); HRMS calculated for $C_{16}H_{22}N_2O_8$: 370.1336, found: 370.1337.

(3*R,3a*S**,6a*R**)-Triethyl 5-benzyl-4,6-dioxohexahydropyrrolo-[3,4-*c*]pyrrole-1,1,3(2*H*)-tricarboxylate *endo*-1b.** Sticky pale yellow oil; R_f 0.39 (*n*-hexane–ethyl acetate 7 : 3); IR (neat) ν_{max} 2939, 2984, 2341, 2360, 1734, 1708 cm^{-1}; ^1H NMR δ_H: 1.24–1.34 (m, 9H, 3 × $CO_2CH_2CH_3$), 3.62 [deform. dd, J = 8.5 and 8.5 Hz, 1H, C*H*CH(CO_2Et)NH], 3.88 [d, J = 8.5 Hz, 1H, C*H*C(CO_2Et) NH], 4.14–4.43 [m, 7H, 3 × $CO_2CH_2CH_3$ and C*H*(CO_2Et)$_2$NH], 4.59 (s, 2H, CH_2Ph), 7.32–7.26 (m, 5H, Ar*H*), N*H* nd; ^{13}C NMR δ_C: 14.0 ($CHCO_2CH_2CH_3$), 14.1 (2 × $CO_2CH_2CH_3$), 43.1 (CH_2Ph), 49.3 [*C*HCH(CO_2Et)NH], 51.8 [*C*HC(CO_2Et)$_2$NH], 61.7 [*C*H(CO_2Et)NH], 62.2, 63.0, 63.1 (3 × $CO_2CH_2CH_3$), 75.7 [*C*(CO_2Et)$_2$], 128.1, 128.6, 128.7, 135.2 (Ar*C*), 166.2, 168.6, 168.7 (3 × $CO_2CH_2CH_3$), 174.2, 174.4 (2 × CON); MS (EI-GC) *m*/*z*: 446 (M^+ + 1, <1%), 374 (21), 373 (100), 227 (11), 166 (33), 94 (11), 91 (42); HRMS calculated for $C_{22}H_{26}N_2O_8$: 446.1689, found: 446.1688.

(3*R,3a*S**,6a*R**)-Triethyl 4,6-dioxo-5-phenylhexahydropyrrolo-[3,4-*c*]pyrrole-1,1,3(2*H*)-tricarboxylate *endo*-1c.** Sticky pale yellow oil; R_f 0.29 (*n*-hexane–ethyl acetate 7 : 3); IR (neat) ν_{max} 2983, 2939, 2906, 1714 cm^{-1}; ^1H NMR δ_H: 1.25–1.37 (m, 9H, 3 × $CO_2CH_2CH_3$), 3.64 (d, J = 10.0 Hz, 1H, N*H*), 3.78 [dd, J = 8.4, 7.9 Hz, 1H, C*H*CH(CO_2Et)NH], 4.00 [dd, J = 10.0, 8.4 Hz, 1H, C*H*C(CO_2Et)NH], 4.16–4.45 [m, 7H, 3 × $CO_2CH_2CH_3$ and C*H*-(CO_2Et)$_2$NH], 7.15–7.23 (m, 2H, Ar*H*), 7.47–7.33 (m, 3H, Ar*H*), N*H* nd; ^{13}C NMR δ_C: 14.0 ($CHCO_2CH_2CH_3$), 14.1 (2 × $CO_2CH_2CH_3$), 49.6 [*C*HCH(CO_2Et)NH], 52.1 [*C*HC(CO_2Et)$_2$NH], 62.1 [*C*H(CO_2Et)NH], 62.3, 63.1, 63.2 (3 × $CO_2CH_2CH_3$), 76.2 [*C*(CO_2Et)$_2$], 126.7, 129.1, 129.4, 131.5 (Ar*C*), 166.4, 168.7, 169.0 (3 × $CO_2CH_2CH_3$), 173.8, 174.0 (2 × CON); MS (EI-GC) *m*/*z*: 432 (M^+ + 1, <1%), 360 (20), 359 (100), 166 (58), 138 (12), 94 (19); HRMS calculated for $C_{21}H_{24}N_2O_8$: 432.1533, found: 432.1544.

(3*S,4*S**,5*R**)-2,2,5-Triethyl 3,4-dimethyl pyrrolidine-2,2,3,4,5-pentacarboxylate *endo*-1d.** Yellow pale oil; R_f 0.34 (*n*-hexane–ethyl acetate 7 : 3); IR (neat) ν_{max} 2984, 2956, 2910, 1732 cm^{-1}; ^1H NMR δ_H: 1.20–1.30 (m, 9H, 3 × $CO_2CH_2CH_3$), 3.56 [deform. dd, J = 9.0, 8.0 Hz, 1H, C*H*CH(CO_2Et)NH], 3.68–3.75 [m with 2 × s, 7H, 2 × CO_2CH_3, C*H*C(CO_2Et)NH], 4.08 [d, J = 9.0 Hz, 1H, C*H*(CO_2Et)$_2$], 4.10–4.32 (m, 6H, 3 × $CO_2CH_2CH_3$), N*H* nd; ^{13}C NMR δ_C: 13.9 ($CHCO_2CH_2CH_3$), 14.0, 14.2 (2 × $CO_2CH_2CH_3$), 50.5 [*C*HCH(CO_2Et)NH], 52.6 [*C*HC-(CO_2Et)$_2$NH], 52.7, 53.4 (2 × CO_2CH_3), 61.8 [*C*H(CO_2Et)NH], 61.9, 62.7, 62.7 (3 × $CO_2CH_2CH_3$), 74.6 [*C*(CO_2Et)$_2$], 168.7, 168.9, 170.3, 171.0, 171.2 (5 × CO_2CH_3); MS (EI-GC) *m*/*z*: 403 (M^+ + 1, <1%), 299 (15), 298 (100), 198 (23), 166 (47), 152 (15), 138 (10), 119 (10), 94 (11); HRMS calculated for $C_{17}H_{25}NO_{10}$: 403.1478, found: 403.1490.

(3*R,4*R**,5*S**)-Triethyl 3,4-bis(phenylsulfonyl)pyrrolidine-2,2,5-tricarboxylate *endo*-1e.** Pale yellow prisms, mp = 49–51 °C (from hexane–ethyl acetate); R_f 0.11 (*n*-hexane–ethyl acetate 7 : 3); IR (neat) ν_{max} 3105, 2360, 2341, 1747, 1265, 1153 cm^{-1}; ^1H NMR δ_H: 1.10 (t, J = 7.1 Hz, 3H, $CO_2CH_2CH_3$), 1.27 (t, J = 7.1 Hz, 3H, $CO_2CH_2CH_3$), 1.34 (t, J = 7.1 Hz, 3H, $CO_2CH_2CH_3$), 4.04 (q, J = 7.1 Hz, 2H, $CO_2CH_2CH_3$), 4.16 [d, J = 4.7 Hz, 1H, C*H* (CO_2Et)NH], 4.29–4.40 (m, 4H, 2 × $CO_2CH_2CH_3$), 4.64 [dd, J = 4.7, 3.7 Hz, 1H, C*H*CH(CO_2Et)NH], 5.15 [d, J = 3.7 Hz, 1H, C*H*(CO_2Et)$_2$NH], 7.45–7.74 (m, 8H, Ar*H*), 7.84–7.96 (m, 2H, Ar*H*), N*H* nd; ^{13}C NMR δ_C: 13.6 ($CHCO_2CH_2CH_3$), 13.8, 13.9 (2 × $CO_2CH_2CH_3$), 60.4 [*C*HCH-(CO_2Et)NH], 62.2, 63.3, 63.4 (3 × $CO_2CH_2CH_3$), 63.5 [*C*HC-(CO_2Et)$_2$NH], 68.3 [*C*H(CO_2Et)NH], 76.1 [*C*(CO_2Et)$_2$], 128.7, 129.0, 129.2, 129.3, 134.2, 134.3, 137.5, 138.2 (Ar*C*), 165.4, 167.5, 168.7 (3 × $CO_2CH_2CH_3$); MS (EI-GC) *m*/*z*: 567 (M^+ + 1, <1%), 495 (10), 494 (35), 353 (14), 352 (73), 306 (41), 280 (50), 235 (13), 234 (100), 212 (19), 166 (17), 141 (16), 140 (20), 125 (18), 120 (11), 112 (22), 94 (32), 77 (42), 68 (16); HRMS calculated for $C_{25}H_{29}NO_{10}S_2$–$C_3H_5O_2$: 494.0943, found: 494.0929.

(4*S,5*R**)-2,2,5-Triethyl 4-methylpyrrolidine-2,2,4,5-tetracarboxylate *endo*-1f and compound *exo*-1f.** Pale yellow oil; R_f 0.41 (*n*-hexane–ethyl acetate 7 : 3); IR (neat) ν_{max} 2985, 1735 cm^{-1}; ^1H NMR δ_H: 1.20–1.29 (m, 2 × 9H, 3 × $CO_2CH_2CH_3$ *endo* + *exo*), 2.31–2.83 [m, 2 × 2H, CH_2C(CO_2Et)$_2$ *endo* + *exo*], 3.10 (br. s, 1H, NH), 3.64, 3.65 (2 × s, 2 × 3H, CO_2CH_3 *endo* + *exo*), 3.76 [deform. dd, J = 7.4, 7.2 Hz, 1H, C*H*CH(CO_2Et)NH *exo*], 3.88 [dd, 1H, J = 8.2, 6.9 Hz, C*H*CH(CO_2Et)NH *endo*], 4.09 [d, J = 8.2 Hz, 1H, C*H*(CO_2Et)NH *endo*], 4.12–4.30 [m, 13H, 6 × $CO_2CH_2CH_3$ *endo* + *exo* C*H*(CO_2Et)NH *exo*]; ^{13}C NMR δ_C: 14.0, 14.1, 14.1, 14.2, 14.2, 14.3 (6 × $CO_2CH_2CH_3$ *endo* + *exo*), 33.5, 34.6 [2 × CH_2C(CO_2Et)$_2$NH *endo* + *exo*], 46.8, 49.5 [2 × *C*H-(CO_2Et)NH *endo* + *exo*], 52.2, 52.3 [2 × *C*HCH(CO_2Et)NH *endo* + *exo*], 59.1, 62.7 (2 × CO_2CH_3 *endo* + *exo*), 61.5, 61.6, 62.3, 62.5, 62.5, 62.6 (6 × $CO_2CH_2CH_3$ *endo* + *exo*), 71.6, 75.31 [2 × *C*(CO_2Et)$_2$ *endo* + *exo*], 168.9, 169.7, 170.3, 171.0, 171.3, 171.5, 171.9, 172.4 (8 × CO_2 *endo* + *exo*); MS (EI-GC) *m*/*z*: 345 (M^+ + 1, <1%), 273 (14), 272 (100), 140 (10), 170 (12), 94 (10), 68 (14); HRMS calculated for $C_{15}H_{23}NO_8$: 345.1434, found: 345.1441.

(*R*/*S*)-2,2,3,4,5-Pentaethyl 1*H*-pyrrole-2,2,3,4,5(5*H*)-pentacarboxylate 1g. Yellow oil; R_f 0.10 (*n*-hexane–ethyl acetate 7 : 3); IR (neat) ν_{max} 2981, 2360, 2341, 1741 cm^{-1}; ^1H NMR δ_H 1.33–1.24 (m, 15H, 5 × $CO_2CH_2CH_3$), 4.14–4.32 (m, 10H, 5 × $CO_2CH_2CH_3$), 5.51 [s, 1H, C*H*(CO_2Et)NH], N*H* nd; ^{13}C NMR δ_C: 13.9, 14.0, 14.1, 14.1, 14.3 (5 × $CO_2CH_2CH_3$), 59.8, 62.1, 62.2, 62.5, 62.5 (5 × $CO_2CH_2CH_3$), 77.24 [*C*(CO_2Et)$_2$], 92.91 [*C*HC-(CO_2Et)$_2$NH], 146.9 [*C*CH(CO_2Et)NH], 147.0 [*C*C(CO_2Et)$_2$NH], 163.4, 166.7, 166.7, 166.8, 169.3 (5 × CO_2); MS (EI-GC) *m*/*z*: 429 (M^+ + 1, <1%), 345 (18), 300 (15), 299 (16), 273 (12), 272 (84), 227 (29), 226 (100), 199 (10), 198 (79), 181 (20), 170 (33), 154 (11), 142 (14), 125 (10), 124 (19), 87 (16), 69 (13), 68 (12);

microanalysis calculated for $C_{19}H_{27}NO_{10}$: C, 53.1; H, 6.3; N, 3.4%; found: C, 53.0; H, 6.0; N, 3.4%.

(*R*/*S*)-2,2,5-Triethyl 4-methyl 1*H*-pyrrole-2,2,4,5(5*H*)-tetracarboxylate 1h. Yellow oil; R_f 0.49 (*n*-hexane–ethyl acetate 7 : 3); IR (neat) ν_{max} 2981, 2914, 1734, 1608 cm^{-1}; ^1H NMR δ_H: 1.19–1.33 (m, 9H, 3 × $CO_2CH_2CH_3$), 3.63 (s, 3H, CO_2CH_3), 4.09–4.31 (m, 6H, 3 × $CO_2CH_2CH_3$), 4.83 [d, *J* = 1.7 Hz, 1H, C*H*(CO$_2$Et)NH], 6.86 [d, *J* = 1.7 Hz, 1H, C*H*C(CO$_2$Et)$_2$], N*H* nd; ^{13}C NMR δ_C: 13.9 (3 × $CO_2CH_2CH_3$), 61.5 ($CO_2CH_2CH_3$), 62.6 (2 × $CO_2CH_2CH_3$), 62.8 (CO_2CH_3), 67.0 [*C*H(CO$_2$Et)NH], 79.0 [*C*(CO$_2$Et)$_2$NH], 150.8 [CHC(CO$_2$Et)$_2$NH], 150.9 [*C*CH(CO$_2$Et)NH], 162.60, 168.1, 168.2, 170.5 (4 × *C*O$_2$CH$_3$); MS (EI-GC) *m*/*z*: 343 (M^+ + 1, <1%), 270 (25), 226 (10), 198 (100), 170 (30), 166 (30), 152 (60), 126 (19), 122 (13), 120 (54), 94 (14); HRMS calculated for $C_{15}H_{21}NO_8$–$C_3H_5O_2$: 270.0980, found: 270.0995.

(*R*/*S*)-2,2,5-Triethyl 3-methyl 1*H*-pyrrole-2,2,3,5(5*H*)-tetracarboxylate 1i. Yellow oil; R_f 0.40 (*n*-hexane–ethyl acetate 7 : 3); IR (neat) ν_{max} 2953, 1730, 1608 cm^{-1}; ^1H NMR δ_H: 1.19–1.33 (m, 9H, 3 × $CO_2CH_2CH_3$), 3.74 (s, 3H, CO_2CH_3), 4.09–4.31 (m, 6H, 3 × $CO_2CH_2CH_3$), 4.54 [d, *J* = 13.0 Hz, 1H, C*H*(CO$_2$Et)NH], 7.42 [d, *J* = 13.0 Hz, 1H, C*H*CH(CO$_2$Et)NH], N*H* nd; ^{13}C NMR δ_C: 13.9 (2 × $CO_2CH_2CH_3$), 14.0 (CHCO$_2$CH$_2$*C*H$_3$), 62.4 (CHCO$_2$*C*H$_2$CH$_3$), 62.5 (2 × $CO_2CH_2CH_3$), 62.8 (CO_2CH_3), 66.2 [*C*H(CO$_2$Et)NH], 83.0 [*C*(CO$_2$Et)$_2$NH], 136.8 [*C*HCH(CO$_2$Et)NH], 162.6 [*C*C(CO$_2$Et)$_2$NH], 168.2, 168.5, 168.6, 170.3 (4 × *C*O$_2$); MS (EI-GC) *m*/*z*: 343 (M^+ + 1, <1%), 270 (20), 226 (10), 198 (100), 170 (30), 166 (20), 152 (65), 126 (25), 122 (10), 120 (50), 94 (12); HRMS calculated for $C_{15}H_{21}NO_8$–$C_3H_5O_2$: 270.0980, found: 270.0995.

(1*R,3*S**,3a*R**,6a*S**)-Diethyl 5-methyl-4,6-dioxooctahydropyrrolo[3,4-*c*]pyrrole-1,3-dicarboxylate *endo-cis*-2a.** Sticky yellow oil; R_f 0.14 (*n*-hexane–ethyl acetate 7 : 3); IR (neat) ν_{max} 2984, 1699, 1595 cm^{-1}; ^1H NMR δ_H: 1.33 (t, *J* = 7.2 Hz, 6H, 2 × $CO_2CH_2CH_3$), 2.94 (s, 3H, NC*H*$_3$), 3.57 [m, 2H, 2 × C*H*CH(CO$_2$Et)NH], 3.97 [m, 2H, 2 × *CH*(CO$_2$Et)NH], 4.30 (q, *J* = 7.2 Hz, 4H, 2 × $CO_2CH_2CH_3$), N*H* nd; ^{13}C NMR δ_C: 14.2 (2 × $CO_2CH_2CH_3$), 25.5 (NCH$_3$), 50.0 [2 × *C*HCH(CO$_2$Et)NH], 61.9 (2 × $CO_2CH_2CH_3$), 63.1 [2 × *C*H(CO$_2$Et)NH], 169.0 (2 × *C*O$_2$CH$_2$CH$_3$), 175.0 (2 × CON); MS (EI-GC) *m*/*z*: 298 (M^+ + 1, 1%), 226 (12), 225 (100), 179 (32), 151 (53), 94 (44), 67 (12); HRMS calculated for $C_{13}H_{18}N_2O_6$: 298.1155, found: 298.1148.

(1*R,3*R**,3a*R**,6a*S**)-Diethyl 5-methyl-4,6-dioxooctahydropyrrolo[3,4-*c*]pyrrole-1,3-dicarboxylate *endo-trans*-2a.** Sticky yellow oil; R_f 0.25 (*n*-hexane–ethyl acetate 7 : 3); IR (neat) ν_{max} 2984, 1774, 1731, 1595 cm^{-1}; ^1H NMR δ_H: 1.33 (t, *J* = 7.2 Hz, 3H, $CO_2CH_2CH_3$), 1.35 (t, *J* = 7.2 Hz, 3H, $CO_2CH_2CH_3$), 2.98 (s, 3H, NC*H*$_3$), 3.56 [deform. dd, *J* = 8.0, 8.0 Hz, 1H, C*H*CH(CO$_2$Et)NH], 3.64 [dd, *J* = 8.0, 1.2 Hz, 1H, C*H*CH(CO$_2$Et)NH], 4.13 [d, *J* = 8.0 Hz, 1H, C*H*(CO$_2$Et)NH], 4.24 (q, *J* = 7.2 Hz, 2H, $CO_2CH_2CH_3$), 4.27–4.35 [m, 3H, $CO_2CH_2CH_3$ and C*H*(CO$_2$Et)NH], N*H* nd; ^{13}C NMR δ_C: 14.2, 14.3 (2 × $CO_2CH_2CH_3$), 25.5 (NCH$_3$), 47.6 [*C*HCH(CO$_2$Et)NH], 48.8 [*C*HCH(CO$_2$Et)NH], 61.8, 62.0 (2 × $CO_2CH_2CH_3$), 62.2 [*C*H(CO$_2$Et)NH], 62.4 [*C*H(CO$_2$Et)NH], 169.7, 171.7 (2 × *C*O$_2$), 175.4, 176.6 (2 × CON); MS (EI-GC) *m*/*z*: 298 (M^+ + 1, 1%), 226 (12), 225 (100), 179 (17), 151 (40), 94 (40), 68 (10), 67 (13); HRMS calculated for $C_{13}H_{18}N_2O_6$: 298.1155, found: 298.1148.

(1*R,3*S**,3a*R**,6a*S**)-Diethyl 5-benzyl-4,6-dioxooctahydropyrrolo[3,4-*c*]pyrrole-1,3-dicarboxylate *endo-cis*-2b.** Sticky yellow oil; R_f 0.15 (*n*-hexane–ethyl acetate 7 : 3); IR (neat) ν_{max} 2984, 1740, 1705 cm^{-1}; ^1H NMR δ_H: 1.28 (t, *J* = 7.1 Hz, 6H, 2 × $CO_2CH_2CH_3$), 3.54 [m, 2H, C*H*CH(CO$_2$Et)NH], 3.94 [m, 2H, C*H*(CO$_2$Et)NH], 4.24 (q, *J* = 7.1 Hz, 4H, 2 × $CO_2CH_2CH_3$), 4.58 (s, 2H, CH_2Ph), 7.18–7.38 (m, 5H, Ar*H*); ^{13}C NMR δ_C: 14.1 (2 × $CO_2CH_2CH_3$), 43.0 (CH_2Ph), 49.8 [2 × *C*HCH(CO$_2$Et)NH], 62.0 (2 × $CO_2CH_2CH_3$), 63.0 [2 × *C*H(CO$_2$Et)NH], 128.1, 128.6, 128.7, 135.2 (Ar*C*), 168.8 (2 × *C*O$_2$CH$_2$CH$_3$), 174.6 (CON); MS (EI-GC) *m*/*z*: 374 (M^+ + 1, 2%), 302 (18), 301 (100), 227 (50), 94 (23), 91 (47), 68 (11); HRMS calculated for $C_{19}H_{22}N_2O_6$: 374.1478, found: 374.1470.

(1*R,3*R**,3a*R**,6a*S**)-Diethyl 5-benzyl-4,6-dioxooctahydropyrrolo[3,4-*c*]pyrrole-1,3-dicarboxylate *endo-trans*-2b.** Sticky yellow oil; R_f 0.22 (*n*-hexane–ethyl acetate 7 : 3); IR (neat) ν_{max} 2990, 1740, 1700 cm^{-1}; ^1H NMR δ_H: 1.23–1.38 (m, 6H, 2 × $CO_2CH_2CH_3$), 3.64 (dd, *J* = 8.0, 1.4 Hz, 1H, C*H*CH(CO$_2$Et)NH), 4.10–4.33 [m, 6H, C*H*CH(CO$_2$Et)NH and C*H*(CO$_2$Et)NH and 2 × $CO_2CH_2CH_3$], 4.52–4.69 (m, 3H, CH_2Ph and C*H*(CO$_2$Et)NH), 7.18–7.40 (m, 5H, Ar*H*); ^{13}C NMR δ_C: 14.2, 14.3 (2 × $CO_2CH_2CH_3$), 43.1 (CH_2Ph), 48.8 [*C*HCH(CO$_2$Et)NH], 49.9 [*C*HCH(CO$_2$Et)NH], 61.8, 62.0 (2 × $CO_2CH_2CH_3$), 62.2 [*C*H-(CO$_2$Et)NH], 62.5 [*C*H(CO$_2$Et)NH], 128.1, 128.8, 129.1, 135.4 (Ar*C*), 169.6, 171.7 (2 × *C*O$_2$CH$_2$CH$_3$), 175.0, 176.3 (2 × CON); MS (EI-GC) *m*/*z*: 374 (M^+ + 1, 2%), 302 (18), 301 (100), 227 (31), 94 (20), 91 (44), 68 (13); HRMS calculated for $C_{19}H_{22}N_2O_6$: 374.1478, found: 374.1470.

(1*R,3*S**,3a*R**,6a*S**)-Diethyl 4,6-dioxo-5-phenyloctahydropyrrolo[3,4-*c*]pyrrole-1,3-dicarboxylate *endo-cis*-2c.** Colorless needles, mp = 123–125 °C (from hexane/$CDCl_3$); R_f 0.11 (*n*-hexane–ethyl acetate 7 : 3); IR (neat) ν_{max} 2980, 1741, 1732, 1708 cm^{-1}; ^1H NMR δ_H: 1.32 (t, *J* = 7.2 Hz, 6H, 2 × $CO_2CH_2CH_3$), 3.05 (t, *J* = 12.7 Hz, 1H, N*H*), 3.71 [m, 2H, 2 × *CH*CH(CO$_2$Et)NH], 4.06 [m, 2H, C*H*(CO$_2$Et)NH], 4.29 (q, *J* = 7.2 Hz, 4H, 2 × $CO_2CH_2CH_3$), 7.19–7.22 (m, 2H, Ar*H*), 7.37–7.46 (m, 3H, Ar*H*); ^{13}C NMR δ_C: 14.0 (2 × $CO_2CH_2CH_3$), 49.9 [2 × *C*HCH(CO$_2$Et)NH], 62.1 (2 × $CO_2CH_2CH_3$), 63.4 [2 × *C*H(CO$_2$Et)-NH], 126.5, 128.9, 129.2, 131.3 (Ar*C*), 169.0 (2 × *C*O$_2$CH$_2$CH$_3$), 174.1 (2 × CON); MS (EI-GC) 360 *m*/*z* (M^+ + 1, 3%), 288 (19), 287 (100), 94 (45), 68 (13), 67 (11); HRMS calculated for $C_{18}H_{20}N_2O_6$: 360.1301, found: 360.1291.

(1*R,3*R**,3a*R**,6a*S**)-Diethyl 4,6-dioxo-5-phenyloctahydropyrrolo[3,4-*c*]pyrrole-1,3-dicarboxylate *endo-trans*-2c.** Colorless needles, mp = 105–107 °C (from hexane/$CDCl_3$); R_f 0.14 (*n*-hexane–ethyl acetate 7 : 3); IR (neat) ν_{max} 2976, 1712 cm^{-1}; ^1H NMR δ_H: 1.20–1.32 (m, 6H, 2 × $CO_2CH_2CH_3$), 2.85 (br. s, 1H, N*H*), 3.68 [deform. dd, *J* = 8.1, 8.1 Hz, 1H, C*H*CH(CO$_2$Et)NH], 3.83 [d, *J* = 8.1, 1H, C*H*CH(CO$_2$Et)NH], 4.25 [m, 5H, 2 × $CO_2CH_2CH_3$ and C*H*(CO$_2$Et)NH], 4.42 [s, 1H, C*H*(CO$_2$Et)NH], 7.23–7.27 (m, 2H, Ar*H*), 7.38–7.47 (m, 3H, Ar*H*); ^{13}C NMR δ_C: 14.0, 14.1 (2 × $CO_2CH_2CH_3$), 47.6 [*C*HCH(CO$_2$Et)NH], 49.9 [*C*HCH(CO$_2$Et)NH], 61.9, 62.1 (2 × $CO_2CH_2CH_3$), 62.3 [*C*H-(CO$_2$Et)NH], 62.9 [*C*H(CO$_2$Et)NH], 126.4, 128.8, 129.1, 131.5 (Ar*C*), 169.8, 171.4 (2 × *C*O$_2$CH$_2$CH$_3$), 174.6, 175.6 (2 × CON); MS (EI-GC) 360 *m*/*z*: (M^+ + 1, 4%), 67 (10), 68 (13), 94 (40),

287 (100), 288 (17); HRMS calculated for $C_{18}H_{20}N_2O_6$: 360.1301, found: 360.1291.

(1*S,3*R**,3a*S**,6a*R**)-3-Ethyl 1-methyl 1,5-dimethyl-4,6-dioxooctahydropyrrolo[3,4-*c*]pyrrole-1,3-dicarboxylate *endo-cis*-3a.** Sticky pale yellow oil; R_f 0.38 (*n*-hexane–ethyl acetate 6 : 4); IR (neat) ν_{max} 2983, 2955, 1777, 1735, 1697 cm^{-1}; ^1H NMR δ_H: 1.36 (t, *J* = 7.2 Hz, 3H, $CO_2CH_2CH_3$), 1.49 [s, 3H, $C(CO_2CH_3)CH_3$], 2.93 (s, 3H, NCH_3), 3.25 [d, *J* = 8.0 Hz, 1H, $CHC(CO_2Me)CH_3$], 3.37 (d, *J* = 12.5 Hz, 1H, N*H*), 3.63 [deform. dd, *J* = 8.0, 8.0 Hz, 1H, $CHCH(CO_2Et)NH$], 3.83 (s, 3H, CO_2CH_3), 4.14 [dd, *J* = 12.5, 8.0 Hz, 1H, $CH(CO_2Et)NH$], 4.30 (q, *J* = 7.2 Hz, 2H, $CO_2CH_2CH_3$); ^{13}C NMR δ_C: 14.2 ($CO_2CH_2CH_3$), 24.6 [$C(CO_2CH_3)CH_3$], 25.4 (NCH_3), 50.4 [$CHCH(CO_2Et)NH$], 53.1 [$CHC(CO_2Me)CH_3$], 62.0 (CO_2CH_3), 62.1 ($CO_2CH_2CH_3$), 69.4 [$CH(CO_2Me)CH_3$], 169.5, 171.7 (2 × CO_2), 175.0, 175.2 (2 × CON); MS (EI-GC) *m*/*z*: 298 (M^+ + 1, <1%), 239 (67), 225 (39), 165 (100), 108 (43), 81 (10), 80 (21); HRMS calculated for $C_{13}H_{18}N_2O_6$: 298.1165, found: 298.1163.

(2*R,3*S**,5*S**)-2-Ethyl 3,5-dimethyl 5-methylpyrrolidine-2,3,5-tricarboxylate *endo-cis*-3f.** Yellowish oil; R_f 0.41 (*n*-hexane–ethyl acetate 7 : 3); IR (neat) ν_{max} 2983, 2954, 1731, 1725, 1700 cm^{-1}; ^1H NMR δ_H: 1.26 (t, *J* = 7.2 Hz, 3H, $CO_2CH_2CH_3$), 1.49 [s, 3H, $C(CO_2CH_3)CH_3$], 2.01 [dd, *J* = 12.9, 9.8 Hz, 1H, $CHHC(CO_2Me)CH_3$], 2.64 [dd, *J* = 12.9, 8.3 Hz, 1H, $CHHC(CO_2Me)CH_3$], 3.19 [ddd, *J* = 9.8, 8.3, 7.1 Hz, 1H, $CH(CO_2Me)$], 3.71, 3.73 (2s, 3H, CO_2CH_3), 3.77 [d, *J* = 7.1 Hz, 1H, $CH(CO_2Et)NH$], 4.16 (q, *J* = 7.2 Hz, 2H, $CO_2CH_2CH_3$, N*H* nd; ^{13}C NMR δ_C: 14.3 ($CO_2CH_2CH_3$), 25.9 [$C(CO_2CH_3)CH_3$], 40.7 [$CH_2C(CO_2Me)CH_3$], 47.4 [$CHCH(CO_2Et)NH$], 52.4, 52.7 (2 × CO_2CH_3), 61.6 ($CO_2CH_2CH_3$), 63.0 [$CH(CO_2Et)NH$], 66.3 [$C(CO_2Me)CH_3$], 172.8, 173.5, 176.3 (3 × CO_2); MS (EI-GC) *m*/*z*: 273 (M^+ + 1, <2%), 215 (11), 214 (100), 200 (30), 168 (13), 140 (33), 108 (19), 82 (21); HRMS calculated for $C_{12}H_{19}NO_6$: 273.1212, found: 273.1214.

(2*R,3*S**,5*R**)-2-Ethyl 3,5-dimethyl 5-methylpyrrolidine-2,3,5-tricarboxylate *endo-trans*-3f.** Yellowish oil; R_f 0.22 (*n*-hexane–ethyl acetate 7 : 3); IR (neat) ν_{max} 2983, 2953, 1732, 1725, 1703 cm^{-1}; ^1H NMR δ_H: 1.25 (t, *J* = 7.2 Hz, 3H, $CO_2CH_2CH_3$), 1.37 [s, 3H, $C(CO_2CH_3)CH_3$], 2.01 [dd, *J* = 13.5, 8.0 Hz, 1H, $CHHC(CO_2Me)CH_3$], 2.68 [dd, *J* = 13.5, 7.2 Hz, 1H, $CHHC(CO_2Me)CH_3$], 3.30 [ddd, *J* = 8.0, 7.2, 7.0 Hz, 1H, $CHCH(CO_2Et)$], 3.62, 3.73 (2s, 3H, CO_2CH_3), 4.03 [d, *J* = 7.0 Hz, 1H, $CH(CO_2Et)NH$], 4.15 (q, *J* = 7.2 Hz, 2H, $CO_2CH_2CH_3$), N*H* nd; ^{13}C NMR δ_C: 14.2 ($CO_2CH_2CH_3$), 28.3 [$C(CO_2CH_3)CH_3$], 39.1 [$CH_2C(CO_2Me)CH_3$], 47.1 [$CHCH(CO_2Et)NH$], 53.3, 53.4 (2 × CO_2CH_3), 61.4 ($CO_2CH_2CH_3$), 62.8 [$CH(CO_2Et)NH$], 65.4 [$C(CO_2Me)CH_3$], 172.3, 173.6, 176.4 (3 × CO_2); MS (EI-GC) *m*/*z*: 273 (M^+ + 1, <2%), 215 (12), 214 (100), 200 (33), 140 (62), 108 (20), 99 (24), 82 (23); HRMS calculated for $C_{12}H_{19}NO_6$: 273.1212, found: 273.1215.

(2*S,3*R**,5*R**)-5-Ethyl 2,3-dimethyl 2-methylpyrrolidine-2,3,5-tricarboxylate *endo-cis*-3f'.** Yellowish oil; R_f 0.21 (*n*-hexane–ethyl acetate 7 : 3); IR (neat) ν_{max} 2983, 2955, 1730, 1726, 1700 cm^{-1}; ^1H NMR δ_H: 1.26 (t, *J* = 7.1 Hz, 3H, $CO_2CH_2CH_3$), 1.51 [s, 3H, $C(CO_2CH_3)CH_3$], 2.29–2.57 [m, 2H, $CH_2CH(CO_2Et)$], 2.87 [dd, *J* = 9.5, 8.1 Hz, 1H, $CHC(CO_2Me)CH_3$], 3.65, 3.66 (2s, 3H, CO_2CH_3), 3.87 [dd, *J* = 8.6, 7.6 Hz, 1H, $CH(CO_2Et)NH$], 4.15 (q, *J* = 7.1 Hz, 2H, $CO_2CH_2CH_3$), N*H* nd; ^{13}C NMR δ_C: 14.3 ($CO_2CH_2CH_3$), 25.5 [$CHC(CO_2Me)CH_3$], 32.3 [$CH_2CH(CO_2Et)NH$], 52.0, 52.1 (2 × CO_2CH_3), 52.5 [$CHC(CO_2Me)Me$], 58.0 [$CH(CO_2Et)NH$], 61.4 ($CO_2CH_2CH_3$), 68.3 [$C(CO_2Me)Me$], 171.6, 172.2, 174.3 (3 × CO_2); MS (EI-GC) *m*/*z*: 273 (M^+ + 1, <2%), 215 (12), 214 (100), 200 (32), 140 (62), 108 (20), 99 (27), 82 (23); HRMS calculated for $C_{12}H_{19}NO_6$: 273.1212, found: 273.1214.

(2*S,3*S**,4*S**,5*R**)-5-Ethyl 2,3,4-trimethyl 2-methylpyrrolidine-2,3,4,5-tetracarboxylate *endo-cis*-3d.** Pale yellow oil; R_f 0.20 (*n*-hexane–ethyl acetate 7 : 3); IR (neat) ν_{max} 2986, 2954, 2907, 1730, 1729 cm^{-1}; ^1H NMR δ_H: 1.27 (t, *J* = 7.1 Hz, 3H, $CO_2CH_2CH_3$), 1.60 [s, 3H, $C(CO_2CH_3)CH_3$], 3.24 [d, *J* = 10.0 Hz, 1H, $CHC(CO_2Me)Me$], 3.64, 3.68, 3.74 (3s, 3H, CO_2CH_3), 3.78 [dd, *J* = 10.0, 8.1 Hz, 1H, $CHCH(CO_2Et)NH$], 4.02 [d, *J* = 8.1 Hz, 1H, $CH(CO_2Et)NH$], 4.15 (q, *J* = 7.1 Hz, 2H, $CO_2CH_2CH_3$), N*H* nd; ^{13}C NMR δ_C: 14.2 ($CO_2CH_2CH_3$), 24.9 [$C(CO_2CH_3)CH_3$], 49.6 [$CHC(CO_2Me)Me$], 52.3, 52.6 52.7 (3 × CO_2CH_3), 56.8 [$CHCH(CO_2Et)NH$], 61.7 [$CH(CO_2Et)NH$], 61.8 ($CO_2CH_2CH_3$), 68.4 [$C(CO_2Me)Ph$], 170.6, 172.3, 173.0, 173.8 (4 × CO_2); MS (EI-GC) *m*/*z*: 331 (M^+ + 1, <2%), 272 (65), 258 (19), 262 (19), 241 (10), 240 (82), 226 (99), 212 (80), 198 (60), 180 (10), 167 (11), 166 (100), 154 (25), 140 (72), 139 (10), 136 (10), 122 (10), 108 (58), 94 (11), 81 (22), 80 (27), 59 (24); HRMS calculated for $C_{14}H_{21}NO_8$: 331.1267, found: 331.1274.

(2*R,3*R**,4*R**,5*S**)-5-Ethyl 2-methyl 2-methyl-3,4-bis(phenylsulfonyl)pyrrolidine-2,5-dicarboxylate *endo-cis*-3e.** Orange oil; R_f 0.11 (*n*-hexane–ethyl acetate 7 : 3); IR (neat) ν_{max} 2985, 2956, 2905, 1735, 1710, 1308, 1146 cm^{-1}; ^1H NMR δ_H: 1.00 (t, *J* = 7.1 Hz, 3H, $CO_2CH_2CH_3$), 1.72 [s, 3H, $C(CO_2CH_3)CH_3$], 3.72 (s, 3H, CO_2CH_3), 3.94 (q, *J* = 7.1 Hz, 2H, $CO_2CH_2CH_3$), 4.27 [d, *J* = 6.5 Hz, 1H, $CH(CO_2Et)NH$], 4.28 [d, *J* = 4.5 Hz, 1H, $CHC(CO_2Me)Me$], 5.01 [dd, *J* = 6.5, 4.5 Hz, 1H, $CHCHCO_2Et$], 7.51–7.71 (m, 6H, Ar*H*), 7.81–8.02 (m, 4H, Ar*H*), N*H* nd; ^{13}C NMR δ_C: 14.0 ($CO_2CH_2CH_3$), 23.7 [$CHC(CO_2Me)CH_3$], 52.7 [$CH(CO_2Et)NH$], 61.5 (CO_2CH_3), 62.2 ($CO_2CH_2CH_3$), 69.4 [$C(CO_2Me)Me$], 69.5 [$CHC(CO_2Me)Me$], 73.0 [$CHCH(CO_2Et)NH$], 128.4, 128.9, 129.3, 129.4, 134.2, 134.4, 138.1, 140.4 (Ar*C*), 170.1, 171.2 (2 × CO_2); MS (EI-GC) *m*/*z*: 495 (M^+ + 1, <1%), 294 (32), 279 (21), 248 (39), 237 (14), 236 (100), 222 (26), 221 (10), 156 (11), 128 (17), 125 (11), 108 (23), 96 (26), 95 (10), 94 (11), 81 (46), 80 (21), 77 (14); HRMS calculated for $C_{22}H_{25}NO_8S_2$: 495.1022, found: 495.1015.

(1*S,3*R**,3a*S**,6a*R**)-Diethyl 1-benzyl-5-methyl-4,6-dioxooctahydropyrrolo[3,4-*c*]pyrrole-1,3-dicarboxylate *endo-cis*-4a.** Sticky pale yellow oil; R_f 0.22 (*n*-hexane–ethyl acetate 7 : 3); IR (neat) ν_{max} 3030, 2982, 2936, 1779, 1734, 1699 cm^{-1}; ^1H NMR δ_H: 1.32, 1.34 (2t, *J* = 7.2 Hz, 3H, $CO_2CH_2CH_3$), 2.88, 3.30 (2d, *J* = 13.8 Hz, 2H, CH_2Ph), 2.92 (s, 3H, NCH_3), 3.38 [d, *J* = 8.0 Hz, 1H, $CHC(CO_2Et)Bn$], 3.55 [deform. dd, *J* = 8.4, 8.0 Hz, 1H, $CHCH(CO_2Et)NH$], 4.09 [d, *J* = 8.4 Hz, 1H, $CH(CO_2Et)NH$], 4.24 (q, *J* = 7.2 Hz, 2H, $CO_2CH_2CH_3$), 4.26 (q, *J* = 7.2 Hz, 2H, $CO_2CH_2CH_3$), N*H* nd; ^{13}C NMR δ_C: 14.0 (2 × $CO_2CH_2CH_3$), 25.4 (NCH_3), 42.2 (CH_2Ar), 50.4 [$CHCH(CO_2Et)NH$], 56.6 [$CHC(CO_2Et)Bn$], 62.0 [$CH(CO_2Et)NH$], 62.1 ($CO_2CH_2CH_3$),

62.3 ($CO_2CH_2CH_3$), 73.6 [$C(CO_2Et)Bn$], 127.2, 128.3, 130.4, 135.7 (Ar*C*), 169.6, 170.1 (2 × CO_2), 175.0, 175.1 (2 × CON); MS (EI-GC) *m*/*z*: 388 (M^+ + 1, <1%), 315 (13), 298 (14), 297 (100), 223 (11), 166 (45), 94 (11), 91 (17); HRMS calculated for $C_{20}H_{24}N_2O_6$: 388.1634, found: 388.1631.

(1*S,3*R**,3a*S**,6a*R**)-Diethyl 1,5-dibenzyl-4,6-dioxooctahydropyrrolo[3,4-*c*]pyrrole-1,3-dicarboxylate *endo-cis*-4b.** Colorless prisms, mp = 127–130 °C (from hexane/$CDCl_3$); R_f 0.39 (*n*-hexane–ethyl acetate 7 : 3); IR (neat) ν_{max} 3030, 2989, 1741, 1719, 1699 cm^{-1}; ^1H NMR δ_H: 1.23 (t, *J* = 7.2 Hz, 3H, $CO_2CH_2CH_3$), 1.28 (t, *J* = 7.2 Hz, 3H, $CO_2CH_2CH_3$), 2.89, 3.31 (2 × d, *J* = 13.9 Hz, 2H, CH_2Ph), 3.38 [d, *J* = 7.8 Hz, 1H, C*H*C(CO$_2$Et)Bn], 3.55 [deform. dd, *J* = 7.8, 7.8 Hz, 1H, C*H*CH(CO$_2$Et)NH], 4.03–4.27 [m, 5H, 2 × $CO_2CH_2CH_3$ and C*H*(CO$_2$Et)NH], 4.54, 4.60 (d, *J* = 14.3 Hz, 2H), 7.20–7.35 (m, 10H, 2 × CH_2Ph), N*H* nd; ^{13}C NMR δ_C: 14.0, 14.1 (2 × $CO_2CH_2CH_3$), 42.2, 43.0 (2 × CH_2Ph), 50.4 [*C*HCH(CO$_2$Et)NH], 56.6 [*C*HCH(CO$_2$Et)NH], 61.9, 62.1 (2 × $CO_2CH_2CH_3$), 62.3 [*C*H(CO$_2$Et)NH], 73.7 [*C*Bn(CO$_2$Et)NH], 127.2, 128.0, 128.3, 128.6, 128.7, 130.5, 135.2, 135.8 (ArC), 169.4, 169.9 (2 × $CO_2CH_2CH_3$), 174.6, 174.7 (2 × CON); MS (EI-GC) *m*/*z*: 464 (M^+ + 1, <1%), 391 (14), 374 (22), 373 (100), 166 (22), 91 (73); HRMS calculated for $C_{26}H_{28}N_2O_6$–C_7H_7: 373.1400, found: 373.1401.

(1*S,3*R**,3a*S**,6a*R**)-Diethyl 1-benzyl-4,6-dioxo-5-phenyloctahydropyrrolo[3,4-*c*]pyrrole-1,3-dicarboxylate *endo-cis*-4c.** Colorless prisms, mp = 169–172 °C (from hexane/$CDCl_3$); R_f 0.34 (*n*-hexane–ethyl acetate 7 : 3); IR (neat) ν_{max} 2979, 2937, 1729, 1714 cm^{-1}; ^1H NMR δ_H: 1.25–1.30 (m, 6H, 2 × $CO_2CH_2CH_3$), 2.96, 3.36 (2 × d, *J* = 13.9 Hz, 2H, CH_2Ph), 3.51 (s, 1H, N*H*), 3.55 [d, *J* = 7.8 Hz, 1H, C*H*C(CO$_2$Et)Bn], 3.73 [deform. dd, *J* = 7.8, 7.8 Hz, 1H, C*H*CH(CO$_2$Et)NH], 4.15–4.30 [m, 5H, 2 × $CO_2CH_2CH_3$ and C*H*(CO$_2$Et)NH], 7.15–7.49 (m, 10H, Ar*H*); ^{13}C NMR δ_C: 13.9, 14.0 ($CO_2CH_2CH_3$), 42.3 (CH_2Ph), 50.4 [*C*HCH(CO$_2$Et)NH], 56.6 [*C*HCH(CO$_2$Et)NH], 62.1, 62.2 (2 × $CO_2CH_2CH_3$), 62.3 [CH(CO$_2$Et)NH], 74.1 [*C*Bn(CO$_2$Et)NH], 126.6, 127.2, 128.0, 128.2, 128.9, 129.2, 130.4, 135.6 (ArC), 169.7, 170.1 (2 × CO_2), 174.0, 174.2 (2 × CON); MS (EI-GC) *m*/*z*: 450 (M^+ + 1, <1%), 377 (14), 360 (22), 359 (100), 207 (44), 166 (40), 156 (10), 119 (10), 94 (13), 91 (45); HRMS calculated for $C_{25}H_{26}N_2O_6$: 450.1791, found: 450.1801.

(2*S,3*S**,4*S**,5*R**)-5-Ethyl 2,3,4-trimethyl 2-benzylpyrrolidine-2,3,4,5-tetracarboxylate *endo-cis*-4d.** Colorless oil; R_f 0.35 (*n*-hexane–ethyl acetate 7 : 3); IR (neat) ν_{max} 2983, 2954, 2906, 1732, 1727 cm^{-1}; ^1H NMR δ_H: 1.22, 1.26 (2t, *J* = 7.1 Hz, 3H, $CO_2CH_2CH_3$), 3.13, 3.37 (2d, *J* = 13.8 Hz, 2H, CH_2Ph), 3.34 [d, *J* = 10.1 Hz, 1H, C*H*C(CO$_2$Et)Bn], 3.65 [dd, *J* = 10.1, 8.5 Hz, 1H, C*H*CH(CO$_2$Et)NH], 3.70, 3.78 (2s, 3H, CO_2CH_3), 3.86 [d, *J* = 8.5 Hz, 1H, C*H*(CO$_2$Et)NH], 4.05–4.25 (m, 4H, 2 × $CO_2CH_2CH_3$), 7.24–7.36 (m, 5H, Ar*H*), N*H* nd; ^{13}C NMR δ_C: 14.0, 14.2 (2 × $CO_2CH_2CH_3$), 42.6 (CH_2Ar), 49.3 [CHC(CO$_2$Et)Bn], 52.4, 52.6 (2 × CO_2CH_3), 54.8 [*C*HCH(CO$_2$Et)NH], 61.6 [*C*H(CO$_2$Et)NH], 62.0, 61.7 (2 × $CO_2CH_2CH_3$), 72.3 [*C*(CO$_2$Et)Bn], 127.1, 128.3, 130.9, 135.9 (Ar*C*), 170.5, 171.9, 172.3, 172.9 (4 × CO_2); MS (EI-GC) *m*/*z*: 407 (M^+ + 1, <1%), 348 (18), 330 (48), 316 (44), 298 (100), 166 (32), 138 (11), 91 (60); HRMS calculated for $C_{20}H_{25}NO_8$: 407.1580, found: 407.1586.

(2*R,3*S**,4*S**,5*S**)-Diethyl 2-benzyl-3,4-bis(phenylsulfonyl)-pyrrolidine-2,5-dicarboxylate *exo-cis*-4e.** Pale yellow prisms, mp = 85–86 °C (from *n*-hexane–ethyl acetate); R_f 0.22 (7 : 3 *n*-hexane–ethyl acetate); IR (neat) ν_{max} 2971, 1741, 1235, 1149 cm^{-1}; ^1H NMR δ_H: 1.04 (t, *J* = 7.2 Hz, 1H, $CO_2CH_2CH_3$), 1.21 (t, *J* = 7.2 Hz, 1H, $CO_2CH_2CH_3$), 3.29, 3.40 (2 × d, *J* = 14.2 Hz, 2H, CH_2Ph), 3.88–4.29 (m, 4H, 2 × $CO_2CH_2CH_3$), 4.20 [C*H*(CO$_2$Et)NH], 4.43 (br. s, 1H, N*H*), 4.51 [d, *J* = 5.2 Hz, 1H, C*H*C(CO$_2$Et)Bn], 4.89 [deform. dd, *J* = 5.2, 5.2 Hz, 1H, C*H*CH(CO$_2$Et)NH], 7.18–7.33 (m, 5H, Ar*H*), 7.44–7.82 (m, 8H, Ar*H*), 7.88–7.98 (m, 2H, Ar*H*); ^{13}C NMR δ_C: 13.8, 14.0 (2 × $CO_2CH_2CH_3$), 41.0 (CH_2Ph), 61.1, 62.2 (2 × $CO_2CH_2CH_3$), 62.3 [*C*HCH(CO$_2$Et)NH], 69.4 [*C*HCBn(CO$_2$Et)NH], 72.0 [*C*H(CO$_2$Et)-NH], 73.8 [*C*Bn(CO$_2$Et)NH], 127.4, 128.4, 128.8, 129.1, 129.2, 129.4, 130.7, 134.3, 134.4, 134.7, 138.5, 139.5 (Ar*C*), 169.6, 169.6 (2 × CO_2); MS (EI-GC) *m*/*z*: 585 (M^+ + 1, <1%), 512 (10), 494 (34), 370 (14), 353 (13), 352 (69), 306 (33), 298 (10), 280 (26), 235 (10), 234 (82), 157 (13), 156 (23), 141 (10), 125 (15), 112 (11), 94 (16), 91 (100), 80 (12), 77 (29); HRMS calculated for $C_{29}H_{31}NO_8S_2$–$C_3H_5O_2$: 512.1202, found: 512.1215.

(1*R,3*R**,3a*S**,6a*R**)-3-Ethyl 1-methyl 5-methyl-4,6-dioxo-1-phenyloctahydropyrrolo[3,4-*c*]pyrrole-1,3-dicarboxylate *endo-cis*-5a.** Sticky pale yellow oil; R_f 0.21 (*n*-hexane–ethyl acetate 7 : 3); IR (neat) ν_{max} 2982, 2954, 1779, 1736, 1698 cm^{-1}; ^1H NMR δ_H: 1.25 (t, *J* = 7.2 Hz, 3H, $CO_2CH_2CH_3$), 2.91 (s, 3H, NCH_3), 3.37 [deform. dd, *J* = 8.5, 7.5 Hz, 1H, C*H*CHCO$_2$Et], 3.69 (s, 3H, CO_2CH_3), 3.76 [d, *J* = 8.5, 1H, C*H*(CO$_2$Et)NH], 3.96 [d, *J* = 7.5 Hz, 1H, C*H*(CO$_2$Me)Ph], 4.20 (qd, *J* = 7.2, 1.1 Hz, 2H, $CO_2CH_2CH_3$), 7.22–7.36 (m, 3H, Ar*H*), 7.58–7.63 (m, 2H, Ar*H*), N*H* nd; ^{13}C NMR δ_C: 14.2 ($CO_2CH_2CH_3$), 25.5 (NCH_3), 50.3 [*C*HCH(CO$_2$Et)NH], 53.4 [*C*HC(CO$_2$Me)Ph], 56.5 (*C*HCO$_2$Et), 61.6 (CO_2CH_3), 62.1 ($CO_2CH_2CH_3$), 74.8 [*C*(CO$_2$Me)Ph], 127.4, 128.5, 128.7, 138.1 (Ar*C*), 169.6, 170.2 (2 × CO_2), 175.1, 175.4 (2 × CON); MS (EI-GC) *m*/*z*: 360 (M^+ + 1, <1%), 302 (17), 301 (100), 228 (14), 227 (72), 170 (19), 143 (18), 142 (27); HRMS calculated for $C_{18}H_{20}N_2O_6$: 360.1321, found: 360.1322.

(1*S,3*R**,3a*S**,6a*R**)-3-Ethyl 1-methyl 5-methyl-4,6-dioxo-1-phenyloctahydropyrrolo[3,4-*c*]pyrrole-1,3-dicarboxylate *endo-trans*-5a.** Sticky pale yellow oil; R_f 0.12 (*n*-hexane–ethyl acetate 7 : 3); IR (neat) ν_{max} 2983, 2954, 2926, 1781, 1729, 1702 cm^{-1}; ^1H NMR δ_H: 1.39 (t, *J* = 7.2 Hz, 3H, $CO_2CH_2CH_3$), 2.79 (s, 3H, NCH_3), 3.08 (d, *J* = 3.5 Hz, 1H, N*H*), 3.55 [deform. dd, *J* = 7.6, 7.6 Hz, 1H, C*H*CHCO$_2$Et], 3.79 (s, 3H, CO_2CH_3), 3.86 [dd, *J* = 7.6, 3.5 Hz, 1H, C*H*(CO$_2$Et)NH], 4.25 [d, *J* = 7.6 Hz, 1H, C*H*C(CO$_2$Me)Ph], 4.30–4.41 (m, 2H, $CO_2CH_2CH_3$), 7.33–7.41 (m, 3H, Ar*H*), 7.47–7.54 (m, 2H, Ar*H*); ^{13}C NMR δ_C: 14.2 ($CO_2CH_2CH_3$), 25.2 (NCH_3), 45.3 [*C*HCH(CO$_2$Et)NH], 50.4 [*C*HC(CO$_2$Me)Ph], 53.7 (*C*HCO$_2$Et), 59.8 (CO_2CH_3), 61.7 ($CO_2CH_2CH_3$), 74.1 [*C*(CO$_2$Me)Ph], 126.0, 128.5, 128.9, 135.4 (Ar*C*), 169.3, 173.5 (2 × CO_2), 174.1, 175.6 (2 × CON); MS (EI-GC) *m*/*z*: 360 (M^+ + 1, <1%), 302 (18), 301 (100), 228 (13), 227 (63), 170 (20), 143 (22), 142 (30), 115 (15); HRMS calculated for $C_{18}H_{20}N_2O_6$: 360.1321, found: 360.1336.

(2*R,3*R**,5*R**)-5-Ethyl 2,3-dimethyl 2-phenylpyrrolidine-2,3,5-tricarboxylate *endo-cis*-5f.** Yellowish oil; R_f 0.41 (*n*-hexane–ethyl acetate 7 : 3); IR (neat) ν_{max} 2985, 2953, 1734,

1700 cm^{-1}; ^1H NMR δ_H: 1.29 (t, J = 7.1 Hz, 3H, $CO_2CH_2CH_3$), 2.29–2.36 [m, 2H, $CH_2CH(CO_2Et)$], 3.51 [dd, J = 7.6, 4.5 Hz, 1H, $CHC(CO_2Me)Ph$], 3.68, 3.70 (2s, 3H, CO_2CH_3), 3.85 [dd, J = 9.0, 5.7 Hz, 1H, $CH(CO_2Et)NH$], 4.23 (q, J = 7.1 Hz, 2H, $CO_2CH_2CH_3$), 7.25–7.35 (m, 3H, Ar*H*), 7.73–7.77 (m, 2H, Ar*H*), N*H* nd; ^{13}C NMR δ_C: 14.3 ($CO_2CH_2CH_3$), 33.8 [$CH_2CH(CO_2Et)$-NH], 52.2, 52.9 (2 × CO_2CH_3), 54.0 [$CHC(CO_2Me)Ph$], 58.6 [$CH(CO_2Et)NH$], 61.5 ($CO_2CH_2CH_3$), 75.5 [$C(CO_2Me)Ph$], 126.9, 128.1, 128.4, 140.2 (Ar*C*), 172.2, 173.1, 173.6 (3 × CO_2); MS (EI-GC) *m*/z: 335 (M^+ + 1, <2%), 277 (18), 276 (100), 262 (19), 202 (41), 170 (19), 144 (20), 143 (14), 115 (10), 99 (15); HRMS calculated for $C_{17}H_{21}NO_6$: 335.1369, found: 335.1313.

(2*S,3*R**,5*R**)-5-Ethyl 2,3-dimethyl 2-phenylpyrrolidine-2,3,5-tricarboxylate *endo-trans*-5f.** Yellowish oil; R_f 0.29 (*n*-hexane–ethyl acetate 7 : 3); IR (neat) ν_{max} 2984, 2953, 1727, 1658 cm^{-1}; ^1H NMR δ_H: 1.30 (t, J = 7.1 Hz, 3H, $CO_2CH_2CH_3$), 2.36–2.46 [m, 2H, $CH_2CH(CO_2Et)$], 3.19, 3.72 (2s, 3H, CO_2CH_3), 3.92 [deform. dd, J = 8.0, 7.6 Hz, Ph1H, $CHC(CO_2Me)Ph$], 4.04 [deform. dd, J = 6.5, 5.9 Hz, 1H, $CH(CO_2Et)NH$], 4.26 (q, J = 7.1 Hz, 2H, $CO_2CH_2CH_3$), 7.24–7.37 (m, 3H, Ar*H*), 7.49–7.53 (m, 2H, Ar*H*), N*H* nd; ^{13}C NMR δ_C: 14.3 ($CO_2CH_2CH_3$), 32.7 [$CH_2CH(CO_2Et)$-NH], 50.6, 51.5 (2 × CO_2CH_3), 53.4 [$CHC(CO_2Me)Ph$], 58.5 [CH-$(CO_2Et)NH$], 61.3 ($CO_2CH_2CH_3$), 76.0 [$C(CO_2Me)Ph$], 126.3, 128.3, 128.5, 137.5 (Ar*C*), 172.6, 173.0, 173.9 (3 × CO_2); MS (EI-GC) *m*/z: 335 (M^+ + 1, <2%), 277 (21), 276 (100), 262 (15), 202 (38), 201 (10), 170 (25), 144 (13), 143 (11), 115 (11), 99 (17); HRMS calculated for $C_{17}H_{21}NO_6$: 335.1369, found: 335.1308.

(2*R,3*S**,4*S**,5*R**)-5-Ethyl 2,3,4-trimethyl 2-phenylpyrrolidine-2,3,4,5-tetracarboxylate *endo-cis*-5d.** Colorless oil; R_f 0.25 (*n*-hexane–ethyl acetate 7 : 3); IR (neat) ν_{max} 2984, 2954, 1735, 1716, 1713, 1700 cm^{-1}; ^1H NMR δ_H: 1.14 (t, J = 7.1 Hz, 3H, $CO_2CH_2CH_3$), 3.64, 3.67, 3.75 (3s, 3H, CO_2CH_3), 3.82 [dd, J = 10.1, 8.5 Hz, 1H, $CHCH(CO_2Et)NH$], 3.98 [d, J = 8.5 Hz, 1H, CH-$(CO_2Et)NH$], 4.04 (q, J = 7.1 Hz, 2H, $CO_2CH_2CH_3$), 4.38 [d, J = 10.1 Hz, 1H, $CHC(CO_2Me)Ph$], 7.26–7.38 (m, 2H, Ar*H*), 7.51 (dd, J = 8.5, 2.8 Hz, 1H, Ar*H*), 7.70 (dd, J = 8.5, 2.8 Hz, 2H, Ar*H*), N*H* nd; ^{13}C NMR δ_C: 14.0 ($CO_2CH_2CH_3$), 51.1, 52.3, 52.6 (3 × CO_2CH_3), 53.3 [$CHC(CO_2Me)Ph$], 53.5 [$CHCH(CO_2Et)NH$], 60.7 [$CH(CO_2Et)NH$], 61.4 ($CO_2CH_2CH_3$), 75.0 [$C(CO_2Me)Ph$], 127.0, 128.1, 128.3, 140.9 (Ar*C*), 170.8, 171.3, 171.7, 172.8 (4 × CO_2); MS (EI-GC) *m*/z: 393 (M^+ + 1, <2%), 335 (19), 334 (100), 302 (24), 288 (11), 274 (35), 260 (25), 242 (13), 228 (51), 202 (25), 201 (11), 170 (11), 143 (26), 115 (16); HRMS calculated for $C_{19}H_{23}NO_8$: 393.1424, found: 393.1421.

(2*R,3*R**,4*R**,5*R**)-5-Ethyl 2,3,4-trimethyl 2-phenylpyrrolidine-2,3,4,5-tetracarboxylate *exo-cis*-5d.** Colorless oil; R_f 0.30 (*n*-hexane–ethyl acetate 7 : 3); IR (neat) ν_{max} 2990, 2950, 1748, 1733, 1730, 1715 cm^{-1}; ^1H NMR δ_H: 1.30 (t, J = 7.1 Hz, 3H, $CO_2CH_2CH_3$), 3.56, 3.69, 3.72 (3s, 3H, CO_2CH_3), 3.64 [deform. dd, J = 6.9, 6.7 Hz, 1H, $CHCH(CO_2Et)NH$], 3.89 [d, J = 6.7 Hz, 1H, $CHC(CO_2Me)Ph$], 4.17 [d, J = 6.9 Hz, 1H, $CH(CO_2Et)NH$], 4.26 (q, J = 7.1 Hz, 2H, $CO_2CH_2CH_3$), 7.28–7.38 (m, 2H, Ar*H*), 7.51 (dd, J = 7.0, 2.3 Hz, 1H, Ar*H*), 7.70 (dd, J = 7.0, 2.3 Hz, 2H, Ar*H*), N*H* nd; ^{13}C NMR δ_C: 14.3 ($CO_2CH_2CH_3$), 51.8, 52.6, 52.8 (3 × CO_2CH_3), 53.6 [$CHC(CO_2Me)Ph$], 54.7 [$CHCH(CO_2Et)NH$], 61.6 [$CH(CO_2Et)NH$], 61.9 ($CO_2CH_2CH_3$), 75.2 [$C(CO_2Me)Ph$], 126.4, 128.1, 128.2, 139.7 (Ar*C*), 171.1, 171.6, 172.0, 172.1 (4 × CO_2); MS (EI-GC) *m*/z: 393 (M^+ + 1, <1%), 335 (19), 334 (100), 303 (11), 302 (60), 274 (14), 260 (25), 242 (11), 228 (27), 202 (21), 170 (56), 143 (24), 115 (14); HRMS calculated for $C_{19}H_{23}NO_8$: 393.1424, found: 393.1426.

(2*R,3*R**,4*R**,5*S**)-5-Ethyl 2-methyl 2-phenyl-3,4-bis(phenylsulfonyl)pyrrolidine-2,5-dicarboxylate *exo-trans*-5e.** Orange oil; R_f 0.10 (*n*-hexane–ethyl acetate 7 : 3); IR (neat) ν_{max} 2981, 2954, 2926, 1738, 1692, 1309, 1147 cm^{-1}; ^1H NMR δ_H: 1.04 (t, J = 7.2 Hz, 3H, $CO_2CH_2CH_3$), 3.74 (s, 3H, CO_2CH_3), 4.01 (q, J = 7.2 Hz, 2H, $CO_2CH_2CH_3$), 4.35 [d, J = 5.0 Hz, 1H, $CH(CO_2Et)NH$], 4.86 [d, J = 5.3 Hz, 1H, $CHC(CO_2Me)Ph$], 4.91 [deform. dd, J = 5.3, 5.0 Hz, 1H, $CHCHCO_2Et$], 7.35–8.05 (m, 15H, Ar*H*), N*H* nd; ^{13}C NMR δ_C: 14.0 ($CO_2CH_2CH_3$), 53.2 [$CH(CO_2Et)NH$], 60.9 (CO_2CH_3), 62.3 ($CO_2CH_2CH_3$), 69.4 [$CHCH(CO_2Et)NH$], 74.6 [$CHC(CO_2Me)Ph$], 75.1 [$C(CO_2Me)Ph$], 128.2, 128.3, 128.6, 128.8, 128.9, 129.2, 129.3, 134.0, 134.3, 136.8, 138.6, 140.1 (Ar*C*), 170.0, 170.1 (2 × CO_2); MS (EI-GC) *m*/z: 557 (M^+ + 1, <1%), 357 (11), 356 (51), 342 (10), 310 (15), 299 (11), 298 (54), 284 (17), 283 (21), 215 (37), 158 (11), 157 (11), 144 (11), 143 (100), 142 (11), 115 (24), 77 (11); HRMS calculated for $C_{27}H_{27}NO_8S_2$: 557.1168, found: 557.1173.

(2*S,5*R**)-3,4,5-Triethyl 2-methyl 2-methyl-2,5-dihydro-1*H*-pyrrole-2,3,4,5-tetracarboxylate *cis*-3g.** Yellowish oil; R_f 0.20 (*n*-hexane–ethyl acetate 7 : 3); IR (neat) ν_{max} 3021, 2988, 1732, 1720, 1676, 1619 cm^{-1}; ^1H NMR δ_H: 1.20–1.38 (m, 9H, $CO_2CH_2CH_3$), 1.85 [s, 3H, $C(CO_2CH_3)CH_3$], 3.67 (s, 3H, CO_2CH_3), 4.05–4.35 (m, 7H, $CH(CO_2Et)NH$ and 3 × $CO_2CH_2CH_3$), N*H* nd; ^{13}C NMR δ_C: 14.1, 14.2, 15.4 (3 × $CO_2CH_2CH_3$), 24.9 [$CC(CO_2Me)CH_3$], 53.0 (CO_2CH_3), 61.9 [CH-$(CO_2Et)NH$], 62.1, 62.2, 62.8 (3 × $CO_2CH_2CH_3$), 70.0 [$C(CO_2Me)$-Me], 142.0 [$CC(CO_2Me)Me$], 143.9 [$CCH(CO_2Et)NH$], 168.6, 168.8, 169.3, 169.6 (4 × CO_2); MS (EI-GC) *m*/z: 357 (M^+ + 1, <5%), 285 (10), 284 (100), 256 (24), 239 (14), 226 (11), 212 (26), 211 (15), 180 (60), 166 (40), 140 (10), 134 (15), 108 (10), 73 (10); HRMS calculated for $C_{16}H_{23}NO_8$: 357.1424, found: 357.1419.

(2*S,5*R**)-3,4,5-Triethyl 2-methyl 2-benzyl-2,5-dihydro-1*H*-pyrrole-2,3,4,5-tetracarboxylate *cis*-4g.** Pale yellow oil; R_f 0.10 (*n*-hexane–ethyl acetate 7 : 3); IR (neat) ν_{max} 3030, 2982, 1734, 1728, 1656, 1609 cm^{-1}; ^1H NMR δ_H: 1.20–1.38 (m, 12H, $CO_2CH_2CH_3$), 2.91, 3.09 (2d, J = 13.8 Hz, 2H, CH_2Ph), 3.78 [s, 1H, $CH(CO_2Et)NH$], 4.05–4.30 (m, 8H, $CO_2CH_2CH_3$), 7.24–7.30 (m, 5H, Ar*H*), N*H* nd; ^{13}C NMR δ_C: 14.2, 14.3, 14.3, 15.4 (4 × $CO_2CH_2CH_3$), 40.8 (CH_2Ar), 59.5, 61.1, 61.4, 62.0 (4 × $CO_2CH_2CH_3$), 60.7 [$CH(CO_2Et)NH$], 77.1 [$C(CO_2Me)Ph$], 127.0, 128.7, 129.6, 137.1 (Ar*C*), 144.9 [$CCH(CO_2Et)NH$], 145.5[CC-$(CO_2Me)Ph$], 168.2, 168.8, 169.0, 170.6 (4 × CO_2); MS (EI-GC) *m*/z: 447 (M^+ + 1, <1%), 363 (17), 281 (15), 207 (28), 177 (15), 176 (100), 148 (18), 131 (24), 119 (24), 91 (28), 77 (10); HRMS calculated for $C_{23}H_{29}NO_8$: 447.1893, found: 447.1889.

(2*S,5*R**)-3,4,5-Triethyl 2-methyl 2-phenyl-2,5-dihydro-1*H*-pyrrole-2,3,4,5-tetracarboxylate *cis*-5g.** Colorless oil; R_f 0.11 (*n*-hexane–ethyl acetate 7 : 3); IR (neat) ν_{max} 3068, 2925, 1743, 1727, 1656, 1606 cm^{-1}; ^1H NMR δ_H: 1.20, 1.21, 1.28 (3t, J = 7.2 Hz, 9H, 3 × $CO_2CH_2CH_3$), 3.71 (s, 3H, CO_2CH_3), 3.48, 4.13, 4.19 (3 × q, J = 7.2 Hz, 6H, $CO_2CH_2CH_3$), 5.70 [s, 1H,

C*H*(CO_2Et)NH], 7.31–7.37 (m, 5H, Ar*H*), N*H* nd; ^{13}C NMR δ_C: 14.0, 14.5, 15.4 (3 × $CO_2CH_2CH_3$), 52.9 (CO_2CH_3), 59.8, 62.1, 66.0 (3 × $CO_2CH_2CH_3$), 60.7 [*C*H(CO_2Et)NH], 77.2 [*C*(CO_2Me)Ph], 127.5, 128.6, 129.1, 137.7 (Ar*C*), 146.0 [*C*CH(CO_2Et)NH], 146.5[*C*C(CO_2Me)Ph], 168.3, 168.8, 169.2, 171.7 (4 × *C*O_2); MS (EI-GC) *m*/*z*: 419 (M^+ + 1, <1%), 342 (10), 277 (18), 276 (100), 249 (21), 202 (10), 171 (10), 170 (38), 77 (11), 73 (10); HRMS calculated for $C_{21}H_{25}NO_8$: 419.1580, found: 495.1596.

Synthesis of aminoalcohols 6 and 7

To a solution of *endo-cis*-**4b** (928 mg, 2 mmol) in DMF (2 ml) was added benzoyl chloride (707 µl, 6 mmol) and Et_3N (278 µl, 2 mmol). After stirring (0.5 h at 25 °C) the resulting suspension was heated at 100 °C for an additional 12 h. Then the DMF was evaporated and dry THF was added.[17] The resulting solution was added into a $LiAlH_4$ suspension (390.6 mg, 10 mmol, 97%) in dry THF. The resulting suspension was stirred for 0.5 h at 25 °C and then refluxed for 12 h. The mixture was cooled at 0 °C and NaOH 10% was added, stirring the emulsion for 30 min. The resulting mixture was filtered off and extracted with ethyl acetate (2 × 8 mL). The organic layer was dried over $MgSO_4$, and the solvent evaporated giving a residue, which was purified by flash chromatography obtaining 215 mg of **6** and 162 mg of **7** (65% overall yield).

(1*R,3*S**,3a*R**,6a*S**)-1,2,5-Tribenzyloctahydropyrrolo[3,4-*c*]pyrrole-1,3-diol 6a.** Sticky oil; R_f 0.45 (ethyl acetate–methanol 9 : 1); IR (neat) ν_{max} 3300, 2923, 1650, 1615 cm^{-1}; ^{1}H NMR δ_H: 2.18–2.26 (m, 2H, C*H*CHCH$_2$OH and C*H*CCH$_2$OH), 2.73–2.87 (2d, *J* = 13.2 Hz, 4H, C*CH*$_2$Ph,), 3.05–3.27 (m, 4H, 2 × C*H*$_2$NBn), 3.30–3.61 [m with 2d at 3.53 and 3.57, *J* = 14.2 Hz, 7H, N*CH*$_2$Ph, 2 × C*H*$_2$OH, C*H*(CH$_2$OH)NBn], 7.15–7.35 (m, 13H, Ar*H*), 7.46–7.52 (m, 2H, Ar*H*), O*H* nd; ^{13}C NMR δ_C: 44.3 (CH$_2$Ph), 46.0 (*C*HCHCH$_2$OH), 48.3 (*C*HCCH$_2$OH), 52.9 (*C*HCH$_2$OH), 55.1, 57.8 (2 × CH$_2$NBn), 60.3, 61.5 (2 × NCH$_2$Ph), 63.1 (CCH$_2$Ph), 64.1, 65.0 (2 × CH$_2$OH), 126.5, 127.5, 127.6, 128.2, 128.8, 128.9, 129.2, 130.0, 130.6, 135.5, 137.6, 137.9 (Ar*C*); MS (EI-GC) *m*/*z* 442 (M^+ + 1, <1%), 281 (10), 247 (10), 207 (16), 171 (38), 158 (24), 156 (15), 134 (15), 133 (35), 132 (15), 92 (18), 91 (100); microanalysis calculated for $C_{29}H_{34}N_2O_2$: C, 79.0; H, 8.0; N, 6.0%; found: C, 78.6; H, 7.9; N, 6.2%.

Also product **6** was obtained from **7**. To a solution of **7** (162 mg, 0.46 mmol) in MeCN was added K_2CO_3 (190 mg, 1.40 mmol) and BnBr (54.83 µl, 0.46 mmol). After stirring for 0.5 h at 25 °C the resulting suspension was refluxed for an additional 12 h. Then the solvent was evaporated and the resulting crude was extracted with ethyl acetate (2 × 10 mL) and was washed with brine. After drying over $MgSO_4$, the solvent was evaporated and the residue purified by flash chromatography obtaining 146 mg of **6** (72% yield).

(1*S,3*R**,3a*R**,6a*S**)-1,5-Dibenzyl-1,3-bis(hydroxymethyl) octahydropyrrolo[3,4-*c*]pyrrole 7a.** Sticky oil; R_f 0.33 (ethyl acetate–methanol 9 : 1); IR (neat) ν_{max} 3300, 2923 cm^{-1}; ^{1}H NMR δ_H: 2.27–2.33 and 2.95–3.05 (m, 4H, 2 × C*H*$_2$NBn), 2.62–2.90 (m with 2d at 2.65 and 2.83, *J* = 13.4, 4H, *CH*$_2$Ph, C*H*CHCH$_2$OH, and C*H*CH$_2$OH), 3.44–3.75 (m with 2d at 3.48 and 3.63, *J* = 11.4, 7H, N*CH*$_2$Ph, 2 × C*H*$_2$OH, C*H*CCH$_2$OH), 7.17–7.35 (m, 10H, Ar*H*); ^{13}C NMR δ_C: 44.3 (*C*H$_2$Ph), 45.8 (*C*HCHCH$_2$OH), 50.5 (*C*HCH$_2$OH), 54.3, 55.5 (2 × CH$_2$NBn), 59.7 (*C*HCCH$_2$OH), 60.2 (NCH$_2$Ph), 62.4, 64.8 (2 × *C*H$_2$OH), 67.1 [*C*Bn(CH$_2$OH)NH], 127.5, 128.3, 128.5, 128.8, 128.9, 130.5, 137.5, 137.6 (Ar*C*); MS (EI-GC) *m*/*z* 352 (M^+ + 1, <1%), 243 (41), 207 (11), 158 (14), 134 (10), 133 (13), 132 (13), 92 (11), 91 (100), 65 (12); microanalysis calculated for $C_{22}H_{28}N_2O_2$: C, 75.0; H, 8.0; N, 8.0%; found: C, 74.8; H, 8.0; N, 8.3%.

Synthesis of molecule 8

A solution of **6** (120 mg, 0.27 mmol) in dichloromethane was cooled at 0 °C. Then MsCl (21.5 µl, 0.27 mmol, 98%) and Et_3N (38 µl, 0.27 mmol) were added. After stirring for 1 h at 25 °C, the solvent was evaporated and MeCN was added. Then $BnNH_2$ (30 µl, 0.27 mmol, 98%) was added and the resulting solution was refluxed for an additional 15 h. Then the solvent was evaporated and the resulting crude was extracted with ethyl acetate (2 × 8 mL). The organic phase was washed with brine, dried over $MgSO_4$, evaporated *in vacuo*, and the residue purified by flash chromatography obtaining 74 mg of **8** (53% yield).

(3a*S,4*S**,8*R**,8a*R**)-2,4,6,9-Tetrabenzyldecahydro-4,8-epiminopyrrolo[3,4-*d*]azepine (8).** Sticky brown oil; R_f 0.30 (*n*-hexane–ethyl acetate 7 : 3); IR (neat) ν_{max} 3060, 2925, 1669, 1602 cm^{-1}; ^{1}H NMR δ_H: 2.52, 2.72 (2d, *J* = 12.8, 2H, C*CH*$_{2A}$Ph), 2.90–3.05 (m with d at 3.01, *J* = 13.9, 3H, *CH*$_{2K}$, C*H*$_E$ and C*H*$_F$), 3.25–3.41 (m with d at 3.30, *J* = 13.9, 3H, *CH*$_{2K}$, *CH*$_{2J}$ and C*H*$_G$), 3.42–3.70 (4d at 3.47, 3.48, 3.64, 3.65, *J* = 12.9 and 13.0 Hz, 4H, *CH*$_{2B}$Ph and C*H*$_{2D}$Ph), 3.70–4.15 (m, 5H, *CH*$_{2H}$, C*H*$_{2I}$ and C*H*$_{2J}$), 4.30 (s, 2H, *CH*$_{2C}$Ph), 7.15–7.50 (m, 20H, 4 × Ar*H*); ^{13}C NMR δ_C: 40.0 (C_FH), 44.2 (C_KH$_2$), 44.5 (C_EH), 47.2 (C_CH$_2$Ph), 49.9 (C_AH$_2$Ph), 56.5 (C_GH), 60.3, 60.8 (C_BH$_2$Ph and C_DH$_2$Ph), 61.6 (C_JH$_2$), 65.1, 65.4 (C_HH$_2$ and C_IH$_2$), 69.5 (C_L), 127.3, 128.1, 128.2, 128.4, 128.6, 128.7, 128.9, 128.9, 129.5, 130.5, 131.1, 132.2, 134.7, 135.0, 136.4, 137.2 (Ar*C*); MS (EI-GC) *m*/*z* 513 (M^+ + 1, <1%), 195 (17), 194 (17), 106 (100), 105 (23), 104 (49), 132 (13), 92 (20), 91 (94), 79 (28), 78 (15), 77 (29), 65 (18), 51 (17), 43 (10); HRMS calculated for $C_{36}H_{39}N_3$: 513.3144, found: 513.3130.

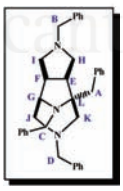

Acknowledgements

This work has been supported by the Spanish Ministerio de Ciencia e Innovación (MICINN) (Consolider INGENIO 2010 CSD2007-00006, CTQ2010-20387), FEDER, Generalitat Valenciana (PROMETEO/2009/039), and by the University of Alicante.

Notes and references

1 For examples of reviews concerning multicomponent reactions, see: (*a*) *Multicomponent Reactions*, ed. J. Zhu and H. Bienaymé, Wiley-VCH, Weinheim, 2005; (*b*) G. Guillena, D. J. Ramón and M. Yus, *Tetrahedron: Asymmetry*, 2007, **18**, 693; (*c*) L. H. Choudhury and T. Parvin, *Tetrahedron*, 2011, **67**, 8213; (*d*) H. Pellissier, *Adv. Synth. Catal.*, 2012, **354**, 237; (*e*) S. S. Van Berkel, B. G. M. Bögels, M. A. Wijdeven, B. Westermann and F. P. J. T. Rutjes, *Eur. J. Org. Chem.*, 2012, 3543.

2 For general reviews dealing with general 1,3-DC, see: (*a*) *Synthetic Applications of 1,3-Dipolar Cycloaddition Chemistry Towards Heterocycles and Natural Products*, ed. A. Padwa and W. H. Pearson, John Wiley & Sons, New Jersey, 2003; (*b*) C. Nájera and J. M. Sansano, *Curr. Org. Chem.*, 2003, **7**, 1105; (*c*) W. Eberbach, *Sci. Synth.*, 2004, **27**, 441–498, ch. 11; (*d*) I. Coldham and R. Hufton, *Chem. Rev.*, 2005, **105**, 2765; (*e*) V. Nair and T. D. Suja, *Tetrahedron*, 2007, **63**, 12247; (*f*) A. Padwa and S. K. Bur, *Tetrahedron*, 2007, **63**, 5341.

3 See for example: (*a*) M. I. Calaza and C. Cativiela, *Eur. J. Org. Chem.*, 2008, 3427; (*b*) X. Companyó, A. N. Alba and R. Ríos, *Targets in Heterocyclic Systems*, ed. O. A. Attanasi and D. Spinelli, RSC, Cambridge, 2009, vol. 13, p. 147–185.

4 (*a*) S. K. Panday, *Tetrahedron: Asymmetry*, 2011, **22**, 1817; (*b*) J. Ferreira da Costa, O. Caamaño, F. Fernández, X. García-Mera, P. Midón and J. E. Rodríguez-Borges, *Tetrahedron*, 2010, **66**, 6797.

5 The enantioselective 1,3-DC of azomethine ylides is a prolific area in organic synthesis and it is frequently being reviewed. For selected recent examples, see: (*a*) H. Pellissier, *Tetrahedron*, 2007, **63**, 3235; (*b*) C. Nájera and J. M. Sansano, in *Topics in Heterocyclic Chemistry*, ed. A. Hassner, Springer-Verlag, Berlin-Heidelberg, 2008, vol. 12, p. 117; (*c*) L. M. Stanley and M. P. Sibi, *Chem. Rev.*, 2008, **108**, 2887; (*d*) M. Álvarez-Corral, M. Muñoz-Dorado and I. Rodríguez-García, *Chem. Rev.*, 2008, **108**, 3174; (*e*) M. Naodovic and H. Yamamoto, *Chem. Rev.*, 2008, **108**, 3132; (*f*) C. Nájera, J. M. Sansano and M. Yus, *J. Braz. Chem. Soc.*, 2010, **21**, 377; (*g*) M. Kissane and A. R. Maguire, *Chem. Soc. Rev.*, 2010, **39**, 845; (*h*) J. Adrio and J. C. Carretero, *Chem. Commun.*, 2011, **47**, 6784.

6 (*a*) S. L. Schreiber, *Science*, 2000, **287**, 1964; (*b*) S. L. Schreiber, *Chem. Eng. News*, 2003, **81**, 51; (*c*) M. D. Burke and S. L. Schreiber, *Angew. Chem., Int. Ed.*, 2004, **43**, 46.

7 See for example: (*a*) J. L. Vicario, S. Reboredo, D. Badía and L. Carrillo, *Angew. Chem.*, 2007, **119**, 5260; (*b*) I. Ibrahem, R. Ríos, J. Vesely and A. Córdova, *Tetrahedron Lett.*, 2007, **48**, 6252; (*c*) J. Yu, L. He, X.-H. Chen, J. Song, W.-J. Chen and L.-Z. Gong, *Org. Lett.*, 2009, **11**, 4946; (*d*) A. Iza, L. Carrillo, J. L. Vicario, D. Badía, E. Reyes and J. I. Martínez, *Org. Biomol. Chem.*, 2010, **8**, 2238; (*e*) M. Martín-Rodríguez, C. Nájera, J. M. Sansano, P. R. R. Costa, E. Crizanto de Lima and A. G. Dias, *Synlett*, 2010, 962; (*f*) M. R. Chaulagain and Z. D. Aron, *J. Org. Chem.*, 2010, **75**, 8271; (*g*) F. Shi, S.-W. Luo, Z.-L. Tao, J. Yu, S.-J. Tu and L.-Z. Gong, *Org. Lett.*, 2011, **13**, 4680; (*h*) L. He, X.-H. Chen, D.-N. Wang, S.-W. Luo, W.-Q. Zhang, J. Yu, L. Ren and L.-Z. Gong, *J. Am. Chem. Soc.*, 2011, **133**, 13504; (*i*) F. Shi, Z.-L. Tao, J. Yu and S.-J. Tu, *Tetrahedron: Asymmetry*, 2011, **22**, 2056.

8 Ethyl glyoxylate was employed in a diastereoselective process where the dipole was generated by the iminium route. C. Wittland, U. Flörke and N. Risch, *Synthesis*, 1997, 1291.

9 (*a*) *Microwaves in Organic Synthesis*, ed. A. Loupy, Wiley-VCH, Weinheim, 2006; (*b*) M. Piñeiro and T. M. V. D. Pinho e Melo, *Eur. J. Org. Chem.*, 2009, 5287; (*c*) *Microwave Heating as a Tool for Sustainable Chemistry*, ed. N. E. Leadbeater, CRC Press, Boca Ratón, 2010.

10 O. Tsuge, S. Kanemasa, M. Ohe, K. Yorozu, S. Takenaka and K. Ueno, *Bull. Chem. Soc. Jpn.*, 1987, **60**, 4067.

11 See ESI.‡ The following crystal structure has been deposited at the Cambridge Crystallographic Data Centre and allocated the deposition number: CCDC 906384.

12 Y. Shi, L. Gan, X. Wei, S. J. S. Zhang, F. Meng, Z. Wang and C. Yan, *Org. Lett.*, 2000, **2**, 667.

13 ChemBioOffice ultra 2010, Perkin Elmer Informatics.

14 See for example: D. Peters, J. P. Redrobe and E. O. Nielsen, *Pat.*, WO 2009 109517, Apr. 2009, CAN 2009:1107687.

15 Attempts to perform direct *N*-benzylation of cycloadduct *endo*-**4b** using benzyl bromide failed.

16 L. J. Huang and D. W. Teng, *Chin. Chem. Lett.*, 2011, **22**, 523.

17 W. Zhang, Y. Lu, C. H.-T. Chen, L. Zeng and D. B. Kassel, *J. Comb. Chem.*, 2006, **8**, 687.

***endo*-1a**

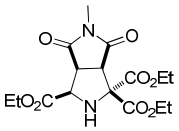

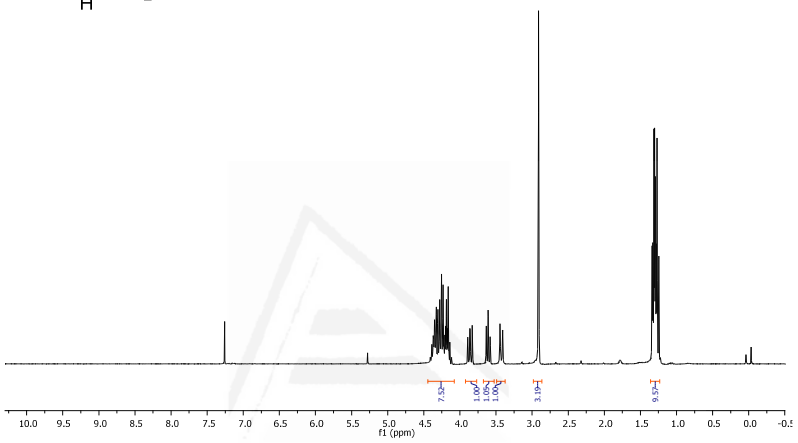

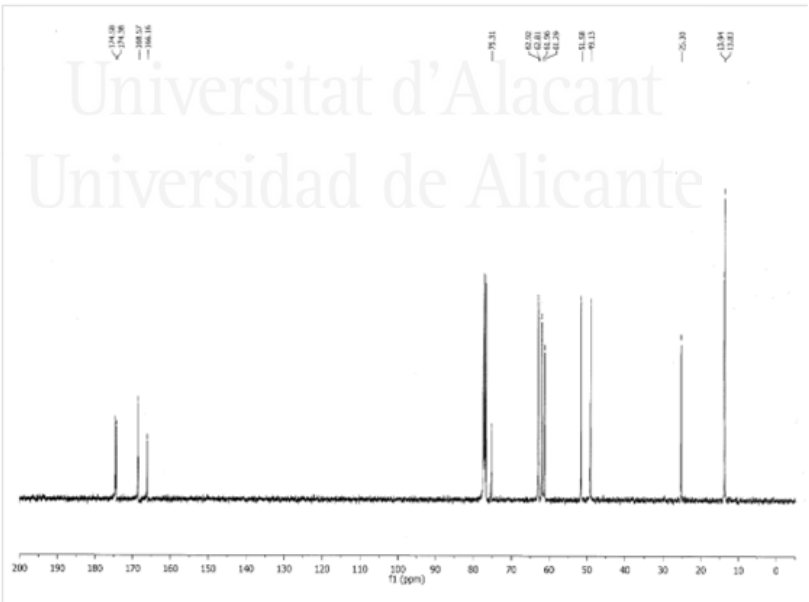

Electronic Supplementary Material (ESI) for Organic & Biomolecular Chemistry

***endo*-1b**

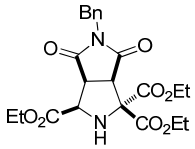

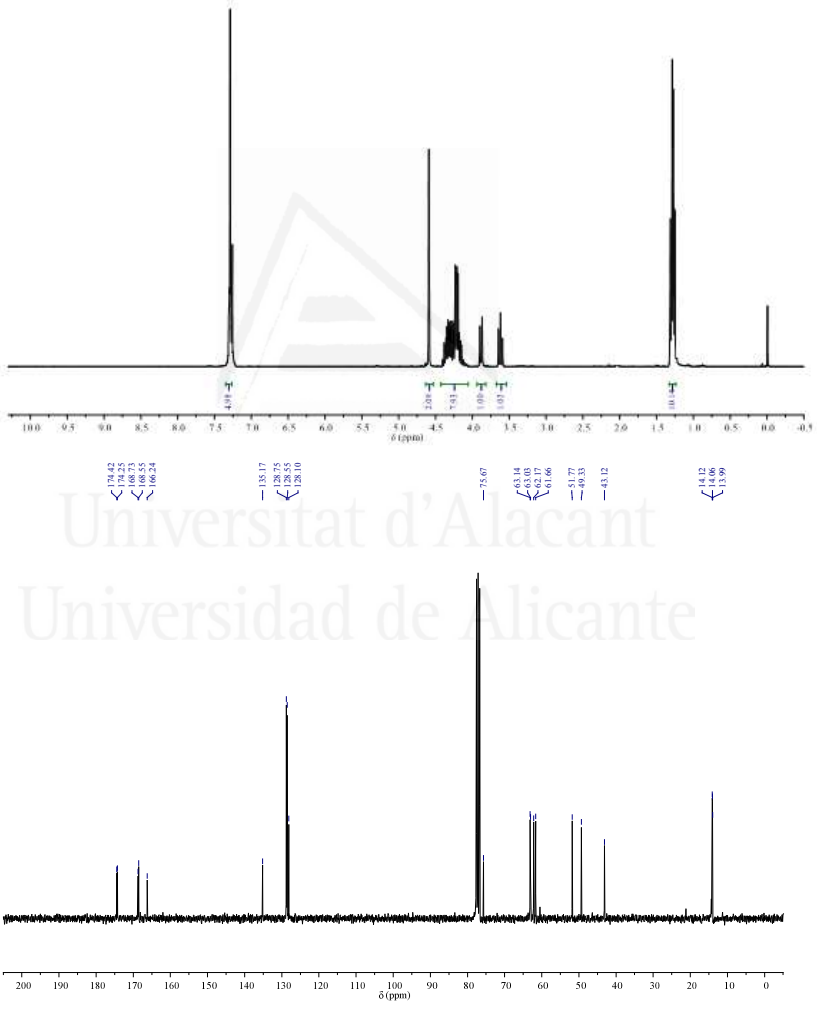

Electronic Supplementary Material (ESI) for Organic & Biomolecular Chemistry

***endo*-1c**

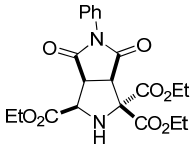

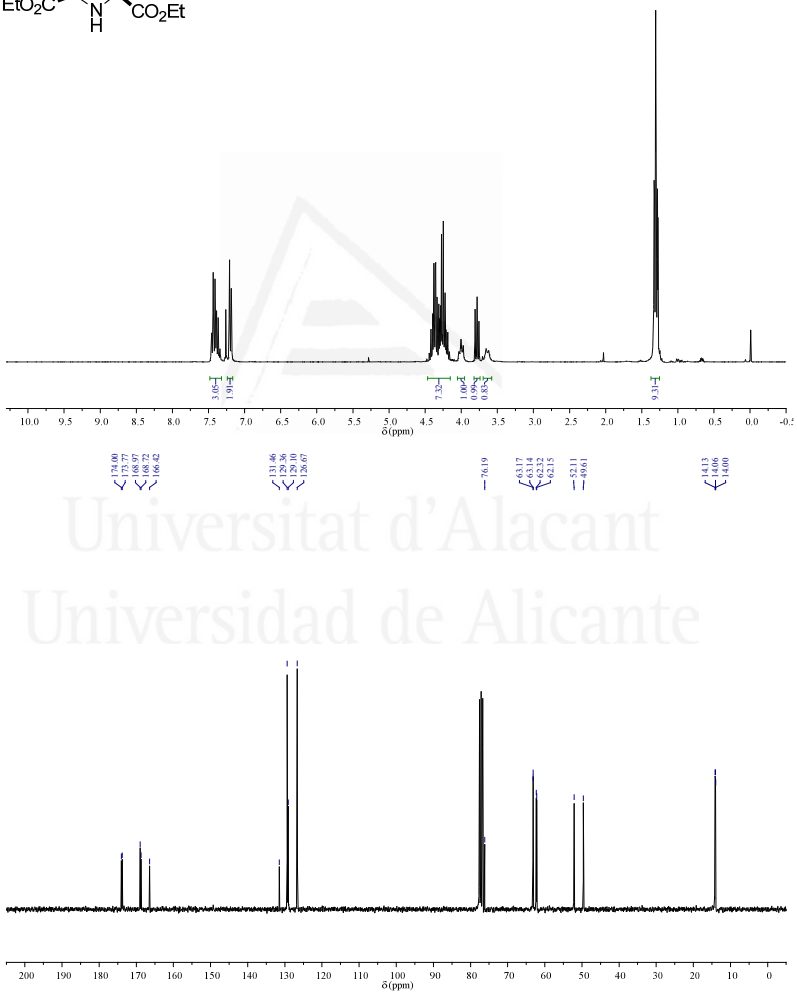

Electronic Supplementary Material (ESI) for Organic & Biomolecular Chemistry

***endo*-1d**

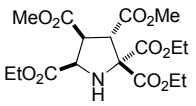

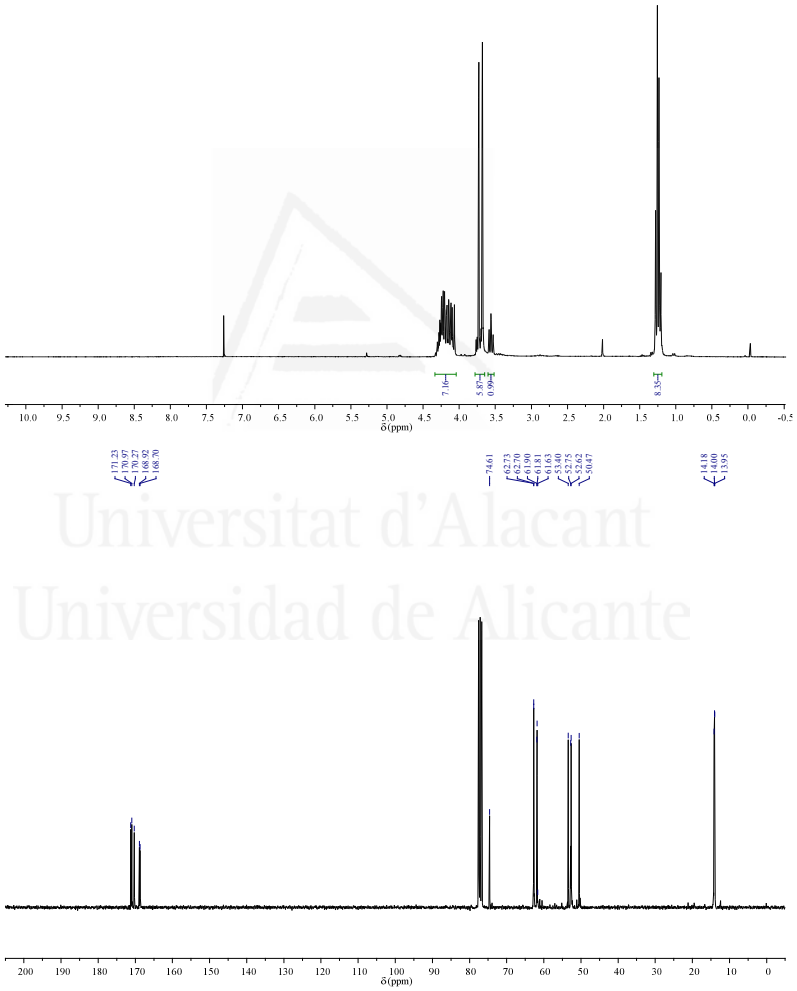

***endo*-1e**

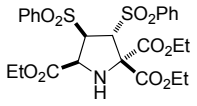

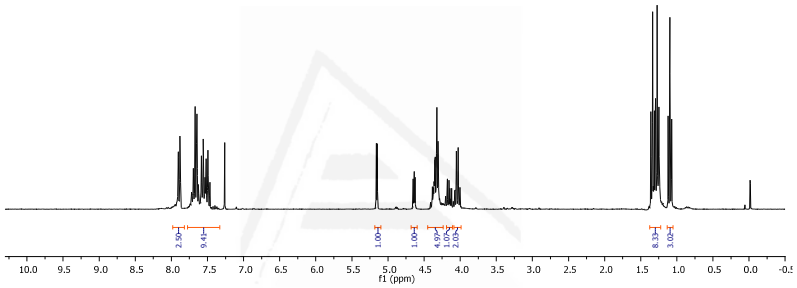

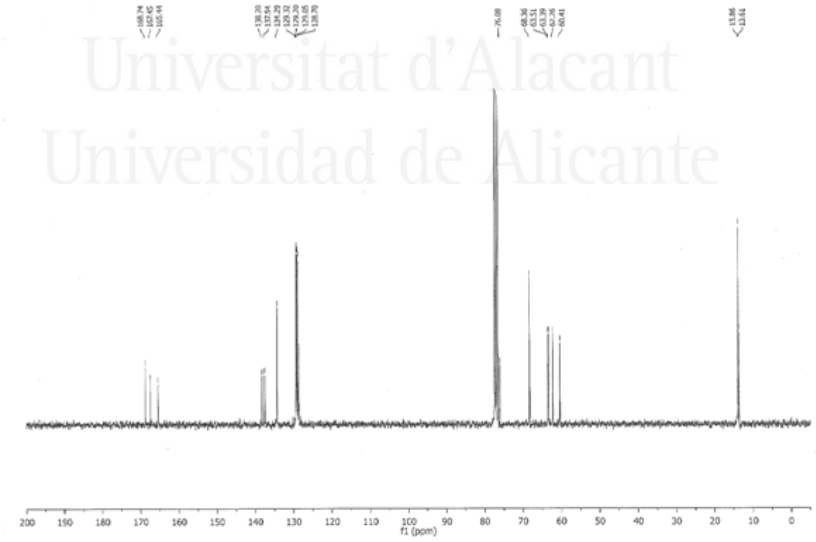

***endo*-1f**, ***exo*-1f** and ***endo*-1f´**

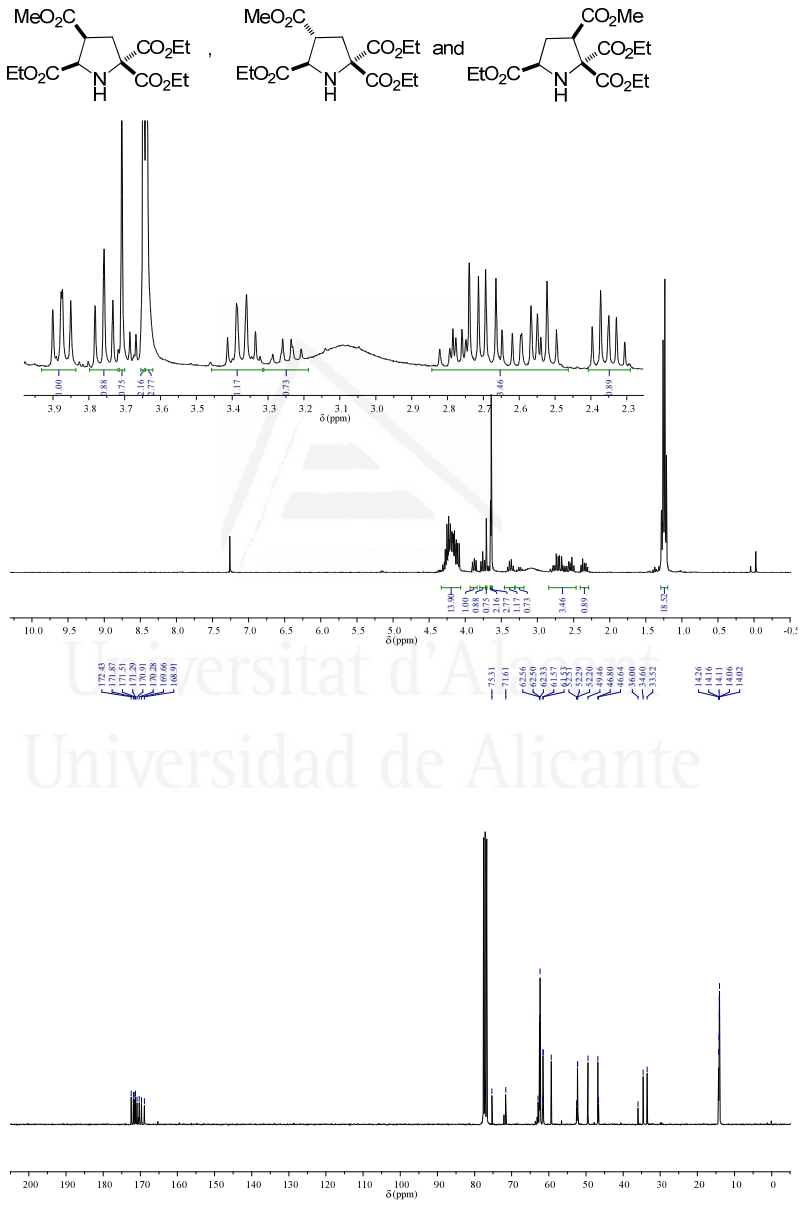

1g

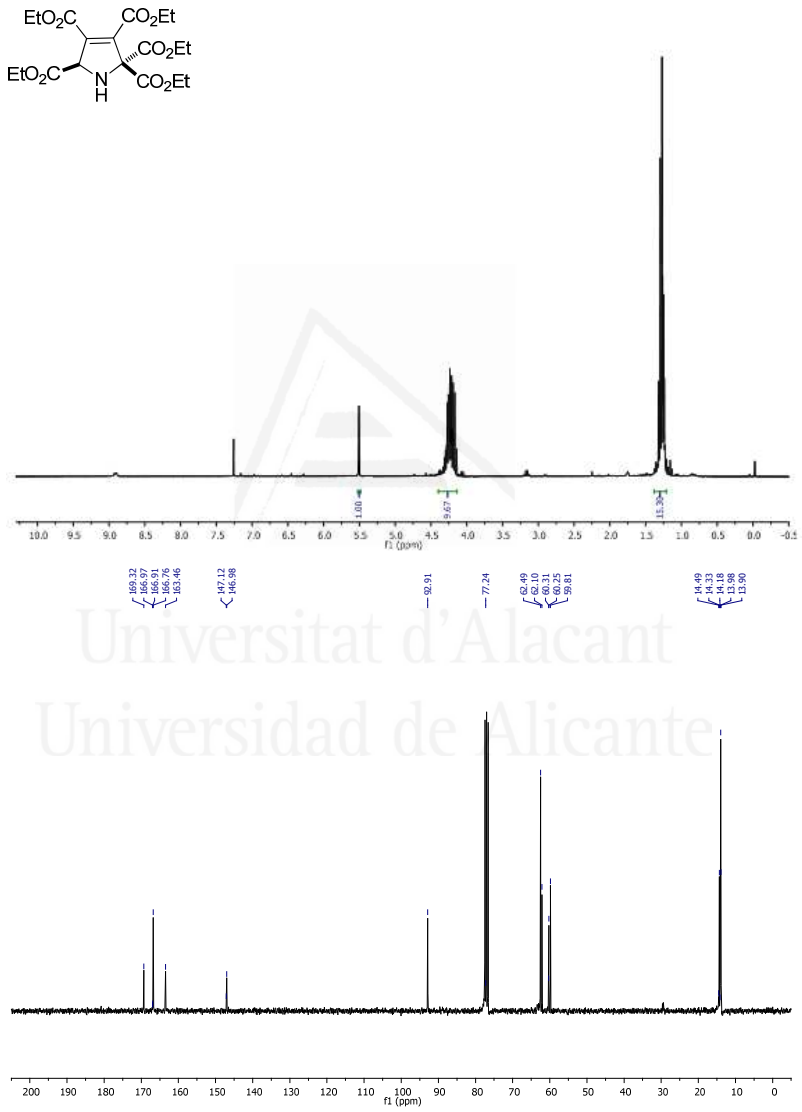

Electronic Supplementary Material (ESI) for Organic & Biomolecular Chemistry

1h and **1i**

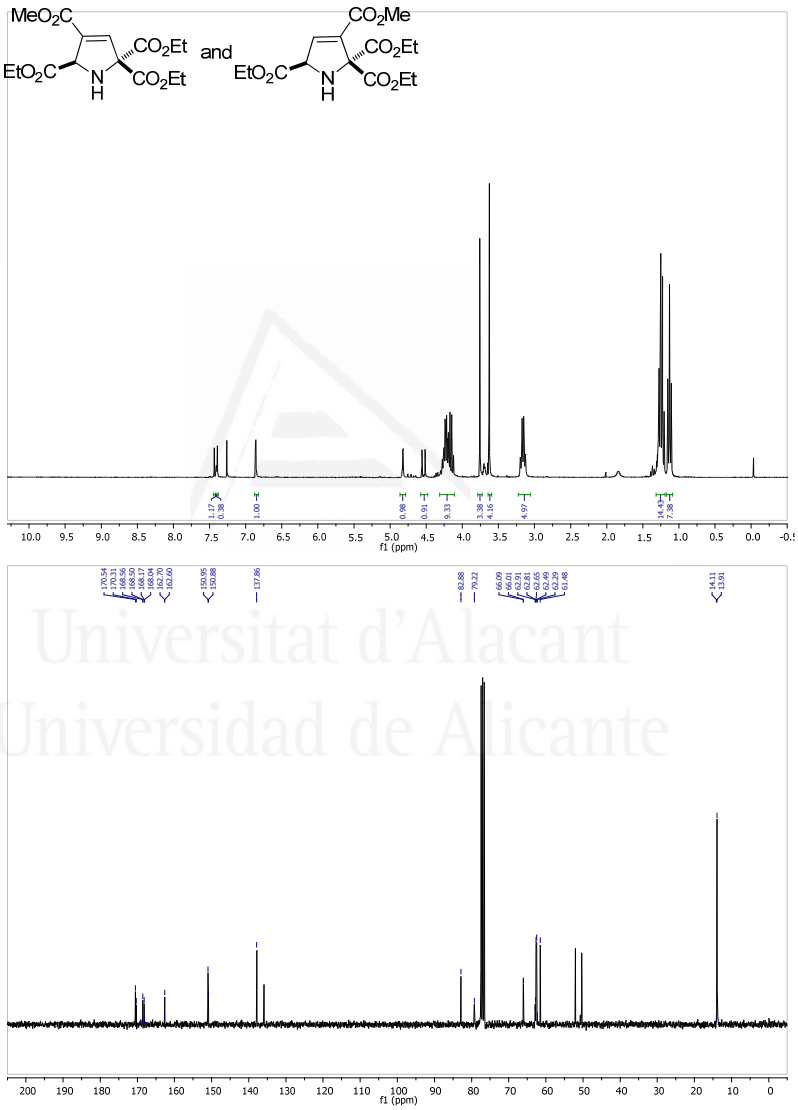

Electronic Supplementary Material (ESI) for Organic & Biomolecular Chemistry

***endo-cis*-2a** and ***endo-trans*-2a**

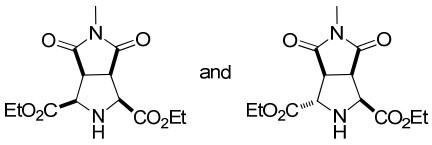

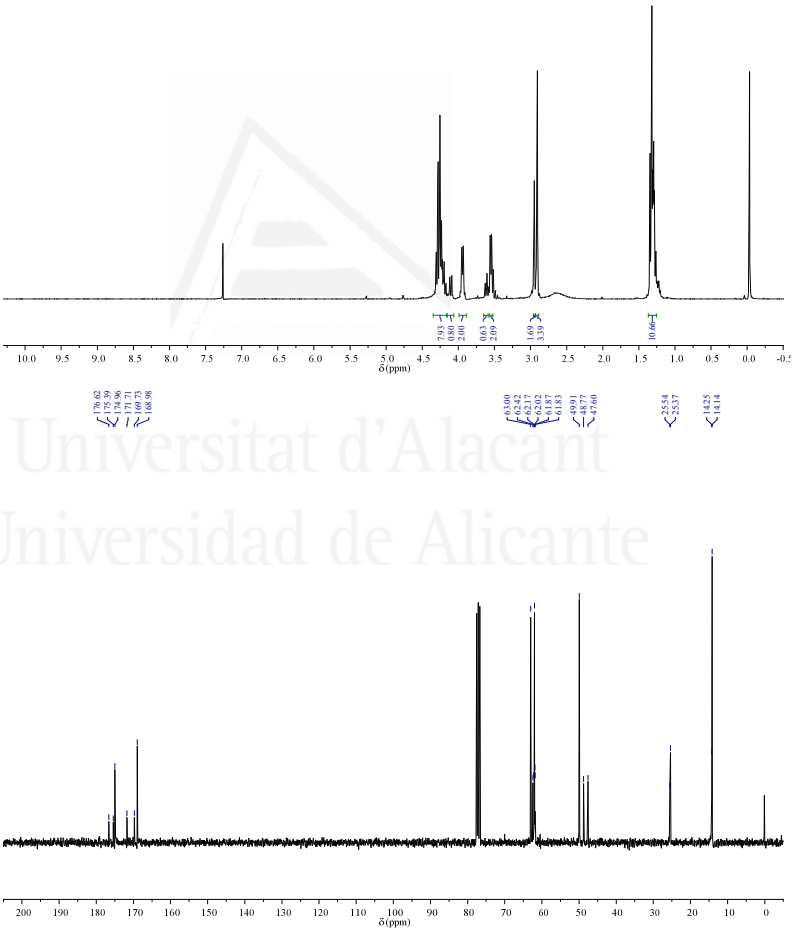

Electronic Supplementary Material (ESI) for Organic & Biomolecular Chemistry

endo-cis-2b

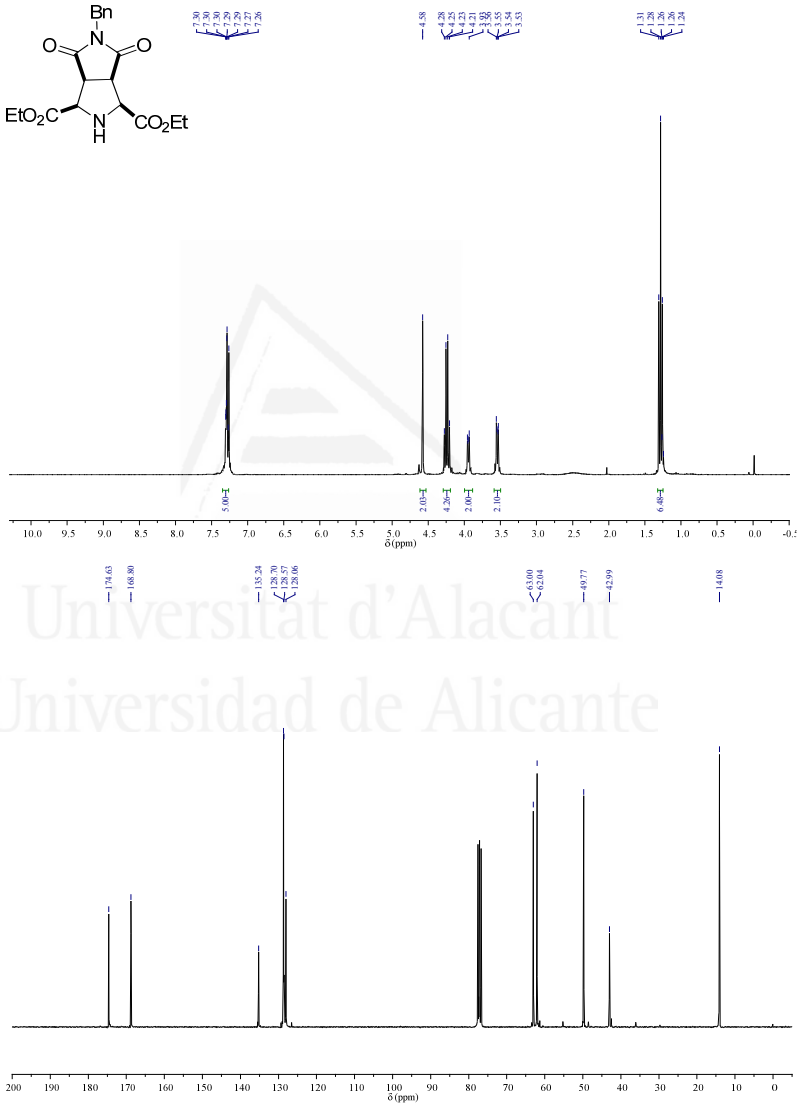

Electronic Supplementary Material (ESI) for Organic & Biomolecular Chemistry

***endo-cis*-2c**

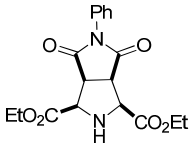

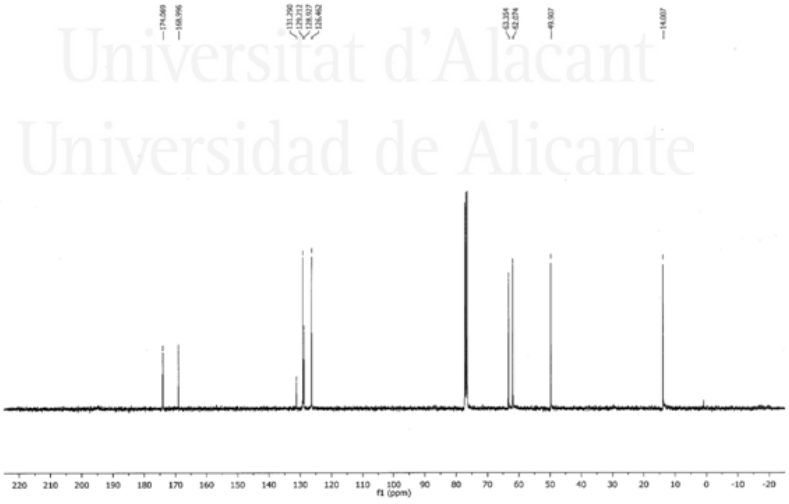

***endo-trans*-2c**

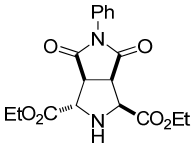

Electronic Supplementary Material (ESI) for Organic & Biomolecular Chemistry

***endo-cis*-3a**

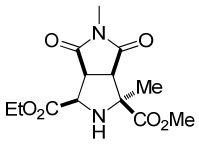

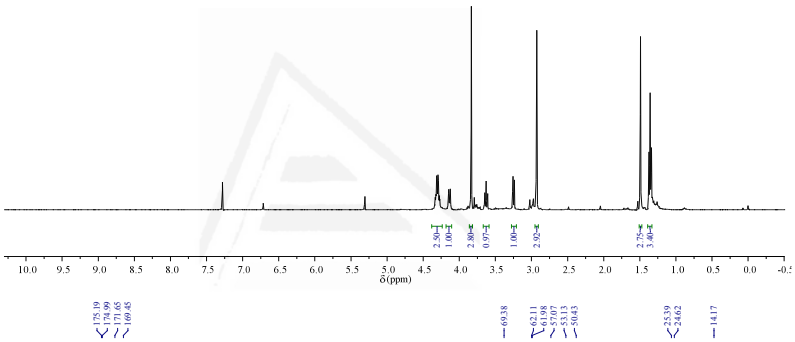

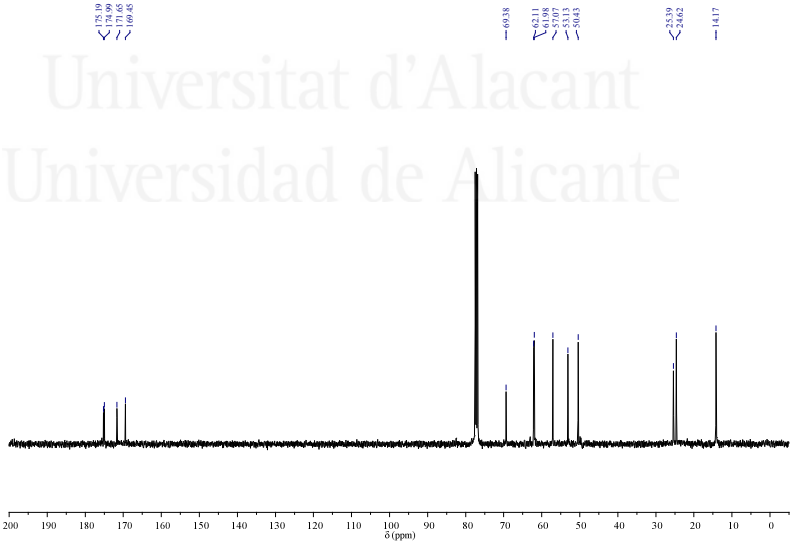

Electronic Supplementary Material (ESI) for Organic & Biomolecular Chemistry

***endo-cis*-3f**

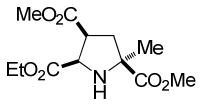

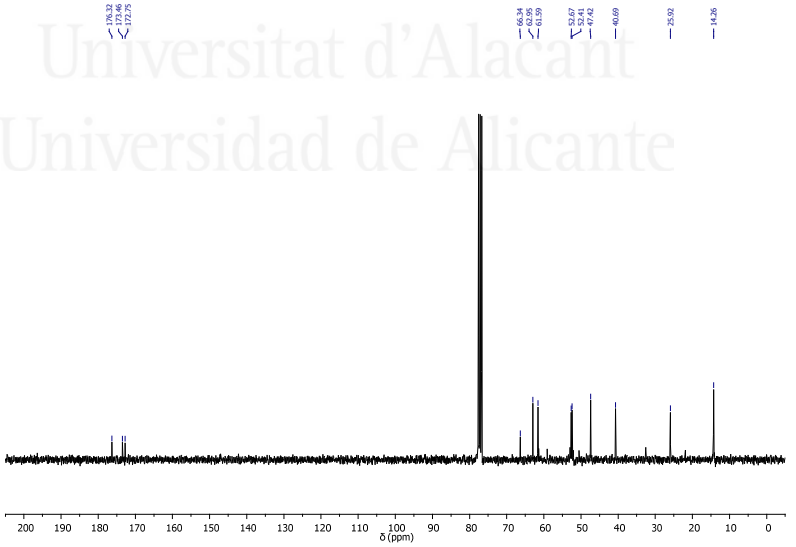

Electronic Supplementary Material (ESI) for Organic & Biomolecular Chemistry

***endo-trans*-3f** and ***endo-cis*-3f´**

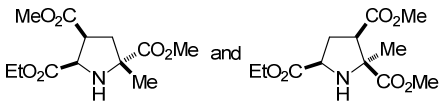

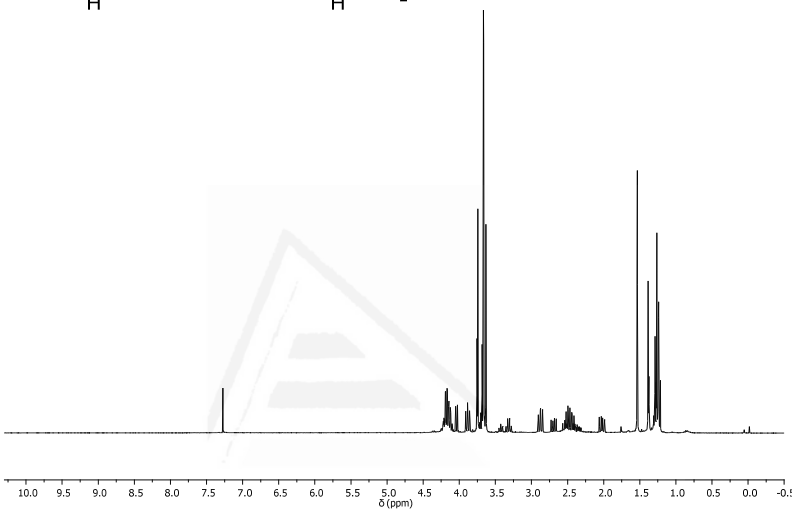

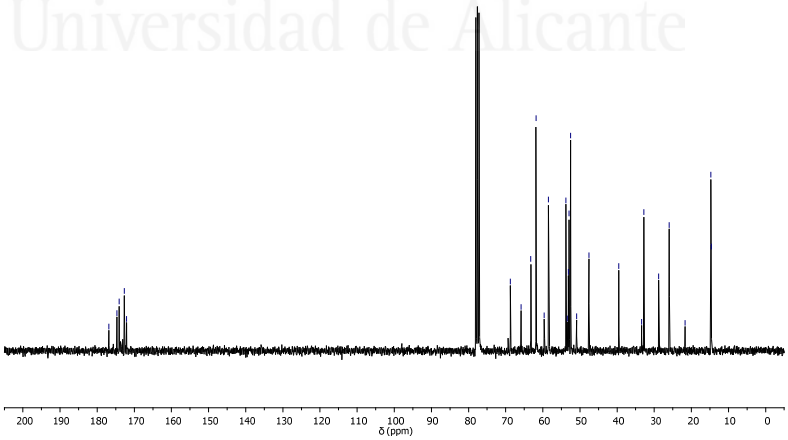

***endo-cis*-3d**

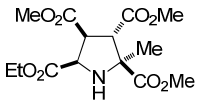

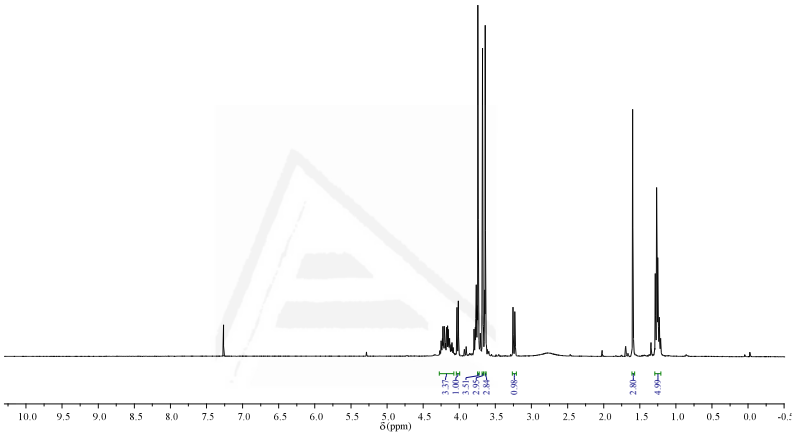

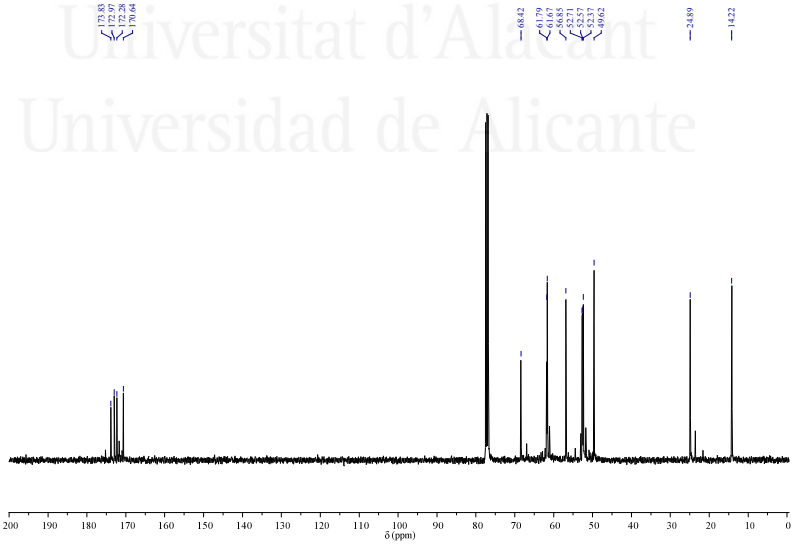

Electronic Supplementary Material (ESI) for Organic & Biomolecular Chemistry

***endo-cis*-3e**

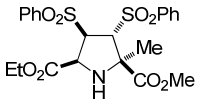

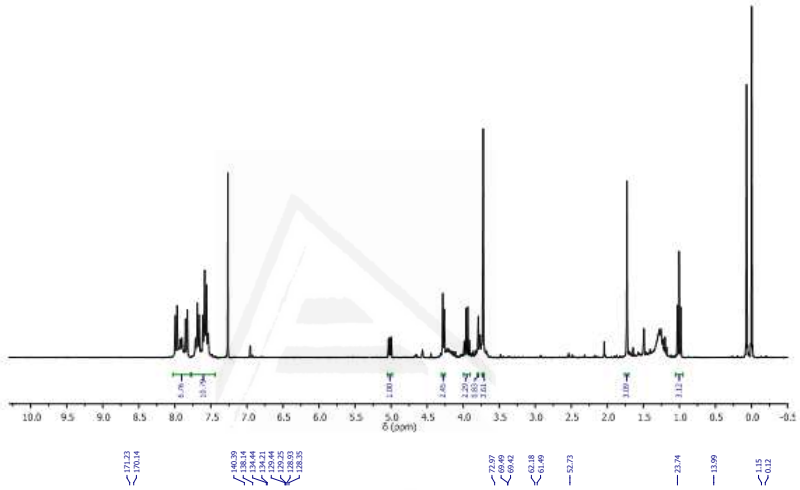

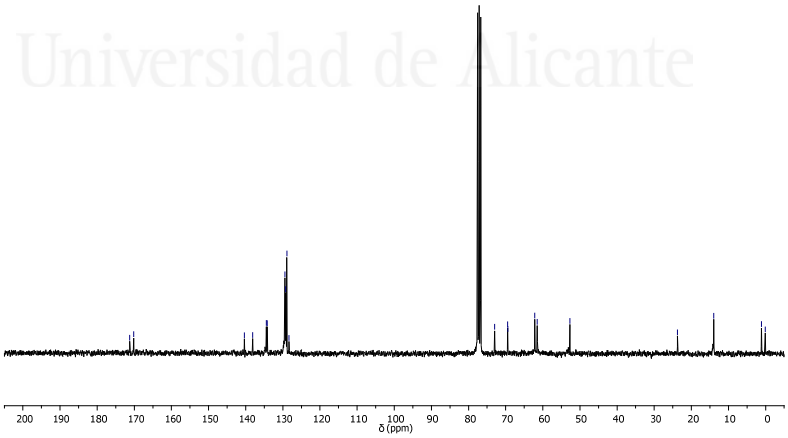

Electronic Supplementary Material (ESI) for Organic & Biomolecular Chemistry

***endo-cis*-4a**

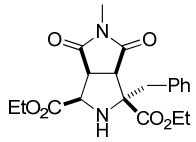

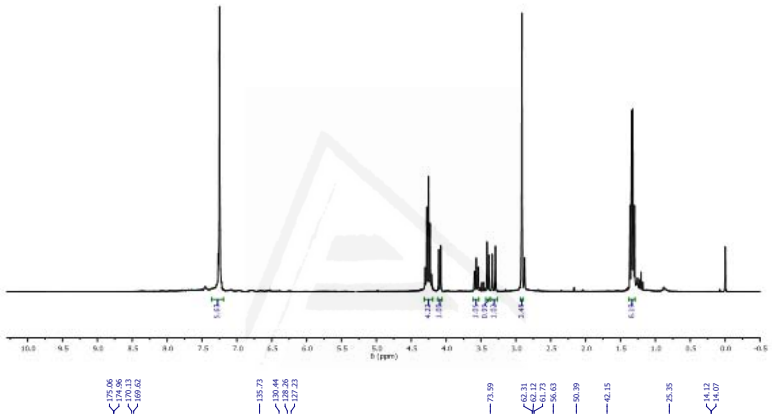

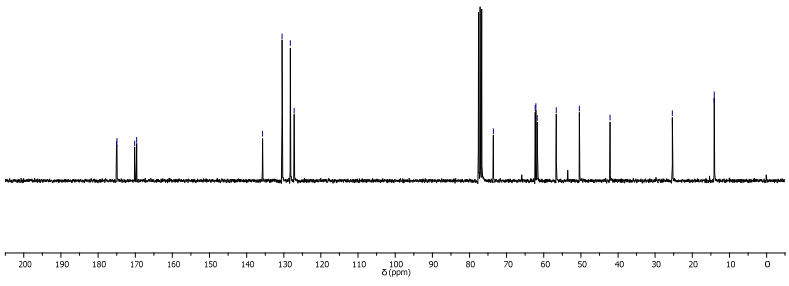

Electronic Supplementary Material (ESI) for Organic & Biomolecular Chemistry

***endo-cis*-4b**

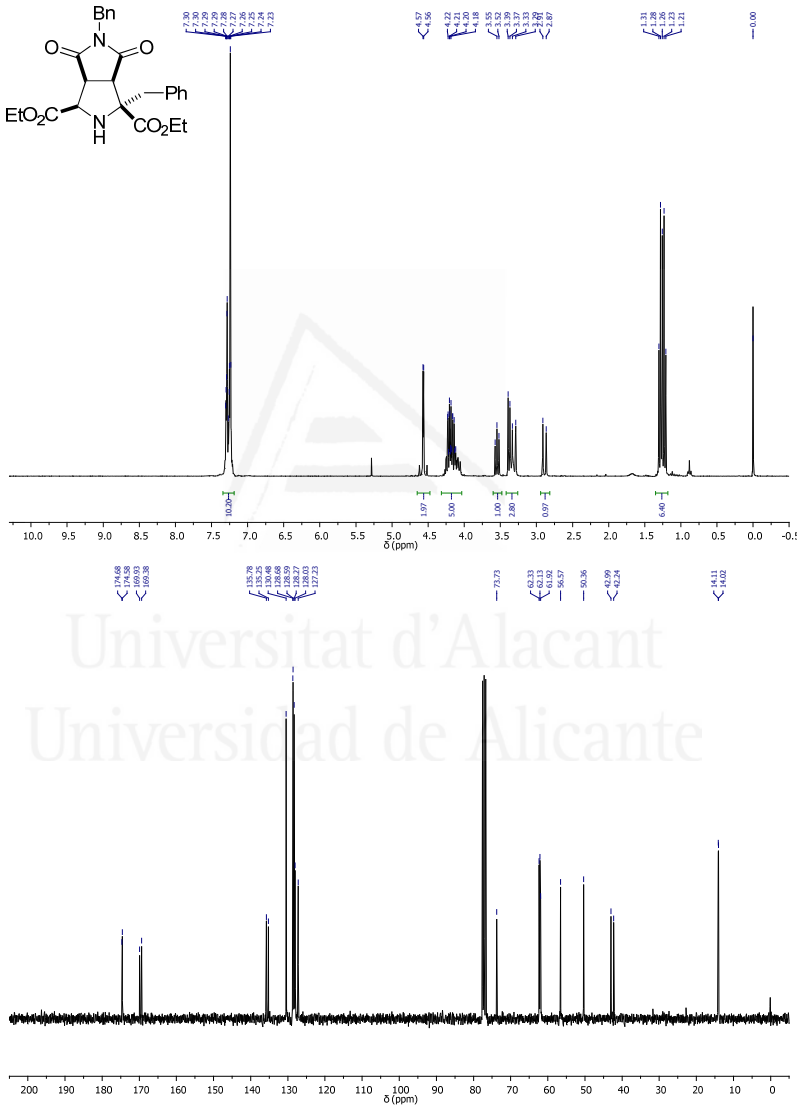

Electronic Supplementary Material (ESI) for Organic & Biomolecular Chemistry

***endo-cis*-4c**

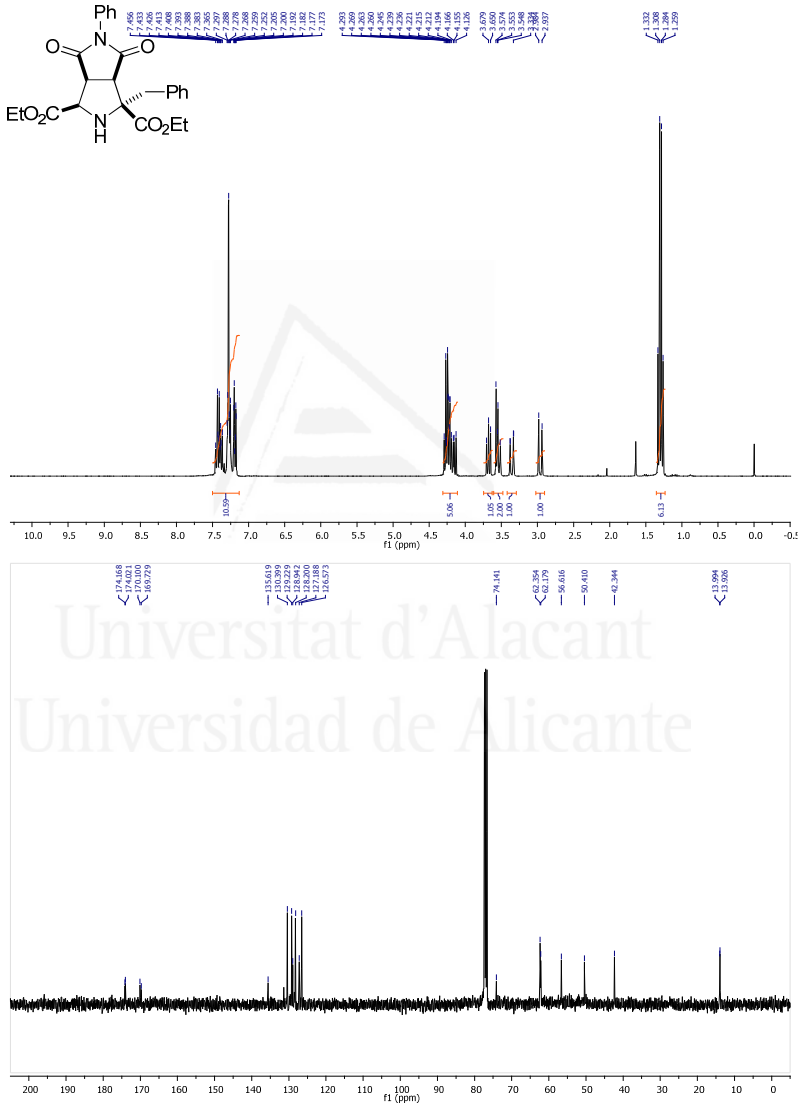

***endo-cis*-4d**

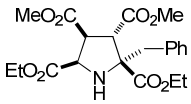

***exo-cis*-4e**

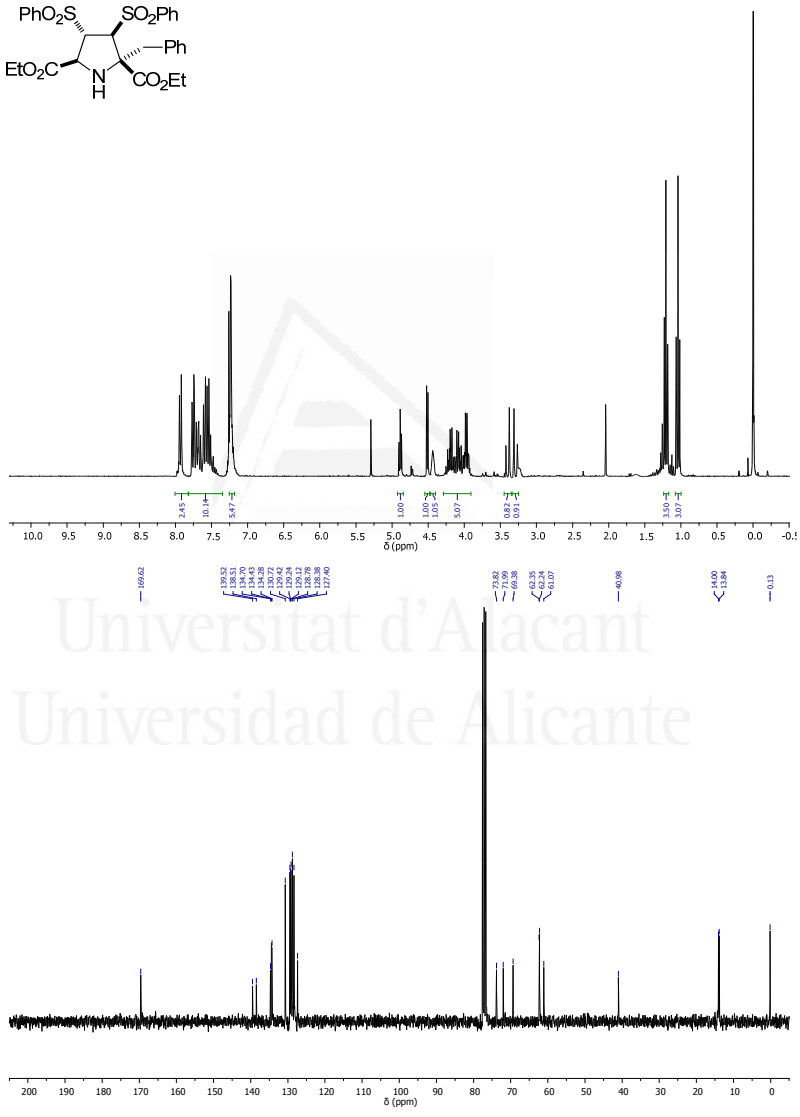

Electronic Supplementary Material (ESI) for Organic & Biomolecular Chemistry

***endo-cis*-5a**

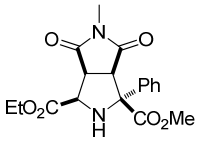

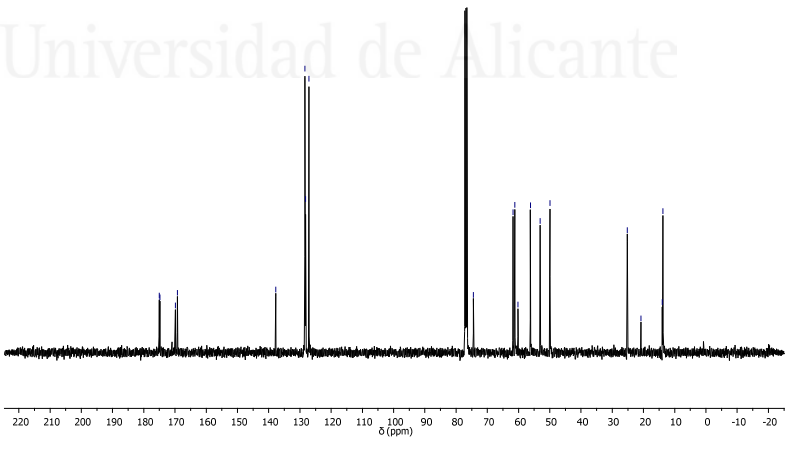

Electronic Supplementary Material (ESI) for Organic & Biomolecular Chemistry

***endo-trans*-5a**

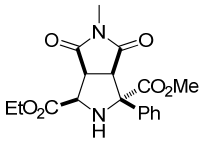

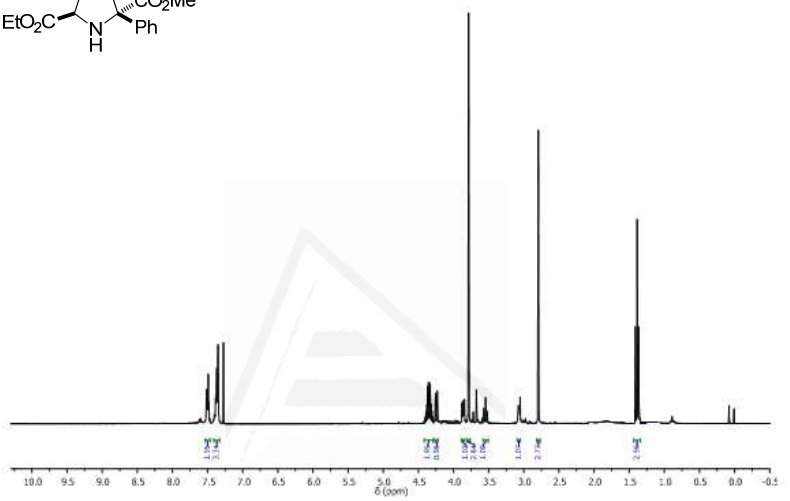

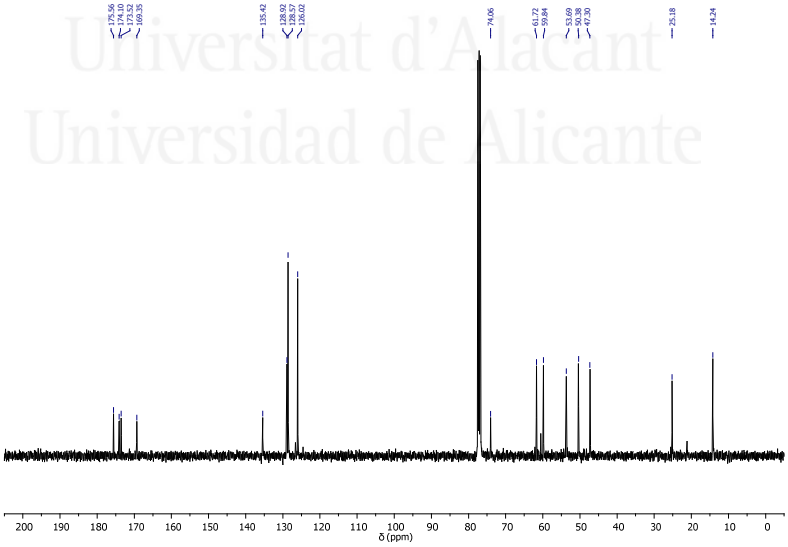

***endo-cis*-5f**

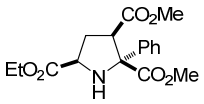

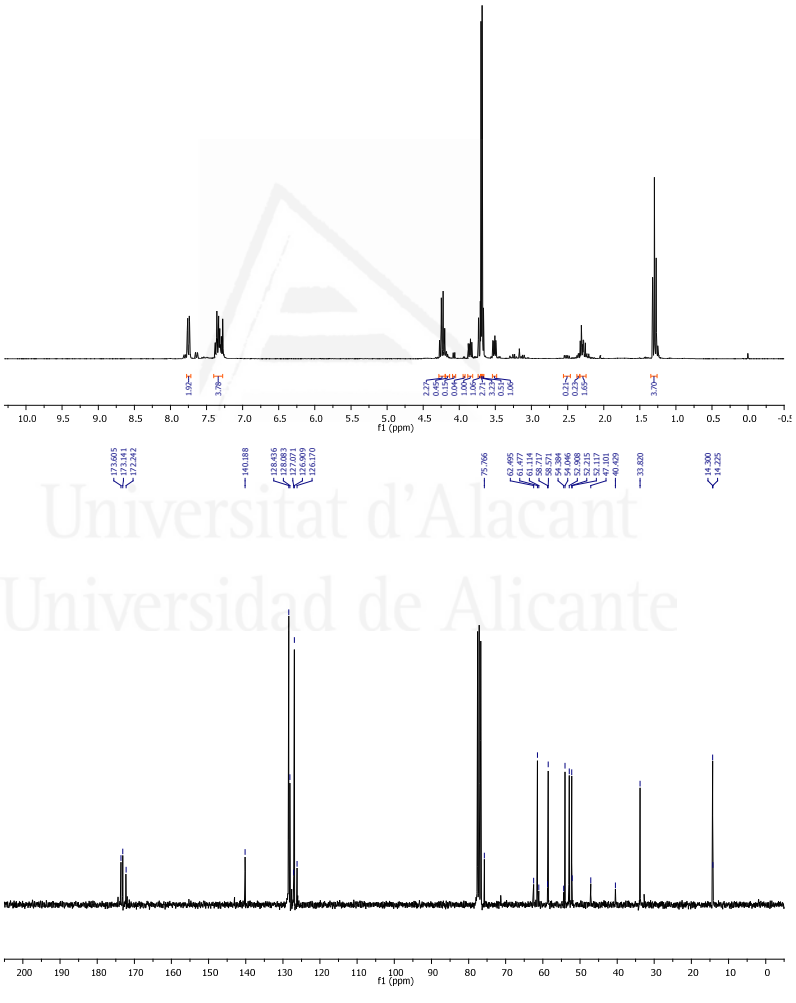

Electronic Supplementary Material (ESI) for Organic & Biomolecular Chemistry

***endo-trans*-5f**

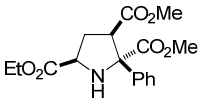

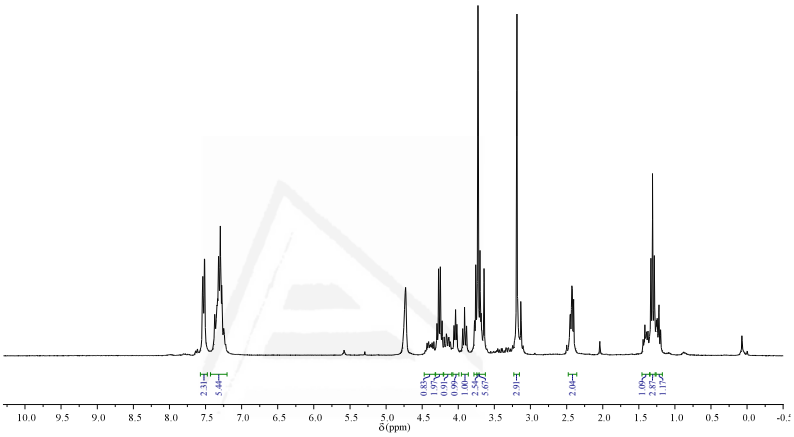

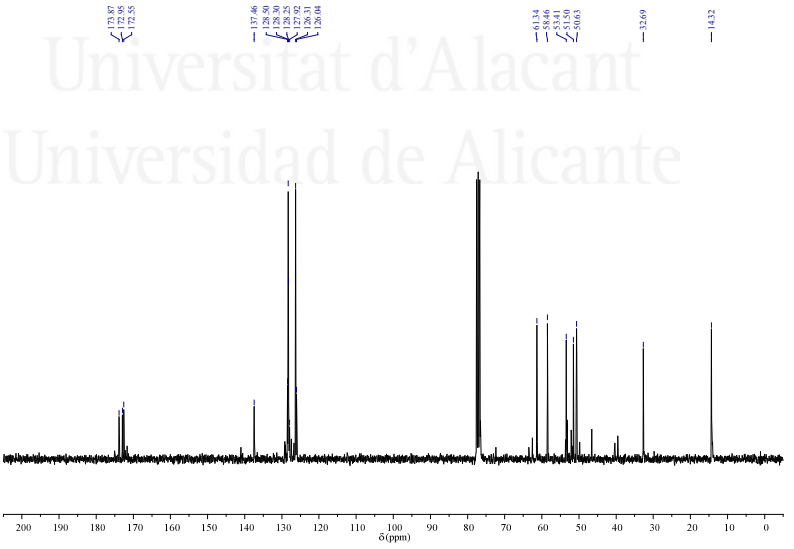

Electronic Supplementary Material (ESI) for Organic & Biomolecular Chemistry

***endo-cis*-5d**

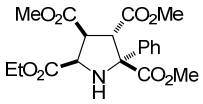

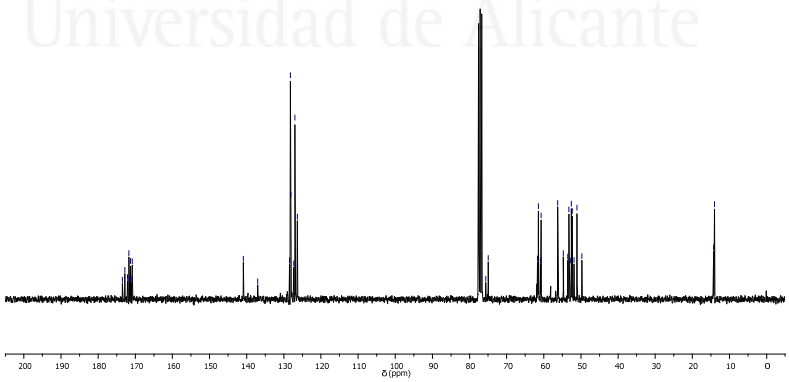

***exo-cis*-5d**

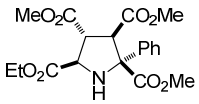

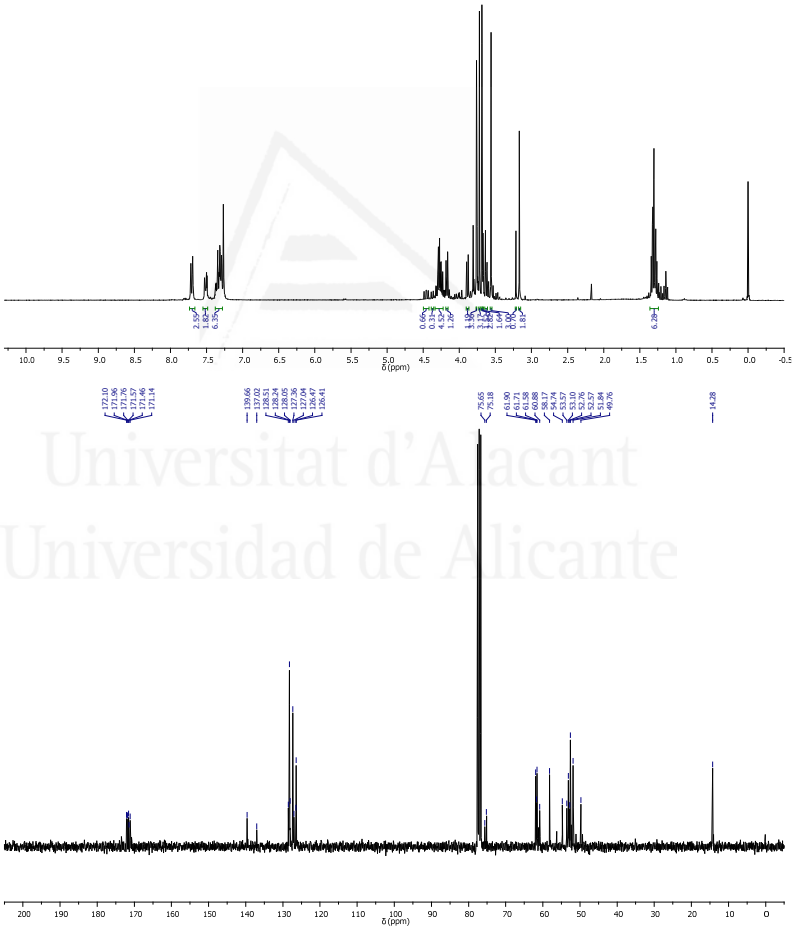

***exo-trans*-5e**

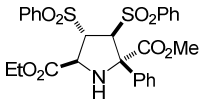

Electronic Supplementary Material (ESI) for Organic & Biomolecular Chemistry

8

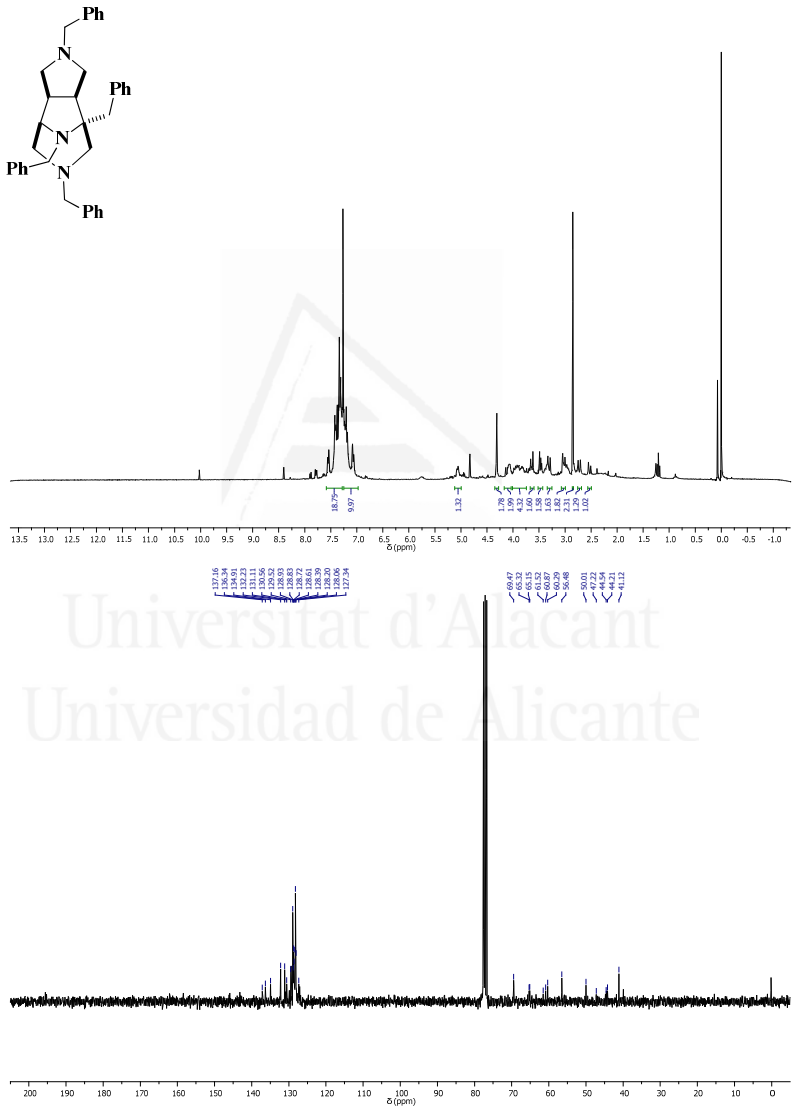

V.3.- CAPÍTULO II-2: CICLOADICIÓN 1,3-DIPOLAR MULTICOMPONENTE CATALIZADA POR PLATA (I) A PARTIR DE GLIOXILATO DE ETILO Y 2,2-DIMETOXIACETALDEHÍDO COMO PRECURSORES DEL ILURO DE AZOMETINO

V.3.5.- Antecedentes Bibliográficos

Como se detalló en la introducción general, a finales de los años setenta y principio de la década de los ochenta, comenzó a estudiarse en profundidad el uso de metales para la cicloadición 1,3-dipolar o reacción de Huisgen. Dado que los metales pueden inducir o estabilizar la carga de un fragmento orgánico, no es de extrañar que existan numerosos ejemplos en la bibliografía de cicloadiciones 1,3-dipolares con metales, donde el rol de este último es el de estabilizar y activar el 1,3-dipolo existente.[61] Un metal puede además inducir un "comportamiento 1,3-dipolar" en moléculas orgánicas que a priori no debieran mostrarlo. Esto sumado a que con determinados ligandos orgánicos pueden llegar a formarse complejos voluminosos, los convierte en una herramienta sencilla, versátil y muy eficiente de realizar la versión asimétrica de esta reacción, como se detalla en el **Capítulo II-3**.

Son numerosos los ejemplos en los que se emplean diferentes metales para tal efecto, pero son los metales de transición los que con más frecuencia se han utilizado y dentro de estos, las sales de Ag(I), Cu(I) y Cu(II). En 1982, Grigg publicó que los ácidos de Lewis, aceleraban notablemente esta reacción con alquinos.[62] Desde entonces, su grupo ha dedicado gran esfuerzo al uso de iminas aromaticas con diferentes sales de plata(I) en cantidades estequiométricas. [63] Esta metodología se ha extendido también a otras iminas que no provienen de aminoesteres. Por ejemplo el iminofosfonato **78**, en presencia de **DBU** como base y acetato de plata(I), forma la pirrolidina **79** con acrilato de metilo como dipolarófilo (**Esquema 20**).[64] La configuración relativa es 2,5-*cis* debido a la conformación W del metalodipolo. Además el metal favorece la aproximación *endo* del dipolarófilo. Como resultado de este comportamiento del metal el aducto resultante tiene configuración relativa 2,4,5-*all cis.*

[61] Frühauf, H.W.; *Chem. Rev.* **1997**, *97*, 523.
[62] Grigg, R.; Gunaratne, H.; *J. Chem. Soc., Chem. Commun.* **1982**, 384.
[63] **a)** Grigg, R.; Gunaratne, H. ; Sridharan, V.; *Tetrahedron* **1987**, *43*, 5887. **b)** Amornraksa, K.; Barr, D.; Donegan, G.; Grigg, R.; Ratananukul, P.; Sridharan, V.; *Tetrahedron* **1989**, *45*, 4649.
[64] Dondas, H.A.; Durust, Y.; Grigg, R.; Slater, M.J.; Sarker, M.; *Tetrahedron* **2005**, *61*, 10667.

Esquema 20

78 **5** **79**

R^1= H, Me, Ph, Bn, CH_2OH, CH_2OTBS
R^2= Me, Et
R^3= 2-naftilo, 2-ciclohexilo, 2-tienilo, 4-nitrofenilo, 2-yodofenilo, 2-piridilo

Por otro lado la cicloadición de iminas con estructura de 2-amino-γ-lactonas y tiolactonas **80** con acrilato de metilo y AgOAc o Ag_2O genera las espirolactonas (tiolactonas) **81** con buen rendimiento, regio- y estéreo selectividad (**Esquema 21**).[65]

Esquema 21

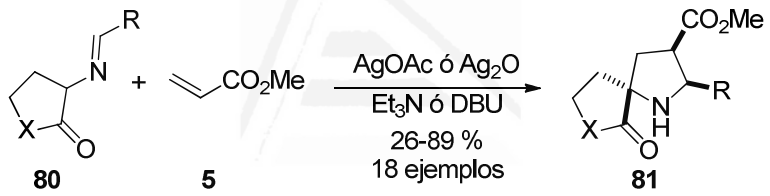

80 **5** **81**

X= O, S
R= alquilo o arilo

En esta misma línea, la reacción de 3-ariliden-4-cromanonas **83**, con la imina apropiada y en tolueno, forma las espiropirrolidinas **84** con una selectividad completa (**Esquema 22**).[66] Esta estrategia sintética ha sido utilizada además en la síntesis de 4-(5-pirrolidinil)-β-lactamas. [67]

[65] Grigg, R.; Sarker, M.; *Tetrahedron* **2006**, *62*, 10332.
[66] Subramaniyan, G.; Raghunathan, R. *Tetrahedron* **2001**, *57*, 2909.
[67] Subramaniyan, G.; Raghunathan, R.; Castro, A.; *Tetrahedron* **2003**, *59*, 335.

Esquema 22

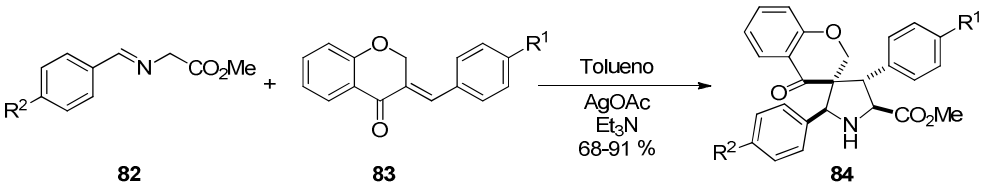

82 **83** **84**

R^1= H, Cl, OMe, Me, NO_2
R^2= H, Cl, OMe

También se ha utilizado como estrategia sintética el uso de iluros de azometino cíclicos como muestra el **Esquema 23**. El grupo de Pandey[68] ha utilizado este tipo de iluros no estables, generados in situ tras desililación de aminas cíclicas con dos grupos trimetilsililo (**85**) para construir *X*-aza-biciclo[*m*.2.1]alcanos (**86**) en el que predomina el aducto *exo*. La rígidez estructural del recién formado iluro de azometino induce a la elevada diasteroselectividad.

Esquema 23

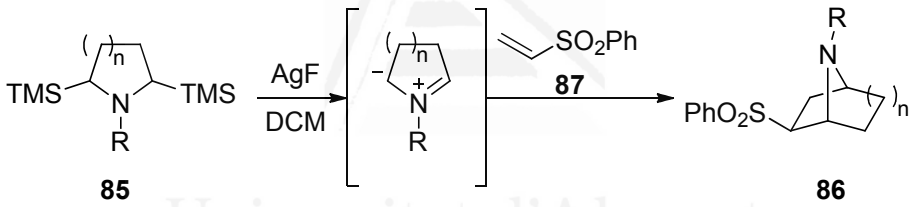

85 **86**
de > 98 %

n= 1, R= Bn, 75 %
n= 2, R= Me, 73 %
n= 3, R= Bn, 70 %

Como puede verse en los ejemplos anteriores, existen diferentes metodologías que utilizan sales de plata(I) para llegar a cicloaductos complejos variando la naturaleza de los reactivos. Sin embargo, no se han encontrado ejemplos de reacción 1,3-dipolar multicomponente con iluros de azometino catalizadas por una sal de plata (síntesis aquiral) En nuestro grupo de investigación, se ha podido llevar a cabo esta cicloadición multicomponente asimétrica utilizando binap **96**/AgSbF6 como catalizador.[69]

[68] Pandey, G.; Laha, J.K.; Lakshmaiah, G.; *Tetrahedron* **2002**, *58*, 3525.
[69] Martín, M.; Univesidad de Alicante, Tesis Doctoral, Alicante, **2012**.

V.3.6.- Objetivos

De acuerdo con lo expuesto en relación a las cicloadiciones 1,3-dipolares con iluros de azometino catalizadas por plata(I), y tras los resultados obtenidos en el **Capítulo II-1**, se plantearon los siguientes objetivos:

- Llevar a cabo la reacción 1,3-dipolar multicomponente catalizada por una sal de plata(I) a partir de glioxilato de etilo como precursor del iluro de azometino con el fin de incrementar especialmente la diasteroselectividad de los cicloaductos obtenidos.
- Utilizar en la reacción 1,3-dipolar multicomponente el 2,2-dimetoxiacetaldehído como precursor del iluro de azometino mediante catálisis por plata(I), obteniendo así una nueva funcionalidad en la posición cinco de la pirrolidina final.

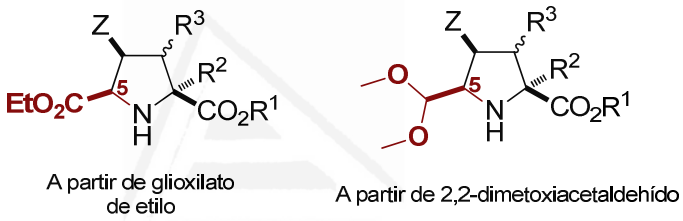

V.3.7.- Discusión de Resultados

Tras el trabajo realizado mostrado en el **Capítulo II-1**, se prodeció a estudiar esta reacción, a temperatura ambiente, usando una sal de plata como catalizador. Para optimizar la reacción, se eligió como dipolarófilo la *N*-metilmaleimida, junto con glioxilato de etilo y el clorhidrato del éster etílico de glicina. Se probaron diferentes sales de plata sin que la reacción mostrase especial selectividad por ninguna de ellas, si bien es cierto que usando AgOAc se obtuvo una conversión casi cuantitativa (**Esquema 24**). La presencia de la sal de plata es crucial ya que en ausencia de ésta la reacción no tiene lugar tras 24 horas a temperatura ambiente.

Esquema 24

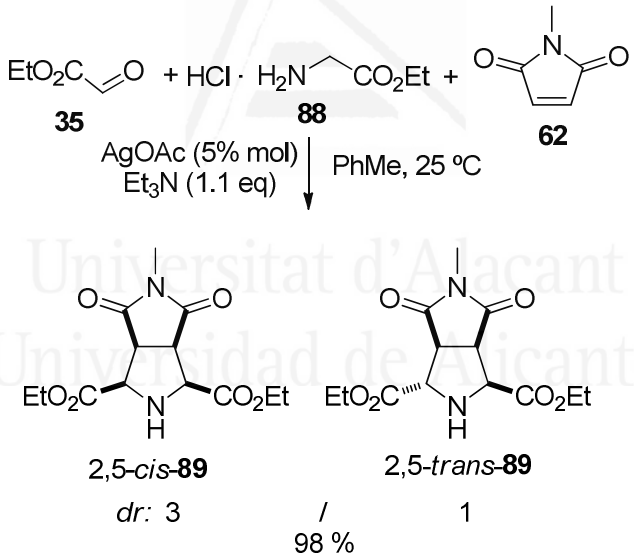

Como en el estudio mostrado en el **Capítulo II-1**, se probaron diferentes α-aminoésteres como son el clorhidrato del éster metílico de alanina, el clorhidrato del éster etílico de fenilalanina y el clorhidrato del éster metílico de fenilglicina, con diferentes dipolarófilos. En general los resultados fueron similares a los obtenidos mediante condiciones térmicas. Sin embargo en algunos caso la diastereoselectividad se incrementó usando AgOAc a favor de los aductos 2,5-*cis*.

El control de la geometría en el producto mayoritario de todos los ejemplos se muestra en el **Esquema 25** donde podemos ver que el metalodipolo presenta una conformación W,W más estable que las conformaciones tipo S.

Esquema 25

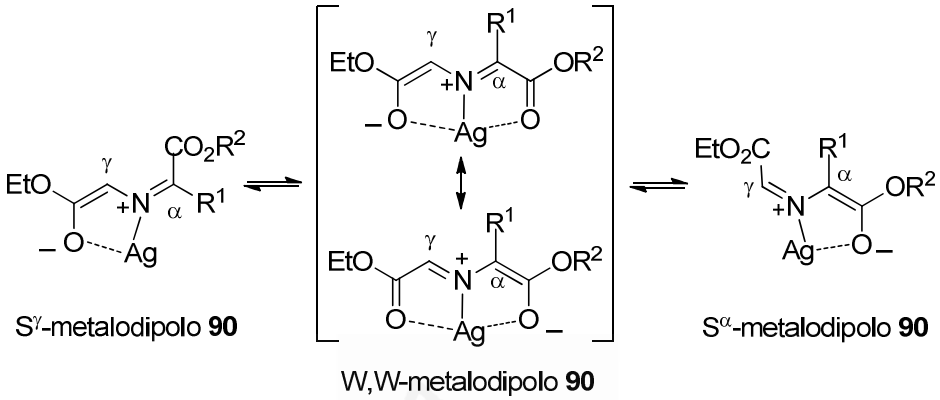

A través de la disposición que muestra la forma de W,W-metalodipolo se explica la preferencia en general para que se dé la reacción obteniéndose los productos correspondientes 2,5-*cis*.

Siguiendo la misma estrategia sintética, basada en la idea de introducir una nueva función en la posición 5 de la pirrolidina formada, se realizó un estudio similar al mostrado usando como precursor del iluro de azometino el 2,2-dimetoxiacetaldehído. Cabe destacar que este aldehído no ha sido nunca utilizado como precursor para la formación del iluro de azometino en una cicloadición 1,3-dipolar.

Se llevó cabo la reacción de este aldehído, junto con el clorhidrato del éster etílico de glicina y *N*-metilmaleimida en presencia de AgOAc y en ausencia de plata(I) bajo condiciones de calentamiento por microondas. Los resultados fueron sorprendentes ya que, mientras térmicamente, se obtiene una mezcla de aductos endo de 2:1 *cis* y *trans*, en presencia de AgOAc se obtuvo exclusivamente el aducto *endo-cis*-**92a** (**Esquema 26**).

Esquema 26

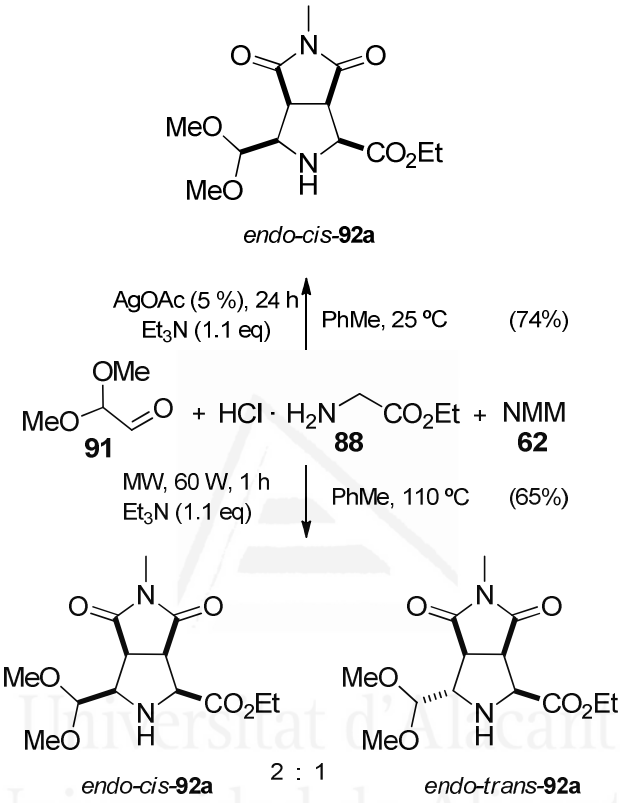

Debido a estos resultados se descartó hacer un estudio paralelo en condiciones térmicas, y se siguió con la metodología en la que se usaba un 5% mol de AgOAc. En este caso, con el 2,2-dimetoxiacetaldehído como precursor del iluro de azometino, puede observarse una coordinación más fuerte con el átomo de Ag(I), que en el caso del glioxilato de etilo, dando lugar al W,W-metalodipolo con mayor preferencia que el S-metalodipolo, lo cual resulta muy interesante desde el punto de vista de la diasteroselección (**Esquema 27**).

Esquema 27

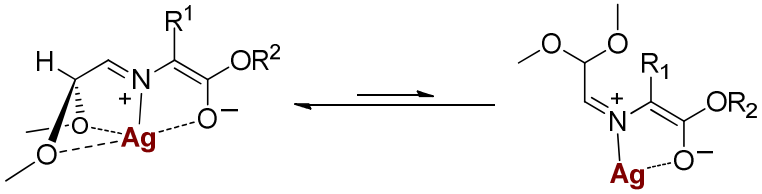

W,W-metallodipole **93** S-dipole **94**

Así pues como en el estudio usando glioxilato de etilo, se llevó a cabo la síntesis de pirrolidinas con 2,2-dimetoxiacetaldehído como precursor del iluro de azometino usando diferentes dipolarófilos y α-aminoesteres. En general, se obtuvieron rendimientos que iban de moderados a muy buenos, y en la mayoría de los casos un solo diasteroisómero (*endo*-2,5-*cis*).

Un estudio más detallado de lo resumido anteriormente se encuentra en el siguiente apartado.

V.3.8.- Org. Chem. Front, enviado

Organic Chemistry Frontiers

Dynamic Article Links ►

Cite this: DOI: 10.1039/c0xx00000x

www.rsc.org/xxxxxx

RESEARCH ARTICLE

Multicomponent Diastereoselective Silver-Catalyzed 1,3-Dipolar Cycloadditions using Ethyl Glyoxylate and 2,2-Dimethoxyacetaldehyde derived Azomethine Ylides[#,§]

Juan Mancebo-Aracil,[a] Carmen Nájera,[a,*] and José M. Sansano[a,*]

Received (in XXX, XXX) Xth XXXXXXXXX 20XX, Accepted Xth XXXXXXXXX 20XX
DOI: 10.1039/b000000x

The silver-catalyzed multicomponent reaction between ethyl glyoxylate or 2,2-dimethoxyacetaldehyde, an α-amino ester hydrochloride, and a dipolarohile in the presence of triethylamine is studied. This domino process takes place by *in situ* liberation of the α-amino ester followed and the formation of the imino ester, which is the precursor of a metalloazomethine ylide. The cycloaddition of this species and the corresponding dipolarophile affords polysubstituted proline derivatives. Ethyl glyoxylate reacts with glycinate, alaninate, phenylalaninate and phenylglycinate at room temperature in the presence of the most representative known dipolarophiles affording *endo*-cycloadducts in good yields and high 2,5-*cis*-diastereoselection. In addition, 2,2-dimethoxyacetaldehyde is evaluated with the same amino esters and dipolarophiles, under the same mild conditions, generating the corresponding *endo*-*cis*-cycloadducts with higher diastereoselections than the obtained in the same reactions using ethyl glyoxylate.

2

1. Introduction

Multicomponent process[1]-atom economy[2]-catalysis[3] constitutes three paramount milestones in organic chemistry today. Methodologies involving them constitute a clear trend of innovation in both laboratory and industrial scale. Many reactions do not waste atoms during their whole process, cycloadditions being the most frequently employed.[4] In addition, a large number of domino/multicomponent cycloadditions are found in the literature with very interesting perspectives and applications, especially when a multifunctionalization can be introduced in the final structure. 1,3-Dipolar cycloadditions (1,3-DC)[5,6] involving metallo-azomethine ylides and electrophilic alkenes are candidates to execute this three concepts with high efficiency. However, examples of multicomponent 1,3-DC involving azomethine ylides as intermediates are not frequently described.[7] Firstly, the 1,3-metallodipole precursor (normally an imino ester) can be obtained *in situ* by imine formation from the corresponding aldehyde and the α–amino ester. Second, the metal catalyst fixs the geometry of the metallodipole favouring a high stereocontrol during the dipolarophile approach and operates under milder conditions. The result of these cycloadditions are polysubstituted pyrrolidines or proline derivatives with an aromatic or heteroaromatic ring at the 5-position, which are very interesting molecules in many scientific areas.[8]

The introduction of a different functionality at the 5-position is crucial to achieve a broader synthetic scope of the resulting proline derivatives as chiral or racemic building blocks. In this way small functionalized aldehydes are advisable. Ethyl glyoxylate, for example, was employed as aldehyde together with ethyl *N*-(1-phenylethyl)glycinate, in thermal iminium route-1,3-DC affording a mixture of pyrrolidines with very low diastereoselections.[9] Also, following this iminium route, the diastereoselective synthesis of pyrrolizidines was achieved using enantiomerically enriched *O*-protected 3,4-dihydroxyprolines.[10] In our group, ethyl glyoxylate has been employed in the thermal multicomponent 1,3-DC with diethyl aminomalonate or α-amino esters and dipolarophiles by our group following the sequence imine formation-[1,2]-prototropy-cycloaddition.[11] However, to the best of our knowledge, the employment of 2,2-dimethoxyacetaldehyde as 1,3-dipole precursor has not been reported to date. The consequence of this incorporation to the final heterocyclic structure would be a very attractive protected formyl group at the 5-position.

In this work study the silver mediated multicomponent 1,3-DC between α-amino esters, dipolarophiles and functionalized aldehydes such as ethyl glyoxylate and 2,2-dimethoxyacetaldehyde will be considered.

2. Results and Discussion

2.1. 1,3-DC with ethyl glyoxylate

For the optimization, the selected reaction combines ethyl glyoxylate, *N*-methylmaleimide (NMM) and glycine ethyl ester hydrochloride in the presence of triethylamine (1.1 equiv) and silver salt (5 mol%) in toluene as solvent at room temperature (Scheme 1, Table 1). The presence of silver salt was crucial because in its absence the reaction failed (Table 1, entry 1). When the reaction was performed in toluene as solvent, compound **1a** was obtained as a *cis*/*trans* 3:1 pure mixture independently of the silver salt employed (Table 1, entries 2-7). All the silver salts tested such as $AgSbF_6$, AgOTf (OTf = triflate), AgOTfa (OTfa = trifluoroacetate), AgOBz, and Ag_2CO_3 afforded good conversions with very pure crude products. AgOAc was selected due to the high conversion achieved (>98%, Table 1, entry 5). The effect of the reaction temperature in the diastereomeric ratio of the product **1a** was also surveyed finding identical *dr* at 0 ºC (Table 1, entry 8). This crude mixture was not so pure when the reaction was run in DCM, THF, Et_2O, or EtOH (Table 1, entries 9-12). Copper(II) perchlorate and copper(II) triflate did not give any improvement neither yields nor diastereoselections, generating secondary unidentified products (Table 1, entries 13, and 14).

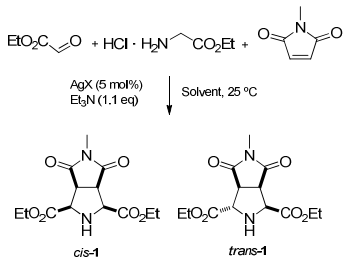

Scheme 1. Optimization of the 1,3-DC between ethyl glycinate, ethyl glyoxylate, and NMM catalyzed by silver salts in different solvents.

Table 1. Optimization of the 1,3-DC between ethyl glycinate, ethyl glyoxylate, and NMM catalyzed by silver salts (5 mol%).[a]

Entry	AgX	Solvent	Conv. (%)[b]	*cis*-**1**/*trans*-**1**[c]
1	——	PhMe	<5	—
2	$AgSbF_6$	PhMe	86[d]	3/1
3	AgOTf	PhMe	89[d]	3/1
4	AgOTfa	PhMe	91[d]	3/1
5	AgOAc	PhMe	>98[d]	3/1
6	AgOBz	PhMe	95[d]	3/1
7	Ag_2CO_3	PhMe	95[d]	3/1
8	AgOAc	PhMee	95[d]	3/1
9	AgOAc	DCM	95[f]	3/1
10	AgOAc	THF	92[f]	3/1
11	AgOAc	EtOH	89[f]	2.5/1
12	AgOAc	Et_2O	95[d]	3/1
13	$Cu(ClO_4)_2$	PhMe	90[f]	<3/1
14	$Cu(OTf)_2$	PhMe	90[f]	<3/1

[a] Ethyl glyoxylate (50% w solution in toluene), ethyl aminoglycinate hydrochloride and NMM (1:1:1), triethylamine (1.1 equiv) and the silver salt (5 mol%) were dissolved in toluene and the mixture allowed to react at 25 ºC for 19 h. [b] Obtained by analysis of crude ^{1}H NMR spectra. [c] Determined by ^{1}H NMR analysis. [d] Crude product was very pure by ^{1}H NMR. [e] Reaction performed at 0 ºC. [f] Several impurities were observed by ^{1}H NMR.

With the selected reaction conditions in hand we study the scope of this multicomponent catalyzed process starting from the reaction of ethyl glyoxylate with different maleimides, and ethyl aminoglycinate (Scheme 2 and Table 2, entries 1-3). *N*-Benzylmaleimide (NBM) afforded a *cis*/*trans* 3:1 pure mixture of **1b** in excellent yield (Table 2, entry 2). In both examples (NMM and NBM), chemical yields and diastereomeric ratios were higher than the previously reported ones in the thermal reactions.[11] However, with *N*-phenylmaleimide (NPM) the same diastereomeric ratio in **1c** was identified (*cis*/*trans* 4:1) independently of the thermal or catalyzed used method being the chemical yield sensibly higher for the silver-mediated reaction (Table 2, entry 3). The relative stereochemistry of the stereoisomers involving reactions with ethyl glyoxylate was drawn according to the comparison with previously published data (X-ray diffraction analysis and NMR experiments). The control of the geometry of the 1,3-metallodipole by the silver cation is noticeable in this reaction allowing the reaction course through a W,W-shape metallodipole **A**, which afforded *cis*-adducts **1** rather than the W,S-shape

Journal Name

Dynamic Article Links ►

Cite this: DOI: 10.1039/c0xx00000x

www.rsc.org/xxxxxx

ARTICLE TYPE

metallodipole **A** giving *trans*-adducts **1** (Scheme 3).

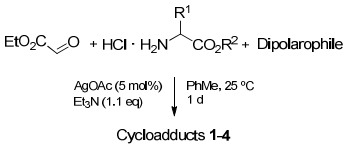

Scheme 2. Silver-catalyzed 1,3-DC of α-amino esters and ethyl glyoxylate with dipolarophiles.

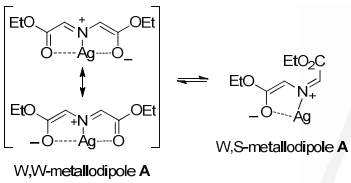

Scheme 3. Metallodipole conformations derived from glycine ethyl ester and ethyl glyoxylate

Due to the importance of the quaternary α-amino acids in many scientific areas, the multicomponent 1,3-DC employing several α-substituted α-amino esters was tested. When alanine methyl ester hydrochloride was allowed to react with ethyl glyoxylate and NMM under the optimized reaction conditions *endo-cis*-cycloadduct **2a** was isolated in 59% yield as unique diastereoisomer with lower yield than the obtained in the thermal process (Scheme 2, Table 2, entry 4). No difference was observed in the reactions (thermal[11] and silver-catalyzed) involving methyl acrylate, dimethyl fumarate, and 1,2-bis(phenylsulfonyl)ethylene (Scheme 2, Table 2, entries 5-7). The diastereoselective transformation occurred for both (*E*)-configured alkenes furnishing *endo-cis*-**2d** and *endo-cis*-**2e** in 55 and 65% yields, respectively (Table 2, entries 5 and 6).A mixture of three stereoisomers (*cis*- and *trans*-**2f** and **2f'**) was obtained in 45% yield in the case of methyl acrylate and alanine methyl ester hydrochloride (Scheme 2, Table 2, entry 7). According to these results W,W-shape metallodipole **B** (Scheme 4) is mainly originated by the silver cation. We can assume that the preferred attack occurred through the γ-position when methyl acrylate was employed as dipolarophile.

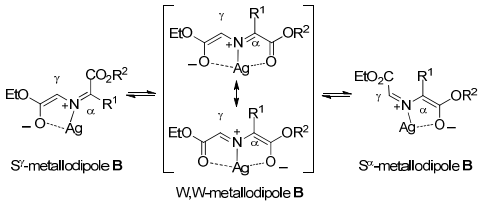

Scheme 4. Metallodipole conformations derived from α-substituted amino esters and ethyl glyoxylate.

Phenylalanine ethyl ester hydrochloride smoothly reacted with maleimides at room temperature using ethyl glyoxylate and silver acetate (5 mol%). Again, *endo-cis* cycloadducts **3a-c** were isolated diastereoselectively in good chemical yields (Scheme 2, Table 2, entries 8-10). However, when more sterically hindered dimethyl fumarate and 1,2-bis(phenylsulfonyl)ethylene (BPSE) were employed as dipolarophiles, following the silver-catalyzed conditions, the chemical yields were lower than the obtained under thermal conditions. The reaction was diastereoselective affording *exo-cis*-cycloadduct **3d** and *endo-cis*-cycloadduct **3e**, respectively (Scheme 2, Table 2, entries 11 and 12). With all this information W,W-shape type metallodipole **B** (Scheme 4) was mainly generated during the reaction course employing the phenylalaninate.

In the case of phenylglycine methyl ester, the major *endo-cis* compound **4a** was obtained through a W,W-shape metallodipole **B** geometry (Scheme 4). The chemical yield of the reaction carried out with methyl acrylate was 45% affording a 1:1 mixture of the *cis*- and *trans*-adducts **4f**, which demonstrated a higher proportion of the S^{γ}-shape metallodipole **B** during the reaction course (Scheme 2 and 4, Table 2, entry 14). In both examples, the diastereomeric ratio was slightly higher than the originally reported for the analogous thermal processes[11] 2.5:1 *vs* 2:1 and 2:1 *vs* 1:1, respectively. *E*-1,2-Disubstituted electrophilic alkenes were not very appropriate reagents for the cycloaddition using the phenylglycine derivative. In both diastereoselective transformations chemical yields were lower than the results obtained for the thermal processes.[11] The *exo*-adducts **4d** and **4e** predominated (Scheme 2, Table 2, entries 15 and 16). The bulkier phenylsulfonyl group, presumably preferred to react through the S-shape metallodipoles **B** rather than W-shaped one (Scheme 4). Working with different ester groups at 2- and 5- positions as occurred in final α-substituted prolines **2**, and **4** would allow to transform chemoselectively one of them (less sterically hindered) leaving the other ester group unaltered.

2.2. 1,3-DC with 2,2-dimethoxyacetaldehyde

Following the same strategy and with the idea to introduce a new functionality at the 5-position of the pyrrolidine ring, we next evaluated the scope of the multicomponent process using 2,2-dimethoxyacetaldehyde as imine precursor. The result of this transformation will introduce a protected formyl group at that

position.

Ethyl glycinate-maleimides-2,2-dimethoxyacetaldehyde was an appropriate combination to be catalyzed by AgOAc. In general, the reaction was diastereoselective (>50:1 ratio by ^{1}H NMR) and the chemical yields of *endo*-*cis*-adducts **5** were satisfactory (71-74%) (Scheme 5, Table 3, entries 1-3). These results indicated that stabilization of the W,W-shape metallodipole type-**C** during the reaction course is very important, probably due to a stronger coordination between the two OMe groups rather than the carbonyl group of the glyoxylate (Scheme 6). However, the microwave-assisted reaction was performed using NMM as example. This thermal transformation produced a 2:1 mixture of *cis*:*trans endo*-cycloadducts **5a** in 65% yield (Scheme 7). In this last example, the thermal [1,2]-prototropy did not control the geometry of the dipole as expected due to the existence of S-dipole **D** in high proportions (Scheme 8). The contrast of this low diastereoselection with the good result achieved in the silver-catalyzed process justified that a new parallel study of the thermal reaction was discarded.

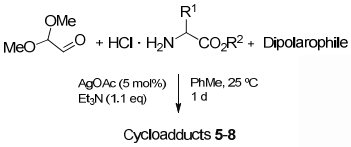

Scheme 5. Silver-catalyzed 1,3-DC of α-amino esters and 2,2-dimethoxyacetaldehyde with dipolarophiles.

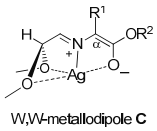

Scheme 6. Metallodipole conformation derived from 1,3-DC of α-substituted amino esters and 2,2-dimethoxyacetaldehyde.

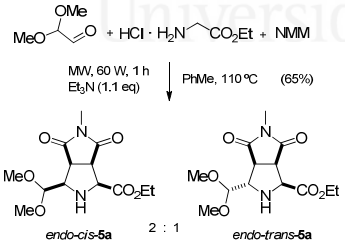

Scheme 7. Thermal 1,3-DC of ethyl glycinate, NMM and 2,2-dimethoxyacetaldehyde.

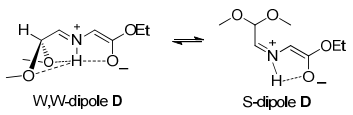

Scheme 8. Dipole conformation for thermal 1,3-DC of ethyl glycinate, NMM and 2,2-dimethoxyacetaldehyde.

Almost complete diastereoselection was detected when alanine derivative and 2,2-dimethoxyacetaldehyde were allowed to react with NMM and dimethyl fumarate. Compound *endo*-*cis*-**6a** was isolated in 89% yield whilst *endo*-*cis*-**6d** was obtained in a lower 43% yield (Scheme 5, Table 3, entries 4 and 5). In this last reaction, apart from starting reagents, small amounts of other secondary products were hardly detected. When methyl acrylate was tested as dipolarophile an equimolar mixture of *endo*-*cis*- and *exo*-*cis*-stereoisomers **6f**, together with an unidentified diastereoisomer was obtained. The overall yield of the mixture of stereoisomers **6f** was 85% (Scheme 5, Table 3, entry 6).

Phenylalanine ethyl ester derivative afforded *endo*-*cis*-compounds **7a-c** in very good chemical yields and excellent diastereoselections upon domino reaction with a maleimide and 2,2-dimethoxyacetaldehyde (Scheme 5, Table 3, 7-9). The crude reaction ^{1}H NMR spectra revealed that any other stereoisomer was formed.

Besides, a considerable lower diastereoselection was obtained when dimethyl fumarate was employed as dipolarophile. The 3:1 *endo*-*cis*-**7d**:*exo*-*cis*-**7d** ratio was determined by ^{1}H NMR and the relative configuration assigned according to nOe experiments (Scheme 5, entry 10). At this point the reaction with 1,2-bis(phenylsulfonyl)ethylene completely failed, which confirms the low chemical yield observed in precedent reactions possibly due to stereoelectronic reasons. The reactions dealing with phenylglycine derivative were surveyed obtaining very complex crude reaction products with many side products.

Unlike the behaviour observed with ethyl glyoxylate, 2,2-dimethoxyacetaldehyde reacted in the presence of NMM and diethyl aminomalonate in good yield (70%) and high diastereomeric ratio affording mainly *all*-*cis* compound **8** (Scheme 5, Table 3, entry 11).

3. Conclusions

The silver catalyzed *endo*-diastereoselective multicomponent 1,3-DC using α-amino esters, dipolarophiles and functionalized aldehydes such as ethyl glyoxylate or 2,2-dimethoxyacetaldehyde was successfully accomplished. In general, in the catalyzed process with ethyl glyoxylate the *endo*-*cis*-diastereoselections and chemical yields were better or similar than those obtained under thermal conditions. When the reaction was performed with 2,2-dimethoxyacetaldehyde the silver-catalyzed conditions for the cycloaddition gave the best results. In this case, higher 2,5-*cis*-diastereoselections than in the reactions involving ethyl glyoxylate were obtained, possibly due to the most favoured W,W-metallodipole geometry.

Journal Name

Dynamic Article Links ►

Cite this: DOI: 10.1039/c0xx00000x

www.rsc.org/xxxxxx

ARTICLE TYPE

Table 2. Scope of the silver catalyzed 1,3-DC between ethyl glyoxylate with different α-imino esters and dipolarophiles, *via* Scheme 2.[a]

Entry	R^1	R^2	Dipolarophile	Product	Yield (%)[b], *dr*	Yield (%)[b,c], *dr*[c]
1	H	Et	NMM[d]	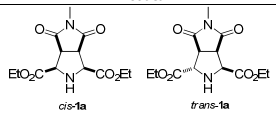 *cis*-**1a** *trans*-**1a**	84, 3/1	80, 2/1
2	H	Et	NBM[e]	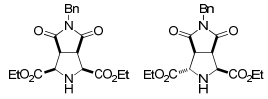 *cis*-**1b** *trans*-**1b**	95, 3/1	64, 1/1
3	H	Et	NPM[f]	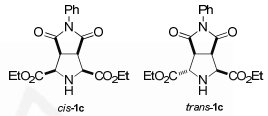 *cis*-**1c** *trans*-**1c**	85, 4/1	71, 4/1
4	Me	Me	NMM[d]	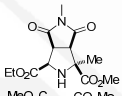 *endo-cis*-**2a**	59	85
5	Me	Me	Dimethyl fumarate	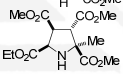 *endo-cis*-**2d**	55	70
6	Me	Me	BPSE[g]	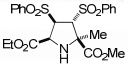 *endo-cis*-**2e**	65	66
7	Me	Me	Methyl acrylate	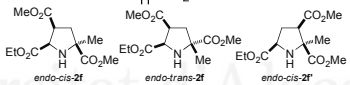 *endo-cis*-**2f** *endo-trans*-**2f** *endo-cis*-**2f'**	53, 1/1/1.5	60, 1/1/1.5
8	Bn	Et	NMM[d]	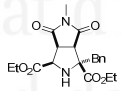 *endo-cis*-**3a**	83	96
9	Bn	Et	NBM[e]	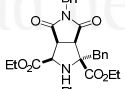 *endo-cis*-**3b**	68	75
10	Bn	Et	NPM[f]	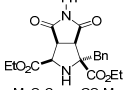 *endo-cis*-**3c**	85	80
11	Bn	Et	Dimethyl fumarate	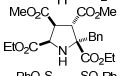 *endo-cis*-**3d**	38	80
12	Bn	Et	BPSE[g]	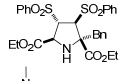 *exo-cis*-**3e**	48	60
13	Ph	Me	NMM[d]	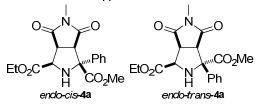 *endo-cis*-**4a** *endo-trans*-**4a**	90, 2.5/1	87, 2/1

6						
14	Ph	Me	Methyl acrylate	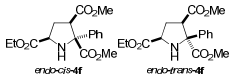 *endo-cis*-**4f** *endo-trans*-**4f**	45, 2/1	67, 1/1
15	Ph	Me	Dimethyl fumarate	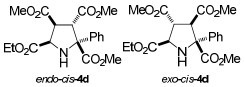 *endo-cis*-**4d** *exo-cis*-**4d**	45, 2/3	87, 1/1
16	Ph	Me	BPSE[g]	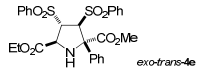 *exo-trans*-**4e**	25	68

[a] Ethyl glyoxylate (1M solution in toluene), amino ester hydrochloride and the dipolarophile (1:1:1), triethylamine (1.1 equiv) and the silver salt (5 mol%) were dissolved in toluene and the mixture allowed to react at 25 ºC for 1 d. [b] Isolated yield after column chromatography. [c] Data of the already reported synthesis under thermal conditions (ref. 11). [d] NMM = *N*-Methylmaleimide. [e] NBM = *N*-Benzylmaleimide. [f] NPM = *N*-Phenylmaleimide. [g] BDSE 1,2-bis(phenylsulfonyl)ethylene.

Journal Name

Dynamic Article Links ►

Cite this: DOI: 10.1039/c0xx00000x

www.rsc.org/xxxxxx

ARTICLE TYPE

Table 3. Scope of the silver catalyzed 1,3-DC between 2,2-dimethoxyacetaldehyde with different α-imino esters and dipolarophiles *via* Scheme 7.[a]

Entry	R^1	R^2	Dipolarophile	Product	Yield (%)[b]
1	H	Et	NMM[c]	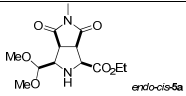 *endo-cis*-**5a**	74[d,e]
2	H	Et	NBM[f]	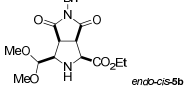 *endo-cis*-**5b**	73[e]
3	H	Et	NPM[g]	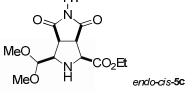 *endo-cis*-**5c**	71[e]
4	Me	Me	NMM[c]	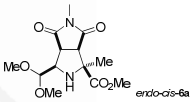 *endo-cis*-**6a**	89[e]
5	Me	Me	Dimethyl fumarate	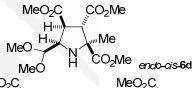 *endo-cis*-**6d**	43[e]
6	Me	Me	Methyl acrylate	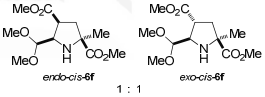 *endo-cis*-**6f** : *exo-cis*-**6f** 1 : 1	85
7	Bn	Et	NMM[c]	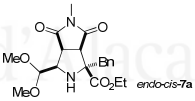 *endo-cis*-**7a**	87[e]
8	Bn	Et	NBM[f]	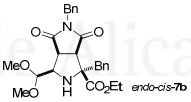 *endo-cis*-**7b**	96[e]
9	Bn	Et	NPM[g]	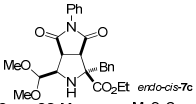 *endo-cis*-**7c**	85[e]
10	Bn	Et	Dimethyl fumarate	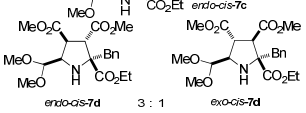 *endo-cis*-**7d** : *exo-cis*-**7d** 3 : 1	66
11	CO_2Et	Et	NMM[c]	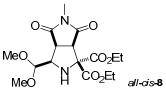 *all-cis*-**8**	70[e]

[a] 2,2-Dimethoxyacetaldehyde, amino ester hydrochloride and the dipolarophile (1:1:1), triethylamine (1.1 equiv) and the silver salt (5 mol%) were dissolved in toluene and the mixture allowed to react at 25 ºC for 1 d. [b] Isolated yield after column chromatography. [c] NMM = *N*-Methylmaleimide. [d] Thermal MW-reaction. afforded a 2:1 mixture of diastereoisomers (see text). [e] *dr* >50:1, determined by ^{1}H NMR analysis. [f] NBM = *N*-Benzylmaleimide. [g] NPM = *N*-Phenylmaleimide.

8

Organic Chemistry Frontiers

Dynamic Article Links ►

Cite this: DOI: 10.1039/c0xx00000x

www.rsc.org/xxxxxx

RESEARCH ARTICLE

4. Experimental section

4.1. General

The structurally most important peaks of the IR spectra (recorded using a Nicolet 510 P-FT and a Jasco FTIR 4100) are listed. ^{1}H NMR (300 MHz) and ^{13}C NMR (75 MHz) spectra were obtained using a Bruker AC-300 with $CDCl_3$ as solvent and TMS as internal standard unless otherwise stated. Low-resolution electron impact (GC-EI) mass spectra were obtained at 70 eV using a Shimadzu QP-5000, and high-resolution mass spectra were obtained using a Finnigan VG Platform. HRMS (GC-EI) were recorded using a Finnigan MAT 95S instrument. Analytical TLC was performed using Schleicher & Schuell F1400/LS silica gel plates, and the spots were visualized under UV light (λ=254 nm). Melting points were determined with a Reichert Thermovar hot plate apparatus and are uncorrected. For flash chromatography, we employed Merck silica gel 60 (0.040–0.063 mm).

4.2.General procedure for the microwave-assisted synthesis of cycloadducts

Ethyl glyoxylate (100 µL, 0.5 mmol, 50% in toluene) or 2,2-dimethoxyacetaldehyde (75µL, 0.5 mmol, 50% in water), diethyl aminomalonate hydrochloride or the amino acid ethyl ester hydrochloride (0.5 mmol), the corresponding dipolarophile (0.5 mmol), AgOAc (4.1 mg, 0.025 mmol) and triethylamine (90 µL, 0.55 mmol) were dissolved in toluene (4 mL). The reaction vessel was covered with an aluminum foil in order to prevent the light exposure. Once the reaction was judged complete after a TLC test the solvent was evaporated under reduced pressure and the residue was dissolved in ethyl acetate, washed with brine and dried over $MgSO_4$. After evaporation the residue was purified by flash chromatography (silica gel) to afford the corresponding product.

4.2.1. (1R,3S*,3aR*,6aS*)-Diethyl 5-methyl-4,6-dioxooctahydro pyrrolo[3,4-c]pyrrole-1,3-dicarboxylate (endo-cis-**1a**).*[9] Sticky yellow oil; IR (neat) ν_{max} 2984, 1699, 1595 cm^{-1}; ^{1}H NMR δ_H: 1.33 (t, *J* = 7.2 Hz, 6H, 2x$CO_2CH_2CH_3$), 2.94 (s, 3H, NCH_3), 3.57 [m, 2H, 2x*CH*CH(CO_2Et)NH], 3.97 [m, 2H, 2xC*H*(CO_2Et)NH], 4.30 (q, *J* = 7.2 Hz, 4H, 2x$CO_2CH_2CH_3$), N*H* nd; ^{13}C NMR δ_C: 14.2 (2x$CO_2CH_2CH_3$), 25.5 (NCH_3), 50.0 [2x*C*HCH(CO_2Et)NH], 61.9 (2x$CO_2CH_2CH_3$), 63.1 [2x*C*H(CO_2Et)NH], 169.0 (2x$CO_2CH_2CH_3$), 175.0 (2xCON); MS (EI-GC) *m/z*: 298 (M^++1, 1%), 226 (12), 225 (100), 179 (32), 151 (53), 94 (44), 67 (12); HRMS calculated for $C_{13}H_{18}N_2O_6$: 298.1155, found: 298.1148.

4.2.2. (1R,3R*,3aR*,6aS*)-Diethyl 5-methyl-4,6-dioxooctahydro pyrrolo[3,4-c]pyrrole-1,3-dicarboxylate (endo-trans-**1a**).*[9] Sticky yellow oil; IR (neat) ν_{max} 2984, 1774, 1731, 1595 cm^{-1}; ^{1}H NMR δ_H: 1.33 (t, *J* = 7.2 Hz, 3H, $CO_2CH_2CH_3$), 1.35 (t, *J* = 7.2 Hz, 3H, $CO_2CH_2CH_3$), 2.98 (s, 3H, NCH_3), 3.56 [deform. dd, *J* = 8.0, 8.0 Hz, 1H, C*H*CH(CO_2Et)NH], 3.64 [dd, *J* = 8.0, 1.2 Hz, 1H, C*H*CH(CO_2Et)NH], 4.13 [d, *J* = 8.0 Hz, 1H, C*H*(CO_2Et)NH], 4.24 (q, *J* = 7.2 Hz, 2H, $CO_2CH_2CH_3$), 4.27–4.35 (m, 3H, $CO_2CH_2CH_3$ and C*H*(CO_2Et)NH], N*H* nd; ^{13}C NMR δ_C: 14.2, 14.3 (2x$CO_2CH_2CH_3$), 25.5 (NCH_3), 47.6 [*C*HCH(CO_2Et)NH], 48.8 [*C*HCH(CO_2Et)NH], 61.8, 62.0 (2x$CO_2CH_2CH_3$), 62.2 [*C*H(CO_2Et)NH], 62.4 [CH(CO_2Et)NH], 169.7, 171.7 (2xCO_2), 175.4, 176.6 (2xCON); MS (EI-GC) *m/z*: 298 (M^++1, 1%), 226 (12), 225 (100), 179 (17), 151 (40), 94 (40), 68 (10), 67 (13),; HRMS calculated for $C_{13}H_{18}N_2O_6$: 298.1155, found: 298.1148.

4.2.3. (1R,3S*,3aR*,6aS*)-Diethyl 5-benzyl-4,6-dioxooctahydro pyrrolo[3,4-c]pyrrole-1,3-dicarboxylate (endo-cis-**1b**).*[9] Sticky yellow oil; IR (neat) ν_{max} 2984, 1740, 1705 cm^{-1}; ^{1}H NMR δ_H: 1.28 (t, *J* = 7.1 Hz, 6H, 2x$CO_2CH_2CH_3$), 3.54 [m, 2H, C*H*CH(CO_2Et)NH], 3.94 [m, 2H, C*H*(CO_2Et)NH], 4.24 (q, *J* = 7.1 Hz, 4H, 2x$CO_2CH_2CH_3$), 4.58 (s, 2H, CH_2Ph), 7.18–7.38 (m, 5H, Ar*H*); ^{13}C NMR δ_C: 14.1 (2x$CO_2CH_2CH_3$), 43.0 (CH_2Ph), 49.8 [2x*C*HCH(CO_2Et)NH], 62.0 (2x$CO_2CH_2CH_3$), 63.0 [2x*C*H(CO_2Et)NH], 128.1, 128.6, 128.7, 135.2 (Ar*C*), 168.8 (2x$CO_2CH_2CH_3$), 174.6 (CON); MS (EI-GC) *m/z*: 374 (M^++1, 2%), 302 (18), 301 (100), 227 (50), 94 (23), 91 (47), 68 (11); HRMS calculated for $C_{19}H_{22}N_2O_6$: 374.1478, found: 374.1470.

4.2.4. (1R,3R*,3aR*,6aS*)-Diethyl 5-benzyl-4,6-dioxooctahydro pyrrolo[3,4-c]pyrrole-1,3-dicarboxylate (endo-trans-**1b**).*[9] Sticky yellow oil; IR (neat) ν_{max} 2990, 1740, 1700 cm^{-1}; ^{1}H NMR δ_H: 1.23–1.38 (m, 6H, 2x$CO_2CH_2CH_3$), 3.64 (dd, *J* = 8.0, 1.4 Hz,1H, C*H*CH(CO_2Et)NH), 4.10–4.33 [m, 6H, C*H*CH(CO_2Et)NH and C*H*(CO_2Et)NH and 2x$CO_2CH_2CH_3$], 4.52–4.69 (m, 3H, CH_2Ph and C*H*(CO_2Et)NH), 7.18–7.40 (m, 5H,Ar*H*); ^{13}C NMR δ_C: 14.2, 14.3 (2x$CO_2CH_2CH_3$), 43.1 (CH_2Ph), 48.8 [*C*HCH(CO_2Et)NH], 49.9 [*C*HCH(CO_2Et)NH], 61.8, 62.0 (2x$CO_2CH_2CH_3$), 62.2 [*C*H(CO_2Et)NH], 62.5 [*C*H(CO_2Et)NH], 128.1, 128.8, 129.1, 135.4 (Ar*C*), 169.6, 171.7 (2x$CO_2CH_2CH_3$), 175.0, 176.3 (2xCON); MS (EI-GC) *m/z*: 374 (M^++1, 2%), 302 (18), 301 (100), 227 (31), 94 (20), 91 (44), 68 (13); HRMS calculated for $C_{19}H_{22}N_2O_6$: 374.1478, found: 374.1470.

4.2.5. (1R,3S*,3aR*,6aS*)-Diethyl 4,6-dioxo-5-phenyloctahydro pyrrolo[3,4-c]pyrrole-1,3-dicarboxylate (endo-cis-**1c**).*[9] Colorless needles, mp = 123-125 ºC (from hexane/$CDCl_3$); IR (neat) ν_{max} 2980, 1741, 1732, 1708 cm^{-1}; ^{1}H NMR δ_H: 1.32 (t, *J* = 7.2 Hz, 6H, 2x$CO_2CH_2CH_3$), 3.05 (t, *J* = 12.7 Hz, 1H, N*H*), 3.71 [m, 2H, 2x*CH*CH(CO_2Et)NH], 4.06 [m, 2H, C*H*(CO_2Et)NH], 4.29 (q, *J* = 7.2 Hz, 4H, 2x$CO_2CH_2CH_3$), 7.19–7.22 (m, 2H, Ar*H*), 7.37–7.46 (m, 3H, Ar*H*); ^{13}C NMR δ_C: 14.0 (2x$CO_2CH_2CH_3$), 49.9 [2x*C*HCH(CO_2Et)NH], 62.1 (2x$CO_2CH_2CH_3$), 63.4 [2x*C*H(CO_2Et)NH], 126.5, 128.9, 129.2, 131.3 (Ar*C*), 169.0 (2x$CO_2CH_2CH_3$), 174.1 (2xCON); MS (EI-GC) 360 *m/z* (M^++1, 3%), 288 (19), 287 (100), 94 (45), 68 (13), 67 (11); HRMS calculated for $C_{18}H_{20}N_2O_6$: 360.1301, found: 360.1291.

4.2.6. (1R,3R*,3aR*,6aS*)-Diethyl 4,6-dioxo-5-phenyloctahydro pyrrolo[3,4-c]pyrrole-1,3-dicarboxylate endo-trans-**1c**).*[9] Colorless needles mp = 105-107 ºC (from hexane/$CDCl_3$); IR (neat) ν_{max} 2976, 1712 cm^{-1}; ^{1}H NMR δ_H:

1.20–1.32 (m, 6H, 2x$CO_2CH_2CH_3$), 2.85 (br. s, 1H, N*H*), 3.68 [deform. dd, *J* = 8.1, 8.1 Hz, 1H, C*H*CH(CO_2Et)NH], 3.83 [d, *J* = 8.1, 1H, C*H*CH(CO_2Et)NH], 4.25 [m, 5H, 2x$CO_2CH_2CH_3$ and C*H*(CO_2Et)NH], 4.42 [s, 1H, C*H*(CO_2Et)NH], 7.23–7.27 (m, 2H, Ar*H*), 7.38–7.47 (m, 3H, Ar*H*); ^{13}C NMR δ_C: 14.0, 14.1 (2x$CO_2CH_2CH_3$), 47.6 [*C*HCH(CO_2Et)NH], 49.9 [CHCH(CO_2Et)NH], 61.9, 62.1 (2x$CO_2CH_2CH_3$), 62.3 [CH(CO_2Et)NH], 62.9 [CH(CO_2Et)NH], 126.4, 128.8, 129.1, 131.5 (Ar*C*), 169.8, 171.4 (2x$CO_2CH_2CH_3$), 174.6, 175.6 (2xCON); MS (EI-GC) 360 *m/z*: (M^++1, 4%), 67 (10), 68 (13), 94 (40), 287 (100), 288 (17); HRMS calculated for $C_{18}H_{20}N_2O_6$: 360.1301, found: 360.1291.

4.2.7. (1S,3R*,3aS*,6aR*)-3-Ethyl 1-methyl 1,5-dimethyl-4,6-dioxooctahydropyrrolo[3,4-c]pyrrole-1,3-dicarboxylate endo-cis-**2a**).*[9] Sticky pale yellow oil; IR (neat) ν_{max} 2983, 2955, 1777, 1735, 1697 cm^{-1}; ^{1}H NMR δ_H: 1.36 (t, *J* = 7.2 Hz, 3H, $CO_2CH_2CH_3$), 1.49 [s, 3H, C(CO_2CH_3)CH_3], 2.93 (s, 3H, NCH_3), 3.25 [d, *J* = 8.0 Hz, 1H, C*H*C(CO_2Me)CH_3], 3.37 (d, *J* = 12.5 Hz, 1H, N*H*), 3.63 [deform. dd, *J* = 8.0, 8.0 Hz, 1H, C*H*CH(CO_2Et)NH], 3.83 (s, 3H, CO_2CH_3), 4.14 [dd, *J* = 12.5, 8.0, Hz, 1H, C*H*(CO_2Et)NH], 4.30 (q, *J* = 7.2 Hz, 2H, $CO_2CH_2CH_3$); ^{13}C NMR δ_C: 14.2 ($CO_2CH_2CH_3$), 24.6 [C(CO_2CH_3)CH_3], 25.4 (NCH_3), 50.4 [*C*HCH(CO_2Et)NH], 53.1 [CHC(CO_2Me)CH_3], 62.0 (CO_2CH_3), 62.1 ($CO_2CH_2CH_3$), 69.4 [CH(CO_2Me)CH_3], 169.5, 171.7 (2xCO_2), 175.0, 175.2 (2xCON); MS (EI-GC) *m/z*: 298 (M^++1, <1%), 239 (67), 225 (39), 165 (100), 108 (43), 81 (10), 80 (21); HRMS calculated for $C_{13}H_{18}N_2O_6$: 298.1165, found: 298.1163.

4.2.8. (2S,3S*,4S*,5R*)-5-Ethyl 2,3,4-trimethyl 2-methylpyrrolidine-2,3,4,5-tetracarboxylate (endo-cis-**2d**).*[9] Pale yellow oil; IR (neat) ν_{max} 2986, 2954, 2907, 1730, 1729 cm^{-1}; ^{1}H NMR δ_H: 1.27 (t, *J* = 7.1 Hz, 3H, $CO_2CH_2CH_3$), 1.60 [s, 3H, C(CO_2CH_3)CH_3], 3.24 [d, *J* = 10.0 Hz, 1H, C*H*C(CO_2Me)Me], 3.64, 3.68, 3.74 (3s, 3H, CO_2CH_3), 3.78 [dd, *J* = 10.0, 8.1 Hz, 1H, C*H*CH(CO_2Et)NH], 4.02 [d, *J* = 8.1 Hz, 1H, C*H*(CO_2Et)NH], 4.15 (q, *J* = 7.1, Hz, 2H, $CO_2CH_2CH_3$), N*H* nd; ^{13}C NMR δ_C: 14.2 ($CO_2CH_2CH_3$), 24.9 [C(CO_2CH_3)CH_3], 49.6 [CHC(CO_2Me)Me], 52.3, 52.6 52.7 (3xCO_2CH_3), 56.8 [CHCH(CO_2Et)NH], 61.7 [CH(CO_2Et)NH], 61.8 ($CO_2CH_2CH_3$), 68.4 [*C*(CO_2Me)Ph], 170.6, 172.3, 173.0, 173.8 (4xCO_2); MS (EI-GC) *m/z*: 331 (M^++1, <2%), 272 (65), 258 (19), 262 (19), 241 (10), 240 (82), 226 (99), 212 (80), 198 (60), 180 (10), 167 (11), 166 (100), 154 (25), 140 (72), 139 (10), 136 (10), 122 (10), 108 (58), 94 (11), 81 (22), 80 (27), 59 (24); HRMS calculated for $C_{14}H_{21}NO_8$: 331.1267, found: 331.1274.

4.2.9. (2R,3R*,4R*,5S*)-5-Ethyl 2-methyl 2-methyl-3,4-bis(phenylsulfonyl)pyrrolidine-2,5-dicarboxylate (endo-cis-**2e**).*[9] Orange oil; IR (neat) ν_{max} 2985, 2956, 2905, 1735, 1710, 1308, 1146 cm^{-1}; ^{1}H NMR δ_H: 1.00 (t, *J* = 7.1 Hz, 3H, $CO_2CH_2CH_3$), 1.72 [s, 3H, C(CO_2CH_3)CH_3], 3.72 (s, 3H, CO_2CH_3), 3.94 (q, *J* = 7.1 Hz, 2H, $CO_2CH_2CH_3$), 4.27 [d, *J* = 6.5 Hz, 1H, C*H*(CO_2Et)NH], 4.28 [d, *J* = 4.5 Hz, 1H, C*H*C(CO_2Me)Me], 5.01 [dd, *J* = 6.5, 4.5 Hz, 1H, C*H*CHCO$_2$Et], 7.51–7.71 (m, 6H, Ar*H*), 7.81–8.02 (m, 4H, Ar*H*), N*H* nd; ^{13}C NMR δ_C: 14.0 ($CO_2CH_2CH_3$), 23.7 [CHC(CO_2Me)CH_3], 52.7 [*C*H(CO_2Et)NH], 61.5 (CO_2CH_3), 62.2 ($CO_2CH_2CH_3$), 69.4 [*C*(CO_2Me)Me], 69.5 [CHC(CO_2Me)Me], 73.0 [*C*HCH(CO_2Et)NH], 128.4, 128.8, 129.3, 129.4, 134.2, 134.4, 138.1, 140.4 (Ar*C*), 170.1, 171.2 (2xCO_2); MS (EI-GC) *m/z*: 495 (M^++1, <1%), 294 (32), 279 (21), 248 (39), 237 (14), 236 (100), 222 (26), 221 (10), 156 (11), 128 (17), 125 (11), 108 (23), 96 (26), 95 (10), 94 (11), 81 (46), 80 (21), 77 (14); HRMS calculated for $C_{22}H_{25}NO_8S_2$: 495.1022, found: 495.1015.

4.2.10. (2R,3S*,5S*)-2-Ethyl 3,5-dimethyl 5-methylpyrrolidine-2,3,5-tricarboxylate (endo-cis-**2f**).*[9] Yellowish oil; IR (neat) ν_{max} 2983, 2954, 1731, 1725, 1700 cm^{-1}; ^{1}H NMR δ_H: 1.26 (t, *J* = 7.2 Hz, 3H, $CO_2CH_2CH_3$), 1.49 [s, 3H, C(CO_2CH_3)CH_3], 2.01 [dd, *J* = 12.9, 9.8 Hz, 1H, C*H*HC(CO_2Me)CH_3], 2.64 [dd, *J* = 12.9, 8.3 Hz, 1H, C*H*HC(CO_2Me)CH_3], 3.19 [ddd, *J* = 9.8, 8.3, 7.1 Hz, 1H, C*H*(CO_2Me)], 3.71, 3.73 (2s, 3H, CO_2CH_3), 3.77 [d, *J* = 7.1 Hz, 1H, C*H*(CO_2Et)NH], 4.16 (q, *J* = 7.2, Hz, 2H, $CO_2CH_2CH_3$, N*H* nd; ^{13}C NMR δ_C: 14.3 ($CO_2CH_2CH_3$), 25.9 [C(CO_2CH_3)CH_3], 40.7 [CH_2C(CO_2Me)CH_3], 47.4 [*C*HCH(CO_2Et)NH], 52.4, 52.7 (2xCO_2CH_3), 61.6 ($CO_2CH_2CH_3$), 63.0 [*C*H(CO_2Et)NH], 66.3 [C(CO_2Me)CH_3], 172.8, 173.5, 176.3 (3xCO_2); MS (EI-GC) *m/z*: 273 (M^++1, <2%), 215 (11), 214 (100), 200 (30), 168 (13), 140 (33), 108 (19), 82 (21); HRMS calculated for $C_{12}H_{19}NO_6$: 273.1212, found: 273.1214.

4.2.11. (2R,3S*,5R*)-2-Ethyl 3,5-dimethyl 5-methylpyrrolidine-2,3,5-tricarboxylate (endo-trans-**2f**).* [9] Yellowish oil; IR (neat) ν_{max} 2983, 2953, 1732, 1725, 1703 cm^{-1}; ^{1}H NMR δ_H: 1.25 (t, *J* = 7.2 Hz, 3H, $CO_2CH_2CH_3$), 1.37 [s, 3H, C(CO_2CH_3)CH_3], 2.01 [dd, *J* = 13.5, 8.0 Hz, 1H, C*H*HC(CO_2Me)CH_3], 2.68 [dd, *J* = 13.5, 7.2 Hz, 1H, C*H*HC(CO_2Me)CH_3], 3.30 [ddd, *J* = 8.0, 7.2, 7.0 Hz, 1H, C*H*CH(CO_2Et)], 3.62, 3.73 (2s, 3H, CO_2CH_3), 4.03 [d, *J* = 7.0 Hz, 1H, C*H*(CO_2Et)NH], 4.15 (q, *J* = 7.2, Hz, 2H, $CO_2CH_2CH_3$, N*H* nd; ^{13}C NMR δ_C: 14.2 ($CO_2CH_2CH_3$), 28.3 [C(CO_2CH_3)CH_3], 39.1 [CH_2C(CO_2Me)CH_3], 47.1 [*C*HCH(CO_2Et)NH], 53.3, 53.4 (2xCO_2CH_3), 61.4 ($CO_2CH_2CH_3$), 62.8 [*C*H(CO_2Et)NH], 65.4 [C(CO_2Me)CH_3], 172.3, 173.6, 176.4 (3xCO_2); MS (EI-GC) *m/z*: 273 (M^++1, <2%), 215 (12), 214 (100), 200 (33), 140 (62), 108 (20), 99 (24), 82 (23); HRMS calculated for $C_{12}H_{19}NO_6$: 273.1212, found: 273.1215.

4.2.12. (2S,3R*,5R*)-5-Ethyl 2,3-dimethyl 2-methylpyrrolidine-2,3,5-tricarboxylate (endo-cis-**2f´**).*[9] Yellowish oil; IR (neat) ν_{max} 2983, 2955, 1730, 1726, 1700 cm^{-1}; ^{1}H NMR δ_H: 1.26 (t, *J* = 7.1 Hz, 3H, $CO_2CH_2CH_3$), 1.51 [s, 3H, C(CO_2CH_3)CH_3], 2.29–2.57 [m, 2H, CH_2CH(CO_2Et)], 2.87 [dd, *J* = 9.5, 8.1 Hz, 1H, C*H*C(CO_2Me)CH_3], 3.65, 3.66 (2s, 3H, CO_2CH_3), 3.87 [dd, *J* = 8.6, 7.6 Hz, 1H, C*H*(CO_2Et)NH], 4.15 (q, *J* = 7.1, Hz, 2H, $CO_2CH_2CH_3$), N*H* nd; ^{13}C NMR δ_C: 14.3 ($CO_2CH_2CH_3$), 25.5 [CHC(CO_2Me)CH_3], 32.3 [CH_2CH(CO_2Et)NH], 52.0, 52.1 (2xCO_2CH_3), 52.5 [*C*HC(CO_2Me)Me], 58.0 [*C*H(CO_2Et)NH], 61.4 ($CO_2CH_2CH_3$), 68.3 [*C*(CO_2Me)Me], 171.6, 172.2, 174.3 (3xCO_2); MS (EI-GC) *m/z*: 273 (M^++1, <2%), 215 (12), 214 (100), 200 (32), 140 (62), 108 (20), 99 (27), 82 (23); HRMS calculated for $C_{12}H_{19}NO_6$: 273.1212, found: 273.1214.

4.2.13. (1S,3R*,3aS*,6aR*)-Diethyl 1-benzyl-5-methyl-4,6-dioxooctahydropyrrolo[3,4-c]pyrrole-1,3-dicarboxylate (endo-cis-**3a**).* [9] Sticky pale yellow oil; IR (neat) ν_{max} 3030, 2982, 2936, 1779, 1734, 1699 cm^{-1}; ^{1}H NMR δ_H: 1.32, 1.34 (2t, *J* = 7.2 Hz, 3H, $CO_2CH_2CH_3$), 2.88, 3.30 (2d, *J* = 13.8 Hz, 2H, CH_2Ph) 2.92 (s, 3H, NCH_3), 3.38 [d, *J* = 8.0 Hz, 1H, C*H*C(CO_2Et)Bn], 3.55 [deform. dd, *J* = 8.4, 8.0 Hz, 1H, C*H*CH(CO_2Et)NH], 4.09 [d, *J* = 8.4, Hz, 1H, C*H*(CO_2Et)NH], 4.24 (q, *J* = 7.2 Hz, 2H, $CO_2CH_2CH_3$), 4.26 (q, *J* = 7.2 Hz, 2H, $CO_2CH_2CH_3$), N*H* nd;

^{13}C NMR δ_C: 14.0 (2x$CO_2CH_2CH_3$), 25.4 (NCH_3), 42.2 (CH_2Ar), 50.4 [*C*HCH(CO_2Et)NH], 56.6 [*C*HC(CO_2Et)Bn], 62.0 [*C*H(CO_2Et)NH], 62.1 ($CO_2CH_2CH_3$), 62.3 ($CO_2CH_2CH_3$) 73.6 [*C*(CO_2Et)Bn], 127.2, 128.3, 130.4, 135.7 (Ar*C*)169.6, 170.1 (2xCO_2), 175.0, 175.1 (2xCON); MS (EI-GC) *m/z*: 388 (M^++1, <1%), 315 (13), 298 (14), 297 (100), 223 (11), 166 (45), 94 (11), 91 (17); HRMS calculated for $C_{20}H_{24}N_2O_6$: 388.1634, found: 388.1631.

4.2.14. (1S,3R*,3aS*,6aR*)-Diethyl 1,5-dibenzyl-4,6-dioxoocta hydropyrrolo[3,4-c]pyrrole-1,3-dicarboxylate (endo-cis-3b).*[9] Colorless prisms, mp = 127-130 ºC (from hexane/$CDCl_3$); IR (neat) ν_{max} 3030, 2989, 1741, 1719, 1699 cm^{-1}; ^{1}H NMR δ_H: 1.23 (t, *J* = 7.2 Hz, 3H, $CO_2CH_2CH_3$), 1.28 (t, *J* = 7.2 Hz, 3H, $CO_2CH_2CH_3$), 2.89, 3.31 (2d, *J* = 13.9 Hz, 2H, CH_2Ph), 3.38 [d, *J* = 7.8 Hz, 1H, C*H*C(CO_2Et)Bn], 3.55 [deform. dd, *J* = 7.8, 7.8 Hz, 1H, C*H*CH(CO_2Et)NH], 4.03–4.27 (m, 5H, 2x$CO_2CH_2CH_3$ and C*H*(CO_2Et)NH], 4.54, 4.60 (d, *J* = 14.3 Hz, 2H), 7.20–7.35 (m, 10H, 2xCH_2*Ph*), N*H* nd; ^{13}C NMR δ_C: 14.0, 14.1 (2x$CO_2CH_2CH_3$), 42.2, 43.0 (2xCH_2Ph), 50.4 [*C*HCH(CO_2Et)NH], 56.6 [*C*HCH(CO_2Et)NH], 61.9, 62.1 (2x$CO_2CH_2CH_3$), 62.3 [*C*H(CO_2Et)NH], 73.7 [*C*Bn(CO_2Et)NH], 127.2, 128.0, 128.3, 128.6, 128.7, 130.5, 135.2, 135.8 (ArC), 169.4, 169.9 (2x$CO_2CH_2CH_3$), 174.6, 174.7 (2xCON); MS (EI-GC) *m/z*: 464 (M^++1, <1%), 391 (14), 374 (22), 373 (100), 166 (22), 91 (73); HRMS calculated for $C_{26}H_{28}N_2O_6$ – C_7H_7: 373.1400, found: 373.1401.

4.2.15. (1S,3R*,3aS*,6aR*)-Diethyl 1-benzyl-4,6-dioxo-5-phenyl octahydropyrrolo[3,4-c]pyrrole-1,3-dicarboxylate (endo-cis-**3c**).*[9] Colorless prisms, mp = 169-172 ºC (from hexane/$CDCl_3$); IR (neat) ν_{max} 2979, 2937, 1729, 1714 cm^{-1}; ^{1}H NMR δ_H: 1.25–1.30 (m, 6H, 2x$CO_2CH_2CH_3$), 2.96, 3.36 (2xd, *J* = 13.9 Hz, 2H, CH_2Ph), 3.51 (s, 1H, N*H*), 3.55 [d, *J* = 7.8 Hz, 1H, C*H*C(CO_2Et)Bn], 3.73 [deform. dd, *J* = 7.8, 7.8 Hz, 1H, C*H*CH(CO_2Et)NH], 4.15–4.30 [m, 5H, 2x$CO_2CH_2CH_3$ and C*H*(CO_2Et)NH], 7.15–7.49 (m, 10H, Ar*H*); ^{13}C NMR δ_C: 13.9, 14.0 ($CO_2CH_2CH_3$), 42.3 (CH_2Ph), 50.4 [*C*HCH(CO_2Et)NH], 56.6 [*C*HCH(CO_2Et)NH], 62.1, 62.2 (2x$CO_2CH_2CH_3$), 62.3 [*C*H(CO_2Et)NH], 74.1 [*C*Bn(CO_2Et)NH], 126.6, 127.2, 128.0, 128.2, 128.9, 129.2, 130.4, 135.6 (ArC), 169.7, 170.1 (2xCO_2), 174.0, 174.2 (2xCON); MS (EI-GC) *m/z*: 450 (M^++1, <1%), 377 (14), 360 (22), 359 (100), 207 (44), 166 (40), 156 (10), 119 (10), 94 (13), 91 (45); HRMS calculated for $C_{25}H_{26}N_2O_6$: 450.1791, found: 450.1801.

4.2.16. (2S,3S*,4S*,5R*)-5-Ethyl 2,3,4-trimethyl 2-benzylpyrrolidine-2,3,4,5-tetracarboxylate (endo-cis-**3d**).* [9] Colorless oil; IR (neat) ν_{max} 2983, 2954, 2906, 1732, 1727 cm^{-1}; ^{1}H NMR δ_H: 1.22, 1.26 (2t, *J* = 7.1 Hz, 3H, $CO_2CH_2CH_3$), 3.13, 3.37 (2d, *J* = 13.8 Hz, 2H, CH_2Ph), 3.34 [d, *J* = 10.1 Hz, 1H, C*H*C(CO_2Et)Bn], 3.65 [dd, *J* = 10.1, 8.5 Hz, 1H, C*H*CH(CO_2Et)NH], 3.70, 3.78 (2s, 3H, CO_2CH_3), 3.86 [d, *J* = 8.5 Hz, 1H, C*H*(CO_2Et)NH], 4.05–4.25 (m, 4H, 2x$CO_2CH_2CH_3$), 7.24–7.36 (m, 5H, Ar*H*), N*H* nd; ^{13}C NMR δ_C: 14.0, 14.2 (2x$CO_2CH_2CH_3$), 42.6 (CH_2Ar), 49.3 [*C*HC(CO_2Et)Bn], 52.4, 52.6 (2xCO_2CH_3), 54.8 [*C*HCH(CO_2Et)NH], 61.6 [*C*H(CO_2Et)NH], 62.0, 61.7 (2x$CO_2CH_2CH_3$), 72.3 [*C*(CO_2Et)Bn], 127.1, 128.3, 130.9, 135.9 (Ar*C*), 170.5, 171.9, 172.3, 172.9 (4xCO_2); MS (EI-GC) *m/z*: 407 (M^++1, <1%), 348 (18), 330 (48), 316 (44), 298 (100), 166 (32), 138 (11), 91 (60); HRMS calculated for $C_{20}H_{25}NO_8$: 407.1580, found: 407.1586.

4.2.17. (2R,3S*,4S*,5S*)-Diethyl 2-benzyl-3,4-bis(phenylsulfonyl) pyrrolidine-2,5-dicarboxylate (exo-cis-**3e**).* [9] Pale yellow prisms, mp = 85-86ºC (from *n*-hexane/ethyl acetate); IR (neat) ν_{max} 2971, 1741, 1235, 1149 cm^{-1}; ^{1}H NMR δ_H: 1.04 (t, *J* = 7.2 Hz, 1H, $CO_2CH_2CH_3$), 1.21 (t, *J* = 7.2 Hz, 1H, $CO_2CH_2CH_3$), 3.29, 3.40 (2xd, *J* = 14.2 Hz, 2H, CH_2Ph), 3.88–4.29 (m, 4H, 2x$CO_2CH_2CH_3$), 4.20 [C*H*(CO_2Et)NH], 4.43 (br. s, 1H, N*H*), 4.51 [d, *J* = 5.2 Hz, 1H, C*H*C(CO_2Et)Bn], 4.89 [deform. dd, *J* = 5.2, 5.2 Hz, 1H, C*H*CH(CO_2Et)NH], 7.18–7.33 (m, 5H, Ar*H*), 7.44 – 7.82 (m, 8H, Ar*H*), 7.88–7.98 (m, 2H, Ar*H*); ^{13}C NMR δ_C: 13.8, 14.0 (2x$CO_2CH_2CH_3$), 41.0 (CH_2Ph), 61.1, 62.2 (2x$CO_2CH_2CH_3$), 62.3 [CHCH(CO_2Et)NH], 69.4 [*C*HCBn(CO_2Et)NH], 72.0 [*C*H(CO_2Et)NH], 73.8 [*C*Bn(CO_2Et)NH], 127.4, 128.4, 128.8, 129.1, 129.2, 129.4, 130.7, 134.3, 134.4, 134.7, 138.5, 139.5 (Ar*C*), 169.6, 169.6 (2x*C*O_2); MS (EI-GC) *m/z*: 585 (M^++1, <1%), 512 (10), 494 (34), 370 (14), 353 (13), 352 (69), 306 (33), 298 (10), 280 (26), 235 (10), 234 (82), 157 (13), 156 (23), 141 (10), 125 (15), 112 (11), 94 (16), 91 (100), 80 (12), 77 (29); HRMS calculated for $C_{29}H_{31}NO_8S_2$–$C_3H_5O_2$: 512.1202, found: 512.1215.

4.2.18. (1R,3R*,3aS*,6aR*)-3-Ethyl 1-methyl 5-methyl-4,6-dioxo-1-phenyloctahydropyrrolo[3,4-c]pyrrole-1,3-dicarboxylate (endo-cis-**4a**).*[9] Sticky pale yellow oil; IR (neat) ν_{max} 2982, 2954, 1779, 1736, 1698 cm^{-1}; ^{1}H NMR δ_H: 1.25 (t, *J* = 7.2 Hz, 3H, $CO_2CH_2CH_3$), 2.91 (s, 3H, NCH_3), 3.37 [deform. dd, *J* = 8.5, 7.5 Hz, 1H, C*H*CHCO$_2$Et], 3.69 (s, 3H, CO_2CH_3), 3.76 [d, *J* = 8.5, 1H, C*H*(CO_2Et)NH], , 3.96 [d, *J* = 7.5, Hz, 1H, C*H*(CO_2Me)Ph], 4.20 (qd, *J* = 7.2, 1.1 Hz, 2H, $CO_2CH_2CH_3$), 7.22–7.36 (m, 3H, Ar*H*), 7.58–7.63 (m, 2H, Ar*H*), N*H* nd; ^{13}C NMR δ_C: 14.2 ($CO_2CH_2CH_3$), 25.5 (NCH_3), 50.3 [*C*HCH(CO_2Et)NH], 53.4 [*C*HC(CO_2Me)Ph], 56.5 (*C*HCO$_2$Et), 61.6 (CO_2CH_3), 62.1 ($CO_2CH_2CH_3$), 74.8 [*C*(CO_2Me)Ph], 127.4, 128.5, 128.7, 138.1 (Ar*C*), 169.6, 170.2 (2xCO_2), 175.1, 175.4 (2xCON); MS (EI-GC) *m/z*: 360 (M^++1, <1%), 302 (17), 301 (100), 228 (14), 227 (72), 170 (19), 143 (18), 142 (27); HRMS calculated for $C_{18}H_{20}N_2O_6$: 360.1321, found: 360.1322.

4.2.19. (1S,3R*,3aS*,6aR*)-3-Ethyl 1-methyl 5-methyl-4,6-dioxo-1-phenyloctahydropyrrolo[3,4-c]pyrrole-1,3-dicarboxylate (endo-trans-**4a**).*[9] Sticky pale yellow oil; IR (neat) ν_{max} 2983, 2954, 2926, 1781, 1729, 1702 cm^{-1}; ^{1}H NMR δ_H: 1.39 (t, *J* = 7.2 Hz, 3H, $CO_2CH_2CH_3$), 2.79 (s, 3H, NCH_3), 3.08 (d, *J* = 3.5 Hz, 1H, N*H*), 3.55 [deform. dd, *J* = 7.6, 7.6 Hz, 1H, C*H*CHCO$_2$Et], 3.79 (s, 3H, CO_2CH_3), 3.86 [dd, *J* = 7.6, 3.5 Hz, 1H, C*H*(CO_2Et)NH], 4.25 [d, *J* = 7.6, Hz, 1H, C*H*C(CO_2Me)Ph], 4.30–4.41 (m, 2H, $CO_2CH_2CH_3$), 7.33–7.41 (m, 3H, Ar*H*), 7.47–7.54 (m, 2H, Ar*H*); ^{13}C NMR δ_C: 14.2 ($CO_2CH_2CH_3$), 25.2 (NCH_3), 45.3 [*C*HCH(CO_2Et)NH], 50.4 [*C*HC(CO_2Me)Ph], 53.7 (*C*HCO$_2$Et), 59.8 (CO_2CH_3), 61.7 ($CO_2CH_2CH_3$), 74.1 [*C*(CO_2Me)Ph], 126.0, 128.5, 128.9, 135.4 (Ar*C*), 169.3, 173.5 (2xCO_2), 174.1, 175.6 (2xCON); MS (EI-GC) *m/z*: 360 (M^++1, <1%), 302 (18), 301 (100), 228 (13), 227 (63), 170 (20), 143 (22), 142 (30), 115 (15); HRMS calculated for $C_{18}H_{20}N_2O_6$: 360.1321, found:360.1336.

4.2.20. (2R,3S*,4S*,5R*)-5-Ethyl 2,3,4-trimethyl 2-phenylpyrrolidine-2,3,4,5-tetracarboxylate (endo-cis-**4d**).*[9] Colorless oil; IR (neat) ν_{max} 2984, 2954, 1735, 1716, 1713, 1700 cm^{-1}; ^{1}H NMR δ_H: 1.14 (t, *J* = 7.1 Hz, 3H, $CO_2CH_2CH_3$), 3.64,

3.67, 3.75 (3s, 3H, CO_2CH_3), 3.82 [dd, *J* = 10.1, 8.5 Hz, 1H, C*H*CH(CO_2Et)NH], 3.98 [d, *J* = 8.5 Hz, 1H, C*H*(CO_2Et)NH], 4.04 (q, *J* = 7.1, Hz, 2H, $CO_2CH_2CH_3$), 4.38 [d, *J* = 10.1 Hz, 1H, C*H*(CO_2Me)Ph], 7.26–7.38 (m, 2H, Ar*H*), 7.51 (dd, *J* = 8.5, 2.8 Hz, 1H, Ar*H*), 7.70 (dd, *J* = 8.5, 2.8 Hz, 2H, Ar*H*), N*H* nd; ^{13}C NMR δ_C: 14.0 ($CO_2CH_2CH_3$), 51.1, 52.3, 52.6 (3xCO_2CH_3), 53.3 [CHC(CO_2Me)Ph], 53.5 [CHCH(CO_2Et)NH], 60.7 [*C*H(CO_2Et)NH], 61.4 ($CO_2CH_2CH_3$), 75.0 [*C*(CO_2Me)Ph], 127.0, 128.1, 128.3, 140.9 (Ar*C*), 170.8, 171.3, 171.7, 172.8 (4xCO_2); MS (EI-GC) *m/z*: 393 (M^++1, <2%), 335 (19), 334 (100), 302 (24), 288 (11), 274 (35), 260 (25), 242 (13), 228 (51), 202 (25), 201 (11), 170 (11), 143 (26), 115 (16); HRMS calculated for $C_{19}H_{23}NO_8$: 393.1424, found: 393.1421.

4.2.21. (2R,3R*,4R*,5R*)-5-Ethyl 2,3,4-trimethyl 2-phenylpyrrolidine-2,3,4,5-tetracarboxylate (exo-cis-**4d**)*.[9] Colorless oil; IR (neat) ν_{max} 2990, 2950, 1748, 1733, 1730, 1715 cm^{-1}; ^{1}H NMR δ_H: 1.30 (t, *J* = 7.1 Hz, 3H, $CO_2CH_2CH_3$ CO_2Et)NH], 4.86 [d, *J* = 5.3 Hz, 1H, C*H*(CO_2Me)Ph], 4.91 [deform. dd, *J* = 5.3, 5.0 Hz, 1H, C*H*CHCO$_2$Et], 7.35–8.05 (m, 15H, Ar*H*), N*H* nd; ^{13}C NMR δ_C: 14.0 ($CO_2CH_2CH_3$), 53.2 [CH(CO_2Et)NH], 60.9 (CO_2CH_3), 62.3 ($CO_2CH_2CH_3$), 69.4 [CHCH(CO_2Et)NH], 74.6 [CHC(CO_2Me)Ph], 75.1 [*C*(CO_2Me)Ph], 128.2, 128.3, 128.6, 128.8, 128.9, 129.2, 129.3, 134.0, 134.3, 136.8, 138.6, 140.1 (Ar*C*), 170.0, 170.1 (2xCO_2); MS (EI-GC) *m/z*: 557 (M^++1, <1%), 357 (11), 356 (51), 342 (10), 310 (15), 299 (11), 298 (54), 284 (17), 283 (21), 215 (37), 158 (11), 157 (11), 144 (11), 143 (100), 142 (11), 115 (24), 77 (11); HRMS calculated for $C_{27}H_{27}NO_8S_2$:557.1168, found: 557.1173.

4.2.22. (2R,3R*,5R*)-5-Ethyl 2,3-dimethyl 2-phenylpyrrolidine-2,3,5-tricarboxylate (endo-cis-**4f**)*.[9] Yellowish oil; IR (neat) ν_{max} 2985, 2953, 1734, 1700 cm^{-1}; ^{1}H NMR δ_H: 1.29 (t, *J* = 7.1 Hz, 3H, $CO_2CH_2CH_3$), 2.29–2.36 [m, 2H, CH_2CH(CO_2Et)], 3.51 [dd, *J* = 7.6, 4.5 Hz, 1H, C*H*C(CO_2Me)Ph], 3.68, 3.70 (2s, 3H, CO_2CH_3), 3.85 [dd, *J* = 9.0, 5.7 Hz, 1H, C*H*(CO_2Et)NH], 4.23 (q, *J* = 7.1, Hz, 2H, $CO_2CH_2CH_3$), 7.25–7.35 (m, 3H, Ar*H*), 7.73–7.77 (m, 2H, Ar*H*), N*H* nd; ^{13}C NMR δ_C: 14.3 ($CO_2CH_2CH_3$), 33.8 [*C*H_2CH(CO_2Et)NH], 52.2, 52.9 (2xCO_2CH_3), 54.0 [CHC(CO_2Me)Ph], 58.6 [*C*H(CO_2Et)NH], 61.5 ($CO_2CH_2CH_3$), 75.5 [*C*(CO_2Me)Ph], 126.9, 128.1, 128.4, 140.2 (Ar*C*), 172.2, 173.1, 173.6 (3x*C*O_2); MS (EI-GC) *m/z*: 335 (M^++1, <2%), 277 (18), 276 (100), 262 (19), 202 (41), 170 (19), 144 (20), 143 (14), 115 (10), 99 (15); HRMS calculated for $C_{17}H_{21}NO_6$: 335.1369, found:335.1313.

4.2.23. (2S,3R*,5R*)-5-Ethyl 2,3-dimethyl 2-phenylpyrrolidine-2,3,5-tricarboxylate (endo-trans-**4f**)*.[9] Yellowish oil; R_f 0.29 (*n*-hexane/ethyl acetate 7/3); IR (neat) ν_{max} 2984, 2953, 1727, 1658 cm^{-1}; ^{1}H NMR δ_H: 1.30 (t, *J* = 7.1 Hz, 3H, $CO_2CH_2CH_3$), 2.36–2.46 [m, 2H, CH_2CH(CO_2Et)], 3.19, 3.72 (2s, 3H, CO_2CH_3), 3.92 [deform. dd, *J* = 8.0, 7.6 Hz, Ph1H, C*H*C(CO_2Me)Ph], 4.04 [deform. dd, *J* = 6.5, 5.9 Hz, 1H, C*H*(CO_2Et)NH], 4.26 (q, *J* = 7.1, Hz, 2H, $CO_2CH_2CH_3$), 7.24–7.37 (m, 3H, Ar*H*), 7.49–7.53 (m, 2H, Ar*H*), N*H* nd; ^{13}C NMR δ_C: 14.3 ($CO_2CH_2CH_3$), 32.7 [CH_2CH(CO_2Et)NH], 50.6, 51.5 (2xCO_2CH_3), 53.4 [CHC(CO_2Me)Ph], 58.5 [*C*H(CO_2Et)NH], 61.3 ($CO_2CH_2CH_3$), 76.0 [*C*(CO_2Me)Ph], 126.3, 128.3, 128.5, 137.5 (Ar*C*), 172.6, 173.0, 173.9 (3x*C*O_2); MS (EI-GC) *m/z*: 335 (M^++1, <2%), 277 (21), 276 (100), 262 (15), 202 (38), 201 (10), 170 (25), 144 (13), 143 (11), 115 (11), 99 (17); HRMS calculated for $C_{17}H_{21}NO_6$: 335.1369, found: 335.1308.

4.2.24. (1S,3R*,3aS*,6aR*)-Ethyl 3-(dimethoxymethyl)-5-methyl-4,6-dioxooctahydropyrrolo[3,4-c]pyrrole-1-carboxylate (endo-cis-**5a**)*. Yellow prisms, mp: 105-108ºC (from hexane/CH_2Cl_2); IR (neat) ν_{max} 2980, 1719, 1696 cm^{-1}; ^{1}H NMR δ_H: 1.35 (t, J = 7.2 Hz, 3H, $CO_2CH_2CH_3$), 2.50 (br. s, 1H, NH), 2.95 (s, 3H, NCH_3), 3.27 [deform. dd, J = 7.9, 7.6 Hz, 1H, CHCH(CH(), 3.56, 3.69, 3.72 (3s, 3H, CO_2CH_3), 3.64 [deform. dd, J = 6.9, 6.7 Hz, 1H, CHCH(CO_2Et)NH], 3.89 [d, J = 6.7 Hz, 1H, CHC(CO_2Me)Ph], 4.17 [d, J = 6.9 Hz, 1H, CH(CO_2Et)NH], 4.26 (q, J = 7.1, Hz, 2H, $CO_2CH_2CH_3$), 7.28–7.38 (m, 2H, ArH), 7.51 (dd, J = 7.0, 2.3 Hz, 1H, ArH), 7.70 (dd, J = 7.0, 2.3 Hz, 2H, ArH), NH nd; ^{13}C NMR δ_C: 14.3 ($CO_2CH_2CH_3$), 51.8, 52.6, 52.8 (3xCO_2CH_3), 53.6 [CHC(CO_2Me)Ph], 54.7 [CHCH(CO_2Et)NH], 61.6 [CH(CO_2Et)NH], 61.9 ($CO_2CH_2CH_3$), 75.2 [C(CO_2Me)Ph], 126.4, 128.1, 128.2, 139.7 (ArC), 171.1, 171.6, 172.0, 172.1 (4xCO_2); MS (EI-GC) m/z: 393 (M^++1, <1%), 335 (19), 334 (100), 303 (11), 302 (60), 274 (14), 260 (25), 242 (11), 228 (27), 202 (21), 170 (56), 143 (24), 115 (14); HRMS calculated for $C_{19}H_{23}NO_8$: 393.1424, found: 393.1426.

4.2.25. (2R,3R*,4R*,5S*)-5-Ethyl 2-methyl 2-phenyl-3,4-bis(phenylsulfonyl)pyrrolidine-2,5-dicarboxylate (exo-trans-**4e**)*.[9] Orange oil; R_f 0.10 (*n*-hexane/ethyl acetate 7/3); IR (neat) ν_{max} 2981, 2954, 2926, 1738, 1692, 1309, 1147 cm^{-1}; ^{1}H NMR δ_H: 1.04 (t, *J* = 7.2 Hz, 3H, $CO_2CH_2CH_3$), 3.74 (s, 3H, CO_2CH_3), 4.01 (q, *J* = 7.2 Hz, 2H, $CO_2CH_2CH_3$), 4.35 [d, *J* = 5.0 Hz, 1H, C*H*($OMe)_2$)NH], 3.40 [dd, *J* = 7.6, 4.8 Hz, 1H, C*H*CH($OMe)_2$NH], 3.42, 3.54 (2s, 6H, 2xOCH_3), 3.51 [deform. dd, *J* = 7.9, 7.6 Hz, 1H, C*H*CH(CO_2Et)NH], 3.85 [d, *J* = 7.6 Hz, 1H, C*H*(CO_2Et)NH], 4.30 (q, *J* = 7.2 Hz, 2H, $CO_2CH_2CH_3$), 4.69 [d, *J* = 4.8 Hz, 1H, C*H*($OMe)_2$]; ^{13}C NMR δ_C: 14.2 ($CO_2CH_2CH_3$), 25.2 (NCH_3), 45.5 [*C*HCH($OMe)_2$NH], 49.1 [*C*HCH(CO_2Et)NH], 55.8, 56.0 (2xOCH_3), 61.7 ($CO_2CH_2CH_3$), 62.3 [*C*H(CH($OMe)_2$)NH], 63.4 [*C*H(CO_2Et)NH], 102.6 [*C*H($OMe)_2$], 169.6 (*C*O_2Et), 175.6, 175.9 (2xCON); MS (EI-GC) *m/z*: 300 (M^+, <1%), 269 (13), 225 (27), 195 (34), 179 (10), 151 (18), 94 (16), 75 (100); HRMS calculated for $C_{13}H_{20}N_2O_6$+1: 301.1399, found: 301.1399.

4.2.26. (1S,3R*,3aS*,6aR*)-Ethyl 5-benzyl-3-(dimethoxymethyl)-4,6-dioxooctahydropyrrolo[3,4-c]pyrrole-1-carboxylate (endo-cis-**5b**)*. Sticky pale yellow oil; IR (neat) ν_{max} 2968, 2308, 1716, 1695 cm^{-1}; ^{1}H NMR δ_H: 1.32 (t, J = 7.2 Hz, 3H, $CO_2CH_2CH_3$), 2.50 (br. s, 1H, NH), 3.16, 3.47 (2s, 6H, 2xOCH_3), 3.25 [deform. dd, J = 8.0, 7.7 Hz, 1H, CHCH(CH($OMe)_2$)NH], 3.40 [dd, J = 8.0, 4.0 Hz, 1H, CHCH($OMe)_2$NH], 3.51 [deform. dd, J = 7.7, 7.6 Hz, 1H, CHCH(CO_2Et)NH], 3.87 [d, J = 7.6 Hz, 1H, CH(CO_2Et)NH], 4.29 (q, J = 7.2 Hz, 2H, $CO_2CH_2CH_3$), 4.54 (d, J = 14.3 Hz, 1H, NCHHPh), 4.65 [d, J = 4.0 Hz, 1H, CH($OMe)_2$], 4.68 (d, J = 14.3 Hz, 1H, NCHHPh) 7.23-7.34 (m, 5H, ArH); ^{13}C NMR δ_C: 14.2 ($CO_2CH_2CH_3$), 42.7 (NCH_2Ph), 46.8 [CHCH(CH($OMe)_2$)NH], 49.4 [CHCH(CO_2Et)NH], 55.4, 55.7 (2xOCH_3), 61.6 ($CO_2CH_2CH_3$), 62.7 [CH(CH($OMe)_2$)NH], 63.7

[$CH(CO_2Et)NH$], 102.0 [$CH(OMe)_2$], 127.9, 128.5, 128.6, 135.6 (ArC), 169.4 (CO_2Et), 175.3, 175.5 (2xCON); MS (EI-GC) m/z: 376 (M^+, <1%), 301 (29), 271 (15), 243 (10), 227 (18), 94 (10), 75 (100); HRMS calculated for $C_{19}H_{24}N_2O_6$+1: 377.1712, found: 377.1701.

4.2.27. (1S,3R*,3aS*,6aR*)-Ethyl 3-(dimethoxymethyl)-4,6-dioxo-5-phenyloctahydropyrrolo[3,4-c]pyrrole-1-carboxylate (endo-cis-**5c**).* Yellowish prisms, mp: 98-102ºC (from hexane/CH_2Cl_2); IR (neat) ν_{max} 2995, 2939, 2310, 1718, 1700 cm^{-1}; ^1H NMR δ_H: 1.32 (t, J = 7.2 Hz, 3H, $CO_2CH_2CH_3$), 2.55 (br. s, 1H, NH), 3.39 (s, 3H, OCH_3), 3.43 [deform. dd, J = 7.7, 7.2 Hz, 1H, $CHCH(CH(OMe)_2)NH$], 3.50-3.55 (m, 4H, $CHCH(OMe)_2NH$, OCH_3), 3.66 [deform. dd, J = 7.7, 7.2 Hz, 1H, $CHCH(CO_2Et)NH$], 3.97 [d, J = 7.7 Hz, 1H, $CH(CO_2Et)NH$], 4.28 (q, J = 7.2 Hz, 2H, $CO_2CH_2CH_3$), 4.79 [d, J = 4.0 Hz, 1H, $CH(OMe)_2$], 7.24-7.51 (m, 5H, ArH); ^{13}C NMR δ_C: 14.2 ($CO_2CH_2CH_3$), 47.1 [$CHCH(CH(OMe)_2)NH$], 49.5 [$CHCH(CO_2Et)NH$], 55.8, 55.9 (2xOCH$_3$), 61.8 ($CO_2CH_2CH_3$), 62.9 [$CH(CH(OMe)_2)NH$], 64.1 [$CH(CO_2Et)NH$], 102.2 [$CH(OMe)_2$], 126.7, 128.9, 129.3, 131.9 (ArC), 169.6 (CO_2Et), 174.8, 175.0 (2xCON); MS (EI-GC) m/z: 362 (M^+, <1%), 331 (11), 287 (29), 257 (24), 94 (21), 75 (100); HRMS calculated for $C_{18}H_{22}N_2O_6$+1: 363.1556, found: 363.1550.

4.2.28. (1S,3R*,3aS*,6aR*)-Methyl 3-(dimethoxymethyl)-1,5-dimethyl-4,6-dioxooctahydropyrrolo[3,4-c]pyrrole-1-carboxylate (endo-cis-**6a**).* Yellow solid, mp: 120-123ºC (from hexane/CH_2Cl_2); IR (neat) ν_{max} 2976, 1720, 1702 cm^{-1}; ^1H NMR δ_H: 1.47 [s, 3H, $C(CO_2CH_3)CH_3$], 2.92 (s, 3H, NCH_3), 3.20 [d, J = 7.7 Hz, 1H, $CHC(CO_2Me)CH_3$], 3.34 [deform. dd, J = 8.6, 7.7 Hz, 1H, $CHCH(CH(OMe)_2)NH$], 3.38 3.51 (2s, 6H, 2xOCH$_3$), 3.68 (dd, J = 8.6, 3.0 Hz, 1H, $CHCH(OMe)_2NH$), 3.83 (s, 3H, CO_2CH_3), 4.76 [d, J = 3.0 Hz, 1H, $CH(OMe)_2$], NH nd; ^{13}C NMR δ_C: 24.1 [$C(CO_2CH_3)CH_3$], 25.1 (NCH_3), 47.6 [$CHCH(CH(OMe)_2)NH$], 52.9 [$CHC(CO_2Me)CH_3$], 55.7, 56.0 (2xOCH$_3$), 56.7 (CO_2CH_3), 62.4 [$CH(CH(OMe)_2)NH$], 68.3 [$C(CO_2Me)CH_3$], 101.9 [$CH(OMe)_2$], 172.3 (CO_2Me), 175.7, 176.1 (2xCON); MS (EI-GC) m/z: 300 (M^+, <1%), 241 (13), 225 (37), 209 (24), 165 (40), 108 (20), 75 (100); HRMS calculated for $C_{13}H_{20}N_2O_6$+1: 301.1399, found: 301.1392.

4.2.29. (2S,3S*,4S*,5R*)-Trimethyl 5-(dimethoxymethyl)-2-methylpyrrolidine-2,3,4-tricarboxylate (endo-cis-**6d**).* Sticky pale yellow oil; IR (neat) ν_{max} 2987, 1715, 1713, 1692 cm^{-1}; ^1H NMR δ_H: 1.60 [s, 3H, $C(CO_2CH_3)CH_3$], 3.25 [deform. dd, *J* = 10.5, 8.3 Hz, 1H, $CHCH(CH(OMe)_2)NH$], 3.34 [d, *J* = 10.5 Hz, 1H, $CHC(CO_2Me)CH_3$], 3.40 (s, 6H, 2xOCH_3), 3.60 (dd, *J* = 8.3, 6.2 Hz, 1H, $CHCH(OMe)_2NH$), 3.68 (s, 6H, 2xCO_2CH_3), 3.74 (s, 3H, CO_2CH_3), 4.33 [d, *J* = 6.2 Hz, 1H, $CH(OMe)_2$], N*H* nd; ^{13}C NMR δ_C: 25.6 [$C(CO_2CH_3)CH_3$], 49.2 [*C*HCH(CH(OMe)$_2$)NH], 52.2 [*C*HC(CO$_2$Me)CH$_3$], 52.3, 52.4 (2xOCH$_3$), 54.5, 55.5, 58.0 (3xCO_2CH_3), 62.3 [*C*H(CH(OMe)$_2$)NH], 67.9 [*C*(CO$_2$Me)CH$_3$], 106.1 [CH(OMe)$_2$], 171.0, 173.4, 174.4 (3x*C*O$_2$Me); MS (EI-GC) *m/z*: 333 (M^+, <1%), 258 (11), 215 (15), 200 (12), 156 (31), 75 (100); HRMS calculated for $C_{14}H_{23}NO_8$+1: 334.1502, found: 334.1525.

4.2.30. (1S,3R*,3aS*,6aR*)-Ethyl 1-benzyl-3-(dimethoxymethyl)-5-methyl-4,6-dioxooctahydropyrrolo[3,4-c]pyrrole-1-carboxylate (endo-cis-**7a**).* Yellowish prisms, mp: 85-88ºC (from hexane/CH_2Cl_2); IR (neat) ν_{max} 2988, 2335, 1717, 1699 cm^{-1}; ^1H NMR δ_H: 1.34 (t, J = 7.2 Hz, 3H, $CO_2CH_2CH_3$), 2.79 (br s, 1H, NH), 2.92 (d, J = 13.7 Hz, 1H, CHHPh), 2.93 (s, 3H, NCH_3), 3.30-3.35 [m, 6H, CHHPh, $CHCH(CH(OMe)_2)NH$, $CHC(CO_2Et)BnNH$, OCH_3], 3.49 (s, 3H, OCH_3), 3.66 [m, 1H, $CHCH(OMe)_2NH$], 4.26 (q, J = 7.2 Hz, 2H, $CO_2CH_2CH_3$), 4.68 [d, J = 4.1 Hz, 1H, $CH(OMe)_2$], 7.19-7.30 (m, 5H, ArH); ^{13}C NMR δ_C: 14.2 ($CO_2CH_2CH_3$), 24.2 (NCH_3), 41.0 [$CHC(CO_2Et)BnNH$], 47.1 [$CHCH(CH(OMe)_2)NH$], 55.0 (CH_2Ph), 55.7, 55.8 (2xOCH$_3$), 61.5 ($CO_2CH_2CH_3$), 61.9 [$CH(CH(OMe)_2)NH$], 74.2 [$C(CO_2Et)BnNH$], 102.1 [$CH(OMe)_2$], 127.3, 128.5, 130.2, 135.8 (ArC), 170.7 (CO_2Et), 175.5, 175.9 (2xCON); MS (EI-GC) m/z: 390 (M^+, <1%), 315 (26), 299 (27), 285 (13), 269 (14), 268 (14), 267 (100), 91 (13), 75 (13); HRMS calculated for $C_{20}H_{26}N_2O_6$+1: 391.1869, found: 391.1875.

*4.2.31. (1S,3R,3aS,6aR)-Ethyl 1,5-dibenzyl-3-(dimethoxymethyl)-4,6-dioxooctahydropyrrolo[3,4-c]pyrrole-1-carboxylate (endo-cis-**7b**).* Yellowish prisms, mp: 92-94ºC (from hexane/CH_2Cl_2); IR (neat) ν_{max} 2996, 2938, 2310, 1715, 1700 cm^{-1}; ^1H NMR δ_H: 1.29 (t, J = 7.2 Hz, 3H, $CO_2CH_2CH_3$), 2.86 (br s, 1H, NH), 2.92 (d, J = 13.8 Hz, 1H, CHHPh), 3.08, 3.41 (2s, 6H, 2xOCH$_3$), 3.28-3.35 [m, 3H, CHHPh, $CHCH(CH(OMe)_2)NH$, $CHC(CO_2Et)BnNH$], 3.63 [dd, J = 7.4, 3.8 Hz, 1H, $CHCH(OMe)_2NH$], 4.23 (q, J = 7.2 Hz, 2H, $CO_2CH_2CH_3$), 4.54, 4.66 (d, J = 14.4 Hz, 2H, NCH_2Ph), 4.61 [d, J = 3.8 Hz, 1H, $CH(OMe)_2$], 7.20-7.33 (m, 10H, ArH); ^{13}C NMR δ_C: 14.1 ($CO_2CH_2CH_3$), 41.1, 42.7 (CH_2Ph, NCH_2Ph), 47.1 [$CHC(CO_2Et)BnNH$], 54.5 [$CHCH(CH(OMe)_2)NH$], 55.4, 55.6 (2xOCH$_3$), 61.8 [$CH(CH(OMe)_2)NH$], 62.0 ($CO_2CH_2CH_3$), 72.5 [$C(CO_2Et)BnNH$], 101.7 [$CH(OMe)_2$], 127.2, 127.9, 128.4, 128.5, 128.6, 130.2, 135.6, 135.9 (ArC), 170.6 (CO_2Et), 175.2, 175.5 (2xCON); MS (EI-GC) m/z: 466 (M^+, <1%), 308 (12), 307 (55), 290 (16), 289 (100), 281 (11), 215 (14), 207 (21), 187 (12), 174 (15), 119 (11), 91 (64); HRMS calculated for $C_{26}H_{30}N_2O_6$+1: 467.2182, found: 467.2175.

4.2.32. (1S,3R*,3aS*,6aR*)-Ethyl 1-benzyl-3-(dimethoxymethyl)-4,6-dioxo-5-phenyloctahydropyrrolo[3,4-c]pyrrole-1-carboxylate (endo-cis-**7c**).* Yellowish solid, mp: 118-121ºC (from hexane/CH_2Cl_2); IR (neat) ν_{max} 2992, 2945, 2315, 1718, 1689 cm^{-1}; ^1H NMR δ_H: 1.33 (t, J = 7.2 Hz, 3H, $CO_2CH_2CH_3$), 3.01, 3.39 (2d, J = 13.7 Hz, 2H, CH_2Ph), 3.34, (s, 3H, OCH_3), 3.47-3.53 [m, 5H, $CHCH(CH(OMe)_2)NH$, $CHC(CO_2Et)BnNH$, OCH_3], 3.74 [dd, J = 7.8, 3.4 Hz, 1H, $CHCH(OMe)_2NH$], 4.26 (qd, J = 7.2, 2.1 Hz, 2H, $CO_2CH_2CH_3$), 4.82 [d, J = 3.8 Hz, 1H, $CH(OMe)_2$], 7.23-7.50 (m, 10H, ArH), NH nd; ^{13}C NMR δ_C: 14.0 ($CO_2CH_2CH_3$), 41.3 (CH_2Ph), 47.5 [$CHC(CO_2Et)BnNH$], 54.7 [$CHCH(CH(OMe)_2)NH$], 55.6, 56.0 (2xOCH$_3$), 62.0 [$CH(CH(OMe)_2)NH$], 62.2 ($CO_2CH_2CH_3$), 72.8 [$C(CO_2Et)BnNH$], 101.6 [$CH(OMe)_2$], 126.6, 127.2, 128.3, 128.8, 129.2, 130.2, 131.8, 135.8 (ArC), 170.6 (CO_2Et), 174.6, 174.9 (2xCON); MS (EI-GC) m/z: 452 (M^+, <1%), 315 (23), 299 (24), 285 (13), 269 (15), 268 (15), 267 (100), 241 (10), 91 (29),

75 (35); HRMS calculated for $C_{25}H_{28}N_2O_6$+1: 453.2025, found: 453.2014.

4.2.33. (2S,3R*,4R*,5R*)-2-Ethyl 3,4-dimethyl 2-benzyl-5-(dimethoxymethyl)pyrrolidine-2,3,4-tricarboxylate (exo-cis-**7d**).* Sticky pale yellow oil; IR (neat) ν_{max} 2985, 2947, 1714, 1712, 1691 cm^{-1}; ^1H NMR δ_H: 1.26 (t, *J* = 7.1 Hz, 3H, $CO_2CH_2CH_3$), 2.76, 2.95 (d, *J* = 13.0 Hz, 2H, CH_2Ph), 3.29, 3.34 (s, 6H, 2xOCH_3), 3.68-3.73 [m, 6H, C*H*CH(CH(OMe)$_2$)NH, C*H*C(CO_2Et)BnNH, C*H*CH(OMe)$_2$NH, CO_2CH_3], 3.79 (s, 3H, CO_2CH_3), 4.07-4.23 [m, 3H, C*H*(OMe)$_2$, $CO_2CH_2CH_3$], 7.16-7.22 (m, 5H, Ar*H*), N*H* nd; ^{13}C NMR δ_C: 14.2 ($CO_2CH_2CH_3$), 42.0 (CH_2Ph), 47.9 [*C*HC(CO_2Et)BnNH], 52.0 [CHCH(CH(OMe)$_2$)NH], 52.4, 53.1 (2x$COCH_3$), 54.5, 54.8 (2xOCH_3), 59.7 [*C*H(CH(OMe)$_2$)NH], 61.7 ($CO_2CH_2CH_3$), 69.9 [*C*(CO_2Et)BnNH], 103.8 [*C*H(OMe)$_2$], 126.8, 128.0, 130.6, 136.3 (ArC), 171.3, 171.6 (2xCO_2Me), 174.1 (*C*O_2Et); MS (EI-GC) *m/z*: 423 (M^+, <1%), 392 (14), 350 (19), 348 (45), 332 (36), 318 (21), 317 (13), 316 (68), 301 (11), 300 (76), 288 (39), 286 (11), 268 (59), 258 (26), 256 (15), 242 (16), 240 (15), 226 (20), 224 (11), 216 (11), 210 (18), 196 (13), 194 (17), 166 (11), 91 (100), 75 (28); HRMS calculated for $C_{21}H_{29}NO_8$+1: 424.1971, found: 424.1968.

4.2.34. (2S,3S*,4S*,5R*)-2-ethyl 3,4-dimethyl 2-benzyl-5-(dimethoxymethyl)pyrrolidine-2,3,4-tricarboxylate (endo-cis-**8d**).* Sticky pale yellow oil; IR (neat) ν_{max} 2987, 2955, 1719, 1716, 1696 cm^{-1}; ^1H NMR δ_H: 1.24 (t, *J* = 7.1 Hz, 3H, $CO_2CH_2CH_3$), 2.61 (br s, 1H, N*H*), 3.12-1.19 [m, 2H, C*H*HPh, C*H*CH(CH(OMe)$_2$)NH], 3.29-3.40 [m, 9H, C*H*HPh, C*H*C(CO_2Et)BnNH, C*H*CH(OMe)$_2$NH, 2xOCH_3], 3.69 (s, 3H, CO_2CH_3), 3.77 (s, 3H, CO_2CH_3), 4.05-4.15 [m, 2H, $CO_2CH_2CH_3$], 4.36 [d, *J* = 6.4 Hz, 1H, C*H*(OMe)$_2$], 7.17-7.27 (m, 5H, Ar*H*); ^{13}C NMR δ_C: 14.1 ($CO_2CH_2CH_3$), 43.1 (CH_2Ph), 49.0 [CHC(CO_2Et)BnNH], 52.2, 52.3 (2x$COCH_3$), 53.8 [CHCH(CH(OMe)$_2$)NH], 55.2, 55.7 (2xOCH_3), 61.7 [CH(CH(OMe)$_2$)NH], 61.9 ($CO_2CH_2CH_3$), 72.0 [C(CO_2Et)BnNH], 105.9 [CH(OMe)$_2$], 127.1, 128.3, 130.7, 136.1 (ArC), 171.1, 173.1 (2xCO_2Me), 173.4 (*C*O_2Et); MS (EI-GC) *m/z*: 423 (M^+, <1%), 348 (11), 333 (11), 332 (65), 316 (33), 300 (45), 288 (46), 286 (11), 268 (61), 258 (33), 256 (14), 242 (14), 240 (17), 226 (21), 216 (12), 210 (17), 194 (16), 166 (10), 91 (100), 75 (27); HRMS calculated for $C_{21}H_{29}NO_8$+1: 424.1971, found: 424.1959.

4.2.35. (3R,3aS*,6aR*)-Diethyl 3-(dimethoxymethyl)-5-methyl-4,6-dioxohexahydropyrrolo[3,4-c]pyrrole-1,1(2H)-dicarboxylate (all-cis-**8**).* Sticky pale yellow oil; IR (neat) ν_{max} 2999, 1718, 1713, 1691 cm^{-1}; ^1H NMR δ_H: 1.29 (t, J = 7.1 Hz, 3H, $CO_2CH_2CH_3$), 1.33 (t, J = 7.1 Hz, 3H, $CO_2CH_2CH_3$), 2.97 (s, 3H, NCH_3), 3.32 (deform. dd, J = 7.8, 7.5 Hz, 1H, CHCHNH), 3.42, 3.54 (2s, 6H, 2xOCH_3), 4.08 [d, J = 7.5 Hz, 1H, CHC(CO_2Et)$_2$NH], 4.18-4.40 (m, 5H, CHNH, 2x$CO_2CH_2CH_3$), 4.56 [d, J = 6.1 Hz, 1H, CH(OMe)$_2$], NH nd; ^{13}C NMR δ_C: 14.1, 14.2 (2x$CO_2CH_2CH_3$), 25.4 (NCH_3), 45.5 (CHCHNH), 50.6 [CHC(CO_2Et)$_2$NH], 55.5, 56.2 (2xOCH_3), 60.9 (CHNH), 62.6, 62.9 (2x$CO_2CH_2CH_3$), 74.1 [C(CO_2Et)$_2$], 103.5 [CH(OMe)$_2$], 166.9, 169.3 (2xCO_2Et), 175.2, 175.4 (2xCON); MS (EI-GC) m/z: 372 (M^+, <1%), 341 (14), 299 (24), 298 (10), 297 (52), 268 (10), 267 (65), 166 (30), 75 (100); HRMS calculated for $C_{16}H_{24}N_2O_8^{+1}$: 373.1611, found: 373.1599.

Acknowledgments

This work has been supported by the DGES of the Spanish Ministerio de Ciencia e Innovación (MICINN) (Consolider INGENIO 2010 CSD2007-00006, CTQ2010-20387), FEDER Generalitat Valenciana (PROMETEO/2009/039), and by the University of Alicante.

Notes and references

[a] Department of Organic Chemistry and Institute of Organic Synthesis.Faculty of Sciences, University of Alicante, E-03080 Alicante, Spain.
Fax: +34 965903549.
E-mail: cnajera@ua.es, jmsansano@ua.es

 # Dedicated to Prof. Max Malacria on the occasion of his 65th birthday

§ Electronic Supplementary Information (ESI) available: [details of any supplementary information available should be included here]. See DOI: 10.1039/b000000x/

1 For recent reviews, see: (*a*) Multicomponent Reactions, (Eds. J. Zhu and H. Bienaymé), Wiley-VCH, Weinheim, 2005; (*b*) G. Guillena, D. J. Ramón, and M. Yus, *Tetrahedron: Asymmetry* 2007, **18**, 693-700; (*c*) L. H. Choudhury, and T. Parvin, *Tetrahedron*, 2011, **67**, 8213-8228; (*d*) H. Pellissier, *Adv. Synth. Catal*. 2012, **354**, 237-294; (*e*) S. S. Van Berkel, B. G. M. Bögels, M. A. Wijdeven, B. Westermann, and F. P. J. T. Rutjes, *Eur. J. Org. Chem*. 2012, 3543-3559; (*f*) G. van der Heijden, E. Ruijter, and R. V. A. Orru, *Synlett* 2013, 24, 666-685; (*g*) S. Brauch, S. S. van Berkel, and B. Westermann, *Chem. Soc. Rev.*, 2013, **42**, 4948-4692.

2 For a very recent review, see: B. M. Trost, *Handbook of Green Chemistry* 2012, **7**, 1-33.

3 Catalysis from A to Z: A Concise Encyclopedia (Eds.: B. Cornils, W. A. Herrmann, M. Muhler, and C.-H. Wong), Wiley-VCH, Weinheim, 2013.

4 Cycloaddition Reactions in Organic Synthesis (Eds.: S. Kobayashi, and K. A. Jorgensen), Wiley-VCH, Weinheim, 2002.

5 For general reviews dealing with general 1,3-DC, see: (*a*) Synthetic Applications of 1,3-Dipolar Cycloaddition Chemistry Toward Heterocycles and Natural Products, (Eds. A. Padwa, W. H. Pearson), John Wiley & Sons, New Jersey, 2003; (*b*) C. Nájera, J. M. Sansano, *Curr. Org. Chem.* 2003, **7**, 1105-1150; (*c*) W. Eberbach, *Sci. Synth.* 2004, **27**, chp. 11, 441-498; (*d*) I. Coldham, and R. Hufton, *Chem. Rev*. 2005, **105**, 2765-2810; (*e*) V. Nair, and T. D. Suja, *Tetrahedron* 2007, **63**, 12247-12275; (*f*) A. Padwa, and S. K. Bur, *Tetrahedron* 2007, **63**, 5341-5378.

6 This can be exemplified by the numerous asymmetric 1,3-DC reported. For recent reviews, see: (*a*) H. Pellissier, *Tetrahedron* 2007, **63**, 3235-3285; (*b*) C. Nájera, and J. M. Sansano in *Topics in Heterocyclic Chemistry*, *vol. 12* (Ed.: A. Hassner), Springer-Verlag: Berlin-Heidelberg, 2008, pp. 117-145; (*c*) L. M. Stanley,

and M. P. Sibi, *Chem. Rev.* 2008, **108**, 2887-2902; (*d*) M. Álvarez-Corral, M. Muñoz-Dorado, and I. Rodríguez-García, *Chem. Rev.* 2008, **108**, 3174-3198; (*e*) M. Naodovic, and H. Yamamoto, *Chem. Rev*. 2008, 108, 3132-3148; (*f*) C. Nájera, J. M. Sansano, and M. Yus, *J. Braz. Chem. Soc*. 2010, **21**, 377-412; (*g*) M. Kissane, and A. R. Maguire, *Chem. Soc. Rev*. 2010, **39**, 845-883; (*h*) J. Adrio, J. C. Carretero, *Chem. Commun*. 2011, **47**, 6784-6794.

7 See for example: (*a*) I. Ibrahem, R. Ríos, J. Vesely, and A. Córdova, *Tetrahedron Lett*. 2007, **48**, 6252-6257; (*b*) W.-J. Liu, X.-H. Chen, and L.-Z. Gong, *Org. Lett.* 2008, **10**, 5357-5360; (*c*) X.-H. Chen, W. Q. Zhang, and L.-Z. Gong, *J. Am. Chem. Soc*. 2008, **130**, 5652-5653; (*d*) X.-H. Chen, Q. Wei, S.-W. Luo, H. Xiao, and L.-Z. Gong, *J. Am. Chem. Soc.* 2009, **131**, 13819-13825; (*f*) J. Yu, L. He, X.-H. Chen, J. Song, W.-J. Chen, and L.-Z. Gong, *Org. Lett*. 2009, **11**, 4946-4949; (*g*) N. Li, J. Song, X.-F. Tu, B. Liu, X.-H. Chen, and L.-Z. Gong, *Org. Biomol. Chem.* 2010, **8**, 2016-2019; (*h*) A. Iza, L. Carrillo, J. L. Vicario, D. Badía, E. Reyes, and J. I. Martínez, *Org. Biomol. Chem*. 2010, 8, 2238-2244; (*i*) M. Martín-Rodríguez, C. Nájera, J. M. Sansano, P. R. R. Costa, E. Crizanto de Lima, and A. G. Dias, *Synlett* 2010, 962-967; (*j*) M. R. Chaulagain and Z. D. Aron, *J. Org. Chem*. 2010, **75**, 8271-8274; (*k*) F. Shi, S.-W. Luo, Z.-L. Tao, J. Yu, S.-J. Tu and L.-Z. Gong, *Org. Lett*. 2011, **13**, 4680-4683; (*l*) F. Shi, S.-W. Luo, Z.-L. Tao, L. He, S.-J. Tu, and L.-Z. Gong *Org. Lett.* 2011, **13**, 4680-4683; (*m*) L. He, X.-H. Chen, D.-N. Wang, S.-W. Luo, W.-Q. Zhang, J. Yu, L. Ren, and L.-Z. Gong, *J. Am. Chem. Soc.* 2011, **133**, 13504-13518; (*n*) F. Shi, Z.-L. Tao, J. Yu and S.-J. Tu, *Tetrahedron: Asymmetry*, 2011, **22**, 2056-2064. (*o*) S. Reboredo, E. Reyes, J. L. Vicario, D. Badía, L. Carrillo, A. de Cózar, and F. P. Cossío, *Chem. Eur. J*. 2012, **18**, 7179 - 7188; (*p*) F. Shi, S.-W. Luo, S.-J. Tu, and L.-Z. Gong *Chem. Eur. J*. 2012, **18**, 6885-6894; (*q*) F. Shi, G.-J. Xing, W. Tan, R.-Y. Zhu, and S. Tu, *Org. Biomol. Chem.* 2013, **11**, 1482-1489; (*r*) L. Tian, X.-Q. Hu, Y.-H. Li, and P.-F. Xu, *Chem. Commun*. 2013, **49**, 7213-7215.

8 (*a*) M. I. Calaza, and C. Cativiela, *Eur. J. Org. Chem*. 2008, 3427-3488; (*b*) X. Companyó, A. N. Alba, and R. Ríos, *Targets in Heterocyclic Systems, vol 13*, (Eds.: O. A. Attanasi, D. Spinelli), RSC, Cambridge 2009, pp. 147-185; (*c*) *Privileged Ligands and Catalysts*, (Ed. Q.-L. Zhou), Wiley-VCH, Weinheim, 2011; (*d*) C. Nájera, J. M. Sansano, *L'Actualité Chim.* 2013, **370**, 28-30.

9 C. Wittland, U. Flörke, and N. Risch, *Synthesis* 1997, 1291-1295.

10 N. G. Argyropoulos, V. C. Sarli, and M. Gdaniec, *Eur. J. Org. Chem*. 2006, 3738-3745.

11 For a recent work using thermal induced multicomponent 1,3-DC with ethyl glyoxylate, see: J. Mancebo-Aracil, C. Nájera, and J. M. Sansano, *Org. Biomol. Chem.* 2013, **11**, 662-675.

SUPPORTING INFORMATION

Table of contents

1. General

The structurally most important peaks of the IR spectra (recorded using a Nicolet 510 P-FT and a Jasco FTIR 4100) are listed. ^{1}H NMR (300 MHz) and ^{13}C NMR (75 MHz) spectra were obtained using a Bruker AC-300 with $CDCl_3$ as solvent and TMS as internal standard unless otherwise stated. Low-resolution electron impact (GC-EI) mass spectra were obtained at 70 eV using a Shimadzu QP-5000, and high-resolution mass spectra were obtained using a Finnigan VG Platform. HRMS (GC-EI) were recorded using a Finnigan MAT 95S instrument. Analytical TLC was performed using Schleicher & Schuell F1400/LS silica gel plates, and the spots were visualized under UV light (λ=254 nm). Melting points were determined with a Reichert Thermovar hot plate apparatus and are uncorrected. For flash chromatography, we employed Merck silica gel 60 (0.040–0.063 mm).

2. General procedure for the microwave-assisted synthesis of cycloadducts

Ethyl glyoxylate (100 μL, 0.5 mmol, 50% in toluene) or dimethoxyacetaldehyde (75μL, 0.5 mmol, 50% in water), diethyl aminomalonate hydrochloride or the amino acid ethyl ester hydrochloride (0.5 mmol), the corresponding dipolarophile (0.5 mmol), AgOAc (4.1 mg, 0.025 mmol) and triethylamine (90 μL, 0.55 mmol) were dissolved in toluene (4 mL). The reaction vessel was covered with an aluminum foil in order to prevent the light exposure. Once the reaction was judged complete after a TLC test the solvent was evaporated under reduced pressure and the residue was dissolved in ethyl acetate, washed with brine and dried over $MgSO_4$. After evaporation the residue was purified by flash chromatography (silica gel) to afford the corresponding product.

(1*R,3*S**,3a*R**,6a*S**)-Diethyl 5-methyl-4,6-dioxooctahydro pyrrolo[3,4-*c*]pyrrole-1,3-dicarboxylate *endo*-*cis*-1a:**[1] Sticky yellow oil; IR (neat) ν_{max} 2984, 1699, 1595 cm^{-1}; ^{1}H NMR δ_H: 1.33 (t, *J* = 7.2 Hz, 6H, 2x$CO_2CH_2CH_3$), 2.94 (s, 3H, NCH_3), 3.57 [m, 2H, 2x*CH*CH(CO_2Et)NH], 3.97 [m, 2H, 2x*CH*(CO_2Et)NH], 4.30 (q, *J* = 7.2 Hz, 4H, 2x$CO_2CH_2CH_3$), N*H* nd; ^{13}C NMR δ_C: 14.2 (2x$CO_2CH_2CH_3$), 25.5 (NCH_3), 50.0 [2x*C*HCH(CO_2Et)NH], 61.9

(2x$CO_2CH_2CH_3$), 63.1 [2x*C*H(CO_2Et)NH], 169.0 (2x*C*$O_2CH_2CH_3$), 175.0 (2xCON); MS (EI-GC) *m/z*: 298 (M^++1, 1%), 226 (12), 225 (100), 179 (32), 151 (53), 94 (44), 67 (12); HRMS calculated for $C_{13}H_{18}N_2O_6$: 298.1155, found: 298.1148.

(1*R,3*R**,3a*R**,6a*S**)-Diethyl 5-methyl-4,6-dioxooctahydro pyrrolo[3,4-*c*]pyrrole-1,3-dicarboxylate *endo-trans*-1a:[1]** Sticky yellow oil; IR (neat) ν_{max} 2984, 1774, 1731, 1595 cm^{-1}; ^{1}H NMR δ_H: 1.33 (t, *J* = 7.2 Hz, 3H, $CO_2CH_2CH_3$), 1.35 (t, *J* = 7.2 Hz, 3H, $CO_2CH_2CH_3$), 2.98 (s, 3H, NCH_3), 3.56 [deform. dd, *J* = 8.0, 8.0 Hz, 1H, C*H*CH(CO_2Et)NH], 3.64 [dd, *J* = 8.0, 1.2 Hz, 1H, C*H*CH(CO_2Et)NH], 4.13 [d, *J* = 8.0 Hz, 1H, C*H*(CO_2Et)NH], 4.24 (q, *J* = 7.2 Hz, 2H, $CO_2CH_2CH_3$), 4.27–4.35 (m, 3H, $CO_2CH_2CH_3$ and C*H*(CO_2Et)NH], N*H* nd; ^{13}C NMR δ_C: 14.2, 14.3 (2x$CO_2CH_2CH_3$), 25.5 (NCH_3), 47.6 [*C*HCH(CO_2Et)NH], 48.8 [*C*HCH(CO_2Et)NH], 61.8, 62.0 (2x$CO_2CH_2CH_3$), 62.2 [*C*H(CO_2Et)NH], 62.4 [*C*H(CO_2Et)NH], 169.7, 171.7 (2x*C*O_2), 175.4, 176.6 (2xCON); MS (EI-GC) *m/z*: 298 (M^++1, 1%), 226 (12), 225 (100), 179 (17), 151 (40), 94 (40), 68 (10), 67 (13),; HRMS calculated for $C_{13}H_{18}N_2O_6$: 298.1155, found: 298.1148

(1*R,3*S**,3a*R**,6a*S**)-Diethyl 5-benzyl-4,6-dioxooctahydro pyrrolo[3,4-*c*]pyrrole-1,3-dicarboxylate *endo-cis*-1b:[1]** Sticky yellow oil; IR (neat) ν_{max} 2984, 1740, 1705 cm^{-1}; ^{1}H NMR δ_H: 1.28 (t, *J* = 7.1 Hz, 6H, 2x$CO_2CH_2CH_3$), 3.54 [m, 2H, C*H*CH(CO_2Et)NH], 3.94 [m, 2H, C*H*(CO_2Et)NH], 4.24 (q, *J* = 7.1 Hz, 4H, 2x$CO_2CH_2CH_3$), 4.58 (s, 2H, CH_2Ph), 7.18–7.38 (m, 5H, Ar*H*); ^{13}C NMR δ_C: 14.1 (2x$CO_2CH_2CH_3$), 43.0 (CH_2Ph), 49.8 [2x*C*HCH(CO_2Et)NH], 62.0 (2x$CO_2CH_2CH_3$), 63.0 [2x*C*H(CO_2Et)NH], 128.1, 128.6, 128.7, 135.2 (Ar*C*), 168.8 (2x*C*$O_2CH_2CH_3$), 174.6 (CON); MS (EI-GC) *m/z*: 374 (M^++1, 2%), 302 (18), 301 (100), 227 (50), 94 (23), 91 (47), 68 (11); HRMS calculated for $C_{19}H_{22}N_2O_6$: 374.1478, found: 374.1470.

(1*R,3*R**,3a*R**,6a*S**)-Diethyl 5-benzyl-4,6-dioxooctahydro pyrrolo[3,4-*c*]pyrrole-1,3-dicarboxylate *endo-trans*-1b:[1]** Sticky yellow oil; IR (neat) ν_{max} 2990, 1740, 1700 cm^{-1}; ^{1}H NMR δ_H: 1.23–1.38 (m, 6H, 2x$CO_2CH_2CH_3$), 3.64 (dd, *J* = 8.0, 1.4 Hz,1H, C*H*CH(CO_2Et)NH), 4.10–4.33 [m, 6H, C*H*CH(CO_2Et)NH and C*H*(CO_2Et)NH and 2x$CO_2CH_2CH_3$], 4.52–4.69 (m, 3H, CH_2Ph and C*H*(CO_2Et)NH), 7.18–7.40 (m, 5H,Ar*H*); ^{13}C NMR δ_C: 14.2, 14.3 (2x$CO_2CH_2CH_3$), 43.1 (CH_2Ph), 48.8 [*C*HCH(CO_2Et)NH], 49.9 [*C*HCH(CO_2Et)NH], 61.8, 62.0 (2x$CO_2CH_2CH_3$), 62.2 [*C*H(CO_2Et)NH], 62.5 [*C*H(CO_2Et)NH], 128.1, 128.8, 129.1, 135.4 (Ar*C*), 169.6, 171.7 (2x*C*$O_2CH_2CH_3$), 175.0, 176.3 (2xCON); MS (EI-GC) *m/z*: 374 (M^++1, 2%), 302 (18), 301 (100), 227 (31), 94 (20), 91 (44), 68 (13); HRMS calculated for $C_{19}H_{22}N_2O_6$: 374.1478, found: 374.1470.

(1*R,3*S**,3a*R**,6a*S**)-Diethyl 4,6-dioxo-5-phenyloctahydro pyrrolo[3,4-*c*]pyrrole-1,3-dicarboxylate *endo-cis*-1c:[1]** Colorless needles, mp = 123-125 ºC (from hexane/$CDCl_3$); IR (neat) ν_{max} 2980, 1741, 1732, 1708 cm^{-1}; ^{1}H NMR δ_H: 1.32 (t, *J* = 7.2 Hz, 6H, 2x$CO_2CH_2CH_3$), 3.05 (t, *J* = 12.7 Hz, 1H, N*H*), 3.71 [m, 2H, 2x*C*HCH(CO_2Et)NH], 4.06 [m, 2H, C*H*(CO_2Et)NH], 4.29 (q, *J* = 7.2 Hz, 4H, 2x$CO_2CH_2CH_3$), 7.19–7.22 (m, 2H, Ar*H*), 7.37–7.46 (m, 3H, Ar*H*); ^{13}C NMR δ_C: 14.0 (2x$CO_2CH_2CH_3$), 49.9 [2x*C*HCH(CO_2Et)NH], 62.1 (2x$CO_2CH_2CH_3$), 63.4 [2x*C*H(CO_2Et)NH], 126.5, 128.9, 129.2, 131.3 (Ar*C*), 169.0 (2x*C*$O_2CH_2CH_3$), 174.1 (2xCON); MS (EI-GC) 360 *m/z* (M^++1, 3%), 288 (19), 287 (100), 94 (45), 68 (13), 67 (11); HRMS calculated for $C_{18}H_{20}N_2O_6$: 360.1301, found: 360.1291.

(1*R,3*R**,3a*R**,6a*S**)-Diethyl 4,6-dioxo-5-phenyloctahydro pyrrolo[3,4-*c*]pyrrole-1,3-dicarboxylate *endo-trans*-1c:[1]** Colorless needles mp = 105-107 ºC (from hexane/$CDCl_3$); IR (neat) ν_{max} 2976, 1712 cm^{-1}; ^{1}H NMR δ_H: 1.20–1.32 (m, 6H, 2x$CO_2CH_2CH_3$), 2.85 (br. s, 1H, N*H*), 3.68 [deform. dd, *J* = 8.1, 8.1 Hz, 1H, C*H*CH(CO_2Et)NH], 3.83 [d, *J* = 8.1, 1H, C*H*CH(CO_2Et)NH], 4.25 [m, 5H, 2x$CO_2CH_2CH_3$ and C*H*(CO_2Et)NH], 4.42 [s, 1H, C*H*(CO_2Et)NH], 7.23–7.27 (m, 2H, Ar*H*), 7.38–7.47 (m, 3H, Ar*H*); ^{13}C NMR δ_C: 14.0, 14.1 (2x$CO_2CH_2CH_3$), 47.6 [*C*HCH(CO_2Et)NH], 49.9 [*C*HCH(CO_2Et)NH], 61.9, 62.1 (2x$CO_2CH_2CH_3$), 62.3 [*C*H(CO_2Et)NH], 62.9 [*C*H(CO_2Et)NH], 126.4, 128.8, 129.1, 131.5 (Ar*C*), 169.8, 171.4 (2x*C*$O_2CH_2CH_3$), 174.6, 175.6 (2xCON); MS (EI-

GC) 360 *m/z*: (M^++1, 4%), 67 (10), 68 (13), 94 (40), 287 (100), 288 (17); HRMS calculated for $C_{18}H_{20}N_2O_6$: 360.1301, found: 360.1291.

(1*S,3*R**,3a*S**,6a*R**)-3-Ethyl 1-methyl 1,5-dimethyl-4,6-dioxooctahydropyrrolo[3,4-*c*]pyrrole-1,3-dicarboxylate *endo-cis*-2a:**[1] Sticky pale yellow oil; IR (neat) ν_{max} 2983, 2955, 1777, 1735, 1697 cm^{-1}; ^1H NMR δ_H: 1.36 (t, *J* = 7.2 Hz, 3H, $CO_2CH_2CH_3$), 1.49 [s, 3H, $C(CO_2CH_3)CH_3$], 2.93 (s, 3H, NCH_3), 3.25 [d, *J* = 8.0 Hz, 1H, $CHC(CO_2Me)CH_3$], 3.37 (d, *J* = 12.5 Hz, 1H, NH), 3.63 [deform. dd, *J* = 8.0, 8.0 Hz, 1H, $CHCH(CO_2Et)NH$], 3.83 (s, 3H, CO_2CH_3), 4.14 [dd, *J* = 12.5, 8.0, Hz, 1H, $CH(CO_2Et)NH$], 4.30 (q, *J* = 7.2 Hz, 2H, $CO_2CH_2CH_3$); ^{13}C NMR δ_C: 14.2 ($CO_2CH_2CH_3$), 24.6 [$C(CO_2CH_3)CH_3$], 25.4 (NCH_3), 50.4 [$CHCH(CO_2Et)NH$], 53.1 [$CHC(CO_2Me)CH_3$], 62.0 (CO_2CH_3), 62.1 ($CO_2CH_2CH_3$), 69.4 [$CH(CO_2Me)CH_3$], 169.5, 171.7 (2xCO_2), 175.0, 175.2 (2xCON); MS (EI-GC) *m/z*: 298 (M^++1, <1%), 239 (67), 225 (39), 165 (100), 108 (43), 81 (10), 80 (21); HRMS calculated for $C_{13}H_{18}N_2O_6$: 298.1165, found: 298.1163.

(2*S,3*S**,4*S**,5*R**)-5-Ethyl 2,3,4-trimethyl 2-methylpyrrolidine-2,3,4,5-tetracarboxylate *endo-cis*-2d:**[1] pale yellow oil; IR (neat) ν_{max} 2986, 2954, 2907, 1730, 1729 cm^{-1}; ^1H NMR δ_H: 1.27 (t, *J* = 7.1 Hz, 3H, $CO_2CH_2CH_3$), 1.60 [s, 3H, $C(CO_2CH_3)CH_3$], 3.24 [d, *J* = 10.0 Hz, 1H, $CHC(CO_2Me)Me$], 3.64, 3.68, 3.74 (3s, 3H, CO_2CH_3), 3.78 [dd, *J* = 10.0, 8.1 Hz, 1H, $CHCH(CO_2Et)NH$], 4.02 [d, *J* = 8.1 Hz, 1H, $CH(CO_2Et)NH$], 4.15 (q, *J* = 7.1, Hz, 2H, $CO_2CH_2CH_3$), NH nd; ^{13}C NMR δ_C: 14.2 ($CO_2CH_2CH_3$), 24.9 [$C(CO_2CH_3)CH_3$], 49.6 [$CHC(CO_2Me)Me$], 52.3, 52.6 52.7 (3xCO_2CH_3), 56.8 [$CHCH(CO_2Et)NH$], 61.7 [$CH(CO_2Et)NH$], 61.8 ($CO_2CH_2CH_3$), 68.4 [$C(CO_2Me)Ph$], 170.6, 172.3, 173.0, 173.8 (4xCO_2); MS (EI-GC) *m/z*: 331 (M^++1, <2%), 272 (65), 258 (19), 262 (19), 241 (10), 240 (82), 226 (99), 212 (80), 198 (60), 180 (10), 167 (11), 166 (100), 154 (25), 140 (72), 139 (10), 136 (10), 122 (10), 108 (58), 94 (11), 81 (22), 80 (27), 59 (24); HRMS calculated for $C_{14}H_{21}NO_8$: 331.1267, found: 331.1274.

(2*R,3*R**,4*R**,5*S**)-5-Ethyl 2-methyl 2-methyl-3,4-bis(phenylsulfonyl)pyrrolidine-2,5-dicarboxylate *endo-cis*-2e:**[1] Orange oil; IR (neat) ν_{max} 2985, 2956, 2905, 1735, 1710, 1308, 1146 cm^{-1}; ^1H NMR δ_H: 1.00 (t, *J* = 7.1 Hz, 3H, $CO_2CH_2CH_3$), 1.72 [s, 3H, $C(CO_2CH_3)CH_3$], 3.72 (s, 3H, CO_2CH_3), 3.94 (q, *J* = 7.1 Hz, 2H, $CO_2CH_2CH_3$), 4.27 [d, *J* = 6.5 Hz, 1H, $CH(CO_2Et)NH$], 4.28 [d, *J* = 4.5 Hz, 1H, $CHC(CO_2Me)Me$], 5.01 [dd, *J* = 6.5, 4.5 Hz, 1H, $CHCHCO_2Et$], 7.51–7.71 (m, 6H, ArH), 7.81–8.02 (m, 4H, ArH), NH nd; ^{13}C NMR δ_C: 14.0 ($CO_2CH_2CH_3$), 23.7 [$CHC(CO_2Me)CH_3$], 52.7 [$CH(CO_2Et)NH$], 61.5 (CO_2CH_3), 62.2 ($CO_2CH_2CH_3$), 69.4 [$C(CO_2Me)Me$], 69.5 [$CHC(CO_2Me)Me$], 73.0 [$CHCH(CO_2Et)NH$], 128.4, 128.9, 129.3, 129.4, 134.2, 134.4, 138.1, 140.4 (ArC), 170.1, 171.2 (2xCO_2); MS (EI-GC) *m/z*: 495 (M^++1, <1%), 294 (32), 279 (21), 248 (39), 237 (14), 236 (100), 222 (26), 221 (10), 156 (11), 128 (17), 125 (11), 108 (23), 96 (26), 95 (10), 94 (11), 81 (46), 80 (21), 77 (14); HRMS calculated for $C_{22}H_{25}NO_8S_2$: 495.1022, found: 495.1015.

(2*R,3*S**,5*S**)-2-Ethyl 3,5-dimethyl 5-methylpyrrolidine-2,3,5-tricarboxylate *endo-cis*-2f:**[1] Yellowish oil; IR (neat) ν_{max} 2983, 2954, 1731, 1725, 1700 cm^{-1}; ^1H NMR δ_H: 1.26 (t, *J* = 7.2 Hz, 3H, $CO_2CH_2CH_3$), 1.49 [s, 3H, $C(CO_2CH_3)CH_3$], 2.01 [dd, *J* = 12.9, 9.8 Hz, 1H, $CHHC(CO_2Me)CH_3$], 2.64 [dd, *J* = 12.9, 8.3 Hz, 1H, $CHHC(CO_2Me)CH_3$], 3.19 [ddd, *J* = 9.8, 8.3, 7.1 Hz, 1H, $CH(CO_2Me)$], 3.71, 3.73 (2s, 3H, CO_2CH_3), 3.77 [d, *J* = 7.1 Hz, 1H, $CH(CO_2Et)NH$], 4.16 (q, *J* = 7.2, Hz, 2H, $CO_2CH_2CH_3$, NH nd; ^{13}C NMR δ_C: 14.3 ($CO_2CH_2CH_3$), 25.9 [$C(CO_2CH_3)CH_3$], 40.7 [$CH_2C(CO_2Me)CH_3$], 47.4 [$CHCH(CO_2Et)NH$], 52.4, 52.7 (2xCO_2CH_3), 61.6 ($CO_2CH_2CH_3$), 63.0 [$CH(CO_2Et)NH$], 66.3 [$C(CO_2Me)CH_3$], 172.8, 173.5, 176.3 (3xCO_2); MS (EI-GC) *m/z*: 273 (M^++1, <2%), 215 (11), 214 (100), 200 (30), 168 (13), 140 (33), 108 (19), 82 (21); HRMS calculated for $C_{12}H_{19}NO_6$: 273.1212, found: 273.1214.

(2*R,3*S**,5*R**)-2-Ethyl 3,5-dimethyl 5-methylpyrrolidine-2,3,5-tricarboxylate *endo-trans*-2f:**[1] Yellowish oil; IR (neat) ν_{max} 2983, 2953, 1732, 1725, 1703 cm^{-1}; ^1H NMR δ_H: 1.25 (t, *J* = 7.2 Hz, 3H, $CO_2CH_2CH_3$), 1.37 [s, 3H, $C(CO_2CH_3)CH_3$], 2.01 [dd, *J* = 13.5, 8.0 Hz, 1H, $CHHC(CO_2Me)CH_3$], 2.68 [dd, *J* = 13.5, 7.2 Hz, 1H, $CHHC(CO_2Me)CH_3$], 3.30 [ddd, *J* = 8.0, 7.2, 7.0 Hz, 1H, $CHCH(CO_2Et)$], 3.62, 3.73 (2s, 3H, CO_2CH_3), 4.03 [d, *J* =

7.0 Hz, 1H, C*H*(CO_2Et)NH], 4.15 (q, *J* = 7.2, Hz, 2H, $CO_2CH_2CH_3$, N*H* nd; ^{13}C NMR δ_C: 14.2 ($CO_2CH_2CH_3$), 28.3 [C(CO_2CH_3)CH_3], 39.1 [$CH_2C(CO_2Me)CH_3$], 47.1 [*C*HCH(CO_2Et)NH], 53.3, 53.4 (2xCO_2CH_3), 61.4 ($CO_2CH_2CH_3$), 62.8 [*C*H(CO_2Et)NH], 65.4 [C(CO_2Me)CH_3], 172.3, 173.6, 176.4 (3x*C*O_2); MS (EI-GC) *m/z*: 273 (M^++1, <2%), 215 (12), 214 (100), 200 (33), 140 (62), 108 (20), 99 (24), 82 (23); HRMS calculated for $C_{12}H_{19}NO_6$: 273.1212, found: 273.1215.

(2*S,3*R**,5*R**)-5-Ethyl 2,3-dimethyl 2-methylpyrrolidine-2,3,5-tricarboxylate *endo-cis*-2f´:[1]** Yellowish oil; IR (neat) ν_{max} 2983, 2955, 1730, 1726, 1700 cm^{-1}; ^{1}H NMR δ_H: 1.26 (t, *J* = 7.1 Hz, 3H, $CO_2CH_2CH_3$), 1.51 [s, 3H, C(CO_2CH_3)CH_3], 2.29–2.57 [m, 2H, CH_2CH(CO_2Et)], 2.87 [dd, *J* = 9.5, 8.1 Hz, 1H, C*H*C(CO_2Me)CH_3], 3.65, 3.66 (2s, 3H, CO_2CH_3), 3.87 [dd, *J* = 8.6, 7.6 Hz, 1H, C*H*(CO_2Et)NH], 4.15 (q, *J* = 7.1, Hz, 2H, $CO_2CH_2CH_3$), N*H* nd; ^{13}C NMR δ_C: 14.3 ($CO_2CH_2CH_3$), 25.5 [CHC(CO_2Me)CH_3], 32.3 [CH_2CH(CO_2Et)NH], 52.0, 52.1 (2xCO_2CH_3), 52.5 [*C*HC(CO_2Me)Me], 58.0 [*C*H(CO_2Et)NH], 61.4 ($CO_2CH_2CH_3$), 68.3 [*C*(CO_2Me)Me], 171.6, 172.2, 174.3 (3xCO_2); MS (EI-GC) *m/z*: 273 (M^++1, <2%), 215 (12), 214 (100), 200 (32), 140 (62), 108 (20), 99 (27), 82 (23); HRMS calculated for $C_{12}H_{19}NO_6$: 273.1212, found: 273.1214.

(1*S,3*R**,3a*S**,6a*R**)-Diethyl 1-benzyl-5-methyl-4,6-dioxooctahydropyrrolo[3,4-*c*]pyrrole-1,3-dicarboxylate *endo-cis*-3a:[1]** Sticky pale yellow oil; IR (neat) ν_{max} 3030, 2982, 2936, 1779, 1734, 1699 cm^{-1}; ^{1}H NMR δ_H: 1.32, 1.34 (2t, *J* = 7.2 Hz, 3H, $CO_2CH_2CH_3$), 2.88, 3.30 (2d, *J* = 13.8 Hz, 2H, CH_2Ph) 2.92 (s, 3H, NCH_3), 3.38 [d, *J* = 8.0 Hz, 1H, C*H*C(CO_2Et)Bn], 3.55 [deform. dd, *J* = 8.4, 8.0 Hz, 1H, C*H*CH(CO_2Et)NH], 4.09 [d, *J* = 8.4, Hz, 1H, C*H*(CO_2Et)NH], 4.24 (q, *J* = 7.2 Hz, 2H, $CO_2CH_2CH_3$), 4.26 (q, *J* = 7.2 Hz, 2H, $CO_2CH_2CH_3$), N*H* nd; ^{13}C NMR δ_C: 14.0 (2x$CO_2CH_2CH_3$), 25.4 (NCH_3), 42.2 (CH_2Ar), 50.4 [*C*HCH(CO_2Et)NH], 56.6 [*C*HC(CO_2Et)Bn], 62.0 [*C*H(CO_2Et)NH], 62.1 ($CO_2CH_2CH_3$), 62.3 ($CO_2CH_2CH_3$) 73.6 [*C*(CO_2Et)Bn], 127.2, 128.3, 130.4, 135.7 (Ar*C*)169.6, 170.1 (2x*C*O_2), 175.0, 175.1 (2xCON); MS (EI-GC) *m/z*: 388 (M^++1, <1%), 315 (13), 298 (14), 297 (100), 223 (11), 166 (45), 94 (11), 91 (17); HRMS calculated for $C_{20}H_{24}N_2O_6$: 388.1634, found: 388.1631.

(1*S,3*R**,3a*S**,6a*R**)-Diethyl 1,5-dibenzyl-4,6-dioxoocta hydropyrrolo[3,4-*c*]pyrrole-1,3-dicarboxylate *endo-cis*-3b:[1]** Colorless prisms, mp = 127-130 ºC (from hexane/$CDCl_3$); IR (neat) ν_{max} 3030, 2989, 1741, 1719, 1699 cm^{-1}; ^{1}H NMR δ_H: 1.23 (t, *J* = 7.2 Hz, 3H, $CO_2CH_2CH_3$), 1.28 (t, *J* = 7.2 Hz, 3H, $CO_2CH_2CH_3$), 2.89, 3.31 (2d, *J* = 13.9 Hz, 2H, CH_2Ph), 3.38 [d, *J* = 7.8 Hz, 1H, C*H*C(CO_2Et)Bn], 3.55 [deform. dd, *J* = 7.8, 7.8 Hz, 1H, C*H*CH(CO_2Et)NH], 4.03–4.27 (m, 5H, 2x$CO_2CH_2CH_3$ and C*H*(CO_2Et)NH], 4.54, 4.60 (d, *J* = 14.3 Hz, 2H), 7.20–7.35 (m, 10H, 2xCH_2*Ph*), N*H* nd; ^{13}C NMR δ_C: 14.0, 14.1 (2x$CO_2CH_2CH_3$), 42.2, 43.0 (2xCH_2Ph), 50.4 [*C*HCH(CO_2Et)NH], 56.6 [*C*HCH(CO_2Et)NH], 61.9, 62.1 (2x$CO_2CH_2CH_3$), 62.3 [*C*H(CO_2Et)NH], 73.7 [*C*Bn(CO_2Et)NH], 127.2, 128.0, 128.3, 128.6, 128.7, 130.5, 135.2, 135.8 (ArC), 169.4, 169.9 (2x*C*$O_2CH_2CH_3$), 174.6, 174.7 (2xCON); MS (EI-GC) *m/z*: 464 (M^++1, <1%), 391 (14), 374 (22), 373 (100), 166 (22), 91 (73); HRMS calculated for $C_{26}H_{28}N_2O_6 - C_7H_7$: 373.1400, found: 373.1401.

(1*S,3*R**,3a*S**,6a*R**)-Diethyl 1-benzyl-4,6-dioxo-5-phenyl octahydropyrrolo[3,4-*c*]pyrrole-1,3-dicarboxylate *endo-cis*-3c:[1]** Colorless prisms, mp = 169-172 ºC (from hexane/$CDCl_3$); IR (neat) ν_{max} 2979, 2937, 1729, 1714 cm^{-1}; ^{1}H NMR δ_H: 1.25–1.30 (m, 6H, 2x$CO_2CH_2CH_3$), 2.96, 3.36 (2xd, *J* = 13.9 Hz, 2H, CH_2Ph), 3.51 (s, 1H, N*H*), 3.55 [d, *J* = 7.8 Hz, 1H, C*H*C(CO_2Et)Bn], 3.73 [deform. dd, *J* = 7.8, 7.8 Hz, 1H, C*H*CH(CO_2Et)NH], 4.15–4.30 [m, 5H, 2x$CO_2CH_2CH_3$ and C*H*(CO_2Et)NH], 7.15–7.49 (m, 10H, Ar*H*); ^{13}C NMR δ_C: 13.9, 14.0 ($CO_2CH_2CH_3$), 42.3 (CH_2Ph), 50.4 [*C*HCH(CO_2Et)NH], 56.6 [*C*HCH(CO_2Et)NH], 62.1, 62.2 (2x$CO_2CH_2CH_3$), 62.3 [*C*H(CO_2Et)NH], 74.1 [*C*Bn(CO_2Et)NH], 126.6, 127.2, 128.0, 128.2, 128.9, 129.2, 130.4, 135.6 (ArC), 169.7, 170.1 (2x*C*O_2), 174.0, 174.2 (2xCON); MS (EI-GC) *m/z*: 450 (M^++1, <1%), 377 (14), 360 (22), 359 (100), 207 (44), 166 (40), 156 (10), 119 (10), 94 (13), 91 (45); HRMS calculated for $C_{25}H_{26}N_2O_6$: 450.1791, found: 450.1801.

(2*S,3*S**,4*S**,5*R**)-5-Ethyl 2,3,4-trimethyl 2-benzylpyrrolidine-2,3,4,5-tetracarboxylate *endo-cis*-3d:[1]** Colorless oil; IR (neat) ν_{max} 2983, 2954, 2906, 1732, 1727 cm^{-1}; ^{1}H NMR δ_H: 1.22, 1.26 (2t, *J* = 7.1 Hz, 3H,

$CO_2CH_2CH_3$), 3.13, 3.37 (2d, *J* = 13.8 Hz, 2H, CH_2Ph), 3.34 [d, *J* = 10.1 Hz, 1H, C*H*C(CO_2Et)Bn], 3.65 [dd, *J* = 10.1, 8.5 Hz, 1H, C*H*CH(CO_2Et)NH], 3.70, 3.78 (2s, 3H, CO_2CH_3), 3.86 [d, *J* = 8.5 Hz, 1H, C*H*(CO_2Et)NH], 4.05–4.25 (m, 4H, 2x$CO_2CH_2CH_3$), 7.24–7.36 (m, 5H, Ar*H*), N*H* nd; ^{13}C NMR δ_C: 14.0, 14.2 (2x$CO_2CH_2CH_3$), 42.6 (CH_2Ar), 49.3 [*C*HC(CO_2Et)Bn], 52.4, 52.6 (2xCO_2CH_3), 54.8 [*C*HCH(CO_2Et)NH], 61.6 [*C*H(CO_2Et)NH], 62.0, 61.7 (2x$CO_2CH_2CH_3$), 72.3 [*C*(CO_2Et)Bn], 127.1, 128.3, 130.9, 135.9 (Ar*C*), 170.5, 171.9, 172.3, 172.9 (4xCO_2); MS (EI-GC) *m/z*: 407 (M^++1, <1%), 348 (18), 330 (48), 316 (44), 298 (100), 166 (32), 138 (11), 91 (60); HRMS calculated for $C_{20}H_{25}NO_8$: 407.1580, found: 407.1586.

(2*R,3*S**,4*S**,5*S**)-Diethyl 2-benzyl-3,4-bis(phenylsulfonyl) pyrrolidine-2,5-dicarboxylate *exo-cis*-3e:[1]** Pale yellow prisms, mp = 85-86ºC (from *n*-hexane/ethyl acetate); IR (neat) ν_{max} 2971, 1741, 1235, 1149 cm^{-1}; ^{1}H NMR δ_H: 1.04 (t, *J* = 7.2 Hz, 1H, $CO_2CH_2CH_3$), 1.21 (t, *J* = 7.2 Hz, 1H, $CO_2CH_2CH_3$), 3.29, 3.40 (2xd, *J* = 14.2 Hz, 2H, CH_2Ph), 3.88–4.29 (m, 4H, 2x$CO_2CH_2CH_3$), 4.20 [C*H*(CO_2Et)NH], 4.43 (br. s, 1H, N*H*), 4.51 [d, *J* = 5.2 Hz, 1H, C*H*C(CO_2Et)Bn], 4.89 [deform. dd, *J* = 5.2, 5.2 Hz, 1H, C*H*CH(CO_2Et)NH], 7.18–7.33 (m, 5H, Ar*H*), 7.44 – 7.82 (m, 8H, Ar*H*), 7.88–7.98 (m, 2H, Ar*H*); ^{13}C NMR δ_C: 13.8, 14.0 (2x$CO_2CH_2CH_3$), 41.0 (CH_2Ph), 61.1, 62.2 (2x$CO_2CH_2CH_3$), 62.3 [*C*HCH(CO_2Et)NH], 69.4 [*C*HCBn(CO_2Et)NH], 72.0 [*C*H(CO_2Et)NH], 73.8 [*C*Bn(CO_2Et)NH], 127.4, 128.4, 128.8, 129.1, 129.2, 129.4, 130.7, 134.3, 134.4, 134.7, 138.5, 139.5 (Ar*C*), 169.6, 169.6 (2x*C*O_2); MS (EI-GC) *m/z*: 585 (M^++1, <1%), 512 (10), 494 (34), 370 (14), 353 (13), 352 (69), 306 (33), 298 (10), 280 (26), 235 (10), 234 (82), 157 (13), 156 (23), 141 (10), 125 (15), 112 (11), 94 (16), 91 (100), 80 (12), 77 (29); HRMS calculated for $C_{29}H_{31}NO_8S_2$–$C_3H_5O_2$: 512.1202, found: 512.1215.

(1*R,3*R**,3a*S**,6a*R**)-3-Ethyl 1-methyl 5-methyl-4,6-dioxo-1-phenyloctahydropyrrolo[3,4-*c*]pyrrole-1,3-dicarboxylate *endo-cis*-4a:[1]** Sticky pale yellow oil; IR (neat) ν_{max} 2982, 2954, 1779, 1736, 1698 cm^{-1}; ^{1}H NMR δ_H: 1.25 (t, *J* = 7.2 Hz, 3H, $CO_2CH_2CH_3$), 2.91 (s, 3H, NCH_3), 3.37 [deform. dd, *J* = 8.5, 7.5 Hz, 1H, C*H*CHCO$_2$Et], 3.69 (s, 3H, CO_2CH_3), 3.76 [d, *J* = 8.5, 1H, C*H*(CO_2Et)NH], , 3.96 [d, *J* = 7.5, Hz, 1H, C*H*(CO_2Me)Ph], 4.20 (qd, *J* = 7.2, 1.1 Hz, 2H, $CO_2CH_2CH_3$), 7.22–7.36 (m, 3H, Ar*H*), 7.58–7.63 (m, 2H, Ar*H*), N*H* nd; ^{13}C NMR δ_C: 14.2 ($CO_2CH_2CH_3$), 25.5 (NCH_3), 50.3 [*C*HCH(CO_2Et)NH], 53.4 [*C*HC(CO_2Me)Ph], 56.5 (*C*HCO$_2$Et), 61.6 (CO_2CH_3), 62.1 ($CO_2CH_2CH_3$), 74.8 [*C*(CO_2Me)Ph], 127.4, 128.5, 128.7, 138.1 (Ar*C*), 169.6, 170.2 (2x*C*O_2), 175.1, 175.4 (2xCON); MS (EI-GC) *m/z*: 360 (M^++1, <1%), 302 (17), 301 (100), 228 (14), 227 (72), 170 (19), 143 (18), 142 (27); HRMS calculated for $C_{18}H_{20}N_2O_6$: 360.1321, found: 360.1322.

(1*S,3*R**,3a*S**,6a*R**)-3-Ethyl 1-methyl 5-methyl-4,6-dioxo-1-phenyloctahydropyrrolo[3,4-*c*]pyrrole-1,3-dicarboxylate *endo-trans*-4a:[1]** Sticky pale yellow oil; IR (neat) ν_{max} 2983, 2954, 2926, 1781, 1729, 1702 cm^{-1}; ^{1}H NMR δ_H: 1.39 (t, *J* = 7.2 Hz, 3H, $CO_2CH_2CH_3$), 2.79 (s, 3H, NCH_3), 3.08 (d, *J* = 3.5 Hz, 1H, N*H*), 3.55 [deform. dd, *J* = 7.6, 7.6 Hz, 1H, C*H*CHCO$_2$Et], 3.79 (s, 3H, CO_2CH_3), 3.86 [dd, *J* = 7.6, 3.5 Hz, 1H, C*H*(CO_2Et)NH], 4.25 [d, *J* = 7.6, Hz, 1H, C*H*C(CO_2Me)Ph], 4.30–4.41 (m, 2H, $CO_2CH_2CH_3$), 7.33–7.41 (m, 3H, Ar*H*), 7.47–7.54 (m, 2H, Ar*H*); ^{13}C NMR δ_C: 14.2 ($CO_2CH_2CH_3$), 25.2 (NCH_3), 45.3 [*C*HCH(CO_2Et)NH], 50.4 [*C*HC(CO_2Me)Ph], 53.7 (*C*HCO$_2$Et), 59.8 (CO_2CH_3), 61.7 ($CO_2CH_2CH_3$), 74.1 [*C*(CO_2Me)Ph], 126.0, 128.5, 128.9, 135.4 (Ar*C*), 169.3, 173.5 (2x*C*O_2), 174.1, 175.6 (2xCON); MS (EI-GC) *m/z*: 360 (M^++1, <1%), 302 (18), 301 (100), 228 (13), 227 (63), 170 (20), 143 (22), 142 (30), 115 (15); HRMS calculated for $C_{18}H_{20}N_2O_6$: 360.1321, found:360.1336.

(2*R,3*S**,4*S**,5*R**)-5-Ethyl 2,3,4-trimethyl 2-phenylpyrrolidine-2,3,4,5-tetracarboxylate *endo-cis*-4d:[1]** Colorless oil; IR (neat) ν_{max} 2984, 2954, 1735, 1716, 1713, 1700 cm^{-1}; ^{1}H NMR δ_H: 1.14 (t, *J* = 7.1 Hz, 3H, $CO_2CH_2CH_3$), 3.64, 3.67, 3.75 (3s, 3H, CO_2CH_3), 3.82 [dd, *J* = 10.1, 8.5 Hz, 1H, C*H*CH(CO_2Et)NH], 3.98 [d, *J* = 8.5 Hz, 1H, C*H*(CO_2Et)NH], 4.04 (q, *J* = 7.1, Hz, 2H, $CO_2CH_2CH_3$), 4.38 [d, *J* = 10.1 Hz, 1H, C*H*C(CO_2Me)Ph], 7.26–7.38 (m, 2H, Ar*H*), 7.51 (dd, *J* = 8.5, 2.8 Hz, 1H, Ar*H*), 7.70 (dd, *J* = 8.5, 2.8 Hz, 2H, Ar*H*), N*H* nd; ^{13}C NMR δ_C: 14.0 ($CO_2CH_2CH_3$), 51.1, 52.3, 52.6 (3xCO_2CH_3), 53.3 [*C*HC(CO_2Me)Ph], 53.5 [*C*HCH(CO_2Et)NH], 60.7 [*C*H(CO_2Et)NH], 61.4 ($CO_2CH_2CH_3$), 75.0 [*C*(CO_2Me)Ph], 127.0, 128.1, 128.3, 140.9 (Ar*C*), 170.8, 171.3, 171.7, 172.8 (4x*C*O_2); MS (EI-GC) *m/z*: 393 (M^++1, <2%), 335 (19), 334 (100), 302 (24), 288 (11), 274 (35), 260 (25), 242

(13), 228 (51), 202 (25), 201 (11), 170 (11), 143 (26), 115 (16); HRMS calculated for $C_{19}H_{23}NO_8$: 393.1424, found: 393.1421.

(2*R,3*R**,4*R**,5*R**)-5-Ethyl 2,3,4-trimethyl 2-phenylpyrrolidine-2,3,4,5-tetracarboxylate *exo-cis*-4d:**[1] Colorless oil; IR (neat) ν_{max} 2990, 2950, 1748, 1733, 1730, 1715 cm^{-1}; ^1H NMR δ_H: 1.30 (t, *J* = 7.1 Hz, 3H, $CO_2CH_2CH_3$), 3.56, 3.69, 3.72 (3s, 3H, CO_2CH_3), 3.64 [deform. dd, *J* = 6.9, 6.7 Hz, 1H, C*H*CH(CO_2Et)NH], 3.89 [d, *J* = 6.7 Hz, 1H, C*H*C(CO_2Me)Ph], 4.17 [d, *J* = 6.9 Hz, 1H, C*H*(CO_2Et)NH], 4.26 (q, *J* = 7.1, Hz, 2H, $CO_2CH_2CH_3$), 7.28–7.38 (m, 2H, Ar*H*), 7.51 (dd, *J* = 7.0, 2.3 Hz, 1H, Ar*H*), 7.70 (dd, *J* = 7.0, 2.3 Hz, 2H, Ar*H*), N*H* nd; ^{13}C NMR δ_C: 14.3 ($CO_2CH_2CH_3$), 51.8, 52.6, 52.8 (3xCO_2CH_3), 53.6 [*C*HC(CO_2Me)Ph], 54.7 [*C*HCH(CO_2Et)NH], 61.6 [*C*H(CO_2Et)NH], 61.9 ($CO_2CH_2CH_3$), 75.2 [*C*(CO_2Me)Ph], 126.4, 128.1, 128.2, 139.7 (Ar*C*), 171.1, 171.6, 172.0, 172.1 (4xCO_2); MS (EI-GC) *m/z*: 393 (M^++1, <1%), 335 (19), 334 (100), 303 (11), 302 (60), 274 (14), 260 (25), 242 (11), 228 (27), 202 (21), 170 (56), 143 (24), 115 (14); HRMS calculated for $C_{19}H_{23}NO_8$: 393.1424, found: 393.1426.

(2*R,3*R**,4*R**,5*S**)-5-Ethyl 2-methyl 2-phenyl-3,4-bis(phenylsulfonyl)pyrrolidine-2,5-dicarboxylate *exo-trans*-4e:**[1] Orange oil; R_f 0.10 (*n*-hexane/ethyl acetate 7/3); IR (neat) ν_{max} 2981, 2954, 2926, 1738, 1692, 1309, 1147 cm^{-1}; ^1H NMR δ_H: 1.04 (t, *J* = 7.2 Hz, 3H, $CO_2CH_2CH_3$), 3.74 (s, 3H, CO_2CH_3), 4.01 (q, *J* = 7.2 Hz, 2H, $CO_2CH_2CH_3$), 4.35 [d, *J* = 5.0 Hz, 1H, C*H*(CO_2Et)NH], 4.86 [d, *J* = 5.3 Hz, 1H, C*H*C(CO_2Me)Ph], 4.91 [deform. dd, *J* = 5.3, 5.0 Hz, 1H, C*H*CHCO_2Et], 7.35–8.05 (m, 15H, Ar*H*), N*H* nd; ^{13}C NMR δ_C: 14.0 ($CO_2CH_2CH_3$), 53.2 [*C*H(CO_2Et)NH], 60.9 (CO_2CH_3), 62.3 ($CO_2CH_2CH_3$), 69.4 [*C*HCH(CO_2Et)NH], 74.6 [*C*HC(CO_2Me)Ph], 75.1 [*C*(CO_2Me)Ph], 128.2, 128.3, 128.6, 128.8, 128.9, 129.2, 129.3, 134.0, 134.3, 136.8, 138.6, 140.1 (Ar*C*), 170.0, 170.1 (2xCO_2); MS (EI-GC) *m/z*: 557 (M^++1, <1%), 357 (11), 356 (51), 342 (10), 310 (15), 299 (11), 298 (54), 284 (17), 283 (21), 215 (37), 158 (11), 157 (11), 144 (11), 143 (100), 142 (11), 115 (24), 77 (11); HRMS calculated for $C_{27}H_{27}NO_8S_2$:557.1168, found: 557.1173.

(2*R,3*R**,5*R**)-5-Ethyl 2,3-dimethyl 2-phenylpyrrolidine-2,3,5-tricarboxylate *endo-cis*-4f:**[1] Yellowish oil; IR (neat) ν_{max} 2985, 2953, 1734, 1700 cm^{-1}; ^1H NMR δ_H: 1.29 (t, *J* = 7.1 Hz, 3H, $CO_2CH_2CH_3$), 2.29–2.36 [m, 2H, CH_2CH(CO_2Et)], 3.51 [dd, *J* = 7.6, 4.5 Hz, 1H, C*H*C(CO_2Me)Ph], 3.68, 3.70 (2s, 3H, CO_2CH_3), 3.85 [dd, *J* = 9.0, 5.7 Hz, 1H, C*H*(CO_2Et)NH], 4.23 (q, *J* = 7.1, Hz, 2H, $CO_2CH_2CH_3$), 7.25–7.35 (m, 3H, Ar*H*), 7.73–7.77 (m, 2H, Ar*H*), N*H* nd; ^{13}C NMR δ_C: 14.3 ($CO_2CH_2CH_3$), 33.8 [CH_2CH(CO_2Et)NH], 52.2, 52.9 (2xCO_2CH_3), 54.0 [*C*HC(CO_2Me)Ph], 58.6 [*C*H(CO_2Et)NH], 61.5 ($CO_2CH_2CH_3$), 75.5 [*C*(CO_2Me)Ph], 126.9, 128.1, 128.4, 140.2 (Ar*C*), 172.2, 173.1, 173.6 (3xCO_2); MS (EI-GC) *m/z*: 335 (M^++1, <2%), 277 (18), 276 (100), 262 (19), 202 (41), 170 (19), 144 (20), 143 (14), 115 (10), 99 (15); HRMS calculated for $C_{17}H_{21}NO_6$: 335.1369, found:335.1313.

(2*S,3*R**,5*R**)-5-Ethyl 2,3-dimethyl 2-phenylpyrrolidine-2,3,5-tricarboxylate *endo-trans*-4f:**[1] Yellowish oil; R_f 0.29 (*n*-hexane/ethyl acetate 7/3); IR (neat) ν_{max} 2984, 2953, 1727, 1658 cm^{-1}; ^1H NMR δ_H: 1.30 (t, *J* = 7.1 Hz, 3H, $CO_2CH_2CH_3$), 2.36–2.46 [m, 2H, CH_2CH(CO_2Et)], 3.19, 3.72 (2s, 3H, CO_2CH_3), 3.92 [deform. dd, *J* = 8.0, 7.6 Hz, Ph1H, C*H*C(CO_2Me)Ph], 4.04 [deform. dd, *J* = 6.5, 5.9 Hz, 1H, C*H*(CO_2Et)NH], 4.26 (q, *J* = 7.1, Hz, 2H, $CO_2CH_2CH_3$), 7.24–7.37 (m, 3H, Ar*H*), 7.49–7.53 (m, 2H, Ar*H*), N*H* nd; ^{13}C NMR δ_C: 14.3 ($CO_2CH_2CH_3$), 32.7 [CH_2CH(CO_2Et)NH], 50.6, 51.5 (2xCO_2CH_3), 53.4 [*C*HC(CO_2Me)Ph], 58.5 [*C*H(CO_2Et)NH], 61.3 ($CO_2CH_2CH_3$), 76.0 [*C*(CO_2Me)Ph], 126.3, 128.3, 128.5, 137.5 (Ar*C*), 172.6, 173.0, 173.9 (3xCO_2); MS (EI-GC) *m/z*: 335 (M^++1, <2%), 277 (21), 276 (100), 262 (15), 202 (38), 201 (10), 170 (25), 144 (13), 143 (11), 115 (11), 99 (17); HRMS calculated for $C_{17}H_{21}NO_6$: 335.1369, found: 335.1308.

(1*S,3*R**,3a*S**,6a*R**)-Ethyl 3-(dimethoxymethyl)-5-methyl-4,6-dioxooctahydropyrrolo[3,4-*c*]pyrrole-1-carboxylate *endo-cis*-5a:** Yellow prisms, mp: 105-108ºC (from hexane/CH_2Cl_2); IR (neat) ν_{max} 2980, 1719, 1696 cm^{-1}; ^1H NMR δ_H: 1.35 (t, *J* = 7.2 Hz, 3H, $CO_2CH_2CH_3$), 2.50 (br. s, 1H, N*H*), 2.95 (s, 3H, NCH_3), 3.27 [deform. dd, *J* = 7.9, 7.6 Hz, 1H, C*H*CH(CH($OMe)_2$)NH], 3.40 [dd, *J* = 7.6, 4.8 Hz, 1H, C*H*CH($OMe)_2$NH], 3.42, 3.54 (2s, 6H, 2xOCH_3), 3.51 [deform. dd, *J* = 7.9, 7.6 Hz, 1H, C*H*CH(CO_2Et)NH], 3.85 [d, *J* = 7.6 Hz, 1H, C*H*(CO_2Et)NH], 4.30

(q, *J* = 7.2 Hz, 2H, $CO_2CH_2CH_3$), 4.69 [d, *J* = 4.8 Hz, 1H, C*H*$(OMe)_2$]; ^{13}C NMR δ_C: 14.2 ($CO_2CH_2CH_3$), 25.2 (NCH_3), 45.5 [*C*HCH$(OMe)_2$NH], 49.1 [*C*HCH(CO_2Et)NH], 55.8, 56.0 (2xOCH_3), 61.7 ($CO_2CH_2CH_3$), 62.3 [*C*H$(CH(OMe)_2)$NH], 63.4 [*C*H(CO_2Et)NH], 102.6 [*C*H$(OMe)_2$], 169.6 (*C*O_2Et), 175.6, 175.9 (2xCON); MS (EI-GC) *m/z*: 300 (M^+, <1%), 269 (13), 225 (27), 195 (34), 179 (10), 151 (18), 94 (16), 75 (100); HRMS calculated for $C_{13}H_{20}N_2O_6$+1: 301.1399, found: 301.1399.

(1*S,3*R**,3a*S**,6a*R**)-Ethyl 5-benzyl-3-(dimethoxymethyl)-4,6-dioxooctahydropyrrolo[3,4-*c*]pyrrole-1-carboxylate *endo-cis*-5b:** Sticky pale yellow oil; IR (neat) ν_{max} 2968, 2308, 1716, 1695 cm^{-1}; ^1H NMR δ_H: 1.32 (t, *J* = 7.2 Hz, 3H, $CO_2CH_2CH_3$), 2.50 (br. s, 1H, N*H*), 3.16, 3.47 (2s, 6H, 2xOCH_3), 3.25 [deform. dd, *J* = 8.0, 7.7 Hz, 1H, C*H*CH$(CH(OMe)_2)$NH], 3.40 [dd, *J* = 8.0, 4.0 Hz, 1H, C*H*CH$(OMe)_2$NH], 3.51 [deform. dd, *J* = 7.7, 7.6 Hz, 1H, C*H*CH(CO_2Et)NH], 3.87 [d, *J* = 7.6 Hz, 1H, C*H*(CO_2Et)NH], 4.29 (q, *J* = 7.2 Hz, 2H, $CO_2CH_2CH_3$), 4.54 (d, *J* = 14.3 Hz, 1H, NC*H*HPh), 4.65 [d, *J* = 4.0 Hz, 1H, C*H*$(OMe)_2$], 4.68 (d, *J* = 14.3 Hz, 1H, NC*H*HPh) 7.23-7.34 (m, 5H, Ar*H*); ^{13}C NMR δ_C: 14.2 ($CO_2CH_2CH_3$), 42.7 (NCH_2Ph), 46.8 [*C*HCH$(CH(OMe)_2)$NH], 49.4 [*C*HCH(CO_2Et)NH], 55.4, 55.7 (2xOCH_3), 61.6 ($CO_2CH_2CH_3$), 62.7 [*C*H$(CH(OMe)_2)$NH], 63.7 [*C*H(CO_2Et)NH], 102.0 [*C*H$(OMe)_2$], 127.9, 128.5, 128.6, 135.6 (ArC), 169.4 (*C*O_2Et), 175.3, 175.5 (2xCON); MS (EI-GC) *m/z*: 376 (M^+, <1%), 301 (29), 271 (15), 243 (10), 227 (18), 94 (10), 75 (100); HRMS calculated for $C_{19}H_{24}N_2O_6$+1: 377.1712, found: 377.1701.

(1*S,3*R**,3a*S**,6a*R**)-Ethyl 3-(dimethoxymethyl)-4,6-dioxo-5-phenyloctahydropyrrolo[3,4-*c*]pyrrole-1-carboxylate *endo-cis*-5c:** Yellowish prisms, mp: 98-102ºC (from hexane/CH_2Cl_2); IR (neat) ν_{max} 2995, 2939, 2310, 1718, 1700 cm^{-1}; ^1H NMR δ_H: 1.32 (t, *J* = 7.2 Hz, 3H, $CO_2CH_2CH_3$), 2.55 (br. s, 1H, N*H*), 3.39 (s, 3H, OCH_3), 3.43 [deform. dd, *J* = 7.7, 7.2 Hz, 1H, C*H*CH$(CH(OMe)_2)$NH], 3.50-3.55 (m, 4H, C*H*CH$(OMe)_2$NH, OCH_3), 3.66 [deform. dd, *J* = 7.7, 7.2 Hz, 1H, C*H*CH(CO_2Et)NH], 3.97 [d, *J* = 7.7 Hz, 1H, C*H*(CO_2Et)NH], 4.28 (q, *J* = 7.2 Hz, 2H, $CO_2CH_2CH_3$), 4.79 [d, *J* = 4.0 Hz, 1H, C*H*$(OMe)_2$], 7.24-7.51 (m, 5H, Ar*H*); ^{13}C NMR δ_C: 14.2 ($CO_2CH_2CH_3$), 47.1 [*C*HCH$(CH(OMe)_2)$NH], 49.5 [*C*HCH(CO_2Et)NH], 55.8, 55.9 (2xOCH_3), 61.8 ($CO_2CH_2CH_3$), 62.9 [*C*H$(CH(OMe)_2)$NH], 64.1 [*C*H(CO_2Et)NH], 102.2 [*C*H$(OMe)_2$], 126.7, 128.9, 129.3, 131.9 (ArC), 169.6 (*C*O_2Et), 174.8, 175.0 (2xCON); MS (EI-GC) *m/z*: 362 (M^+, <1%), 331 (11), 287 (29), 257 (24), 94 (21), 75 (100); HRMS calculated for $C_{18}H_{22}N_2O_6$+1: 363.1556, found: 363.1550.

(1*S,3*R**,3a*S**,6a*R**)-Methyl 3-(dimethoxymethyl)-1,5-dimethyl-4,6-dioxooctahydropyrrolo[3,4-*c*]pyrrole-1-carboxylate *endo-cis*-6a:** yellow solid, mp: 120-123ºC (from hexane/CH_2Cl_2); IR (neat) ν_{max} 2976, 1720, 1702 cm^{-1}; ^1H NMR δ_H: 1.47 [s, 3H, C(CO_2CH_3)CH_3], 2.92 (s, 3H, NCH_3), 3.20 [d, *J* = 7.7 Hz, 1H, C*H*C$(CO_2Me)CH_3$], 3.34 [deform. dd, *J* = 8.6, 7.7 Hz, 1H, C*H*CH$(CH(OMe)_2)$NH], 3.38 3.51 (2s, 6H, 2xOCH_3), 3.68 (dd, *J* = 8.6, 3.0 Hz, 1H, C*H*CH$(OMe)_2$NH), 3.83 (s, 3H, CO_2CH_3), 4.76 [d, *J* = 3.0 Hz, 1H, C*H*$(OMe)_2$], N*H* nd; ^{13}C NMR δ_C: 24.1 [C$(CO_2CH_3)CH_3$], 25.1 (NCH_3), 47.6 [*C*HCH$(CH(OMe)_2)$NH], 52.9 [*C*HC$(CO_2Me)CH_3$], 55.7, 56.0 (2xOCH_3), 56.7 (CO_2CH_3), 62.4 [*C*H$(CH(OMe)_2)$NH], 68.3 [*C*$(CO_2Me)CH_3$], 101.9 [*C*H$(OMe)_2$], 172.3 (*C*O_2Me), 175.7, 176.1 (2xCON); MS (EI-GC) *m/z*: 300 (M^+, <1%), 241 (13), 225 (37), 209 (24), 165 (40), 108 (20), 75 (100); HRMS calculated for $C_{13}H_{20}N_2O_6$+1: 301.1399, found: 301.1392.

(2*S,3*S**,4*S**,5*R**)-Trimethyl 5-(dimethoxymethyl)-2-methylpyrrolidine-2,3,4-tricarboxylate *endo-cis*-6d:** Sticky pale yellow oil; IR (neat) ν_{max} 2987, 1715, 1713, 1692 cm^{-1}; ^1H NMR δ_H: 1.60 [s, 3H, C(CO_2CH_3)CH_3], 3.25 [deform. dd, *J* = 10.5, 8.3 Hz, 1H, C*H*CH$(CH(OMe)_2)$NH], 3.34 [d, *J* = 10.5 Hz, 1H, C*H*C$(CO_2Me)CH_3$], 3.40 (s, 6H, 2xOCH_3), 3.60 (dd, *J* = 8.3, 6.2 Hz, 1H, C*H*CH$(OMe)_2$NH), 3.68 (s, 6H, 2xCO_2CH$_3$), 3.74 (s, 3H, CO_2CH_3), 4.33 [d, *J* = 6.2 Hz, 1H, C*H*$(OMe)_2$], N*H* nd; ^{13}C NMR δ_C: 25.6 [C$(CO_2CH_3)CH_3$], 49.2 [*C*HCH$(CH(OMe)_2)$NH], 52.2 [*C*HC$(CO_2Me)CH_3$], 52.3, 52.4 (2xOCH_3), 54.5, 55.5, 58.0 (3xCO_2CH_3), 62.3 [*C*H$(CH(OMe)_2)$NH], 67.9 [*C*$(CO_2Me)CH_3$], 106.1 [*C*H$(OMe)_2$], 171.0, 173.4, 174.4 (3x*C*O_2Me); MS (EI-GC) *m/z*: 333 (M^+, <1%), 258 (11), 215 (15), 200 (12), 156 (31), 75 (100); HRMS calculated for $C_{14}H_{23}NO_8$+1: 334.1502, found: 334.1525.

(1*S,3*R**,3a*S**,6a*R**)-Ethyl 1-benzyl-3-(dimethoxymethyl)-5-methyl-4,6-dioxooctahydropyrrolo[3,4-*c*]pyrrole-1-carboxylate *endo-cis*-7a:** Yellowish prisms, mp: 85-88ºC (from hexane/CH_2Cl_2); IR (neat) ν_{max} 2988, 2335, 1717, 1699 cm^{-1}; ^1H NMR δ_H: 1.34 (t, *J* = 7.2 Hz, 3H, $CO_2CH_2CH_3$), 2.79 (br s, 1H, N*H*), 2.92 (d, *J* = 13.7 Hz, 1H, C*H*HPh), 2.93 (s, 3H, NCH_3), 3.30-3.35 [m, 6H, C*H*HPh, C*H*CH(CH(OMe)$_2$)NH, C*H*C(CO_2Et)BnNH, OCH_3], 3.49 (s, 3H, OCH_3), 3.66 [m, 1H, C*H*CH(OMe)$_2$NH], 4.26 (q, *J* = 7.2 Hz, 2H, $CO_2CH_2CH_3$), 4.68 [d, *J* = 4.1 Hz, 1H, C*H*(OMe)$_2$], 7.19-7.30 (m, 5H, Ar*H*); ^{13}C NMR δ_C: 14.2 ($CO_2CH_2CH_3$), 24.2 (NCH_3), 41.0 [CHC(CO_2Et)BnNH], 47.1 [CHCH(CH(OMe)$_2$)NH], 55.0 (CH_2Ph), 55.7, 55.8 (2xOCH$_3$), 61.5 ($CO_2CH_2CH_3$), 61.9 [CH(CH(OMe)$_2$)NH], 74.2 [C(CO_2Et)BnNH], 102.1 [CH(OMe)$_2$], 127.3, 128.5, 130.2, 135.8 (ArC), 170.7 (CO_2Et), 175.5, 175.9 (2xCON); MS (EI-GC) *m/z*: 390 (M^+, <1%), 315 (26), 299 (27), 285 (13), 269 (14), 268 (14), 267 (100), 91 (13), 75 (13); HRMS calculated for $C_{20}H_{26}N_2O_6$+1: 391.1869, found: 391.1875.

(1S,3R,3aS,6aR)-Ethyl 1,5-dibenzyl-3-(dimethoxymethyl)-4,6-dioxooctahydropyrrolo[3,4-c]pyrrole-1-carboxylate *endo-cis*-7b: Yellowish prisms, mp: 92-94ºC (from hexane/CH_2Cl_2); IR (neat) ν_{max} 2996, 2938, 2310, 1715, 1700 cm^{-1}; ^1H NMR δ_H: 1.29 (t, *J* = 7.2 Hz, 3H, $CO_2CH_2CH_3$), 2.86 (br s, 1H, N*H*), 2.92 (d, *J* = 13.8 Hz, 1H, C*H*HPh), 3.08, 3.41 (2s, 6H, 2xOCH_3), 3.28-3.35 [m, 3H, C*H*HPh, C*H*CH(CH(OMe)$_2$)NH, C*H*C(CO_2Et)BnNH], 3.63 [dd, *J* = 7.4, 3.8 Hz, 1H, C*H*CH(OMe)$_2$NH], 4.23 (q, *J* = 7.2 Hz, 2H, $CO_2CH_2CH_3$), 4.54, 4.66 (d, *J* = 14.4 Hz, 2H, NCH_2Ph), 4.61 [d, *J* = 3.8 Hz, 1H, C*H*(OMe)$_2$], 7.20-7.33 (m, 10H, Ar*H*); ^{13}C NMR δ_C: 14.1 ($CO_2CH_2CH_3$), 41.1, 42.7 (CH_2Ph, NCH_2Ph), 47.1 [CHC(CO_2Et)BnNH], 54.5 [CHCH(CH(OMe)$_2$)NH], 55.4, 55.6 (2xOCH$_3$), 61.8 [CH(CH(OMe)$_2$)NH], 62.0 ($CO_2CH_2CH_3$), 72.5 [C(CO_2Et)BnNH], 101.7 [CH(OMe)$_2$], 127.2, 127.9, 128.4, 128.5, 128.6, 130.2, 135.6, 135.9 (ArC), 170.6 (CO_2Et), 175.2, 175.5 (2xCON); MS (EI-GC) *m/z*: 466 (M^+, <1%), 308 (12), 307 (55), 290 (16), 289 (100), 281 (11), 215 (14), 207 (21), 187 (12), 174 (15), 119 (11), 91 (64); HRMS calculated for $C_{26}H_{30}N_2O_6$+1: 467.2182, found: 467.2175.

(1*S,3*R**,3a*S**,6a*R**)-Ethyl 1-benzyl-3-(dimethoxymethyl)-4,6-dioxo-5-phenyloctahydropyrrolo[3,4-*c*]pyrrole-1-carboxylate *endo-cis*-7c:** Yellowish solid, mp: 118-121ºC (from hexane/CH_2Cl_2); IR (neat) ν_{max} 2992, 2945, 2315, 1718, 1689 cm^{-1}; ^1H NMR δ_H: 1.33 (t, *J* = 7.2 Hz, 3H, $CO_2CH_2CH_3$), 3.01, 3.39 (2d, *J* = 13.7 Hz, 2H, CH_2Ph), 3.34, (s, 3H, OCH_3), 3.47-3.53 [m, 5H, C*H*CH(CH(OMe)$_2$)NH, C*H*C(CO_2Et)BnNH, OCH_3], 3.74 [dd, *J* = 7.8, 3.4 Hz, 1H, C*H*CH(OMe)$_2$NH], 4.26 (qd, *J* = 7.2, 2.1 Hz, 2H, $CO_2CH_2CH_3$), 4.82 [d, *J* = 3.8 Hz, 1H, C*H*(OMe)$_2$], 7.23-7.50 (m, 10H, Ar*H*), N*H* nd; ^{13}C NMR δ_C: 14.0 ($CO_2CH_2CH_3$), 41.3 (CH_2Ph), 47.5 [CHC(CO_2Et)BnNH], 54.7 [CHCH(CH(OMe)$_2$)NH], 55.6, 56.0 (2xOCH$_3$), 62.0 [CH(CH(OMe)$_2$)NH], 62.2 ($CO_2CH_2CH_3$), 72.8 [C(CO_2Et)BnNH], 101.6 [CH(OMe)$_2$], 126.6, 127.2, 128.3, 128.8, 129.2, 130.2, 131.8, 135.8 (ArC), 170.6 (CO_2Et), 174.6, 174.9 (2xCON); MS (EI-GC) *m/z*: 452 (M^+, <1%), 315 (23), 299 (24), 285 (13), 269 (15), 268 (15), 267 (100), 241 (10), 91 (29), 75 (35); HRMS calculated for $C_{25}H_{28}N_2O_6$+1: 453.2025, found: 453.2014.

(2*S,3*R**,4*R**,5*R**)-2-Ethyl 3,4-dimethyl 2-benzyl-5-(dimethoxymethyl)pyrrolidine-2,3,4-tricarboxylate *exo-cis*-7d:** Sticky pale yellow oil; IR (neat) ν_{max} 2985, 2947, 1714, 1712, 1691 cm^{-1}; ^1H NMR δ_H: 1.26 (t, *J* = 7.1 Hz, 3H, $CO_2CH_2CH_3$), 2.76, 2.95 (d, *J* = 13.0 Hz, 2H, CH_2Ph), 3.29, 3.34 (s, 6H, 2xOCH_3), 3.68-3.73 [m, 6H, C*H*CH(CH(OMe)$_2$)NH, C*H*C(CO_2Et)BnNH, C*H*CH(OMe)$_2$NH, CO_2CH_3], 3.79 (s, 3H, CO_2CH_3), 4.07-4.23 [m, 3H, C*H*(OMe)$_2$, $CO_2CH_2CH_3$], 7.16-7.22 (m, 5H, Ar*H*), N*H* nd; ^{13}C NMR δ_C: 14.2 ($CO_2CH_2CH_3$), 42.0 (CH_2Ph), 47.9 [CHC(CO_2Et)BnNH], 52.0 [CHCH(CH(OMe)$_2$)NH], 52.4, 53.1 (2xCOCH_3), 54.5, 54.8 (2xOCH$_3$), 59.7 [CH(CH(OMe)$_2$)NH], 61.7 ($CO_2CH_2CH_3$), 69.9 [C(CO_2Et)BnNH], 103.8 [CH(OMe)$_2$], 126.8, 128.0, 130.6, 136.3 (ArC), 171.3, 171.6 (2xCO_2Me), 174.1 (CO_2Et); MS (EI-GC) *m/z*: 423 (M^+, <1%), 392 (14), 350 (19), 348 (45), 332 (36), 318 (21), 317 (13), 316 (68), 301 (11), 300 (76), 288 (39), 286 (11), 268 (59), 258 (26), 256 (15), 242 (16), 240 (15), 226 (20), 224 (11), 216 (11), 210 (18), 196 (13), 194 (17), 166 (11), 91 (100), 75 (28); HRMS calculated for $C_{21}H_{29}NO_8$+1: 424.1971, found: 424.1968.

(2*S,3*S**,4*S**,5*R**)-2-ethyl 3,4-dimethyl 2-benzyl-5-(dimethoxymethyl)pyrrolidine-2,3,4-tricarboxylate *endo-cis*-8d:** Sticky pale yellow oil; IR (neat) ν_{max} 2987, 2955, 1719, 1716, 1696 cm^{-1}; ^1H NMR δ_H: 1.24 (t, *J* = 7.1 Hz, 3H, $CO_2CH_2CH_3$), 2.61 (br s, 1H, N*H*), 3.12-1.19 [m, 2H, C*H*HPh, C*H*CH(CH(OMe)$_2$)NH], 3.29-3.40 [m, 9H, C*H*HPh, C*H*C(CO_2Et)BnNH, C*H*CH(OMe)$_2$NH, 2xOCH_3], 3.69 (s, 3H, CO_2CH_3), 3.77 (s, 3H, CO_2CH_3), 4.05-4.15 [m, 2H, $CO_2CH_2CH_3$], 4.36 [d, *J* = 6.4 Hz, 1H, C*H*(OMe)$_2$], 7.17-7.27 (m, 5H, Ar*H*); ^{13}C NMR δ_C: 14.1 ($CO_2CH_2CH_3$), 43.1 (CH_2Ph), 49.0 [*C*HC(CO_2Et)BnNH], 52.2, 52.3 (2xCOCH_3), 53.8 [*C*HCH(CH(OMe)$_2$)NH], 55.2, 55.7 (2xOCH_3), 61.7 [*C*H(CH(OMe)$_2$)NH], 61.9 ($CO_2CH_2CH_3$), 72.0 [*C*(CO_2Et)BnNH], 105.9 [*C*H(OMe)$_2$], 127.1, 128.3, 130.7, 136.1 (ArC), 171.1, 173.1 (2x*C*O_2Me), 173.4 (*C*O_2Et); MS (EI-GC) *m/z*: 423 (M^+, <1%), 348 (11), 333 (11), 332 (65), 316 (33), 300 (45), 288 (46), 286 (11), 268 (61), 258 (33), 256 (14), 242 (14), 240 (17), 226 (21), 216 (12), 210 (17), 194 (16), 166 (10), 91 (100), 75 (27); HRMS calculated for $C_{21}H_{29}NO_8$+1: 424.1971, found: 424.1959.

(3*R,3a*S**,6a*R**)-Diethyl 3-(dimethoxymethyl)-5-methyl-4,6-dioxohexahydropyrrolo[3,4-*c*]pyrrole-1,1(2*H*)-dicarboxylate *all-cis*-8:** Sticky pale yellow oil; IR (neat) ν_{max} 2999, 1718, 1713, 1691 cm^{-1}; ^1H NMR δ_H: 1.29 (t, *J* = 7.1 Hz, 3H, $CO_2CH_2CH_3$), 1.33 (t, *J* = 7.1 Hz, 3H, $CO_2CH_2CH_3$), 2.97 (s, 3H, NCH_3), 3.32 (deform. dd, *J* = 7.8, 7.5 Hz, 1H, C*H*CHNH), 3.42, 3.54 (2s, 6H, 2xOCH_3), 4.08 [d, *J* = 7.5 Hz, 1H, C*H*C(CO_2Et)$_2$NH], 4.18-4.40 (m, 5H, C*H*NH, 2x$CO_2CH_2CH_3$), 4.56 [d, *J* = 6.1 Hz, 1H, C*H*(OMe)$_2$], N*H* nd; ^{13}C NMR δ_C: 14.1, 14.2 (2x$CO_2CH_2CH_3$), 25.4 (NCH_3), 45.5 (*C*HCHNH), 50.6 [*C*HC(CO_2Et)$_2$NH], 55.5, 56.2 (2xOCH_3), 60.9 (*C*HNH), 62.6, 62.9 (2x$CO_2CH_2CH_3$), 74.1 [*C*(CO_2Et)$_2$], 103.5 [*C*H(OMe)$_2$], 166.9, 169.3 (2x*C*O_2Et), 175.2, 175.4 (2xCON); MS (EI-GC) *m/z*: 372 (M^+, <1%), 341 (14), 299 (24), 298 (10), 297 (52), 268 (10), 267 (65), 166 (30), 75 (100); HRMS calculated for $C_{16}H_{24}N_2O_8$+1: 373.1611, found: 373.1599.

3. ^{1}H-, ^{13}C-NMR Spectra and Bidimensional Experiments

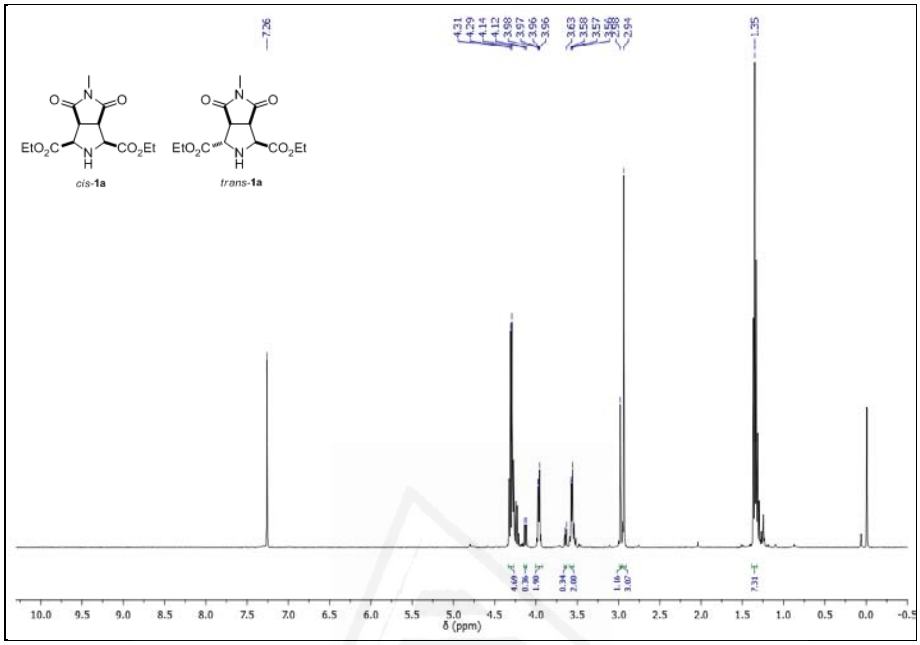

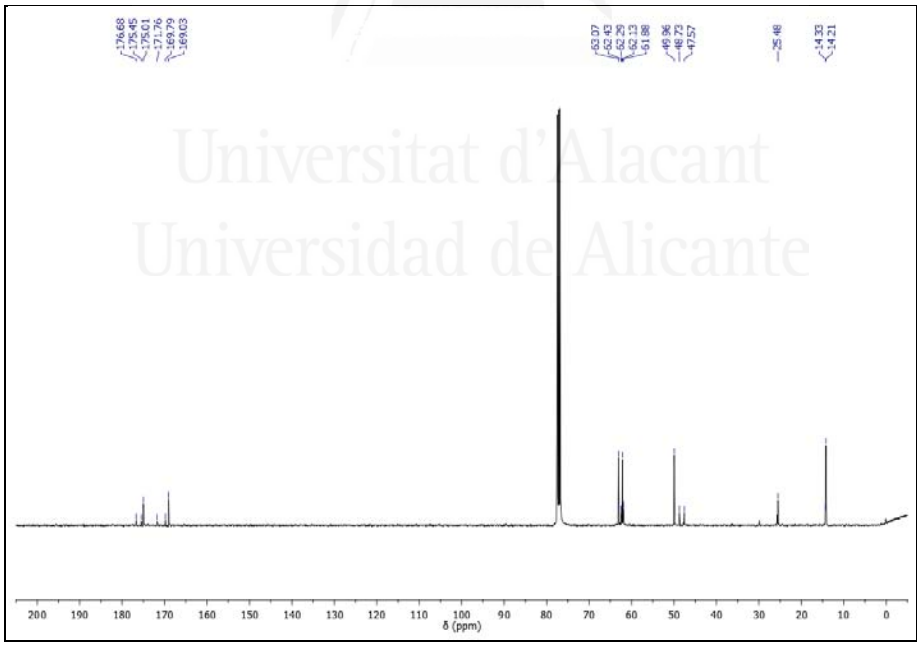

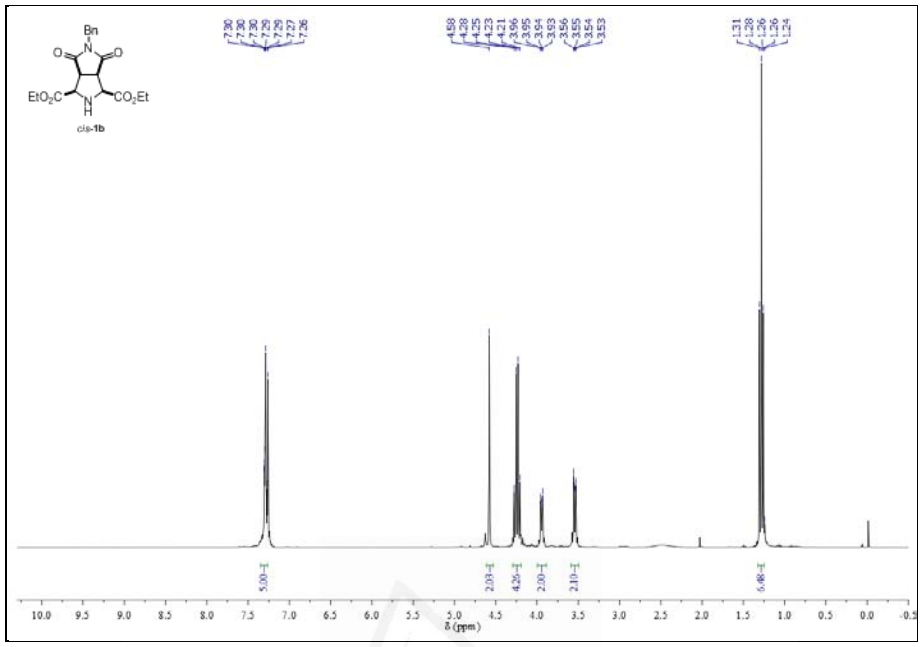

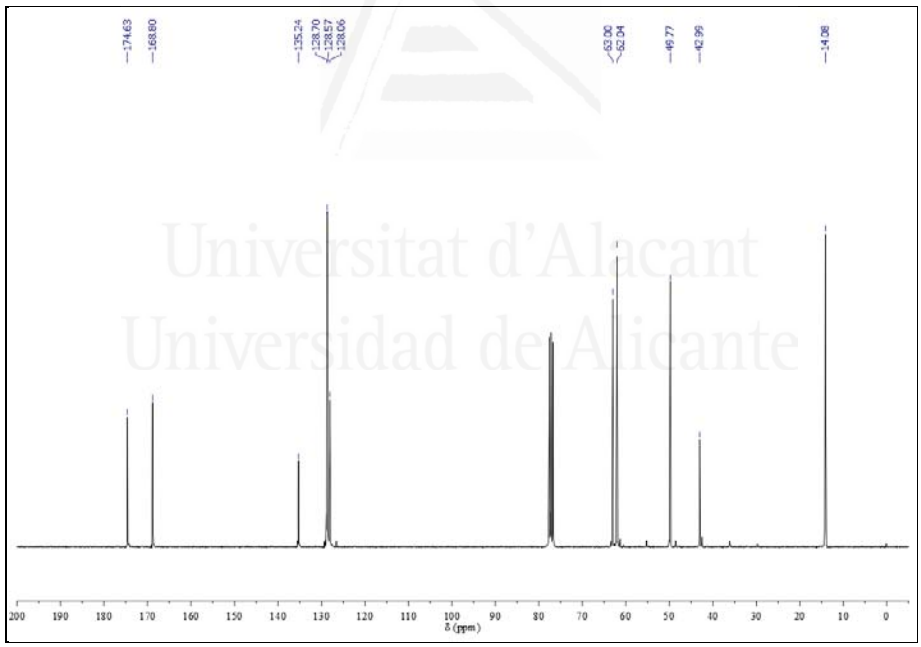

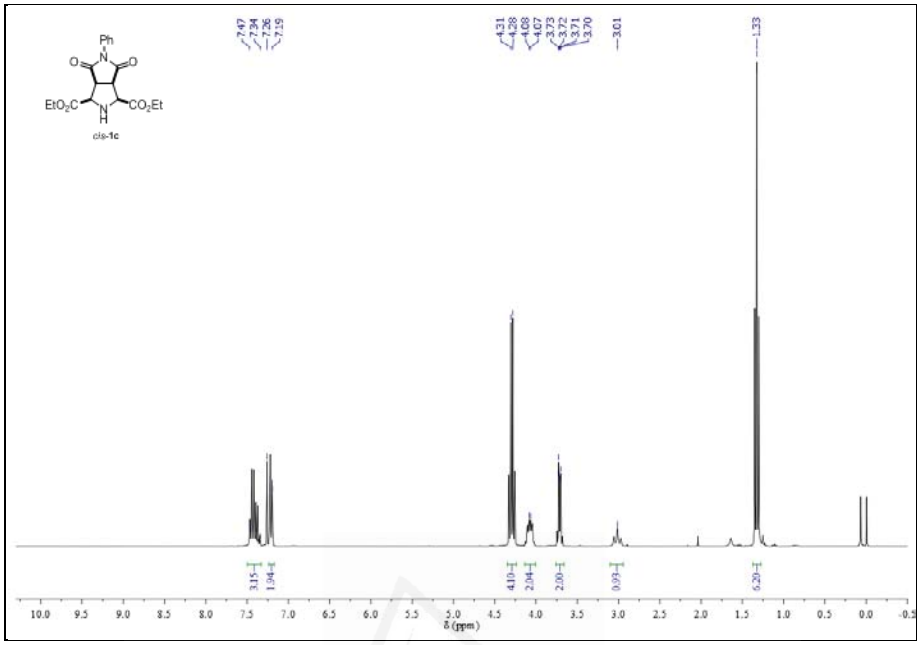

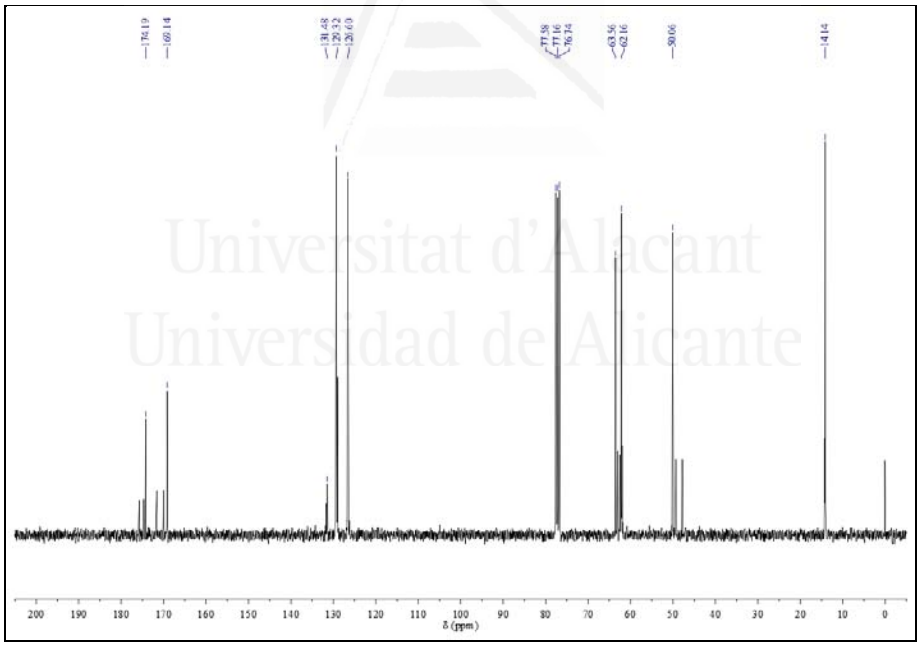

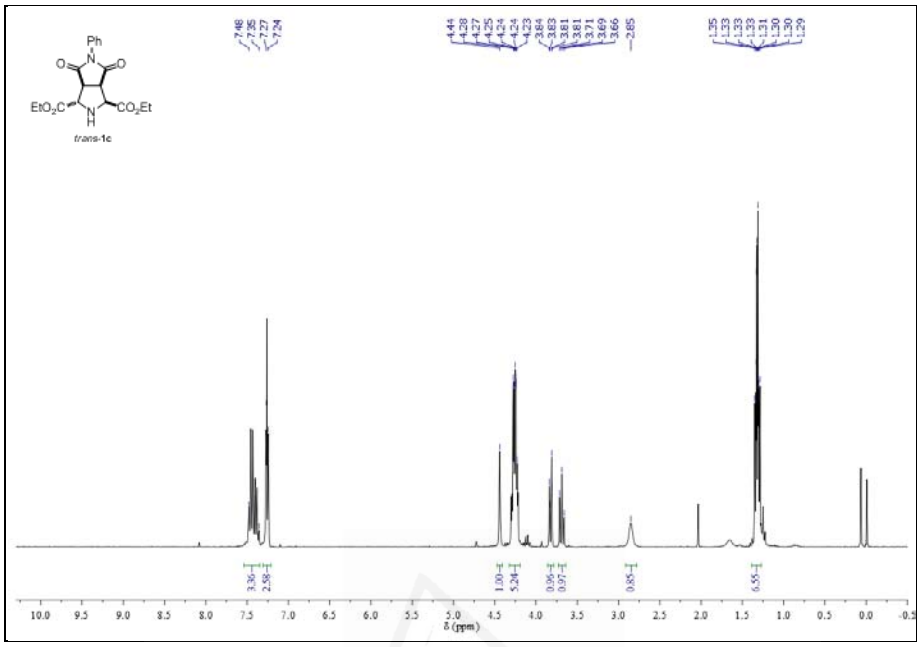

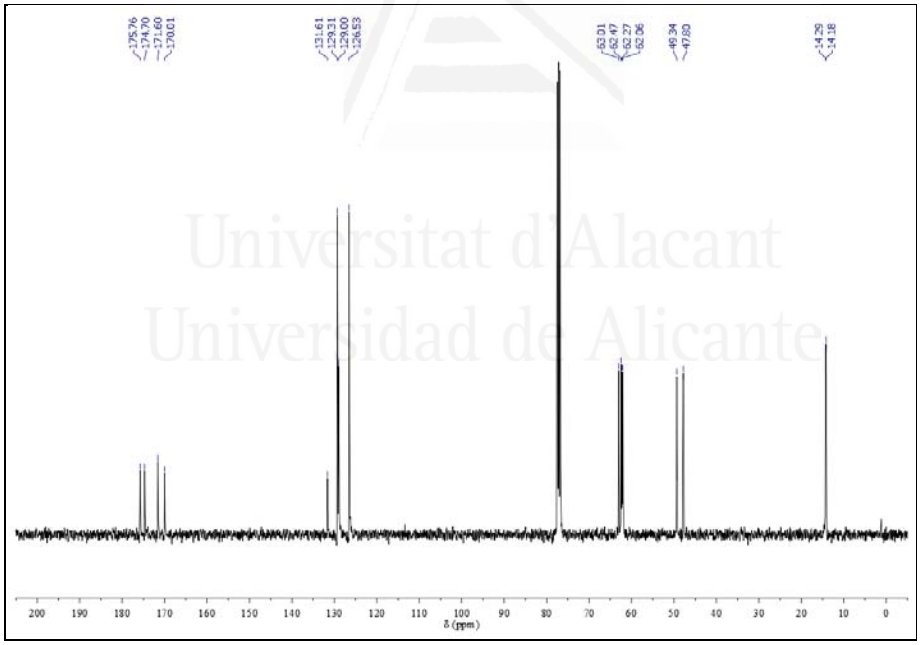

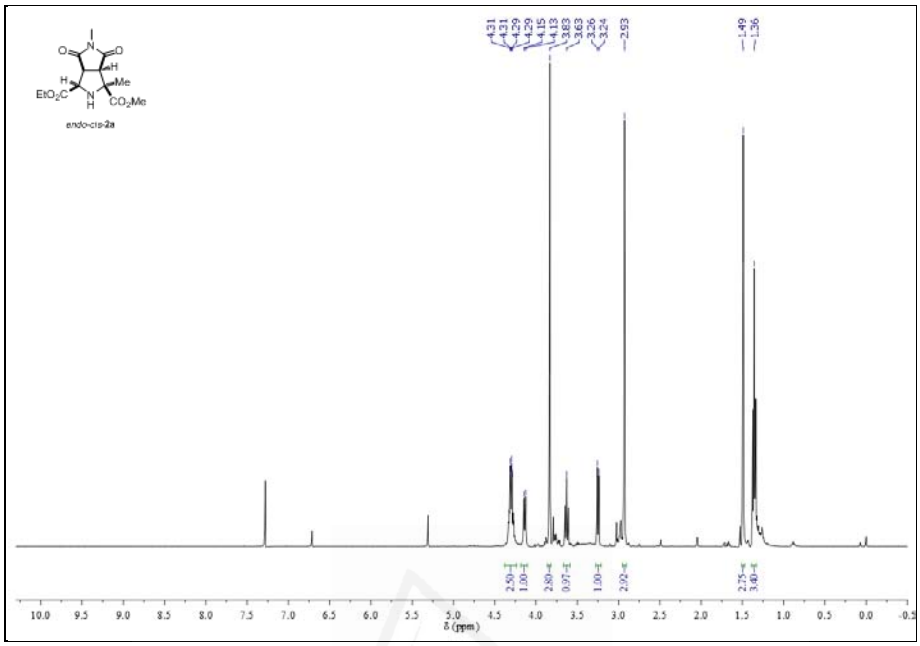

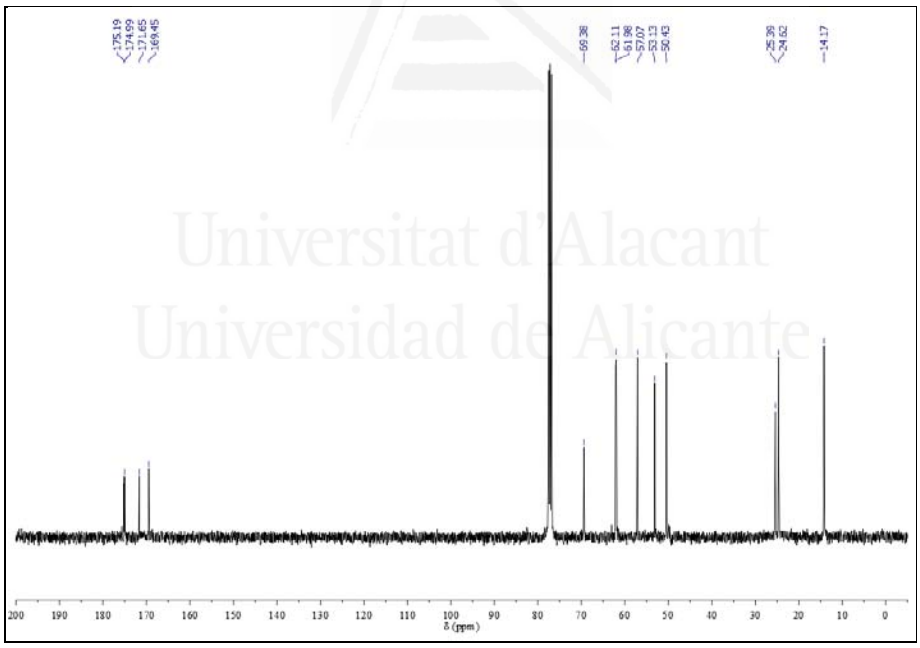

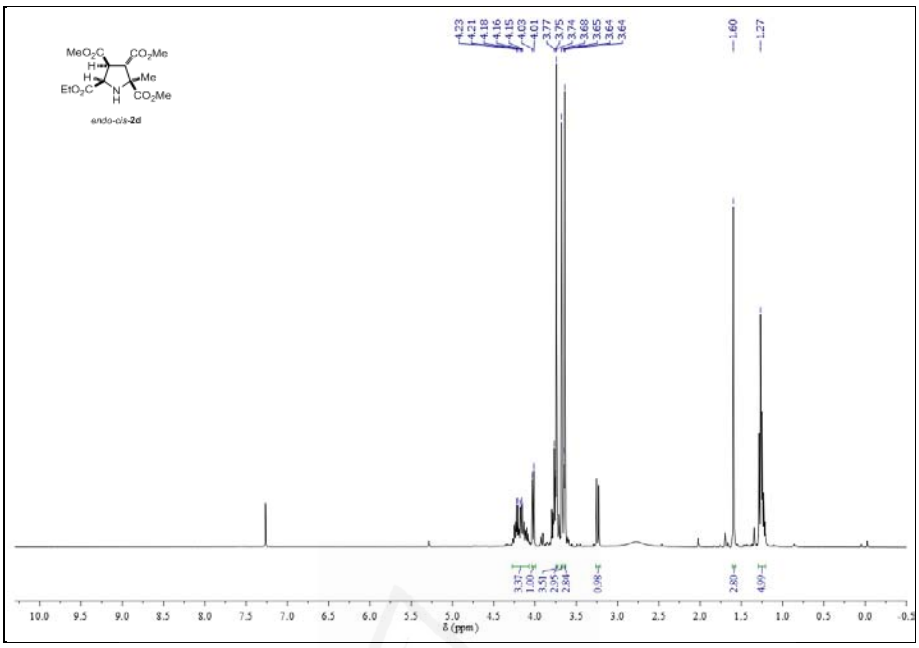

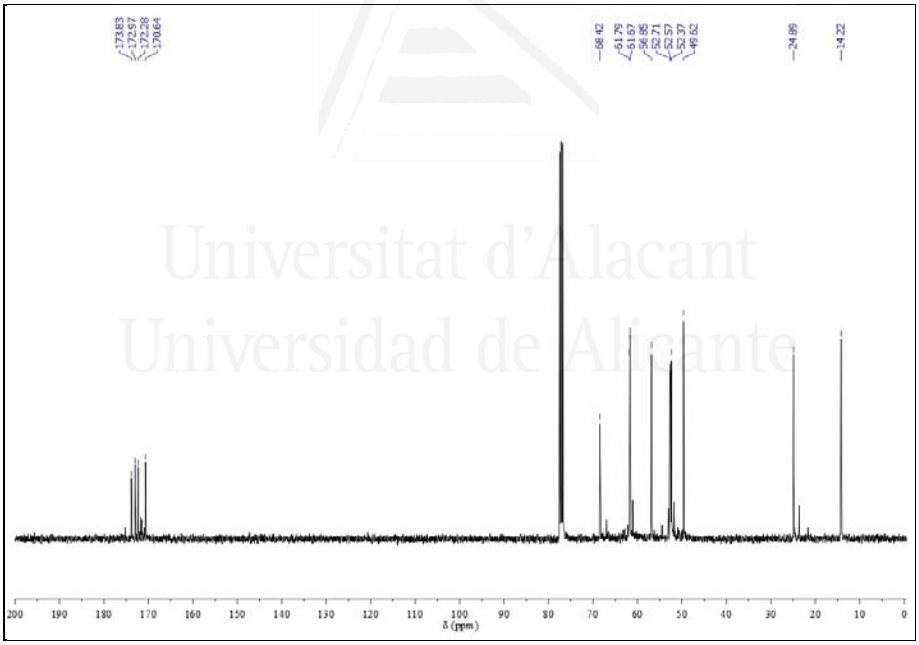

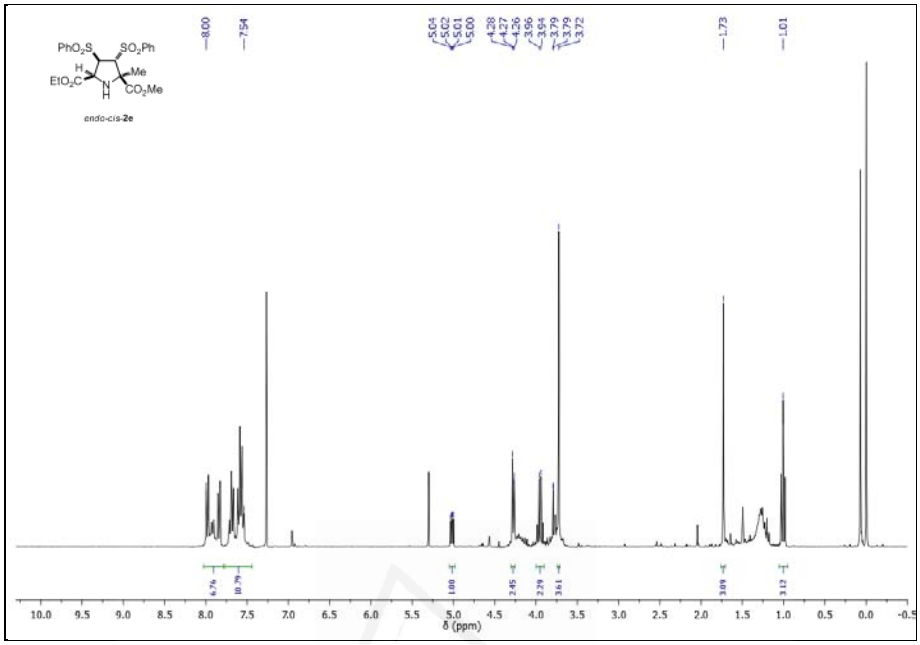

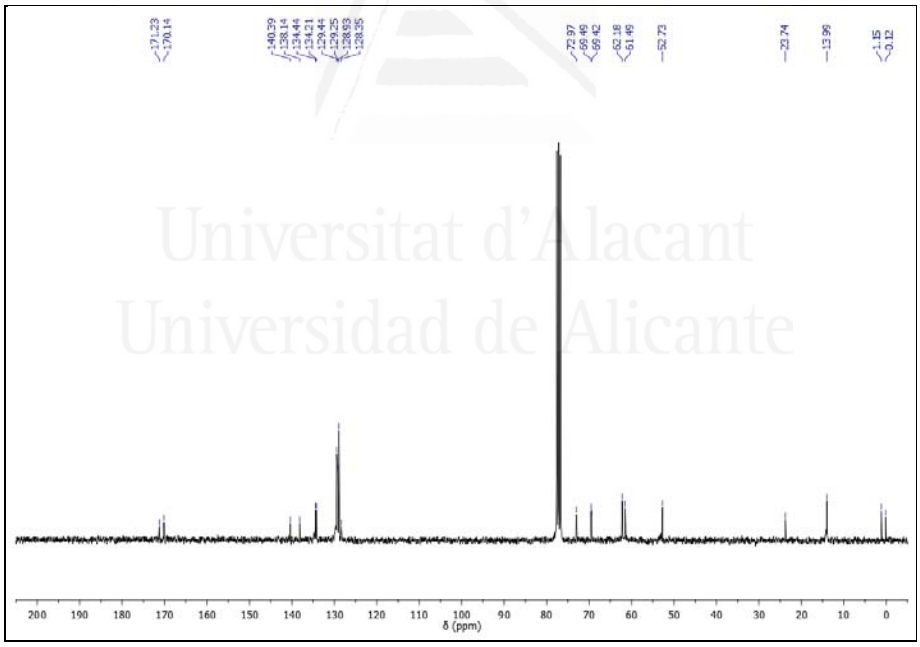

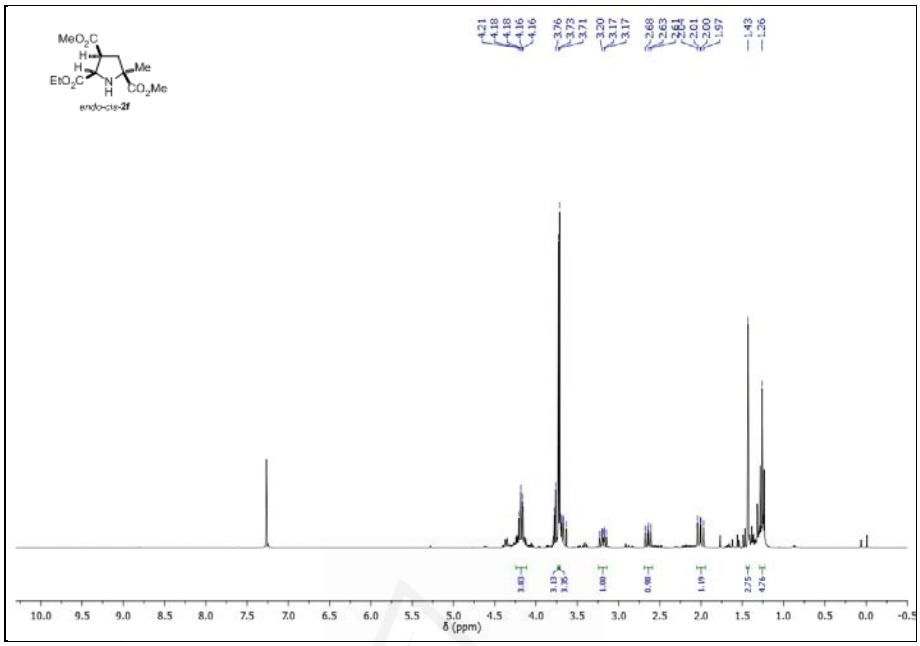

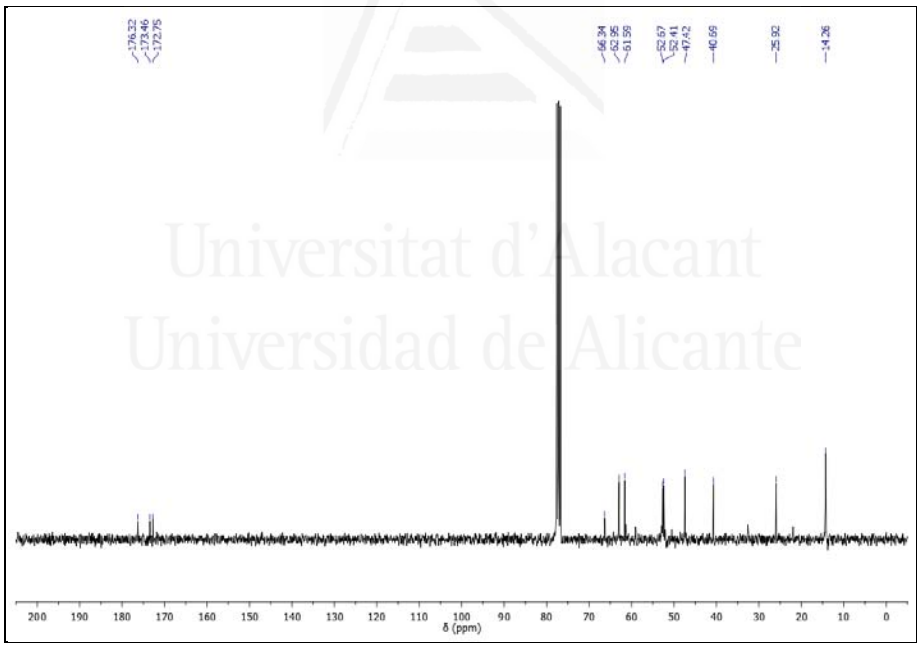

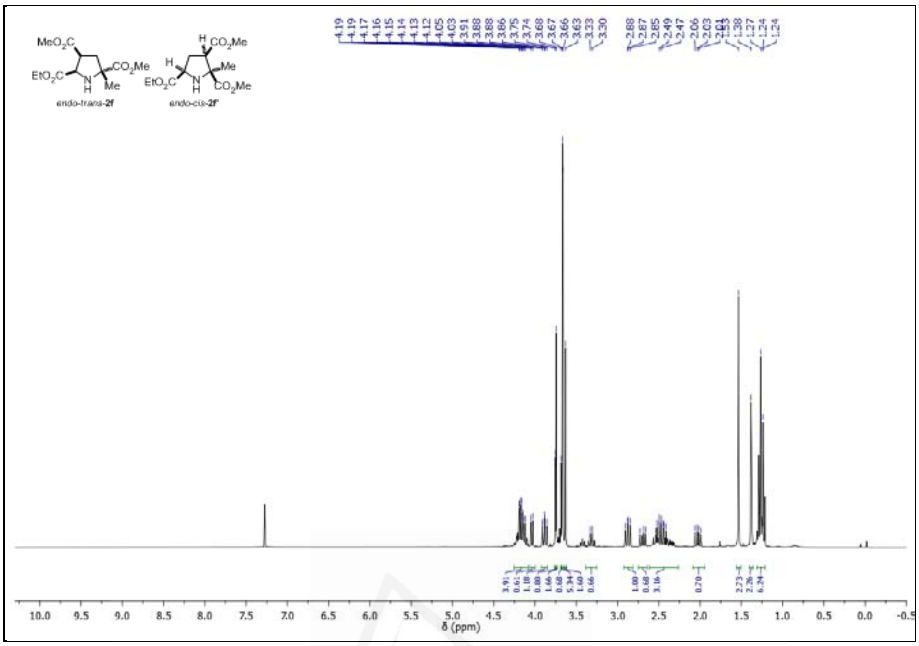

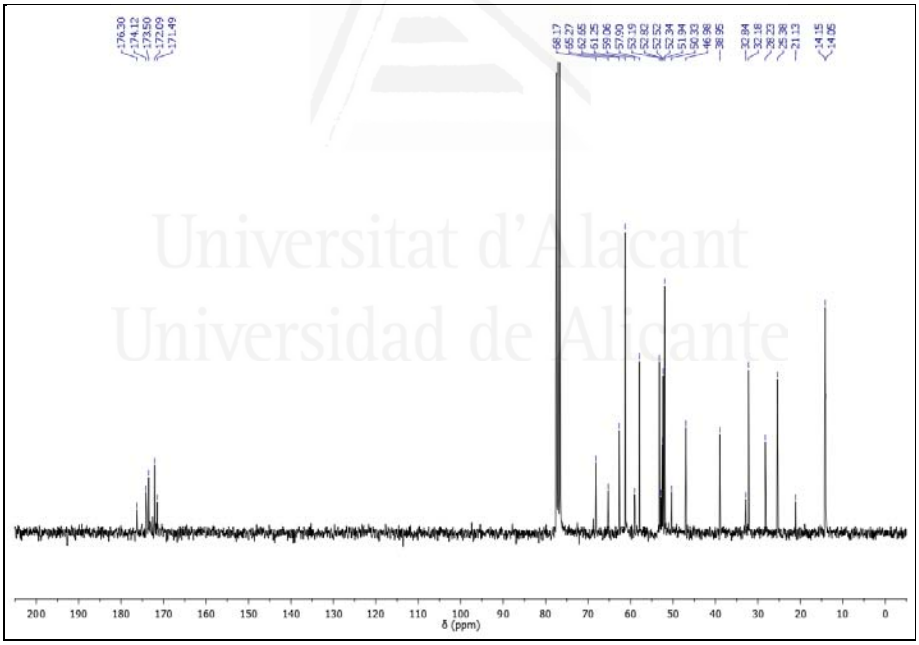

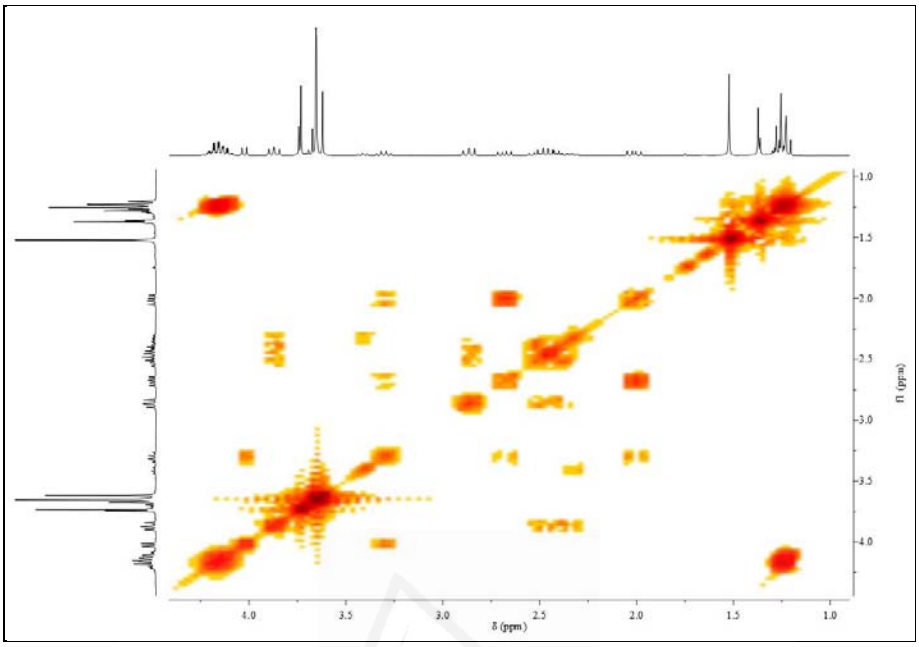

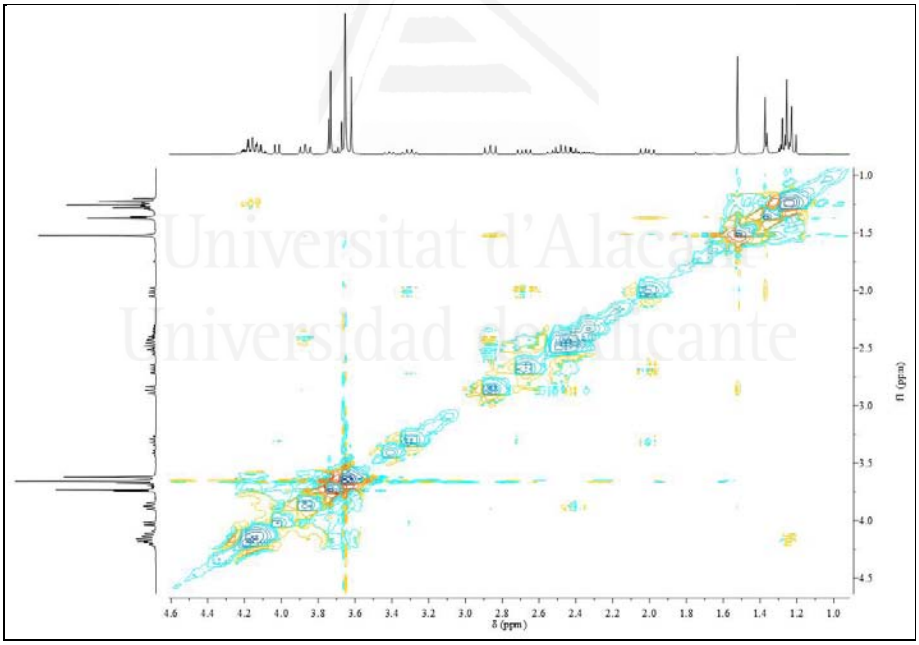

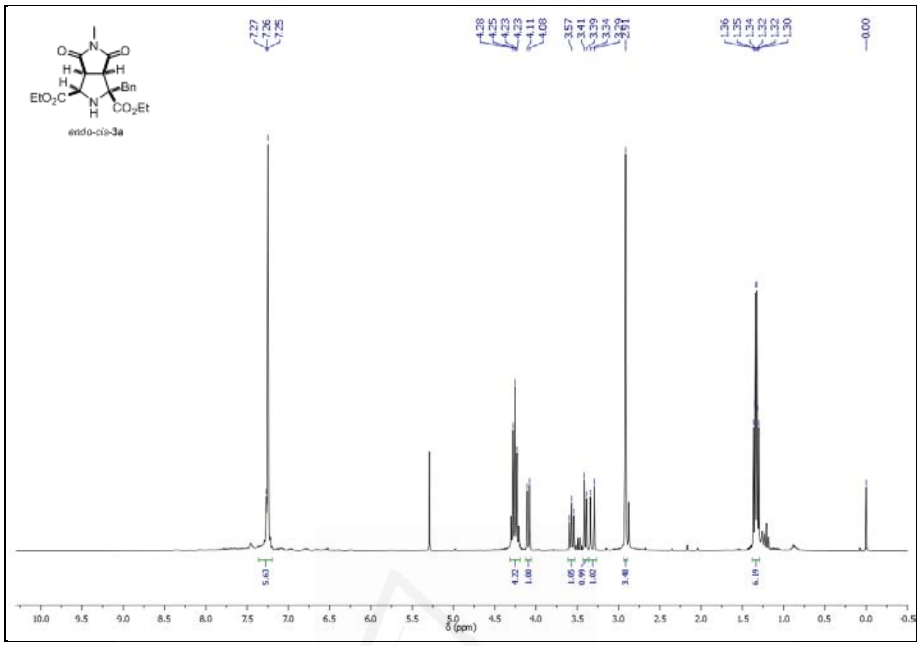

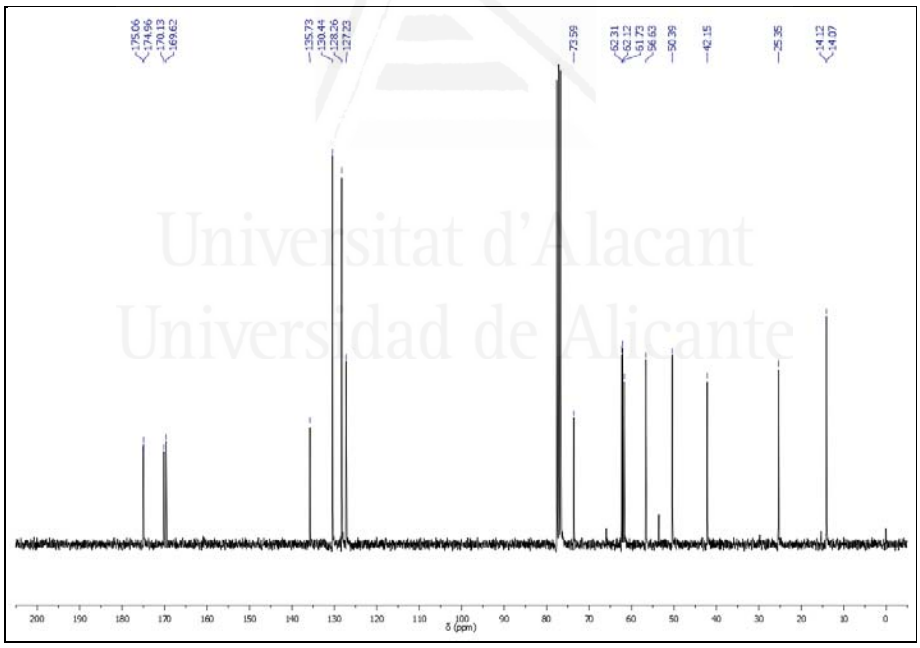

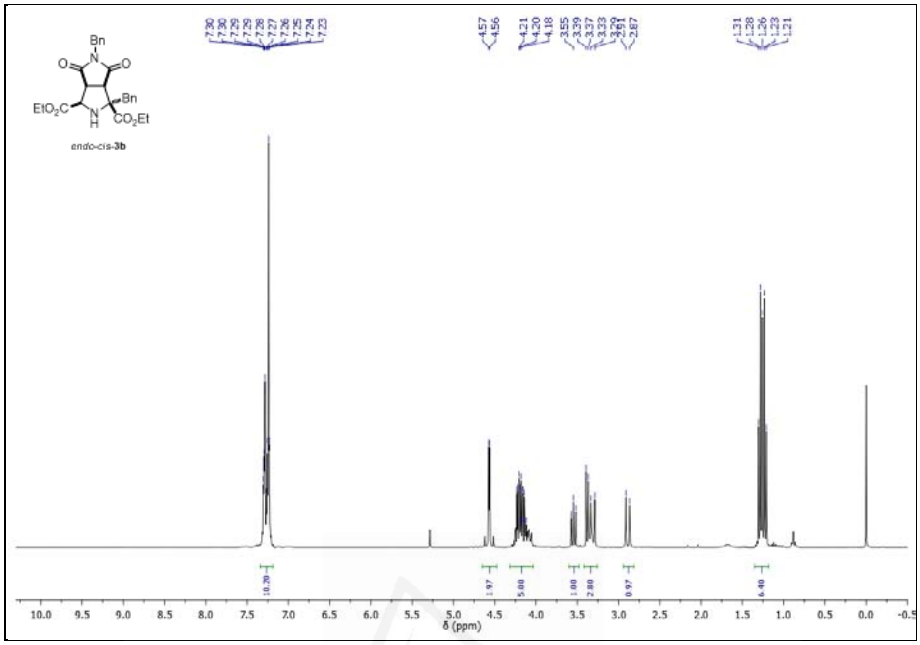

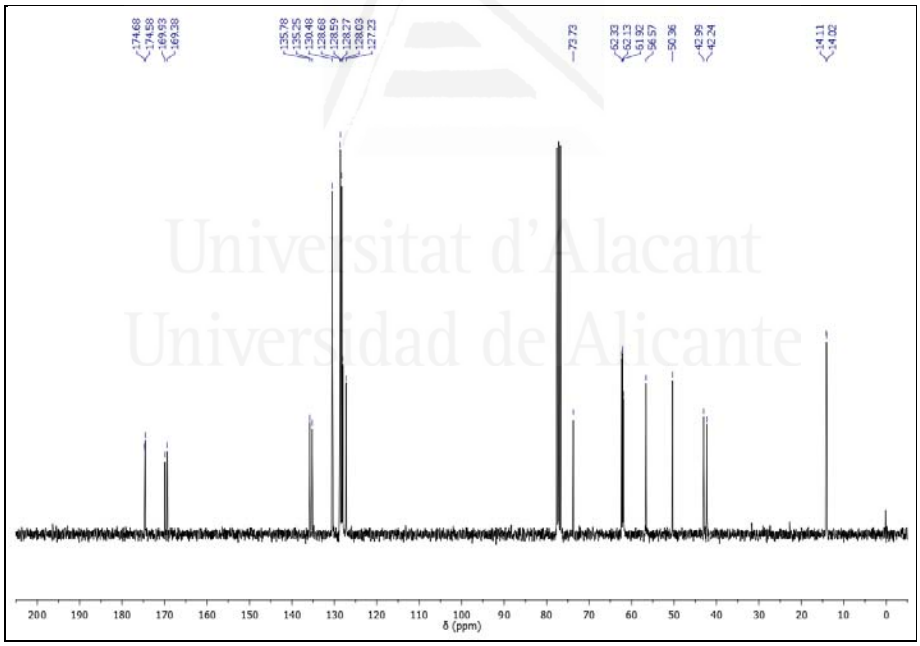

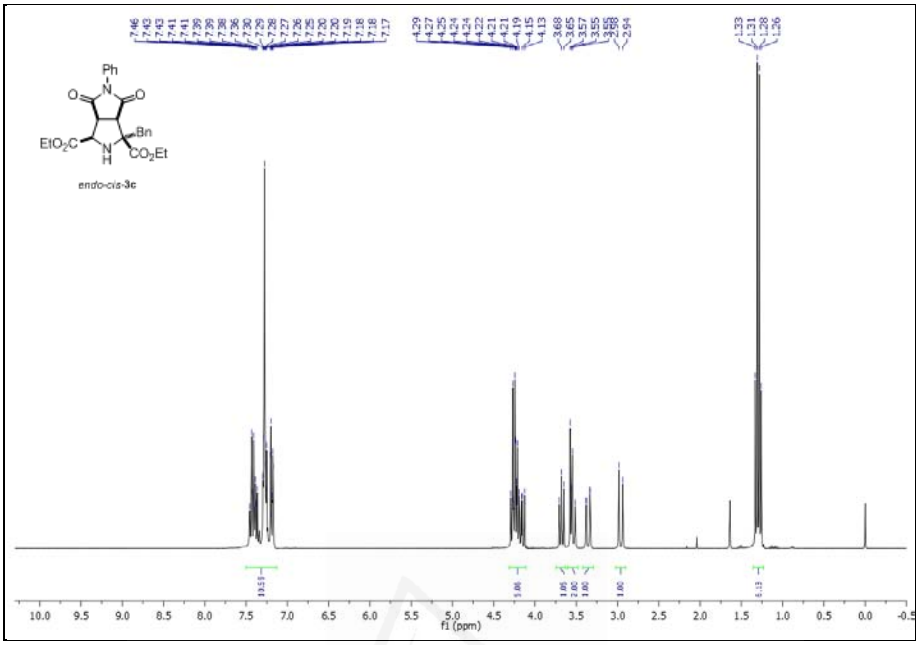

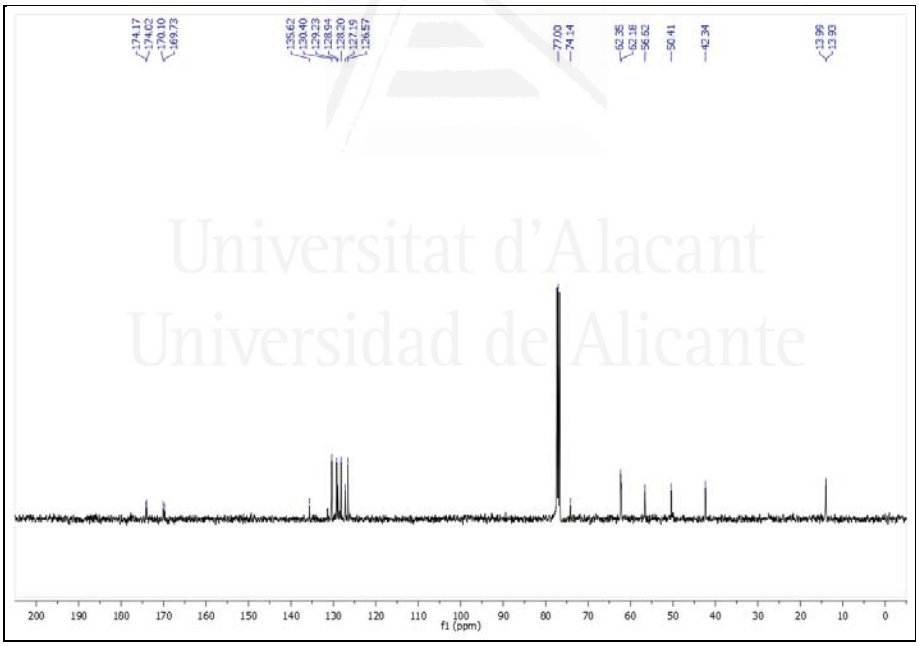

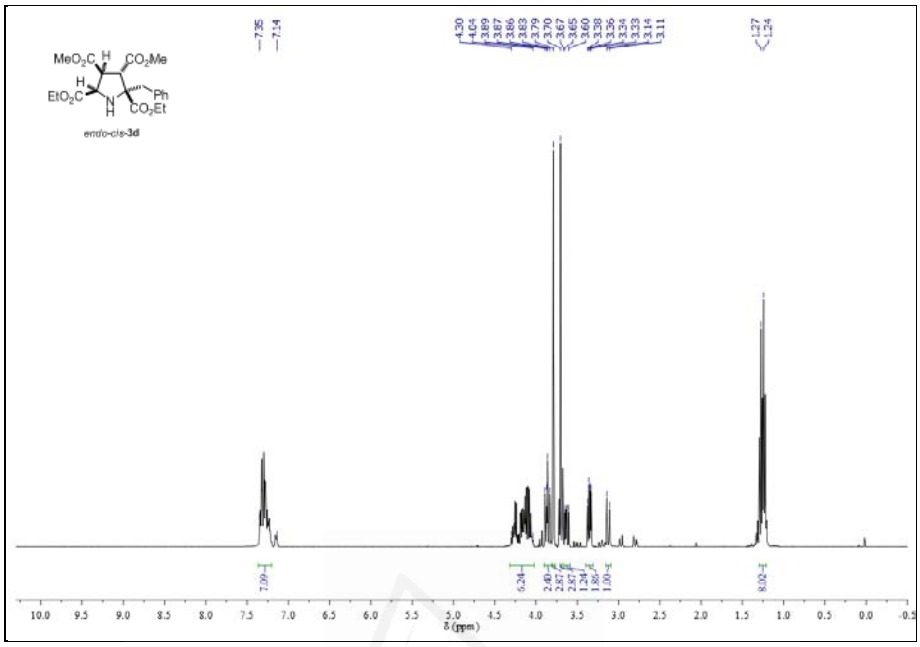

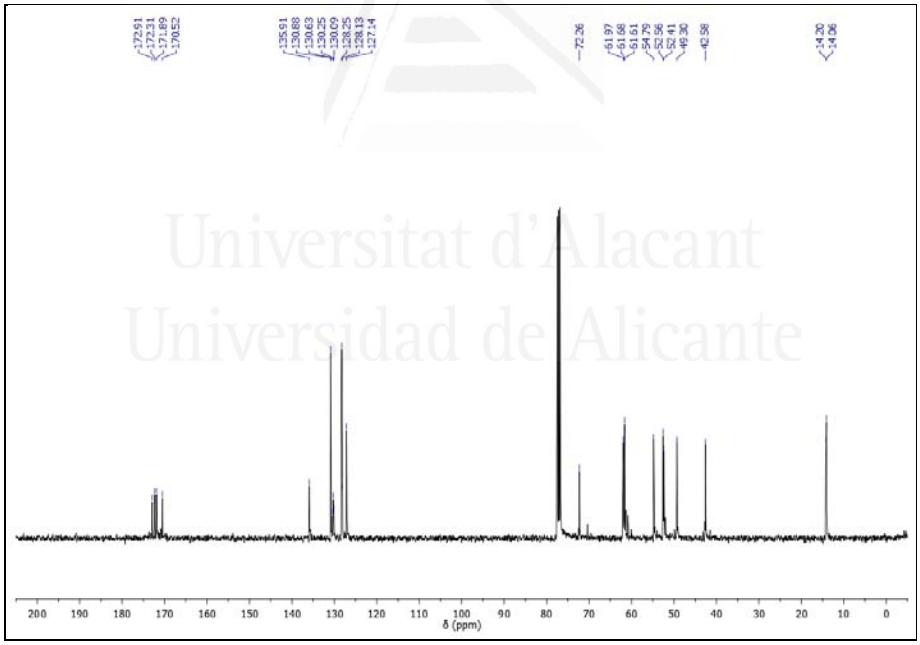

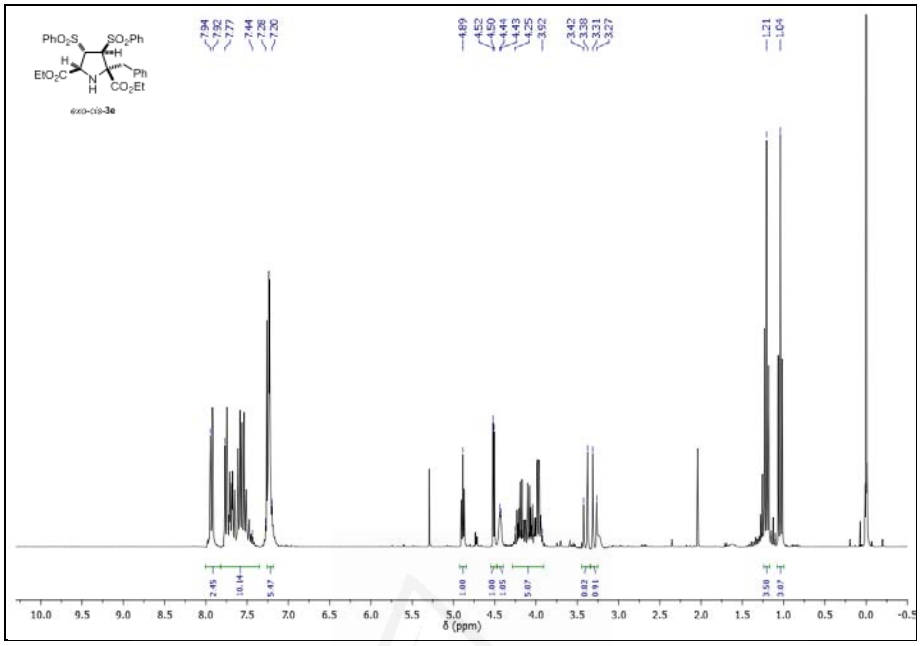

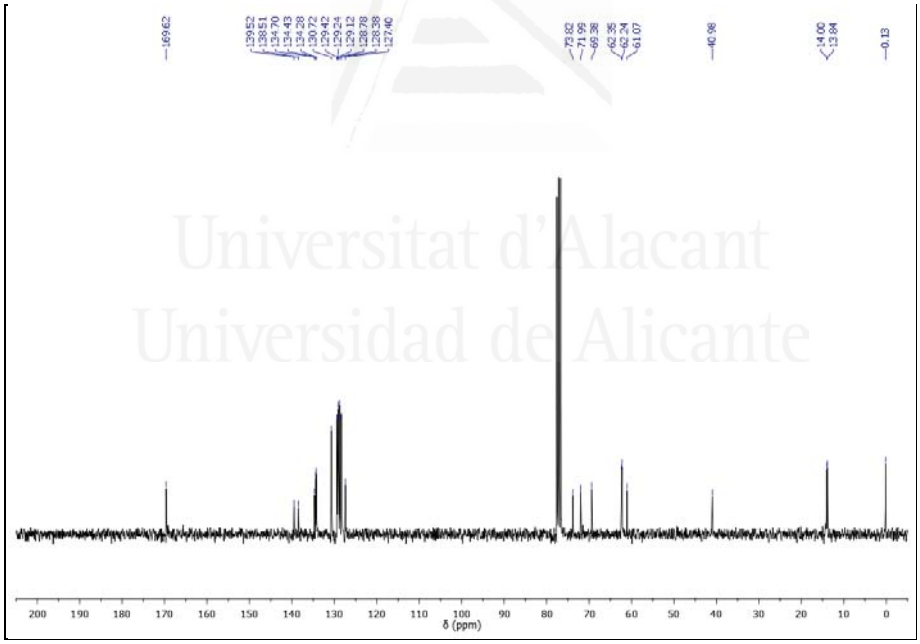

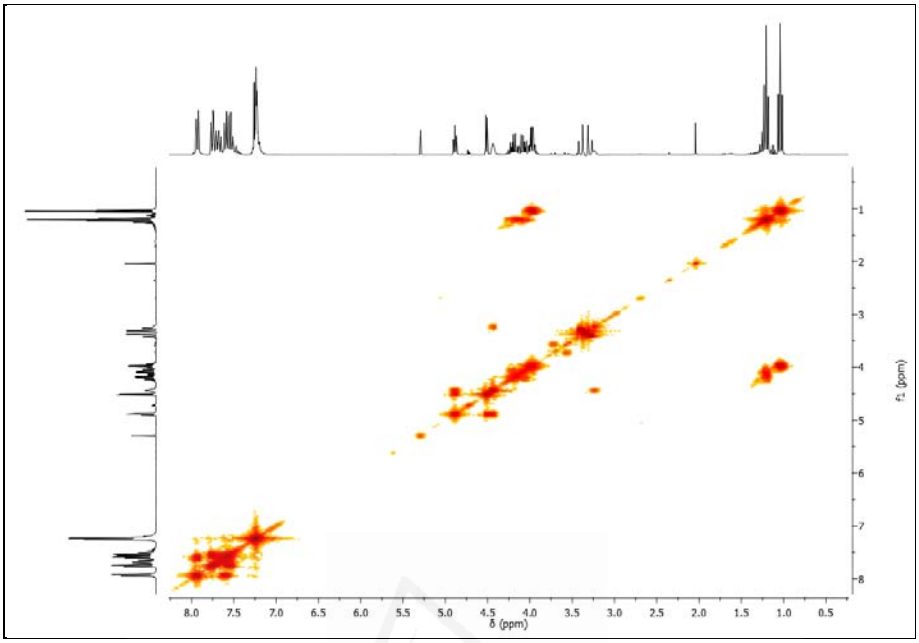

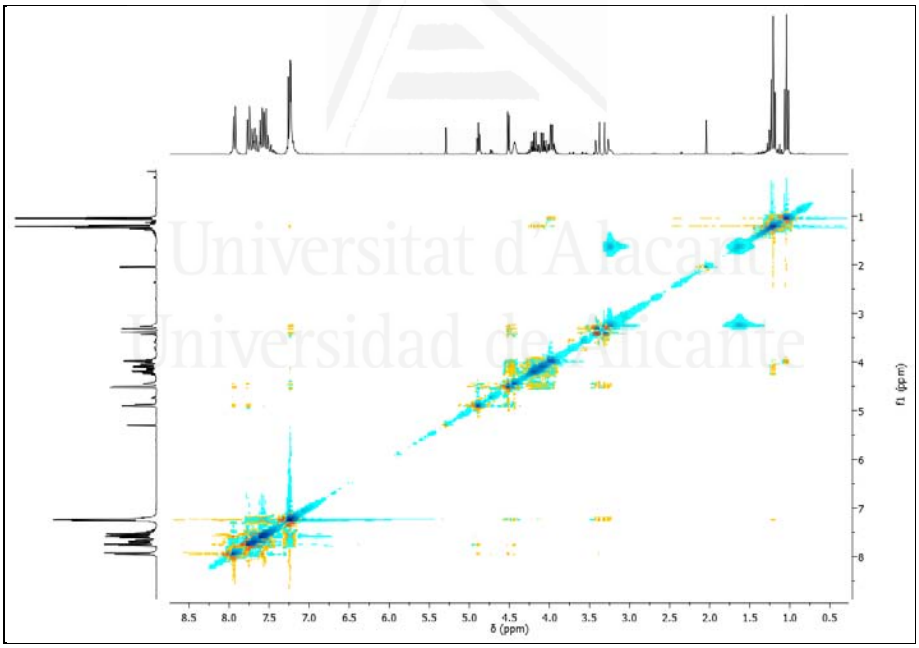

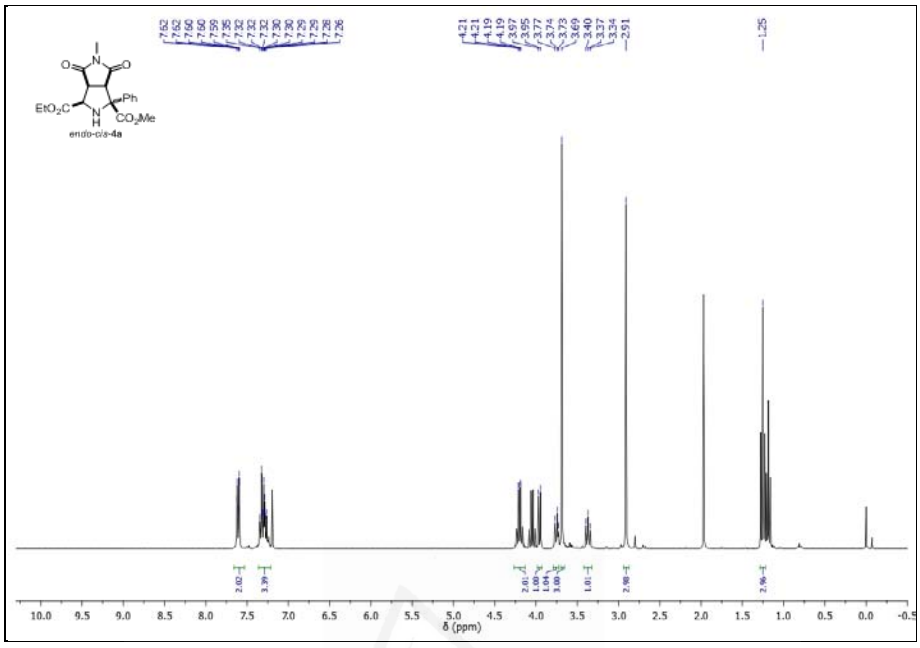

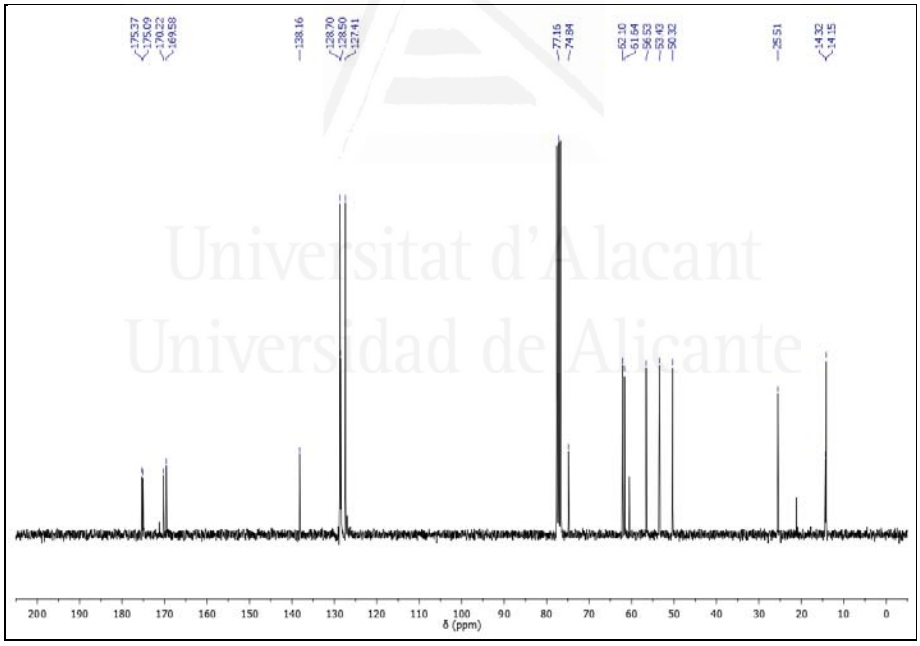

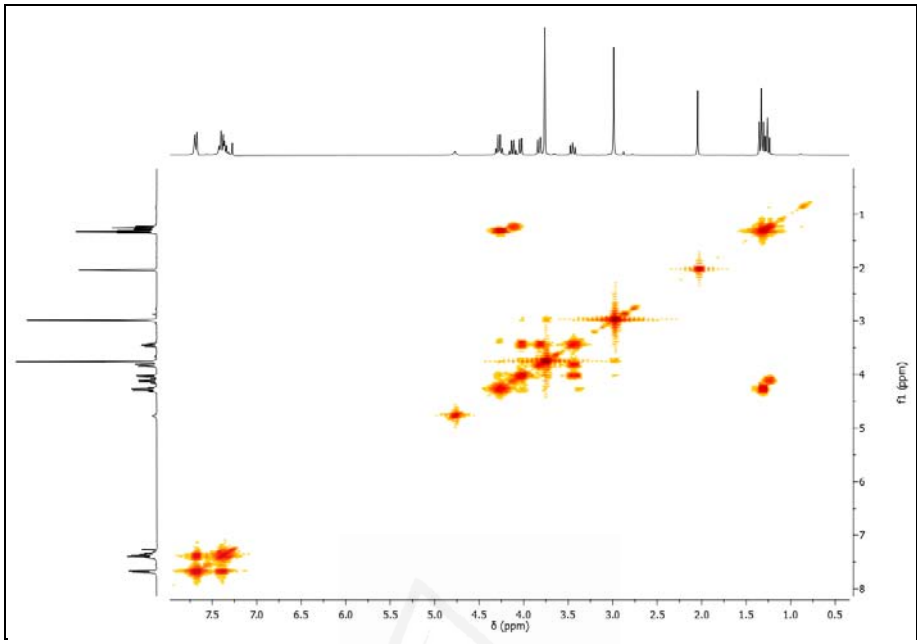

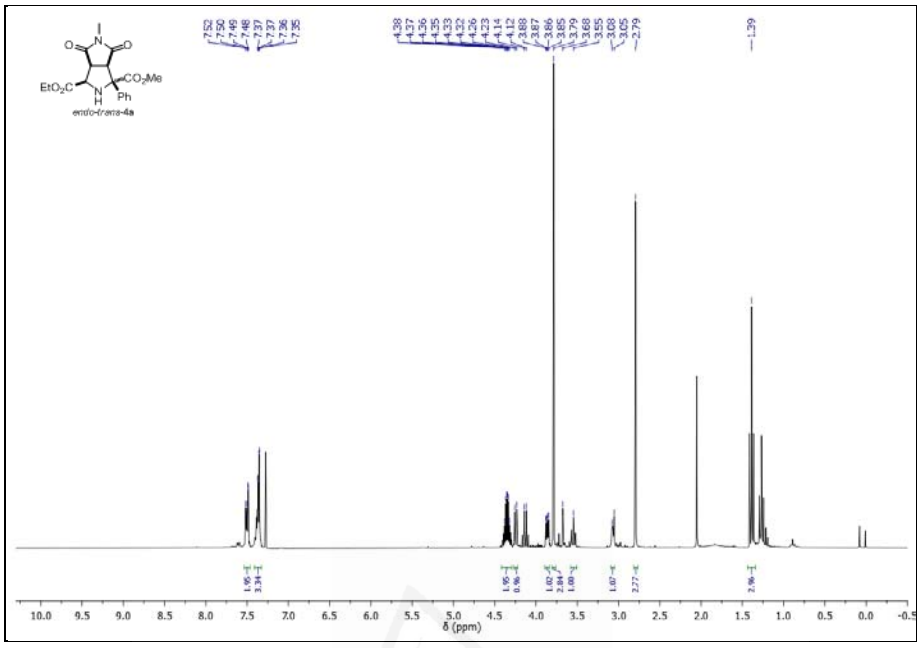

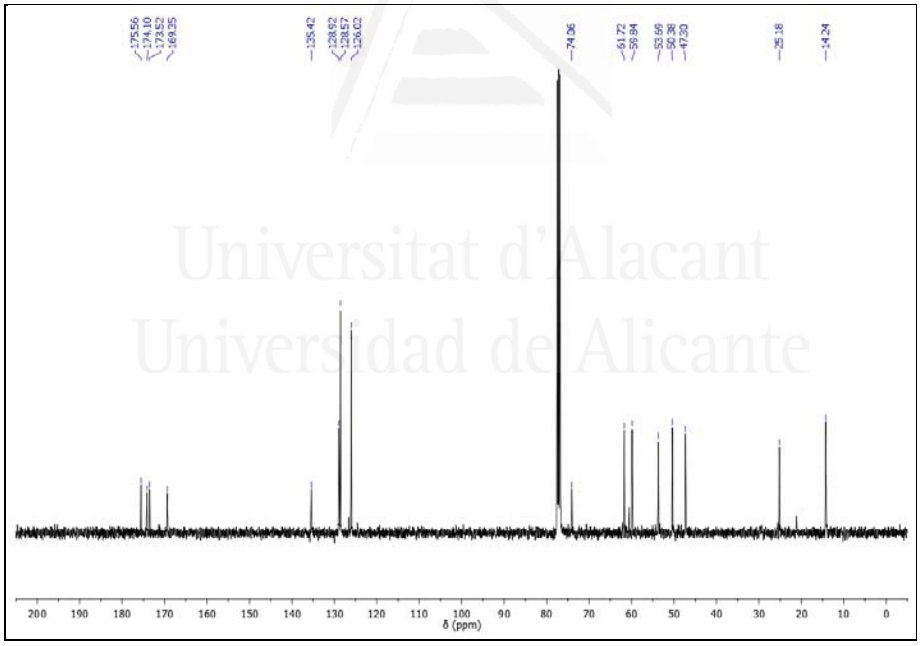

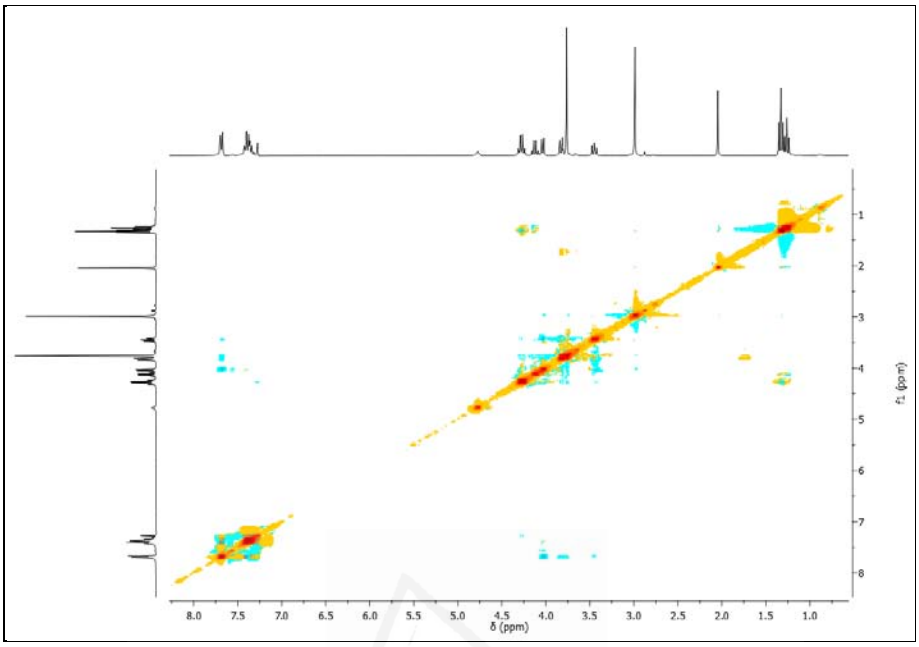

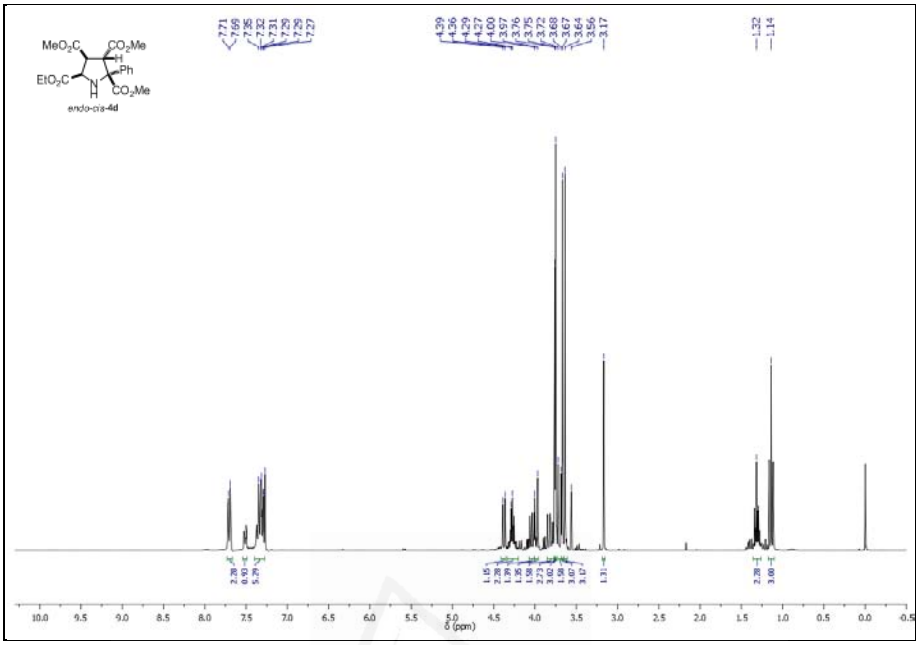

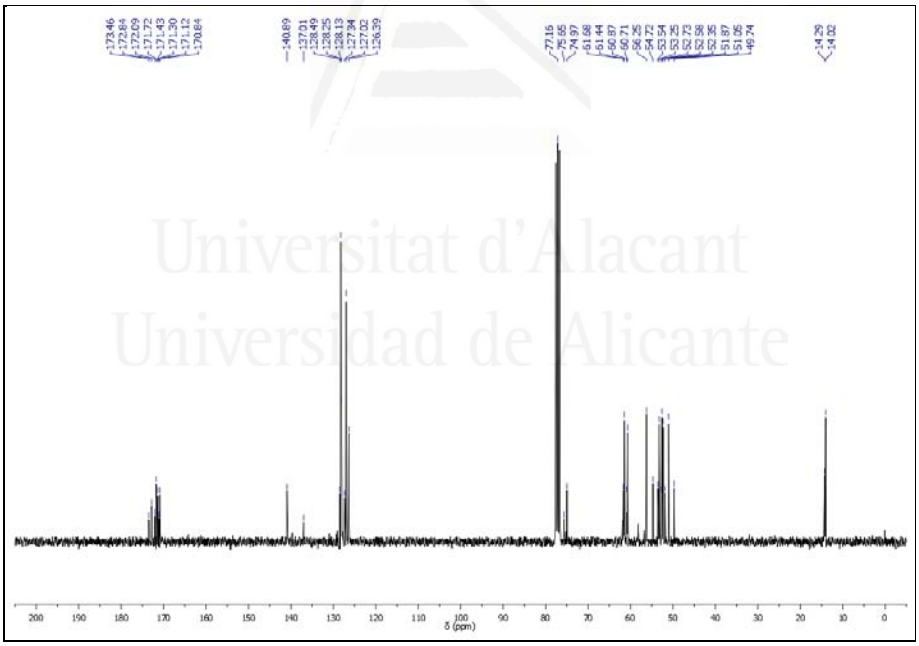

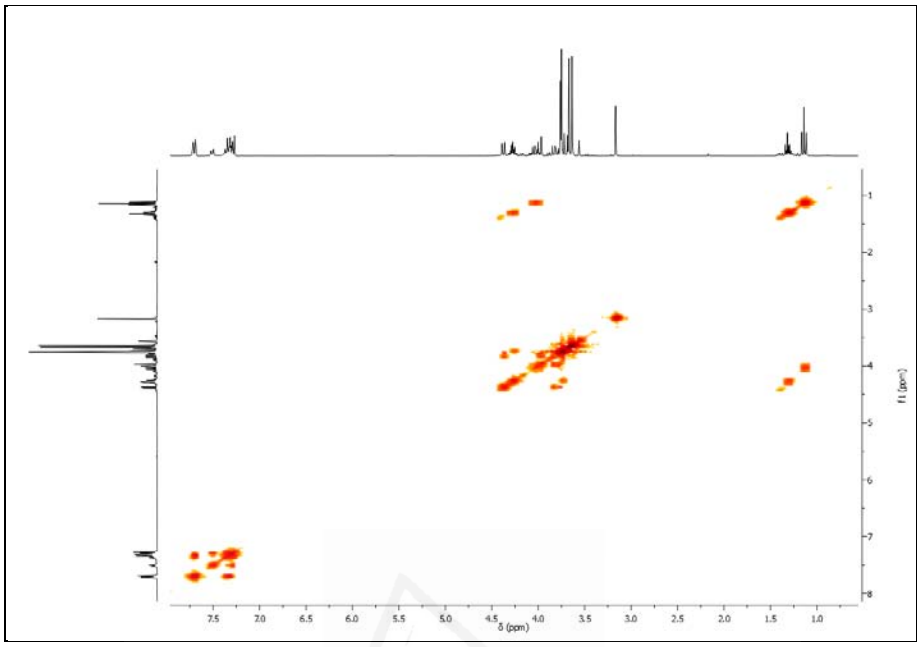

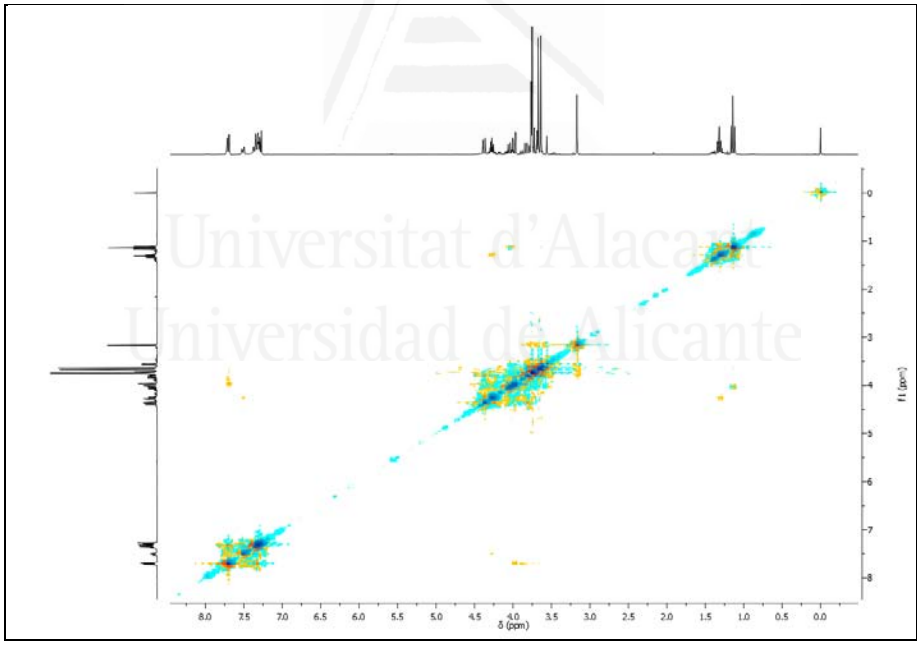

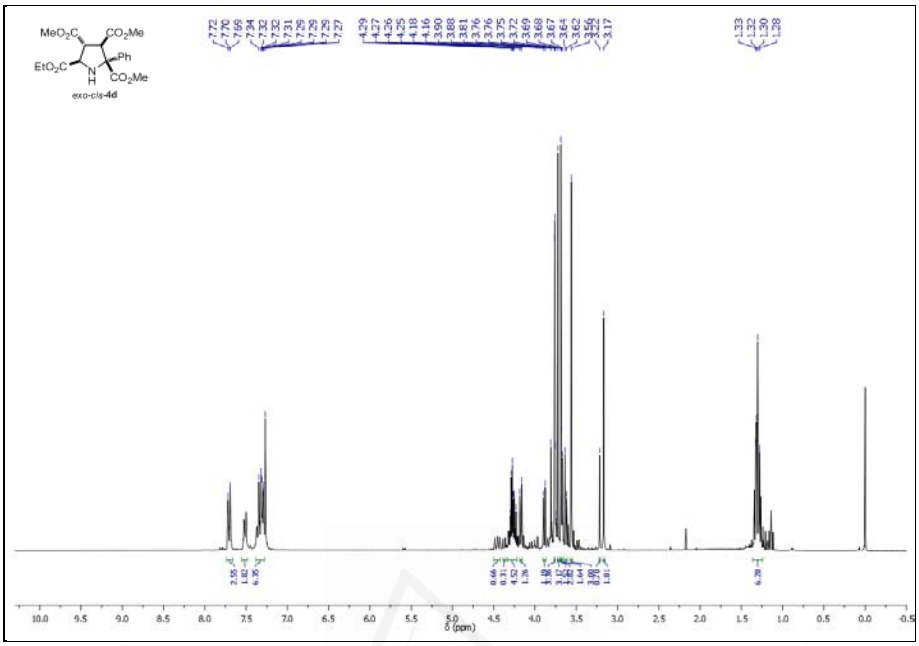

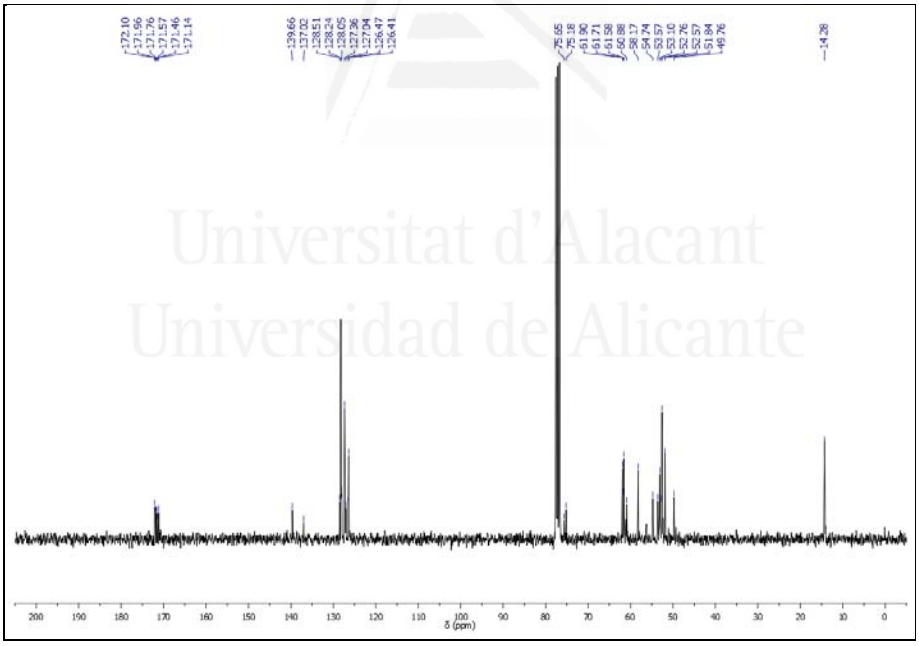

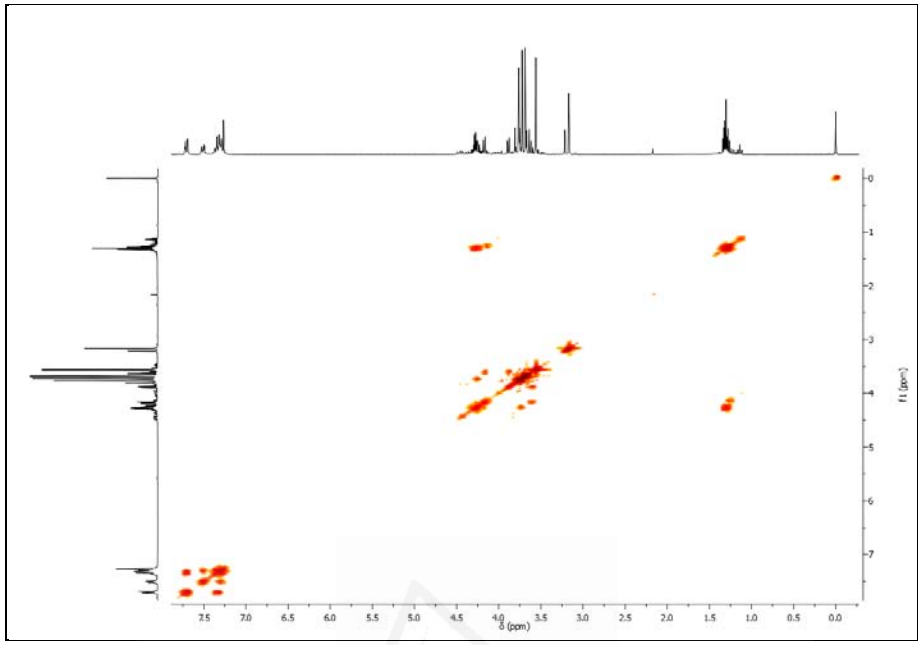

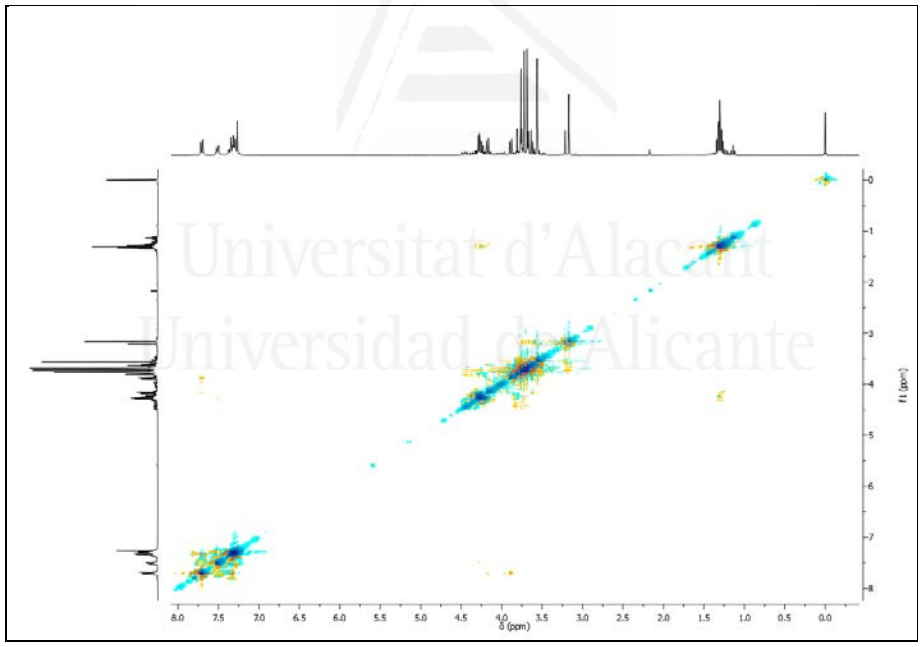

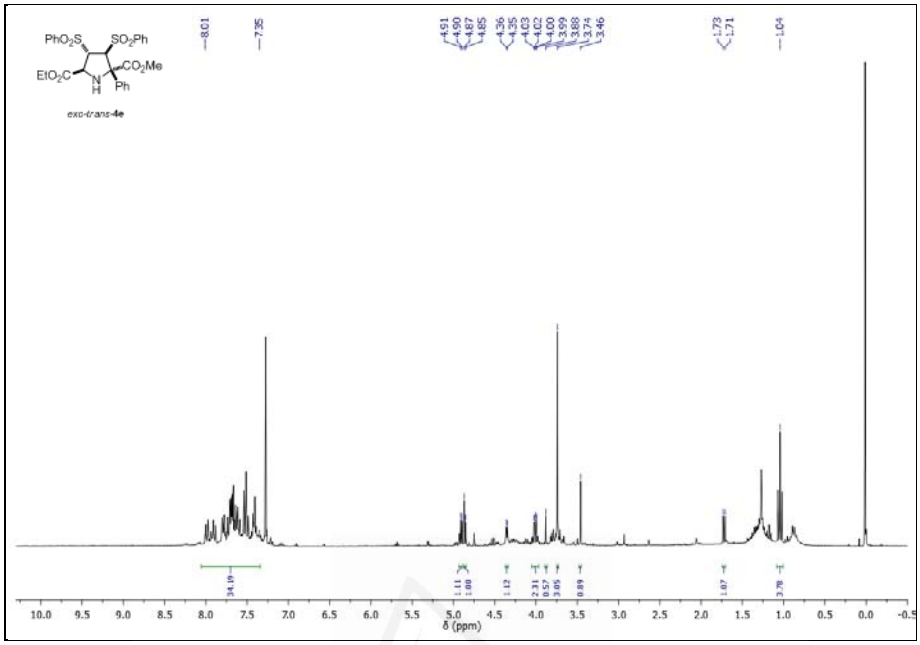

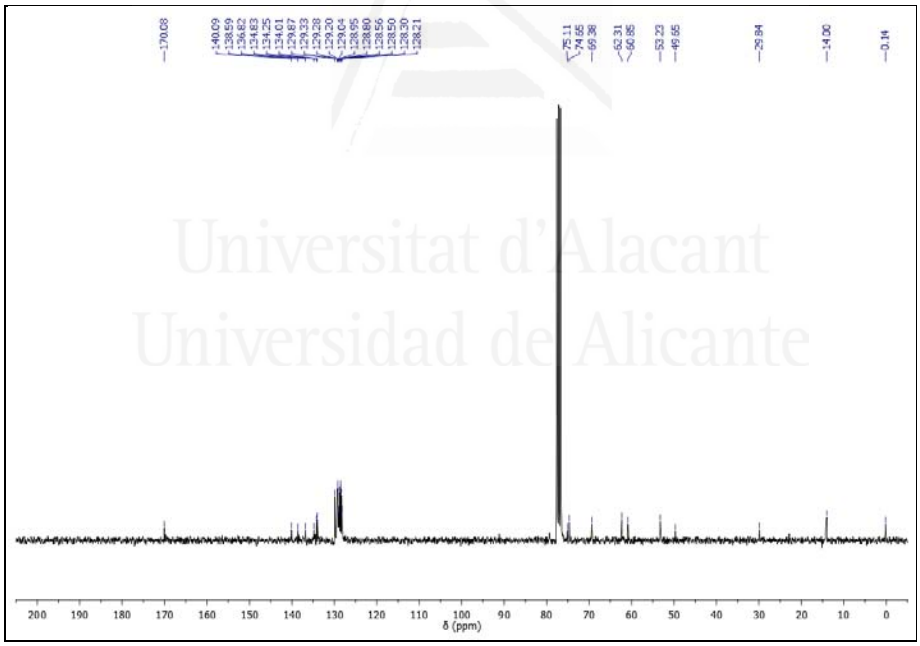

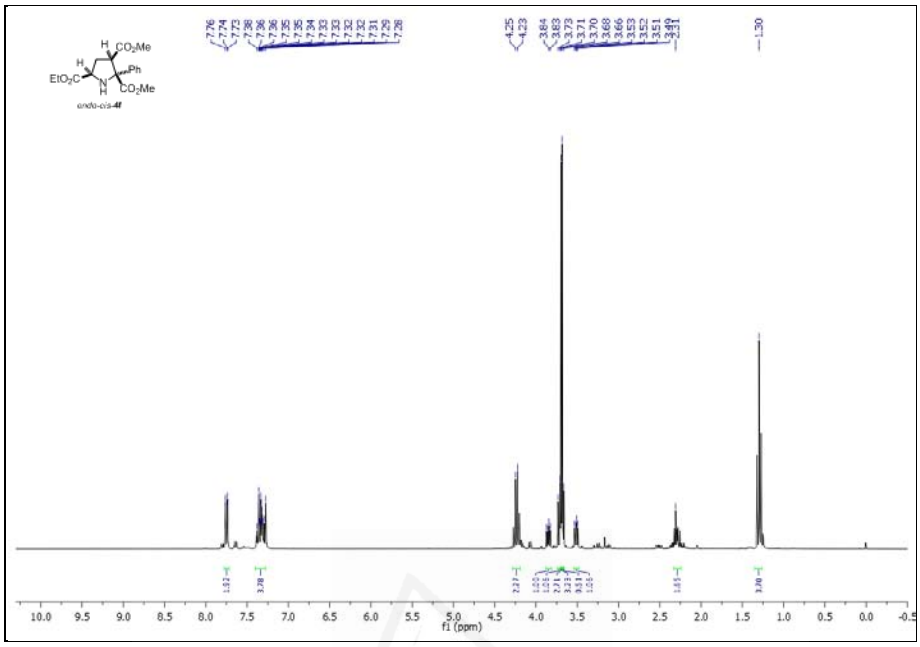

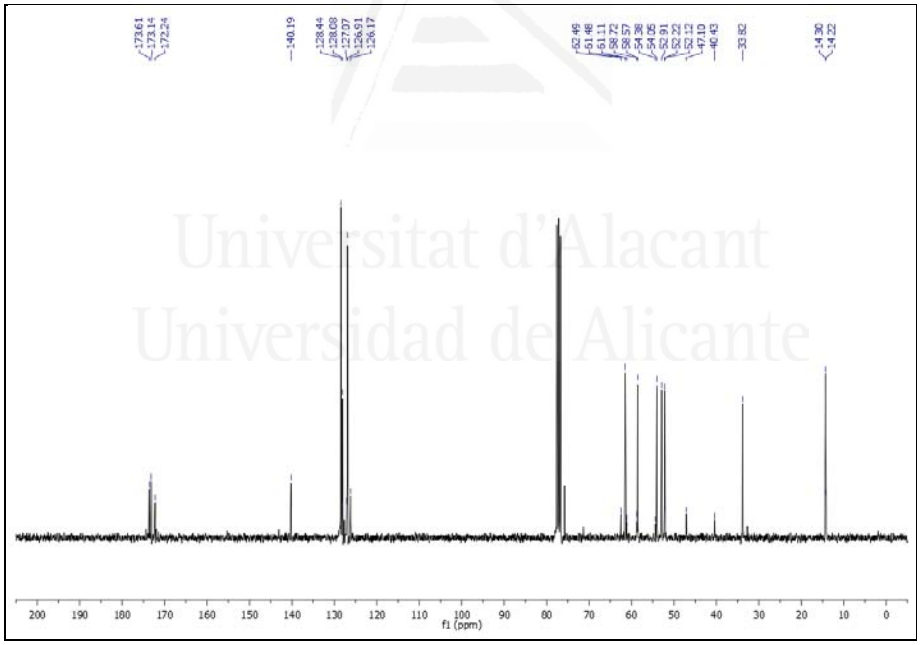

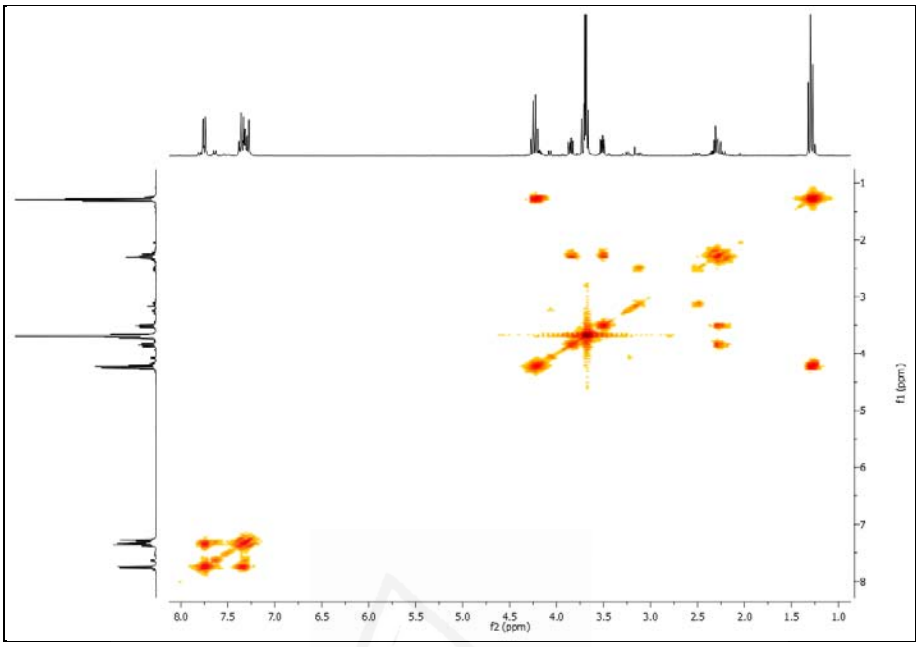

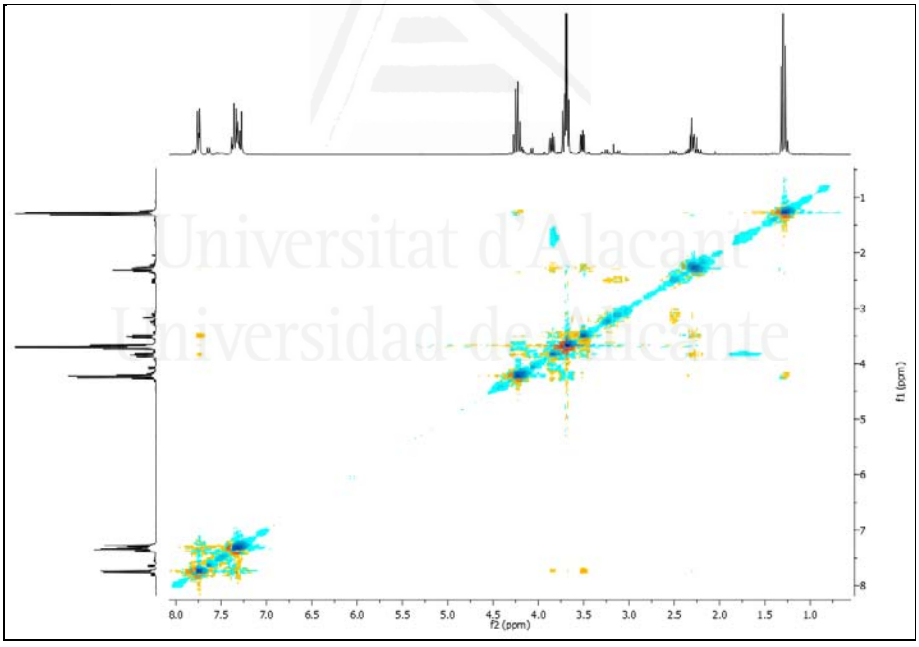

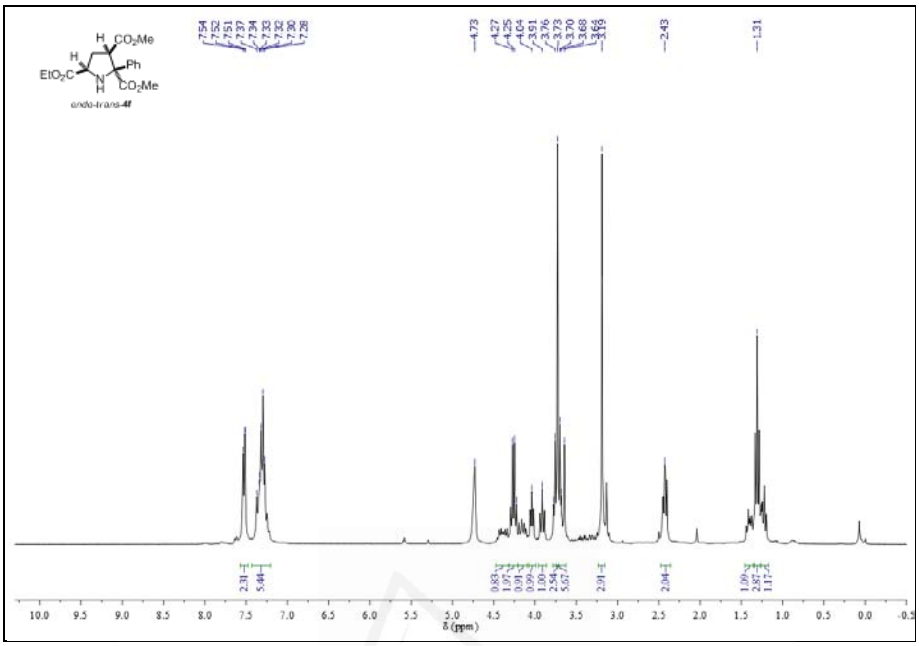

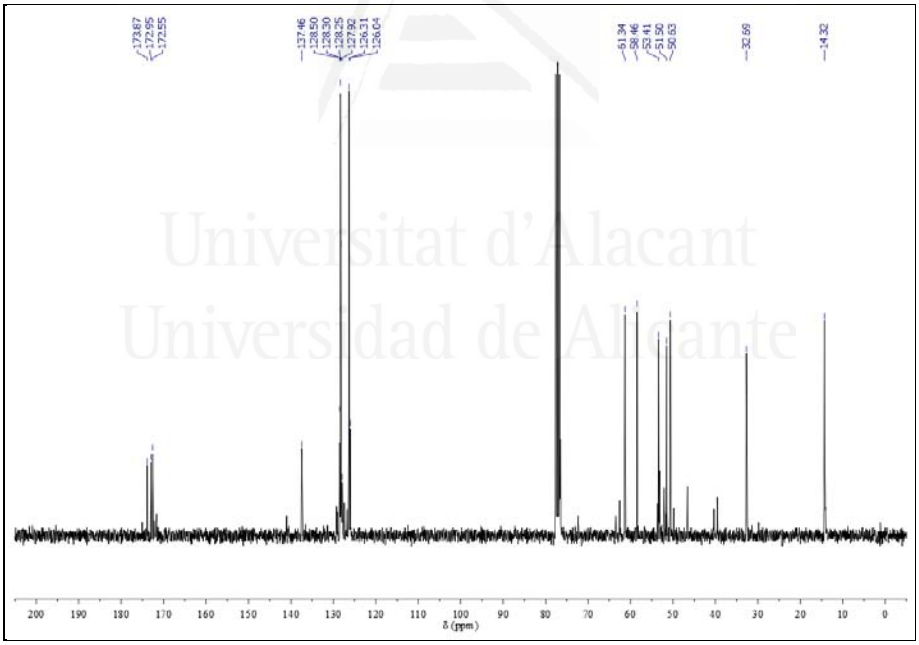

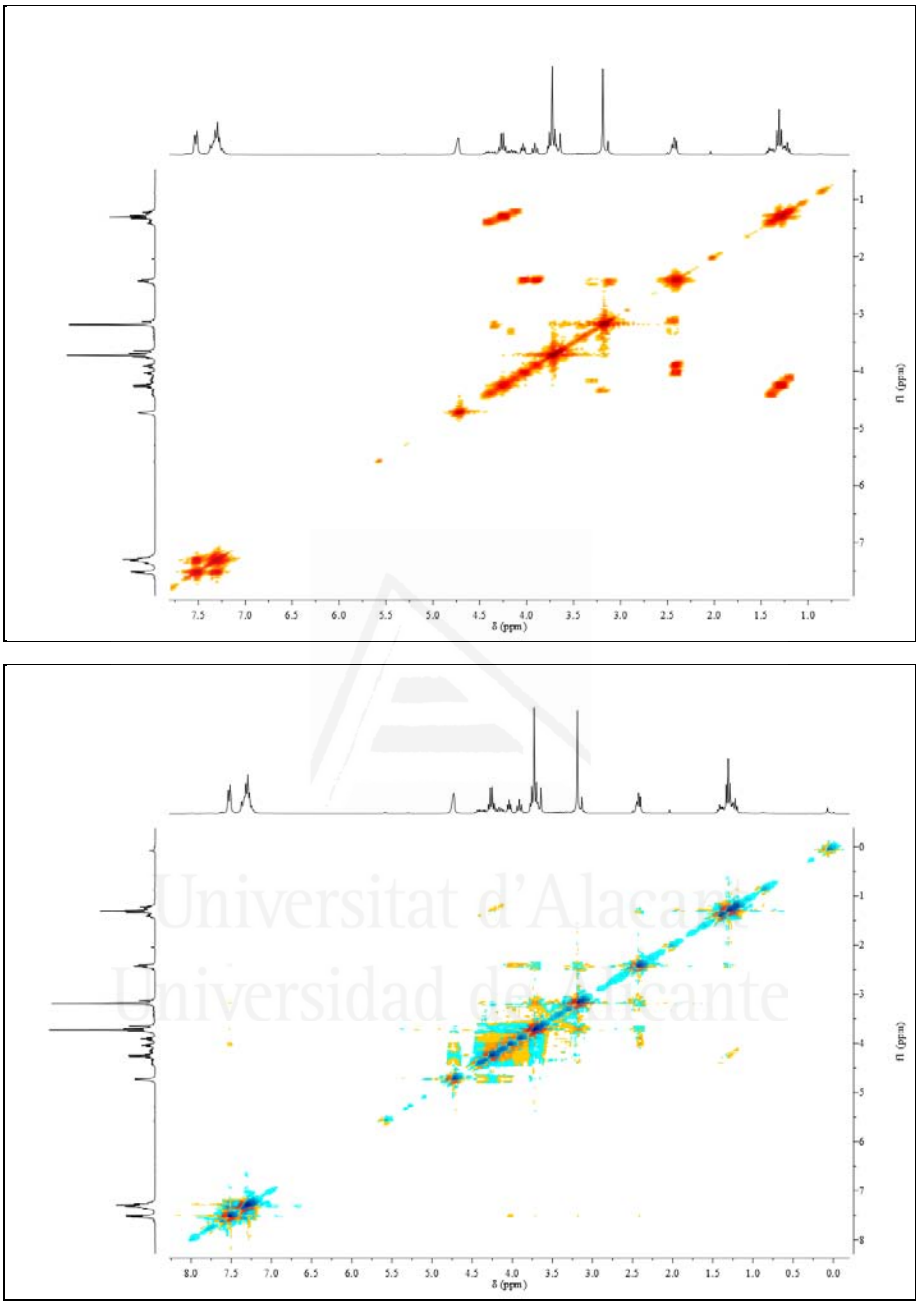

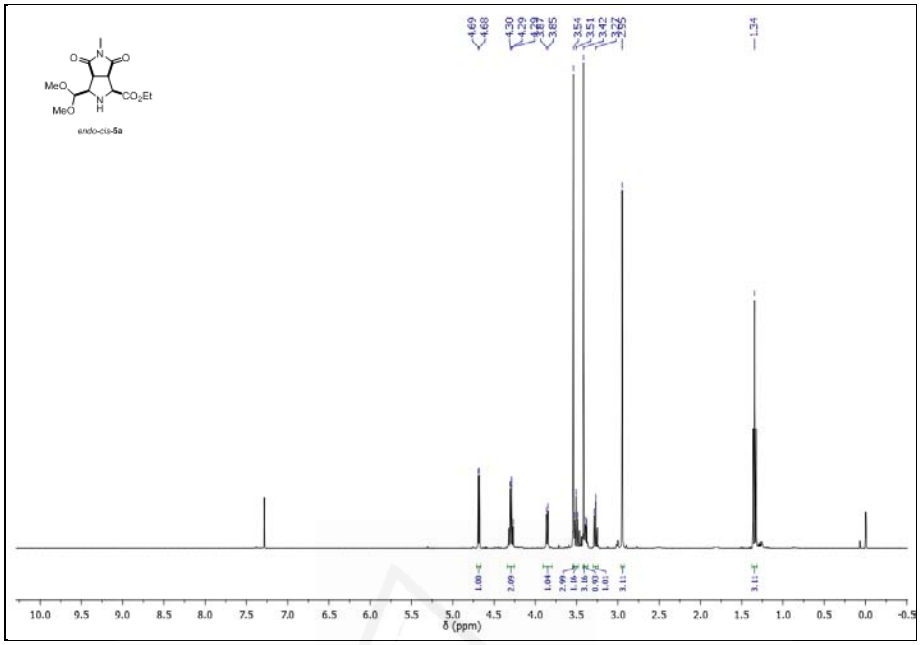

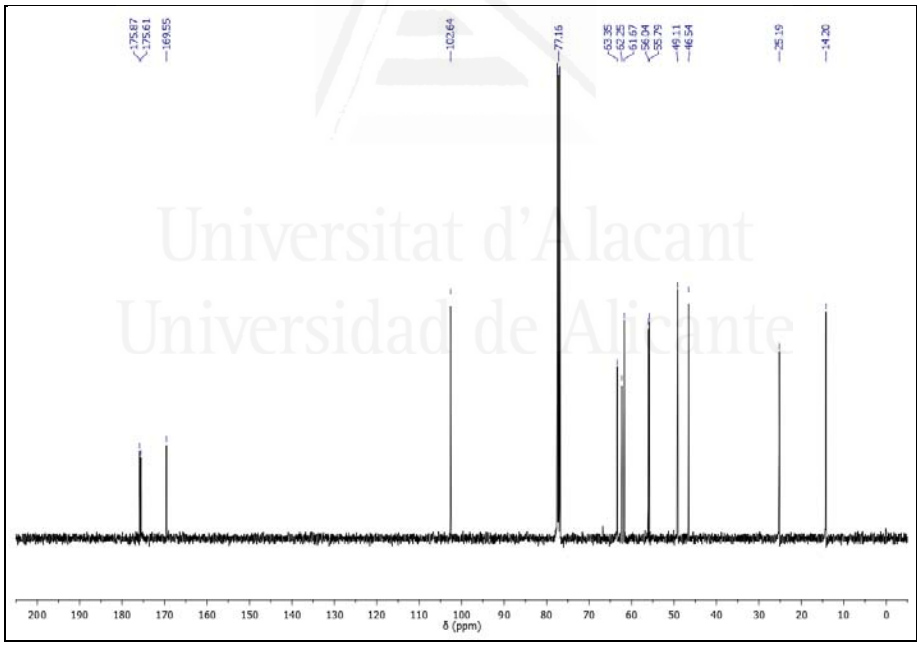

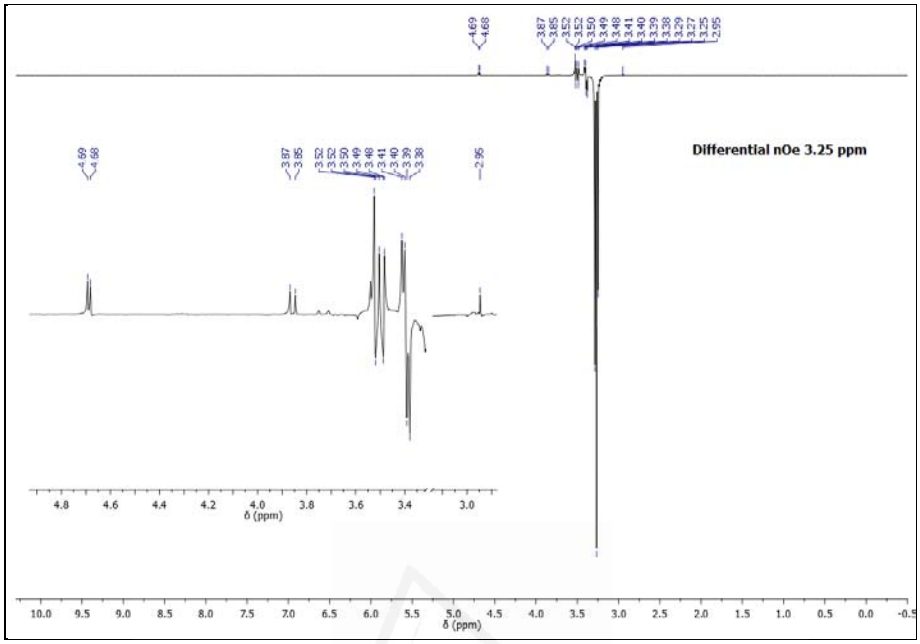

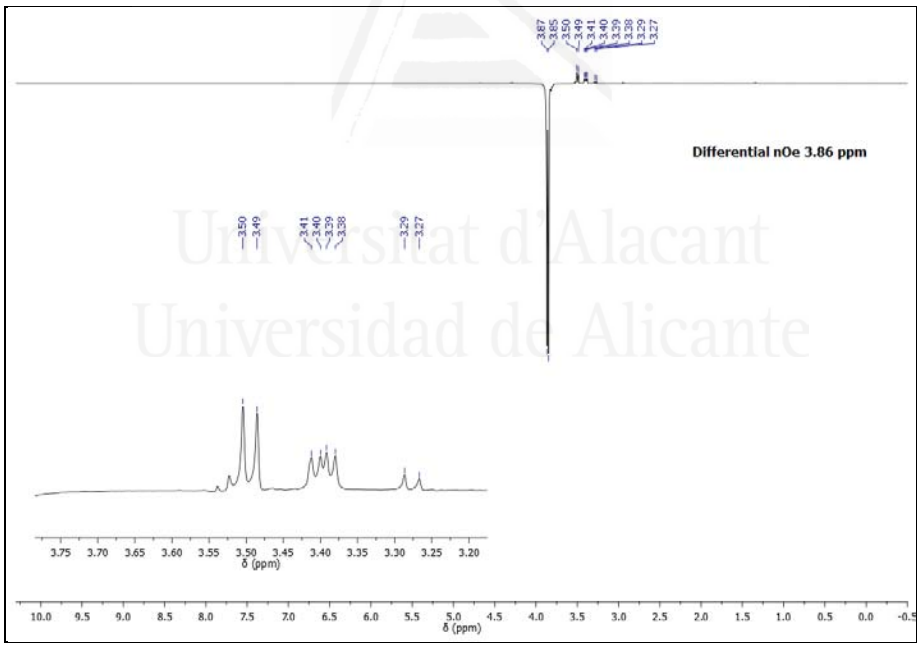

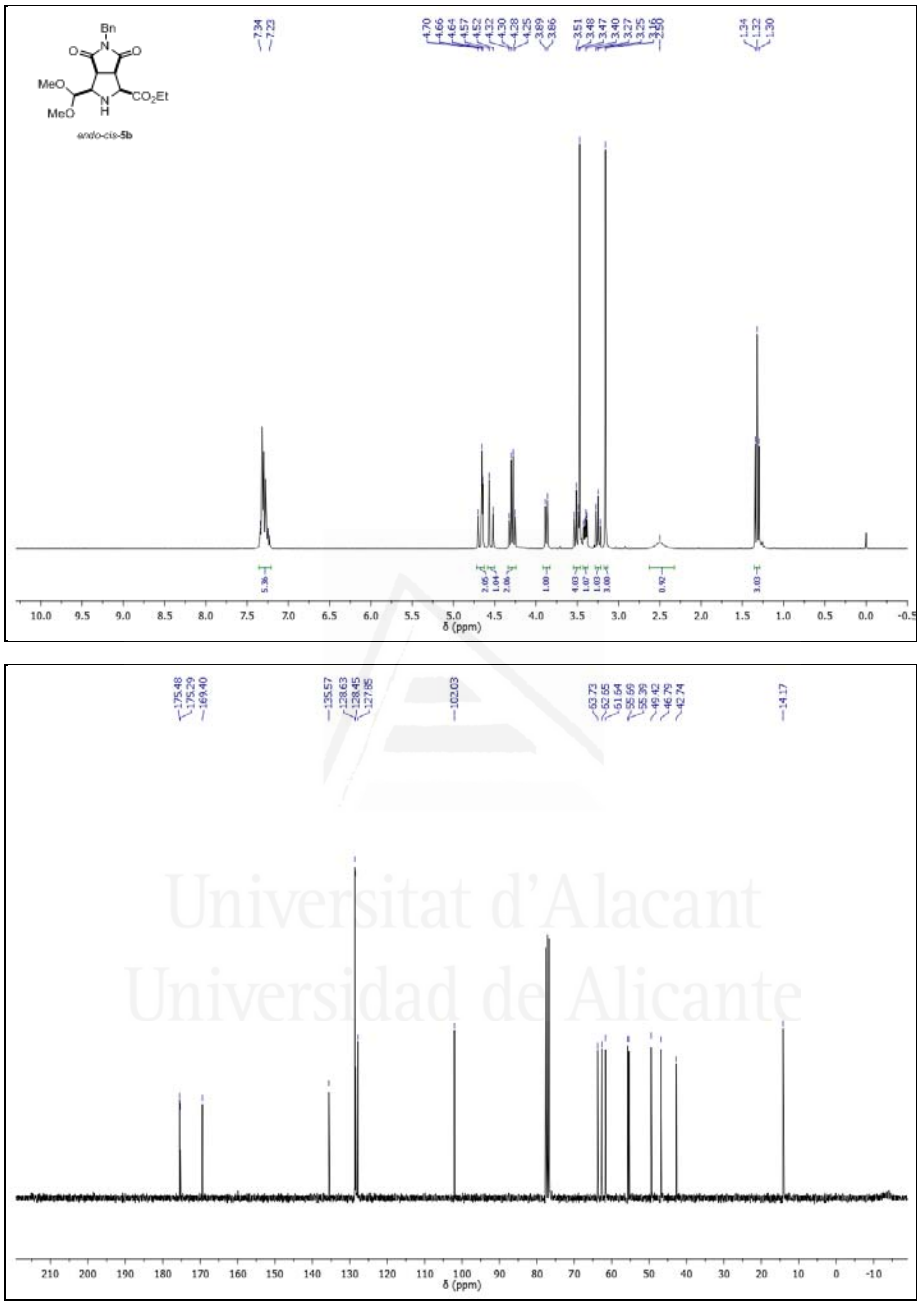

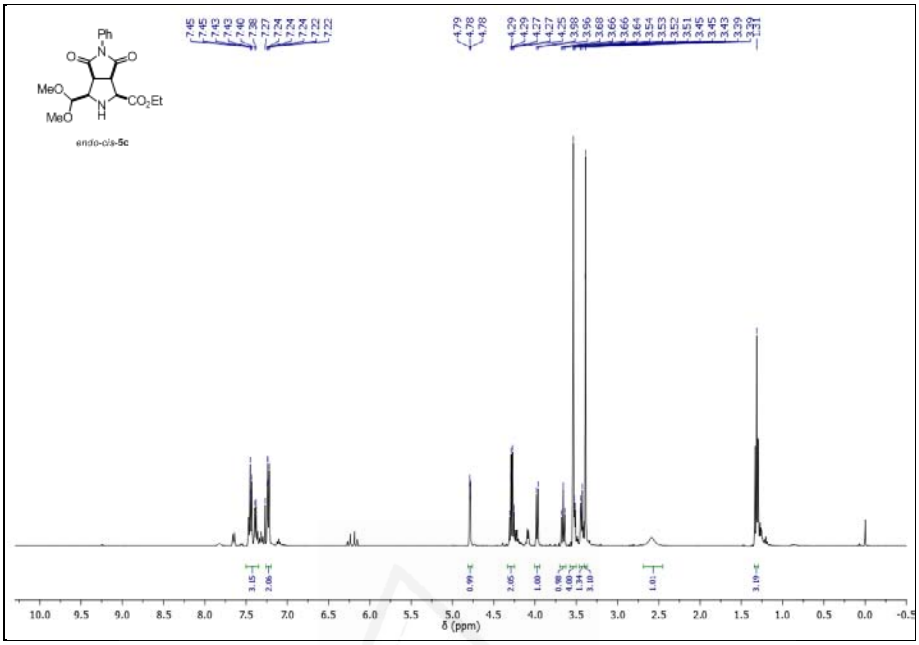

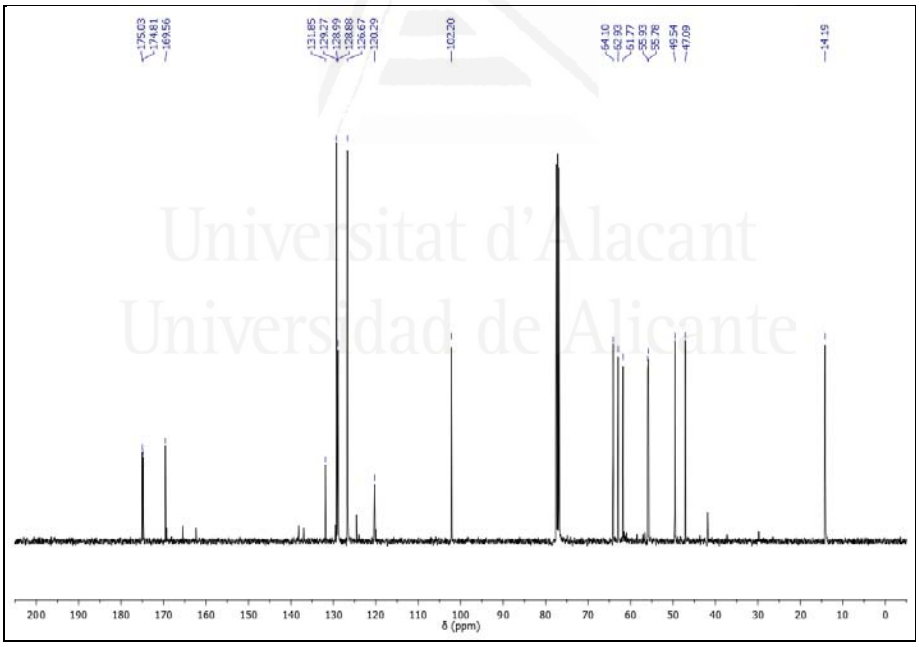

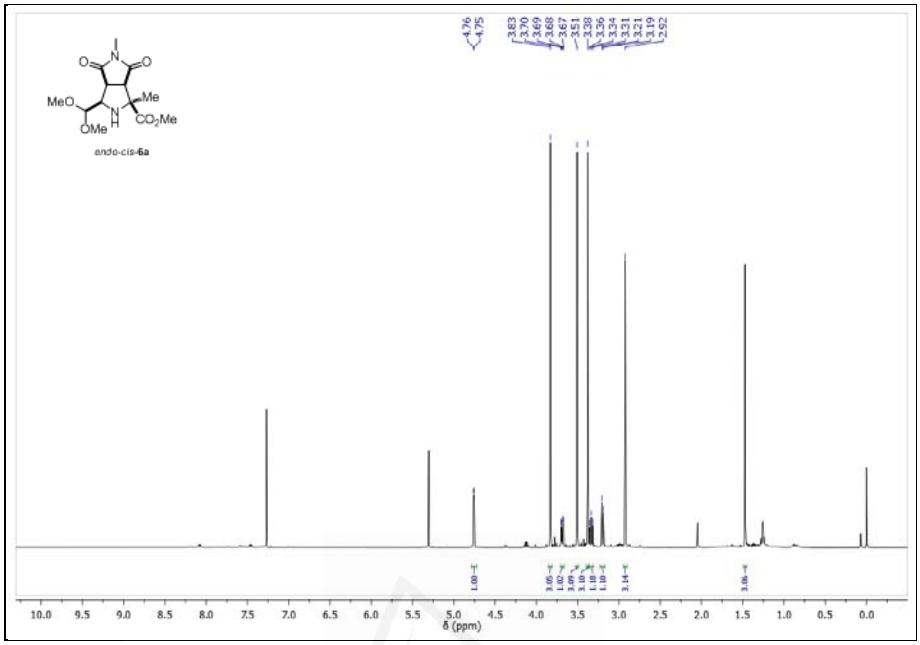

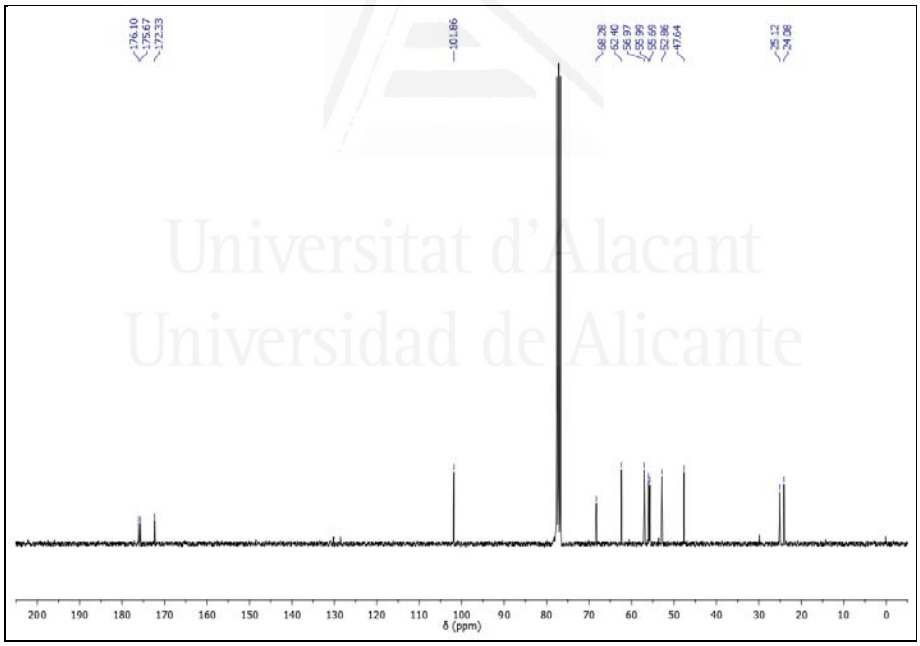

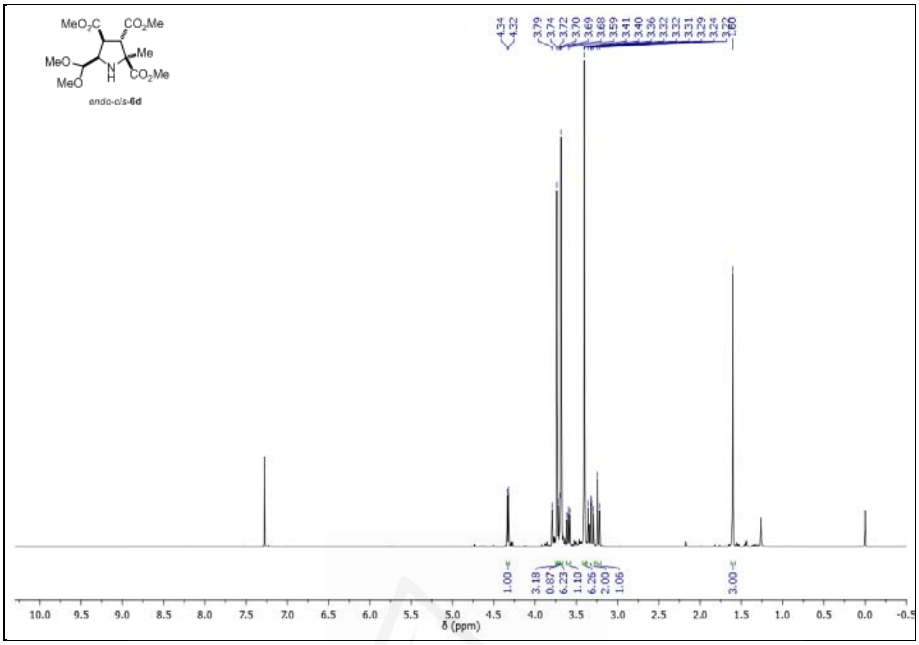

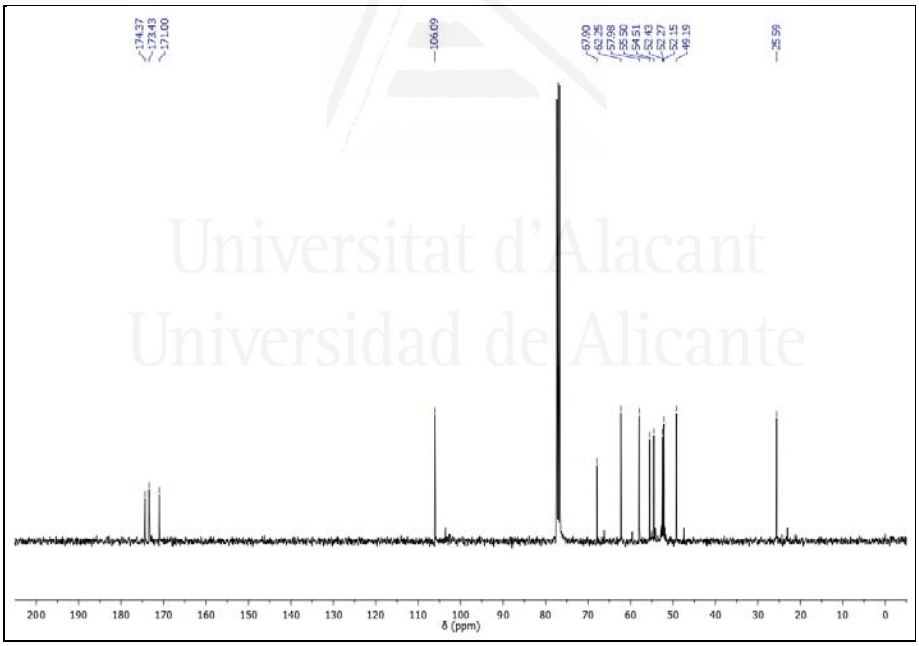

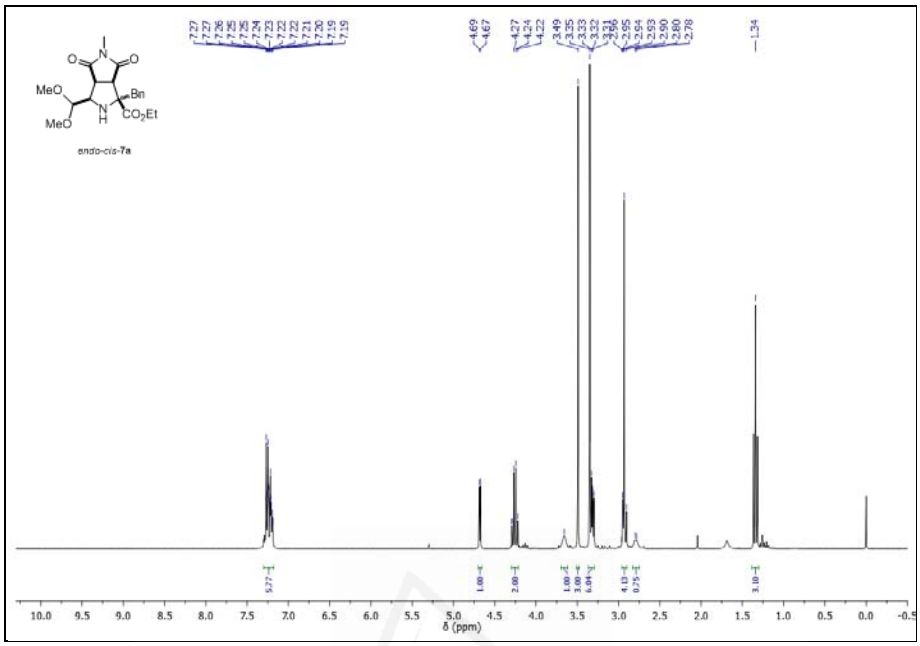

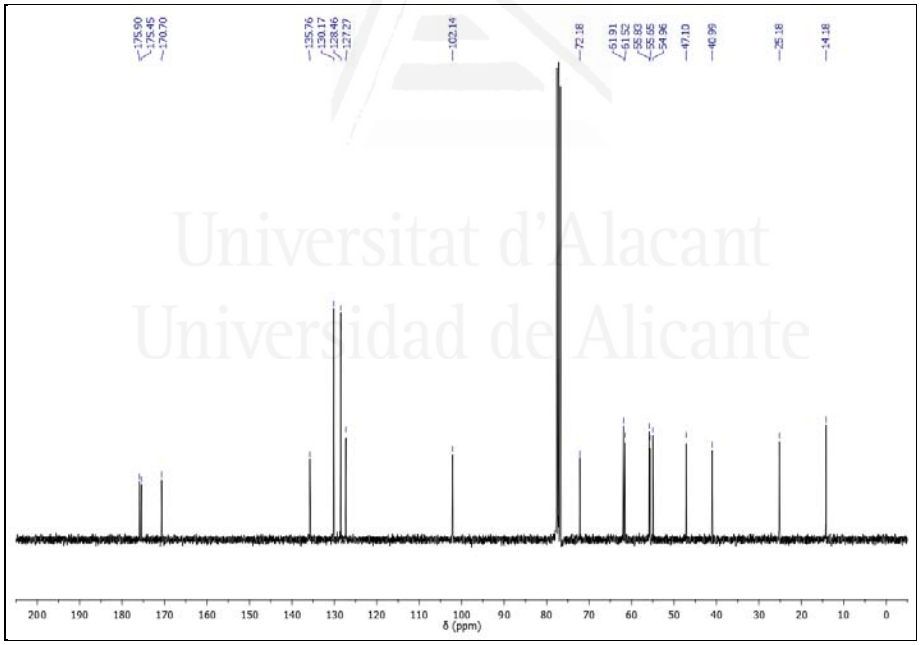

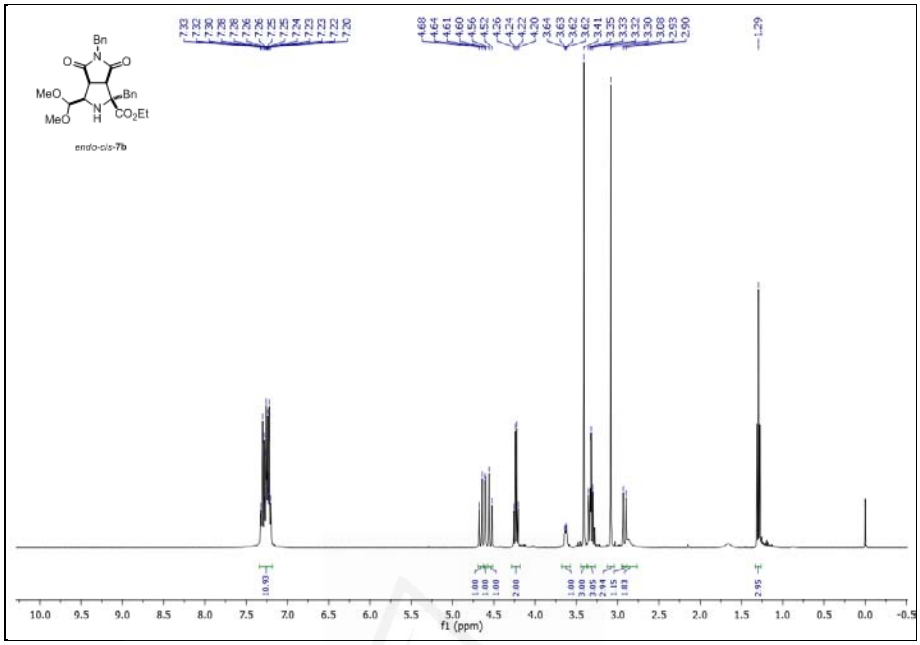

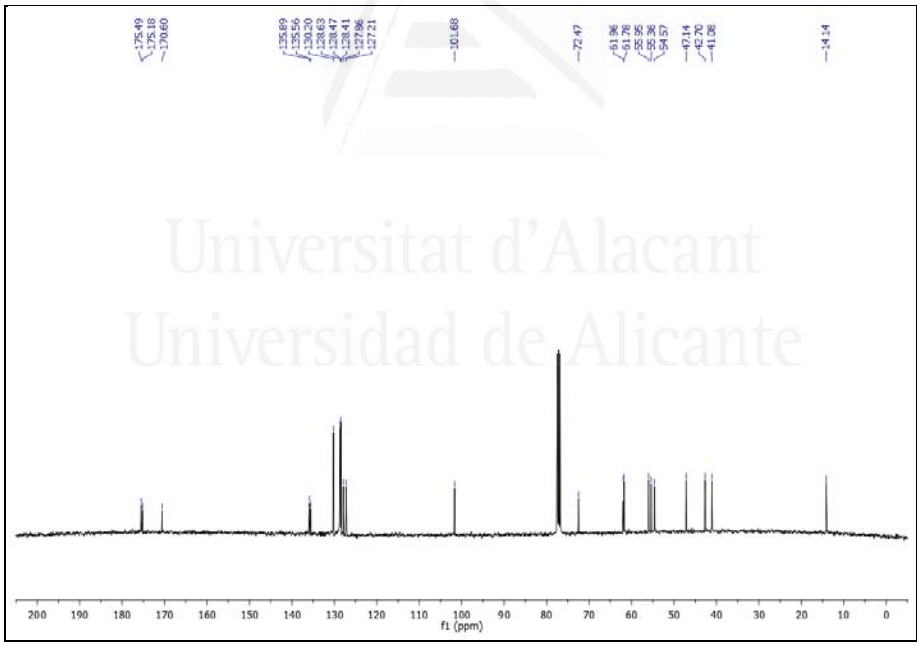

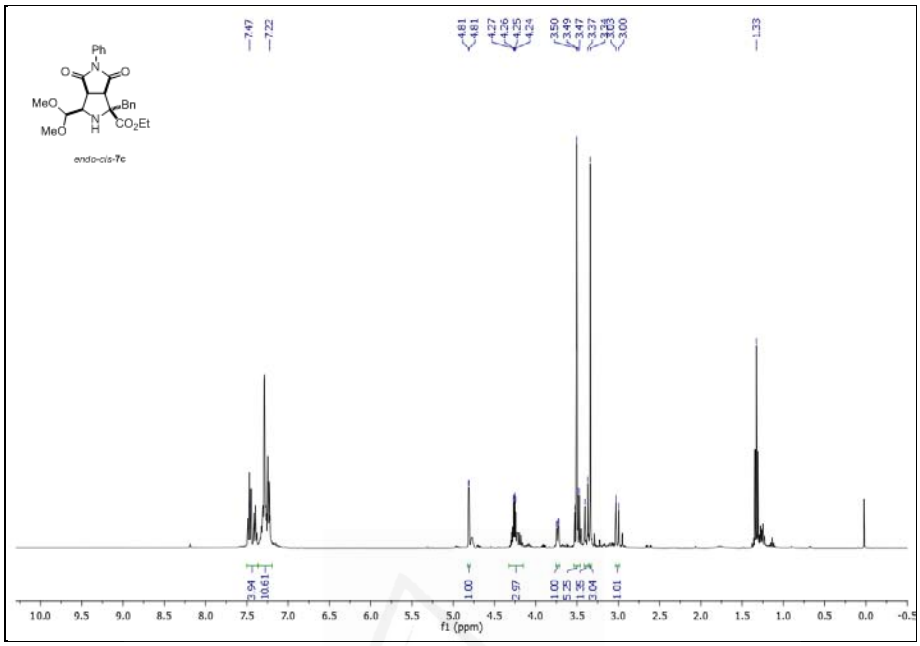

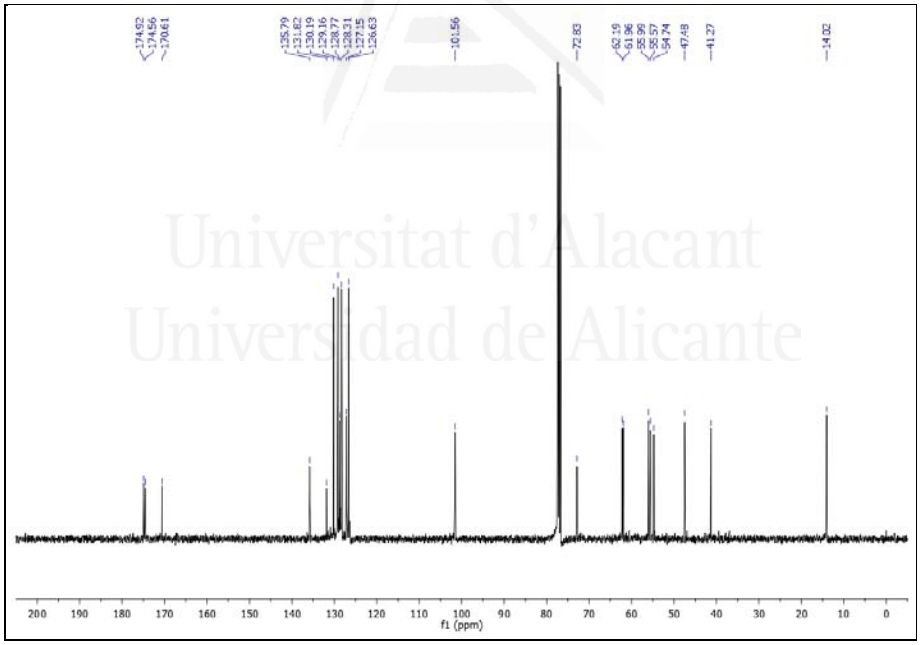

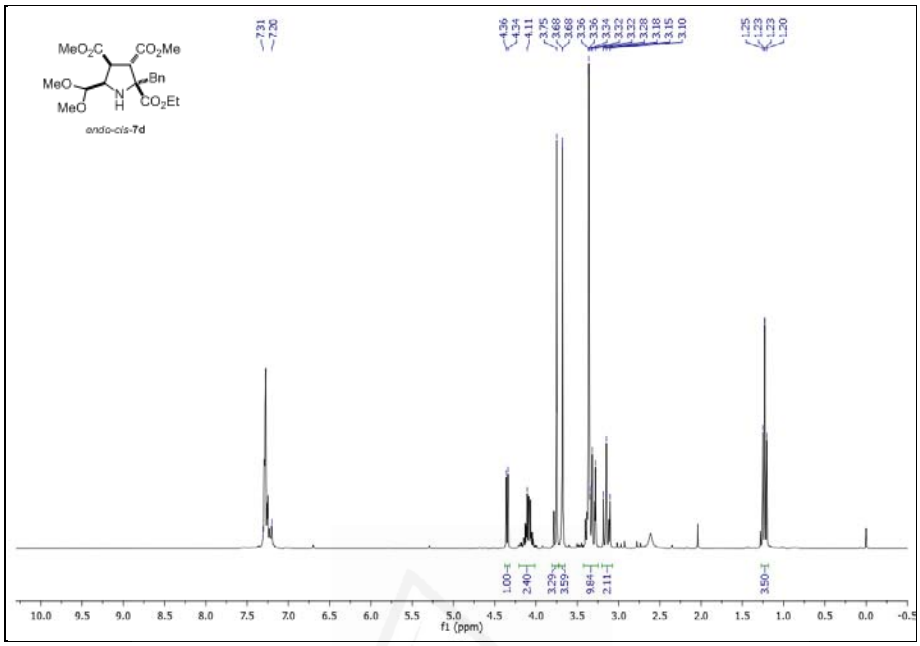

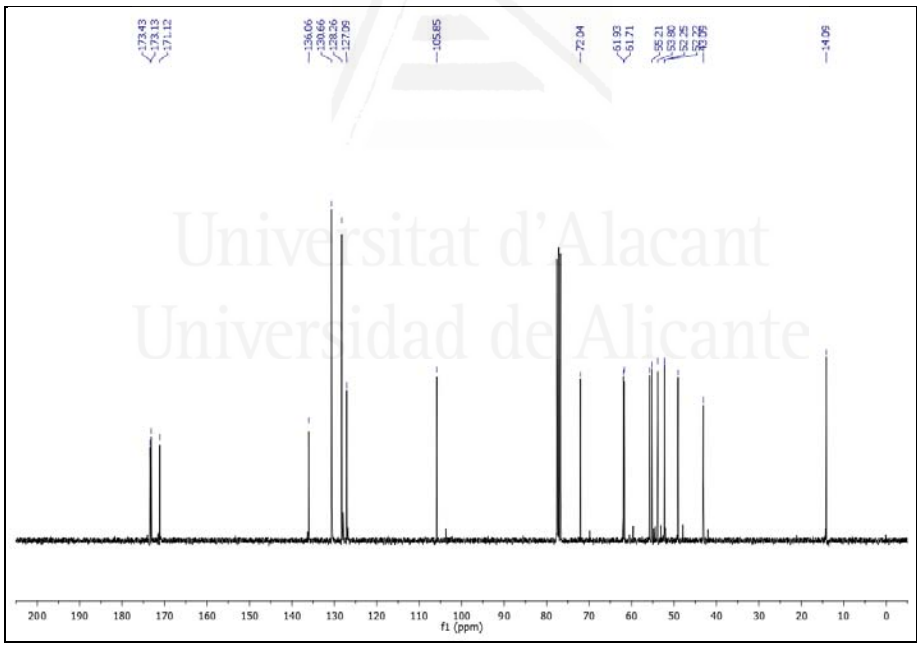

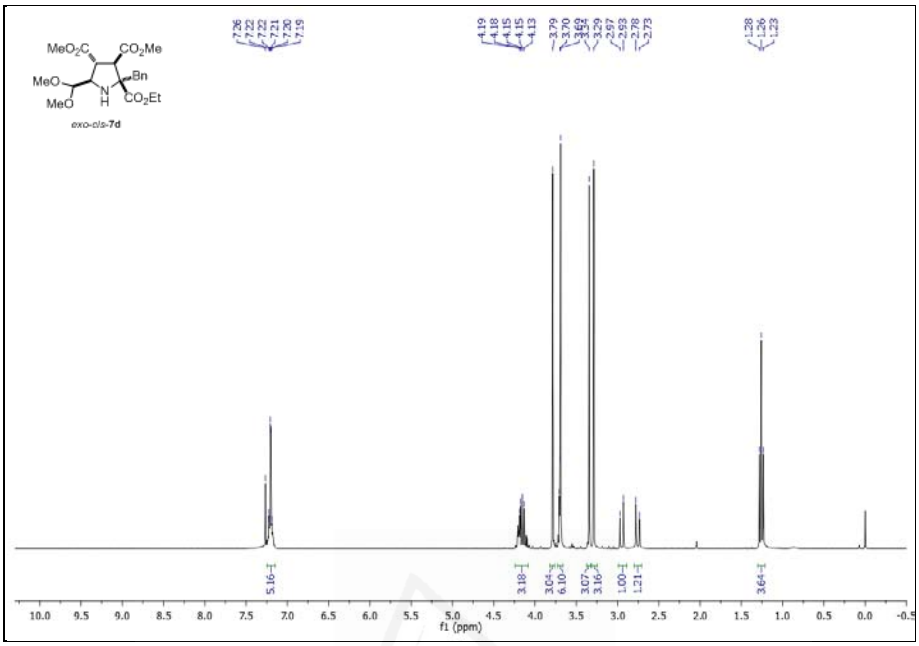

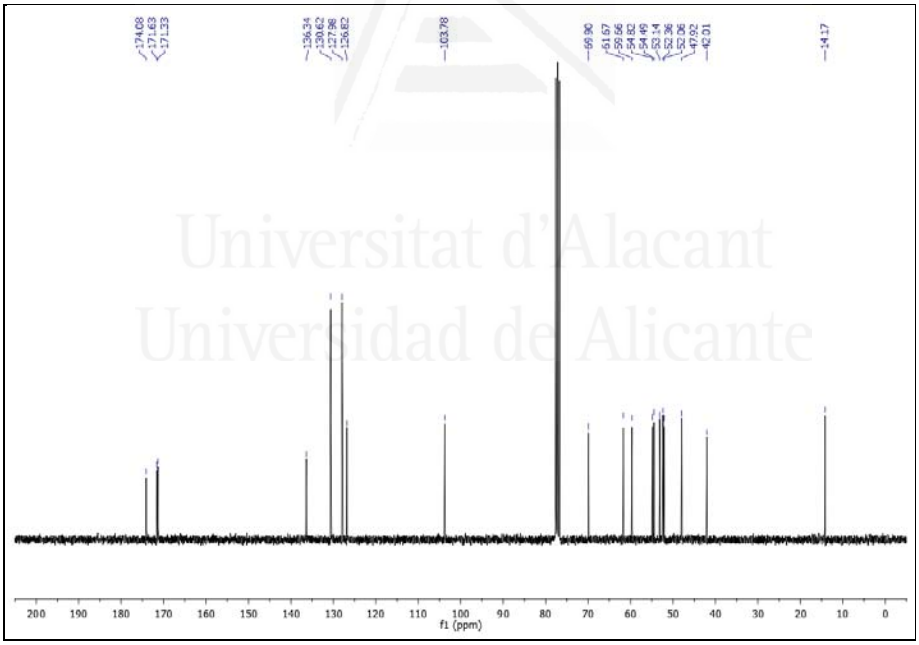

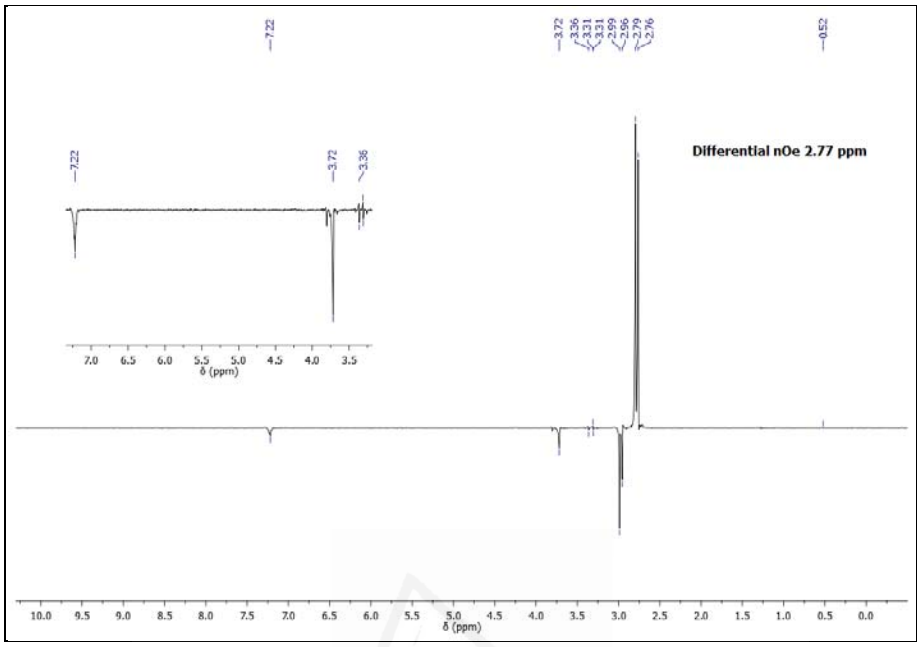

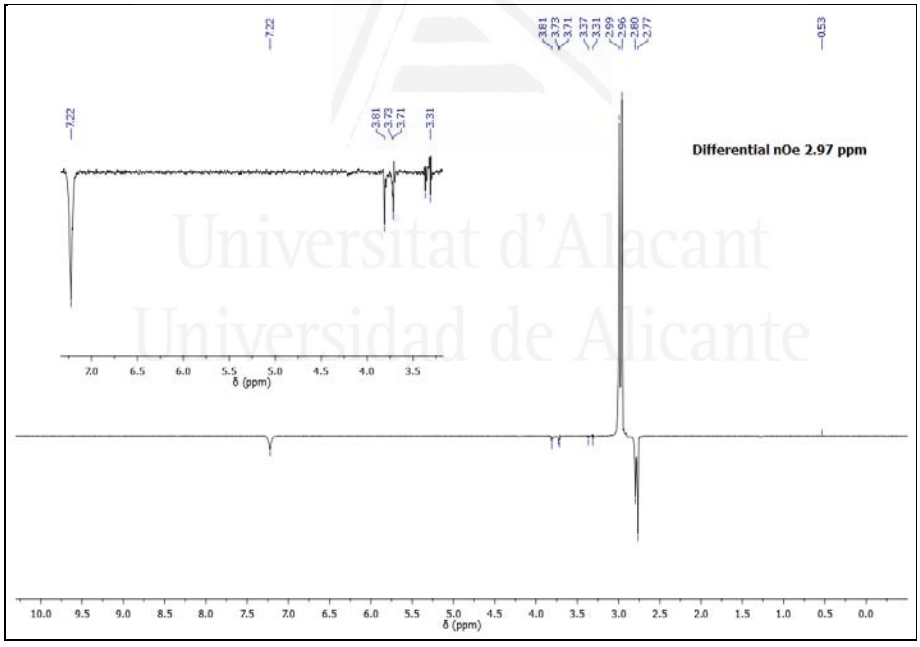

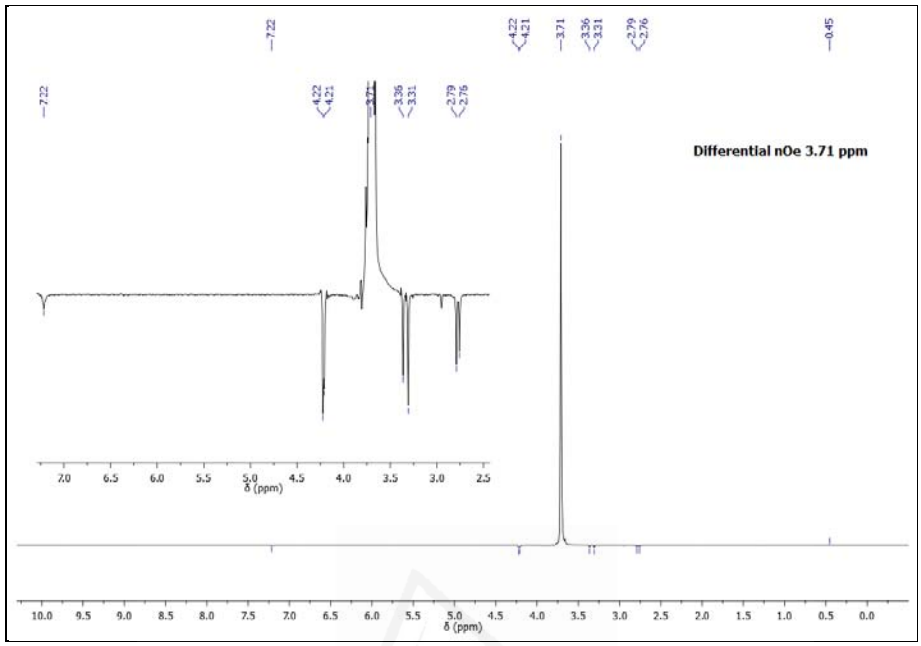

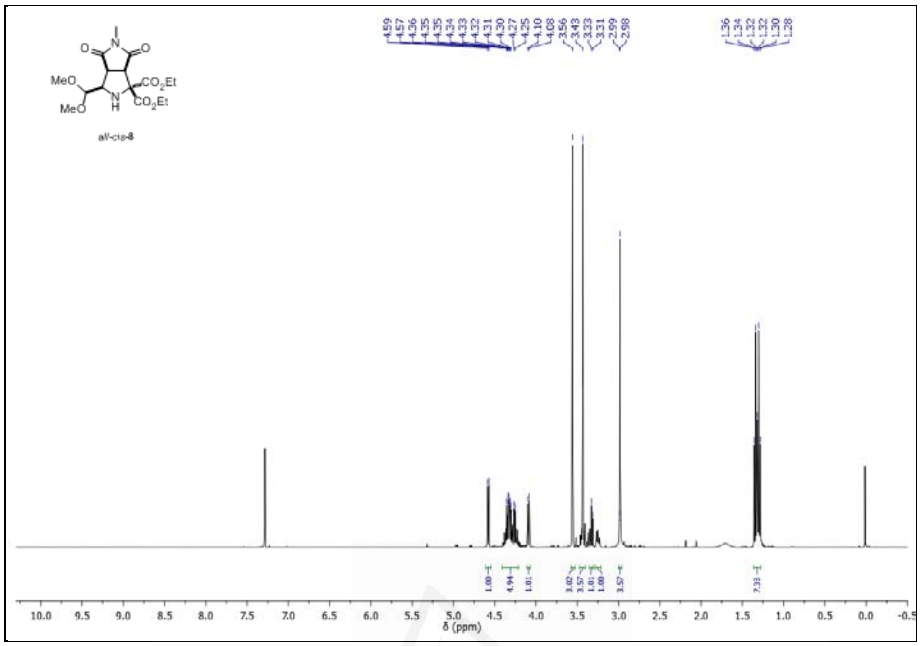

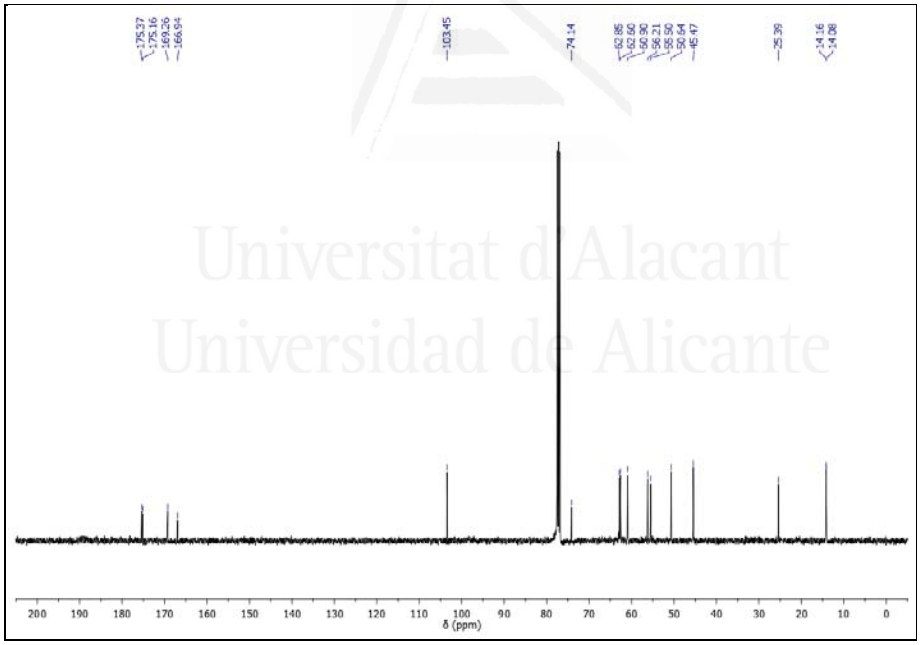

References

[1] J. Mancebo-Aracil, C. Nájera, J. M. Sansano, *Org. Biomol. Chem.* **2013**, *11*, 662-675.

V.4.- CAPÍTULO II-3: SÍNTESIS ASIMÉTRICA A TRAVÉS DE CICLOADICIONES 1,3-DIPOLARES CON ILUROS DE AZOMETINO

V.4.9.- Antecedentes Bibliográficos

La importancia de llevar a cabo una reacción asimétrica de cicloadición 1,3-dipolar con iluros de azometino reside en la formación de cuatro centros asimétricos (como máximo) de forma simultánea, obteniéndose mayoritariamente un único estereoisómero de los 16 posibles. Las revisiones bibliográficas que hacen referencia a esta reacción asimétrica son numerosas,[2] y todas ellas coinciden en que tanto la síntesis diastereoselectiva, como la enantioselectiva, son muy buenas aproximaciones para conseguir elevados excesos diastereo- y enantioméricos, respectivamente, de los derivados de la prolina resultante. De ellas, la más útil actualmente es la última debido a que es necesario emplear cantidades subestequiométricas de una fuente de quiralidad (ligando, organocatalizador o base).

V.4.9.1.- Reacciones 1,3-dipolares enantioselectivas

Grigg y colaboradores, en 1991, fueron los pioneros en la cicloadición 1,3-dipolar enatioselectiva de iluros de azometino y alquenos utilizando cantidades estequiométricas de bases quirales o complejos metálicos quirales.[70] En 2002 se llevó a cabo la misma transformación por Zhang y colaboradores pero esta vez utilizando cantidades subestequiométricas con resultados satisfactorios usando un complejo formado por una difosfina quiral y AgOAc.[71] Posteriormente, aparecieron muchas más contribuciones con resultados extraordinarios en los que se emplearon otros complejos metálicos quirales, bases quirales y organocatalizadores quirales.[72]

[70] Allway, P.; Grigg, R.; *Tetrahedron Lett.* **1991**, *32*, 5817.
[71] Longmire, J.; Wang, B.; Zhang, X.; *J. Am. Chem. Soc.* **2002**, *124*, 13400.
[72] Pellissier, H.; *Adv. Synth. Catal*. **2012**, *354*, 237.

Dentro de todos los complejos metálicos quirales publicados en la bibliografía, los más importantes y frecuentemente utilizados son los de Ag^{I} y Cu^{I} (**Figura 8** y **9**).[73]

Figura 8. Complejos quirales de sales de plata usados para generar ácidos de Lewis quirales empleados en las reacciones 1,3-dipolar entre iluros de azometino y alquenos electrofílicos.[74]

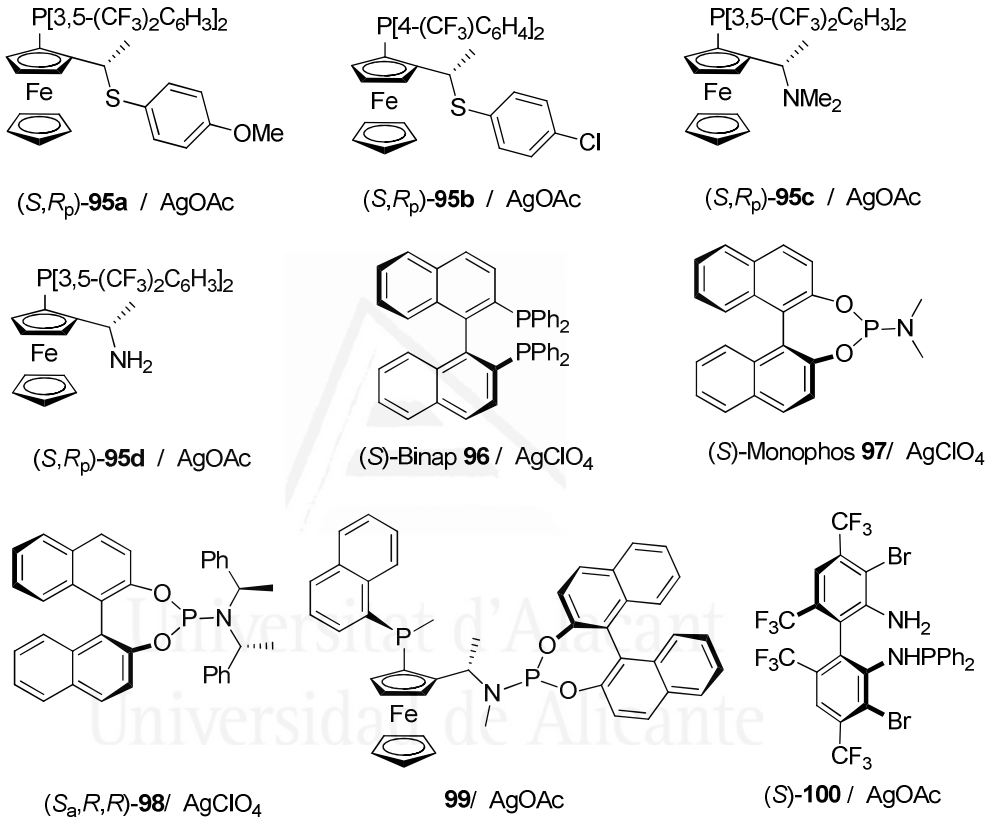

En general, la reacción llevada a cabo con complejos quirales de Ag^{I} dan lugar a los productos *ent*-**102**-*endo* como mayoritarios con excelentes rendimientos y buenas enantioselectividades (**Esquema 28a**).[75]

[73] Oderaotoshi, Y.; Cheng, W.; Fujitomi, S.; Kasano, Y.; Minakata, S.; Komatsu, M.; *Org. Lett.* **2003**, *5*, 5043.

[74] **a)** Chen, C.; Li, X.; Schreiber, S.; *J. Am. Chem. Soc.* **2003**, *125*, 10174; **b)** Knöpfel, T.; Aschwanden, P.; Ichikawa, T.; Watanabe, T.; Carreira, E.; *Angew. Chem. Int. Ed.* **2004**, *43*, 5971; **c)** Zheng, W.; Zhou, Y.; *Org. Lett.* **2005,** *7,* 5055; **d)** Stohler, R.; Wahl, F.; Pfaltz, A.; *Synthesis* **2005**, 1431.

[75] Zeng, W.; Zhou, Y.; *Tetrahedron Lett.* **2007**, *48*, 4619.

Figura 9. Complejos quirales de Cu^{I} utilizados como ácidos de Lewis en las cicloadiciones 1,3-dipolares.

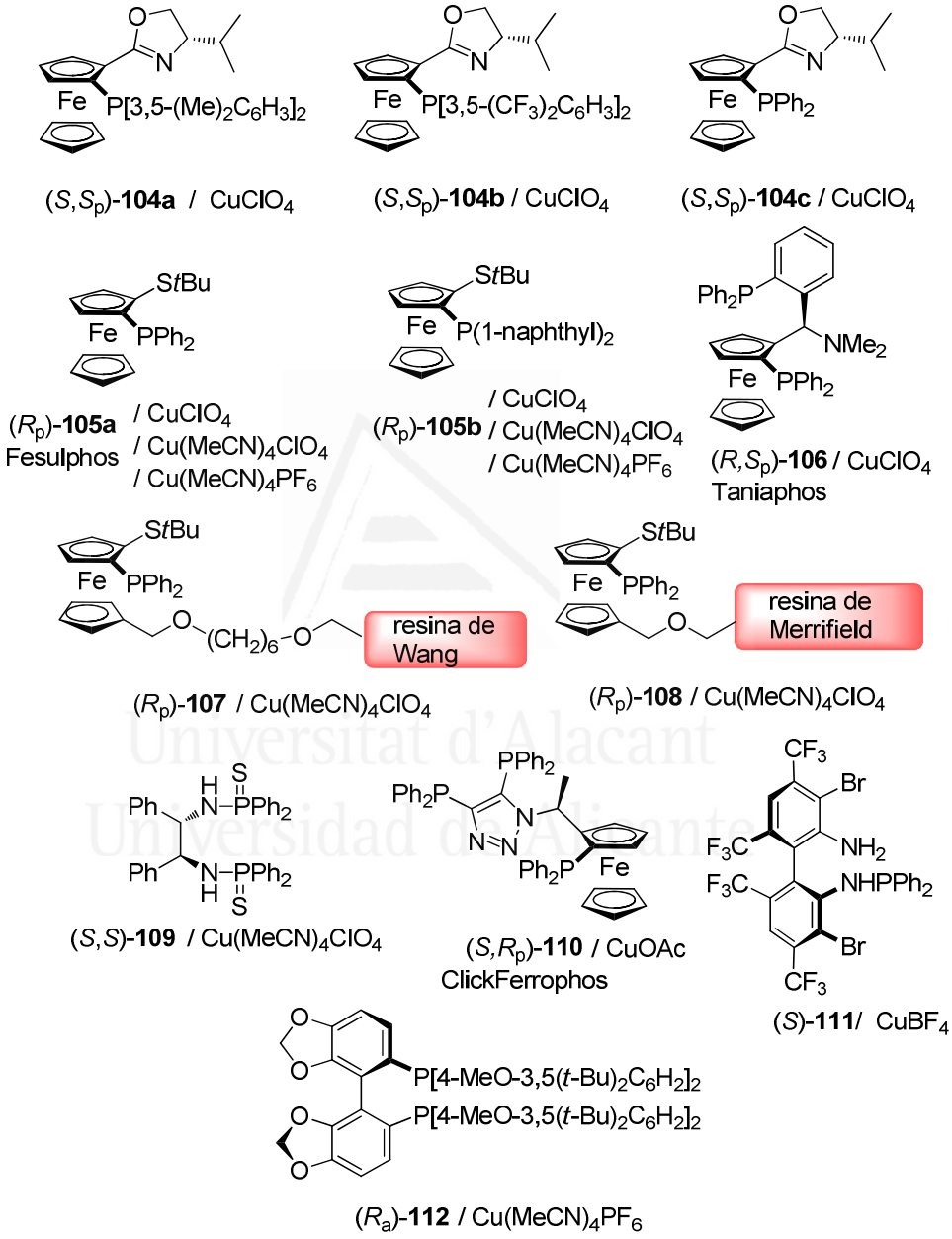

Esquema 28a

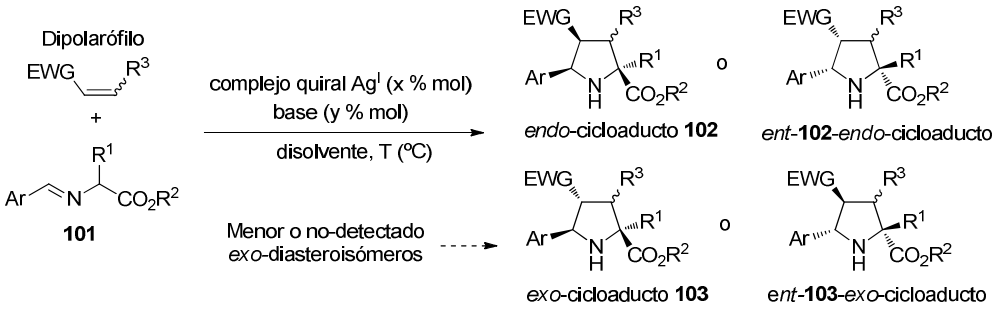

Esquema 28b

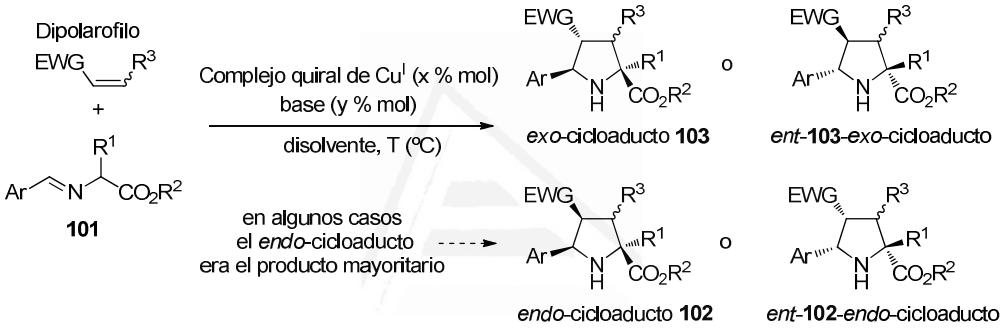

Este tipo de cicloadiciones catalizada por los complejos quirales de Cu^{I} (**Figura 9**) dan como productos mayoritarios, en general, los cicloaductos *exo*-**103** y *ent-exo*-**103** (si bien es cierto que en algunos casos fue la estereoquímica *endo* la obtenida mayoritariamente) (**Esquema 28b**).

Otros catalizadores metálicos quirales como los de zinc(II), calcio(II), niquel(II) y oro(I)[76] (**Figura 10**) dieron lugar al cicloaducto-*endo* con buenos rendimientos pero con menor enantioselectividad y menor campo de aplicación que los complejos de plata(I) y cobre(I) resumidos anteriormente.

Figura 10. Ligandos quirales de los metales: zinc(II), oro(I) o níquel(II) utilizados en las reacciones 1,3-dipolares.

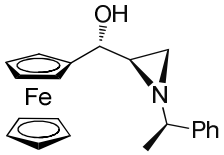

113 / $Zn(OTf)_2$

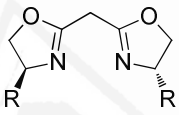

114a, R = Ph / $Ca(OiPr)_2$
114b, R = *i*Pr / $Ca(OiPr)_2$

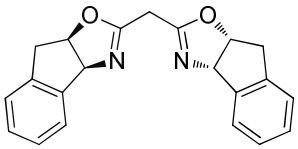

115 / $Ca(OiPr)_2$

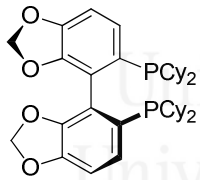

(S_a)-Cy-Segphos **116** / $(AuOBz)_2$

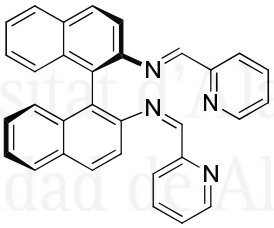

(R_a)-**117**/ $Ni(ClO_4)_2 \cdot 6H_2O$

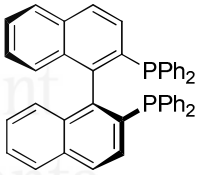

(*S*)-Binap **96** / AuTFA

El interés de esta reacción reside en la síntesis de intermedios ópticamente activos con el fin de preparar productos con gran actividad biológica, como el C-azanucleósido de Schramm **122**(**Esquema 29**) preparado por Carretero y col.[77] Esta molécula se ha utilizado como inhibidor de las hidrolasas de un género de protozoos parásitos denominados tripanosomas, causantes de diferentes enfermedades como la tripanosomiasis africana o enfermedad del sueño.

[76] **a)** Melhado, A.; Luparia, M.; Toste, D.; *J. Am. Chem. Soc.*, **2007**, *129* (42), 12638; **b)** Martín, M.; Nájera, C.; Sansano, J.; Wu, F.; *Tetrahedron: Asymmetry* **2010**, *21*, 1184.
[77] Carretero, J.; López, A.; Adrio, J.; *J. Am. Chem. Soc.* **2008**, *130*, 10085.

Esquema 29. Síntesis del C-azanucleósido de Schramm. **a)** $Cu(MeCN_4)PF_6$ (3 % mol), (R_p)-**105b** Et_3N (20 % mol), CH_2Cl_2, 48h, -78 °C; 94 % *ee*; **b)** $LiAlH_4$, THF, 0 °C; **c)** TIPSOTf, 2,6-lutidina, DCM, 0 °C; **d)** Na(Hg), Na_2HPO_4, MeOH/THF; **e)** OsO_4, TMEDA, DCM, -78°C; **f)** HCl/MeOH, 25 °C.

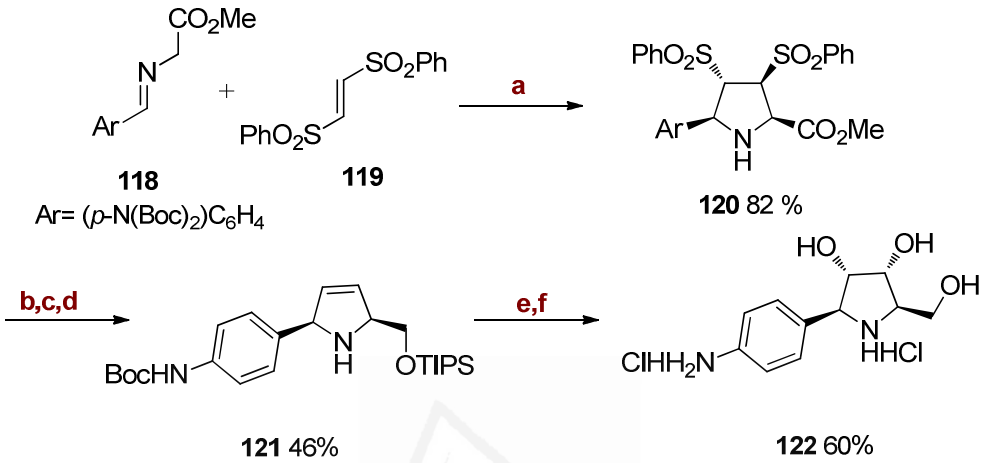

118
Ar= (*p*-N(Boc)$_2$)C_6H_4

119

120 82 %

121 46%

122 60%

Por otro lado, la cicloadición 1,3-dipolar enantioselectiva utilizando iluros de azometino y complejos quirales de plata(I) y oro(I), ha dado lugar a intermedios quirales que se han utilizado en la síntesis de potentes inhibidores del virus causante de la Hepatitis C (**Figura 11**).[78]

[78] Nájera, C.; Sansano, J.; *Org. Biomol. Chem.* **2009**, *7*, 4567.

Figura 11. Inhibidores del virus causante de la hepatitis C, **123** (1ª generación), **124**-**125** (2ª generación) y **126** (3ª generación).

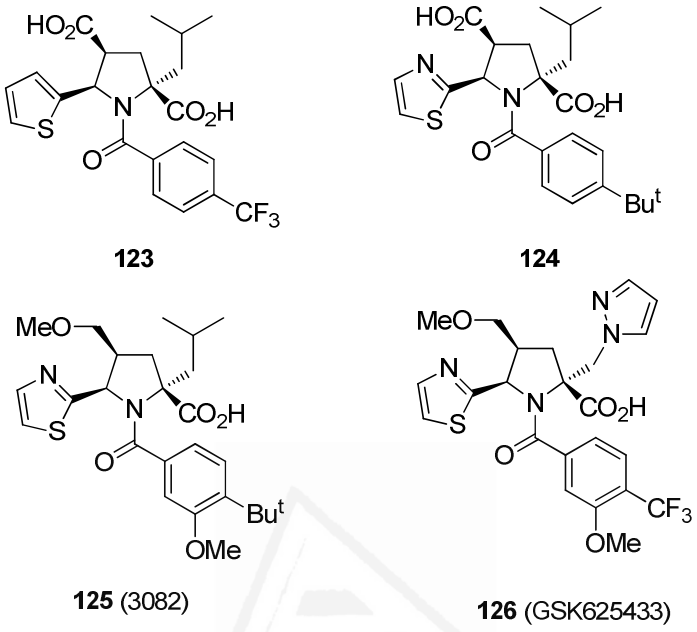

Los productos **123**, **124** y **125** fueron sintetizados a través del intermedio **129,** derivado de iminoésteres de leucina **127** y acrilatos, como se muestra en el **Equema 30**. La primera síntesis enantioselectiva de los anillos de cinco miembros de estas estructuras se realizó mediante el uso de un complejo catalítico formado por el fosforamidito quiral (S_a,*R*,*R*)-**98** y $AgClO_4$ (en cantidades de 5% mol). La reacción se llevó a cabo a -20 °C obteniéndose el compuesto *endo*-**129** con buen rendimiento (**Tabla 4**, entrada 1). La síntesis del producto **123** enantioméricamente enriquecido (82% *ee*) se obtuvo tras la amidación y doble hidrólisis del producto **129** utilizando ácido TFA a 0 °C seguida de KOH-MeOH a 80 °C.[79]

También se sintetizó el intermedio **129** mediante la formación del catalizador compuesto por el ligando quiral **114b** e isopropóxido de calcio teniendo lugar la reacción entre -44 °C y -30 °C en THF como disolvente. Los rendimientos y los excesos enantiómericos fueron altos (**Tabla 4**, entradas 2 y 3).

[79] **a)** Nájera, C.; Martín, M.; Retamosa, M.; Sansano, J.; de Cózar, A.; Cossío, F.; *Eur. J. Org. Chem.*, **2009**, 5622. **b)** Nájera, C.; Retamosa, M.; Sansano, J.;. *Patente Española:P200800908,* Mayo **2008.**

Equema 30

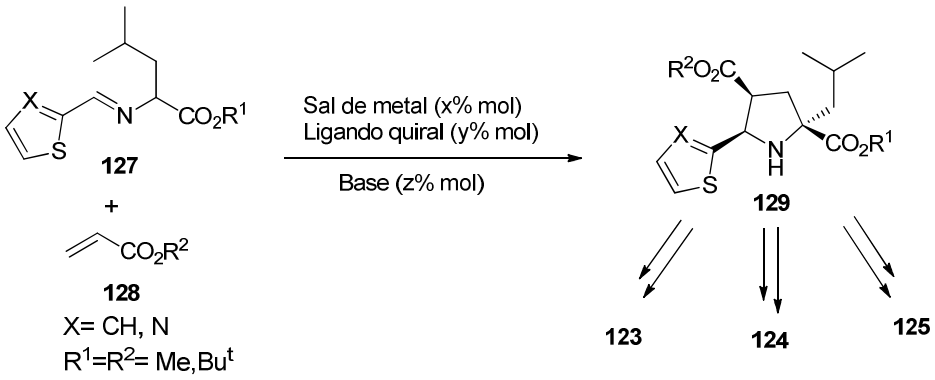

Figura 12

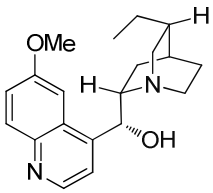

130

Tabla 4. Síntesis enantioselectiva del compuesto **129**.

Entrada	X	R^1	R^2	Sal[a]	L[a]	Base[a]	Tª (ºC)	Rendimiento (%)[b]	*ee*(%)
1	CH	Me	Bu^t	$AgClO_4$ (5)	(*Sa,R,R*)-98 (5)	Et_3N (5)	-20	70	82
2	CH	Bu^t	Bu^t	$Ca(OPr^i)_4$ (10)	**114b** (10)	____	-44	83	85[c]
3	N	Bu^t	Bu^t	$Ca(OPr^i)_4$ (10)	**114b** (10)	____	-30	83	88[c]
4	N	Bu^t	Me	AgOAc (3)	**130**	____	0	84	74

[a]En paréntesis (x, y o z % mol).
[b]Rendimiento del producto aislado.
[c]Se obtuvo el producto *ent*-**129**.

V.4.9.2.- Reacciones 1,3-dipolares enantioselectivas multicomponente

Respecto a la cicloadición 1,3-dipolar multicomponente enantioselectiva, se ha convertido en un área muy estudiada desde hace relativamente poco tiempo, especialmente en el campo de la organocatálisis.[80] La primera cicloadición 1,3-dipolar organocatalizada asimétrica fue publicada por el grupo de Arai en 2006.[81] Sin embargo en este trabajo los resultados fueron modestos, con bajos rendimientos y enantioselectividades. Un año más tarde, en 2007, Vicario y colaboradores llevaron a cabo la primera cicloadición con iluros de azometino obteniendo una excelente enantioselectividad (**Esquema 31**).[82] En ambos trabajos sin embargo, la reacción tenía lugar entre dos componentes.

Esquema 31

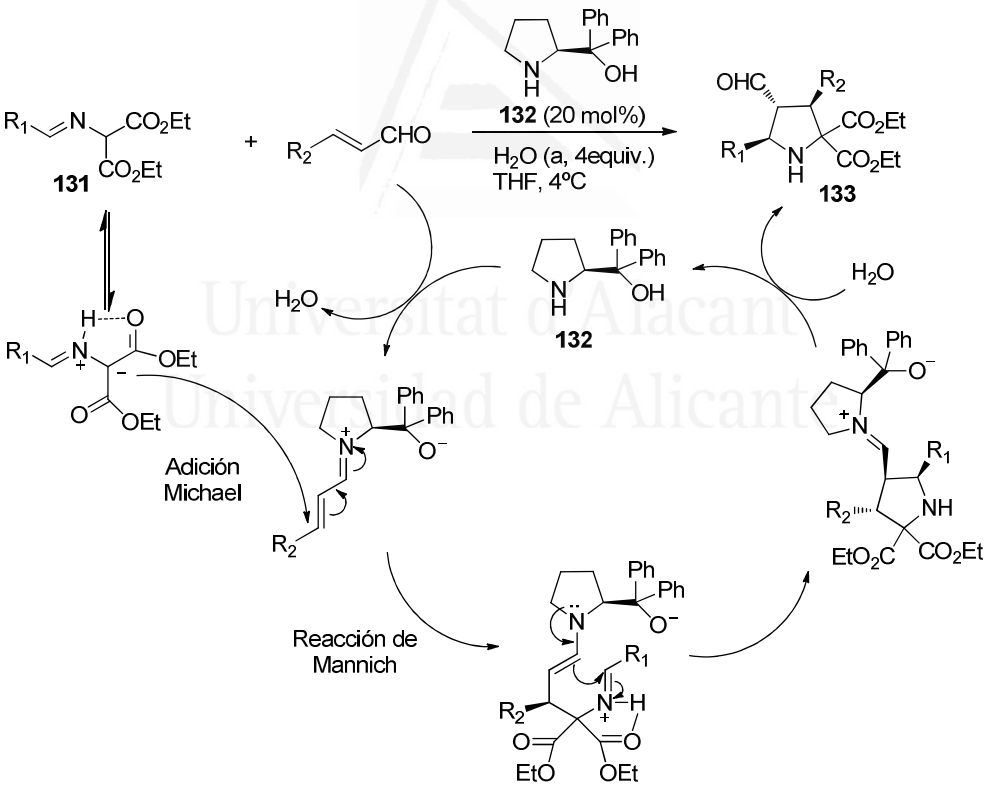

[80] Moyano, A.; Rios, R; *Chem. Rev.* **2011**, *111*, 4703.
[81] Arai, S.; Takahashi, F.; Tsuji, R.; Nishida, A.; *Heterocycles* **2006**, *67*, 495.
[82] Vicario, J.L.; Reboredo, S.; Badia, D.; Carrillo, L.; *Angew. Chem., Int. Ed.* **2007**, *46*, 5168.

Fue el grupo de Córdova el que publicó en el mismo año la cicloadición multicomponente, con los mismos reactivos, sin la necesidad de preformar el (ariliden)aminomalonato.[83] De esta forma, hicieron reaccionar 2-aminomalonato de dietilo con un aldehído, que seguidamente reaccionaba con un aldehído α,β-insaturado actuando como dipolarófilo (**Esquema 32**). Algo más reciente es el trabajo del grupo de Gong, en el que partiendo también de tres componentes, un aldehído, 2-aminomalonato de dietilo y maleato de dialquilo obtienen los cicloaductos correspondientes con buena diasteroselectividad y excelente exceso enantiomérico (**Esquema 33**).[84] Desde entonces hasta hoy, estos tres grupos han continuado con la síntesis enantioselectiva de pirrolidinas, a través de cicloadiciones dipolares multicomponente con iluros de azometino.[85]

Esquema 32

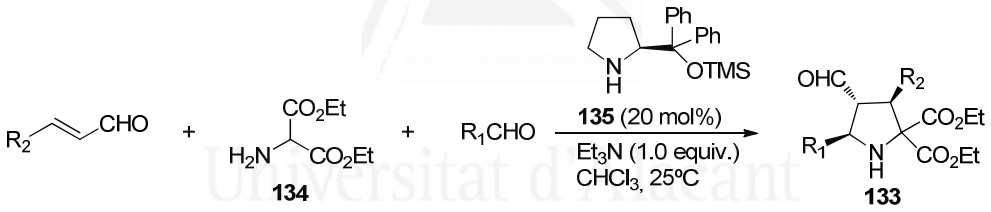

[83] Ibrahem, I.; Rios, R.; Vesely, J.; Córdova, A.; *Tetrahedron Lett.* **2007**, *48*, 6252.

[84] Chen, X.-H.; Zhang, W.-Q.; Gong, L.-Z.; *J. Am. Chem. Soc.* **2008**, *130*, 5652.

[85] **a)** Yu, J.; He, L.; Chen, X.-H.; Song, J.; Chen, W.-J.; Gong L.-Z. *Org. Lett.* **2009**, *11*, 4946. **b)** Iza, A.; Carrillo, L.; Vicario, J.L.; Badía, D.; Reyes, E.; Martínez, J.I.; *Org. Biomol. Chem.* **2010**, *8*, 2238. **c)** Shi,F.; Luo, S.; Tao, Z.-L.; He, L.; Yu, J.; Tu, S.T; Gong, L.-Z.; *Org. Lett.* **2011**, *13*, 4680. **d)** He, L.; Chen, H.X.; Wang, D.; Luo, S.; Zhang, W.Q.; Yu, J.; Ren, L.; Gong, L.-Z.; *J. Am. Chem. Soc.* **2011**, *133*, 13504. **e)** Liu, W.-J.; Chen, H.X.; Gong, L.-Z.; *Org. Lett.* **2008**, *10*, 5357. **f)** Chen, H.X.; Wei, Q.; Luo, S.W.; Xiao, H.; Gong, L.-Z.; *J. Am. Chem. Soc.* **2009**, *131*, 13819. **g)** Reboredo, S.; Reyes, E.; Vicario, J.L.; Badía, D.; Carrillo, L.; Cózar, A.; Cossío, F.; *Chem. Eur. J.* **2012**, *18*, 7179. **h)** Guo, C.; Song, J.; Gong, L.-Z.; *Org. Lett.* **2013**, *15*, 2676.

Esquema 33

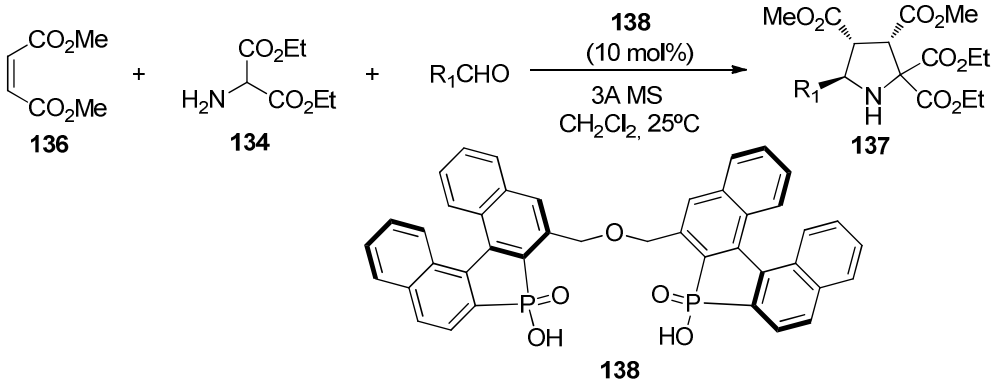

Sin embargo, no son muchos los artículos de este tipo de reacción catalizada por plata. Como ejemplo puede citarse el publicado por nuestro grupo de investigación en 2010. En él, se lleva a cabo la síntesis de pirrolidinas con excelente enantioselectividad, a partir de un aldehído, el clorhidrato del éster metílico de glicina, Et_3N como base, y un dipolarófilo, en presencia de una sal de plata y el ligando quiral (*S*)-Binap **96**.[86]

[86] **a)** Mancebo-Aracil,J.; Martín-Rodríguez,M.; Nájera, C.; Sansano, J.M.; Costa, P.; Crizanto, E.; Dias, A.; *Tet. Asymm.* **2012**, *23*, 1596 **b)** Martín, M.; Nájera, C. Sansano, J.M.; Costa, P.; Crizanto, E.; Dias, A.; *Synlett* **2010**, 0962.

V.4.10.- Objetivos

De acuerdo con lo expuesto anteriormente relativo a las cicloadiciones 1,3-dipolares asimétricas con iluros de azometino y al interés de estas moléculas en la síntesis de productos biológicamente activos, así como a los resultados obtenidos en el **Capítulo II-2** se plantearon los siguientes objetivos:

- Llevar a cabo la reacción 1,3-dipolar multicomponente de forma asímetrica catalizada por complejos quirales de Ag^{I}, a partir de glioxilato de etilo y derivados de aminoácidos.
- Llevar a cabo la síntesis asimétrica de los precursores de los productos naturales (*R*)-(+)-crispina A y (*R*)-(+)-harmicina, a través de una ruta sintética en la que el paso determinante que genera los cuatro centros estereogénicos es una cicloadición 1,3-dipolar, tal como indica el siguiente esquema. Estos nuevos derivados de prolinas sustituidas, **A** y **B**, serán los precursores del anillo de pirrolidina condensada en dichos productos naturales.

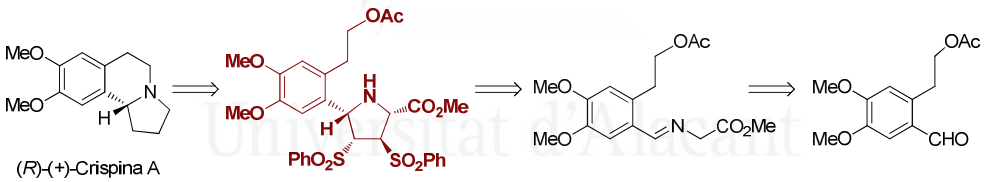

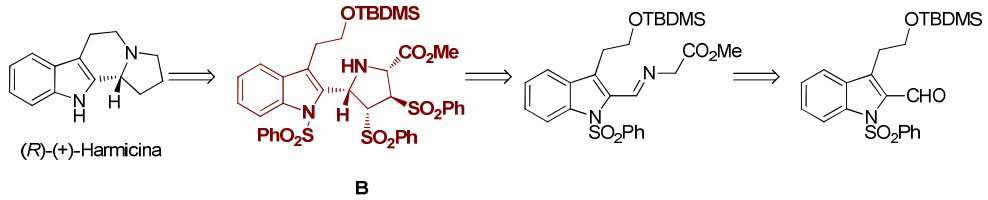

V.4.11.- Discusión de Resultados

V.4.11.1.- Cicloadición 1,3-dipolar multicomponente asimétrica con glioxilato de etilo como precursor del iluro de azometino

De acuerdo con lo estudiado y expuesto en el **Capítulo II-1**, se conoce que puede realizarse la reacción 1,3-dipolar multicomponente entre glioxilato de etilo, derivados de aminoácidos y diferentes dipolarófilos formando el 1,3-dipolo térmicamente con buenos rendimientos y diastereoselectividades. Sin embargo, como se expone en el **Capítulo II-2**, puede mejorarse la diasteroselectividad en algunos casos mediante el uso de sales de Ag^{I}, a temperatura ambiente. Por ello, se propuso entonces llevar a cabo esta misma reacción de forma asimétrica, tratando de obtener las pirrolidinas correspondientes enantioméricamente enriquecidas, mediante el uso de complejos quirales formados a partir de un ligando quiral fosforado "privilegiado" y una sal de plata(I).

Así pues, a la vista de los resultados obtenidos, se decidió optimizar la reacción usando glioxilato de etilo como aldehído, el clorhidrato del éster etílico de L-fenilalanina y *N*-metilmaleimida como dipolarófilo. En primer lugar se realizó el estudio del ligando quiral con trifluoroacetato de plata(I) (AgTFA) en tolueno como disolvente a temperatura ambiente (**Esquema 34**, **Figura 13** y **Tabla 5**). El fenilalaninato de etilo se preparó in situ por tratamiento con K2CO3 del clorhidrato con el fin de evitar la presencia de una base orgánica como la Et3N que pudiera favorecer el proceso racémico.

Esquema 34

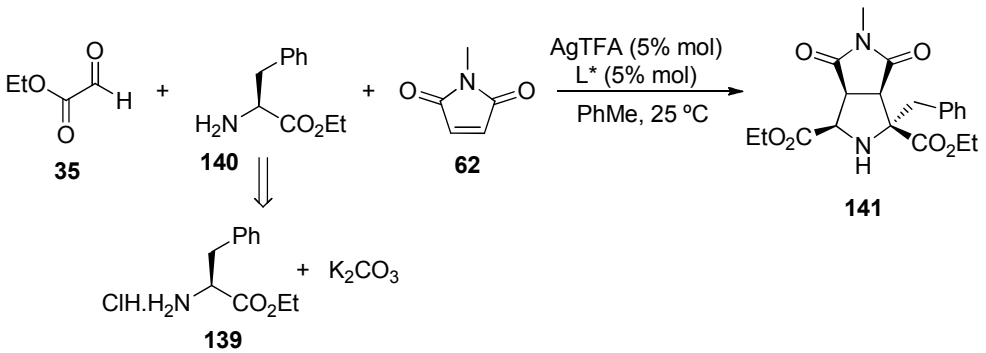

Figura 13. Ligandos quirales (L*)

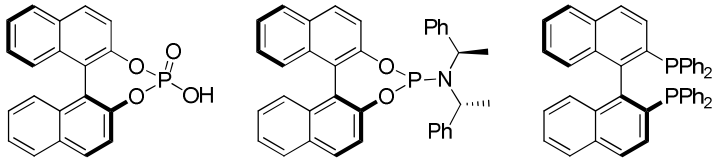

142 (S_a,*R*,*R*)-**98** (*S*)-Binap **96**

Tabla 5. Optimización de ligandos quirales.

Entrada	L* (5% mol)	Conversión[a] (%)	*ee* (%)[b]
1	**142**	100	0[c]
2	(S_a,*R*,*R*)-**98**	100	0
3	(*S*)-Binap **96**	100	0[d]
4	(*S*)-Binap **96**	100	35[e]
5	(*S*)-Binap **96**	100	**70**

[a]Determinado mediante ^{1}H-NMR.
[b]Determinado mediante HPLC quiral.
[c]Sin AgTFA.
[d]Reacción a partir de glioxilato de etilo, y *N*-metilmaleimida, el clorhidrato del éster etílico de fenilalanina y Et_3N.
[e]Adicionando 1 eq. de Et_3N.

Como puede verse en la **Tabla 5**, la reacción con los ligandos **142** y (S_a,*R*,*R*)-**98** (Entradas 1 y 2) dio una conversión química completa, obteniéndose únicamente el diasteroisómero indicado, pero exceso enantiomérico nulo. Sin embargo en el caso del ligando (*S*)-Binap **96** (Entradas 3 a 5), los resultados varían considerablemente en función de la metodología utilizada. Cuando la reacción se llevó a cabo partiendo del clorhidrato de L-fenilalanina, añadiendo un equivalente de Et_3N para liberar el clorhidrato, el producto de reacción fue racémico (Entrada 3). Sin embargo cuando la reacción se trabajó tal y como indica el **Esquema 35**, es decir, mediante el aminoester **140**, aislado en forma de amina libre, en presencia de AgTFA y (*S*)-Binap **96** (Entrada 5), el exceso enantiomérico fue del 70 %. Esto indica, que la sal de trietilamonio formada in situ en el medio de reacción, interfiere notablemente para que la transferencia de quiralidad sea efectiva. Para comprobar si sólo esta sal era la causante del bajo *ee*, y no el exceso de Et_3N presente, se llevó a cabo un experimento (Entrada 4) en el que con la metodología

descrita, se adicionó además un equivalente de esta base (Et_3N). El resultado fue de un 35 % *ee*, con lo que puede concluirse que tanto en presencia de esta base, como del clorhidrato de trietilamonio, el resultado era un producto racémico.

Elegido pues el ligando (*S*)-Binap **96**, se pasó a estudiar el efecto que pudiera tener el uso de diferentes sales de plata, como indica la siguiente tabla:

Esquema 35

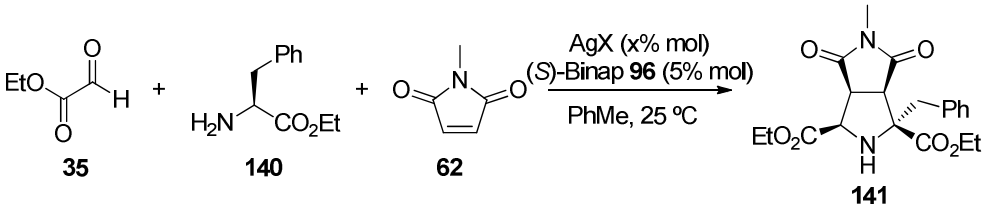

Tabla 6. Estudio de sales de Ag^I en PhMe.

Entrada	AgX (x % mol)	Conversión[a] (%)	*ee* (%)[b]
1	AgOAc (5 %)	100	79
2	AgOBz (5 %)	100	72
3	Ag_2CO_3 (2.5 %)	100	74
4	AgTFA (5 %)	100	70
5	$AgNO_3$ (5 %)	100	74
6	AgOTf (5 %)	100	70
7	$AgBF_4$ (5 %)	100	72
8	Ag_2O (5 %)	85	74
9	AgF (5 %)	100	56
10	$AgClO_4$ (5 %)	95	57
11	$AgSbF_6$ (5 %)	89	18

[a]Determinado mediante ^{1}H-NMR.

[b]Determinado mediante HPLC quiral.

Como puede verse en la **Tabla 6**, la mayoría de sales de plata probadas ofrecían un exceso enantiomérico similar (Entradas 1 a 8). Sin embargo cuando se probó el fluoruro, perclorato y hexafluoroantimoniato de plata(I) (Entradas 9 a 11), el *ee* obtenido era considerablemente menor.

Para el siguiente estudio de disolventes (**Tabla 7**) se escogió el acetato de plata(I) (Entrada 1, **Tabla 7**) por ofrecer en tolueno el mayor *ee*.

Tabla 7. Estudio de disolventes para la cicloadición con (*S*)-Binap **96**/AgOAc

Entrada	Disolvente	Conversión[a]	*ee* (%)[b]
1	Acetona	100	0
2	Acetonitrilo	100	72
3	Etanol	100	76
4	Tetrahidrofurano	100	14
5	Diclorometano	95	70
6	Agua	100	80
7	Tolueno	100	70
8	Dietil éter	100	82
9	Diisopropil éter	100	76
10	*terc*-butil metil éter	100	76

[a]Determinado mediante ^{1}H-NMR.
[b]Determinado mediante HPLC quiral.

A la vista de los resultados es difícil sacar conclusiones sobre qué clase de disolvente es el mejor para esta reacción. En general, los resultados son buenos para disolventes polares como apolares, próticos y apróticos, excepto que en acetona el producto de reacción fue racémico y en THF se obtuvo un *ee* bajo si comparamos con el resto de disolventes. También destaca el resultado en agua presentando muy buena selectividad. Sin embargo, cuando en este mismo disolvente se realizó el ensayo a 4 °C para AgOAc, el *ee* decreció a 34 %.

Llegados a este punto, se decidió probar algunas sales de plata en dietil éter (**Tabla 8**), con el fin de comprobar un posible efecto sinérgico entre el disolvente y la sal de plata correspondiente.

Tabla 8. Estudio de sales de Ag^{I} en dietil éter.

Entrada	AgX (x % mol)	Conversión[a] (%)	*ee* (%)[b]
1	AgOAc (5 %)	100	82
2	AgOBz (5 %)	100	80
3	Ag_2CO_3 (2.5 %)	100	81
4	AgTFA (5 %)	100	66
5	$AgNO_3$ (5 %)	100	66
6	AgOTf (5 %)	100	66

[a]Determinado mediante ^{1}H-NMR.
[b]Determinado mediante HPLC quiral.

Los resultados fueron semejantes a los obtenidos en tolueno, sin embargo, el dietil éter parece discriminar algo más entre las sales de plata probadas.

Debido a que la elección de la sal de plata no era aún definitiva, y tampoco la del disolvente, se decidió hacer un estudio de la temperatura, para ambos disolventes y diferentes sales de plata(I) (**Figuras 14** y **15**).

Figura 14. Estudio de la temperatura en PhMe.

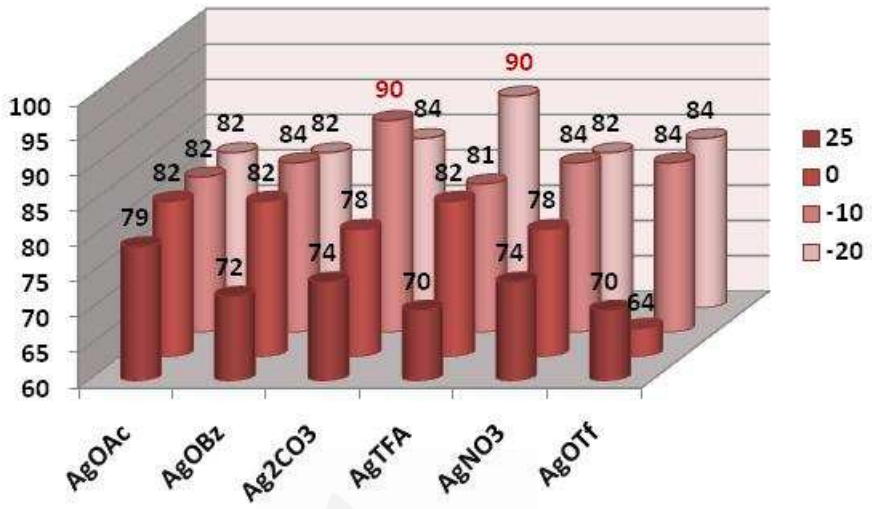

Figura 15. Estudio de la temperatura en dietil éter.

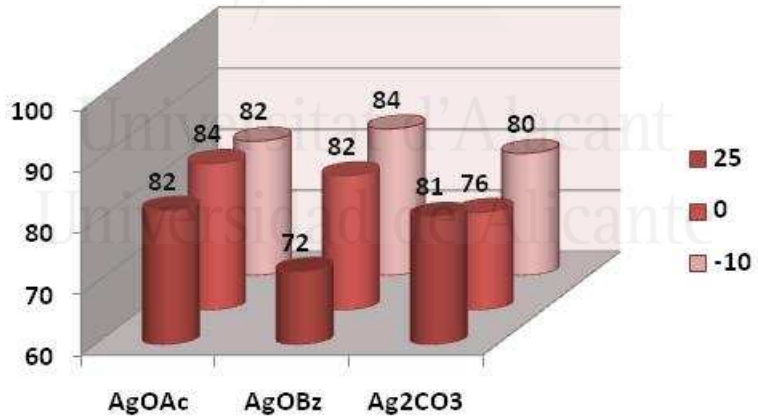

En ambos estudios, la conversión química de todos los ejemplos fue completa. Como puede verse en la **Figura 14**, en tolueno los mejores resultados fueron los obtenidos a -10 °C para el Ag_2CO_3, y -20 °C para AgTFA, con un 90 % de *ee* en ambos casos. En general, la tendencia es la esperada, conforme decrece la temperatura, aumenta el ee, especialmente cuando bajamos de 25 °C a 0 °C o inferior. Sin embargo, a temperaturas menores, la enantioselectividad se mantiene o a penas se incrementa. En el caso del AgOTf incluso decrece

notablemente al disminuir a 0 °C, para luego aumentar a un 84 % *ee*. Las pruebas a baja temperatura realizadas en dietil éter (**Figura 15**) no dieron indicios de mejorar la enantioselectividad para las sales de plata probadas, con *ee* que van desde 72-84 %.

De los dos resultados mejores, se decidió elegir para siguientes ensayos el Ag_2CO_3, ya que es más económica que el AgTFA,[87] permitiendo además realizar los ensayos a 10 °C más de temperatura. Una vez elegidas las condiciones de reacción ((*S*)-Binap **96**, Ag_2CO_3, -10 °C y PhMe) con el fin de optimizar la enantioselectividad, se estudió por último el efecto que pudiera tener la carga de catalizador como muestra la **Tabla 9**:

Tabla 9. Estudio de la carga de catalizador.

Entrada	Ag_2CO_3 + (*S*)-Binap 96 (x% mol)	Conversión[a] (%)	*ee* (%)[b]
1	1	100	74
2	3	100	83
3	5	100	**90**
4	7	100	85

[a]Determinado mediante ^{1}H-NMR.
[b]Determinado mediante HPLC quiral.

Así pues, tras la extensa optimización, se estudiaron distintos dipolarófilos (**Esquema 36**, **Tabla 10**)

Esquema 36

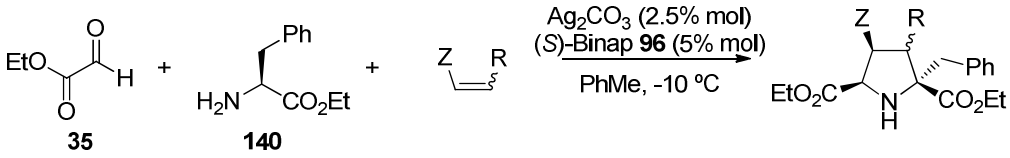

[87] Precios Sigma-Aldrich en **2013** para: Ag_2CO_3 (3.70 €/g, 4.70 €/g Ag), AgTFA (5.60 €/g, 11.40 €/g Ag).

Tabla 10. Estudio de dipolarófilos para el éster etílico de L-fenilalanina.

Entrada	Dipolarófilo	Producto	Conversión[a] (%)	*ee* (%)[b]
1	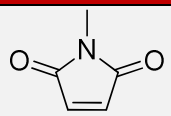	**141**	100	90
2	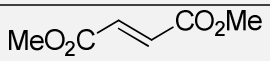	**143**	70	8
3	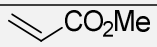	**144**	83	0
4		**145**	75	0
5	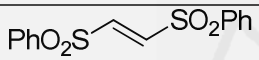	**146**	93	30
6	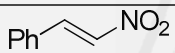	-	-	-

[a]Determinado mediante ^{1}H-NMR.
[b]Determinado mediante HPLC quiral.

En general, las conversiones químicas fueron buenas, salvo para el caso del β–nitroestireno con el que no hubo reacción. La diasteroselectividad fue óptima, obteniéndose, como en el caso de la *N*-metilmaleimida, un solo diasteroisómero. Sin embargo, al variar de dipolarófilo, la enantioselectividad fue baja o nula, siendo el mejor *ee* el del producto de reacción con la 1,2-bis(fenilsulfonil)etileno como dipolarófilo con un 30 %.

Dado que el complejo formado por (*S*)-Binap **96** y Ag_2CO_3, aparentemente presentaba selectividad tan solo para la *N*-metilmaleimida como dipolarófilo, se estudió esta cicloadición 1,3-dipolar con diferentes derivados de aminoácidos como muestra la siguiente tabla:

Esquema 37

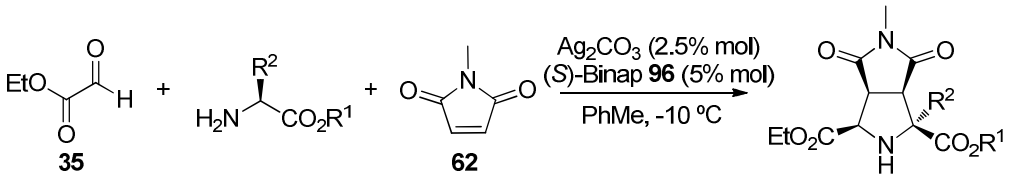

Tabla 11. Estudio de derivados de aminoácidos.

Entrada	Aminoester	Producto	Conversión[a] (%)	*ee* (%)[b]
1	H_2N CO_2Et	**2,5-*cis*-89**	90	0
2	Me, H_2N CO_2Me	**147**	60	11
3	Ph, H_2N CO_2Et	**141**	100	90
4	Ph, H_2N CO_2Me	**148**	85	7

[a]Determinado mediante ^{1}H-NMR.

[b]Determinado mediante HPLC quiral.

Como en el caso del estudio de dipolarófilos, los productos obtenidos presentaban en general un buen rendimiento químico y diasteroselectividad, pero apenas nada de enantioselectividad. Se concluye por tanto que el complejo formado por (*S*)-Binap **96** y Ag_2CO_3, presenta selectividad para la reacción de glioxilato de etilo, éster etílico de L-fenilalanina y *N*-metilmaleimida. Tan solo faltaba por demostrar si esta enantioselectividad era también trasladable a otras maleimidas (**Esquema 38**, **Tabla 12**).

Como puede verse en la **Tabla 12**, tanto el rendimiento de la reacción como la enantioselectividad son muy buenas para maleimidas *N*-sustituidas (Entradas 2 a 6). El *ee* obtenido para la *N*-metilmaleimida fue mejorado hasta un 92 % usando como dipolarófilo la 4-bromofenilmaleimida con un rendimiento casi cuantitativo.

Esquema 38

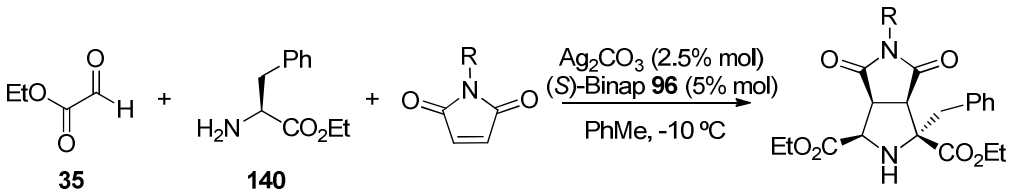

Tabla 12. Estudio de maleimidas *N*-sustituidas.

Entrada	Maleimida	Producto	Conversión[a] (%)	Rto. (%)[b]	*ee* (%)[c]
1	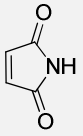	**149**	85	65	30
2	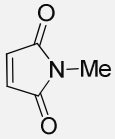	**141**	100	94	90
3	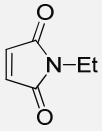	**150**	100	96	85
4	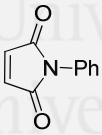	**151**	100	95	88
5	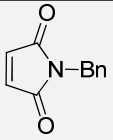	**152**	100	95	77
6	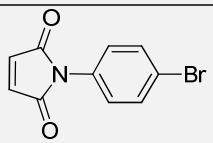	**153**	100	98	**92**

[a]Determinado mediante ^{1}H-NMR.

[b]Rendimiento de producto aislado.

[c]Determinado mediante HPLC quiral.

En conclusión, el catalizador formado a partir del ligando quiral (*S*)-Binap **96** y la sal de plata Ag_2CO_3, mostró excelente rendimiento químico y enantioselectividad para la cicloadición 1,3-dipolar multicomponente entre el iluro de azometino formado a partir de glioxilato de etilo y el éster etílico de L-fenilalanina, y maleimidas *N*-sustituidas como dipolarófilos, con un *ee* de hasta 92 % y rendimientos cuantitativos.

V.4.11.2.- Síntesis asimétrica de los precursores de los productos naturales (*R*)-(+)-crispina A y (*R*)-(+)-harmicina

El alcaloide natural crispina A (**Figura 16**) puede extraerse de la especie de plantas denominadas *Carduus Crispus*, de la familia *Asteraceae*. Este tipo de plantas abundan en Asia y han sido utilizadas en la medicina tradicional China para tratar diferentes males como el resfriado, dolor de estómago o el reumatismo. Se conoce hoy en día además que presenta una actividad citotóxica significante para células tumorales humanas.[88] Por otro lado, la harmicina pertenece al género *Kopsia* de la familia *Kopsia Griffithii* que incluye alrededor de treinta especies que se encuentran en el Asia tropical. Este tipo de alcaloides presentan una fuerte actividad para el tratamiento de la leishmaniasis.[89]

Figura 16

(*R*)-(+)-crispina A (*R*)-(+)-harmicina

Estructuralmente, ambas presentan en su estructura un anillo de pirrolidina condensada con un centro estereogénico, con lo que a priori se pensó que sería posible la síntesis de dichas moléculas con un buen exceso enantiomérico mediante una cicloadición 1,3-dipolar a partir de la ruta sintética mostrada en los **Objetivos**.

V.4.11.2.1.- Síntesis del precursor de la (*R*)-(+)-crispina A

[88] Zhao, Y.; Zhang, Q.; Tu, G. ; Cheng, T.; *Tetrahedron* **2002**, *58*, 6795.
[89] Kam, T.; Sim, K.; *Phytochemistry* **1997**, *47*, 145.

V.4.11.2.1.1.- Primera aproximación: 2-(2-cloroetil)-4,5-dimetoxibenzaldehído como producto de partida

En la primera estrategia sintética que se diseñó, para llegar hasta la crispina A, se utilizó el cloruro **156** (**Esquema 39**) para hacerlo reaccionar posteriormente con 1,2-bis(fenilsulfonil)etileno **119**, y el éster metílico de la glicina **157** bajo diferentes condiciones de reacción, tal y como se indica las **Tablas 13**, **14** y **15** y en el **Esquema 40**. Para ello, se sintetizó el cloruro **156** a partir de 3,4-dimetoxifenetilalcohol a través de dos pasos de reacción tal y como se describió en la bibliografía (**Esquema 39**).[90]

Esquema 39

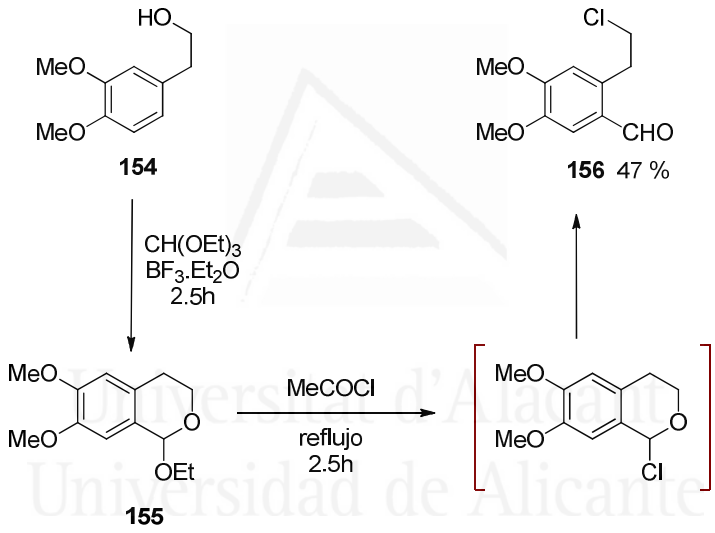

Se obtuvo así el compuesto **156** puro, con un rendimiento global de 47% y se trató de llevar a cabo la reacción 1,3-dipolar con diferentes catalizadores de transferencia de fase quirales o bien de bases quirales (**Figura 17**).[91]

La reacción 1,3-dipolar se realizó mezclando el aldehído **156**, el aminoéster derivado de la glicina **157** y el dipolarófilo en el mismo matraz de reacción para generar la sal de iminio intermedia **158,** la cual se desprotonó en presencia de una base quiral, o bien se usó una mezcla de base

[90] Yamato, M.; Hashigaki, K.; Qais, N.; Ishikawa, S.; *Tetrahedron* **1990**, *46*, 5909.
[91] Tarí, S; Chinchilla, R; Nájera, C; *Tetrahedron: Asymmetry* **2009**, *20*, 2651

inorgánica/catalizador de transferencia de fase quiral (**Esquema 40**), como los indicados en la **Figura 17** derivados de Cinchona.

Esquema 40

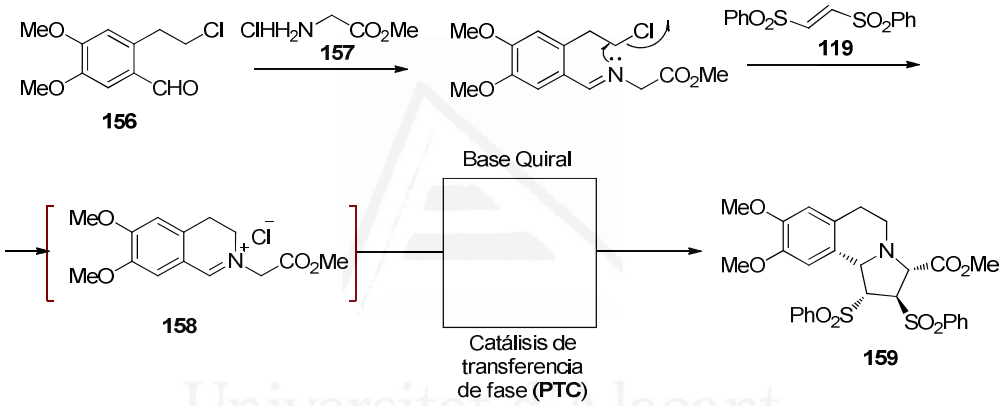

Figura 17

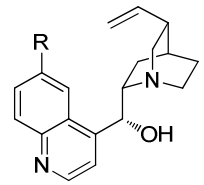

R = H: cinconidina **160a**
R = OMe: quinina **161**
R = OH Cupreína **163**

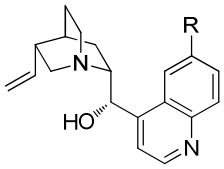

R = H: cinconina **160b**
R = OMe: quinidina **162**

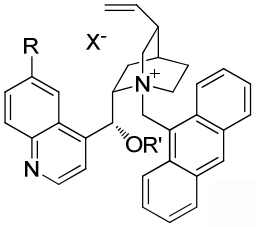

R = H, R' = H, X = Cl **164**
R = H, R' = Alil, X = Br **165**

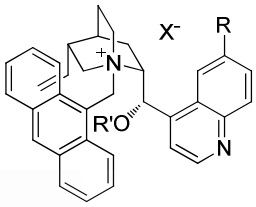

R = H, R' = H, X = Cl **166**
R = H, R' = Alil, X = Br **167**
R = OMe, R' = H, X = Cl **168**

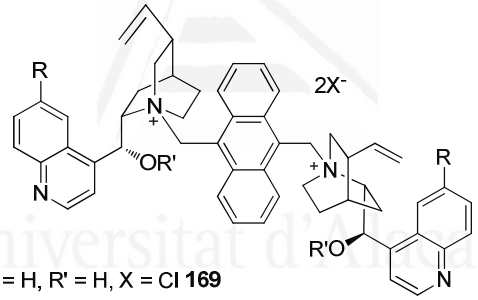

R = H, R' = H, X = Cl **169**
R = H, R' = H, X = BF_4 **170**
R = H, R' = H, X = PF_6 **171**
R = H, R' = Alil, X = Br **172**
R = H, R' = Alil, X = BF_4 **173**
R = H, R' = Alil, X = PF_6:**174**

R = OMe, R' = H, X = Cl **175**
R = OMe, R' = H, X = BF_4 **176**
R = OMe, R' = H, X = PF_6 **177**
R = H, R' = Alil, X = Br **178**

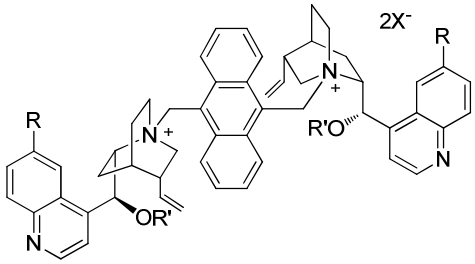

R = H, R' = H, X = Cl **179**
R = H, R' = H, X = BF_4 **180**
R = H, R' = H, X = PF_6 **181**
R = H, R' = Alil, X = Br **182**
R = H, R' = Alil, X = BF_4 **183**
R = H, R' = Alil, X = PF_6 **184**

R = OMe, R' = H, X = Cl **185**
R = OMe, R' = H, X = BF_4 **186**
R = OMe, R' = H, X = PF_6 **187**
R = H, R' = Alil, X = Br **188**

A pesar de haber ensayado todos estos compuestos quirales **160a-188**, solamente el catalizador desarrollado por Lygo **164** y el desarrollado por Corey **165** indujeron algo de quiralidad en el producto final **159**. La **Tabla 13** muestra la reacción 1,3-dipolar del cloruro **156** con la disulfona **119** y el éster metílico de la glicina **157**, utilizando el mencionado catalizador bajo distintas condiciones de reacción, diferentes bases y disolventes. Tan sólo cuando se realizó el experimento con tolueno y Et_3N (**Tabla 13**, entrada 7) y con diclorometano, Et_3N y K_2CO_3 (**Tabla 13**, entrada 3) la reacción funcionó químicamente, obteniéndose unas conversiones del 75 y 44%, respectivamente. Sin embargo el exceso enantiomérico fue casi nulo para ambas.

Esquema 41

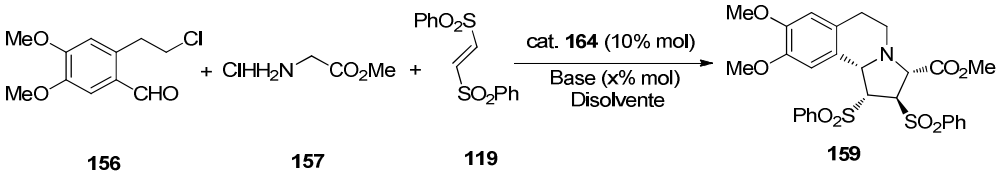

156 **157** **119** **159**

Tabla 13. Cicloadición 1,3-dipolar del producto **156** con el catalizador quiral de transferencia de fase **164**.[a]

Entrada	Base[b]	Disolvente	Conversión (%)[c]	*ee*[d] (%)
1	Et_3N (100) K_2CO_3 (10)	PhMe	____	__
2	Et_3N (100) KOH (10)	PhMe	____	__
3	Et_3N (100) K_2CO_3 (10)	DCM	44	<5
4	Et_3N (110)	DCM	____	__
5	Et_3N (100) DABCO (10)	DCM	____	__
6	K_2CO_3 (200)	PhMe	____	__
7	Et_3N (200)	PhMe	75	<5

[a]Condiciones de reacción: 0.17 mmol de **156**, 0.17 mmol de **119**, 0.17 mmol de **157**, 10 % catalizador **164**, 3 mL de disolvente, 20-25 °C, 44-50 h.
[b]En paréntesis (x % mol).
[c]Determinado mediante ^{1}H-RMN.
[d]Determinado mediante HPLC quiral.

Con estas mismas condiciones, se trabajó con el catalizador desarrollado por Corey **165**, obteniéndose mejores conversiones que con el **164**, pero manteniendo una enantioselección bastante pobre (**Tabla 14**). La mejor conversión, del 85%, se consiguió con las mismas condiciones que habían dado mejor resultado con el catalizador **164** (**Tabla 14**, entrada 7), con dos equivalentes de Et_3N y tolueno como disolvente. El resto de condiciones que dieron lugar al producto **159** lo hicieron con pobres conversiones. En todos los casos, la enantioselectividad fue nula. Incluso utilizando agua como disolvente (**Tabla 14**, entrada 11). También se probaron las condiciones mostradas en la entrada 9 de la **Tabla 14**, ya desarrolladas por nuestro grupo de investigación, en las que se utiliza tolueno como disolvente con un 30% de un disolvente más polar como es el cloroformo, que favorece la disolución del catalizador usado. Por último, se probaron también condiciones similares a las de las **Tablas 13** y **14** con otros catalizadores (**Figura 17**) obteniéndose resultados similares (**Tabla 15**).

Esquema 42

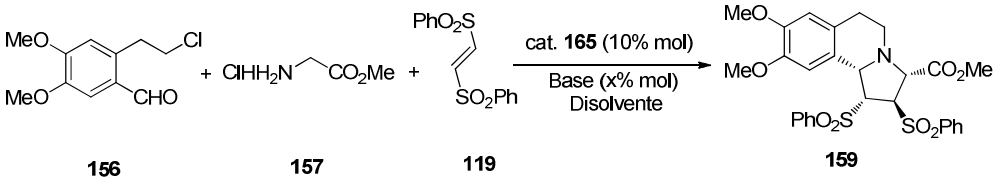

156 **157** **119** **159**

Tabla 14. Cicloadición 1,3-dipolar del producto **156** con el catalizador quiral de transferencia de fase **165.**[a]

Entrada	Base[b]	Disolvente	Conversión (%)[c]	*ee*[d] (%)
1	Et_3N (100) K_2CO_3 (10)	PhMe	33	<5
2	Et_3N (100) KOH (10)	PhMe	50	<5
3	Et_3N (100) K_2CO_3 (10)	DCM	45	<5
4	Et_3N (110)	DCM	____	__
5	Et_3N (100) DABCO (10)	DCM	____	__
6	K_2CO_3 (200)	PhMe	28	<5
7	Et_3N (200)	PhMe	85	<5
8	K_2CO_3 (200)	DCM	15	<5
9	K_2CO_3 (200)	PhMe/ $CHCl_3$ (7/3)	____	__
10	KOH (200)	PhMe	____	__
11	K_2CO_3 (200)	H_2O	____	__

[a]Condiciones de reacción: 0.17 mmol de **156**, 0.17 mmol de **119**, 0.17 mmol de **157**, 10% catalizador **165**, 3 mL de disolvente, 20-25 °C, 44-50 h.
[b]En paréntesis (x% mol).
[c]Determinado mediante ^{1}H-RMN.
[d]Determinado mediante HPLC quiral.

También en esta ocasión las conversiones fueron pobres al igual que los excesos enantioméricos. Destaca el hecho de que se obtuvo producto con una conversión del 66% con cupreína **163** como base quiral (entrada 2, **Tabla 15**) mientras que en iguales condiciones no se obtuvo nada usando como base quiral quinina **161** (entrada 1, **Tabla 15**) el cual difiere en su estructura de la cupreína **163** tan sólo en el grupo R (ver **Figura 17**). Teniendo esto en cuenta se probaron otros catalizadores quirales de transferencia de fase, como los dímeros **168**, **169** y **172** creyendo que pudieran ofrecer una mayor información quiral a la hora de proceder la reacción (entradas de la 8 a la 12, **Tabla 15**). Puede observarse en estas pruebas, que las bases inorgánicas no parecen ofrecer buenos resultados. Se intentó además, como se muestra en la entrada 6 de la **Tabla 15**, el uso del catalizador de transferencia de fase **165** y quinina **163** simultaneamente con el fin de que produjesen un efecto sinérgico o de doble inducción que favoreciese la enantioselectividad, pero sin resultados destacables.

Esquema 43

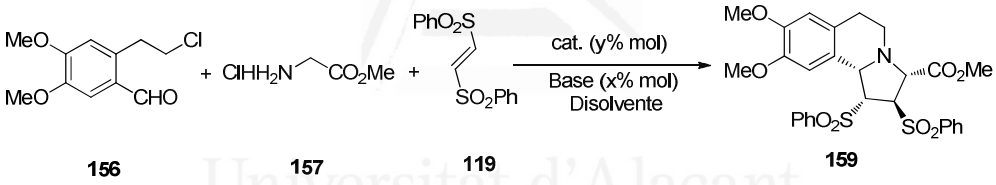

156 **157** **119** **159**

Tabla 15. Cicloadición 1,3-dipolar del producto **156** con diferentes bases quirales como catalizadores.[a]

Entrada	Catalizador[b]	Base[b]	Disolvente	Conversión (%)[c]	*ee* (%)[d]
1	quinina **161** (10)	Et_3N (110)	DCM	____	__
2	cupreína **163** (10)	Et_3N (110)	DCM	66	<5
3	quinina **161** (10)	K_2CO_3 (200)	H_2O	____	__

4	cupreína **163** (10)	K_2CO_3 (200)	H_2O	____	__
5	cupreína **163** (10)	K_2CO_3 (200)	DCM	____	__
6	**165** (10) y quinina **161** (10)	K_2CO_3 (200)	PhMe	____	__
7	**168** (5)	DIPEA (120)	DCM	30	<5
8	**172** (5)	DIPEA (120)	DCM	15	<5
9	**169** (5)	DIPEA (120)	DCM	25	<5
10	**178** (5)	K_2CO_3 (200)	PhMe/ $CHCl_3$ (7/3)	____	__
11	**172** (5)	K_2CO_3 (200)	DCM	___	__
12	**172** (5)	KOH (50 % H_2O) (200)	PhMe/ $CHCl_3$ (7/3)	___	__

[a]Condiciones de reacción: 0.17 mmol de **156**, 0.17 mmol de **119**, 0.17 mmol de **157**, 3 mL de disolvente, 20-25 °C, 44-50 h.
[b]En paréntesis (x o y% mol).
[c]Determinado mediante ^{1}H-RMN.
[d]Determinado mediante HPLC quiral.

En resumen, no se obtuvieron resultados aceptables siendo necesaria la búsqueda de una nueva vía con la que poder ejecutar con más garantías la cicloadición 1,3-dipolar.

V.4.11.2.1.2.- Segunda aproximación: acetato de 2-(2-acetoxietil)-4,5-dimetoxiformaldehído como producto de partida

Tras los resultados obtenidos utilizando los catalizadores de la **Figura 17** y el compuesto **156**, se creyó más oportuno el uso de otro tipo de catalizadores formados por ligandos quirales y plata(I). Para ello, se sintetizó el producto **86**,

como muestra el **Esquema 44**.[92] Se obtuvo así el producto **190** puro, con un rendimiento global del 85%.

Esquema 44

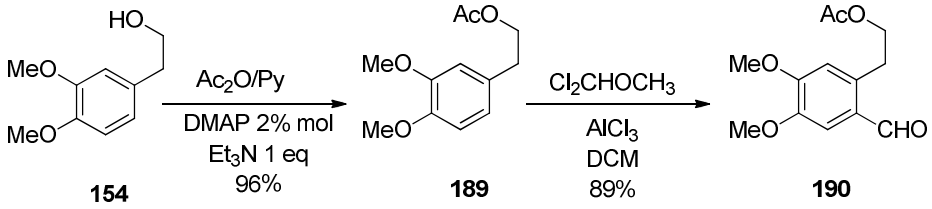

Se intentó primeramente, sin éxito, la reacción multicomponente con el producto **190**, el éster metílico de la glicina **157** y el 1,2-bis(fenilsulfonil)etileno **119** como muestra el **Esquema 45** y la **Tabla 16**.

Esquema 45

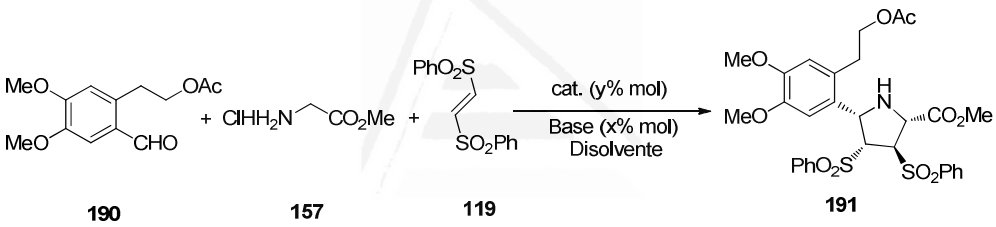

Tabla 16. Cicloadición 1,3-dipolar del producto **190** con diferentes catalizadores.[a]

Entrada	Catalizador[b]	Base[b]	Disolvente	Conversión[c] (%)	*ee* (%)[d]
1	AgOAc (10)	Et_3N (120)	DCM	____	__
2	AgOAc (10)	$NaHCO_3$ (100)	DCM	____	__
3	*rac*-Binap **96**/ AgTFA (10)[e]	Et_3N (120)	PhMe	____	__

[92] Ammendola, S.; Mosca, L.; Bovicelli, P.; *Arkivoc* **2008**, *VIII*, 105.

4	***rac*-Binap 96/ $AgSbF_6$ (10)[e]**	**Et_3N (120)**	**PhMe**	**———**	**—**

[a]Condiciones de reacción: 0.08 mmol de **190**, 0.08 mmol de **119**, 0.08 mmol de **157**, 3 mL de disolvente, 20-25 °C, 44-50 h.
[b]En paréntesis (x o y% mol).
[c]Determinado mediante ^{1}H-RMN.
[d]Determinado mediante HPLC quiral.
[e]Catalizadores generados in situ.

Seguidamente se decidió realizar la cicloadición 1,3-dipolar con la imina formada por el aldehído **190** y el clorhidrato del aminoglicinato de metilo **157**. Tras probar diferentes condiciones, fue la reacción a reflujo de $CHCl_3$, usando Et_3N como base, la que produjo mejor resultado, con una conversión casi completa (**Esquema 46**).

Esquema 46

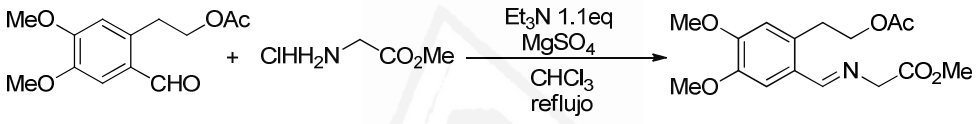

190 **157** **192**

Se usó esta imina **192**, en presencia de catalizadores formados por sales de plata(I) y el ligando quiral (*S*)-Binap **96** (**Esquema 47**, **Tabla 17**). En esta ocasión los resultados fueron mejores que los obtenidos con los catalizadores mostrados en la **Figura 17** y el producto **156**, pero aun así modestos. Pese que hasta el momento el mejor exceso enantiomérico se obtuvo utilizando tolueno como disolvente y DABCO al 10% como base (**Tabla 17**, entrada 2), se probaron bases quirales (**Tabla 17**, entradas 5 a 8,) con el objetivo de incrementar el exceso enantiomérico.[93]

Destacan, por tanto, las entradas 5 y 6, en las que se utilizan dos bases quirales, pseudoenantiómeros entre sí, como son la cinconina **160b** y cinconidina **160a**. Con ambas se obtuvieron conversiones similares, e idéntico exceso enantiomérico. Sin embargo, cuando se realizó el experimento con la pareja de pseudoenantiómeros quinina **161** y quinidina **162** (**Tabla 17**, entradas 7 y 8) se observó que las conversiones sí eran del mismo orden, pero no el exceso enantiomérico, pues éste pasaba de un 45 % en el primer caso, a un -12% en el

[93] **a)** Burton, G.; Ku, T.; Carr, T.; Kiesov, T.; Sarisky, R. ; Lin-Goerke, J.; Hofmann, G.; Slater, M.; Haigh, D.; Dhanak, D.; Johnson, V.; Parry, N.; Thomes, P.; *Bioorg. Med. Chem. Lett.*, **2007**, *17*, 1930; **b)** Slater, M. y colaboradores; *J. Med. Chem*., **2007**, *50*, 897; **c)** Slater, M. y colaboradores; *J. Org. Chem.* **2008**, *73*, 3094.

segundo. Para comprobar hasta qué punto este resultado podía sugerir algo significante se realizaron dos experimentos más, con quinina **161** y quinidina **162** (entradas 9 y 10), idénticos a los realizados en las entradas 7 y 8 de la **Tabla 17**, pero usando (*R*)-Binap **96** como ligando quiral en lugar de (*S*)-Binap **96**. Los excesos enantioméricos fueron coherentes con la tendencia prevista, pero de poca magnitud.

Esquema 47

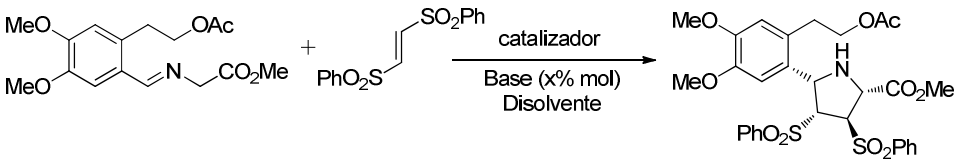

192 **119** **191**

Tabla 17. Cicloadición 1,3-dipolar de la imina **192** con diferentes bases.[a]

Entrada	Base[b]	Disolvente	Conversión (%)[c]	*ee* (%)[d]
1	Et_3N (10)	PhMe	55	35
2	DABCO (10)	PhMe	59	48
3	DIPEA (10)	PhMe	90	30
4	DBU (10)	PhMe	63	24
5	cinconina **160b** (10)	PhMe	87	40
6	cinconidina **160a** (10)	PhMe	81	40
7	quinina **161** (10)	PhMe	71	45
8	quinidina **162** (10)	PhMe	77	-12
9[e]	quinina **161** (10)	PhMe	60	<5
10[e]	quinidina **162** (10)	PhMe	75	-26

[a]Condiciones de reacción: 0.15 mmol de **192**, 0.15 mmol de **119**, (*S*)-Binap **96**/AgTFA (10% mol, generado in situ), 3 mL de disolvente, 20-25 °C, 44-50 h.
[b]En paréntesis (x% mol).
[c]Calculado por ^{1}H-RMN.
[d]Calculado por HPLC quiral.
[e]Realizado con (*R*)-Binap **18**/AgTFA (10% mol, generado in situ).

Se probaron diferentes sales de plata y algunas de las reacciones fueron realizadas sin base (**Tabla 18**, entradas 2-4). En este caso muestra mejor resultado cuando se utiliza acetato de plata(I) (**Tabla 18**, entrada 4) comparado con el trifluoroacetato de plata(I) (**Tabla 18**, entrada 3), probablemente por el carácter más básico del anión acetato. Se realizó una prueba también con el catalizador (*S*)-Binap-AuCl **193**/AgTFA (**Tabla 18**, entrada 2) que había mostrado buenos resultados en este tipo de reacción con la sulfona **119** como se indicó en los antecedentes. Sin embargo los resultados fueron de nuevo modestos.

Por último, y como alternativa a las sales de plata, se intentó también reproducir las mejores condiciones de reacción puestas a punto por nuestro grupo de investigación con complejos quirales de oro(I). La reacción catalizada por el complejo (*S*)-Binap-AuCl **193**/AgTFA generó un rendimiento moderado y un bajo exceso enantiomérico del cicloaducto **191** (**Figura 18** y **Tabla 18**, entrada 5).[76b]

La configuración absoluta del cicloaducto **191** no se pudo determinar por análisis por difracción de Rayos X, y la estereoquímica dibujada se extrapoló de los resultados obtenidos en reacciones de cicloadición previas con la disulfona **119** mediadas por el complejo catalítico (*S*)-Binap **96**/AgTFA y/o (*S*)-Binap **96**/AgOAc. Sin embargo la diasteroselectividad *endo* se pudo demostrar a través de los desplazamientos químicos en experimentos de ^{1}H-RMN y por experimentos NOESY.

Figura 18

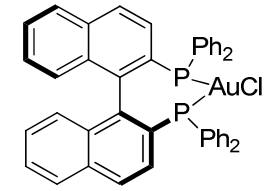

(*S*)-Binap-AuCl **193**/ AgTFA

Esquema 48

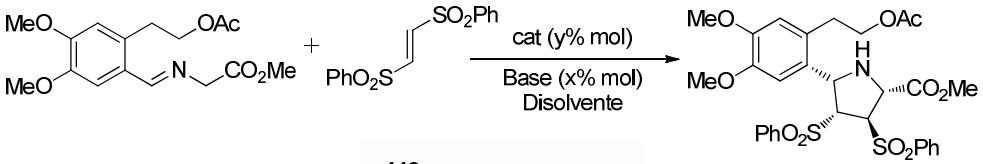

192 **119** **191**

Tabla 18. Cicloadición 1,3-dipolar de la imina **192** con diferentes condiciones de reacción.[a]

Entrada	Catalizador[b]	Base[b]	Disolvente	Conversión (%)[c]	*ee* (%)[d]
1	(*S*)-Binap **96**/ $AgSbF_6$ (10)	Et_3N (10)	PhMe	____	__
2	(*S*)-Binap **96**/ AgTFA (10)	____	DCM	61	6
3	(*S*)-Binap **96**/ AgOAc (10)	____	PhMe	55	32
4	(*S*)-Binap **96**/ AgOAc (10)	____	DCM	69	10
5	(*S*)-Binap-AuCl **193**/ AgTFA (5)	DIPEA (10)	PhMe	45	8

[a]Condiciones de reacción: 0.15 mmol de **192**, 0.15 mmol de **119**, 3 mL de disolvente, 20-25 °C, 44-50 h.
[b]En paréntesis (x o y% mol).
[c]Determinado mediante ^{1}H-RMN.
[d]Determinado mediante HPLC quiral.

V.4.11.2.2.- Síntesis de la harmicina

En analogía con el procedimiento seguido en el apartado anterior para llegar hasta la imina **192**, se planteó la síntesis del mismo tipo de imina con un esqueleto central similar al de la Harmicina, para realizar la cicloadición 1,3-dipolar con ésta. Para ello, se sintetizó primero el aldehído correspondiente **93** a partir de triptofol **90** con un rendimiento global del 60%(**Esquema 49**).[94]

Esquema 49

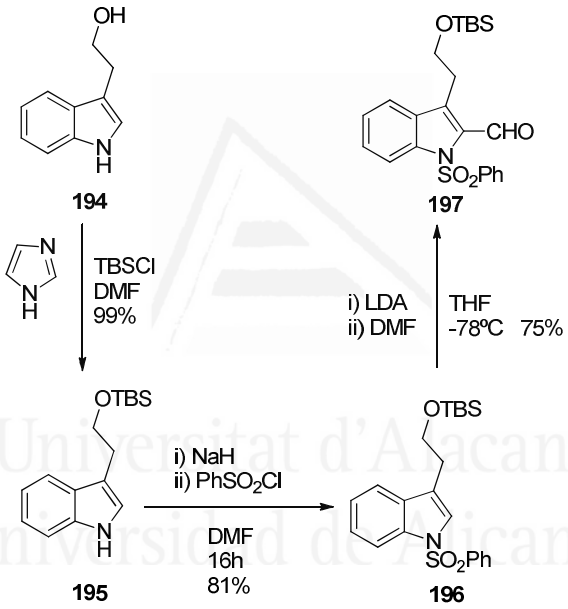

Después se sintetizó la imina **198** correspondiente con las mismas condiciones con las que se sintetizó la imina **192** (ver **Esquema 46**), con una conversión casi completa (**Esquema 50**)

[94] **a)** Nicolau, K. y colaboradores; *J. Am. Chem. Soc.* **1993**, *115*, 12550. **b)** Kuethe, J.; Davies, I.; Dormer, P.; Reamer, R.; Mathre, D.; Reider, P.; *Tetrahedron Lett.* **2002**, *43*, 29.

Esquema 50

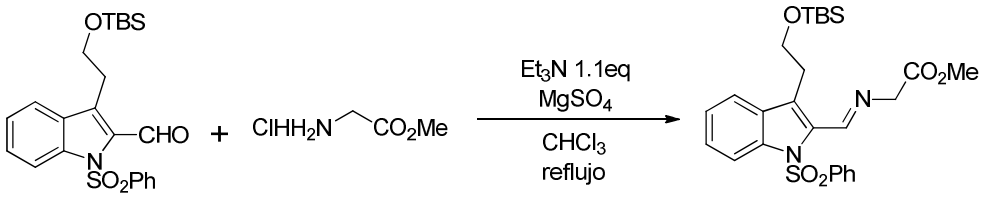

197 **157** **198**

El objetivo siguiente planteado sugería la utilización de las condiciones que ofrecieran mejores resultados en la síntesis del cicloaducto **191** para la síntesis enantioselectiva del producto **199** que se llegó a él a través de la reacción que muestra el **Esquema 51**, de nuevo utilizando como dipolarófilo la sulfona **119** y como catalizador AgTFA con el ligando Binap **96** racémico al 10 % molar. Se obtuvo así el producto racémico **199** puro, con un rendimiento de 63% de la cicloadición 1,3.-dipolar.

Esquema 51

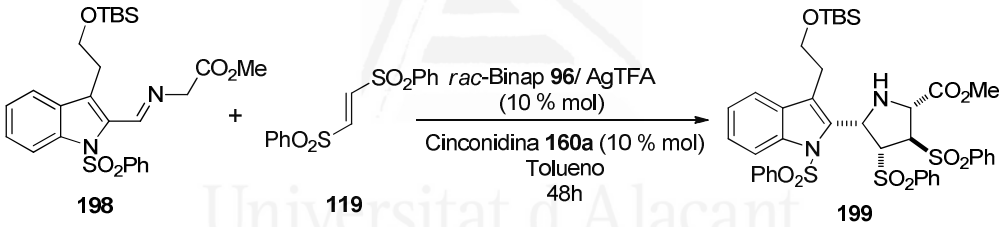

198 **119** **199**

De esta forma, se trató de llevar a cabo la versión enantioselectiva de esta reacción, con las condiciones que ofrecieran mejores resultados para la síntesis del precursor de Crispina A. Sin embargo pese a los rendimientos de moderados a buenos en esta síntesis, en todos los caso se obtuvo el cicloaducto **199** racémico.

V.4.12.- Tet. Asymm. 2012, 23, 1596

Tetrahedron: *Asymmetry* 23 (2012) 1596–1606

Contents lists available at SciVerse ScienceDirect

Tetrahedron: *Asymmetry*

journal homepage: www.elsevier.com/locate/tetasy

Binap-silver salts as chiral catalysts for the enantioselective 1,3-dipolar cycloaddition of azomethine ylides and alkenes

Juan Mancebo-Aracil [a], María Martín-Rodríguez [a], Carmen Nájera [a], José M. Sansano [a,*], Paulo R. R. Costa [b], Evanoel Crizanto de Lima [b], Ayres G. Dias [b]

[a] *Departamento de Química Orgánica e Instituto de Síntesis Orgánica (ISO), Facultad de Ciencias, Universidad de Alicante, E-03080 Alicante, Spain*
[b] *Laboratório de Química Biorgânica, Núcleo de Pesquisas de Produtos Naturais, Centro de Ciencias da Saúde, Universidade Federal do Rio de Janeiro, Cidade Universitária, 21941-590 Rio de Janeiro, Brazil*

ARTICLE INFO

Article history:
Received 3 October 2012
Accepted 12 October 2012

ABSTRACT

Binap-$AgSbF_6$ catalyzed 1,3-dipolar cycloadditions between azomethine ylides and electrophilic alkenes are described and compared with analogous transformations mediated by other Binap-silver(I) salt complexes. Maleimides and 1,2-bis(phenylsulfonyl)ethylene are suitable dipolarophiles for obtaining very good enantioselectivities, even better values are generated by a multicomponent version. There are some very interesting applications of the disulfonylated cycloadducts in the total synthesis of cis-2,5-disubstituted pyrrolidines, precursors of natural products, or valuable intermediates in the synthesis of antiviral compounds.

1. Introduction

Privileged chiral ligands[1] are very efficient enantiomerically pure molecules, incorporating a few core structures, and are used as references for chemists working in the field of asymmetric catalysis. Binap is one such example of this concept, which has been used with ruthenium, rhodium, and palladium in many enantioselective organic transformations.[1] This chiral diphosphine was also tested in the catalytic enantioselective 1,3-dipolar cycloaddition[2] (1,3-DC) of azomethine ylides (derived from imino esters) and electrophilic alkenes.[3] In the first substoichiometric catalytic enantioselective 1,3-DC of azomethine ylides reported by Zhang et al.,[4] the combination of (*S*)-Binap-AgOAc (3 mol %) showed low *ee* values when dipoles derived from imino esters and dimethyl maleate were used (up to 13% *ee*). The change of the counterion of the complex was critical for the success of the reaction. (*S*)-Binap-$AgClO_4$ **1**, a very stable and recyclable complex, is very appropriate for the 1,3-DC of imino esters and maleimides (up to >99% *ee*).[5] In addition to silver(I), copper(I)[6] and (II),[7] gold(I)[8–10] chiral Binap complexes have been studied as catalysts in analogous 1,3-DCs using several dipolarophiles.

The reluctance of chemical companies to use perchlorate salts, prompted us to search another poorly coordinated anion in order to ensure or even improve upon the results obtained from using the (*S*)-Binap-$AgClO_4$ complex. Computational studies of this asynchronous transformation also revealed that in the transition state responsible for the enantiodiscrimination, the perchlorate anion was weakly bonded to the central metal (2.41 Å).[5b] Based on these data, we thought that the weakly coordinating hexafluoroantimonate anion could be used as an alternative to perchlorate as catalyst for this particular cycloaddition. An identical semi-empirical model, but incorporating SbF_6^- instead of ClO_4^-, showed a longer distance (2.46 Å) between the central silver atom and its counterion.[11] Herein we report how important this small distance difference is during the enantioselective catalyzed 1,3-DC between imino esters and electron-deficient alkenes, and the scope of (*S*)-Binap-$AgSbF_6$ catalyst **2** versus other Binap complexes formed with different silver(I) salts.[12]

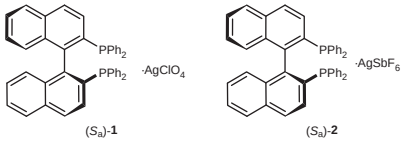

2. Results and discussion

2.1. Optimization of the reaction conditions

The model reaction selected between methyl benzylideneiminoglycinate **3aa** and *N*-methylmaleimide (NMM) **4a** was performed in toluene at room temperature using 5 mol % of

* Corresponding author. Tel./fax: +34 965903549.
E-mail address: jmsansano@ua.es (J.M. Sansano).

0957-4166/$ - see front matter © 2012 Elsevier Ltd. All rights reserved.
http://dx.doi.org/10.1016/j.tetasy.2012.10.015

(S)-Binap and 5 mol % of Ag^I salt as the catalyst precursor (Scheme 1 and Table 1). The reaction was carried out with equimolar amounts of both (S_a)-Binap and several oxygenated silver(I) salts with a weakly coordinating anion, such as AgOAc, AgOTfa (Tfa = trifluoroacetate), AgOTf (Tf = trifluoromethanesulfonate) $AgNO_3$, or $AgBF_4$, (5 mol %). When AgOAc was used, excellent results for compound **5aa** were obtained by using triethylamine rather than DABCO (Table 1, entries 1 and 2), but the crude reaction product was not very clean. Silver trifluoroacetate also gave excellent results for cycloadduct **5aa**, but again the reaction crude product was slightly impure (^{1}H NMR) (Table 1, entry 3). This chiral catalyst can work as an internal base, with the trifluoroacetate anion being the most effective (Table 1, entry 4). In this case, the enantioselection was excellent, although the reaction was slightly slower and a few impurities were detected in the crude product. The bifunctional behavior of acetate derived catalyst was not as effective as the Tfa complex, affording lower yields of the cycloadduct **5aa**. Silver triflate afforded excellent enantioselection (99% *ee*) but with a higher amount of the exo-diastereoisomer (Table 1, entry 5). The rest of the silver salts described in Table 1 were not able to promote the 1,3-DC in the absence of an external base. $AgBF_4$ and $AgNO_3$ catalyzed the reactions but afforded lower chemical yields, diastereo- and enantioselections (Table 1, entries 6 and 7).

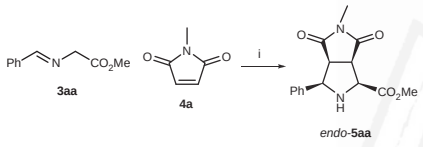

Scheme 1. Reagents and conditions: (i) (S_a)-Binap (5 mol %), Ag^I salt (5 mol %), base (5 mol %), toluene, 25 °C, 16 h.

Table 1
Optimization of the reaction of imino esters **3aa** with NMM **4a**

	Ag^I salt	Base	Product **5aa**[a]		
			Yield[b] (%)	*endo*:*exo*[c]	*ee*[d] (%)
1	AgOAc	Et_3N	89	>98:2	99[e]
2	AgOAc	DABCO	85	>95:5	94
3	AgOTfa	Et_3N	89	>98:2	99[e]
4	AgOTfa	—	78	>98:2	99[e]
5	AgOTf	Et_3N	88	90:10	99
6	$AgNO_3$	Et_3N	65	85:11	67
7	$AgBF_4$	Et_3N	77	89:11	72
8	$AgSbF_6$	Et_3N	90 (89)	>98:2 (>98:2)	>99 (>99)
9	$AgSbF_6$[f]	Et_3N	78 (80)	>98:2 (>98:2)	>99 (>99)
10	$AgSbF_6$	DIPEA	89 (89)	>98:2 (>98:2)	>99 (>99)
11	$AgSbF_6$	DABCO	87 (88)	>90:10 (>90:10)	94 (92)[e]
12	$AgSbF_6$	DBU	87 (80)	>90:10 (>90:10)	90 (91)[e]
13	$AgSbF_6$[g]	Et_3N	90 (90)	90:10 (90:10)	96 (98)[e]
14	$AgSbF_6$[h]	Et_3N	90 (91)	>98:2 (>98:2)	56 (<50)[e]

[a] Conversions were higher than 95% (determined by ^{1}H NMR spectroscopy of the crude product).
[b] Isolated yield after recrystallization. The yields of the analogous reaction performed with $AgClO_4$ are given in parenthesis.[5]
[c] Determined by ^{1}H NMR spectroscopy of the crude product.
[d] Determined by HPLC of the crude product employing chiral columns (Daicel Chiralpak AS). The *ee* of the analogous reaction performed with $AgClO_4$ is given in parenthesis.[5]Identical *ee* values were determined for the purified product in both reaction sets.
[e] Some unidentified impurities were detected in the crude product.
[f] Reaction performed with 3 mol % of the catalyst.
[g] Reaction performed with 2 equiv of Binap and 1 equiv of Ag^I salt.
[h] Reaction performed with 1 equiv of Binap and 2 equiv of Ag^I salt.

Using $AgSbF_6$ and Et_3N as the base, the enantiomerically enriched cycloadduct **5aa** (>99% *ee*) was isolated in very good yield (90%) and with excellent endo-selectivity.[13] This result, and the result obtained when the reaction was performed with $AgClO_4$, were almost identical (Table 1, entry 8). Other solvents, such as Et_2O, DCM, THF, and MeCN, were tested but neither the purity nor the diastereo-/enantioselection of the final product **5aa** were improved upon. The 5 mol % catalyst loading was the most appropriate because the reaction became slower when a 3 mol % charge was used instead (Table 1, entry 9). Bases such as 1,4-diazabicyclo[2.2.2]octane (DABCO) and diazabicyclo[5.4.0]undec-7-ene (DBU) were evaluated in this reaction and afforded lower enantioselections with some unidentified products in the crude mixture (Table 1, entries 10, and 11). However, when the reaction was carried out with *N*,*N*-diisopropylethylamine (DIPEA), it was completely equivalent to the reaction carried out with triethylamine (Table 1, compare entries 8 and 10). Using a different stoichiometry to 1:1 (S_a)-Binap:silver salt, such as 2:1 or 1:2, afforded lower enantioselections and larger amounts of the exo-diastereoisomer in both situations (Table 1, entries 13 and 14).

Thus it can be seen that when the reaction is carried out with silver hexafluoroantimonate in the presence of a small amount of thiethylamine, good chemical yields, excellent enantioselection (>99%), and a very clean material that did not require any additional purification were obtained.

2.2. Characterization of the catalytic species

The reaction was also carried out with the isolated complex formed by the addition of equimolar amounts of (*S*)-Binap and $AgSbF_6$; obtaining almost identical results to those described in entry 8 of the Table 1. However, this $AgSbF_6$ derived complex became darker upon standing since it was much more unstable than the identical complex generated by $AgClO_4$. As a result, the in situ generation of the catalytic complex, which avoided light exposure during the whole process was preferred for all of the transformations described herein.

The presumed catalytic monomeric species in the solution were identical to those reported previously with triflate[14] (Fig. 1) or perchlorate anions.[5b] Complexes formed from silver triflate and (*R*)- or (*S*)-Binap, were isolated at different temperatures and further characterized by X-ray diffraction analysis by Yamamoto et al. These studies revealed that the mixture of structures **6–8**

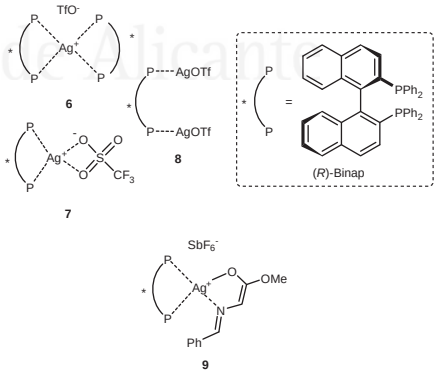

Figure 1. [(*R*)-Binap]AgOTf complexes and catalyst-dipole complex **9**.

were in equilibrium, and at room temperature, the 1:1 complex **7** was the most abundant system (Fig. 1).[14]

The 1:1 (*R*)- or (*S*)-Binap and $AgSbF_6$ complexes were characterized by ESI-MS experiments and ^{31}P NMR. ESI-MS showed an M^++1 signal at 730, and 732 corresponding to the monomeric Binap-Ag^I complex (S_a)-**2** and a tiny one at 1352 and 1354 corresponding to the 2:1 Binap:$AgSbF_6$ (similar to complex **6**). The ^{31}P NMR ($CDCl_3$) spectra of 1:1 (*R*)- or (*S*)-Binap and $AgSbF_6$ (using 10% aqueous polyphosphoric acid as an internal reference) afforded signals at 15.31 ppm and 15.45 ppm (2d, J = 242 Hz) (15.26, and 15.35 ppm for the Binap-$AgClO_4$ complex).

Calculations performed with the Binap-$AgClO_4$ model, which were comparable with the Binap-$AgSbF_6$ model, supported the idea that NMM was the best dipolarophile due to coordination of the nitrogen atom to the metal center. The TS responsible for the enantiodiscrimination was as expected, asynchronous. The steric interaction between one of the phenyl groups of the phosphine moiety of the chiral ligand and the dipolarophile can be considered to be crucial for explaining the experimental findings and providing a rationale for the observed excellent asymmetric induction.

2.3. General scope of the (S_a)-Binap-$AgSbF_6$ catalyzed 1,3-DC

The optimized reaction conditions were employed in the diastereo- and enantioselective transformation of several azomethine ylides, generated from the corresponding methyl arylideneiminoglycinates **3**, and maleimides into the corresponding cycloadducts *endo*-**5**. Reactions employing 5 mol % of an equimolar mixture of (*S*)-Binap and $AgSbF_6$ in the presence of toluene as a solvent and a catalytic amount of triethylamine (5 mol %) were compared directly with the analogous results obtained with the (*S*)-Binap-$AgClO_4$ complex[5] (Scheme 2, and Table 2).

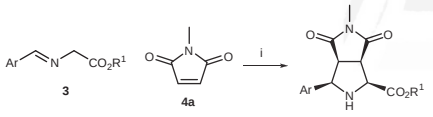

Scheme 2. Reagents and conditions: (i) (S_a)-Binap (5 mol %), Ag^I salt (5 mol %), Et_3N (5 mol %), toluene, 25 °C, 16 h.

In general, we observed that the isolated chemical yields of compounds **5** were identical to each other. For example, for Ar = Ph, 2-naphthyl, and 2-thienyl, there was no difference in terms of enantioselection between both catalytic complexes (Table 2, entries 1, 6 and 12). These three entries were also repeated employing (*S*)-Binap-AgTfa with no added base; similar enantioselections and lower chemical yields of slightly unpurified cycloadducts *endo*-**5** (not shown in Table 2) were obtained. When the reaction was performed with (*R*)-Binap, the corresponding enantiomer of *endo*-**5aa** was isolated in good yield and excellent enantioselectivity (Table 2, entry 2). Modification of the alkyl moiety of the ester group caused a decrease of the diastereoselection, (Table 2, entries 3–5). In all of these cases, the enantioselectivity was lower than that obtained for the methyl ester. For substituted aromatic imino esters, the enantioselection was always higher when $AgSbF_6$ was selected as the co-catalyst, except when *o*-tolyl derivative **3ca** was used (Table 2, entries 7–10). Heteroaromatic groups attached to the 1,3-dipole precursor, influenced the reaction course. Whereas a 2-thienyl derivative furnished **5ha** with very good enantioselection, 3-pyridyl derivative **3ga** was not suitable for this particular transformation (Table 2, entries 11 and 12). Presumably, the basic character of the nitrogen heterocycle promoted the non-asymmetric process.

The absolute configuration of these products **5**, as well as all of the compounds described herein, was determined by comparison with the known data reported in the literature for identical molecules.

When different N-substituted maleimides were compared, we found that *N*-ethylmaleimide (NEM) did not give any difference with respect to those results obtained with the (*S*)-Binap-$AgClO_4$. However, when the reaction was carried out with *N*-phenylmaleimide (NPM), it was much more enantioselective in the presence of (*S*)-Binap-$AgSbF_6$ complex than that obtained with a perchlorate derived chiral complex (82% *ee*, vs 62% *ee*). Computational calculations justified this difference because of the existence of steric hindrance between the phenyl group of the NPM and the Binap-$AgClO_4$ catalyst.[5b] The less coordinating anion in the catalyst Binap-$AgSbF_6$ released the steric congestion of the transition state. In the examples carried out with *N*-benzylmaleimide, the differences in the ee values of the product *endo*-**8** were not important (Scheme 3). Products *endo*-**6**, *endo*-**7**, and *endo*-**8** were isolated in more than a 98:2 *endo*:*exo* ratio independent of the chiral catalyst employed.

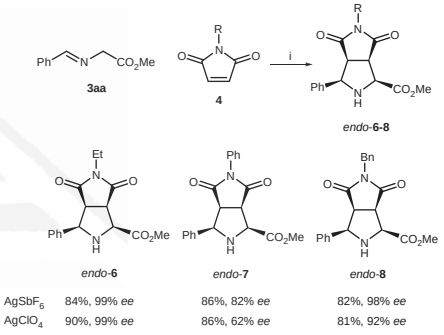

Scheme 3. Reagents and conditions: (i) (S_a)-Binap (5 mol %), Ag^I salt (5 mol %), Et_3N (5 mol %), toluene, 25 °C, 16 h.

The effect of α-substitution in the 1,3-dipole precursor was next evaluated. Alanine, leucine, and phenylalaninates **9** were allowed to react with NMM under the typical reaction conditions, requiring 48 h to reach complete conversions (Scheme 4). Cycloadducts

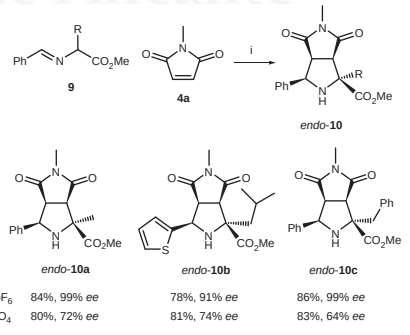

Scheme 4. Reagents and conditions: (i) (S_a)-Binap (5 mol %), Ag^I salt (5 mol %), Et_3N (5 mol %), toluene, 25 °C, 48 h.

endo-**10** were obtained in good yields when both chiral catalysts were used, but the enantioselectivity achieved by (S_a)-Binap-$AgSbF_6$ was noticeably higher. This is further evidence of the ease of the hexafluoroantimonate salt to perform cycloadditions with sterically hindered components.

We also found that dipolarophiles such as alkyl acrylates, dialkyl fumarates, dimethyl maleate, and acrylonitrile exhibited identical behavior with both silver salts, that is, very low enantioselections and good chemical yields were obtained. More polar solvents, such as acetone, acetonitrile, diethyl ether, ethanol, and water were tested but the cycloaddition was not completed and the crude reaction mixtures were notably impure. When small amounts of cycloadducts were isolated, the enantioselections were almost zero.

Large differences were detected when 1,2-bis(phenylsulfonyl)ethylene was employed as low-LUMO alkene (Scheme 5 and Table 3). Although toluene was used as the solvent, the reactions could also be carried out in THF because we observed a very clean reaction mixture, and the crude products *endo*-**12** did not require additional purification. When the reaction was performed with (*S*)-Binap-$AgClO_4$, we saw no improvement in the results generated by intermediacy of (*S*)-Binap-$AgSbF_6$. Phenyl- and 2-naphthyl substituents bonded to the imino group afforded high enantioselections of the products **12aaa** and **12baa**, respectively (Table 3, entries 1–4). The effect of the methyl group in the azomethine ylide caused lower enantioselections in the final products **12bba** (Table 3, entries 5 and 6). The introduction of a substituent in the arylidene moiety of the imino ester was not very profitable because the *ee* of the cycloadducts was very low, except in the case of *para*-methyl substituted derivatives (Table 3, entries 7–14). The presence of an isopropyl ester instead of a methyl group also gave poor enantioselection in heterocycle **12fab** (Table 3, entries 15 and 16). The 3-pyridyl group was the most appropriate heterocycle (Table 3, entries 17 and 18) since the 2-thienyl and 2-thiazolyl imino esters did not afford very high enantioselections despite producing excellent yields (Table 3, entries 19–22). Sterically hindered imino esters such as *ortho*-substituted arylinenes, isopropyl esters, and α-branched amino acid derivatives (alanine and leucine) furnished lower *endo*:*exo* ratios, and this was more pronounced when (*S*)-Binap-$AgClO_4$ was employed (Table 3, entries 5–8, 15, 16, and 19–22).

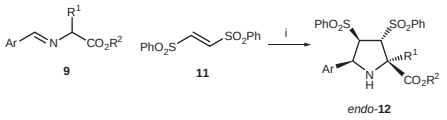

Scheme 5. Reagents and conditions: (i) (S_a)-Binap (5 mol %), Ag^I salt (5 mol %), Et_3N (5 mol %), toluene or THF, 25 °C, 48 h.

Multicomponent reactions were attempted using the best results obtained in Tables 2 and 3. Thus, benzaldehyde/NMM **4a** or 3-pyridinecarbaldehyde/disulfone **11**, glycine methyl ester hydrochloride, triethylamine (1.05 equiv), (*S*)-Binap-$AgSbF_6$ (5 mol %), were put together in toluene and the resulting mixture was allowed to react at 25 °C for 48 h. The results obtained for compound *endo*-**5aa** or *endo*-**12gaa** were good (88% yield, >99% *ee*, or 86% yield, 98% *ee*, respectively, Scheme 6). However, analogous reac-

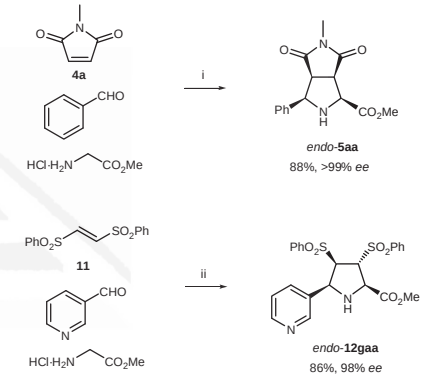

Scheme 6. Reagents and conditions: (i) (S_a)-Binap (5 mol %), $AgSbF_6$ (5 mol %), Et_3N (5 mol %), toluene, 25 °C, 16 h. (ii) (S_a)-Binap (5 mol %), $AgSbF_6$ (5 mol %), Et_3N (5 mol %), toluene, 25 °C, 48 h.

Table 2
1.3-DC of iminoglycinates **3** and NMM **4a**

Entry	N°	Ar	R^1	Product *endo*-**5**			
				No.	Yield[a,b] (%)	*endo*:*exo*[b,c]	ee_{endo}[b,d] (%)
1	**3aa**	Ph	Me	**5aa**	90 (90)	>98:2	>99 (>99)
2	**3aa**[e]	Ph	Me	*ent*-**5aa**	90 (90)	>98:2	>99 (>99)
3	**3ab**	Ph	Et	**5ab**	81 (78)	95:5 (90:10)	92 (91)
4	**3ac**	Ph	Pr^i	**5ac**	80 (81)	90:10	87 (72)
5	**3ad**	Ph	Bu^t	**5ad**	81 (79)	80:20 (75:25)	91 (92)
6	**3ba**	2-Naphthyl	Me	**5ba**	89 (80)	>98:2	>99 (>99)
7	**3ca**	2-$CH_3C_6H_4$	Me	**5ca**	85 (85)	>98:2	70 (75)
8	**3da**	2-ClC_6H_4 [f]	Me	**5da**	85 (88)	>98:2	>99 (85)
9	**3ea**	4-$CH_3C_6H_4$	Me	**5ea**	85 (85)	>98:2	99 (80)
10	**3fa**	4-ClC_6H_4	Me	**5fa**	84 (87)	>98:2	94 (65)
11	**3ga**	3-Pyridyl	Me	**5ga**	77 (81)	80:20	40 (10)
12	**3ha**	2-Thienyl	Me	**5ha**	84 (87)	>98:2 (90:10)	93 (92)

[a] Isolated yield after flash chromatography.
[b] In brackets the result obtained previously with (*S*)-Binap-$AgClO_4$ complex.[5]
[c] Determined by chiral ^1H NMR of the crude product.
[d] Determined by HPLC of the crude product using chiral columns. Identical *ee* was determined after purification of **5**.
[e] Reaction performed with (*R*)-Binap-$AgSbF_6$.
[f] Reaction performed at −20 °C.

Table 3
1.3-DC of iminoglycinates **9** and disulfone **11**

Entry	Ar	R^1	R^2	Solvent	No	Product *endo*-**12**		
						Yield[a,b] (%)	*endo*:*exo*[b,c]	ee_{endo}[b,d] (%)
1	Ph	H	Me	PhMe	**12aaa**	81 (80)	>98:2	90 (88)
2	Ph	H	Me	THF	**12aaa**	82	>98:2	90
3	2-Naphthyl	H	Me	PhMe	**12baa**	91[e] (88)	>98:2	92 (80)
4	2-Naphthyl	H	Me	THF	**12baa**	90	>98:2	80
5	2-Naphthyl	Me	Me	PhMe	**12bba**	95[e] (82)	90:10	24 (10)
6	2-Naphthyl	Me	Me	THF	**12bba**	91[e]	90:10	12
7	2-$CH_3C_6H_4$	H	Me	PhMe	**12caa**	63 (79)	90:10	18 (16)
8	2-$CH_3C_6H_4$	H	Me	THF	**12caa**	68	90:10	6
9	4-$CH_3C_6H_4$	H	Me	PhMe	**12daa**	91[e] (78)	>98:2	88 (28)
10	4-$CH_3C_6H_4$	H	Me	PhMe	**12daa**	78	>98:2	82
11	4-$MeOC_6H_4$	H	Me	PhMe	**12eaa**	58 (60)	>98:2	38 (28)
12	4-$MeOC_6H_4$	H	Me	THF	**12eaa**	78	>98:2	12
13	4-ClC_6H_4	H	Me	PhMe	**12faa**	81 (85)	>98:2	45 (27)
14	4-ClC_6H_4	H	Me	THF	**12faa**	79	>98:2	42
15	4-ClC_6H_4	H	Pr^i	PhMe	**12fab**	64 (71)	80:20	40 (30)
16	4-ClC_6H_4	H	Pr^i	THF	**12fab**	93[e]	80:20	30
17	3-Pyridyl	H	Me	PhMe	**12gaa**	83 (82)	>98:2	93 (78)
18	3-Pyridyl	H	Me	THF	**12gaa**	92[e]	>98:2	90
19	2-Thienyl	Bu^i	Me	PhMe	**12hca**	92 (<50)	90:10 (75:25)	70 (12)
20	2-Thienyl	Bu^i	Me	PhMe	**12hca**	95[e]	90:10 (75:25)	58
21	2-Thiazolyl	Bu^i	Me	PhMe	**12ica**	92[e] (<50)	90:10 (75:25)	10 (8)
22	2-Thiazolyl	Bu^i	Me	PhMe	**12ica**	93[e]	90:10 (75:25)	4

[a] Isolated yield after flash chromatography.
[b] In brackets, the result obtained previously with an (*S*)-Binap–$AgClO_4$ complex.
[c] Determined by chiral ^1H NMR of the crude product.
[d] Determined by HPLC of the crude product using chiral columns. Identical *ee* was determined after purification of **12**.
[e] No additional purification was required.

tions carried out in the presence of the (*S*)-Binap-$AgClO_4$ complex were unsuccessful. Although very activated aminomalonates have been used as one of the three components of enantioselective organocatalyzed 1,3-DC, this was the first occasion in which a three-component transformation was performed enantioselectively in the presence of a chiral Lewis acid.[12] However, the employment of other substrates with these two dipolarophiles did not afford either the expected enantioselections or good chemical yields. The introduction of the free α-amino ester instead of the corresponding hydrochloride did not improve the results.

2.4. Applications of (S_a)-Binap-AgX catalyzed 1,3-DC

As a masked acetylene equivalent, disulfone **11** has been used in this 1,3-DC for the preparation of Schramm's C-azanucleoside,[15] which is a promising trypanosomal nucleoside hydrolase inhibitor. Herein the enantioselective synthesis of the *exo*-cycloadduct (of type **12**) was the key step of the total process, after which the methoxycarbonyl group was reduced with lithium aluminum hydride (LAH) followed by complete desulfonylation with sodium amalgam. In our case, when the enantiomerically enriched *endo*-**12aaa** was allowed to undergo this double reduction protocol (LAH plus amalgam) a very complex reaction mixture was obtained, with pyrrole being the major product observed. Several conditions were tested and we found that the behavior of the *endo*-diastereoisomer was very different to the *exo* one, even in terms of stability upon flash chromatography.

The synthesis of 5-substituted prolines is another interesting application because it gives access to biologically active compounds, such as the nonpeptide cholecystokinin antagonist (+)-RP 66803 **13**.[16] The 5-phenylprolinate fragment was prepared according to the route described in Scheme 7. Isomers **14** and **15** were obtained after desulfonylation with sodium amalgam (10%) and the crude mixture, without purification, was submitted to hydrogenation with Pt/C (10%). The enantiomeric excesses of both prolinates remained unaltered with respect to the starting disulfonylated heterocycle ones. The overall yield of **16** was 47% (Scheme 7). This low yield could be justified by the formation of significant amounts of the pyrrole derivative after the desulfonylation step.

(*R*)-(+)-Crispine A **17** and (*R*)-(+)-harmicine **18** are naturally occurring molecules that are employed in traditional medicine. The anticancer properties of the former and the anti-leishmaniasis effects of the latter have attracted the attention of many scientists.[17,18] Following the approach of Coldham et al., which used a 1,3-DC with disulfone **11** (Scheme 8),[19] new starting aromatic precursors **19** and **20**, that were suitably protected, were prepared.

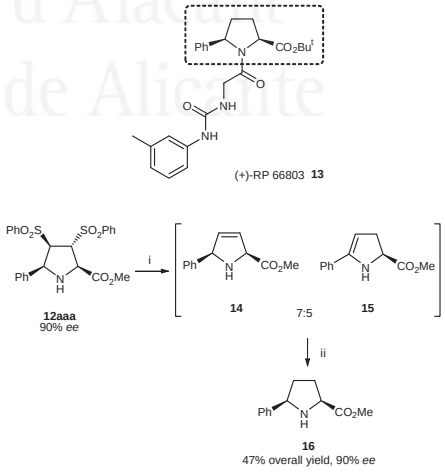

Scheme 7. Reagents and conditions: (i) Na(Hg), 10%, MeOH/THF (3/1), from 0 to 25 °C, 1 h. (ii) Pt/C (10%), H_2 (1 atm), MeOH, 48 h, 25 °C.

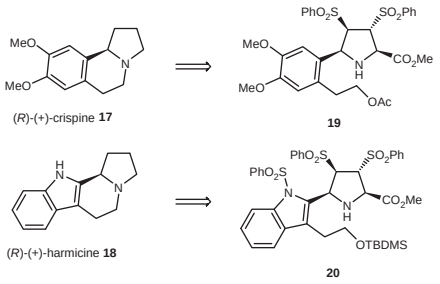

Scheme 8. Retrosynthetic analysis of natural products **19** and **20**.

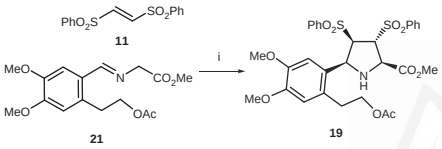

Scheme 9. Reagents and conditions: (i) (S_a)-Binap (10 mol %), Ag^I salt (10 mol %), base (10 mol %), toluene, 20–25 °C, 48 h.

Table 4
Optimization of the reaction of imino ester **21** with **11**

	Ag^I salt	Base	Product **19**	
			Yield[a,b] (%)	*ee*[c] (%)
1	$AgSbF_6$	Et_3N	55	32
2	AgOAc	Et_3N	45	30
3	AgTfa	Et_3N	55	35
4	AgTfa	DIPEA	80	30
5	AgTfa	DABCO	59	50
6	$AgSbF_6$	DABCO	50	30
7	AgTfa	DBU	63	24
8	AgTfa	Cinchonine	87	40
9	AgTfa	Cinchonidine	81	40
10	AgTfa	Quinine	71	45
11	AgTfa	Quinidine	77	−12

[a] Isolated yield of the *endo*-product after flash chromatography.
[b] The *endo*/*exo* ratio could not be determined from the crude product.
[c] Determined by HPLC of the crude product employing chiral column (Daicel Chiralpak AD).

The reaction of imine **21** (obtained from the corresponding aldehyde[20] and methyl glycinate) and disulfone **11** was accomplished at 20–25 °C using toluene as the solvent with 10 mol % of catalyst loading (formed by chiral Binap and a silver salt) and in the presence or absence of a base (Scheme 9 and Table 4). $AgSbF_6$, AgTfa, and AgOAc were tested and the best results were obtained when the trifluoroacetate salt was combined with triethylamine (10 mol %) as the base (Table 4, entries 1–3). Other bases such as DIPEA, DABCO, or DBU were tested and we found a noticeable increase in the enantioselection with AgTfa/DABCO mixture (up to 50% *ee*) (Table 4, entries 4–7). Quinuclidine based alkaloids were tested next for double chiral induction, but the results never overtook 45% *ee* (Table 4, entries 8–11). The transformations carried out with these silver salts in the absence of base were unsuccessful. Cycloadduct **19** (up to 32% *ee*) was obtained with poor enantioselections and in moderate chemical yields (55–65%).

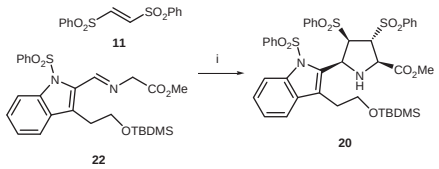

Scheme 10. Reagents and conditions: (i) (S_a)-Binap (10 mol %), AgTfa (10 mol %), DABCO (10 mol %), toluene, 25 °C, 48 h.

Under the best reaction conditions described in Table 4, imino ester **22** was submitted to cycloaddition with disulfone **11** to afford cycloadduct **20** in 60% chemical yield with very poor enantioselectivity Scheme 10 (12% *ee*).

Despite the low enantioselections obtained in the reaction performed between imino ester **3aa** and acrylates, the 1,3-DC of the heterocyclic imino ester **23** and *tert*-butyl acrylate were attempted (Scheme 11 and Table 5). As reported in previous works, molecule **24** is the key intermediate in the elaboration of 2nd generation GSK inhibitors of the virus causing hepatitis C **25**.[9,21] $AgClO_4$, AgTfa, and $AgSbF_6$ were tested (Table 5), and the reactions afforded good chemical yields at 25 °C, for 48 h and with high enantioselections, especially for the reaction carried out with silver perchlorate (88% *ee*) (Table 5, entry 1). The reaction needed 10 mol % of both catalyst loading and triethylamine to occur. Lowering the temperature and using different solvents, bases did not improve upon the results described in Table 5.

3. Conclusion

We conclude that a small variation in the structure of the dipole-dipolarophile or in the reaction parameters can cause a dramatic change in the final enantioselection of the chiral Binap-silver(I) complexes when they catalyze enantioselective 1,3-dipolar cycloadditions between azomethine ylides and electrophilic alkenes. Replacing perchlorate salts with other different anions is also desirable from an industrial point of view. Silver hexafluoroantimonate can efficiently catalyze cycloadditions dealing with maleimides and 1,2-bis(phenylsulfonyl)ethylene and the best results were obtained when using sterically hindered dipole precursors. It should be noted that multicomponent transformations could be carried out in the presence of $AgSbF_6$ while the analogous reaction, mediated by silver(I) perchlorate, was unsuccessful. However, silver trifuoroacetate was much more effective, or as effective as silver(I) perchlorate, in the applications of this methodology into the synthesis of natural (crispine or harmicine precursors) or biologically attractive compounds (e.g. antiviral precursors).

4. Experimental

4.1. General

All reactions were carried out in the absence of light. Anhydrous solvents were freshly distilled under an argon atmosphere. Aldehydes were also distilled prior to use for the elaboration of the imino esters. Melting points were determined with a Reichert Thermovar hot plate apparatus and are uncorrected. Only the structurally most important peaks of the IR spectra (recorded on a Nicolet 510 P-FT) are listed. ^1H NMR (300 MHz) and ^{13}C NMR (75 MHz) spectra were obtained on a Bruker AC-300 using $CDCl_3$ as the solvent and TMS as the internal standard, unless otherwise stated. Optical rotations were measured on a Perkin Elmer 341 polarimeter. HPLC analyses were performed on a JASCO 2000-

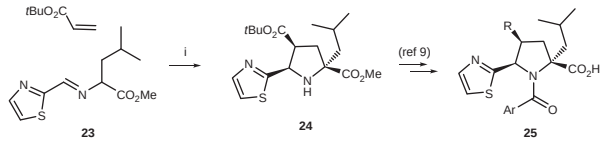

Scheme 11. Reagents and conditions: (i) (S_a)-Binap (10 mol %), AgX (10 mol %), Et_3N (10 mol %), toluene, 25 °C, 48 h.

Table 5
Synthesis of antiviral agent precursor **24**

Entry	AgX	Product **24**	
		Yield[a,b] (%)	*ee*[c] (%)
1	$AgClO_4$	78	88
2	AgTfa	75	88
3	$AgSbF_6$	79	72

[a] Isolated yield of the *endo*-product after flash chromatography.
[b] The *endo*/*exo* ratio was >98:2 (^{1}H NMR).
[c] Determined by HPLC of the crude product employing chiral column (Daicel Chiralpak AD).

series equipped with a chiral column (detailed for each compound in the main text), using mixtures of n-hexane/isopropyl alcohol as mobile phase, at 25 °C. Low-resolution electron impact (EI) mass spectra were obtained at 70 eV on a Shimadzu QP-5000 and high-resolution mass spectra were obtained on a Finnigan VG Platform. HRMS (EI) were recorded on a Finnigan MAT 95S. Microanalyses were performed on a Perkin Elmer 2400 and a Carlo Erba EA1108. Analytical TLC was performed on Schleicher & Schuell F1400/LS silica gel plates and the spots were visualized under UV light (λ = 254 nm). For flash chromatography, we employed Merck silica gel 60 (0.040–0.063 mm).

4.2. 1,3-Dipolar cycloaddition of imino esters 3, 9, 21, 22, or 23 and dipolarophiles. General procedure

A solution of the imino ester (1 mmol) and dipolarophile (1 mmol) in toluene (5 mL) was added to a suspension containing (*R*)- or (*S*)-Binap (0.05 mmol, 31 mg) and AgX (0.05 mmol) in toluene (5 mL). To the resulting suspension triethylamine (0.05 mmol, 7 μL) was added and the mixture was stirred at room temperature and in the absence of the light for 16–48 h (see main text). The precipitate was filtered and the complex was recovered. The organic filtrate was directly evaporated and the residue was purified by recrystallization or by flash chromatography yielding pure *endo*-cycloadducts.

Methyl (1*S*,3*R*,3a*S*,6a*R*)-5-methyl-3-phenyl-4,6-dioxooctahydro pyrrolo [3,4-*c*]pyrrole-1-carboxylate *endo*-**5aa**.[5b]

Ethyl (1*S*,3*R*,3a*S*,6a*R*)-5-methyl-3-phenyl-4,6-dioxooctahydro pyrrolo[3,4-*c*]pyrrole-1-carboxylate *endo*-**5ab**.[5b]

Isopropyl (1*S*,3*R*,3a*S*,6a*R*)-5-methyl-3-phenyl-4,6-dioxoocta hydropyrrolo[3,4-*c*]pyrrole-1-carboxylate *endo*-**5ac**.[5b]

tert-Butyl (1*S*,3*R*,3a*S*,6a*R*)-5-methyl-3-phenyl-4,6-dioxoocta hydropyrrolo[3,4-*c*]pyrrole-1-carboxylate *endo*-**5ad**.[5b]

Methyl (1*S*,3*R*,3a*S*,6a*R*)-5-methyl-3-(2-naphthyl)-4,6-dioxoocta hydropyrrolo[3,4-*c*]pyrrole-1-carboxylate *endo*-**5ba**.[5a]

Methyl (1*S*,3*R*,3a*S*,6a*R*)-5-methyl-4,6-dioxo-3-o-tolyloctahydro pyrrolo[3,4-*c*]pyrrole-1-carboxylate *endo*-**5ca**.[5b]

Methyl (1*S*,3*R*,3a*S*,6a*R*)-3-(2-chlorophenyl)-5-methyl-4,6-dioxo octahydropyrrolo[3,4-*c*]pyrrole-1-carboxylate *endo*-**5da**.[5a]

Methyl (1*S*,3*R*,3a*S*,6a*R*)-5-methyl-3-(4-methylphenyl)-4,6-dioxo octahydropyrrolo[3,4-*c*]pyrrole-1-carboxylate *endo*-**5ea**.[5a]

Methyl (1*S*,3*R*,3a*S*,6a*R*)-3-(4-chlorophenyl)-5-methyl-4,6-dioxo octahydropyrrolo[3,4-*c*]pyrrole-1-carboxylate *endo*-**5fa**.[5a]

Methyl (1*S*,3*R*,3a*S*,6a*R*)-3-(3-pyridyl)-5-methyl-4,6-dioxoocta hydropyrrolo[3,4-*c*]pyrrole-1-carboxylate *endo*-**5ga**.[22]

Methyl (1*S*,3*R*,3a*S*,6a*R*)-5-methyl-4,6-dioxo-3-(2-thienyl)octa hydropyrrolo[3,4-*c*]pyrrole-1-carboxylate *endo*-**5ha**.[5a]

Methyl (1*S*,3*R*,3a*S*,6a*R*)-5-ethyl-4,6-dioxo-3-phenyloctahydro pyrrolo[3,4-*c*]pyrrole-1-carboxylate *endo*-**6**.[23]

Methyl (1*S*,3*R*,3a*S*,6a*R*)-4,6-dioxo-3,5-diphenyloctahydro pyrrolo[3,4-*c*]pyrrole-1-carboxylate *endo*-**7**.[23]

Methyl (1*S*,3*R*,3a*S*,6a*R*)-5-benzyl-4,6-dioxo-3-phenyloctahydro pyrrolo[3,4-*c*]pyrrole-1-carboxylate *endo*-**8**. Pale yellow oil; $[\alpha]_D^{20}$ = +69.4 (*c* 1, $CHCl_3$) 98% *ee* from HPLC; IR ν_{max} 1740–1705, 3260 cm^{-1}; ^{1}H NMR δ_H: 2.10 (s, 1H, NH), 3.33, 3.58 (2×deform. d, *J* = 7.0, Hz, 2H, CH_2Ph), 3,40 (d, *J* = 7,5 Hz, 1H, CCH), 3,58 (dd, *J* = 9.1, and 7.6 Hz, 1H, $CHCHCO_2CH_3$), 3.76 (s, 3H, CO_2Me), 3.58 (d, *J* = 7.1 Hz, 1H, $CHCO_2CH_3$), 4.25 (d, *J* = 6.8 Hz, 1H, CHAr), 7.27–7.48 (m, 10H, Ar*H*); ^{13}C NMR δ_C: 46.2 (CH_2Ph), 47.1, 48.9 (2 × CHCON), 51.9 (CH_3), 61.4, 66.2 (2 × CHN), 128.1, 128.5, 125.9, 140.5, 126.9, 128.6, 126.7, 136.5 (ArC), 176.4, 176.0, 171.6 (3 × CO); MS (EI-GC) *m*/*z*: 364 (M^++1, 2%), 273 (100), 91 (47), 68 (11); HRMS calculated for $C_{21}H_{20}N_2O_4$: 364.1423, found: 364.1430; HPLC (Chiralpak AS, 1 mL/min, *n*-hexane/*i*-PrOH: 20/80, λ 225 nm), t_{Rmaj} = 10.5 min, t_{Rmin} = 26.7 min.

Methyl (1*S*,3*R*,3a*S*,6a*R*)-1,5-dimethyl-4,6-dioxo-3-phenyloctahydro pyrrolo[3,4-*c*]pyrrole-1-carboxylate *endo*-**10a**.[5b]

Methyl (1*S*,3*R*,3a*S*,6a*R*)-1-isobutyl-5-methyl-4,6-dioxo-3-(2-thienyl) octahydropyrrolo[3,4-*c*]pyrrole-1-carboxylate *endo*-**10b**.[5b]

Methyl (1*S*,3*R*,3a*S*,6a*R*)-1-benzyl-5-methyl-4,6-dioxo-3-phenyl octahydropyrrolo[3,4-*c*]pyrrole-1-carboxylate *endo*-**10c**.[5b]

Methyl (2*R*,3*R*,4*R*,5*S*)-5-phenyl-3,4-bis(phenylsulfonyl)pyrrolidine-2-carboxylate *endo*-**12aaa**. Sticky oil, $[\alpha]_D^{20}$ = +1.2 (*c* 1, CH_2Cl_2) 90% *ee* from HPLC; IR (neat) ν_{max}: 3311, 1753 cm^{-1}; ^{1}H NMR δ_H: 2.80 (br s, 1H, NH), 3.68 (s, 3H, CO_2Me), 4.33 (m, 1H, PhCHCHSO$_2$Ph), 4.41 (dd, *J* = 2.4, 6.3 Hz, 1H, NCCHSO$_2$Ph), 4.47 (dd, *J* = 2.4, 6.0 Hz, 1H, $CHCO_2$Me), 4.64 (m, 1H, PhCHN), 7.28–7.26 (m, 2H, Ar*H*), 7.34–7.32 (m, 2H, Ar*H*), 7.46–7.42 (m, 2H, Ar*H*), 7.61–7.52 (m, 3H, Ar*H*), 7.72–7.65 (m, 6H, Ar*H*); ^{13}C NMR δ_C: 38.3 (Me) 48.6 ($CHCO_2$Me), 49.1, 52.7 (2 × CHS), 56.0 (CHPh), 112.3, 112.9, 113.2, 113.3, 113.7, 113.9 114.1, 114.2, 119.2, 121.9, 122.8, 123.1 (ArC), 152.4 (CO); MS (EI) *m*/*z* (%): 485 (M^+, <1%), 284 (11), 203 (15), 202 (100), 170 (18), 144 (27), 143 (60), 115 (14), 77 (14); HRMS calculated for $C_{24}H_{23}NO_6S_2$: 485.0967, found: 485.0990; HPLC (Chiralpak IA, 1 mL/min, *n*-hexane/*i*-PrOH: 80/20, λ 224 nm), t_{Rmaj} = 50.23 min, t_{Rmin} = 30.92 min.

Methyl (2*R*,3*R*,4*R*,5*S*)-5-(naphth-2-yl)-3,4-bis(phenylsulfonyl) pyrrolidine-2-carboxylate *endo*-**12baa**. Sticky oil, $[\alpha]_D^{20}$ = +17.1 (*c* 0.5; CH_2Cl_2) 92% *ee* from HPLC; IR (neat) ν_{max}: 1741, 3340 cm^{-1}; ^{1}H NMR δ_H: 2.20 (br s, 1H, NH), 3.69 (s, 3H, CO_2Me); 4.38 (m, 1H, ArCHCHSO$_2$Ph), 4.45 (dd, *J* = 2.4, 6.4 Hz, 1H, NCCHSO$_2$Ph), 4.49 (dd, *J* = 2.4, 6.0 Hz, 1H, $CHCO_2$Me), 4.79 (m, 1H, CHAr), 7.39–7.35 (m, 2H, Ar*H*), 7.56–7.45 (m, 6H, Ar*H*), 7.72–7.60 (m, 7H, Ar*H*), 7.81–7.77 (m, 2H, Ar*H*); ^{13}C NMR δ_C: 38.5 (Me), 48.6 ($CHCO_2$Me), 49.1, 52.7 (2 × $CHSO_2$), 55.9 (ArCH), 109.3, 111.2, 111.3, 112.0, 112.4, 112.5, 112.9, 113.0, 113.3, 113.4, 113.5, 113.8, 114.2,

114.3, 119.2, 120.0, 121.1, 121.3 (ArC), 152.5 (CO); MS (EI) *m*/*z* (%): 535 (M^+, <1%), 394 (26), 392 (11), 391 (35), 359 (28), 268 (21), 267 (19), 266 (17), 253 (19), 252 (100), 251 (31), 250 (13), 220 (31), 219 (31), 194 (35), 193 (62), 192 (22), 191 (31), 190 (41), 167 (15), 166 (11), 165 (47), 164 (13), 163 (15), 155 (11), 153 (11), 152 (22), 142 (11), 127 (17), 125 (14), 78 (20), 77 (46), 51 (15); HRMS calculated for $C_{28}H_{25}NO_6S_2$: 535.1123; found: 535.1110; HPLC (Chiralpak AD, 1 mL/min, *n*-hexane/*i*-PrOH: 75/25, λ 227 nm), t_{Rmaj} = 57.01 min, t_{Rmin} = 51.97 min.

Methyl (2*R*,3*R*,4*R*,5*S*)-2-methyl-5-(naphth-2-yl)-3,4-bis(phenyl sulfonyl)pyrrolidine-2-carboxylate *endo*-**12bba**: Colorless oil, $[\alpha]_D^{20} = +5.2$ (*c* 1, CH_2Cl_2) 24% *ee* from HPLC; IR (neat) ν_{max}: 1748 3341 cm^{-1}; ^1H NMR δ_H: 1.80 (s, 3H, CH_3), 3.79 (s, 3H, CO_2Me), 3.46–3.43 (m, 1H, NH), 4.48 (d, *J* = 3.9 Hz, 1H, ArCHC*H*SO_2Ph), 4.61 (dd, *J* = 3.9, 7.2 Hz, 1H, NCC*H*SO_2Ph), 4.83–4.77 (m, 1H, ArC*H*), 7.28–7.12 (m, 5H, Ar*H*), 7.51–7.43 (m, 5H, Ar*H*),7.73–7.57 (m, 6H, Ar*H*), 7.90–7.87 (m, 1H, Ar*H*); ^{13}C NMR δ_C: 25.2 (CH_3), 39.2 (CO_2Me), 49.0, 52.1 (2 × $CHSO_2$), 56.9 (ArCH), 73.5 (CMe), 111.7, 112.0, 112.5, 112.9, 113.0, 124.0, 126.3, 126.4, 127.5, 127.6, 128.0, 128.2, 128.8, 129.0, 129.1, 129.4, 134.1, 134.4 (ArC), 171.0 (CO); MS (EI) *m*/*z* (%): 549 (M^+, <1%), 408 (22), 348 (15), 267 (20), 266 (100), 234 (31), 208 (39), 207 (91), 206 (27), 193 (19), 165 (20), 77 (14). HRMS required for $C_{29}H_{27}NO_6S_2$: 549.1280; found: 549.1301; HPLC (Chiralpak AD, 1 mL/min, *n*-hexane/*i*-PrOH: 60/40, λ 227 nm), t_{Rmaj} = 18.21 min, t_{Rmin} = 39.37 min.

Methyl (2*R*,3*R*,4*R*,5*S*)-3,4-bis(phenylsulfonyl)-5-(*o*-tolyl)pyrrolidine-2-carboxylate *endo*-**12caa**: Colorless sticky oil, $[\alpha]_D^{20} = +1.7$ (*c* 0.9, CH_2Cl_2) 18% *ee* from HPLC; IR (neat) ν_{max}: 1749, 3341 cm^{-1}; ^1H NMR δ_H: 2.42 (s, 3H, ArC*H*$_3$); 2.90 (br s, 1H, NH), 3.64 (s, 3H, CO_2*Me*), 4.32 (s, 1H, ArCHC*H*SO_2Ph), 4.48 (dd, *J* = 2.7, 6.2 Hz, 1H, NCC*H*SO_2Ph), 4.65 (dd, *J* = 2.7, 6.9 Hz, 1H, C*H*CO_2Me), 4.97 (s, 1H, ArC*H*), 7.25–7.16 (m, 2H, Ar*H*), 7.41 (t, *J* = 7.6 Hz, 8.0 Hz, 2H, Ar*H*), 7.58–7.54 (m, 5H, Ar*H*), 7.71–7.67 (m, 5H, Ar*H*), ^{13}C NMR δ_C: 37.4 (OMe), 44.3 (Ar*Me*), 50.0 (*C*HCO_2Me), 53.0, 55.5 (2 × *C*HSO_2), 57.8 (ArC*H*), 110.9, 111.9, 113.1, 113.3, 114.2, 114.3, 115.5, 119.1, 119.2, 120.8, 122.0, 122.1, 123.1, 124.6, (ArC),152.3 (CO); MS (EI) *m*/*z* (%): 499 (M^+, <1%), 298 (10), 217 (16), 216 (100), 184 (18), 158 (29), 157 (49), 156 (20), 143 (12), 129 (11), 77 (23); HRMS calculated for $C_{25}H_{25}NO_6S_2$: 499.1123; found: 499.1134; HPLC (Chiralpak AD, 1 mL/min, *n*-hexane/*i*-PrOH: 80/20, λ 227 nm), t_{Rmaj} = 35.89 min, t_{Rmin} = 43.91 min.

Methyl (2*R*,3*R*,4*R*,5*S*)-3,4-bis(phenylsulfonyl)-5-(*p*-tolyl)pyrrolidine-2-carboxylate **12daa**: Colorless sticky oil, $[\alpha]_D^{20} = +2.3$ (*c* 1, CH_2Cl_2) 88% *ee* from HPLC; IR (neat) ν_{max}: 1747, 3341 cm^{-1}; ^1H NMR δ_H: 2.30 (s, 3H, ArC*H*$_3$); 2.20 (br s, 1H, NH), 3.66 (s, 3H, CO_2*Me*), 4.31–4.27 (m, 1H, ArCHC*H*SO_2Ph), 4.35 (dd, *J* = 2.4, 6.4 Hz, 1H, NCC*H*SO_2Ph), 4.41 (dd, *J* = 2.4, 6.0 Hz, 1H, C*H*CO_2Me), 4.61–4.57 (m, 1H, ArC*H*), 7.06 (d, *J* = 8.1 Hz, 1H, Ar*H*), 7.20 (d, *J* = 8.1 Hz, 1H, Ar*H*), 7.54–7.40 (m, 6H, Ar*H*), 7.64–7.57 (m, 2H, Ar*H*), 7.70–7.66 (m, 4H, Ar*H*), ^{13}C NMR δ_C: 21.2 (CH_3Ar), 53.6 (OMe), 63.5, 64.2 (2 × $CHSO_2$), 67.9 (*C*HCO_2Me), 71.2 (ArCH), 127.3, 128.5, 128.6, 129.1, 129.3, 129.4, 129.5, 134.3, 135.0, 138.2, 138.3 (ArC), 167.6 (CO); MS (EI) *m*/*z* (%): 499 (M^+, <1%), 358 (24), 217 (15), 216 (100), 184 (22), 158 (22), 157 (48), 156 (14), 77 (15); HRMS required for $C_{25}H_{25}NO_6S_2$: 499.1123; found: 499.1122; HPLC (Chiralpak AD, 1 mL/min, *n*-hexane/*i*-PrOH: 75/25, λ 220 nm), t_{Rmaj} = 50.08 min, t_{Rmin} = 26.11 min.

Methyl (2*R*,3*R*,4*R*,5*S*)-5-(4-methoxyphenyl)-3,4-bis(phenylsulfonyl) pyrrolidine-2-carboxylate *endo*-**12eaa**: Colorless sticky oil, $[\alpha]_D^{20} = -4.5$ (*c* 1, CH_2Cl_2) 38% *ee* from HPLC; IR (neat) ν_{max}: 1747, 3341 cm^{-1}; ^1H NMR δ_H: 2.70 (br s, 1H, NH), 3.68, 3.80 (2 × s, 6H, CO_2Me); 4.31 (s, 1H, ArCHC*H*SO_2Ph), 4.35 (dd, *J* = 2.4, 6.4 Hz, 1H, NCC*H*SO_2Ph), 4.44 (dd, *J* = 2.4, 6.0 Hz, 1H, C*H*CO_2Me), 4.61 (s, 1H, ArC*H*), 7.29–7.24 (m, 2H, Ar*H*), 7.47–7.43 (m, 2H, Ar*H*), 7.63–7.52 (m, 5H, Ar*H*), 7.72–7.66 (m, 5H, Ar*H*); ^{13}C NMR δ_C: 37.4, 40.1 (2 × OMe), 45.3 (*C*HCO_2Me), 49.0, 52.7 (2 × $CHSO_2$), 56.0 (ArCH), 99.0, 113.4, 113.5, 114.2, 114.3, 119.2, 119.5, 120.8, 121.9, 122.2, 123.0, 144.4 (ArC), 152.4 (CO); MS (EI) *m*/*z* (%): 515 (M^+, <1%), 375 (17), 374 (77), 233 (17), 232 (100), 231 (14), 200 (31), 199 (16), 174 (27), 173 (46), 172 (11), 159 (11), 158 (23), 130 (11), 78 (10), 77 (29); HRMS required for $C_{25}H_{25}NO_7S_2$: 515.1072; found: 515.1082; HPLC (Chiralpak AD, 1 mL/min, *n*-hexane/*i*-PrOH: 70/30, λ 230 nm), t_{Rmaj} = 38.85 min, t_{Rmin} = 43.96 min.

Methyl (2*R*,3*R*,4*R*,5*S*)-5-(4-chlorophenyl)-3,4-bis(phenylsulfonyl) pyrrolidine-2-carboxylate *endo*-**12faa**: Colorless viscous oil, $[\alpha]_D^{20} = +91.6$ (*c* 1, CH_2Cl_2) 45% *ee* from HPLC; IR (neat) ν_{max}: 1750, 3341 cm^{-1}; ^1H NMR δ_H: 2.40 (br s, 1H, NH), 3.67 (s, 3H, CO_2*Me*); 4.30 (dd, *J* = 2.3, 6.3 Hz, 1H, ArCHC*H*SO_2Ph), 4.34 (m, 1H, NCC*H*SO_2Ph), 4.38 (dd, *J* = 2.3, 5.9 Hz, 1H, C*H*CO_2Me), 4.66–4.61 (m, 1H, ArC*H*), 7.30–7.21 (m, 3H, Ar*H*), 7.53–7.43 (m, 4H, Ar*H*), 7.71–7.59 (m, 7H, Ar*H*); ^{13}C NMR δ_C: 37.5 (Me); 45.2 (*C*HCO_2Me), 48.9, 52.6 (2 × $CHSO_2$), 55.9 (ArCH), 113.2, 113.5, 113.8, 113.9, 114.2, 114.3, 114.5, 114.8, 119.2, 119.5, 121.7, 123.0 (ArC), 152.3 (CO); MS (EI) *m*/*z* (%): 519 (M^+, <1%), 238 (32), 237 (17), 236 (100), 235 (12), 204 (19), 203 (15), 179 (17), 178 (19), 177 (48), 143 (21), 140 (14), 125 (16), 115 (13), 77 (29), 152 (13); HRMS required for $C_{24}H_{22}ClNO_6S_2$: 519.0577; found: 519.0585; HPLC (Chiralpak AD, 1 mL/min, *n*-hexane/*i*-PrOH: 70/30, λ 220 nm), t_{Rmaj} = 41.08 min, t_{Rmin} = 34.69 min.

Isopropyl (2*R*,3*R*,4*R*,5*S*)-5-(4-chlorophenyl)-3,4-bis(phenylsulfonyl) pyrrolidine-2-carboxylate *endo*-**12fab**: Colorless needles, mp 178 °C (CH_2Cl_2/*n*-hexane); $[\alpha]_D^{20} = +37.0$ (*c* 0.7, $CHCl_3$) 40% *ee* from HPLC; IR (KBr) ν_{max}: 1735, 3328 cm^{-1}; ^1H NMR δ_H: 1,33, 1.41 [2 × d, *J* = 6.2 Hz, 6H, $CO_2CH(CH_3)_2$], 2.42 (br s, 1H, NH), 4.30 (dd, *J* = 2.3, 6.3 Hz, 1H, ArCHC*H*SO_2Ph), 4.34 (m, 1H, NCC*H*SO_2Ph), 4.38 (dd, *J* = 2.3, 5.9 Hz, 1H, C*H*CO_2Me), 4.66–4.61 (m, 1H, ArC*H*), 5.20 (m, 1H, C*H*Me_2); 7.21–7.81 (m, 7 Hz, 14H, ArH); ^{13}C NMR δ_C: 21.6, 21.9 [CH(*C*H_3)$_2$], 45.2 (*C*HCO_2), 47.5, 48.9 (2 × $CHSO_2$), 55.9 (ArCH), 62.0 [*C*H$(CH_3)_2$], 113.2, 113.5, 113.7, 113.9, 114.0, 114.1, 114.5, 114.6, 119.4, 119.5, 121.7, 123.0 (ArC), 152.3 (CO); MS (EI) *m*/*z* (%): 513 (M^+, 2%), 229 (100), 140 (14); HRMS calculated for $C_{17}H_{20}N_2O_4$: 513.11280; found: 513,11289; Microanalysis for $C_{26}H_{27}NO_6$ S_2: C, 60.8; H, 5.3; N, 2.8%, found: C, 60.5; H, 5.3; N, 2.5; HPLC (Chiralpak OD-H, 1 mL/min, *n*-hexane/*i*-PrOH: 80/20, λ 215 nm), t_{Rmaj} = 20.5 min, t_{Rmin} = 38.4 min.

Methyl (2*R*,3*R*,4*R*,5*S*)-3,4-bis(phenylsulfonyl)-5-(pyrid-3-yl) pyrrolidine-2-carboxylate *endo*-**12gaa**: Colorless sticky oil, $[\alpha]_D^{20} = -63.9$ (*c* 1.2, CH_2Cl_2) 92% *ee* from HPLC; IR (neat) ν_{max}: 1753, 3310 cm^{-1}; ^1H NMR δ_H: 2.25 (br s, 1H, NH), 3.68 (s, 3H, Me); 4.33 (dd, *J* = 2.3, 6.4 Hz, 1H, ArCHC*H*SO_2Ph), 4.35 (s, 1H, NCCHSO_2Ph), 4.43 (dd, *J* = 2.3, 5.9 Hz, 1H, C*H*CO_2Me), 4.66 (d, *J* = 6.4 Hz, 1H, ArC*H*), 7.46 (t, *J* = 7.7 Hz, 8.0 Hz, 2H, Ar*H*), 7.53 (t, *J* = 7.4 Hz, 2H, Ar*H*), 7.61–7.65 (m, 3H, Ar*H*), 7.70 (t, *J* = 7.4 Hz, 5H, Ar*H*), 8.36 (s, 1H, Ar*H*), 8.52 (s, 1H, Ar*H*); ^{13}C NMR δ_C: 34.6, 37.5 (*C*HCO_2*Me*), 48.9, 52.4 (2 × $CHSO_2$), 55.7 (ArCH), 108.7, 113.3, 113.4, 114.3, 114.6, 119.3, 119.6, 119.8, 120.1, 121.5, 122.5 134.0, 134.7 (ArC), 152.3 (CO); MS (EI) *m*/*z* (%): 289 (M^+, 18%); HRMS calculated for $C_{23}H_{22}N_2O_6S_2$: 289.1062; found: 289.1064; HPLC (Chiralpak AD, 1 mL/min, *n*-hexane/*i*-PrOH: 50/50, λ 222 nm), t_{Rmaj} = 15.05 min, t_{Rmin} = 7.91 min.

Methyl (2*R*,3*R*,4*R*,5*S*)-2-isobutyl-3,4-bis(phenylsulfonyl)-5-(thien-2-yl)pyrrolidine-2-carboxylate *endo*-**12hca**: Pale yellow oil, $[\alpha]_D^{20} = 7.1$ (*c* 1, CH_2Cl_2) 70% *ee* from HPLC; IR (neat) ν_{max}: 1779, 3338 cm^{-1}; ^1H NMR δ_H: 0.88 [d, *J* = 6.7 Hz, 3H, C*H*$(CH_3)_2$], 1.08 [d, *J* = 6.4 Hz, 3H, C*H*$(CH_3)_2$], 1.84–1.74 [m, 1H, C*H*$(CH_3)_2$], 1.98 [dd, *J* = 6.4, 14.6 Hz, 1H, CH_2CH$(CH_3)_2$], 2.22 [dd, *J* = 5.7 Hz, 14.6 Hz, 1H, CH_2CH$(CH_3)_2$], 3.10 (br s, 1H, NH), 3.82 (s, 3H, CO_2Me), 4.40 (d, *J* = 3.9 Hz, 1H, ArCHC*H*SO_2Ph), 4.46 (dd, *J* = 3.9 Hz, 7.2 Hz, 1H, NCC*H*SO_2Ph), 4.88 (m, 1H, ArC*H*), 7.21–7.13 (m, 2H, Ar*H*), 7.36–7.26 (m, 4H, Ar*H*), 7.54–7.45 (m, 4H, Ar*H*), 7.65–7.61 (m, 1H, Ar*H*), 7.76–7.23 (m, 1H, Ar*H*), 7.90 (d, *J* = 7.3 Hz, 1H, Ar*H*); ^{13}C NMR δ_C: 24.4, 24.6 [CH$(CH_3)_2$], 28.4 [CH$(CH_3)_2$], 37.7 (CH_2), 39.5,

43.7, 57.8 (OMe and 2 × $CHSO_2$), 58.4, 58.9 (*C*CO, NCH), 110.2, 110.5, 111.1, 111.7, 113.0, 114.0, 114.2, 118.9, 119.2, 123.2, 123.3, 125.7, (Ar*C*), 155.2 (CO). MS (EI) *m*/*z* (%): 547 (M^+, < 1%), 488 (13), 406 (13), 348 (28), 346 (22), 317 (12), 316 (66), 265 (16), 264 (100), 232 (22), 208 (26), 207 (25), 206 (26), 205 (57), 176 (26), 175 (12), 162 (43), 150 (13), 149 (30), 121 (14), 77 (20); HRMS calculated for $C_{26}H_{29}NO_6S_3$: 547.1157; found: 547.1151. HPLC (Chiralpak AD, 1 mL/min, *n*-hexane/*i*-PrOH: 70/30, λ 233 nm), t_{Rmaj} = 19.67 min, t_{Rmin} = 23.43 min.

Methyl (2*R*,3*R*,4*R*,5*S*)-2-isobutyl-3,4-bis(phenylsulfonyl)-5-(thiazol-2-yl)pyrrolidine-2-carboxylate *endo*-**12ica**: Sticky oil, $[\alpha]_D^{20} = +4.1$ (*c* 1, CH_2Cl_2) 10% *ee* from HPLC; IR (neat) ν_{max}: 1735, 3328 cm^{-1}. ^1H NMR δ_H: 0.87, 1.07 [2 × d, *J* = 6.7 Hz, 6H, CH(CH_3)$_2$], 1.86–1.73 [m, 1H, C*H*(CH_3)$_2$], 1.98 (dd, *J* = 6.4 Hz, 14.6 Hz, 1H, CH_2), 2.22 (dd, *J* = 5.7 Hz, 14.6 Hz, 1H, CH_2), 3.79 (s, 3H, OMe), 4.40 (d, *J* = 4.1 Hz, 1H, ArCHC*H*SO_2Ph), 4.97 (dd, *J* = 7.1 Hz, 12.2 Hz, 1H, NCC*H*SO_2Ph), 5.11 (dd, *J* = 4.1 Hz, 7.1 Hz, 1H, ArC*H*), 7.26–7.19 (m, 3H, Ar*H*), 7.38–7.33 (m, 2H, Ar*H*), 7.62–7.50 (m, 5H, Ar*H*), 7.74–7.68 (m, 1H, Ar*H*), 7.88–7.85 (m, 2H, Ar*H*); ^{13}C NMR δ_C: 24.5, 24.7 [CH(CH_3)$_2$], 28.0 [CH(CH_3)$_2$], 37.9 (CH_2), 39.9, 43.9, 57.2 (OMe and 2 × $CHSO_2$), 58.4, 58.4 (CCO, NCH), 110.2, 110.5, 111.7, 113.4, 114.4, 114.2, 118.4, 119.2, 123.1, 123.3, 125.9, (Ar*C*), 155.8 (CO); MS (EI) *m*/*z* (%): 548 (M^+, <1%), 491 (26), 489 (19), 407 (13), 351 (13), 347 (28), 317 (53), 266 (15), 265 (87), 233 (50), 221 (12), 209 (35), 208 (71), 207 (52), 206 (100), 205 (10), 178 (11), 177 (79), 176 (13), 164 (13), 163 (65), 151 (19); 150 (17), 141 (11), 125 (16), 123 (17), 122 (13), 94 (10), 86 (10), 80 (12), 78 (13), 77 (44), 59 (11); HRMS calculated for $C_{25}H_{28}N_2O_6S_2$: 548.1109; found: 548.1118. HPLC (Chiralpak AD, 1 mL/min, *n*-hexane/*i*-PrOH: 70/30, λ 220 nm), t_{Rmaj} = 21.63 min, t_{Rmin} = 12.69 min.

4.3. Multicomponent 1,3-dipolar cycloaddition of glycine methyl ester hydrochloride. General procedure

To a suspension containing (*R*)- or (*S*)-Binap (0.05 mmol, 31 mg) and $AgSbF_6$ (17 mg, 0.05 mmol) in toluene (3 mL), triethylamine (6.6 μL, 0.05 mmol), the corresponding dipolarophile (1 mmol) and glycine methyl ester hydrochloride (126 mg, 1 mmol) were added in this order at 25 °C. The reaction mixture was then stirred at the same temperature for 16 or 48 h (see Scheme 6). The solvent was evaporated in vacuo and the residue was purified by flash chromatography yielding products *endo*-**5aa** or *endo*-**12gaa**.

4.4. Synthesis of pyrrolidine 16

To a solution of methyl (2*R*,3*S*,4*S*,5*S*)-5-phenyl-3,4-bis(phenylsulfonyl) pyrrolidine-2-carboxylate *endo*-**12aaa**, (22.0 mg, 0.04 mmol), in a 3:1 mixture of MeOH/THF (3 ml), 10% Na(Hg) (69.3 mg) and Na_2HPO_4 (22.4 mg, 0.16 mmol) were sequentially added at 0 °C. After stirring for 1 h at room temperature, ethyl acetate (10 ml) was added, and the resulting suspension was filtered and washed with water (2 × 5 ml). The aqueous phase was extracted with ethyl acetate (2 × 5 ml) and the combined organic phases were washed with brine (5 ml), dried, and concentrated. The residue (7:5 mixture of **14** and **15**) was then dissolved in methanol (3 ml) and Pt/C (10%) (30 mg) was added. The reaction was stirred for 48 h under a hydrogen atmosphere (1 atm) at 25 °C and the final mixture was filtered over a Celite pad. The remaining solution was evaporated in vacuo and the residue was purified by flash chromatography to give product **16a** in 47% overall yield.

Methyl 5-phenylpyrrolidine-2-carboxylate **16a**.[16]

4.5. Synthesis of imine 21

To a solution of 3,4-dimethoxyphenethyl alcohol (3.0 g, 16.6 mmol) in pyridine (4 ml), Ac_2O (1.6 ml, 16.6 mmol), DMAP (0.040 g, 0.33 mmol), and Et_3N (2.35 ml, 16.6 mmol) were added in this order. The mixture was then stirred for 4 h. Next, water (5 mL) and ethyl acetate (3 × 6 ml) were added, and the resulting organic layers were washed with brine. The crude product was employed in the next step without purification. This aldehyde [2-(2-acetoxyethyl)-4,5-dimethoxybenzaldehyde][20] (252 mg, 1 mmol), glycine methyl ester hydrochloride (126 mg, 1 mmol), Et_3N (1.1 mmol), and $MgSO_4$ (100 mg) were suspended in chloroform and the mixture was refluxed for 16 h. The mixture was then filtered and the resulting organic phase was washed with water (2 × 5 mL). The organic layer was dried ($MgSO_4$) and evaporated in vacuo to obtain imine **21** in 96% yield.

Methyl (*E*)-2-{[(2-(2-acetoxyethyl)-4,5-dimethoxybenzylidene] amino}acetate **21**: Pale yellow oil; IR (neat) υ_{max}: 1741, 1731, 1634 cm^{-1}; ^1H NMR δ_H: 1.96 (s, 3H, CH_3CO_2), 3.05 (t, *J* = 7.3 Hz, 2H, AcOCH_2), 3.61 (s, 3H, CO_2CH_3), 3.84, 3.85 (2 × s, 6H, 2 × OCH_3), 4.16 (t, *J* = 7.3 Hz, 2H, PhCH_2), 4.36 (s, 2H, NCH_2), 6.61 (s, 1H, Ar*H*), 7.46 (s, 1H, Ar*H*), 8.48 (s, 1H, NC*H*); ^{13}C NMR δ_C: 20.9 (CH_3CO), 31.3 (CH_2Ar), 52.0, 55.8, 56.0 (3 × OMe), 62.1, 65.0 (CH_2CO, CH_2O), 109.7, 112.8, 126.5, 131.3, 148.1, 151.4 (Ar*C*), 162.9 (CN), 170.7, 170.9 (2 × CO); MS (EI) *m*/*z* (%): 323.2 (M^+, 5%), 264 (21), 263 (26), 262 (100), 190 (13), 176 (14), 175 (59); HRMS calculated for $C_{16}H_{21}NO_6$: 323.1369; found: 323.1361.

4.6. Synthesis of cycloadduct 19

A suspension of silver(I) salt (0.01 mmol), and (*S*)-Binap (6 mg, 0.01 mmol) in toluene was stirred at 25 °C for 30 min avoiding exposure to light. Next, imine **21** (32 mg, 0.1 mmol), 1,2-bis(phenylsulfonyl)ethylene (31 mg, 0.1 mmol) and the corresponding base (0.01 mmol, see Table 4) were added in this order. The reaction was stirred for 48 h at 25 °C after which water (5 ml) and the aqueous phase extracted with ethyl acetate (2 × 5 ml). The organic layer was dried ($MgSO_4$) and evaporated in vacuo to obtain cycloadduct **19**.

Methyl (2*R*,3*S*,4*S*,5*S*)-5-[2-(2-acetoxyethyl)-4,5-dimethoxyphenyl]-3,4-bis(phenylsulfonyl)pyrrolidine-2-carboxylate **19**: Colorless needles, mp 92–94 °C (*n*-hexane/ethyl acetate); $[\alpha]_D^{20} = -25.3$ (*c* 1, $CHCl_3$) 50% *ee* from HPLC; IR (KBr) υ_{max}: 1148, 1309, 1738, 3306 cm^{-1}; ^1H NMR δ_H: 2.05 (s, 3H, CH_3CO_2), 2.30 (br s, 1H, NH), 2.85, 3.18 (2 m, 2H, PhCH_2), 3.60 (s, 3H, CO_2CH_3), 3.88, 3.91 (2s, 6H, 2 × OCH_3), 4.25–4.28 (m, 4H, AcOCH_2, C*H*S, C*H*CO_2Me), 4.60 (dd, *J* = 6.3, 1.9 Hz, 1H, C*H*S), 5.04 (d, *J* = 6.3 Hz, 1H, PhC*H*), 6.63 (s, 1H, Ar*H*), 7.31 (s, 1H, Ar*H*), 7.43–7.74 (m, 10H, Ar*H*); ^{13}C NMR δ_C: 21.0 (CH_3CO), 31.9 (CH_2Ar), 45.6, 49.9, 52.4, 55.9, 56.1, 58.6 (CHCO_2Me 3xOMe and 2 CHS), 64.4, 64.8 (CH_2CO, CH_2O), 68.5 (ArCH), 109.8, 112.8, 128.1, 128.4, 129.1, 129.3, 129.5, 134.2, 135.5, 137.3, 137.4, 137.5, 138.3, 148.7 (Ar*C*), 167.4, 171.0 (2 × CO); MS (EI) *m*/*z* (%): 631.1 (M^+, 0.1%), 348 (16), 347 (79), 272 (13), 256 (17), 255 (25), 254 (21), 229 (17), 228 (100), 227 (55), 215 (17), 214 (11), 213 (11), 212 (16), 200 (14), 197 (12), 196 (13), 184 (13); Microanalysis for $C_{30}H_{33}NO_{10}$ S_2: C, 57.0; H, 5.3; N, 2.2%, found: C, 57.3; H, 5.3; N, 2.5; HPLC (Chiralpak AD, 1 mL/min, *n*-hexane/*i*-PrOH: 70/30, λ 217 nm), t_{Rmaj} = 28.20 - min, t_{Rmin} = 21.53.

4.7. Synthesis of imine 22[24]

To a cooled solution (0 °C) of tryptophol (0.5 g, 3.1 mmol) and imidazole (0.46 g, 6.8 mmol) in DMF (3 mL), TBDMCl (0.51 g, 3.4 mmol) was added, and the reaction mixture was stirred for 16 h at 26 °C. Ethyl acetate was then added (10 mL) and the organic phase was washed with brine (3 × 4 ml). The organic phase was dried over $MgSO_4$ and evaporated in vacuo. The residue was purified by flash chromatography to obtain the silyl-protected derivative (0.84 g, 99%). A solution of this derivative (0.84 g, 3.1 mmol)

in anhydrous DMF (3 ml) was slowly added at 0 °C to a suspension of 60% NaH (0.19 g, 9.5 mmol) in anhydrous DMF (2 ml) and stirring was continued at 25 °C for 30 min. Next, $PhSO_2Cl$ (0.53 ml, 4 mmol) was added in one portion and the reaction was maintained at the same temperature for another 19 h. A saturated solution of ammonium chloride was poured out (10 ml) and the aqueous phase was extracted with diethyl ether (3 × 15 ml). The combined organic phases were dried over $MgSO_4$ and evaporated in vacuo. The residue was purified by flash chromatography to obtain the *N*-phenylsulfonyl derivative (0.79 g, 81%). The final formylation was achieved by preparing a solution of the last compound (0.79 g, 1.90 mmol) in anhydrous THF (2 mL), which was cooled to −78 °C and treated with 1.6 M solution of BuLi in hexanes (2.14 mL). After 2 h, the temperature was slowly increased to 25 °C and then immediately cooled to −78 °C. Next, DMF (0.77 ml, 1 mmol) was added and the temperature again was allowed to rise to 25 °C. A saturated solution of ammonium chloride was poured out (10 mL) and the aqueous phase was extracted with ethyl acetate (3 × 15 mL). The combined organic phases were dried over $MgSO_4$ and evaporated in vacuo. The residue was purified by flash chromatography to obtain the desired aldehyde (0.63 g, 75%).[24b]

Imine **22** was prepared in 95% pure crude yield as described for **21** (see above).

(*E*)-Methyl 2-{[3-(2-[(*tert*-butyldimethylsilyloxy)ethyl]-1-(phenyl sulfonyl)-1*H*-indol-2-yl]methylene}aminoacetate **22**: Orange sticky oil; IR (neat) υ_{max}: 1747, 1631, 1371, 1170 cm^{-1}; ^1H NMR δ_H: −0.17, 0.02 (2 × s, 6H, 2 × $SiCH_3$), 0.87 [s, 9H, $SiC(CH_3)_3$], 2.88 (t, *J* = 6.7 Hz, 2H, CCH_2), 3.31 (t, *J* = 6.7 Hz, 2H, OCH_2), 3.81 (s, 3H, CO_2CH_3), 4.53 (s, 2H, NCH_2), 7.41–8.00 (m, 9H, ArC*H*), 8.84 (s, 1H, NC*H*); ^{13}C NMR δ_C: −2.8, −2.6, 18.2, 25.8, 28.5, 52.0, 62.5, 63.2, 113.6, 115.3, 119.5, 120.3, 121.3, 123.0, 124.1, 124.5, 126.6, 128.9, 129.1, 133.5, 158.6, 170.9; MS (EI) *m*/*z* (%): 514 (M^+, 1%), 359 (16), 358 (59), 233 (11), 217 (11), 216 (51), 200 (16), 199 (100). HRMS calculated for $C_{26}H_{34}N_2O_5SSi$: 514.1958; found: 514.1967.

4.8. Synthesis of cycloadduct 20

A suspension of silver(I) trifluoroacetate (3 mg, 0.01 mmol), and (*S*)-Binap (6 mg, 0.01 mmol) in toluene was stirred at 25 °C for 30 min while avoiding exposure to light. Next, imine **22** (51 mg, 0.1 mmol), 1,2-bis(phenylsulfonyl)ethylene (31 mg, 0.1 mmol), and DABCO (2 mg, 0.01 mmol) were added in this order. The reaction was stirred for 48 h at 25 °C and water (5 mL) and the aqueous phase extracted with ethyl acetate (2 × 5 mL). The organic layer was dried ($MgSO_4$) and evaporated in vacuo to obtain cycloadduct **20**.

Methyl (2*R*,3*R*,4*R*,5*S*)-5-{3-[2-((tert-butyldimethylsilyl)oxy)ethyl]-1-(phenylsulfonyl)-1*H*-indol-2-yl}-3,4-bis(phenylsulfonyl)pyrrolidine-2-carboxylate **20**: Colorless needles, mp 155 °C (*n*-hexane/ethyl acetate); $[\alpha]_D^{20} = -4.5$ (*c* 1, $CHCl_3$) 12% *ee* from HPLC; IR (KBr) υ_{max}: 1142, 1309, 1765, 3286 cm^{-1}; ^1H NMR δ_H: −0.137, −0.04 (2 × s, 6H, 2 × $SiCH_3$), 0.79 [s, 9H, $SiC(CH_3)_3$], 2.81 (t, *J* = 6.6 Hz, 2H, $OTBDMSCH_2$), 3.02 (td, *J* = 6.6, 1.9 Hz, 2H, CCH_2), 3.76–3.79 (m, 5H, CO_2CH_3, SC*H*, C*H*CO_2CH_3), 4.26 (d, *J* = 7.1 Hz, 1H, NCH_2), 4.87 (dd, *J* = 7.1, 4.7 Hz, 1H, C*H*N), 5.40 (s, 1H, N*H*), 7.07–8.01 (m, 19H, ArC*H*); ^{13}C-NMR δ_C: −5.5,−5.3, 18.0, 29.9, 30.0, 30.6, 48.4, 51.9, 52.5, 62.5, 64.1, 108.7, 115.8, 115.9, 116.8, 116.9, 117.6, 125.6, 125.7, 126.9, 127.0, 128.00, 128.46, 128.73, 129.13, 129.86, 133.59, 134.09, 134.92, 136.96, 140.37, 171.5; MS (ESI) *m*/*z* (%): 822 (M^+, 2%). Microanalysis for $C_{40}H_{46}N_2O_9S_2Si$: C, 58.4; H, 5.6; N, 3.4%, found: C, 58.3; H, 5.3; N, 3.5; HPLC (Chiralpak OD-H, 1 mL/min, *n*-hexane/*i*-PrOH: 93/7, λ 222 nm), t_{Rmaj} = 24.5 min, t_{Rmin} = 27.8 min.

4.9. Synthesis of the antiviral precursor 24[25]

Compound **24** was prepared according to the procedure described earlier (see Section 4.2).

tert-Butyl methyl (2*S*,4*S*,5*R*)-2-isobutyl-5-(thiazol-2-yl)pyrrolidine-2,4-dicarboxylate **24**: $[\alpha]_D^{20} = +38$ (*c* 1, CH_2Cl_2) 99% *ee* by HPLC Lit.[25] $[\alpha]_D^{20} = +43$ (*c* 1, CH_2Cl_2) 99% *ee* by HPLC.

Acknowledgments

This work has been supported by the Spanish Ministerio de Ciencia e Innovación (MICINN) through the Hispano-Brazilian project PHB2008-0037-PC and CNPq-2878, Consolider INGENIO 2010 CSD2007-00006, CTQ2010-20387, FEDER, Generalitat Valenciana (PROMETEO/2009/039), and by the University of Alicante. MM-R thanks MEC for a predoctoral fellowship. EC thanks CNPq for a predoctoral Doutorado Sanduíche stay.

References

1. *Privileged Chiral Ligands and Catalysts*; Qi-Lin Zhou, Ed.; Wiley-VCH: New York, 2011.
2. For the pioneering catalytic enantioselective 1,3-DC work carried out by Grigg et al., see (a) Allway, P.; Grigg, R. *Tetrahedron Lett.* **1991**, *32*, 5817–5820; (b) Grigg, R. *Tetrahedron: Asymmetry* **1995**, *6*, 2475–2486.
3. The enantioselective 1,3-DC of azomethine ylides is a prolific area in organic synthesis and is frequently reviewed. For selected recent examples, see: (a) Pellissier, H. *Tetrahedron* **2007**, *63*, 3235–3285; (b) Nájera, C.; Sansano, J. M. In *Topics in Heterocyclic Chemistry*; Hassner, A., Ed.; Springer: Berlin, Heidelberg, 2008; Vol. 12, pp 117–145; (c) Stanley, L. M.; Sibi, M. P. *Chem. Rev.* **2008**, *108*, 2887–2902; (d) Álvarez-Corral, M.; Muñoz-Dorado, M.; Rodríguez-García, I. *Chem. Rev.* **2008**, *108*, 3174–3198; (e) Naodovic, M.; Yamamoto, H. *Chem. Rev.* **2008**, *108*, 3132–3148; (f) Nájera, C.; Sansano, J. M.; Yus, M. *J. Braz. Chem. Soc.* **2010**, *21*, 377–412; (g) Kissane, M.; Maguire, A. R. *Chem. Soc., Rev.* **2010**, *39*, 845–883; (h) Adrio, J.; Carretero, J. C. *Chem. Commun.* **2011**, *47*, 6784–6794.
4. Longmire, J. M.; Wang, B.; Zhang, X. *J. Am. Chem. Soc.* **2002**, *124*, 13400–13401.
5. (a) Nájera, C.; Retamosa, M. G.; Sansano, J. M. *Org. Lett.* **2007**, *9*, 4025–4028; (b) Nájera, C.; Retamosa, M. G.; Sansano, J. M.; de Cózar, A.; Cossío, F. P. *Tetrahedron: Asymmetry* **2008**, *19*, 2913–2923.
6. (*R*)-Binap-Cu$(MeCN)_4ClO_4$ catalyzed the reaction with phenyl vinyl sulfone (up to 26% *ee*). Llamas, T.; Gómez-Arrayás, R.; Carretero, J. C. *Org. Lett.* **2006**, *8*, 1795–1798.
7. (*R*)-Binap-Cu$(OTf)_2$ catalyzed the reaction with maleimides (up to 64–65% *ee* of the corresponding *exo*-adduct). Oderaotoshi, Y.; Cheng, W.; Fujitomi, S.; Kasano, Y.; Minakata, S.; Komatsu, M. *Org. Lett.* **2003**, *5*, 5043–5046.
8. $[(S_a)$-Binap-AuTFA$]_2$ catalyzed the reaction with maleimides, maleates, acrylates, vinylic sulfones, etc. (up to 99% *ee*). (a) Martín-Rodríguez, M.; Nájera, C.; Sansano, J. M.; Wu, F. L. *Tetrahedron: Asymmetry* **2010**, *21*, 1184–1186. and corringendum, **2010**, *21*, 2559; (b) Martín-Rodríguez, M.; Nájera, C.; Sansano, J. M.; de Cózar, A.; Cossío, F. P. *Chem. Eur. J.* **2011**, *17*, 14224–14233.
9. The reactivity of the dimeric gold complex $[(S_a)$-Binap-AuTFA$]_2$ has been studied and compared with several silver complexes in the elaboration of the key precursor of the 2nd generation GSK-inhibitors of the virus responsible for hepatitis C: Martín-Rodríguez, M.; Nájera, C.; Sansano, J. M.; de Cózar, A.; Cossío, F. P. *Beilstein J. Org. Chem.* **2011**, *7*, 988–996.
10. For enantioselective gold(I)-catalyzed cycloadditions dealing with azlactones see: (a) Melhado, A. D.; Luparia, M.; Toste, F. D. *J. Am. Chem. Soc.* **2007**, *129*, 12638–12639; (b) Melhado, A. D.; Amarante, G. W.; Wang, Z. J.; Luparia, M.; Toste, F. D. *J. Am. Chem. Soc.* **2011**, *133*, 3517–3527; (c) Martín-Rodríguez, M.; Nájera, C.; Sansano, J. M. *Synlett* **2012**, 62–65.
11. Unpublished estimated data calculated by F. P. Cossío and A. de Cózar (University of the Basque Country).
12. For a preliminary communication, see: Martín-Rodríguez, M.; Nájera, C.; Sansano, J. M.; Costa, P. R. R.; de Lima, E. C.; Dias, A. G. *Synlett* **2010**, 962–967.
13. The *endo* descriptor refers the approach of the electron-withdrawing group to the metalodipole before the cycloaddition.
14. Momiyama, N.; Yamamoto, H. *J. Am. Chem. Soc.* **2004**, *126*, 5360–5361.
15. López-Pérez, A.; Adrio, J.; Carretero, J. C. *J. Am. Chem. Soc.* **2008**, *130*, 10084–10085.
16. See, for example: van Esseveldt, B. C. J.; Vervoort, P. W. H.; van Delft, F. L.; Rutjes, P. J. T. *J. Org. Chem.* **2005**, *70*, 1791–1795.
17. Zhang, Q.; Tu, G.; Zhao, Y.; Cheng, T. *Tetrahedron* **2002**, *58*, 6795–6798.
18. Kam, T.; Sim, K. *Phytochemistry* **1997**, *47*, 145–147.
19. Coldham, I.; Jana, S.; Watson, L.; Martin, N. G. *Org. Biomol. Chem.* **2009**, *7*, 1674–1679.
20. Ammendola, S.; Mosca, L.; Bovicelli, P. *Arkivoc* **2008**, *VIII*, 105–115.
21. Nájera, C.; Sansano, J. M. *Org. Biomol. Chem.* **2009**, *7*, 4567–4581.
22. Nájera, C.; Retamosa, M. G.; Martín-Rodríguez, M.; Sansano, J. M.; de Cózar, A.; Cossío, F. P. *Eur. J. Org. Chem.* **2009**, 5622–5634.

23. (a) Oderaotoshi, Y.; Cheng, W.; Fujitomi, S.; Kasano, Y.; Minakata, S.; Komatsu, M. *Org. Lett.* **2003**, *5*, 5043–5046; (b) Dogan, Ö.; Koyuncu, H.; Garner, P.; Bulut, A.; Youngs, W. J.; Panzner, M. *Org. Lett.* **2006**, *8*, 4687–4690.
24. (a) Hirschmann, R.; Nicolau, K.; Pietranico, S.; Leahy, E.; Salvino, J.; Arison, B.; Cichy, M.; Spoors, P.; Shakespeare, W.; Sprengeler, P.; Hamley, P.; Smith, A.; Reisine, T.; Raynor, K.; Maechler, L.; Donaldson, C.; Vale, W.; Freidinger, R.; Cascieri, M.; Strader, C. *J. Am. Chem. Soc.* **1993**, *115*, 12550–12568; (b) Kuethe, J.; Davies, I.; Dormer, P.; Reamer, R.; Mathre, D.; Reider, P. *Tetrahedron Lett.* **2002**, *43*, 29–32.
25. Martín-Rodríguez, M.; Nájera, C.; Sansano, J. M.; de Cózar, A.; Cossío, F. P. *Beilstein J. Org. Chem.* **2011**, *7*, 988–996.

VI.- CAPÍTULO III: SÍNTESIS DE PIRROLIZIDINAS MEDIANTE CICLOADICIONES 1,3-DIPOLARES MULTICOMPONENTE

VI.1.- ANTECEDENTES BIBLIOGRÁFICOS

El esqueleto de pirrolizidina es una estructura química de gran importancia en la química de productos naturales, presente en muchos de ellos.[95] La mayoría de los alcaloides con estructura de pirrolizidina y los *N*-óxidos de pirrolizidinas se encuentran en más de 6.000 variedades de plantas.[96] En concreto, muchas de las pirrolizidinas funcionalizadas presentan interesantes propiedades y diferente actividad biológica.[97] Por ejemplo las hidronorsecurininas **200**, que se encuentra en la especie *Secrurinega* y *Phylathus genera*, posee una potente actividad antibacteriana y antitumoral[98] (**Figura 19**). La casuarina **201**, perteneciente al grupo de los alcaloides polihidroxilados, que puede aislarse de la corteza de la madera de la especie *Casuarina equisetifolia*, se usa como tratamiento para la disentería y la diarrea.

Figura 19

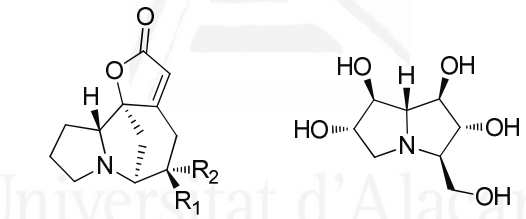

hidronorsecurininas **200** casuarina **201**

Muchos de estos productos naturales, como se ha mencionado antes, pueden clasificarse como alcaloides polihidroxilados. Normalmente estos alcaloides se extraen de la fracción acuosa de plantas y cultivos microbiológicos.[99] Pueden clasificarse de cinco formas de acuerdo a su estructura: pirrolidinas, piperidinas, pirrolizidinas, indolizidinas y *nor*-tropanos. Debido a su semejanza estructural con los carbohidratos, estas moléculas se han empleado en estudios

[95] Kang, T.R.; Cheng, Y.; He. L.; Ye, J.;Liu, Q.Z.; *Tet. Lett.* **2012**, *53*, 2552.
[96] Liddell, J.R.; *Nat. Prod. Rep.* **2002**, *19*, 773.
[97] Pyne, S.G.; Tang, M.Y.; *Curr. Org. Chem.* **2005**, *9*, 1393.
[98] Wang, G.-C.; Wang, Y.; Zhang, X.-Q.; Li, Y.-L.; Yao, X.-S.; Ye, W.-C.; *Chem. Pharm. Bull.* **2010**, *58*, 390.
[99] Tamayo, J.A; Franco, F.; Lo Re, D.; Sánchez, F.; *J. Org. Chem.* **2009**, *74*, 5679.

biológicos de procesos de reconocimiento celular.[100] Algunas de estas estructuras se muestran en la **Figura 20**.

Figura 20

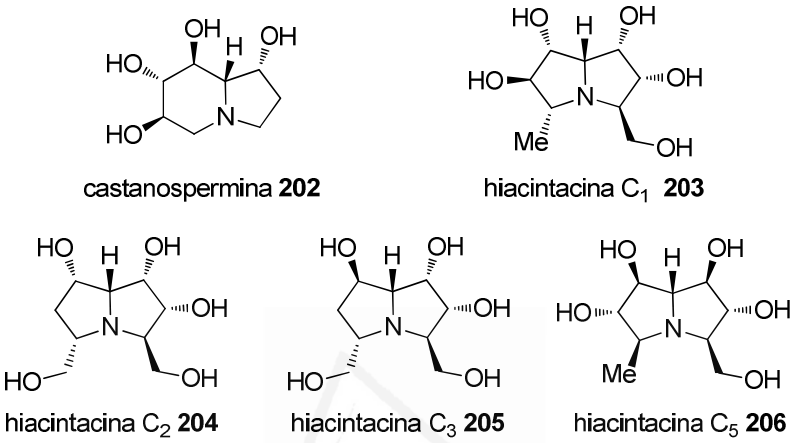

También existen algunos productos naturales con esqueleto de pirrolizidina e indolizidina sin hidroxilar, como muestra la **Figura 21**.

Figura 21

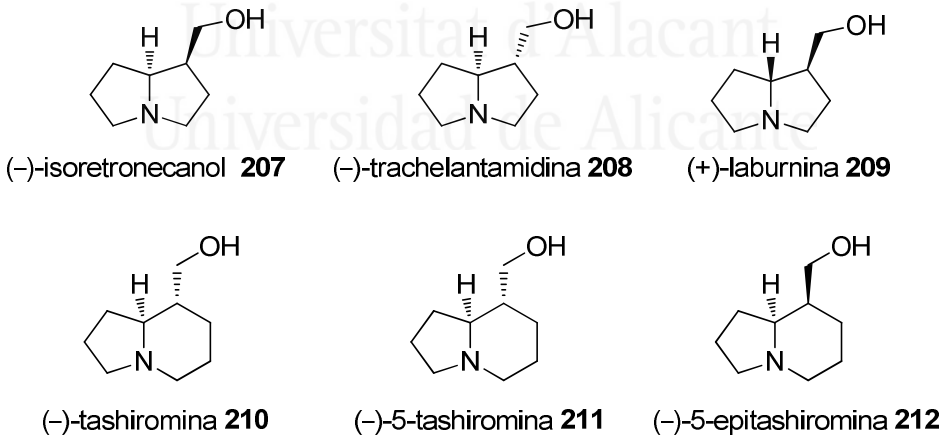

VI.1.1.- Biogénesis del esqueleto de pirrolizidina

Un análisis conciso de la estructura de pirrolizidina indicaría que este esqueleto puede provenir del aminoácido ornitina, en el que dos moléculas de

[100] Sinnot, M.L.; *Chem. Rev.* **1990**, *90*, 1171.

este aminoácido serian necesarias para la biogénesis de los alcaloides con el núcleo bicíclico de pirrolizidina, relativamente frecuentes en especies de géneros tales como *Senecio*, *Crotalaria* y *Heliotropium*.[101] Se ha comprobado mediante experimentos con marcadores isotópicos que el 4-aminopentanal **216** no está implicado en la biosíntesis, pero sí, en cambio la putrescina (**Figura 22**, **Esquema 51**), que experimenta un dimerización a *homospermidina* (1,6,11-triazaundecano) mediada por el par NAD^+/NADH. Ésta se convierte posteriormente en una sal de iminio que se cicla al sistema de pirrolizidina (**Esquema 52**).

Figura 22

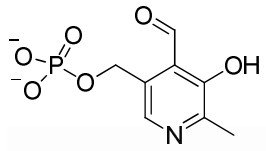

fosfato de piridoxal
(**PLP**) **213**

Esquema 52

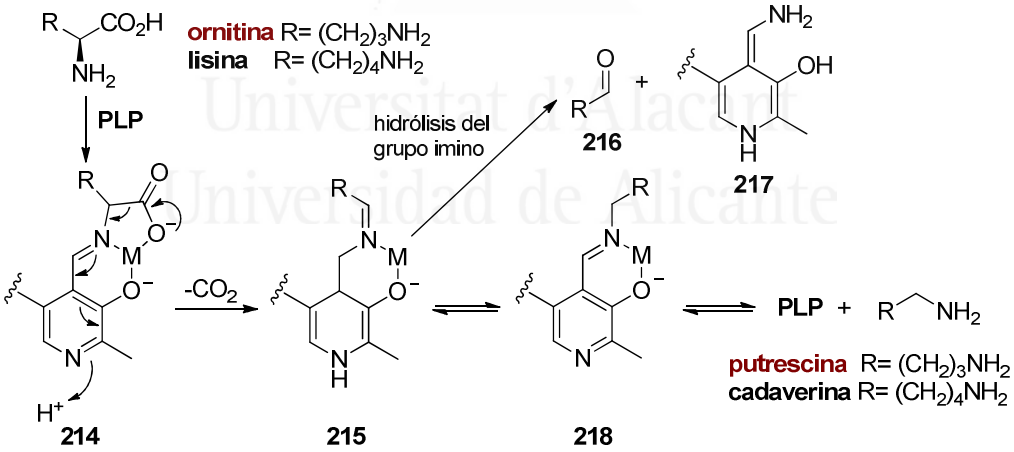

[101] Marco, J.A.; Química de los productos naturales, Ed. Síntesis S.A., **2006**.

Esquema 53

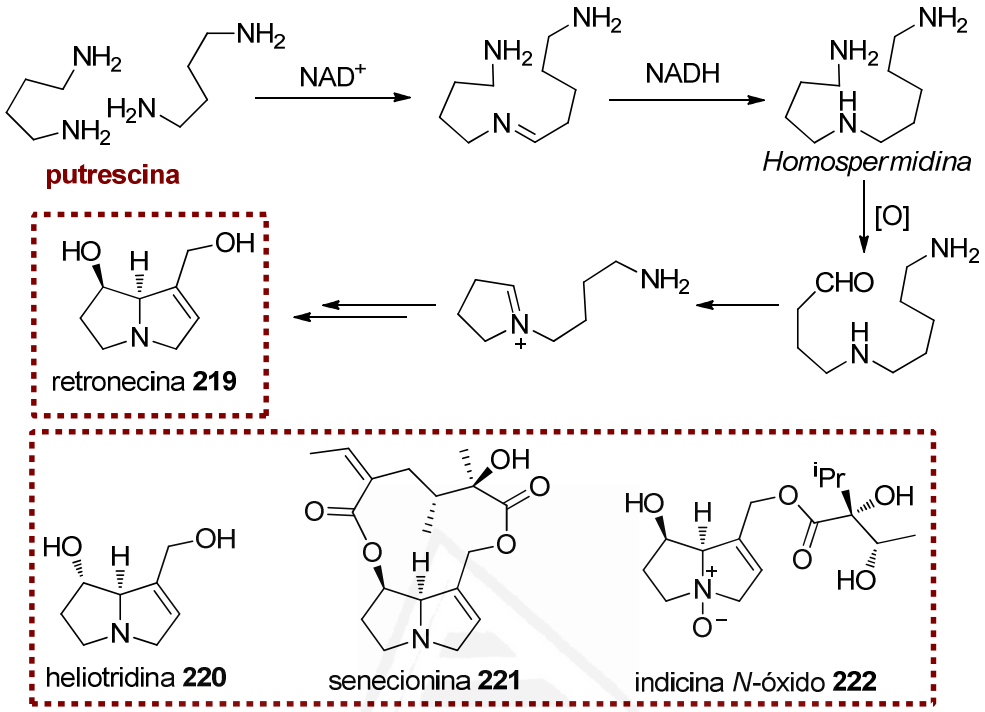

Los alcaloides de este grupo pueden aparecer en forma libre, como la *retronecina* o la *heliotridina*, o más a menudo en forma de mono o diésteres con monoácidos o diácidos estructuralmente complejos (denominados *ácidos nécicos*), como en el caso de la *senecionina*. Con cierta frecuencia, el átomo de nitrógeno está en forma de *N*-óxido, como ocurre en la *indicina*. Muchos de estos compuestos exhiben una intensa hepatotoxicidad y se sabe además que algunas especies de insectos los ingieren en la dieta y los acumulan en sus organismos. Ello probablemente les proporciona un mecanismo de defensa frente a sus depredadores, pues tales alcaloides les confieren mal sabor.

VI.1.2.- Síntesis de pirrolizidinas

Debido a la importancia biológica y farmacéutica de este tipo de compuestos, y a la frecuencia con la que aparecen en la naturaleza, la síntesis de pirrolizidinas se muestra como un campo muy atractivo desde el punto de vista de la química orgánica.

Existen numerosos trabajos en los que se llega al esqueleto final de pirrolizidina tras varios pasos de reacción. Tal es el caso del publicado por el grupo de Davies, en el que sintetizan pirrolizidinas con varios grupos alcohol, a través de

una ruta que incluye una reacción de Grubbs seguida de iodoaminación transanular.[102] También son frecuentes los ejemplos en los que a través de amidoarilación [103] o aminoarilación [104] intramolecular catalizada por Pd(II) sintetizan dicha estructura (**Esquema 54**).

Esquema 54a

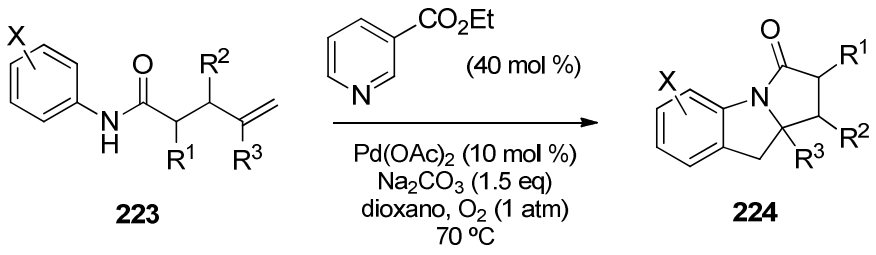

223 **224**

Esquema 54b

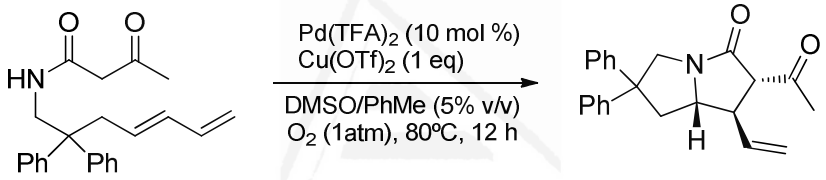

225 **226**

Por otro lado, el trabajo publicado por Liddell[96] se centra en la síntesis de *necinas* y ácidos nécicos que en muchas ocasiones dan lugar a pirrolizidinas polihidroxiladas. En esta línea, es muy interesante el trabajo publicado por Yu, Kato y colaboradores. En él se centran en el estudio de un alcaloide concreto que es la pochonicina, sintetizando ocho diasteroisómeros de esta pirrolizidina con una única metodología.[105]

Un par de ejemplos de síntesis del esqueleto de pirrolizidina con catalizadores no tan habituales en química orgánica[106] es el que publicaron el grupo de Marks. En el primero de ellos, a través de un catalizador formado por samario, llevan a cabo una reacción tándem de hidroaminación/ciclación de

[102] Brock, E. A.; Davies, S.G.; Lee, J.A.; Roberts, P.M.; Thomson,J. E.; *Org. Lett.* **2011**, *13*, 1594.
[103] Yip, K.T.; Yang, D.; *Org. Lett.* **2011**, *13*, 2134.
[104] Xing, D.; Yang, D.; *Org. Lett.* **2013**, *15*, 4370.
[105] Kato, A.; Yu, C.-Y. y colaboradores; *J. Org. Chem.* **2013**, *78*, 10298.
[106] Nakamura, I.; Yamamoto, Y.; *Chem. Rev.* **2004**, *104*, 207.

alenilalquenilaminas con alto rendimiento[107] (**Esquema 55a**). En el segundo de los ejemplos, a través de un catalizador órgano-lantánido realizan la biciclación de aminodiinos, aminoeninos y aminodienos sintetizando derivados de pirrolizidina e indolizidina en un único paso de reacción[108] (**Esquema 55b**).

Esquema 55a

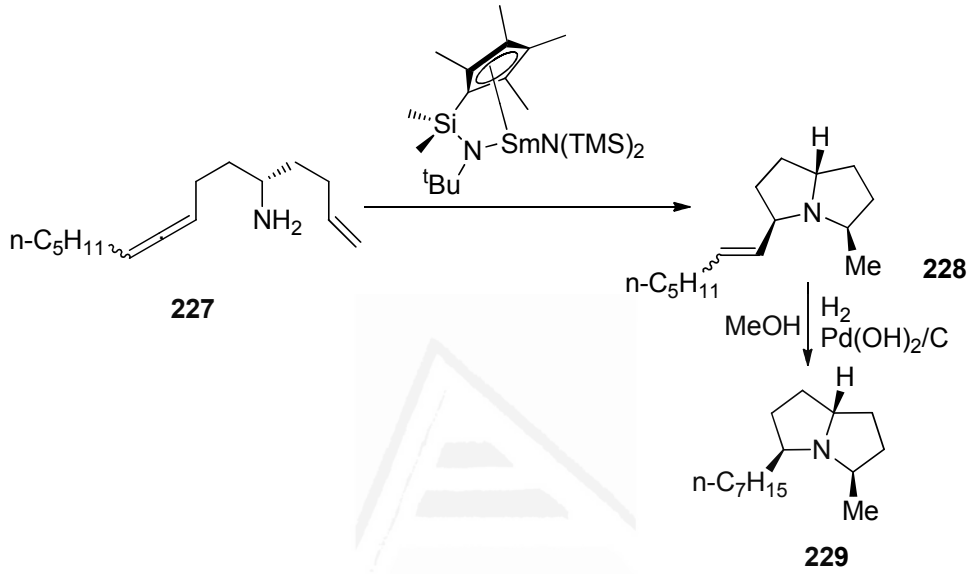

Esquema 55b

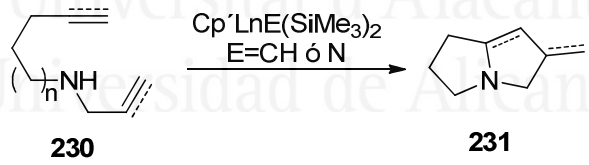

El grupo de Blum, llevó a cabo la catálisis dual con oro(I) y paladio(II) del reordenamiento de alquenil vinil aziridinas cuyo producto de reacción era una pirrolizidina con buenos rendimientos y diasteroselectividades moderadas[109] (**Esquema 56**).

[107] **a)** Arredondo, V.M.; Tian, S.; McDonald, F.E.; Marks, T.J.; *J. Am. Chem. Soc.* **1999**, *121*, 3633; **b)** Tian, S.; Arredondo, V.M.; Stern, C.L.; Marks, T.J.; *Organometallics* **1999**, *18*, 2568.
[108] **a)** Li, Y.; Marks, T J.; *J. Am. Chem. Soc.* **1996**, *118*, 707; **b)** Li, Y.; Marks, T.J.; *J. Am. Chem. Soc.* **1998**, *120*, 1757.
[109] Hirner, J.J.; Roth, K.E.; Shi, Y.; Blum, S.A.; *Organometallics* **2012**, *31*, 6843.

Esquema 56

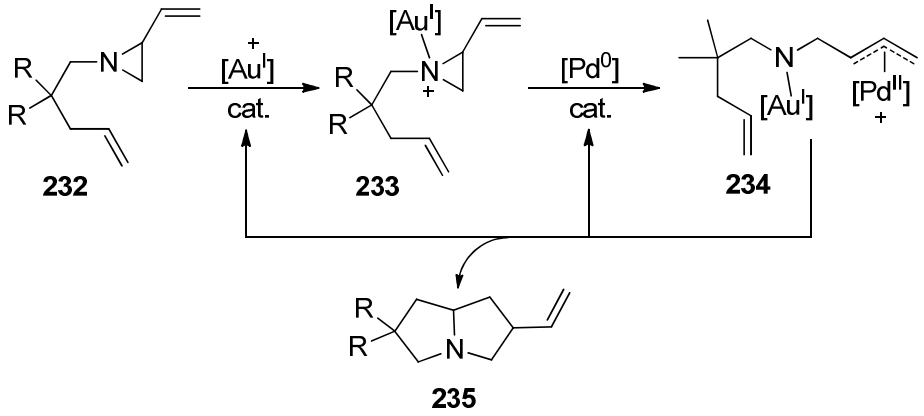

Además de las metodologías de síntesis comentadas, las cicloadiciones 1,3-dipolares se muestran como una de las alternativas más atractivas para la síntesis de pirrolizidinas debido al elevado control que ofrecen en la regio- y estereoselectividad de los productos formados.

VI.1.2.1.- Síntesis de pirrolizidinas mediante cicloadición 1,3-dipolar

Un ejemplo de cicloadición 1,3-dipolar en la síntesis de pirrolizidinas e indolizidinas con varios grupos alcohol es el publicado por Tamayo.[99] En él se describe la síntesis de nitronas para llevar a cabo esta reacción con una metodología que permite la obtención de diversos productos naturales tras pequeñas modificaciones en los grupos funcionales.

En lo que respecta a la cicloadición 1,3-dipolar con iluros de azometino, son varios los ejemplos en la bibliografía en los que a partir de prolina, llevan a cabo esta reacción de manera multicomponente, con un aldehído o cetona y un dipolarófilo, generando el 1,3-dipolo por decarboxilación de la prolina, en un reflujo de DMSO o CH_3CN normalmente[58,95](**Equema 57**).

Equema 57

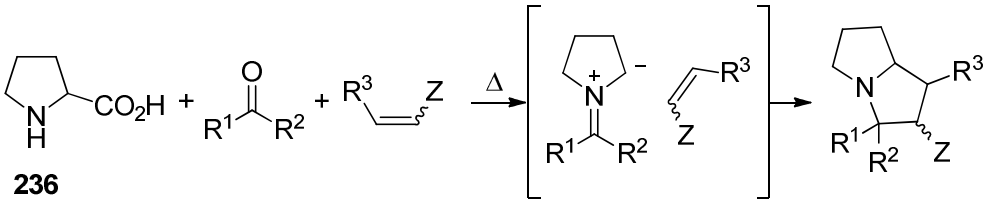

236

Más recientemente, se ha descrito simultáneamente la síntesis de pirrolizidinas a través de la reacción dipolar multicomponente, pero usando un éster alquílico de prolina por el grupo del profesor Maiti[110] y por nuestro grupo.[111] El grupo de Maiti lleva a cabo el estudio utilizando cinamaldehído y derivados de este, en DCM y en poco tiempo (**Esquema 58**).

Esquema 58

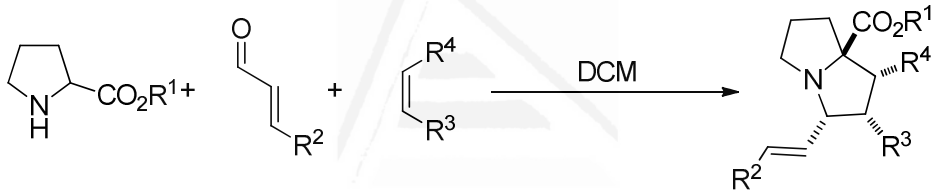

Nuestro grupo de investigación, amplió la síntesis al uso de otros aldehídos α,β-insaturados, así como a aldehídos alifáticos y glioxilato de etilo usando como aditivo una sal de plata(I) que resultó ser necesaria en algunos casos. Obteniendo además pirrolizidinas enantiomericamente enriquecidas cuando se partía del clorhidrato del éster metílico de (2*S*,4*R*)-4-hidroxiprolina **237** como se detalla en la **Discusión de Resultados**.

Por último, una de las contribuciones más importantes a la síntesis de pirrolizidinas es la aportada por el grupo de Reisman.[112] En su trabajo, lleva a cabo la síntesis enantioselectiva de pirrolizidinas, en dos etapas de reacción, obteniendo primero una prolina enantioméricamente enriquecida, pudiendo ser aislada, de la que se parte seguidamente para obtener el producto final con buenos excesos enantioméricos. (**Esquema 59**)

[110] Sengupta, T.; Khamarui, S.; Samanta, S.; Maiti, D.K.; *Chem. Commun.* **2013**, *49*, 9962.
[111] Mancebo-Aracil, J.; Nájera, C.; Sansano, J.M.; *Chem. Commun.* **2013**, *49*, 11218.
[112] Lim, A.D.; Codelli, J.A.; Reisman, S.A.; *Chem. Sci.* **2013**, *4*, 650.

Esquema 59

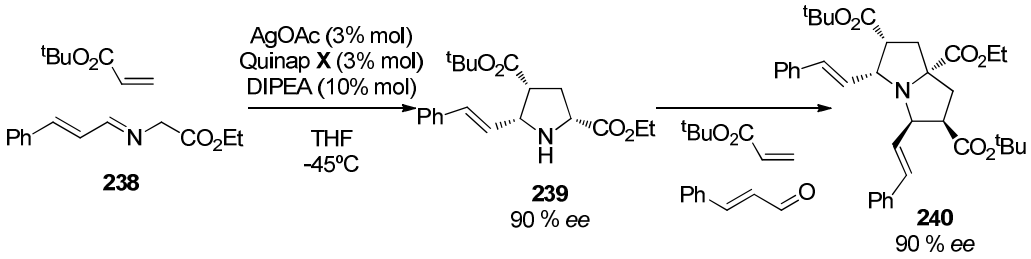

VI.2.- OBJETIVOS

A la vista de lo expuesto en los Antecedentes Bibliográficos, se propusieron los siguientes objetivos:

- Sintetizar mediante una cicloadición 1,3-dipolar multicomponente con iluros de azometino, diferentes ejemplos de pirrolizidina controlando la regio- y la diasteroselectividad de los productos finales a partir de ésteres alquílicos de prolina.
- Mediante la misma metodología, sintetizar el esqueleto de indolizidina, a partir de ésteres alquílicos del ácido pipecolínico utilizando la ruta de la sal de iminio para generar el 1,3-dipolo manteniendo la mayor economía de átomos al no producirse la descarboxilación durante la generación del mismo siguiendo el esquema retrosintético que se muestra a continuación.

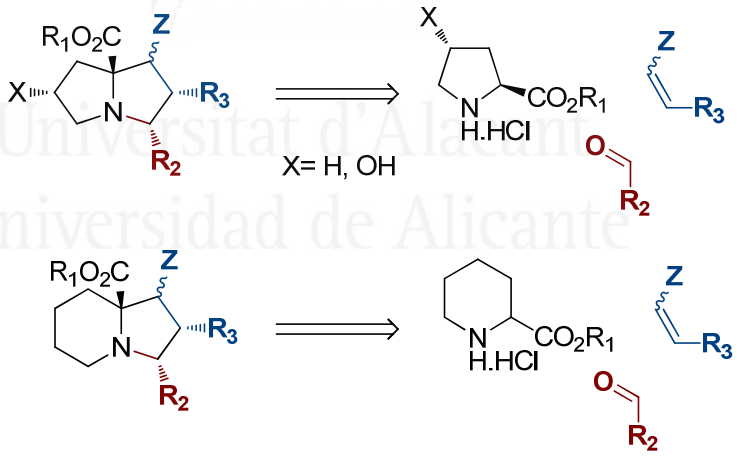

VI.3.- DISCUSIÓN DE RESULTADOS

Siguiendo la metodología descrita en el **Capítulo II**, se llevó a cabo la cicloadición 1,3-dipolar multicomponente, generando el iluro de azometino in situ a partir de un aldehído y el clorhidrato de una amina, en presencia de un dipolarófilo. En esta ocasión, a diferencia del capítulo anterior, el aminoácido utilizado tiene una unidad amina secundaria cíclica.

En primer lugar se realizó la reacción entre el clorhidrato del éster metílico de prolina **241**, Et_3N, acrilato de metilo **5** y cinamaldehído **242** a temperatura ambiente con tolueno, diclorometano y THF como disolventes. Se observó entonces, que con los tres disolventes probados, la conversión era cuantitativa obteniendo mayoritariamente el producto mostrado en el **Esquema 60**. Sin embargo, pese a que en tolueno la reacción era más lenta (unas 5 horas frente a menos de una hora en DCM) la diasteroselectividad era de 99:1 en este disolvente, mayor que en diclorometano o THF (85:15 y 88:12 respectivamente).

Esquema 60

Se probaron entonces, con este mismo aldehído otros dipolarófilos, utilizados frecuentemente como son las maleimidas *N*-sustituidas, otros acrilatos, fumarato de dimetilo, etc.

Con el fin de mejorar los rendimientos y la diasteroselectividad de los productos obtenidos, se probó además dicha reacción añadiendo una sal de plata(I) en cantidades subestequiométricas. Se observó entonces que los resultados eran muy similares y el rol de la plata parecía ser de mero espectador. Sin embargo, cuando se llevo a cabo la reacción con glioxilato de etilo como aldehído con y sin plata(I), se observó que jugaba un papel fundamental en este caso concreto, de manera que sin presencia de ella, la reacción no tenía lugar (**Esquema 61**).

Esquema 61

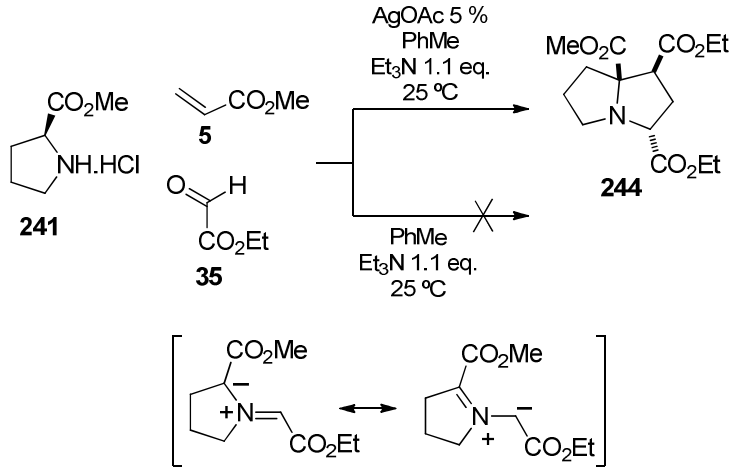

Además el producto final **244** mostraba una diasteroselectividad diferente del producto mayoritario obtenido con cinamaldehído, lo cual puede explicarse debido al equilibrio tautomérico que puede tener lugar en la formación del dipolo en el que la presencia del doble enlace endocíclico es fundamental (**Esquema 61**).

Así pues se decidió llevar a cabo dos estudios paralelos, con y sin acetato de plata(I), observando que en la mayoría de casos no interactuaba en la reacción, pero sin embargo en otros ejemplos incrementaba la diasteroselectividad de los productos e incluso hacía que la reacción tuviera lugar como en el caso ya comentado del glioxilato de etilo **35** y también el isovaleraldehído, en presencia de acrilato de metilo como dipolarófilo.

La función de este ácido de Lewis está aún por determinar, pero se intuye que puede favorecer la generación de una pequeña cantidad de imina necesaria para comenzar el proceso, de hecho, en algunos ejemplos la reacción no se produce en su ausencia. Es importante recordar, que no fue posible aislar la imina generada por condensación entre un aminoéster y glioxilato de etilo.

Por otro lado con el fin de funcionalizar más aun la pirrolizidina obtenida, se decidió usar como reactivo de partida el clorhidrato del éster metílico de (2*S*,4*R*)-4-hidroxiprolina **237**, confiando además en que el grupo hidroxilo pudiera aumentar de alguna forma la diasteroselectividad y obtener pirrolizidinas enantioméricamente enriquecidas. Así la presencia del grupo alcohol en posición

4, permitió obtener una pirrolizidina final enantiomericamente enriquecida sin necesidad de ningún metal ni auxiliar quiral, obteniendo, en algunos casos prácticamente un solo enantiómero (**Esquema 62**).

Esquema 62

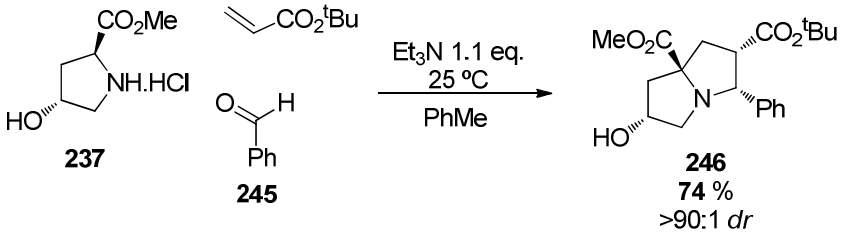

Finalmente, aplicando esta metodología se pudo sintetizar la estructura de indolizidina partiendo del clorhidrato del éster metílico del ácido pipecolínico, con cinamaldehído y acrilato de metilo como dipolarófilo. Esto no fue posible, con y sin presencia de AgOAc. Sin embargo, bajo condiciones térmicas en reflujo de tolueno, la reacción tuvo lugar obteniéndose el producto esperado con buen rendimiento y diasteroselectividad (**Esquema 63**).

Esquema 63

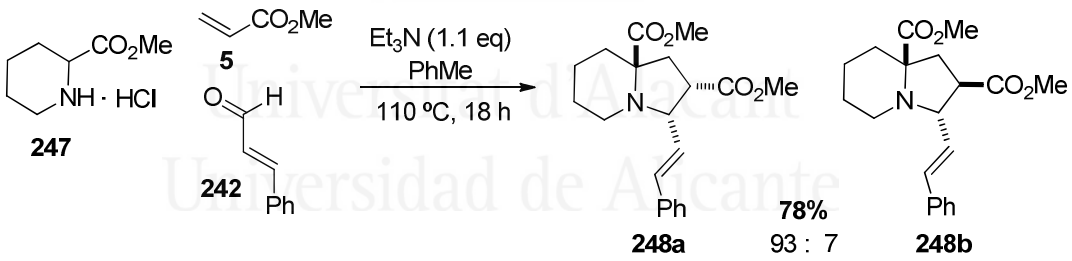

Un estudio más detallado de lo resumido anteriormente se encuentra en el siguiente apartado.

VI.4.- CHEM. COMMUN. 2013, 49, 11218

ChemComm

RSC Publishing

COMMUNICATION

View Article Online
View Journal | View Issue

Multicomponent synthesis of unnatural pyrrolizidines using 1,3-dipolar cycloaddition of proline esters†

Juan Mancebo-Aracil, Carmen Nájera* and José M. Sansano*

Cite this: *Chem. Commun.*, 2013, **49**, 11218

Received 19th September 2013,
Accepted 9th October 2013

DOI: 10.1039/c3cc47184e

www.rsc.org/chemcomm

The synthesis of unnatural pyrrolizidines has been studied using a multicomponent-domino process involving proline or 4-hydroxyproline esters, an aldehyde and a dipolarophile. The formation of the iminium salt promotes the 1,3-dipolar cycloaddition affording highly substituted pyrrolizidines under mild conditions and high regio- and diastereoselectivities.

Pyrrolizidine alkaloids are a group of naturally occurring alkaloids[1] produced by plants as a defense mechanism against insect herbivores. The evolution of pyrrolizidine alkaloid biosynthesis highly conserves the first steps of the pathway whilst the diversification of secondary derived pyrrolizidine alkaloids occurs.[2] This process ensures the appearance of new families of pyrrolizidines over time. Many of them are potent hepatotoxic, mutagenic and tumorigenic agents although some families of pyrrolizidines possess interesting therapeutic and medicinal applications. The synthesis of these natural frameworks has been achieved, for example, employing different strategies such as chain elongation of proline derivatives, followed by cyclization,[3] transannular iodoamination,[4] using lactams,[5] from other natural products,[6] *etc.* However, the most important and straightforward route is to employ a 1,3-dipolar cycloaddition (1,3-DC)[7,8] using mainly nitrones[9] or azomethine ylides.[10,11] The characteristic regio- and diastereoselective control of these cycloadditions contributes to the enhancement of the importance of this strategy for this purpose. In particular, proline has been used as starting material for the *in situ* generation of an azomethyne ylide ready to react with an electrophilic alkene (Scheme 1).

In these examples the generation of the reactive dipole proceeds after decarboxylation of the proline, which reduces the functionalization of the resulting pyrrolizidine. The intermediate dipole, generated from 2,3-butanedione or ethyl pyruvate and proline or (2*S*,4*R*)-4-hydroxyproline, has been trapped using β-nitrostyrene. Unexpectedly, the decarboxylation occurred at room temperature

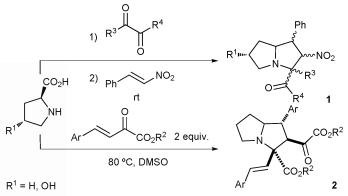

Scheme 1

affording mixtures of pyrrolizidines **1** in good chemical yields (78–90%).[12] More recently, it has been described that the same proline underwent a domino iminium salt formation with β,γ-unsaturated α-keto esters followed by decarboxylation and cycloaddition with the named keto ester at 80 °C in DMSO as solvent.[13]

In this work we describe the multicomponent 1,3-DC between proline esters, aldehydes and dipolarophiles. The generation of the reactive azomethine ylide will be achieved through the iminium salt route[7b] and the cycloaddition will be surveyed at room temperature in the presence or in the absence of silver salts. The aim of this strategy is to maintain the original ester functional group of the proline in order to obtain modified pyrrolizidines with diverse functionalization at the 7a carbon atom of the named fused heterocycle. In this way the access to unnatural alkaloids with unknown biological properties would be ensured.[14]

The synthesis of pyrrolizidines **3** was initially tested at room temperature employing a multicomponent process following the previous methodology developed by our group.[15] Proline methyl ester hydrochloride was allowed to react with cinnamaldehyde and methyl acrylate using triethylamine (1 equiv.). Despite toluene[16] afforded a slower reaction (5 h) with methyl acrylate (96% crude yield of pure **3a**), it was selected as solvent because a higher diastereoselection (99 : 1) was obtained in this example (Scheme 2 and Table 1). Two different processes run in THF (1 h) and DCM (1 h) afforded lower diastereoselectivity of compound **3a** (88 : 12, and 85 : 15, respectively). Different dipolarophiles such as allyl methacrylate, *N*-methylmaleimide (NMM), dimethyl fumarate, β-nitrostyrene, and 1,2-bis(phenylsulfonyl)ethylene afforded the corresponding

Departamento de Química Orgánica e Instituto de Síntesis Orgánica, Universidad de Alicante, E-03080-Alicante, Spain. E-mail: cnajera@ua.es, jmsansano@ua.es; Fax: +34-965903549; Tel: +34-965903549

† Electronic supplementary information (ESI) available. Experimental data. CCDC 961250 and 961570. For ESI and crystallographic data in CIF or other electronic format see DOI: 10.1039/c3cc47184e

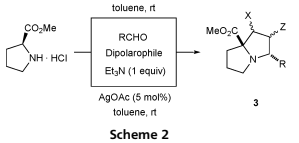

Scheme 2

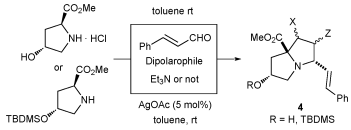

Scheme 3

pyrrolizidines **3b–3f** in good yields and high dr (Table 1, entries 2–6). When the 1,3-DC was carried out in the presence of AgOAc (5 mol%) compound **3a** was obtained after 10 h (Table 1, entry 1). Under identical reaction conditions AgTFA, AgOTf and Ag_2CO_3 afforded similar results for compound **3d**. For these reasons the same reactions described above were also performed at rt in the presence of AgOAc (Table 1, entries 2–6).

The reaction in the absence of silver salts is faster than the analogous silver-mediated processes furnishing the same dr (up to 99 : 1). However, higher diastereoselections were achieved in the presence of AgOAc when other aldehydes such as crotonaldehyde, benzaldehyde, isovaleraldehyde and ethyl glyoxylate were used as iminium salt precursors (Table 1, entries 7–10). Moreover, the last two reactions did not proceed in the absence of silver acetate.

All diastereoisomers were separated by column chromatography and the relative configuration of these new compounds was established according to the X-ray diffraction analysis of molecule **3a**[17] and additional nOe experiments performed for other compounds.

Due to the existence of multiple hydroxy groups as substituents in natural pyrrolizidine alkaloids we surveyed the effect of a stereogenic

Table 1 Synthesis of pyrrolizidines **3** employing L-proline and aldehydes with several dipolarophiles

				Without AgOAc			With AgOAc		
Entry	Aldehyde	Dipolarophile	Product **3**	*t* (h)	Yield[a] (%)	dr	*t* (h)	Yield[a] (%)	dr
1	Cinnamaldehyde	Methyl acrylate	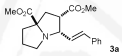 **3a**	5	(95) 80	99 : 1	10	(94) 80	99 : 1
2	Cinnamaldehyde	Allyl methacrylate	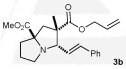 **3b**	3	(93) 82	99 : 1	8	(93) 81	99 : 1
3	Cinnamaldehyde	NMM	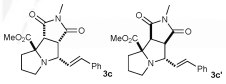 **3c** **3c'**	2	(92) 80	85 : 15	10	(92) 81	85 : 15
4	Cinnamaldehyde	Dimethyl fumarate	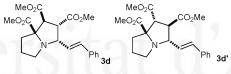 **3d** **3d'**	2	(96) 83	85 : 15	6	(96) 83	85 : 15
5	Cinnamaldehyde	β-Nitrostyrene	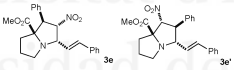 **3e** **3e'**	2	(95) 79	85 : 15	10	(94) 78	85 : 15
6	Cinnamaldehyde	Disulfone	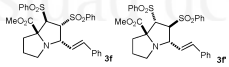 **3f** **3f'**	3	(85) 62	62 : 19 : 19[b]	9	(90) 72	72 : 28
7	Crotonaldehyde	Methyl acrylate	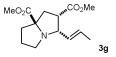 **3g**	1	(96) 85	90 : 10	9	(96) 85	90 : 10
8	Benzaldehyde	Methyl acrylate	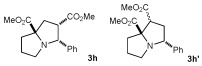 **3h** **3h'**	5	(85) 65	37 : 37 : 26[b]	24	(90) 75	80 : 20
9	Isovaleraldehyde	Methyl acrylate	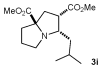 **3i**	3	—	—	24	(96) 80	80 : 20
10	Ethyl glyoxylate	Methyl acrylate	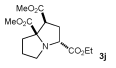 **3j**	6	—	—	24	(88) 59	99 : 1

[a] Isolated yields of the mixture of diastereoisomers (in brackets crude pure yield). [b] The third isomer was not characterized.

Table 2 Synthesis of pyrrolizidines **4** employing (2*S*,4*R*)-4-hydroxyproline and cinnamaldehyde with several dipolarophiles

				Without AgOAc			With AgOAc		
Entry	R	Dipolarophile	Product **4**	*t* (h)	Yield[a] (%)	dr	*t* (h)	Yield[a] (%)	dr
1	H	Methyl acrylate	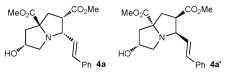	4	(93) 85	80 : 20	6	(92) 85	87 : 13
2	TBDMS	Methyl acrylate	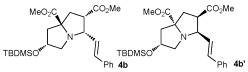	4	(91) 80	78 : 18	6	(92) 79	80 : 20
3	H	*t*-Butyl acrylate	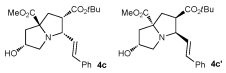	3	(92) 80	90 : 10	6	(92) 82	98 : 2
4	H	NMM	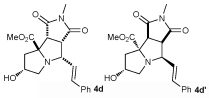	3	(91) 80	75 : 25	6	(94) 81	75 : 25

[a] Isolated yields of the mixture of diastereoisomers (in brackets crude pure yield).

centre at the 4 position of the heterocycle. Thus (2*S*,4*R*)-4-hydroxyproline and its *O*-TBDMS protected derivative were used as starting materials in the title 1,3-DC with acrylates and NMM employing cinnamaldehyde as the iminium salt precursor (Scheme 3, and Table 2). The *O*-TBDMS protected proline ester furnished compound **4b** in lower diastereoselection than the corresponding reaction performed with (2*S*,4*R*)-4-hydroxyproline methyl ester yielding cycloadduct **4a** (Table 2, entries 1 and 2). *tert*-Butyl acrylate gave product **4c** with higher diastereoselection (98 : 2) than methyl acrylate, especially in the presence of silver acetate (Table 2, entry 3). In the case of NMM products **4d** and **4d′** were obtained in a 4 : 1 diastereomeric ratio (Table 2, entry 4). All the diastereoisomers could be separated by column chromatography providing enantiomerically enriched compounds **4**. Pale yellow needles obtained from molecule **4a** were subjected to X-ray diffraction analysis and served for the determination of its absolute configuration.[18] The relative configuration of the rest of products was assigned according to positive nOe experiments.

We can conclude that a very simple multicomponent 1,3-DC from proline methyl esters, aldehydes and dipolarophiles is an appropriate methodology to prepare highly substituted unnatural pyrrolizidine alkaloids. The corresponding enantiomerically pure 1*H*-pyrrolizidin-2-ol skeleton was prepared from natural (2*S*,4*R*)-4-hydroxyproline methyl ester. The presence of AgOAc was crucial when aliphatic aldehydes and ethyl glyoxylate were employed because the reaction failed under standard conditions.

This work has been supported by the DGES of the Spanish Ministerio de Ciencia e Innovación (MICINN) (Consolider INGENIO 2010 CSD2007-00006, CTQ2007-62771/BQU, CTQ2010-20387), FEDER Generalitat Valenciana (PROMETEO/2009/039), and by the University of Alicante.

Notes and references

1 J. R. Liddell, *Nat. Prod. Rep.*, 2002, **19**, 773.
2 (*a*) D. Ober and E. Kaltenegger, *Phytochemistry*, 2009, **70**, 1687; (*b*) D. Langel, D. Ober and P. B. Pelser, *Phytochem. Rev.*, 2011, **10**, 3.
3 (*a*) T. J. Donohoe, R. E. Thomas, M. D. Cheeseman, C. L. Rigby, G. Bhalay and I. D. Linney, *Org. Lett.*, 2008, **10**, 3615; (*b*) A. C. Breman, J. Dijkink, J. H. van Maarseveen, S. S. Kinderman and H. Hiemstra, *J. Org. Chem.*, 2009, **74**, 6327; (*c*) T. Ponpandian and S. Muthusubramanian, *Tetrahedron*, 2013, **69**, 527; (*d*) X. Garrabou, L. Gómez, J. Joglar, S. Gil, T. Parella, J. Bujons and P. Clapes, *Chem.–Eur. J.*, 2010, **16**, 10691; (*e*) I. Izquierdo, M. T. Plaza, J. A. Tamayo, F. Franco and F. Sanchez-Cantalejo, *Tetrahedron*, 2010, **66**, 3788; (*f*) D. Muroni, M. Mucedda and A. Saba, *Tetrahedron Lett.*, 2008, **49**, 2373; (*g*) A. Iza, L. Carrillo, J. L. Vicario, D. Badía, E. Reyes and J. L. Martínez, *Org. Biomol. Chem.*, 2010, **8**, 2238.
4 E. A. Brock, S. G. Davies, J. A. Lee, P. M. Roberts and J. E. Thomson, *Org. Lett.*, 2011, **13**, 1594.
5 P. V. Reddy, J. Smith, A. Kamath, H. Jamet, A. Veyron, P. Koos, C. Philouze, A. E. Greene and P. Delair, *J. Org. Chem.*, 2013, **78**, 4840.
6 R. Lahiri, A. A. Ansanri and Y. D. Vankar, *Chem. Soc. Rev.*, 2013, **42**, 5102.
7 For very recent general reviews dealing with general 1,3-DC, see: (*a*) V. Nair and T. D. Suja, *Tetrahedron*, 2007, **63**, 12247; (*b*) A. Padwa and S. K. Bur, *Tetrahedron*, 2007, **63**, 5341.
8 For recent reviews of asymmetric 1,3-DC, see: (*a*) M. Álvarez-Corral, M. Muñoz-Dorado and I. Rodríguez-García, *Chem. Rev.*, 2008, **108**, 3174; (*b*) M. Naodovic and H. Yamamoto, *Chem. Rev.*, 2008, **108**, 3132; (*c*) C. Nájera, J. M. Sansano and M. Yus, *J. Braz. Chem. Soc.*, 2010, **21**, 377; (*d*) M. Kissane and A. R. Maguire, *Chem. Soc. Rev.*, 2010, **39**, 845; (*e*) J. Adrio and J. C. Carretero, *Chem. Commun.*, 2011, **47**, 6784.
9 (*a*) S. Stecko, M. Jurczak, Z. Urbanczyk-Lipkowska, J. Solecka and M. Chmielewski, *Carbohydr. Res.*, 2008, **343**, 2215; (*b*) A. Brandi, F. Cardona, S. Cicchi, F. M. Cordero and A. Goti, *Chem.–Eur. J.*, 2009, **15**, 7808.
10 (*a*) R. Grigg, M. Jordan and J. F. Malone, *Tetrahedron Lett.*, 1979, **20**, 3877; (*b*) L. Faraji, H. Arvinnezhad, N. Alikami and K. Jadidi, *Lett. Org. Chem.*, 2010, **7**, 472; (*c*) R. M. Gorman, M. A. Little, J. A. Morris and V. Sridharan, *Chem. Commun.*, 2012, **48**, 9537.
11 In some examples proline itself has been generated from a previous 1,3-DC. For selected examples of racemic and non-racemic processes, see: (*a*) P. Cui, L. Xu, Z. Shi and L. Gan, *J. Org. Chem.*, 2011, **76**, 4210; (*b*) J. A. Codelli, A. L. A. Puchlopek and S. E. Reisman, *J. Am. Chem. Soc.*, 2012, **134**, 1930; (*c*) Q. Lu, G. Song, J. P. Jasinski, A. C. Keeley and W. Zhang, *Green Chem.*, 2012, **14**, 3010–3012; (*d*) A. D. Lim, J. A. Codelli and S. E. Reisman, *Chem. Sci.*, 2013, **4**, 650.
12 F. Felluga, C. Forzato, P. Nitti, G. Pitacco, E. Valentin and E. Zangrando, *J. Heterocycl. Chem.*, 2010, **47**, 664.
13 T.-R. Kang, Y. Cheng, L. He, J. Ye and Q.-Z. Liu, *Tetrahedron Lett.*, 2012, **53**, 2552.
14 T. Sengupta, S. Khamarui, S. Samanta and D. K. Maiti, *Chem. Commun.*, 2013, **49**, 9962.
15 J. Mancebo-Aracil, C. Nájera and J. M. Sansano, *Org. Biomol. Chem.*, 2013, **11**, 662.
16 From the industrial point of view toluene is preferred, rather than DCM, THF of ether.
17 CCDC number of molecule **3a**: 961250.
18 CCDC number of molecule **4a**: 961570.

Electronic Supplementary Material (ESI) for Chemical Communications

SUPPORTING INFORMATION

Table of contents

1. General.

Aldehydes were distilled prior to use for the elaboration of the iminoesters. Melting points were determined with a Reichert Thermovar hot plate apparatus and are uncorrected. Only the structurally most important peaks of the IR spectra (recorded on a Nicolet 510 P-FT and on a Jasco FTIR 4100) are listed. ^{1}H NMR (300 MHz) and ^{13}C NMR (75 MHz) spectra were obtained on a Bruker AC-300 using $CDCl_3$ as solvent and TMS as internal standard, unless otherwise stated. Optical rotations were measured on a Perkin Elmer 341 polarimeter. Low-resolution electron impact (EI) mass spectra were obtained at 70eV on a Shimadzu QP-5000 and high-resolution mass spectra were obtained on a Finnigan VG Platform. HRMS (EI) were recorded on a Finnigan MAT 95S. Microanalyses were performed on a Perkin Elmer 2400 and a Carlo Erba EA1108. Analytical TLC was performed on Schleicher & Schuell F1400/LS silica gel plates and the spots were visualized under UV light (λ=254 nm). For flash chromatography we employed Merck silica gel 60 (0.040-0.063 mm). Complexes were prepared according to the reported procedure (see text). All of the transformations performed with silver catalysts were performed in the absence of light.

Electronic Supplementary Material (ESI) for Chemical Communications

2. General procedure for the synthesis of compounds 3 and 4 in the absence of AgOAc.

Methyl ester L-proline hydrochloride (82.8 mg, 0.5 mmol) or L-4-hydroxyproline methyl ester hydrochloride (92.1 mg, 0.5 mmol), the corresponding alkene (0.5 mmol), the aldehyde (0.5 mmol) and triethylamine (90 µL, 0.55 mmol) were dissolved in toluene (3mL). The resulting mixture was stirred for times described in Table 1 and 2. Then the solvent was evaporated under reduced pressure and the residue was purified by flash chromatography (silica gel) to afford the corresponding product **3** or **4**.

3. General procedure for the synthesis of compounds 3 and 4 in the presence of AgOAc.

Methyl ester L-proline hydrochloride (82.8 mg, 0.5 mmol) or L-4-Hydroxyproline methyl ester hydrochloride (92.1 mg, 0.5 mmol), silver acetate (4.15 mg, 0.025 mmol), the corresponding alkene (0.5 mmol), the aldehyde (0.5 mmol) and triethylamine (90 µL, 0.55 mmol) were dissolved in toluene (3mL). The resulting suspension was stirred for the corresponding times (see Tables 1 and 2) avoiding the light exposure. Then the solvent was evaporated under reduced pressure. and the residue was purified by flash chromatography (silica gel) to afford the corresponding product **3** or **4**.

4. Physical and spectroscopic data of compounds 3 and 4

(2*S,3*S**,7a*R**)-Dimethyl 3-[*(E)*-styryl]hexahydro-*1H*-pyrrolizine-2,7a-dicarboxylate 3a:** Pale orange needles, mp: 107-110ºC; IR (neat) ν_{max} 2985, 2939, 2305, 1714, 1691 cm^{-1}; ^{1}H NMR δ_H: 1.72–1.93 (m, 3H, C*H*$_2$CH$_2$N, C*H*HCCO$_2$Me), 2.22 (deform. dd, *J* = 13.0, 12.8 Hz, 1H, C*H*HCHCO$_2$Me), 2.31 (deform. ddd, *J* = 8.6, 6.9 Hz, 1H, C*H*HCCO$_2$Me), 2.64 (dd, *J* = 13.0, 6.7 Hz, 1H, C*H*HCHCO$_2$Me), 2.89 (deform. ddd, *J* = 11.2, 6.7, 2.3 Hz, 1H, C*H*HN), 3.10 (m, 1H, C*H*HN), 3.51-3.58 (m, 4H, CHCO$_2$Me, CHCO$_2$C*H*$_3$), 3.75 (s, 3H, CCO$_2$CH$_3$), 4.19 (dd, *J* = 10.4, 6.4 Hz, 1H, CHN), 5.98 (dd, *J* = 15.5, 10.4 Hz, 1H, C*H*CHN), 6.56 (d, *J* = 15.5 Hz, 1H, C*H*Ph), 7.28-7.35 (m, 5H, Ar*H*); ^{13}C NMR δ_C: 28.0 (*C*H$_2$CH$_2$N), 36.5 (*C*H$_2$CCO$_2$Me), 37.2 (*C*H$_2$CHCO$_2$Me), 48.8 (CH$_2$N), 50.0 (*C*HCO$_2$Me), 51.9 (CHCO$_2$*C*H$_3$), 52.6 (CCO$_2$*C*H$_3$), 67.4 (CHN), 76.4 (*C*CO$_2$Me), 125.7 (*C*HCHN), 126.7, 128.0, 128.7, 136.5 (Ar*C*), 135.5 (*C*HPh), 172.2 (CH*C*O$_2$Me), 177.0 (C*C*O$_2$Me); MS (EI-GC) *m/z*: 329 (M^+, 3%), 271 (19), 270 (100), 243 (13), 238 (21), 210 (17), 184 (40), 123 (10), 115 (10); Microanalysis calculated for $C_{19}H_{23}NO_4$: C, 69.3; H, 7.0; N, 4.3%; found: C, 69.5; H, 7.2; N, 4.5%.

(2*S,3*S**,7a*R**)-2-allyl 7a-methyl 2-methyl-3-(*(E)*-styryl)hexahydro-*1H*-pyrrolizine-2,7a-dicarboxylate 3b:** Brown-yellow solid, mp: 90-95ºC; IR (neat) ν_{max} 2983, 1720, 1699, 2310, 1270 cm^{-1}; ^{1}H NMR δ_H: 1.44 (s, 3H, CCH$_3$), 1.69-2.02 (m, 3H, C*H*$_2$CH$_2$N, C*H*HCCO$_2$Me), 2.15-2.24 (m, 1H, C*H*HCCO$_2$Me), 2.51 [d, *J* = 13.7 Hz, 1H, C*H*HC(CH$_3$)CO$_2$Allyl], 2.64 [d, *J* = 13.7 Hz, 1H, C*H*HC(CH$_3$)CO$_2$Allyl], 2.92-3.01 (m, 1H, C*H*HN), 3.08-3.16 (m, 1H, C*H*HN), 3.77 (s, 3H, CCO$_2$CH$_3$), 3.80 (d, *J* = 10.4, Hz, 1H, CHN), 4.43-4.45 (m, 2H, CO$_2$C*H*$_2$CHCH$_2$), 5.07 (ddd, *J* = 10.4, 2.6, 1.2 Hz, 1H, CO$_2$CH$_2$CHC*H*H), 5.19 (ddd, *J* = 17.2, 2.6, 1.2 Hz, 1H, CO$_2$CH$_2$CHC*H*H), 5.75 (ddt, *J* = 17.2, 10.4, 5.9 Hz, 1H, CO$_2$CH$_2$C*H*CH$_2$), 5.95 (dd, *J* = 15.6, 10.4 Hz, 1H, C*H*CHN), 6.53 (d, *J* = 15.6 Hz, 1H, C*H*Ph), 7.23-7.34 (m, 5H, Ar*H*); ^{13}C NMR δ_C: 23.5 (C*C*H$_3$), 27.5 (*C*H$_2$CH$_2$N), 39.2 (*C*H$_2$CCO$_2$Me), 43.9 [*C*H$_2$C(CH$_3$)CO$_2$Allyl], 49.0 (CH$_2$N), 52.7 (CCO$_2$*C*H$_3$),

Electronic Supplementary Material (ESI) for Chemical Communications

55.5 (CCO_2CH_3), 65.7 ($CO_2CH_2CHCH_2$), 74.6 (CHN), 77.4 [$C(CH_3)CO_2$Allyl], 118.6 ($CO_2CH_2CHCH_2$), 126.1 (*C*HCHN), 126.7, 127.9, 128.7, 136.6 (Ar*C*), 132.1 ($CO_2CH_2CHCH_2$), 135.4 (*C*HPh), 174.4 (CO_2Allyl), 178.0 (CO_2Me); MS (EI-GC) *m/z*: 369 (M^+, <1%), 310 (33), 243 (34), 185 (15), 184 (100), 115 (11); Microanalysis calculated for $C_{22}H_{27}NO_4$: C, 71.5; H, 7.4; N, 3.8%; found: C, 72.2; H, 7.1; N, 4.2%.

(3a*S,4*S**,8a*R**,8b*R**)-methyl 2-methyl-1,3-dioxo-4-(*(E)*-styryl)decahydropyrrolo[3,4-a]pyrrolizine-8a-carboxylate 3c:** Sticky brown oil IR (neat) ν_{max} 2360, 2341, 1699, 1265 cm^{-1}; ^{1}H NMR δ_H: 1.73-1.85, 1.95-2.08 (m, 2H, CH_2CH$_2$N), 2.31-2.40, 2.46-2.59 (m, 3H, CH_2CCO$_2$Me, C*H*HN), 2.97 (s, 3H, NCH_3), 3.08 (m, 1H, C*H*HN), 3.46 (deform. dd, *J* = 8.1 Hz, 1H, C*H*CHN), 3.81 (s, 3H, CO_2CH_3), 3.89 (d, *J* = 8.1 Hz, 1H, CHCCO$_2$Me), 4.20 (dd, *J* = 9.0, 8.1 Hz, 1H, CHN), 6.37 (dd, *J* = 15.6, 9.0 Hz, 1H, C*H*CHN), 6.76 (d, *J* = 15.6 Hz, 1H, C*H*Ph), 7.21-7.42 (m, 5H, Ar*H*); ^{13}C NMR δ_C: 25.0 (N*C*H$_3$), 25.3 (*C*H$_2$CH$_2$N), 30.3 (*C*H$_2$CCO$_2$Me), 48.3 (*C*H$_2$N), 51.2 (*C*HCCO$_2$Me), 52.3 (*C*HCHCCO$_2$Me), 53.2 (CCO$_2$*C*H$_3$), 64.6 (CHN), 78.9 (*C*CO$_2$CH$_3$), 123.4 (*C*HCHN), 126.9, 128.1, 128.6, 136.7 (Ar*C*), 135.9 (*C*HPh), 174.1, 176.7 (2xCON), 177.1 (CO$_2$Me); MS (EI-GC) *m/z*: 354 (M^+, <1%), 296 (25), 295 (100), 243 (30), 242 (10), 241 (10), 228 (11), 184 (13), 115 (12), 91 (11); Microanalysis calculated for $C_{20}H_{22}N_2O_4$: C, 67.8; H, 6.3; N, 7.9%; found: C, 68.2; H, 6.3; N, 8.0%.

(3a*S,4*S**,8a*R**,8b*R**)-methyl 2-methyl-1,3-dioxo-4-(*(E)*-styryl)decahydropyrrolo[3,4-a]pyrrolizine-8a-carboxylate 3c´:** Sticky brown oil; IR (neat) ν_{max} 2370, 2328, 1715 cm^{-1}; ^{1}H NMR δ_H: 1.83-2.02 (m, 3H, CH_2CH$_2$N, C*H*HCCO$_2$Me), 2.72-2.81(m, 1H, C*H*HCCO$_2$Me), 2.98 (s, 3H, NCH_3), 3.02-3.09 (m, 2H, CH_2N), 3.40 (d, *J* = 9.5 Hz, 1H, C*H*CCO$_2$Me), 3.56 (dd, *J* = 9.5, 7.5 Hz, 1H, C*H*CHN), 3.71 (s, 3H, CO_2CH_3), 4.42 (deform. dd, *J* = 7.5, 7.0 Hz, 1H, CHN), 6.32 (dd, *J* = 15.9, 7.0 Hz, 1H, C*H*CHN), 6.85 (d, *J* = 15.9 Hz, 1H, C*H*Ph), 7.22-7.42 (m, 5H, Ar*H*); ^{13}C NMR δ_C: 25.0 (N*C*H$_3$), 25.3 (*C*H$_2$CH$_2$N), 36.3 (*C*H$_2$CCO$_2$Me), 49.3 (*C*H$_2$N), 51.1 (*C*HCCO$_2$Me), 52.7 (*C*HCHCCO$_2$Me), 57.1 (CCO$_2$*C*H$_3$), 67.3 (CHN), 78.8 (*C*CO$_2$CH$_3$), 125.3 (*C*HCHN), 126.7, 128.1, 128.6, 136.3 (Ar*C*), 134.9 (*C*HPh), 172.1, 176.1 (2xCON), 176.3 (CO$_2$Me); MS (EI-GC) *m/z*: 354 (M^+, <1%), 296 (31), 295 (100), 243 (28), 242 (11), 228 (15), 184 (12), 183 (10), 115 (14); Microanalysis calculated for $C_{20}H_{22}N_2O_4$: C, 67.8; H, 6.3; N, 7.9%; found: C, 68.6; H, 6.5; N, 8.1%.

(1*R,2*R**,3*S**,7a*R**)-trimethyl 3-(*(E)*-styryl)hexahydro-*1H*-pyrrolizine-1,2,7a-tricarboxylate 3d:** Sticky yellow oil; IR (neat) ν_{max} 2965, 2915, 2306, 1715, 1713, 1699 cm^{-1}; ^{1}H NMR δ_H: 1.76–1.86 (m, 1H, C*H*HCH$_2$N), 1.93–2.03 (m, 1H, C*H*HCH$_2$N), 2.08–2.17 (m, 1H, C*H*HCCO$_2$Me), 2.52–2.61 (m, 1H, C*H*HCCO$_2$Me), 2.83 (deform. ddd, *J* = 10.8, 6.6, 6.5 Hz, 1H, C*H*HN), 3.09 (deform. ddd, *J* = 10.8, 6.6, 6.5 Hz, 1H, C*H*HN), 3.42 (d, *J* = 11.7 Hz, 1H, C*H*CCO$_2$Me), 3.58, 3.69 (s, 6H, 2xCHCO$_2$C*H*$_3$), 3.70 (s, 3H, CCO$_2$C*H*$_3$), 4.02 (dd, *J* = 11.7, 8.2 Hz, 1H, C*H*CHN), 4.28 (dd, *J* = 10.4, 8.2 Hz, 1H, C*H*N), 5.96 (dd, *J* = 15.5, 10.4 Hz, 1H, C*H*CHN), 6.56 (d, *J* = 15.5 Hz, 1H, C*H*Ph), 7.25-7.35 (m, 5H, Ar*H*); ^{13}C NMR δ_C: 27.6 (*C*H$_2$CH$_2$N), 35.8 (*C*H$_2$CCO$_2$Me), 48.8 (CH$_2$N), 52.1, 52.2 (2x*C*HCO$_2$Me), 52.4, 52.6, 53.6 (3xCO$_2$*C*H$_3$), 65.7 (CHN), 78.2 (*C*CO$_2$Me), 125.3 (*C*HCHN), 126.7, 128.2, 128.7, 136.3 (Ar*C*), 135.8 (*C*HPh), 171.1, 171.7 (2xCH*C*O$_2$Me), 174.1 (C*C*O$_2$Me); MS (EI-GC) *m/z*: 387 (M^+, <1%), 271 (19), 270 (100), 243 (13), 238 (21), 210 (17), 184 (40), 123 (10), 115 (10); Microanalysis calculated for $C_{21}H_{25}NO_6$: C, 65.1; H, 6.5; N, 3.6 %; found: C, 65.4; H, 7.0; N, 3.9%.

Electronic Supplementary Material (ESI) for Chemical Communications

(1*S,2*S**,3*S**,7a*R*)-methyl 2-nitro-1-phenyl-3-((*E*)-styryl)hexahydro-*1H*-pyrrolizine-7a-carboxylate 3e:** Sticky brown oil; IR (neat) ν_{max} 3003, 2983, 2872, 1726, 1536 cm^{-1}; ^1H NMR δ_H: 1.86–2.10 (m, 3H, C*H*$_2$C*H*$_2$N, C*H*HCCO$_2$Me), 2.68-2.76 (m, 1H, C*H*HCCO$_2$Me), 2.92 (ddd, *J* = 10.1, 6.7, 4.5 Hz, 1H, C*H*HN), 3.25 (ddd, *J* = 10.1, 7.5, 6.3 Hz, 1H, C*H*HN), 3.37 (s, 3H, CCO$_2$CH$_3$), 4.17 (d, *J* = 11.3 Hz, 1H, C*H*CCO$_2$Me), 4.79 (dd, *J* = 10.2, 7.9 Hz, 1H, C*H*N), 6.10 (dd, *J* = 11.3, 7.8 Hz, 1H, C*H*NO$_2$), 6.14 (dd, *J* = 15.5, 10.3 Hz, 1H, C*H*CHN), 6.72 (d, *J* = 15.5 Hz, 1H, C*H*Ph), 7.23-7.40 (m, 10H, Ar*H*); ^{13}C NMR δ_C: 27.4 (*C*H$_2$CH$_2$N), 35.5 (*C*H$_2$CCO$_2$Me), 48.6 (CH$_2$N), 52,1 (CCO$_2$*C*H$_3$), 55.4 (*C*HCCO$_2$CH$_3$), 66.2 (CHN), 80.5 (*C*CO$_2$Me), 91.9 (*C*HNO$_2$), 122.7 (*C*HCHN), 127.1, 127.3, 128.3, 128.6, 128.7, 128.9, 134.1, 135.8 (Ar*C*), 138.3 (*C*HPh), 173.6 (C*C*O$_2$Me); MS (EI-GC) *m/z*: 392 (M^+, <1%), 243 (11), 185 (14), 184 (100), 156 (16); HRMS calculated for $C_{23}H_{24}N_2O_4$+1: 393.1814 found: 393.1800.

(1*R,2*S**,3*S**,7a*R**)-methyl 1-nitro-2-phenyl-3-((E)-styryl)hexahydro-1H-pyrrolizine-7a-carboxylate 3e´:** Sticky brown oil; IR (neat) ν_{max} 3015, 2979, 2872, 1725, 1530 cm^{-1}; ^1H NMR δ_H: 1.57-1.63 (m, 1H, C*H*HCH$_2$N), 1.96-2.02 (m, 2H, C*H*HCH$_2$N, C*H*HCCO$_2$Me), 2.46-2.52 (m, 1H, C*H*HCCO$_2$Me), 3.03 (ddd, *J* = 10.8, 8.7, 6.1 Hz, 1H, C*H*HN), 3.13-3.19 (m, 1H, C*H*HN), 4.06 (dd, *J* = 11.6, 10.2 Hz, 1H, C*H*Ph), 4.23 (ddd, *J* = 11.6, 7.6, 0.5 Hz, 1H, C*H*N), 5.94 (d, *J* = 10.2 Hz, 1H, C*H*NO$_2$), 6.18 (dd, *J* = 15.9, 7.6 Hz, 1H, C*H*CHN), 6.44 (dd, *J* = 15.9, 0.5 Hz, 1H, C*H*Ph), 7.24-7.40 (m, 10H, Ar*H*); ^{13}C NMR δ_C: 26.0 (*C*H$_2$CH$_2$N), 32.1 (*C*H$_2$CCO$_2$Me), 50.7 (CH$_2$N), 51.0 (CCO$_2$*C*H$_3$), 53.6 (*C*HPh), 67.8 (CHN), 76.2 (*C*CO$_2$Me), 97.1 (*C*HNO$_2$), 123.8 (*C*HCHN), 126.6, 127.9, 128.0, 128.2, 128.7, 129.2, 136.1, 136.2 (Ar*C*), 136.4 (*C*HPh), 173.5 (C*C*O$_2$Me); MS (EI-GC) *m/z*: 392 (M^+, <1%), 243 (10), 185 (15), 184 (100), 156 (17), 115 (10); HRMS calculated for $C_{23}H_{24}N_2O_4$+1: 393.1814 found: 393.1806.

(1*R,2*R**,3*S**,7a*S**)-methyl 1,2-bis(phenylsulfonyl)-3-((*E*)-styryl)hexahydro-*1H*-pyrrolizine-7a-carboxylatetricarboxylate 3f:** Sticky pale yellow oil; IR (neat) ν_{max} 2991, 2934, 1708, 1310, 1141 cm^{-1}; ^1H NMR δ_H: 1.99–2.05 (m, 2H, C*H*$_2$CH$_2$N), 2.14-2.22 (m, 1H, C*H*HCCO$_2$Me), 3.03-3.07 (m, 1H, C*H*HCCO$_2$Me), 3.14-3.21 (m, 1H, C*H*HN), 3.32-3.38 (m, 1H, C*H*HN), 3.87 (s, 3H, CCO$_2$CH$_3$), 4.51 (d, *J* = 8.1 Hz, 1H, C*H*CCO$_2$Me), 4.71 (dd, *J* = 10.0, 8.2 Hz, 1H, CHN), 5.04 (deform. dd, *J* = 8.2, 8.1 Hz, 1H, CHN), 6.20 (d, *J* = 15.7 Hz, 1H, C*H*Ph), 6.47 (dd, *J* = 15.7, 10.0 Hz, 1H, C*H*CHN), 7.13-8.04 (m, 15H, Ar*H*); ^{13}C NMR δ_C: 25.6 (*C*H$_2$CH$_2$N), 35.1 (*C*H$_2$CCO$_2$Me), 49.1 (CH$_2$N), 53.1 (CHCO$_2$*C*H$_3$), 65.7 (CHN), 73.7 [*C*H(SO$_2$Ph)CH], 74.5 [*C*H(SO$_2$Ph)CCO$_2$Me], 78.8 (*C*CO$_2$Me), 122.7 (*C*HCHN), 126.9, 128.3, 128.6, 128.9, 129.0, 129.6, 133.6, 133.9, 134.5, 135.9, 139.2, 141.5 (Ar*C*), 136.7 (*C*HPh), 170.9 (C*C*O$_2$Me); MS (EI-GC) *m/z*: 493 (10), 492 (11), 410 (10), 310 (11), 244 (31), 243 (100), 128 (15), 115 (17); HRMS calculated for $C_{29}H_{29}NO_6S_2$ +1: 552.1514 found: 552.1548.

(1*S,2*S**,3*S**,7a*S**)-methyl 1,2-bis(phenylsulfonyl)-3-((*E*)-styryl)hexahydro-1H-pyrrolizine-7a-carboxylatetricarboxylate 3f´:** Sticky yellow oil; IR (neat) ν_{max} 2979, 2910, 1715, 1300, 1148 cm^{-1}; ^1H NMR δ_H: 2.02–2.17 (m, 3H, C*H*$_2$CH$_2$N, C*H*HCCO$_2$Me), 2.94-3.16 (m, 3H, C*H*HCCO$_2$Me, C*H*$_2$N), 3.83 (s, 3H, CCO$_2$CH$_3$), 4.03 (deform dd, *J* = 4.3, 4.1 Hz, 1H, C*H*(SO$_2$Ph)CH), 4.38 (dd, *J* = 8.4, 4.3 Hz, 1H, CHN), 5.06 (d, *J* = 4.1 Hz, 1H, C*H*(SO$_2$Ph)CCO$_2$Me), 6.13-6.24 (m, 2H, C*H*CHN, C*H*Ph), 7.14-7.90 (m, 15H, Ar*H*); ^{13}C NMR δ_C: 26.4 (*C*H$_2$CH$_2$N), 32.4 (*C*H$_2$CCO$_2$Me), 47.2 (CH$_2$N), 53.3 (CHCO$_2$*C*H$_3$), 64.7 (CHN), 66.9 [*C*H(SO$_2$Ph)CH], 71.7 [*C*H(SO$_2$Ph)CCO$_2$Me], 79.8 (*C*CO$_2$Me), 125.9 (*C*HCHN), 126.7, 128.2,

Electronic Supplementary Material (ESI) for Chemical Communications

128.6, 128.9, 128.9, 129.3, 129.3, 134.2, 134.3, 135.7, 137.0, 138.5 (Ar*C*), 135.2 (*C*HPh), 173.9 (CCO_2Me); MS (EI-GC) *m/z*: 551 (M^+, <1%), 492 (15), 410 (10), 311 (10), 310 (10), 244 (25), 243 (100), 128 (11), 115 (21); HRMS calculated for $C_{29}H_{29}NO_6S_2$ +1: 552.1514 found: 552.1565.

(2*S,3*S**,7a*R**)-dimethyl 3-((*E*)-prop-1-en-1-yl)hexahydro-*1H*-pyrrolizine-2,7a-dicarboxylatetricarboxylate 3g:** Sticky brown oil; IR (neat) ν_{max} 2985, 2939, 2305, 1714, 1691 cm^{-1}; ^{1}H NMR δ_H: 1.69 (d, *J* = 6.5 Hz, 3H, CHC*H*$_3$), 1.71–1.85 (m, 3H, C*H*$_2$CH$_2$N, C*H*HCCO$_2$Me), 2.02-2.12 (m, 1H, C*H*HCO$_2$Me), 2.20-2.23 (m, 1H, C*H*HCHCO$_2$Me), 2.55 (dd, *J* = 13.2, 6.7 Hz, 1H, C*H*HCHCO$_2$Me), 2.79-2.87 (m, 1H, C*H*HN), 3.02-3.07 (m, 1H, C*H*HN), 3.41 (deform. ddd, *J* = 12.7, 7.5, 6.7 Hz, 1H, C*H*CO$_2$Me), 3.61 (s, 3H, CHCO$_2$C*H*$_3$), 3.72 (s, 3H, CCO$_2$C*H*$_3$), 3.99 (dd, *J* = 10.3, 7.5 Hz, 1H, C*H*N), 5.25 (dd, *J* = 15.0, 10.3 Hz, 1H, C*H*CHN), 5.68 (dq, *J* = 15.0, 6.5 Hz, 1H, C*H*Me); ^{13}C NMR δ_C: 17.9 (CH*C*H$_3$), 27.6 (*C*H$_2$CH$_2$N), 36.4 (*C*H$_2$CHCO$_2$Me), 37.1 (*C*H$_2$CCO$_2$Me), 48.6 (CH$_2$N), 49.8 (*C*HCO$_2$Me), 51.7 (CHCO$_2$C*H*$_3$), 52.6 (CCO$_2$C*H*$_3$), 67.3 (CHN), 76.3 (*C*CO$_2$Me), 126.8 (*C*HCHN), 132.1 (*C*HMe), 172.5 (CH*C*O$_2$Me), 177.0 (C*C*O$_2$Me); MS (EI-GC) *m/z*: 267 (M^+, <1%), 208 (100), 207 (10), 181 (25), 59 (10); Microanalysis calculated for $C_{14}H_{21}NO_4$: C, 62.9; H, 7.9; N, 5.2%; found: C, 63.3; H, 7.4; N, 5.4%.

(2*S,3*R**,7a*R**)-dimethyl 3-phenylhexahydro-*1H*-pyrrolizine-2,7a-dicarboxylate 3h:** Sticky colorless oil; IR (neat) ν_{max} 2900, 1718, 1687 cm^{-1}; ^{1}H NMR δ_H: 1.81–2.00 (m, 3H, C*H*$_2$CH$_2$N, C*H*HCCO$_2$Me), 2.34-2.43 (m, 2H, C*H*HCCO$_2$Me, C*H*HCHCO$_2$Me), 2.54-2.61 (m, 1H, C*H*HCHCO$_2$Me), 2.64-2.76 (m, 2H, CH$_2$N), 3.23 (s, 3H, CHCO$_2$C*H*$_3$), 3.76 (s, 3H, CCO$_2$C*H*$_3$), 3.88 (ddd, *J* = 13.0, 8.8, 7.4 Hz, 1H, CHCO$_2$Me), 4.73 (d, *J* = 8.8 Hz, 1H, CHN), 7.15-7.17, 7.25-7.28 (m, 5H, Ar*H*); ^{13}C NMR δ_C: 28.3 (*C*H$_2$CH$_2$N), 36.3 (*C*H$_2$CHCO$_2$Me), 36.7 (*C*H$_2$CCO$_2$Me), 47.2 (CH$_2$N), 51.4 (*C*HCO$_2$Me), 52.7 (CHCO$_2$C*H*$_3$), 52.5 (CCO$_2$C*H*$_3$), 67.3 (CHN), 76.1 (*C*CO$_2$Me), 127.9, 128.2, 129.3, 138.0 (Ar*C*), 172.2 (CH*C*O$_2$Me), 177.3 (C*C*O$_2$Me); MS (EI-GC) *m/z*: 303 (M^+, <1%), 245 (11), 244 (100), 226 (21), 218 (10), 217 (17), 185 (26), 77 (15); HRMS calculated for $C_{17}H_{21}NO_4$ +1: 304.1549 found: 304.1553.

***(*3*R**,7a*R**)-dimethyl 3-phenylhexahydro-*1H*-pyrrolizine-1,7a-dicarboxylate 3h´:** Sticky colorless oil; IR (neat) ν_{max} 2935, 2903, 1720, 1705 cm^{-1}; ^{1}H NMR δ_H: 1.37–1.48 (m, 1H, C*H*HCCO$_2$Me), 1.65-1.86 (m, 2H, C*H*$_2$CH$_2$N), 2..18 (ddd, *J* = 12.1, 6.7, 4.1 Hz, 1H, C*H*HCHPh), 2.26-2.34 (m, 1H, C*H*HCCO$_2$Me), 2.41-2.55 (m, 3H, C*H*HCHPh, C*H*$_2$N), 3.72 (s, 3H, CHCO$_2$C*H*$_3$), 3.82 (s, 3H, CCO$_2$C*H*$_3$), 3.80 (dd, *J* = 12.1, 6.7 Hz, 1H, CHCO$_2$Me), 4.49 (dd, *J* = 12.8, 4.0 Hz, 1H, CHN), 7.27-7.45 (m, 5H, Ar*H*); ^{13}C NMR δ_C: 25.8 (*C*H$_2$CH$_2$N), 29.2 (*C*H$_2$CHPh), 33.0 (*C*H$_2$CCO$_2$Me), 50.7 (CH$_2$N), 51.0 (*C*HCO$_2$Me), 52.0 (CHCO$_2$C*H*$_3$), 52.9 (CCO$_2$C*H*$_3$), 64.8 (CHN), 76.4 (*C*CO$_2$Me), 127.7, 128.3, 128.9, 137.7 (Ar*C*), 173.1 (CH*C*O$_2$Me), 175.5 (C*C*O$_2$Me); MS (EI-GC) *m/z*: 303 (M^+, <1%), 245 (10), 244 (100), 243 (10), 227 (10), 226 (23), 217 (14), 185 (15), 77 (13); HRMS calculated for $C_{17}H_{21}NO_4$ +1: 304.1549 found: 304.1592.

(2*S,3*S**,7a*R**)-dimethyl 3-isobutylhexahydro-*1H*-pyrrolizine-2,7a-dicarboxylate 3i:** colorless oil; R_f 0.29 (*n*-hexane/ethyl acetate 7/3); IR (neat) ν_{max} 2986, 2956, 2903, 1716, 1700 cm^{-1}; ^{1}H NMR δ_H: 0.93 [d, 6H, *J* = 6.0 Hz, CH(C*H*$_3$)$_2$], 1.35-1.41 [m, 2H, C*H*HCH$_2$N, C*H*(CH$_3$)$_2$], 1.52-1.62 (m, 1H, C*H*HCH$_2$N), 1.74-1.83, 1.87-1.94 (m, 2H, C*H*$_2$CCO$_2$Me), 2.22 (dd, *J* = 13.7, 5.4 Hz, 1H, C*H*HCHCO$_2$Me), 2.41 (ddd, *J* = 12.6, 8.4, 4.0 Hz, 1H, C*H*HCHCO$_2$Me), 2.57 (dd, *J* = 13.7, 9.1 Hz, 1H, C*H*HCHCO$_2$Me), 2.92-3.15 (m, 3H, C*H*N, C*H*HN, C*H*CO$_2$Me), 3.68 (s, 3H, CHCO$_2$CH$_3$), 3.73 (s, 3H, CCO$_2$CH$_3$); ^{13}C NMR δ_C: 22.9 [CH(*C*H$_3$)$_2$], 25.0 (*C*H$_2$CH$_2$N), 26.1

Electronic Supplementary Material (ESI) for Chemical Communications

[*C*H(CH_3)$_2$], 35.8 (*C*H_2CHN) 37.8 (*C*H_2CCO$_2$Me), 39.7 (C*H*$_2$CHCO$_2$Me), 47.4 (CH_2N), 48.6 (CHCO$_2$*C*H$_3$), 51.5 (CCO$_2$*C*H$_3$), 52.9 (*C*HCO$_2$Me), 62.9 (CHN), 76.1 (*C*CO$_2$Me), 176.2 (CH*C*O$_2$Me), 176.3 (C*C*O$_2$Me); MS (EI-GC) *m/z*: 283 (M^+, <1%), 225 (15), 224 (100), 198 (14), 197 (35), 165 (21), 128 (11), 127 (10); Microanalysis calculated for $C_{15}H_{25}NO_4$: C, 63.6; H, 8.9; N, 4.9%; found: C, 63.5; H, 8.4; N, 5.1%.

(1*S,3*R**,7a*R**)-3-ethyl 1,7a-dimethyl hexahydro-*1H*-pyrrolizine-1,3,7a-tricarboxylate 3j:** Sticky yellow oil; IR (neat) ν_{max} 2991, 2910, 1714, 1711, 1699 cm^{-1}; ^{1}H NMR δ_H: 1.30 (t, *J* = 7.1 Hz, 3H, CO$_2$CH$_2$C*H*$_3$), 1.41 (ddd, *J* = 12.7, 11.4, 7.6 Hz, 1H, C*H*HCCO$_2$Me), 1.80-1.90 (m, 2H, CH_2N), 2.15 (ddd, *J* = 12.7, 7.0, 4.8 Hz, 1H, C*H*HCHCO$_2$Et), 2.32-2.47 (m, 2H, C*H*HCHCO2Et, C*H*HCCO$_2$Me), 2.52-2.61 (m, 1H, C*H*HN), 3.11-3.16 (m, 1H, C*H*HN), 3.59 (dd, *J* = 12.2, 7.0 Hz, 1H, CHCO$_2$Me), 3.69 (s, 3H, CHCO$_2$C*H*$_3$), 3.76 (s, 3H, CCO$_2$C*H*$_3$), 4.00 (dd, *J* = 12.2, 4.8 Hz, 1H, CHCO$_2$Et), 4.24 (q, *J* = 7.1 Hz, 2H, CO$_2$C*H*$_2$CH$_3$); ^{13}C NMR δ_C: 14.3 (CO$_2$CH$_2$*C*H$_3$), 26.0 (*C*H$_2$CH$_2$N), 28.8 (*C*H$_2$CHCO$_2$Et), 32.4 (*C*H$_2$CCO$_2$Me), 50.3 (*C*HCO$_2$Me), 51.4 (CO$_2$*C*H$_2$CH$_3$), 52.1 (CHCO$_2$*C*H$_3$), 52.9 (CCO$_2$*C*H$_3$), 61.3 (CH_2N), 64.7 (CHN), 76.7 (*C*CO$_2$Me), 169.9, 172.3, 174.7 (2x*C*O$_2$Me, *C*O$_2$Et); MS (EI-GC) *m/z*: 299 (M^+, <1%), 241 (14), 240 (100), 226 (21), 212 (23), 166 (10), 108 (21); HRMS calculated for $C_{23}H_{24}N_2O_4$ +1: 300.1447 found: 300.1451.

(2*S*,3*S*,6*R*,7a*S*)-dimethyl 6-hydroxy-3-((*E*)-styryl)hexahydro-*1H*-pyrrolizine-2,7a-dicarboxylate 4a: Brown needles, mp: 99-102ºC; $[\alpha]_D^{20}$ = +81.2º (*c* 1, CH_2Cl_2), IR (neat) ν_{max} 3322, 2950, 2305, 1715, 1707 cm^{-1}; ^{1}H NMR δ_H: 1.97 (dd, *J* = 13.5, 4.8 Hz, 1H, C*H*HCCO$_2$Me), 2.42 (deform. dd, *J* = 12.9, 12.3 Hz, 1H, C*H*HCHCO$_2$Me), 2.54-2.61 (m, 2H, C*H*HCHCO$_2$Me, C*H*HCCO$_2$Me), 3.07-3.16 (m, 2H, C*H*$_2$N), 3.50-3.56 (m, 4H, C*H*CO$_2$Me, CHCO$_2$C*H*$_3$), 3.73 (s, 3H, CCO$_2$CH$_3$), 4.21 (dd, *J* = 10.3, 7.8 Hz, 1H, CHN), 4.56 (deform. dddd, *J* = 5.1, 5.0, 4.8, 4.7 Hz, 1H, C*H*OH), 6.23 (dd, *J* = 15.5, 10.4 Hz, 1H, C*H*CHN), 6.51 (d, *J* = 15.5 Hz, 1H, C*H*Ph), 7.23-7.38 (m, 5H, Ar*H*); ^{13}C NMR δ_C: 36.9 (*C*H$_2$CCO$_2$Me), 45.0 (*C*H$_2$CHCO$_2$Me), 50.5 (*C*HCO$_2$Me), 51.9 (CCO$_2$*C*H$_3$), 52.7 (*C*HCO$_2$Me), 56.2 (CH_2N), 66.9 (CHN), 74.2 (CHOH), 75.9 (*C*CO$_2$Me), 126.7, 128.0, 128.7, 136.7 (Ar*C*), 127.5 (*C*HCHN), 136.7 (*C*HPh), 172.4 (CH*C*O$_2$Me), 176.5 (C*C*O$_2$Me); MS (EI-GC) *m/z*: 345 (M^+, <1%), 269 (11), 268 (100), 243 (11), 241 (15), 209 (15), 126 (11), 105 (13); Microanalysis calculated for $C_{19}H_{23}NO_5$: C, 66.1; H, 6.7; N, 4.1%; found: C, 66.5; H, 7.0; N, 4.3%.

(2*R*,3*R*,6*R*,7a*R*)-dimethyl 6-hydroxy-3-((*E*)-styryl)hexahydro-*1H*-pyrrolizine-2,7a-dicarboxylate 4a´: Brown needles, mp: 95-97ºC; $[\alpha]_D^{20}$ = +34.7º (*c* 1, CH_2Cl_2); IR (neat) ν_{max} 3396, 2944, 2315, 1717, 1698 cm^{-1}; ^{1}H NMR δ_H: 2.06 (dd, *J* = 14.0, 6.1 Hz, 1H, C*H*HCCO$_2$Me), 2.24 (dd, *J* = 13.4, 11.7 Hz, 1H, C*H*HCHCO$_2$Me), 2.50 (dd, *J* = 14.0, 1.8 Hz, 1H, C*H*HCCO$_2$Me), 2.63 (dd, *J* = 13.4, 7.0 Hz, 1H, C*H*HCHCO$_2$Me), 2.92 (dd, *J* = 11.7, 2.5 Hz, 1H, C*H*HN), 3.50-3.53 (m, 4H, C*H*CO$_2$Me, CHCO$_2$C*H*$_3$), 3.76 (s, 3H, CCO$_2$CH$_3$), 4.16 (dd, *J* = 10.4, 7.4 Hz, 1H, CHN), 4.44 (m, 1H, C*H*OH), 5.87 (dd, *J* = 15.6, 10.4 Hz, 1H, C*H*CHN), 6.57 (d, *J* = 15.5 Hz, 1H, C*H*Ph), 7.27-7.31 (m, 5H, Ar*H*); ^{13}C NMR δ_C: 36.9 (*C*H$_2$CCO$_2$Me), 46.5 (*C*H$_2$CHCO$_2$Me), 50.7 (*C*HCO$_2$Me), 52.0 (CCO$_2$*C*H$_3$), 53.0 (*C*HCO$_2$Me), 57.0 (CH_2N), 66.5 (CHN), 75.0 (CHOH), 75.5 (*C*CO$_2$Me), 125.3 (*C*HCHN), 126.7, 128.2, 128.8, 136.3 (Ar*C*), 136.0 (*C*HPh), 172.3 (CH*C*O$_2$Me), 177.3 (C*C*O$_2$Me); MS (EI-GC) *m/z*: 345 (M^+, <1%), 269 (13), 268 (100), 243 (10), 241 (31), 209 (22), 105 (11), 59 (10); Microanalysis calculated for $C_{19}H_{23}NO_5$: C, 66.1; H, 6.7; N, 4.1%; found: C, 66.4; H, 6.9; N, 4.1%.

Electronic Supplementary Material (ESI) for Chemical Communications

(2*S*,3*S*,6*R*,7a*S*)-dimethyl 6-((*tert*-butyldimethylsilyl)oxy)-3-((*E*)-styryl)hexahydro-*1H*-pyrrolizine-2,7a-dicarboxylate 4b: Sticky orange oil; $[\alpha]_D^{20} = +4.2^o$ (*c* 1, CH_2Cl_2); IR (neat) ν_{max} 3396, 2944, 2315, 1717, 1698 cm^{-1}; ^1H NMR δ_H: -0.04 (s, 6H, OTBS), 0.81 (s, 9H, OTBS), 1.95 (dd, *J* = 13.0, 6.0 Hz, 1H, C*H*HCCO$_2$Me), 2.28 (deform. dd, *J* = 13.2, 13.0 Hz, 1H, C*H*HCHCO$_2$Me), 2.40-2.51 (m, 2H, C*H*HCHCO$_2$Me, C*H*HCCO$_2$Me), 2.8 (dd, *J* = 11.6, 4.7 Hz, 1H, C*H*HN), 3.20 (dd, *J* = 11.6, 5.4 Hz, 1H, C*H*HN), 3.49-3.56 (m, 4H, C*H*CO$_2$Me, CHCO$_2$C*H*$_3$), 3.74 (s, 3H, CCO$_2$CH$_3$), 4.18 (dd, *J* = 10.5, 7.2 Hz, 1H, CHN), 4.56 (deform. dddd, *J* = 6.0, 5.4, 5.3, 4.7 Hz, 1H, C*H*OH), 5.85 (dd, *J* = 15.6, 10.5 Hz, 1H, C*H*CHN), 6.54 (d, *J* = 15.6 Hz, 1H, C*H*Ph), 7.24-7.30 (m, 5H, Ar*H*); ^{13}C NMR δ_C: -4.8, -4.9 (OTBS), 18.2 (OTBS), 25.9 (OTBS), 37.5 (*C*H$_2$CCO$_2$Me), 46.4 (*C*H$_2$CHCO$_2$Me), 49.4 (*C*HCO$_2$Me), 51.9 (CCO$_2$*C*H$_3$), 52.7 (*C*HCO$_2$Me), 56.3 (CH$_2$N), 66.9 (CHN), 74.5 (CHOH), 74.7 (*C*CO$_2$Me), 125.4 (*C*HCHN), 126.7, 128.2, 128.7, 136.4 (Ar*C*), 136.0 (*C*HPh), 171.9 (CH*C*O$_2$Me), 176.9 (C*C*O$_2$Me); MS (EI-GC) *m/z*: 459 (M^+, <1%), 327 (10), 268 (100), 267 (11), 243 (15), 242 (10), 241 (21), 209 (17), 208 (10), 106 (10), 105 (10); HRMS calculated for $C_{25}H_{37}NO_5Si$ +1: 460.2519 found: 460.2522.

(2*S*,3*S*,6*R*,7a*S*)-2-*tert*-butyl 7a-methyl 6-hydroxy-3-((*E*)-styryl)hexahydro-*1H*-pyrrolizine-2,7a-dicarboxylate 4c: Sticky yellow oil; $[\alpha]_D^{20} = -124.7^o$ (*c* 1, CH_2Cl_2); IR (neat) ν_{max} 2985, 2939, 2305, 1714, 1691 cm^{-1}; ^1H NMR δ_H: 1.26 [s, 1H, CO$_2$C(C*H*$_3$)$_3$], 1.94 (dd, *J* = 13.4, 5.1 Hz, 1H, C*H*HCCO$_2$Me), 2.37 (deform. dd, *J* = 12.6, 12.3 Hz, 1H, C*H*HCHCO$_2$Bu^t), 2.50-2.59 (m, 2H, C*H*HCHCO$_2$Bu^t, C*H*HCCO$_2$Me), 3.08-3.15 (m, 2H, C*H*$_2$N), 3.44 (ddd, *J* = 12.3, 7.5, 6.7 Hz, 1H, C*H*CO$_2$Bu^t), 3.72 (s, 3H, CCO$_2$C*H*$_3$), 4.16 (dd, *J* = 10.4, 7.5 Hz, 1H, CHN), 4.54 (deform. dddd, *J* = 5.5, 5.3, 5.1, 4.9 Hz, 1H, C*H*OH), 6.24 (dd, *J* = 15.6, 10.4 Hz, 1H, C*H*CHN), 6.51 (d, *J* = 15.6 Hz, 1H, C*H*Ph), 7.20-7.38 (m, 5H, Ar*H*); ^{13}C NMR δ_C: 28.2 [CO$_2$C(C*H*$_3$)$_3$], 36.9 (*C*H$_2$CCO$_2$Me), 45.2 (*C*H$_2$CHCO$_2$Bu^t), 51.2 (CCO$_2$*C*H$_3$), 52.6 (*C*HCO$_2$Bu^t), 56.0 (CH$_2$N), 66.9 (CHN), 74.3 (CHOH), 75.7 (*C*CO$_2$Me), 80.9 [CO$_2$*C*(CH$_3$)$_3$], 126.7, 127.9, 128.7, 136.6 (Ar*C*), 127.7 (*C*HCHN), 134.9 (*C*HPh), 171.1 (CH*C*O$_2$Bu^t), 176.7 (C*C*O$_2$Me); MS (EI-GC) *m/z*: 387 (M^+, <1%), 369 (11), 329 (10), 310 (15), 268 (30), 209 (100), 241 (11), 240 (17), 105 (12);Microanalysis calculated for $C_{22}H_{29}NO_5$: C, 68.2; H, 7.5; N, 3.6%; found: C, 68.5; H, 7.3; N, 3.7%.

(2*R*,3*R*,6*R*,7a*R*)-2-*tert*-butyl 7a-methyl 6-hydroxy-3-((*E*)-styryl)hexahydro-*1H*-pyrrolizine-2,7a-dicarboxylate 4c´: Sticky brown oil; $[\alpha]_D^{20} = +43.3^o$ (*c* 1, CH_2Cl_2); IR (neat) ν_{max} 3002, 2955, 2315, 1721, 1708 cm^{-1}; ^1H NMR δ_H: 1.30 [s, 1H, CO$_2$C(C*H*$_3$)$_3$], 2.03 (dd, *J* = 13.9, 6.1 Hz, 1H, C*H*HCCO$_2$Me), 2.16 (dd, *J* = 13.4, 11.9 Hz, 1H, C*H*HCHCO$_2$ Bu^t), 2.49 (dd, *J* = 14.0, 2.0 Hz, 1H, C*H*HCCO$_2$Me), 2.58 (dd, *J* = 13.4, 6.9 Hz, 1H, C*H*HCHCO$_2$Bu^t), 2.91 (dd, *J* = 11.7, 2.5 Hz, 1H, C*H*HN), 3.37 (dd, *J* = 11.7, 5.4 Hz, 1H, C*H*HN), 3.49 (dd, *J* = 11.9, 7.4 Hz, 1H, C*H*CO$_2$Bu^t), 3.78 (s, 3H, CCO$_2$CH$_3$), 4.11 (dd, *J* = 10.4, 7.4 Hz, 1H, CHN), 4.40 (m, 1H, C*H*OH), 5.88 (dd, *J* = 15.6, 10.4 Hz, 1H, C*H*CHN), 6.57 (d, *J* = 15.5 Hz, 1H, C*H*Ph), 7.26-7.37 (m, 5H, Ar*H*); ^{13}C NMR δ_C: 28.2 [CO$_2$C(C*H*$_3$)$_3$], 36.8 (*C*H$_2$CCO$_2$Me), 46.5 (*C*H$_2$CHCO$_2$Bu^t), 51.4 (CCO$_2$*C*H$_3$), 53.0 (*C*HCO$_2$Bu^t), 57.1 (CH$_2$N), 66.6 (CHN), 75.2 (CHOH), 75.5 (*C*CO$_2$Me), 81.1 [CO$_2$*C*(CH$_3$)$_3$], 125.7 (*C*HCHN), 126.7, 128.2, 128.8, 136.0 (Ar*C*), 136.3 (*C*HPh), 171.0 (CH*C*O$_2$Bu^t), 176.5 (C*C*O$_2$Me); MS (EI-GC) *m/z*: 387 (M^+, <1%), 369 (10), 329 (10), 328 (11), 311 (15), 310 (13), 209 (100), 241 (13), 240 (21), 105 (10); Microanalysis calculated for $C_{22}H_{29}NO_5$: C, 68.2; H, 7.5; N, 3.6%; found: C, 68.6; H, 7.4; N, 3.5%.

Electronic Supplementary Material (ESI) for Chemical Communications

(3a*S*,4*S*,7*R*,8a*R*,8b*R*)-methyl 7-hydroxy-2-methyl-1,3-dioxo-4-((*E*)-styryl)decahydropyrrolo[3,4-a]pyrrolizine-8a-carboxylate 4d: Sticky yellow oil; $[\alpha]_D^{20} = -78.1^{o}$ (*c* 1, CH_2Cl_2); IR (neat) ν_{max} 3005, 2980, 2305, 1714, 1710, 1698 cm^{-1}; ^1H NMR δ_H: 2.31-2.41 (m, 1H, C*H*HCCO$_2$Me), 2.71-2.83 (m, 3H, C*H*HCCO$_2$Me, C*H*$_2$N), 2.97 (s, 3H, NCH$_3$), 3.52 (deform. dd, *J* = 8.5, 8.1 Hz, 1H, C*H*CON), 3.85 (s, 3H, CO$_2$CH$_3$), 3.95 (d, *J* = 8.1 Hz, 1H, CHCCO$_2$Me), 4.21 (deform. dd, *J* = 9.1, 8.5 Hz, 1H, C*H*N), 4.36 (m, 1H, CHOH), 6.23 (dd, *J* = 15.6, 9.1 Hz, 1H, C*H*CHN), 6.76 (d, *J* = 15.6 Hz, 1H, C*H*Ph), 7.26-7.40 (m, 5H, Ar*H*); ^{13}C NMR δ_C: 26.1 (NC*H*$_3$), 37.3 (*C*H$_2$CCO$_2$Me), 52.3, 53.1, (2x*C*HCON), 54.4 (CCO$_2$*C*H$_3$), 55.1 (*C*H$_2$N), 65.7 (CHN), 75.3 (CHOH), 77.9 (*C*CO$_2$CH$_3$), 125.3 (*C*HCHN), 126.9, 128.2, 128.7, 135.7 (Ar*C*), 136.0 (*C*HPh), 176.2, 176.3 (2xCON), 177.1 (*C*O$_2$Me); MS (EI-GC) *m/z*: 370 (M^+, <1%), 352 (10), 312 (10), 293 (100), 243 (21), 210 (12), 182 (40), 115 (10); HRMS calculated for $C_{20}H_{22}N_2O_5$ +1: 371.1607 found: 371.1621.

5. NMR spectra

Electronic Supplementary Material (ESI) for Chemical Communications

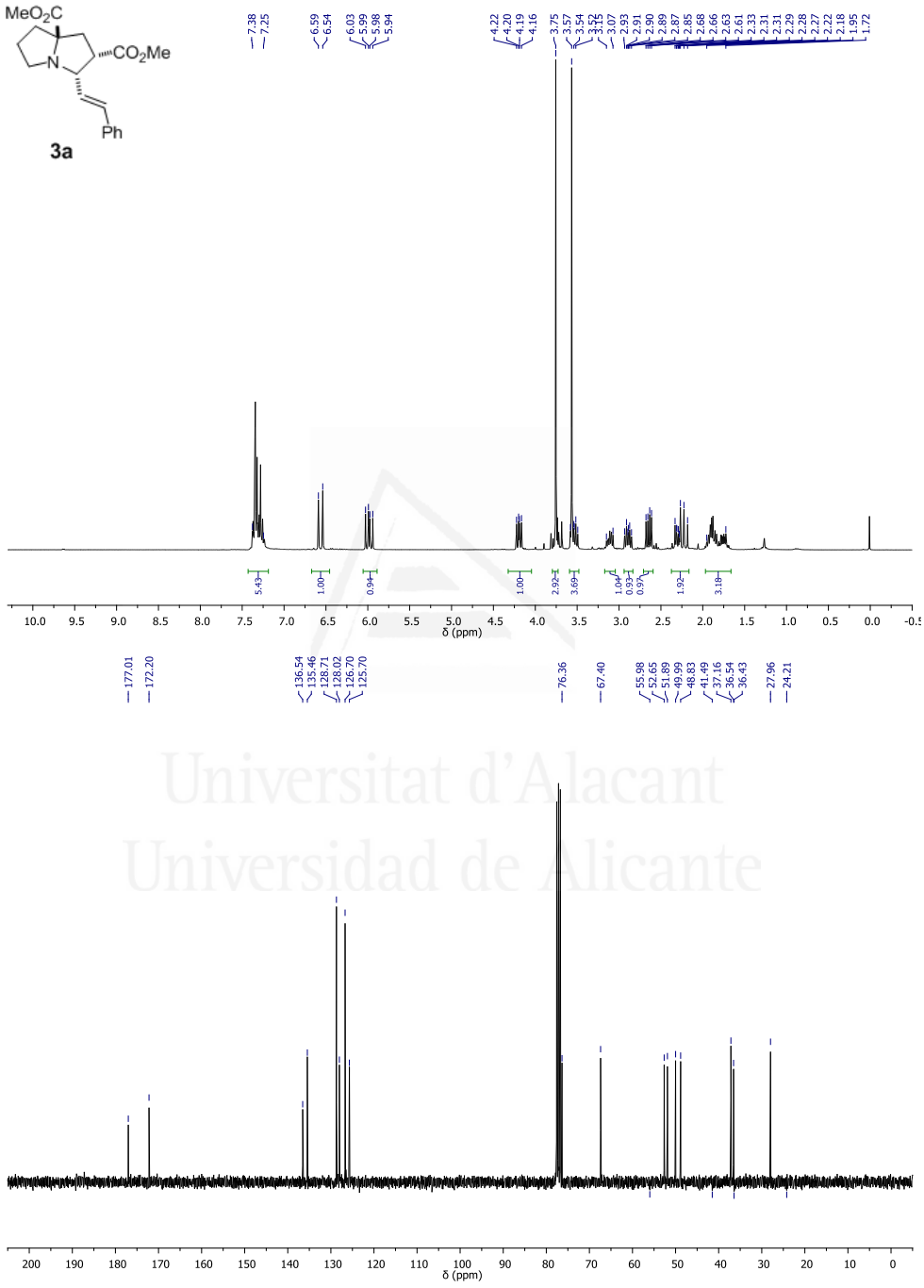

Electronic Supplementary Material (ESI) for Chemical Communications

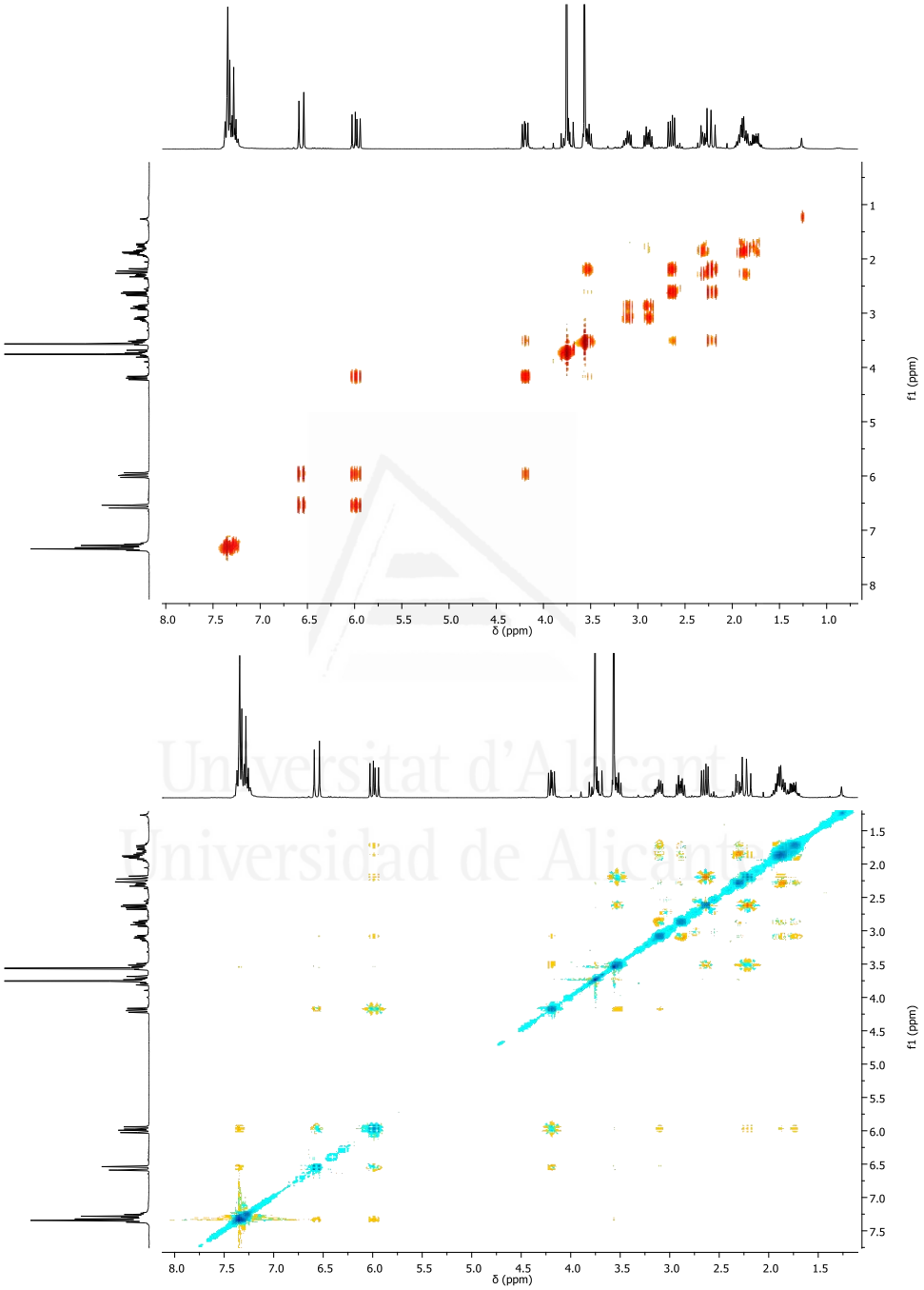

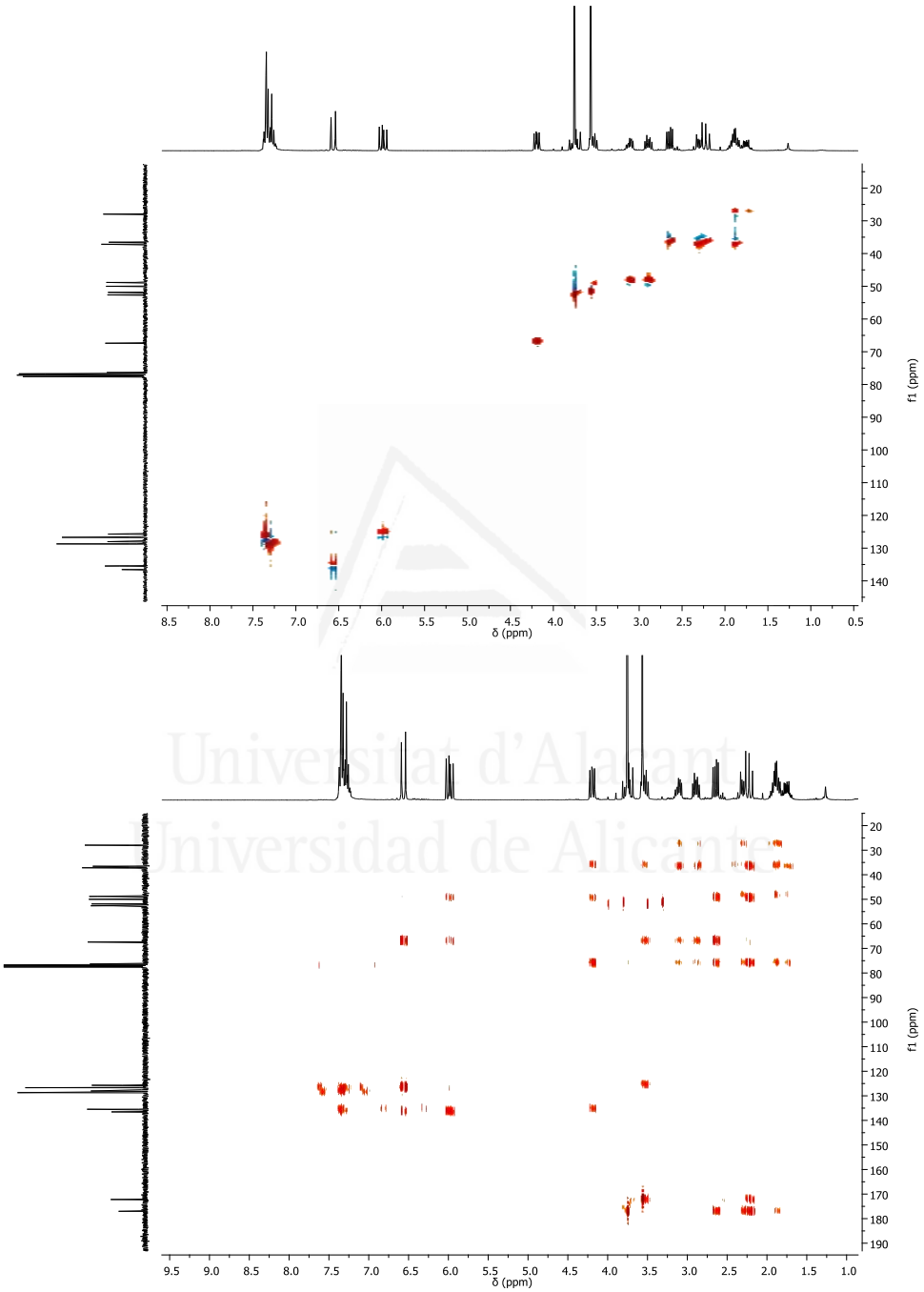

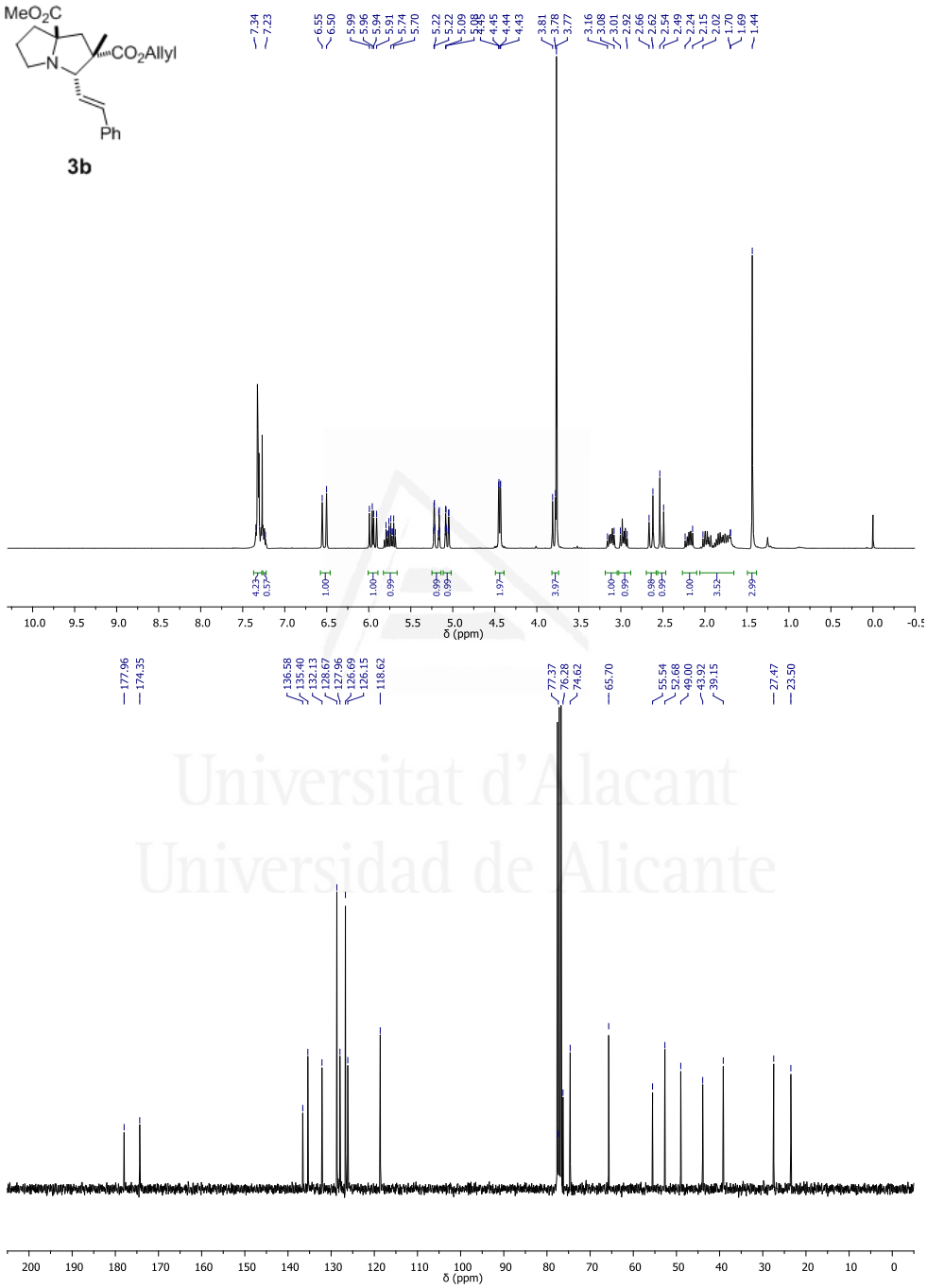

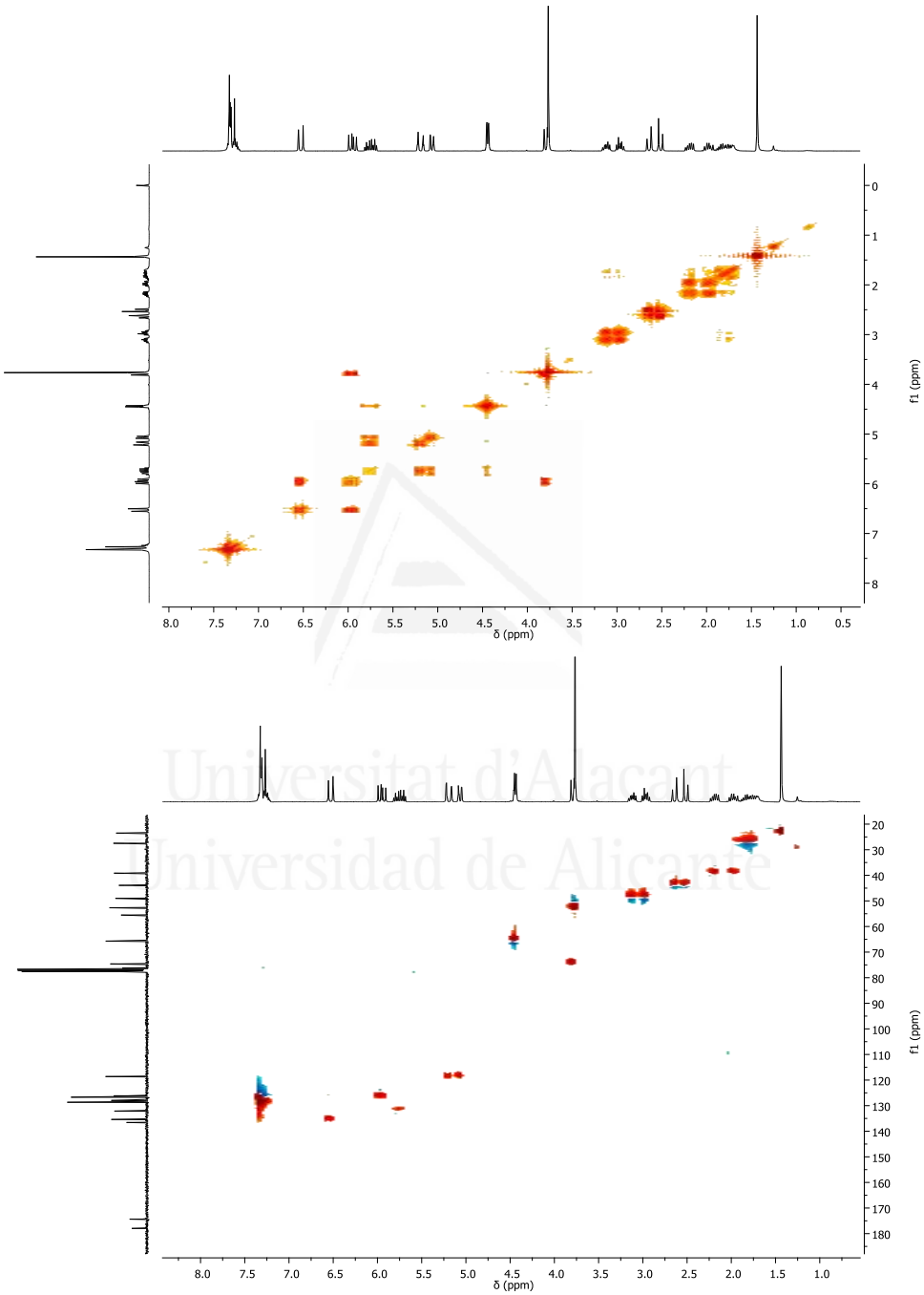

Electronic Supplementary Material (ESI) for Chemical Communications

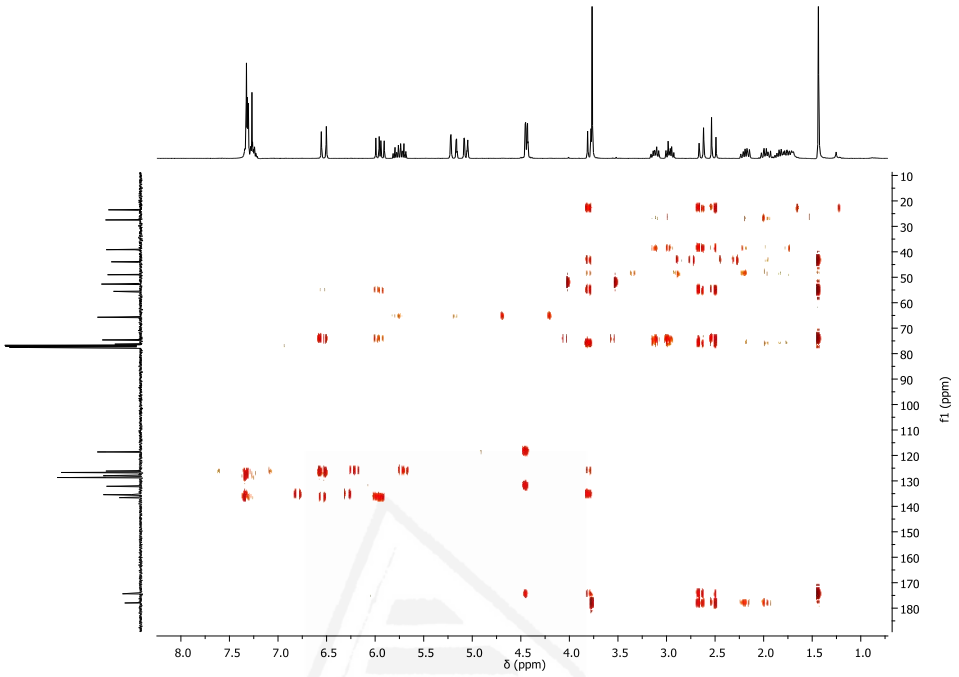

Electronic Supplementary Material (ESI) for Chemical Communications

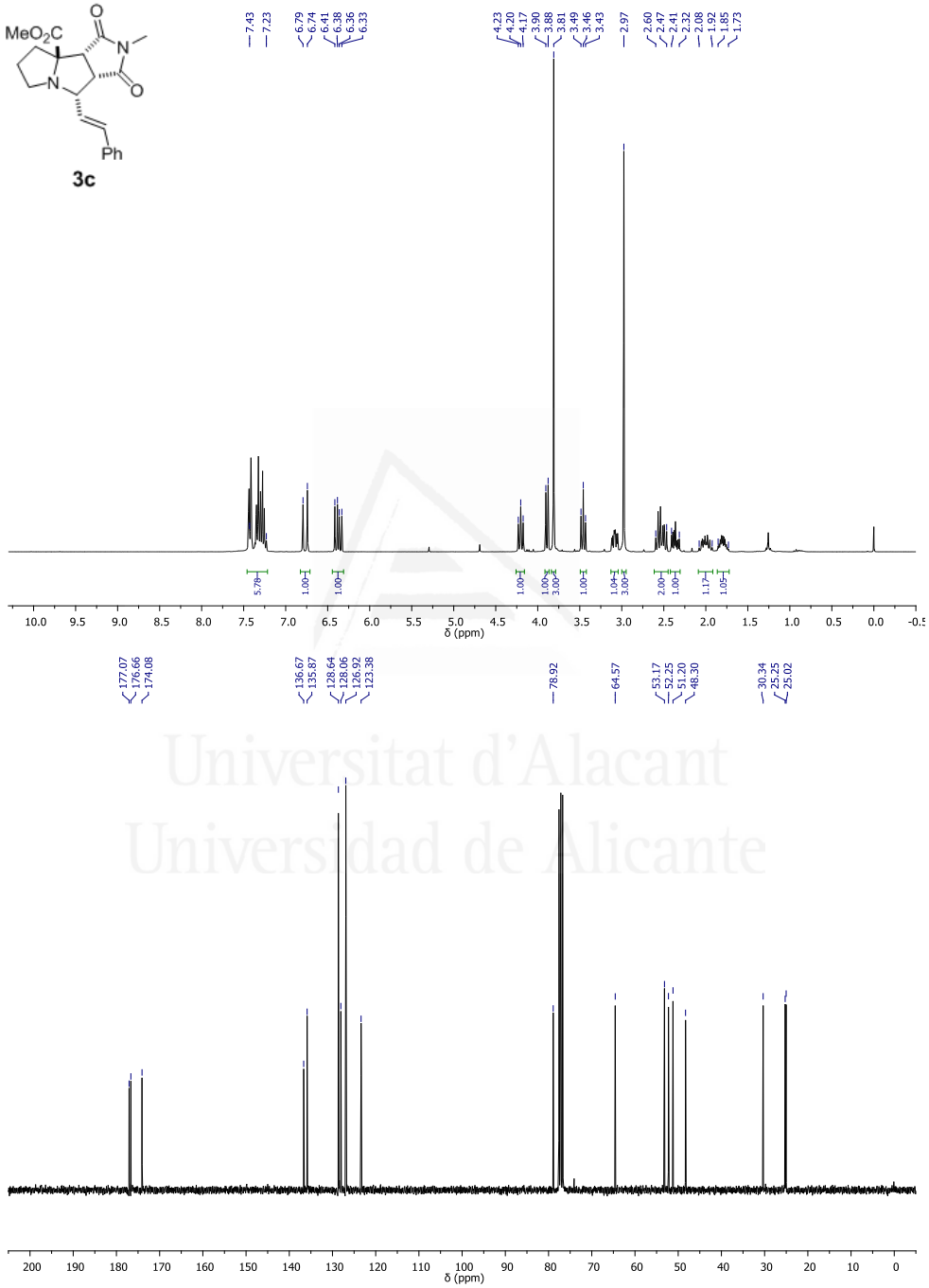

Electronic Supplementary Material (ESI) for Chemical Communications

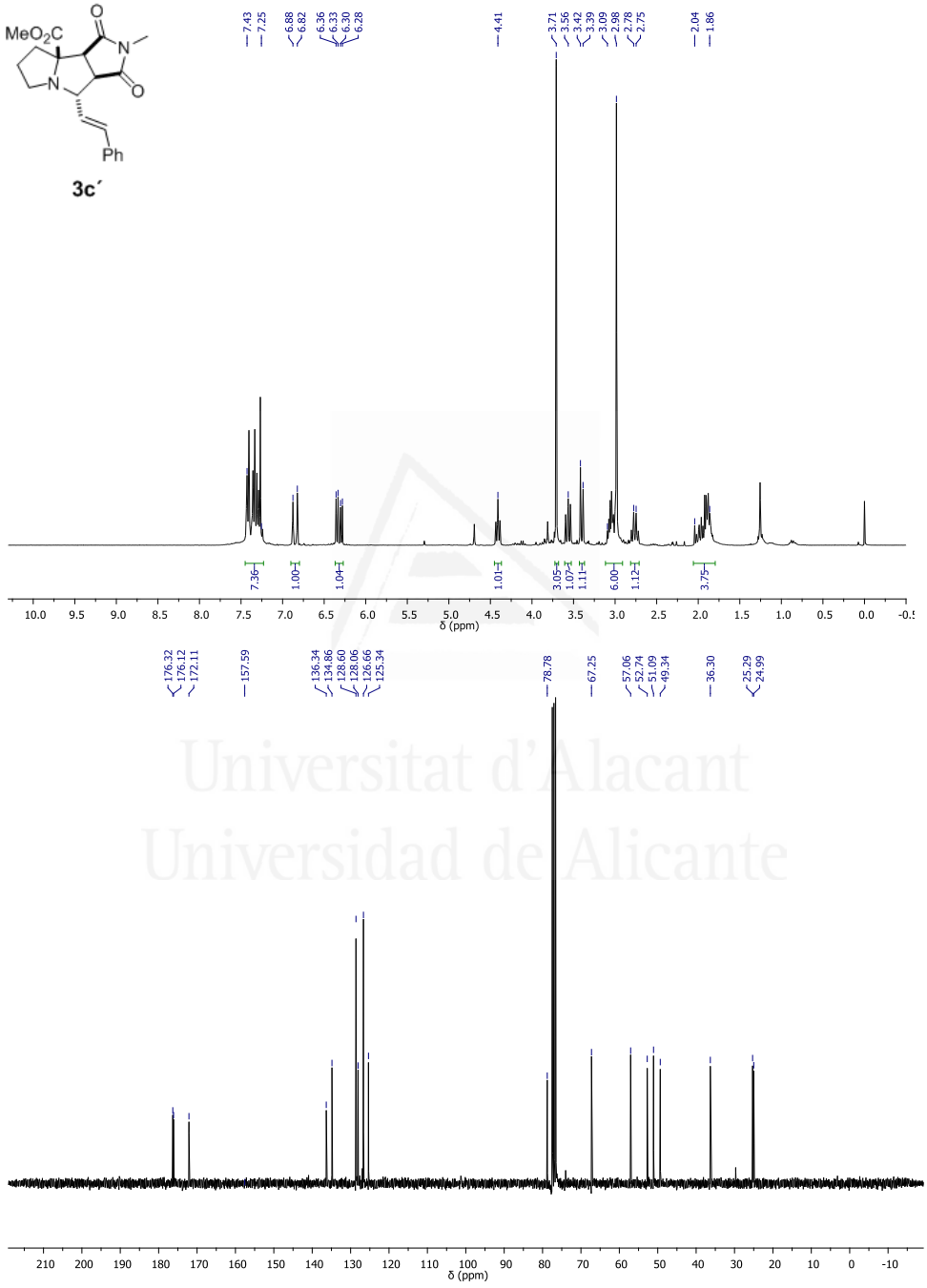

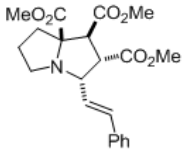

3d

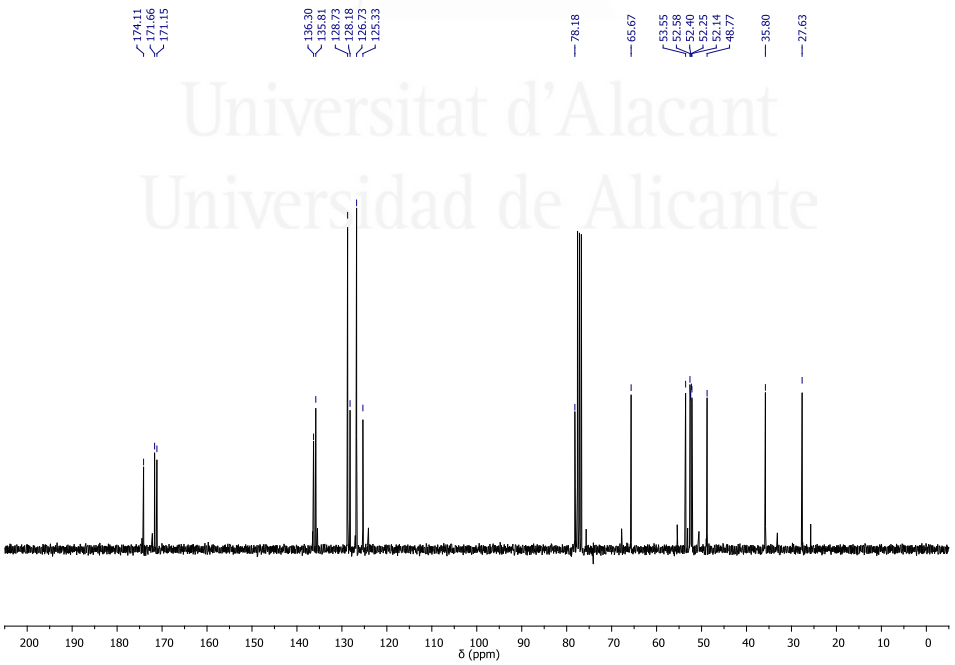

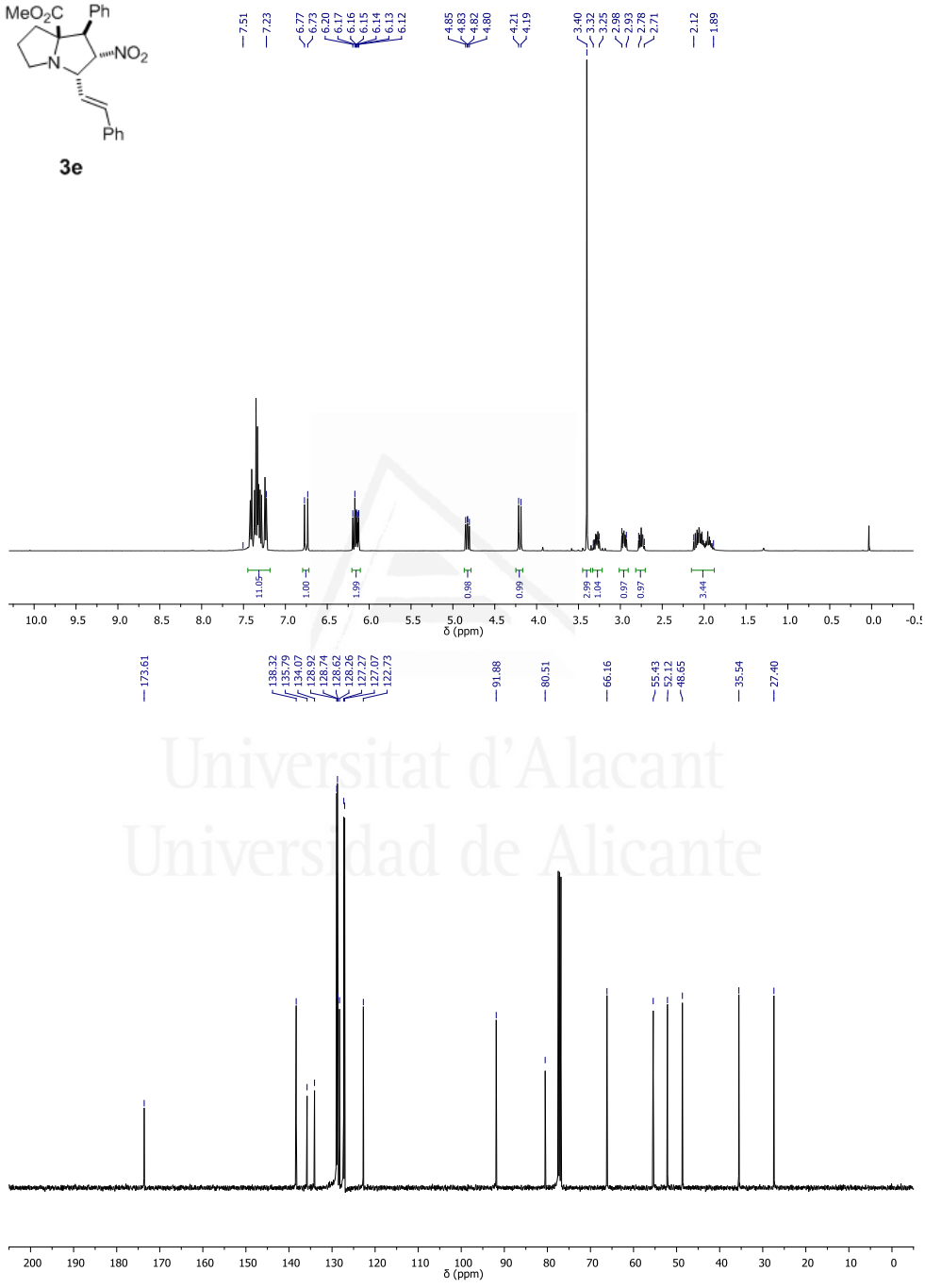

Electronic Supplementary Material (ESI) for Chemical Communications

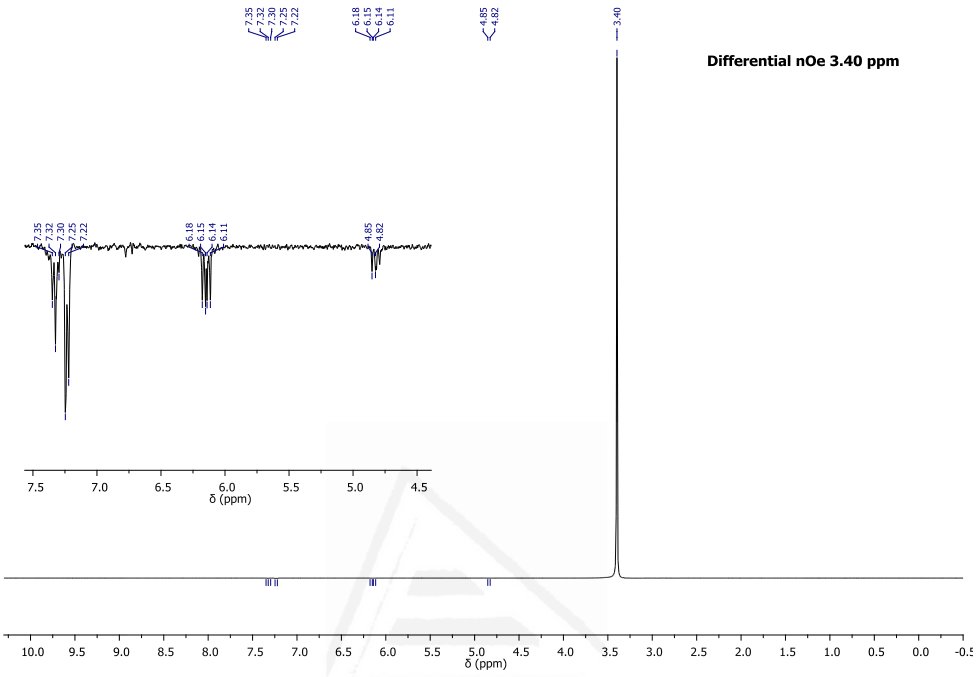

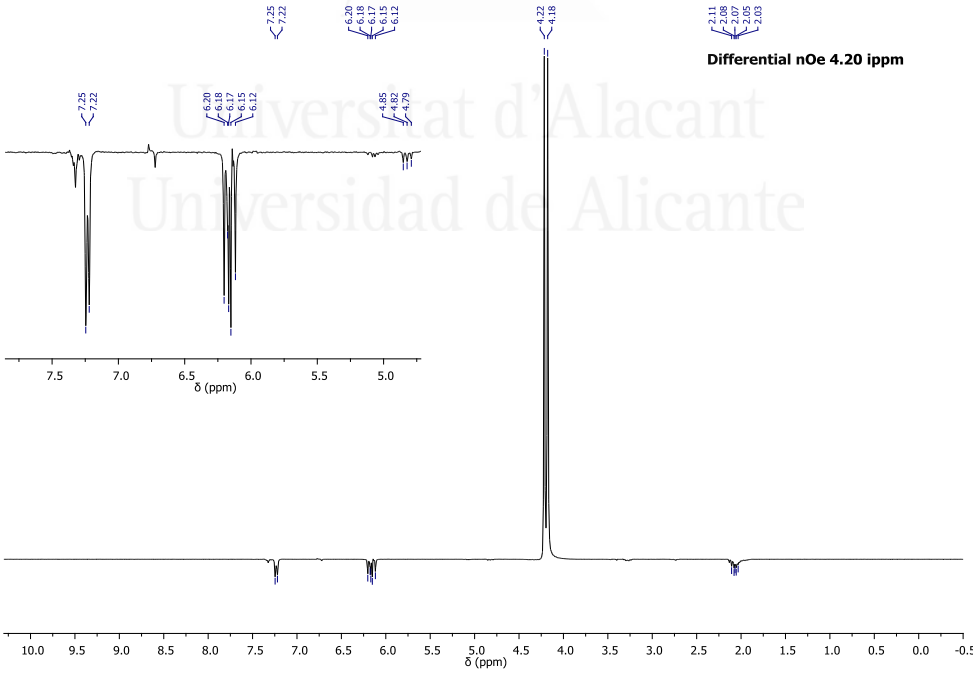

Electronic Supplementary Material (ESI) for Chemical Communications

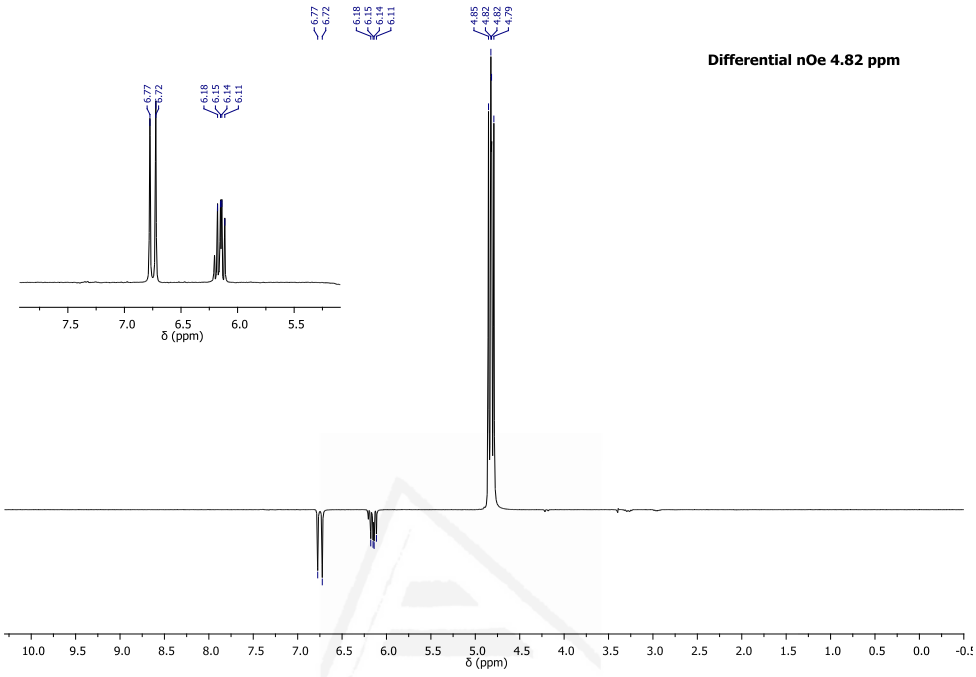

Electronic Supplementary Material (ESI) for Chemical Communications

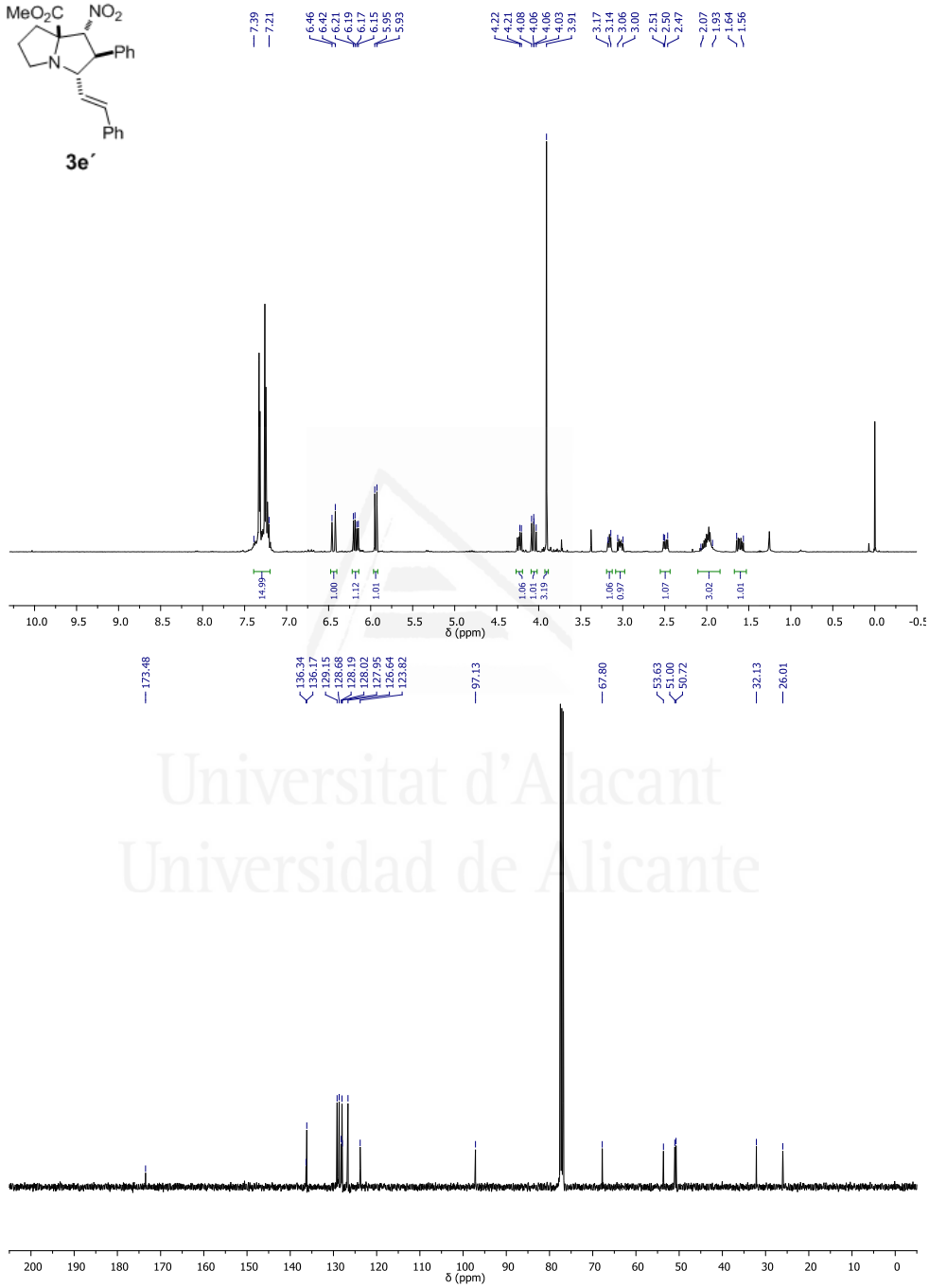

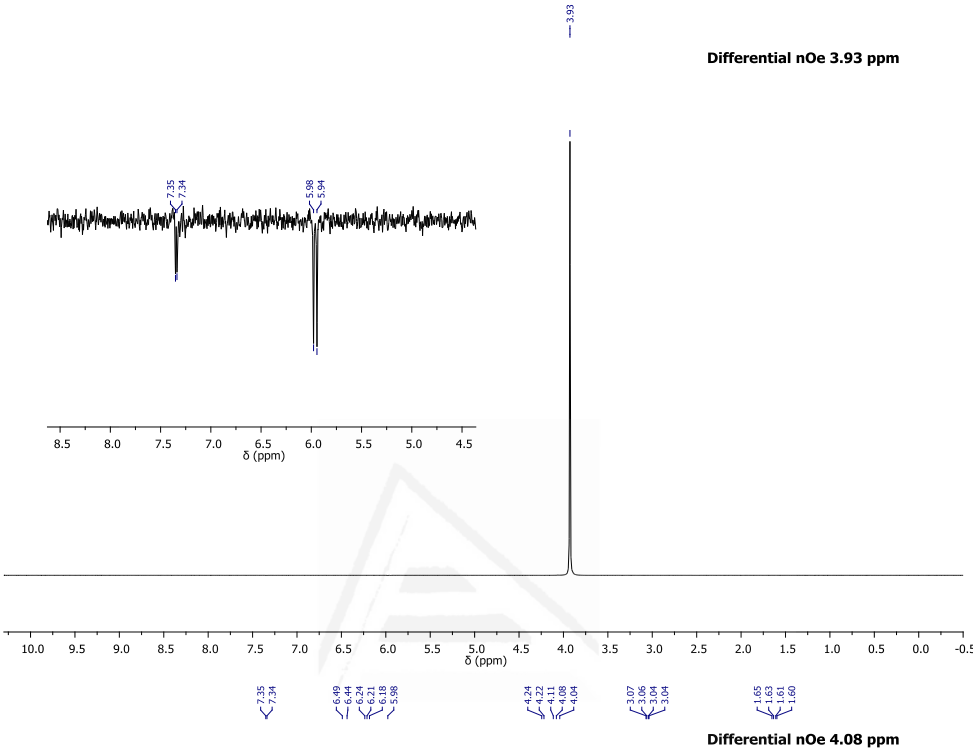

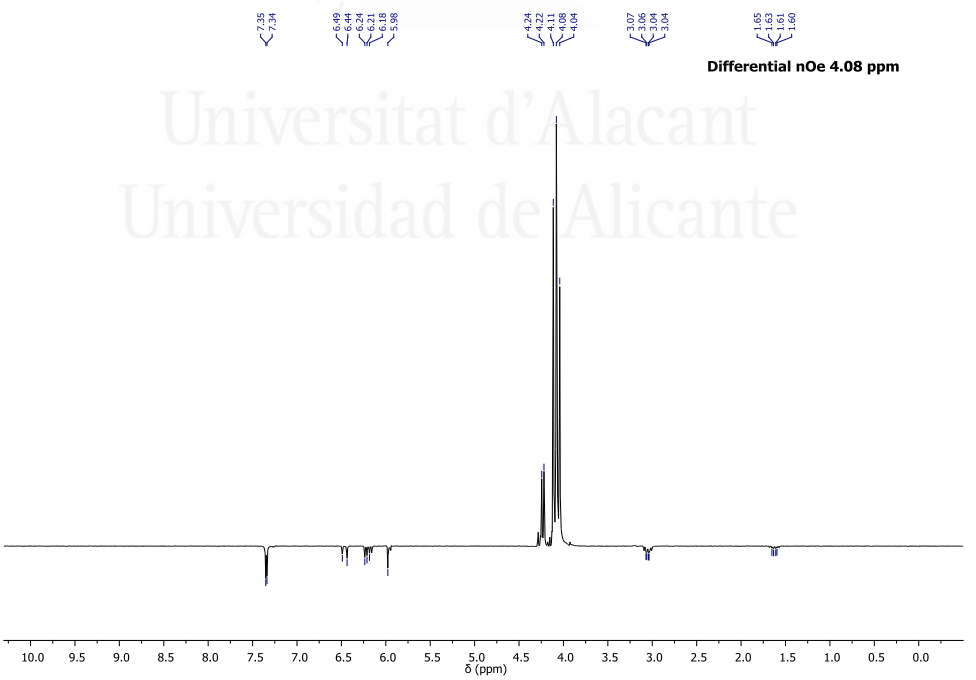

Electronic Supplementary Material (ESI) for Chemical Communications

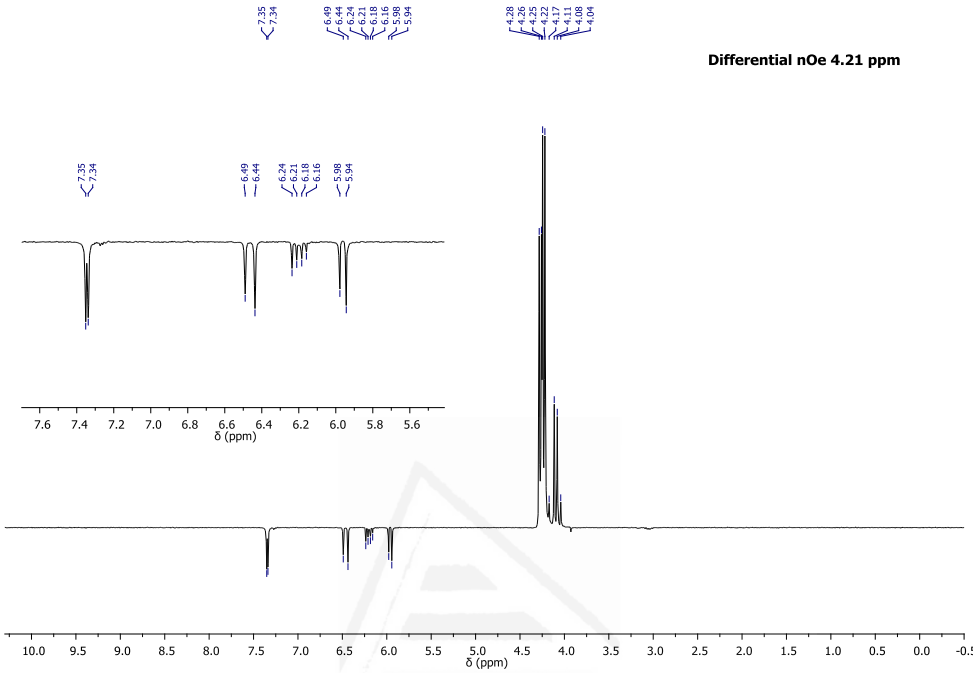

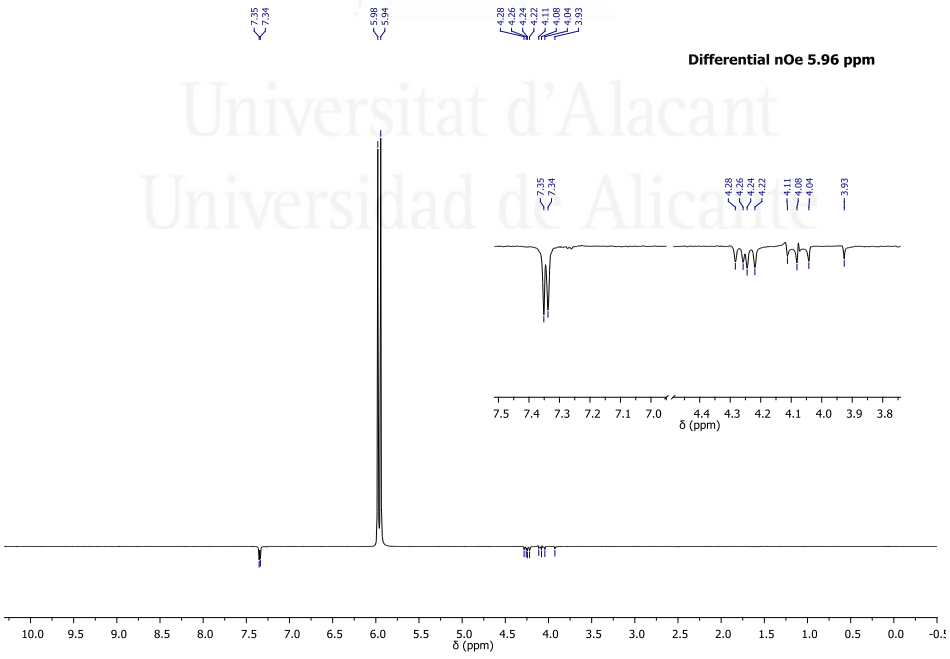

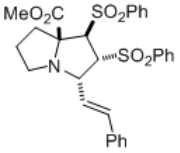

3f

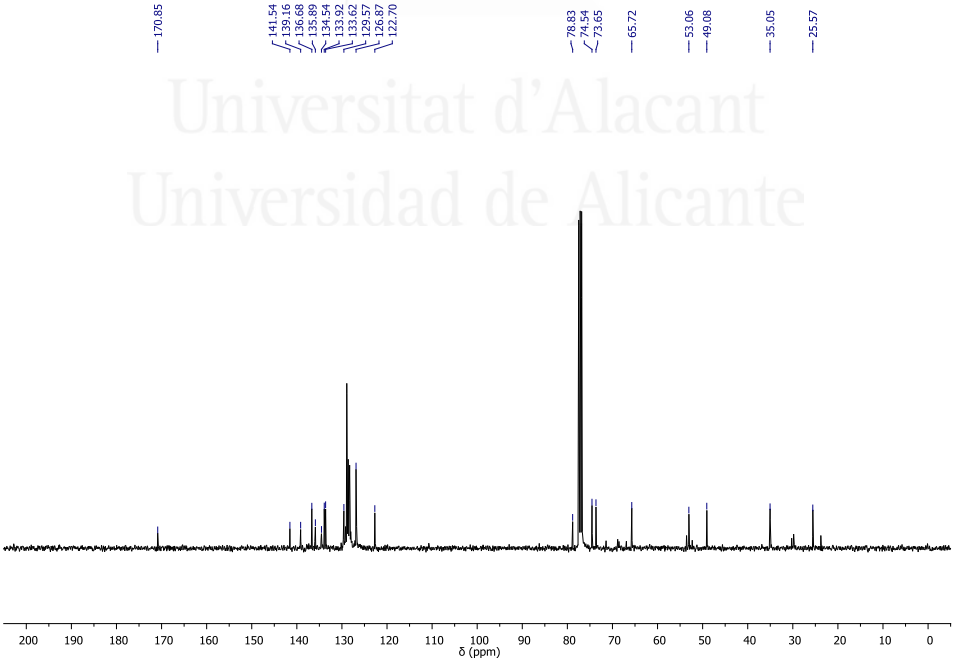

Electronic Supplementary Material (ESI) for Chemical Communications

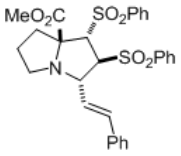

3f´

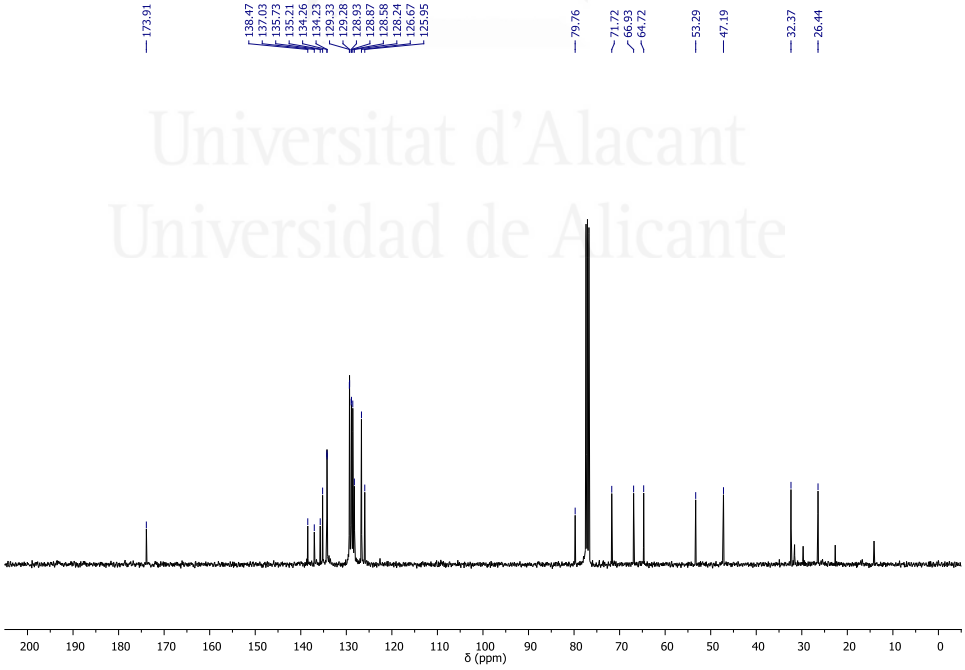

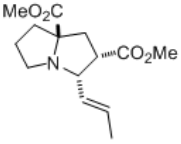

3g

Electronic Supplementary Material (ESI) for Chemical Communications

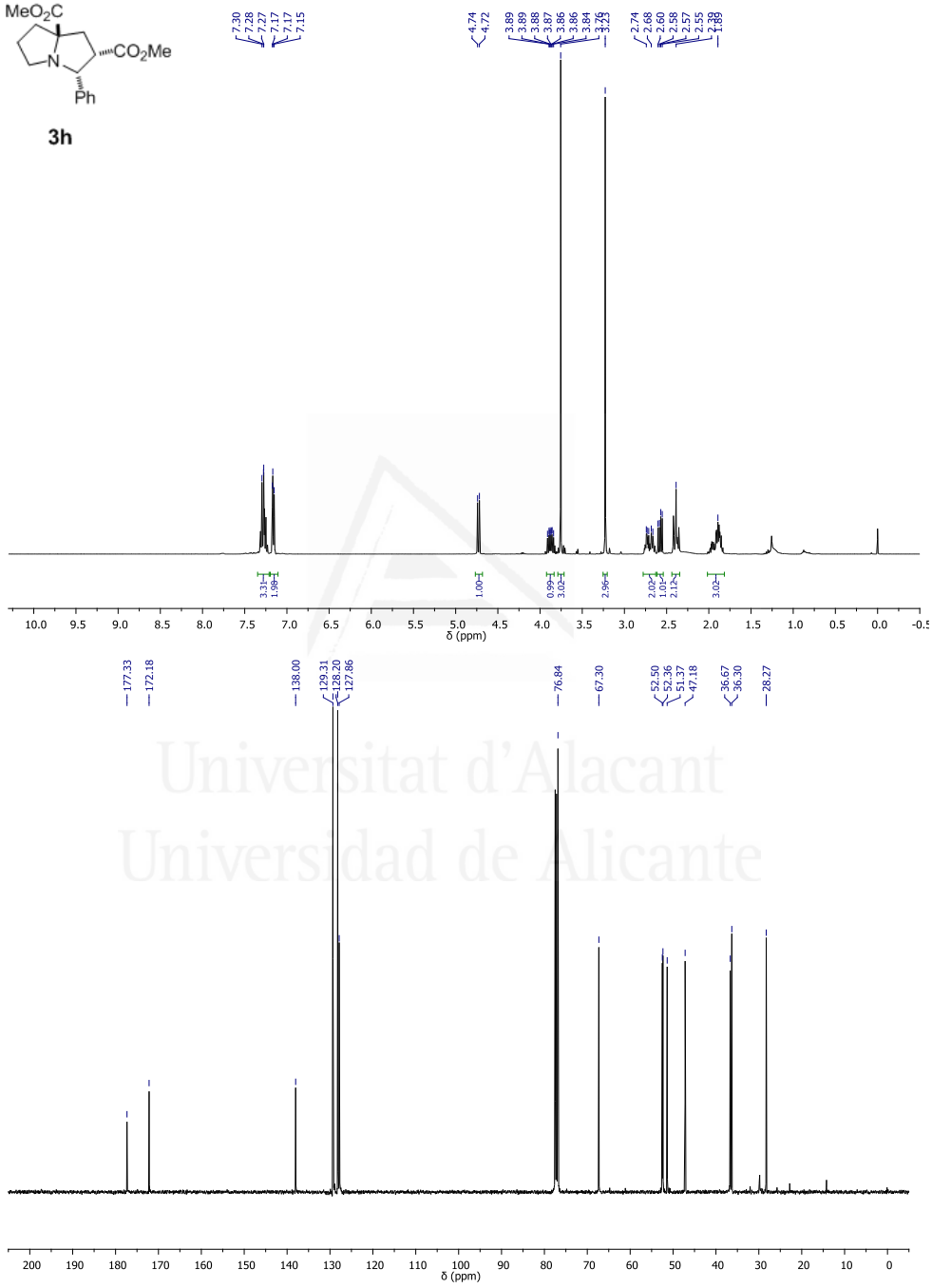

Electronic Supplementary Material (ESI) for Chemical Communications

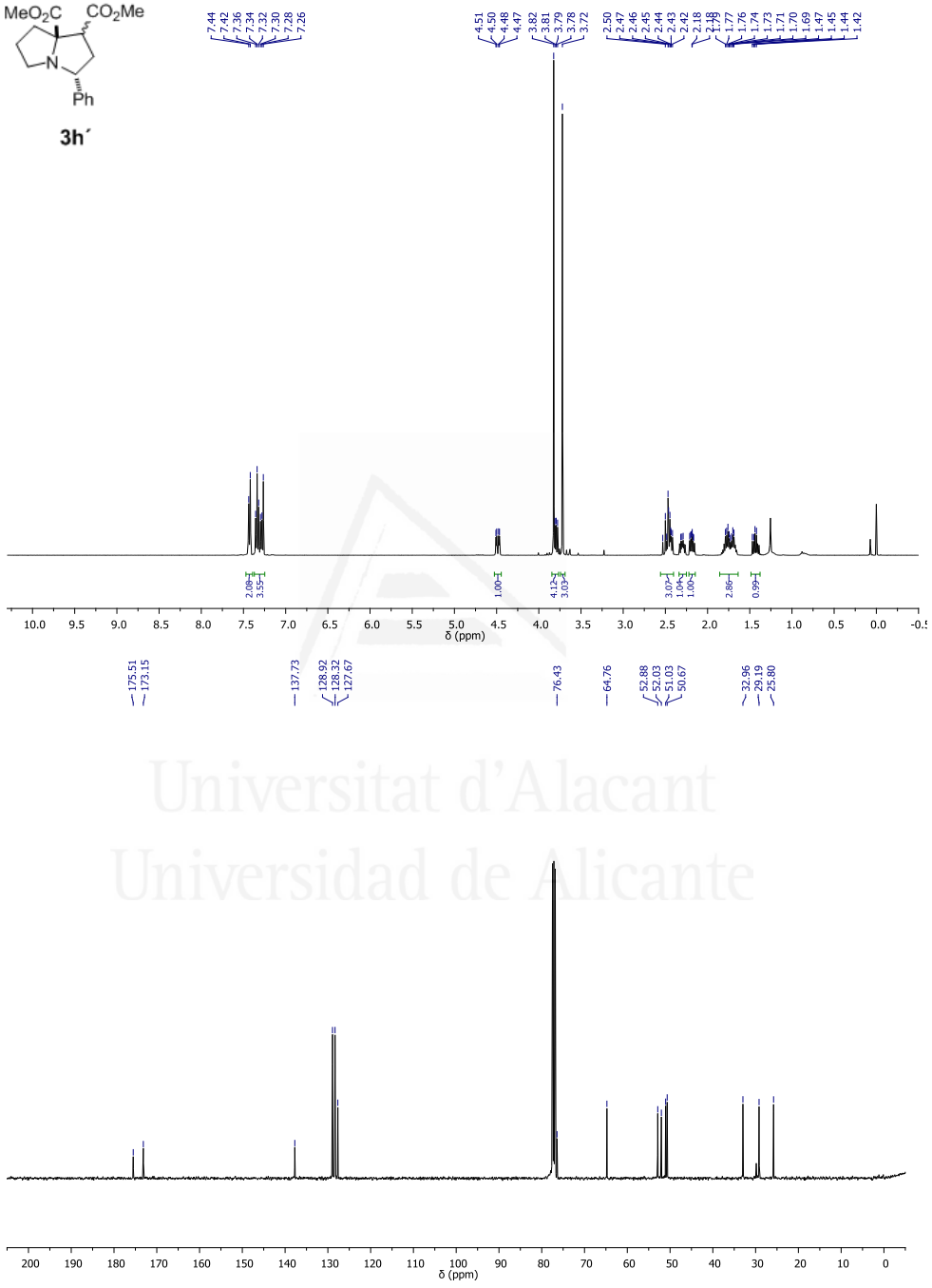

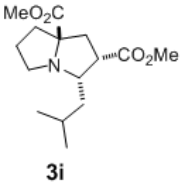

3i

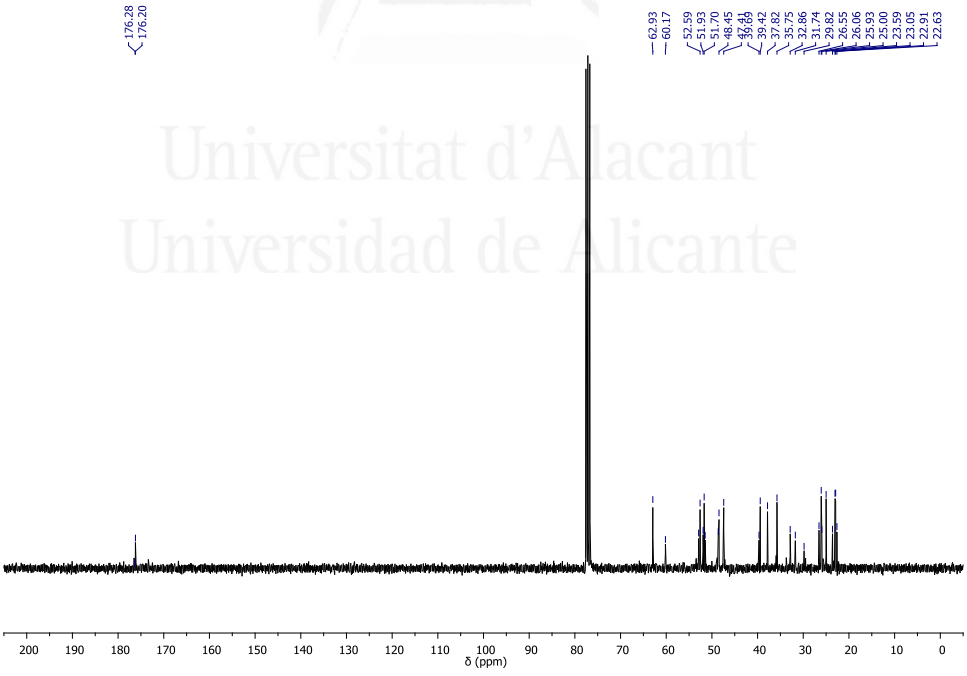

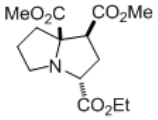

3j

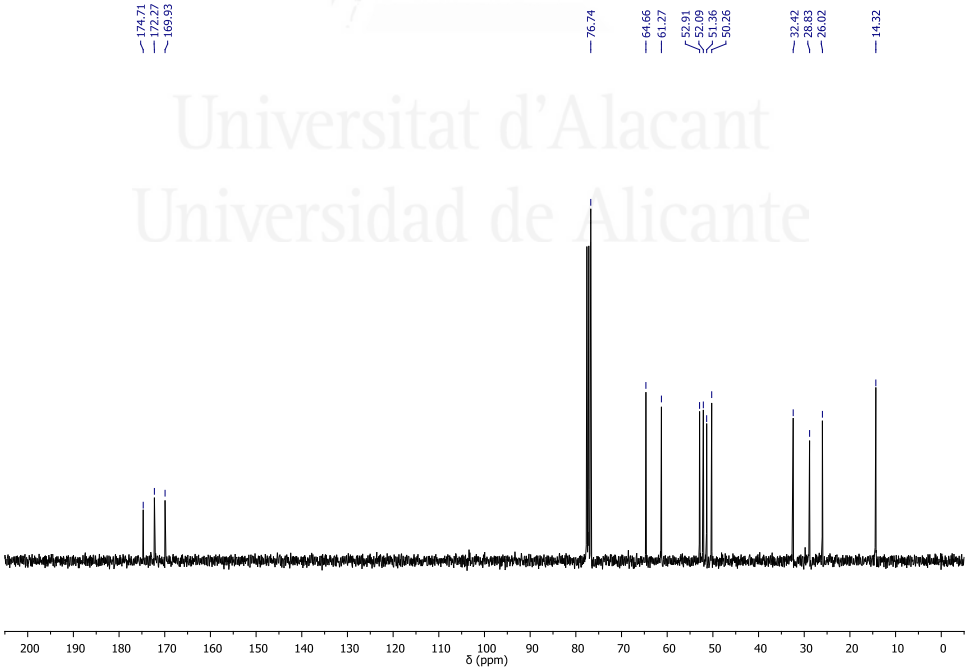

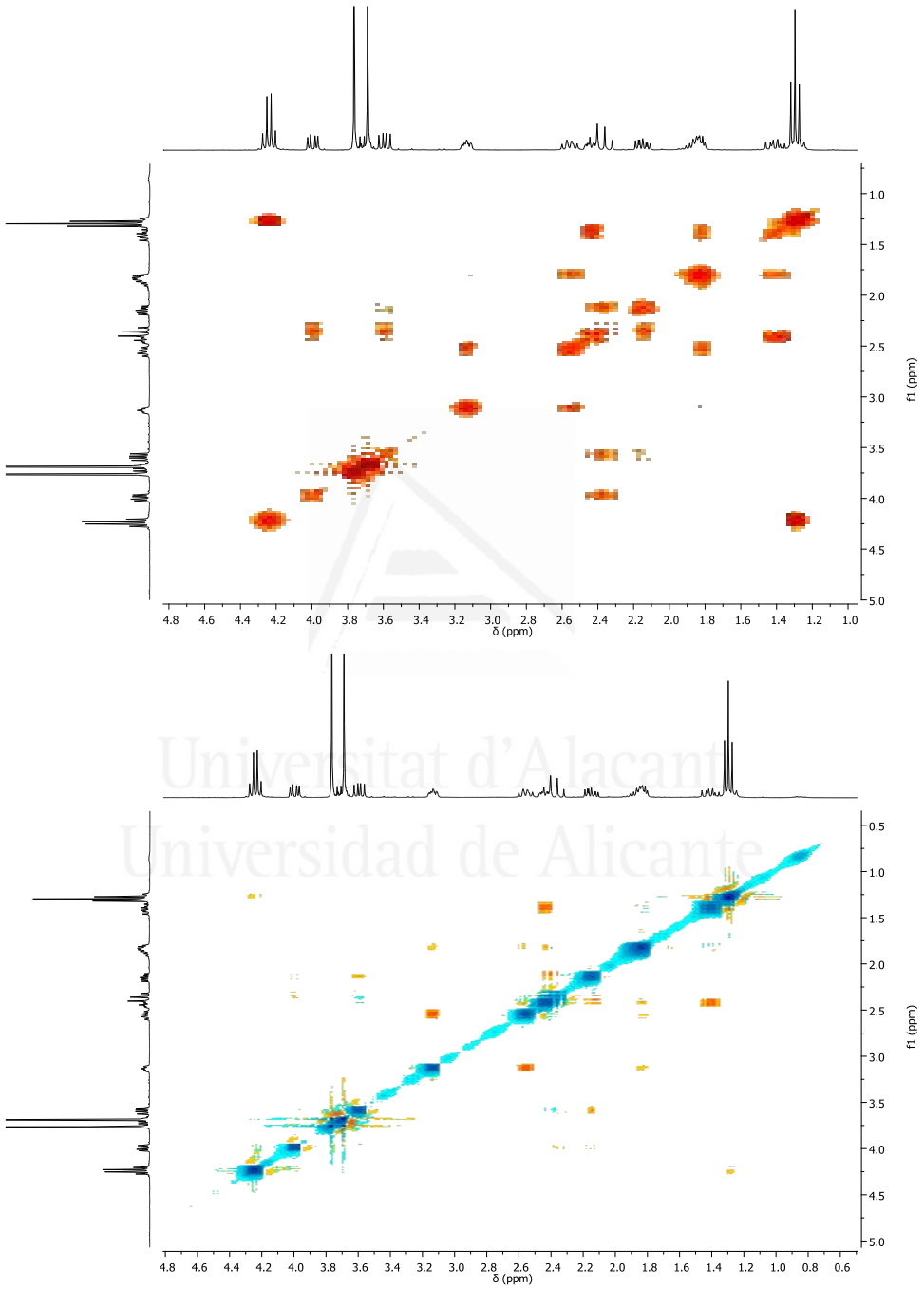

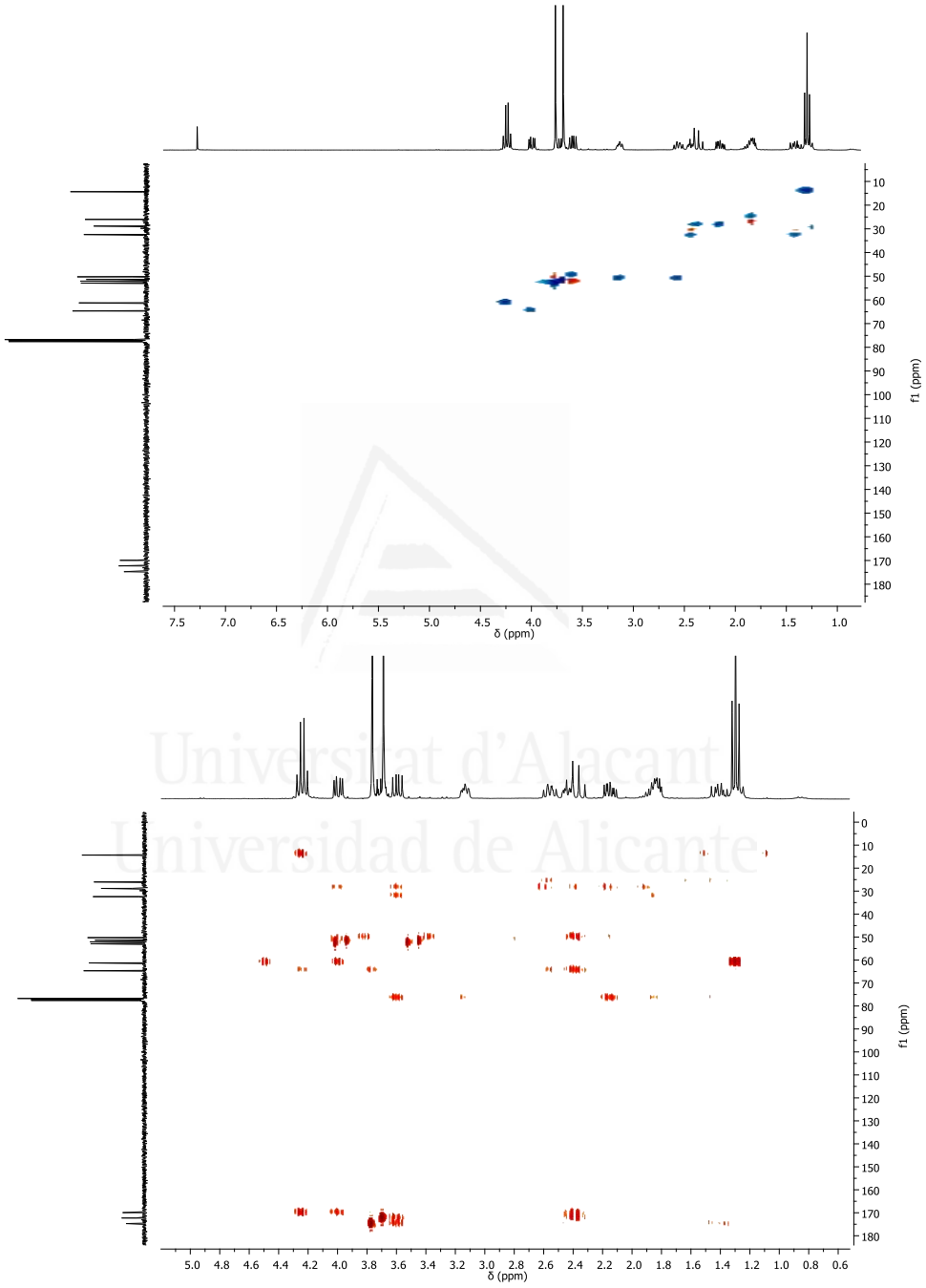

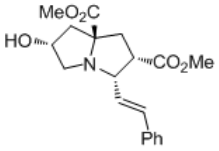

4a

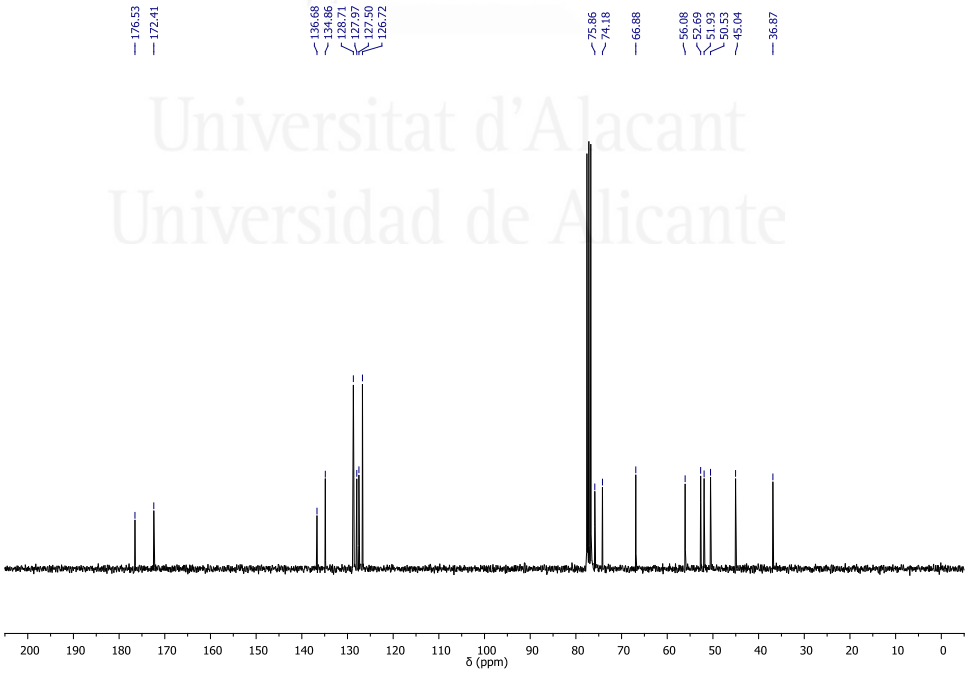

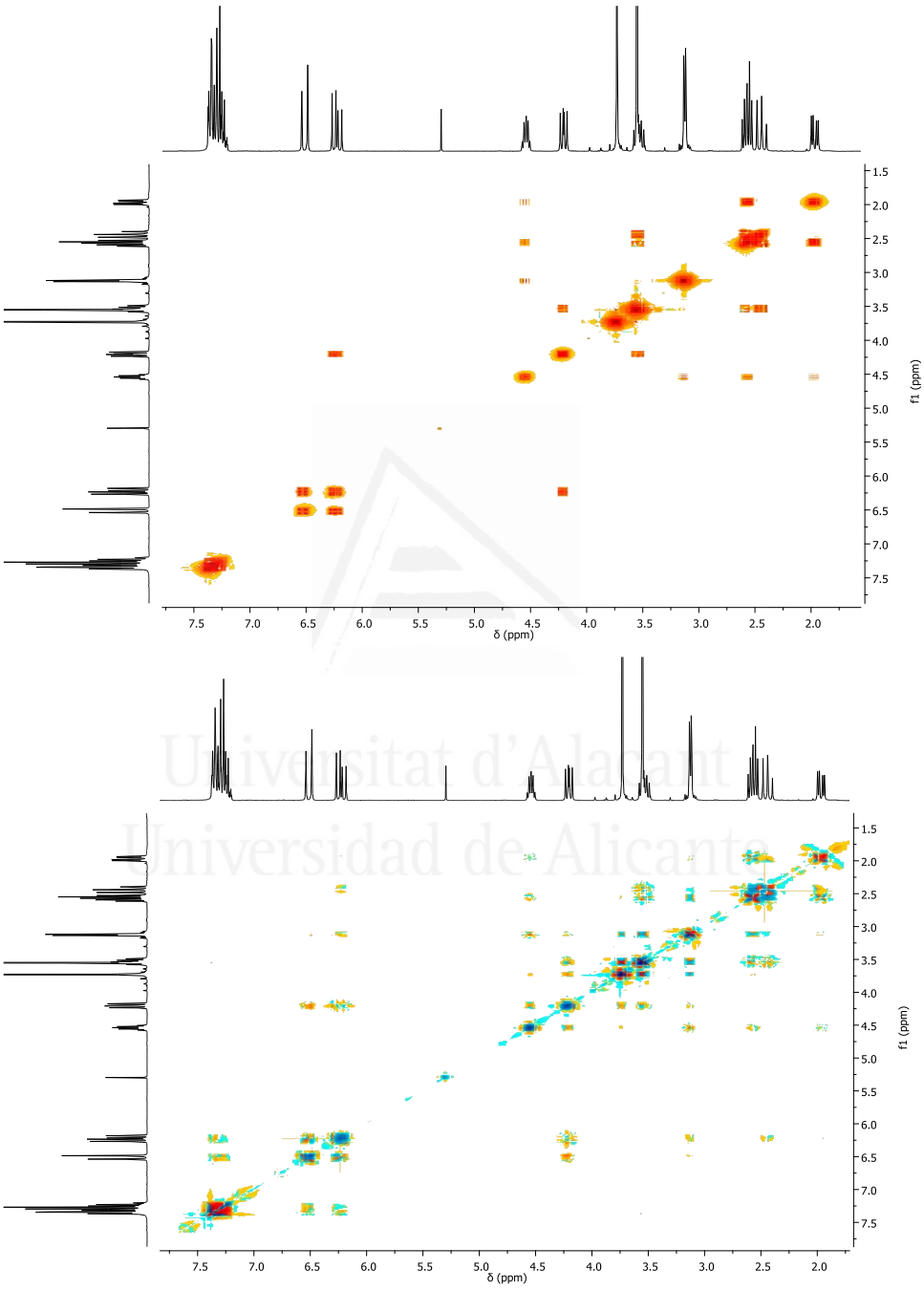

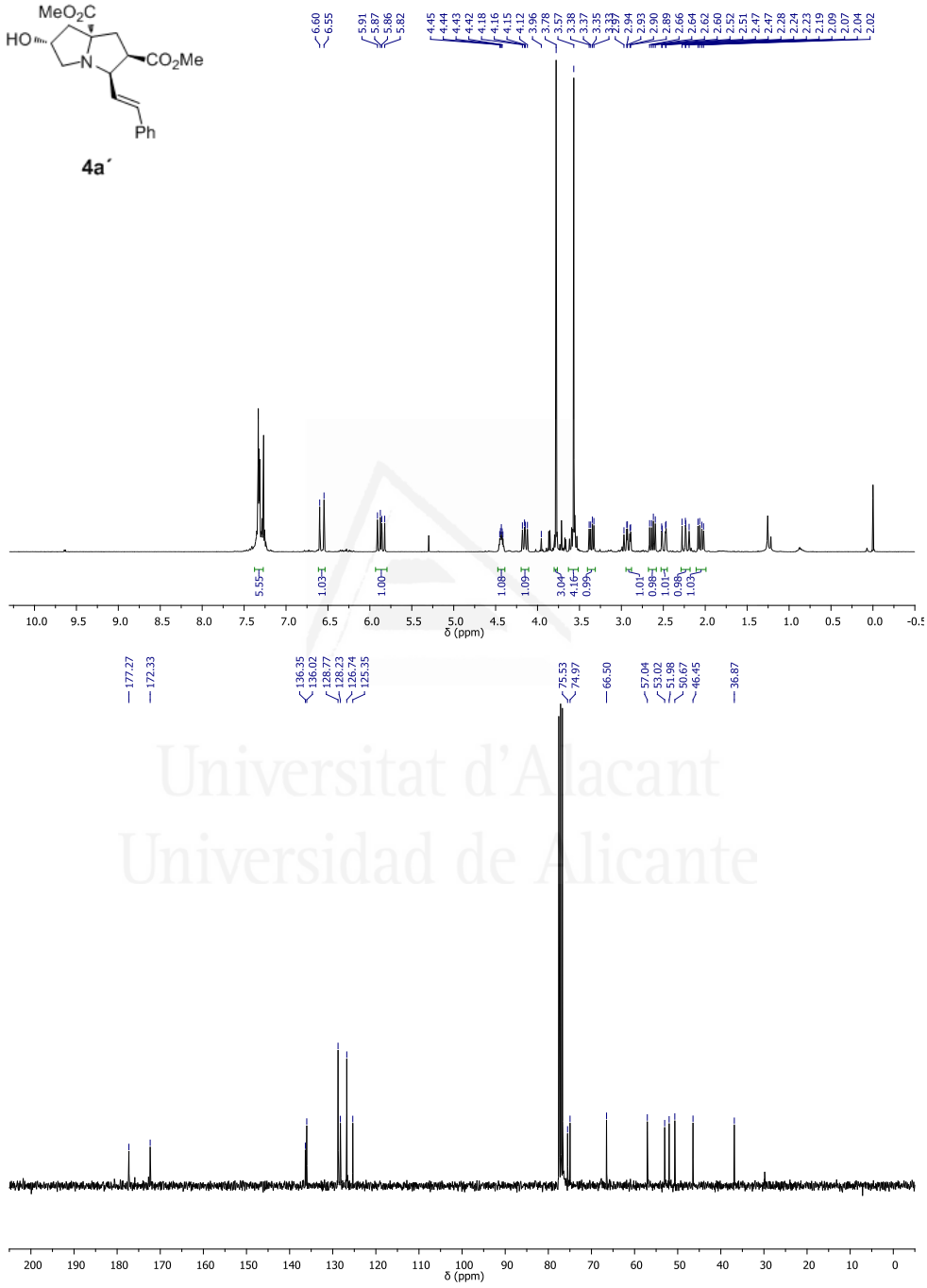

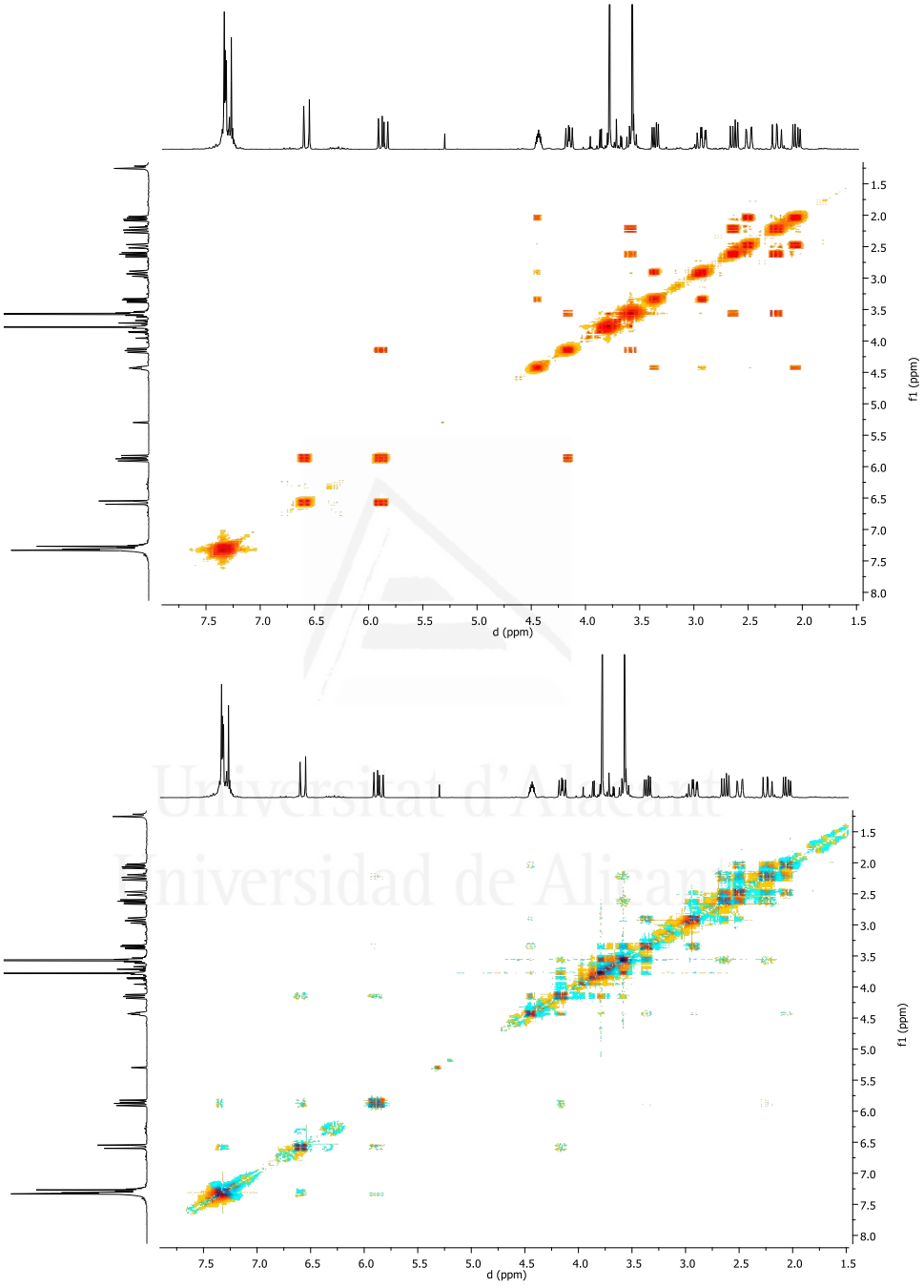

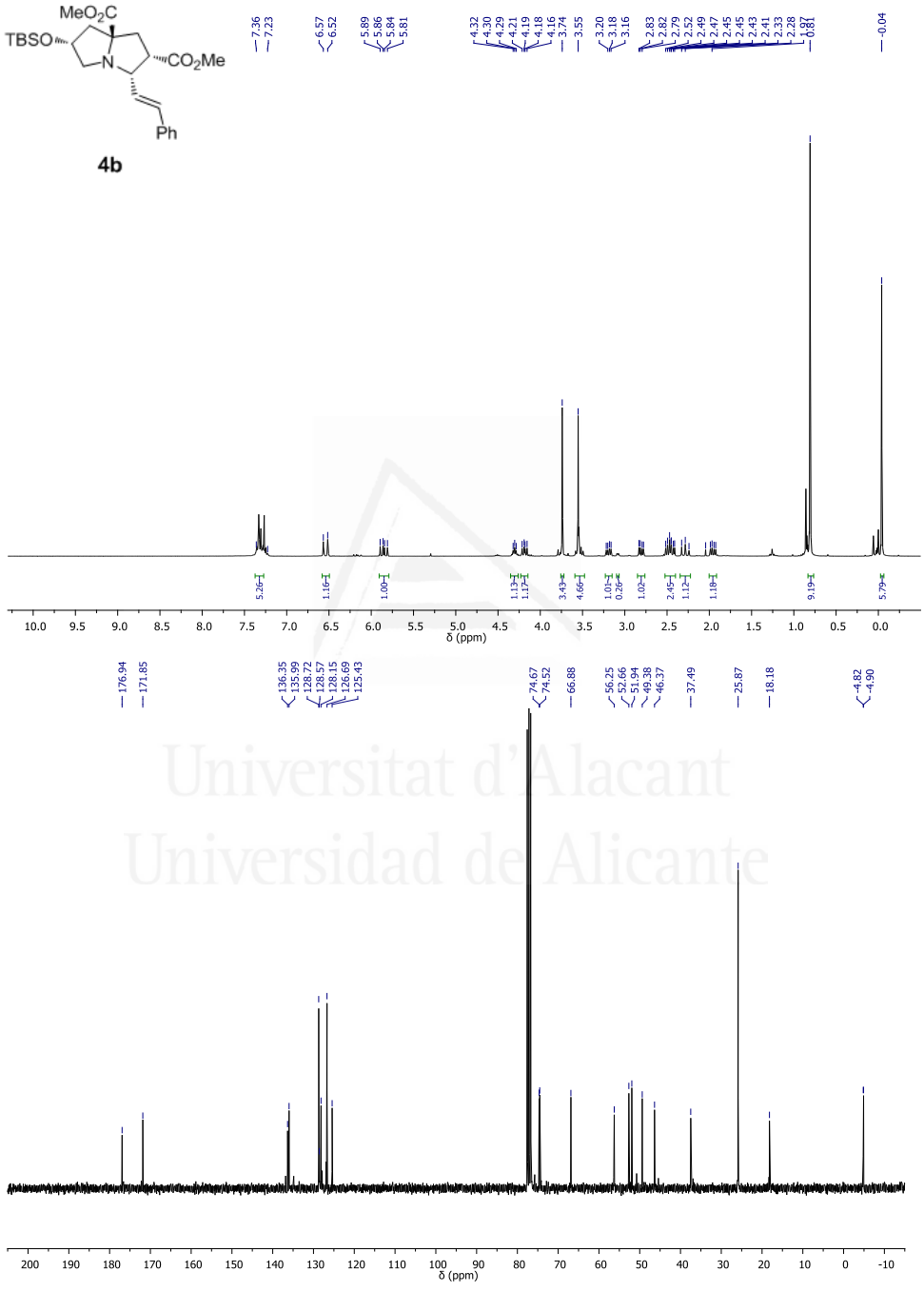

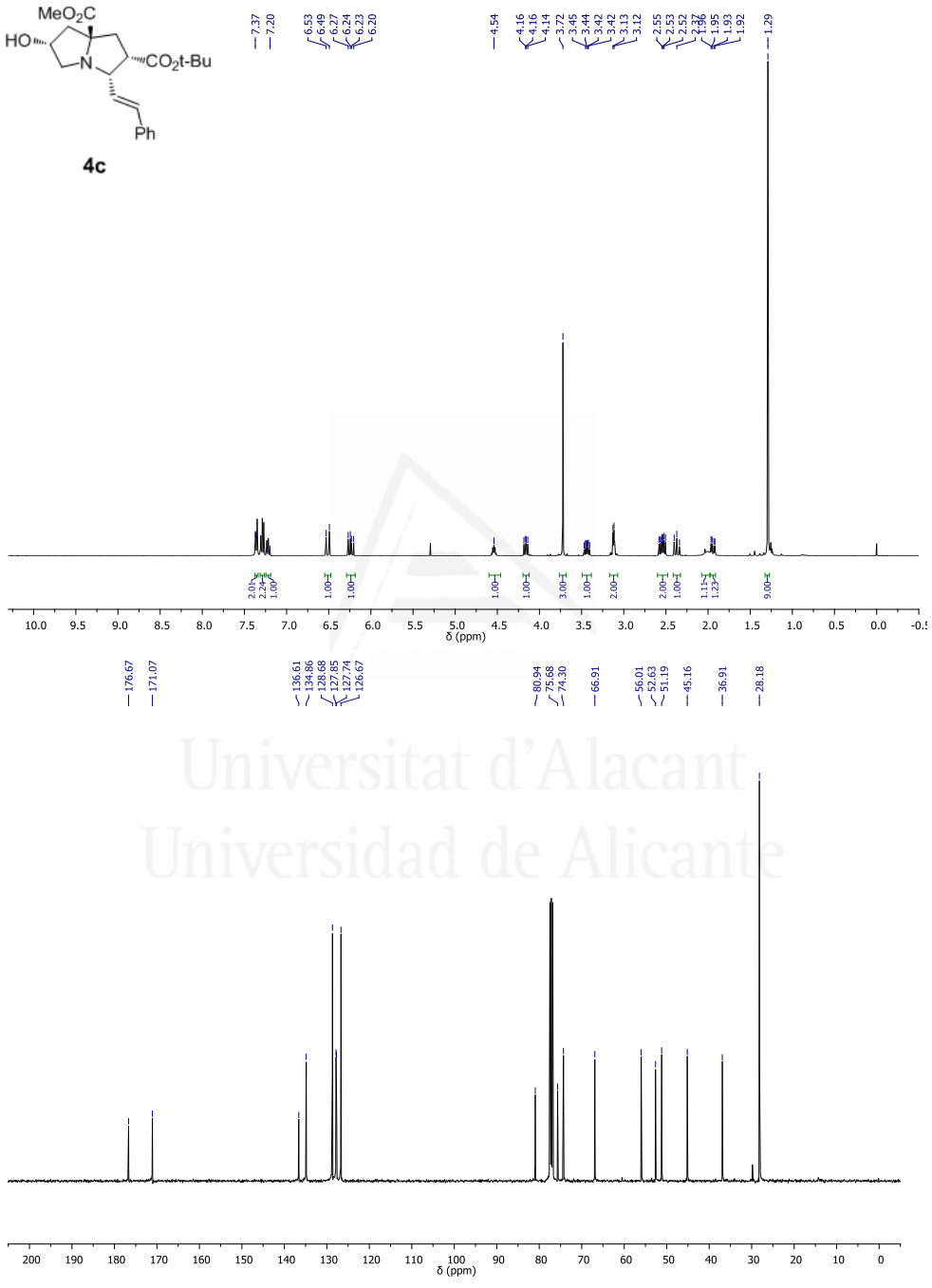

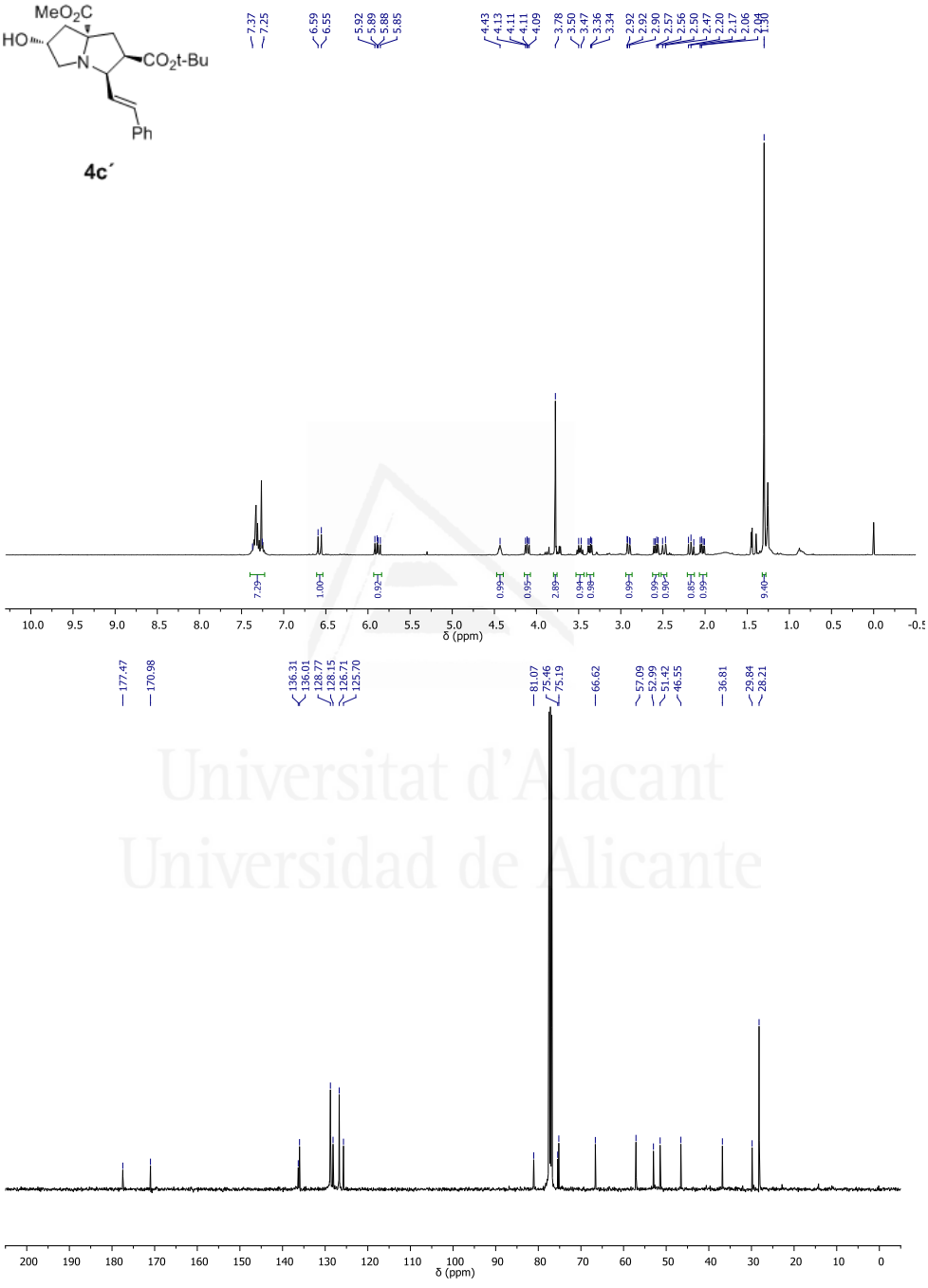

Electronic Supplementary Material (ESI) for Chemical Communications

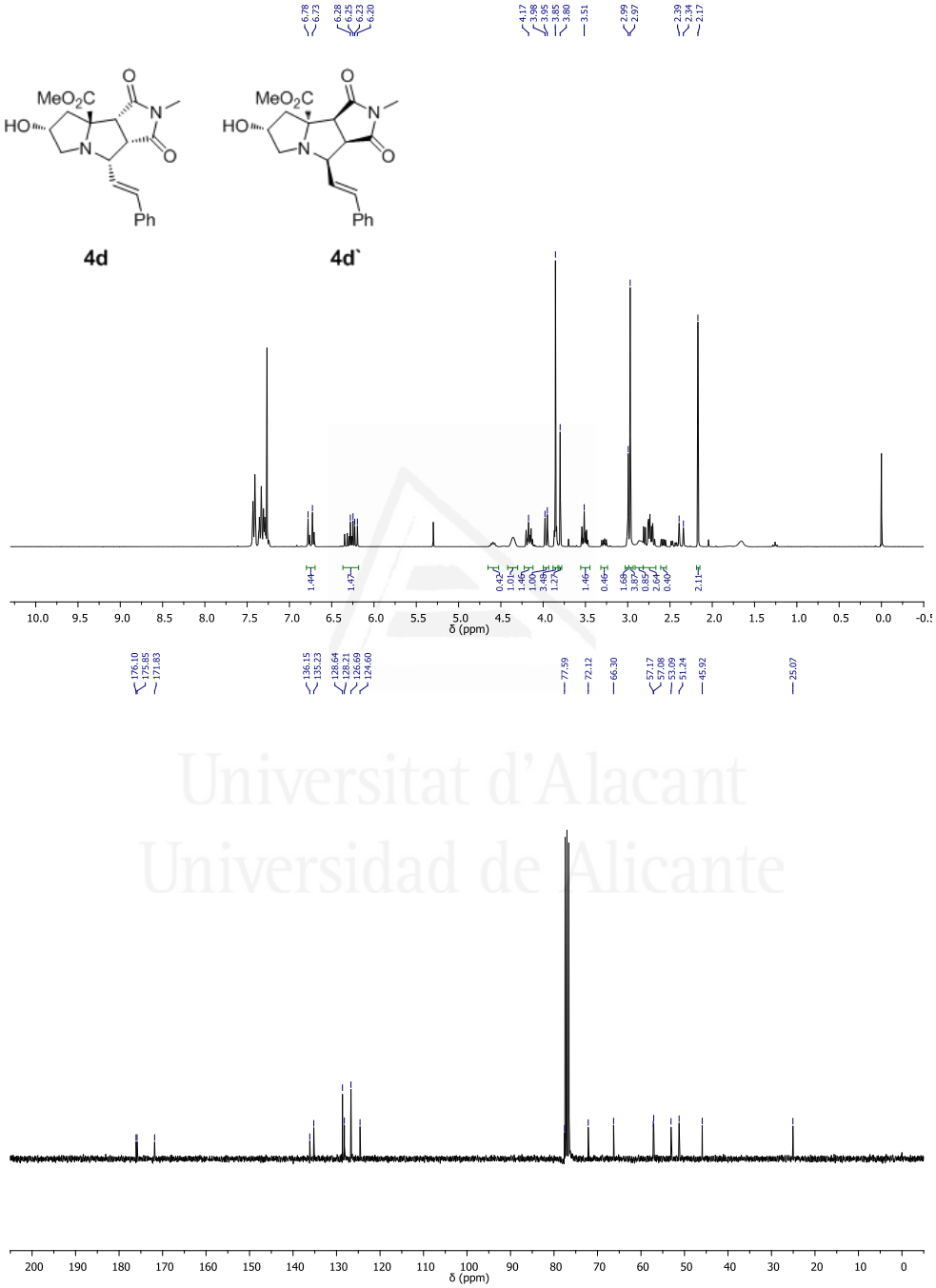

Electronic Supplementary Material (ESI) for Chemical Communications

6. X-Ray diffraction analysis of 3a

checkCIF/PLATON report

Structure factors have been supplied for datablock(s) x

No syntax errors found. CIF dictionary Interpreting this report

Datablock: x

Bond precision: C-C = 0.0070 A Wavelength=0.71073

Cell: a=10.2542(17) b=24.002(4) c=14.842(2)
alpha=90 beta=104.390(5) gamma=90
Temperature: 297 K

	Calculated	Reported
Volume	3538.3(10)	3538.3(10)
Space group	P 21/n	P 21/n
Hall group	-P 2yn	?
Moiety formula	C19 H23 N O4	C19 H23 N O4
Sum formula	C19 H23 N O4	C19 H23 N O4
Mr	329.38	329.38
Dx,g cm-3	1.237	1.237
Z	8	8
Mu (mm-1)	0.086	0.086
F000	1408.0	1408.0
F000'	1408.70	
h,k,lmax	12,28,17	12,28,17
Nref	6320	6296
Tmin,Tmax	0.988,0.996	0.524,0.996
Tmin'	0.986	

Correction method= MULTI-SCAN

Data completeness= 0.996 Theta(max)= 25.130

R(reflections)= 0.0691(2144) wR2(reflections)= 0.1800(6296)

S = 0.923 Npar= 437

The following ALERTS were generated. Each ALERT has the format
test-name_ALERT_alert-type_alert-level.
Click on the hyperlinks for more details of the test.

Alert level B

RINTA01_ALERT_3_B The value of Rint is greater than 0.18
Rint given 0.196
PLAT026_ALERT_3_B Ratio Observed / Unique Reflections too Low .... 34 Perc.
PLAT241_ALERT_2_B Check High Ueq as Compared to Neighbors for C6

Electronic Supplementary Material (ESI) for Chemical Communications

Alert level C

```
PLAT242_ALERT_2_C Check Low       Ueq as Compared to Neighbors for        C18
PLAT242_ALERT_2_C Check Low       Ueq as Compared to Neighbors for        C37
PLAT340_ALERT_3_C Low Bond Precision on  C-C Bonds ..............     0.0070 Ang
PLAT906_ALERT_3_C Large K value in the Analysis of Variance ......     12.450
PLAT906_ALERT_3_C Large K value in the Analysis of Variance ......      3.036
PLAT906_ALERT_3_C Large K value in the Analysis of Variance ......      2.011
PLAT911_ALERT_3_C Missing # FCF Refl Between THmin & STh/L=  0.598        27
```

Alert level G

```
PLAT005_ALERT_5_G No _iucr_refine_instructions_details  in the CIF         ?
PLAT128_ALERT_4_G Alternate Setting of Space-group P21/c   .......     P21/n
PLAT793_ALERT_4_G The Model has Chirality at C1       (Verify) ....        S
PLAT793_ALERT_4_G The Model has Chirality at C2       (Verify) ....        S
PLAT793_ALERT_4_G The Model has Chirality at C4       (Verify) ....        R
PLAT793_ALERT_4_G The Model has Chirality at C20      (Verify) ....        R
PLAT793_ALERT_4_G The Model has Chirality at C21      (Verify) ....        R
PLAT793_ALERT_4_G The Model has Chirality at C23      (Verify) ....        S
```

```
   0 ALERT level A = Most likely a serious problem - resolve or explain
   3 ALERT level B = A potentially serious problem, consider carefully
   7 ALERT level C = Check. Ensure it is not caused by an omission or oversight
   8 ALERT level G = General information/check it is not something unexpected

   0 ALERT type 1 CIF construction/syntax error, inconsistent or missing data
   3 ALERT type 2 Indicator that the structure model may be wrong or deficient
   7 ALERT type 3 Indicator that the structure quality may be low
   7 ALERT type 4 Improvement, methodology, query or suggestion
   1 ALERT type 5 Informative message, check
```

Datablock z - ellipsoid plot

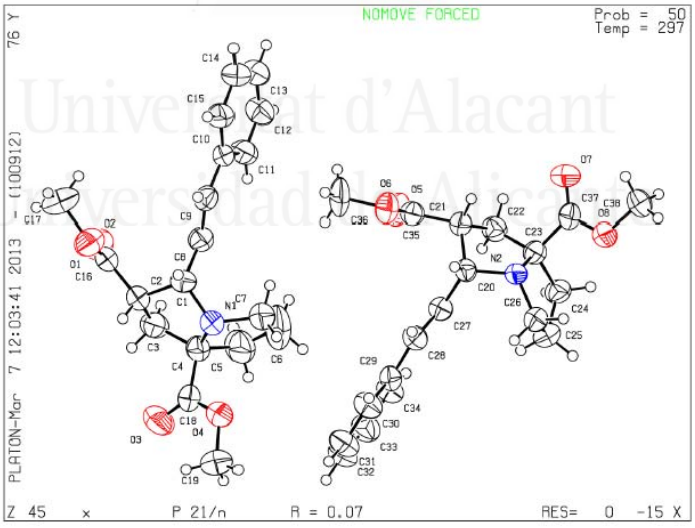

Electronic Supplementary Material (ESI) for Chemical Communications

checkCIF/PLATON report

Structure factors have been supplied for datablock(s) x

THIS REPORT IS FOR GUIDANCE ONLY. IF USED AS PART OF A REVIEW PROCEDURE FOR PUBLICATION, IT SHOULD NOT REPLACE THE EXPERTISE OF AN EXPERIENCED CRYSTALLOGRAPHIC REFEREE.

No syntax errors found. CIF dictionary Interpreting this report

Datablock: x

Bond precision: C-C = 0.0060 A Wavelength=0.71073

Cell: a=11.1442(19) b=5.9143(10) c=13.609(2)
alpha=90 beta=94.567(4) gamma=90
Temperature: 298 K

	Calculated	Reported
Volume	894.1(3)	894.1(3)
Space group	P 21	P 21
Hall group	P 2yb	?
Moiety formula	C19 H23 N O5	C19 H23 N O5
Sum formula	C19 H23 N O5	C19 H23 N O5
Mr	345.38	345.38
Dx,g cm-3	1.283	1.283
Z	2	2
Mu (mm-1)	0.093	0.093
F000	368.0	368.0
F000'	368.19	
h,k,lmax	13,7,16	13,7,16
Nref	3159[1750]	3131
Tmin,Tmax	0.991,0.997	0.928,0.997
Tmin'	0.965	

Correction method= MULTI-SCAN

Data completeness= 1.79/0.99 Theta(max)= 25.060

R(reflections)= 0.0532(1784) wR2(reflections)= 0.1415(3131)

S = 1.002 Npar= 229

The following ALERTS were generated. Each ALERT has the format
test-name_ALERT_alert-type_alert-level.
Click on the hyperlinks for more details of the test.

Electronic Supplementary Material (ESI) for Chemical Communications

Alert level C

```
PLAT089_ALERT_3_C Poor Data / Parameter Ratio (Zmax  <   18) .....       7.64
PLAT230_ALERT_2_C Hirshfeld Test Diff for    C4     --  C8      ..        6.3 su
PLAT242_ALERT_2_C Check Low       Ueq as Compared to Neighbors for         C8
PLAT340_ALERT_3_C Low Bond Precision on  C-C Bonds ..............     0.0060 Ang.
PLAT411_ALERT_2_C Short Inter H...H Contact  H3B    ..  H6      ..       2.06 Ang.
```

Alert level G

```
PLAT005_ALERT_5_G No _iucr_refine_instructions_details  in the CIF          ? Do !
PLAT007_ALERT_5_G Note: Number of Unrefined Donor-H Atoms ........          1
PLAT791_ALERT_4_G Note: The Model has Chirality at C2      (Verify)         R
PLAT791_ALERT_4_G Note: The Model has Chirality at C4      (Verify)         S
PLAT791_ALERT_4_G Note: The Model has Chirality at C6      (Verify)         S
PLAT791_ALERT_4_G Note: The Model has Chirality at C7      (Verify)         S
```

```
  0 ALERT level A = Most likely a serious problem - resolve or explain
  0 ALERT level B = A potentially serious problem, consider carefully
  5 ALERT level C = Check. Ensure it is not caused by an omission or oversight
  6 ALERT level G = General information/check it is not something unexpected

  0 ALERT type 1 CIF construction/syntax error, inconsistent or missing data
  3 ALERT type 2 Indicator that the structure model may be wrong or deficient
  2 ALERT type 3 Indicator that the structure quality may be low
  4 ALERT type 4 Improvement, methodology, query or suggestion
  2 ALERT type 5 Informative message, check
```

PLATON version of 01/06/2013; check.def file version of 24/05/2013

Datablock x - ellipsoid plot

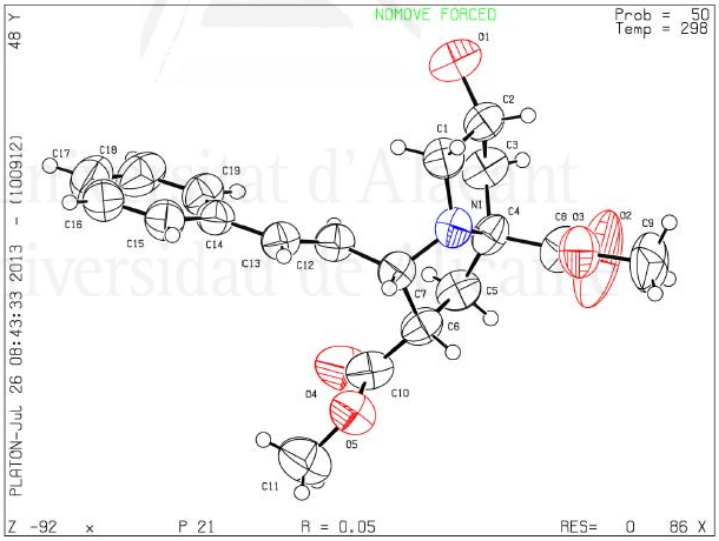

VI.5.- ORG. BIOMOL. CHEM., ENVIADO

Organic and Biomolecular Chemistry RSCPublishing

ARTICLE

Simple and Diastereoselective Multicomponent 1,3-Dipolar Cycloaddition Combining Cyclic α-Amino Esters-Aldehydes-Dipolarophiles for the Synthesis of Pyrrolizidines and Indolizidines

Cite this: DOI: 10.1039/xoxxooooox

Received ooth January 2012,
Accepted ooth January 2012

DOI: 10.1039/xoxxooooox

Dedicated to Prof. Richard Taylor on the occasion of his 65th birthday

www.rsc.org/

J. Mancebo-Aracil,[a] C. Nájera,[a]* and J. M. Sansano[a]*

Abstract: The diastereoselective multicomponent 1,3-dipolar cycloaddition between (2*S*,4*R*)-4-hydroxyproline or (*S*)-proline, an aldehyde and the corresponding dipolarophile affords polysubstituted unnatural pyrrolizidine alkaloids. With these proline derivatives as substrate, reactions take place under at room temperature giving high regioselectivities and good diastereoselections. The influence of adding silver acetate (5 mol%) in the final diastereoselection is also surveyed for each transformation. This methodology is extended to the synthesis of polyfunctionalized indolizidines from pipecolic acid derivative, although it is necessary to increase the reaction temperature.

Introduction

The The mechanisms of defense systems in plants are very complex. The diversification and evolution of secondary metabolites such as pyrrolizidine alkaloids (PAs) constitutes a clear example of the confrontation between plants and microorganisms/insects.[1] PAs are of special interest currently because several of them have been shown to cause toxic, genotoxic and carcinogenic reactions in humans when ingested with foods or herbal medicines.[2,3] Natural PAs are frequently hydroxylated, *O*-alkylated or *O*-acylated in key positions of the bicyclic heterocycle. Thus, for instance, the most common skeletal formula of retronecine **1** (R^1, R^2 = H) is hydroxylated at the C1 whilst the hydoxymethyl group is bonded to the C7. However, few natural PAs bear these oxygenated functional groups at 2-position, such as (+)-crotanecine **2**, madurensine **3** and anacrotine **4**, isolated from Crotalaria species have been widely used for the treatment of bacterial and viral infections as well as for cancer.[4] A rare class of pyrrolizidines (+)-amphorogynines A **5** and D **6**, characterized by substitution at C-1 and C-6 were isolated from *Amphorogynine spicata* were also identified,[5] as well as casuarine, which was extracted from *Casuarina equisitefolia* (Figure 1).[6]

Less structurally sophisticated natural pyrrolizidines and indolizidines shown in Figure 2 also exhibit desirable and potent glycosidase inhibition apart from other biological properties.[2]

The synthesis of all these alkaloids was not so simple, for example, (+)-**2** and (+)-**5**, were prepared by diastereoselective [4+2] cycloadditions using nitroalkenes and a chiral vinyl ether,[4a] and by diastereoselective [2+2] dichloroketene-chiral enol ether cycloaddition,[7] respectively. Besides, (–)-**8** to (–)-**11** scaffolds were prepared by double reductive amination[8] or through a biomimetic Mannich-type reaction,[9] or including a metathesis.[10] Indolizidines **12** and **13** were also obtained in a multi-step sequence involving a ring closing metathesis.[10]

In order to facilitate this synthesis, several diastereoselective approaches to this heterocyclic frameworks has been successfully attempted, for example, employing chain elongations of proline derivatives, followed by cyclization,[11] transanular iodoamination,[12] using lactams,[13] from other natural products,[14] etc. However, the most important and straightforward route is to employ a 1,3-dipolar cycloaddition (1,3-DC)[15,16,17] using mainly nitrones[18,19,20,21,22] or azomethine ylides.[23,24,25]

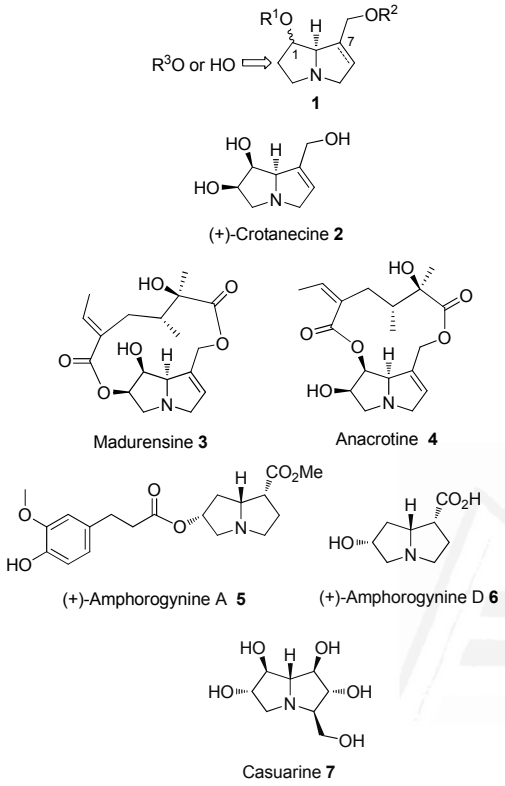

Figure 1. Non common C6 or C2-hydroxylated pyrrolizidines.

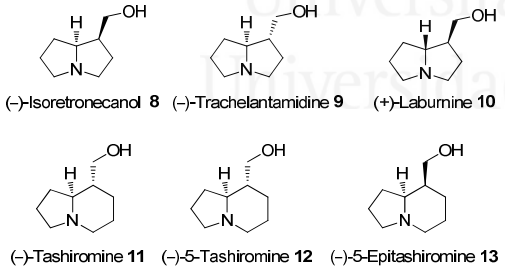

Figure 2. Non-hydroxylated pyrrolizidine and indolizidine alkaloids.

According to all these features, azomethine ylides derived from enantiomerically enriched commercially available (2*S*,4*R*)-4-hydroxyproline methyl ester **14** or proline methyl ester **15** were envisaged to undergo diastereoselective cycloadditions with electrophilic alkenes providing this functional hydroxy group at 6-position of the indolizidine nucleus. Previously, in the literature, the intermediate dipole, generated from decarboxylation of the iminium salt formed with 2,3-butanedione or ethyl pyruvate and proline or (2*S*,4*R*)-4-hydroxyproline, has been trapped using β-nitrostyrene affording mixtures of pyrrolizidines in good chemical yields (78-90%).[26] More recently, it has been described that the proline itself underwent a domino iminium salt formation with α,β-unsaturated β-keto esters followed by decarboxylation and diastereoselective cycloaddition, in good chemical yields (80-90%), with the named keto ester at 80 ºC in DMSO as solvent.[27]

In this work the scope of the synthesis of non-natural pyrrolizidine alkaloids **I** or **II** employing a multicomponent diastereoselective 1,3-DC of azomethine ylides, prepared *in situ* following a non-descarboxylative iminium route starting from chiral hydroxyproline **14** or proline **15**, will be described according to retrosynthetic Scheme 1.[28,29]

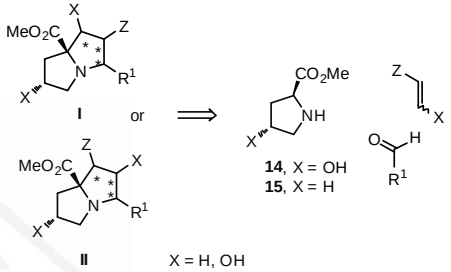

Scheme 1. Retrosynthetic analysis of pyrrolizidines prepared in this work.

Results and discussion

1,3-DC using iminium salts derived from (2S,4R)-4-hydroxyproline methyl ester 14.

According to the literature, the intermediate dipole, generated from 2,3-butanedione and (2*S*,4*R*)-4-hydroxyproline **14**, has been trapped using β-nitrostyrene. Unexpectedly, the decarboxylation occurred at room temperature affording mixtures of pyrrolizidines (three stereosiomers in 1:4:1 proportion) in good chemical yield (78%).[26]

In this work, we tried to follow the concept of atom economy with the aim to increase the functionality in the final pyrrolizidine alkaloid. Thus, the starting 1,3-DC involving (2*S*,4*R*)-4-hydroxyproline **14** was performed employing cinnamaldehyde, as iminium salt precursor, and methyl acrylate as dipolarophile, in toluene at room temperature (25 ºC average). The reaction took place in 4 h obtaining 85% yield of a 80:20 *dr* of compounds **17a** and **17a'**(Scheme 2). These reaction conditions were initially settled due to the previous experience gained from other cycloadditions published by our group.[28,30,31] The employment of other different solvents such as DCM, and THF at room temperature were discarded due to the lower diastereoselection achieved.

The introduction of a bulkier protecting group of the hydroxy functionality was carried out onto molecule **14** to give **16** with the aim to ameliorate de diastereoselection of the corresponding reaction product **17b**, but unfortunately, the final diastereomeric ratio of **17b**:**17b'** was even lower (78:18 *dr*, Scheme 2).

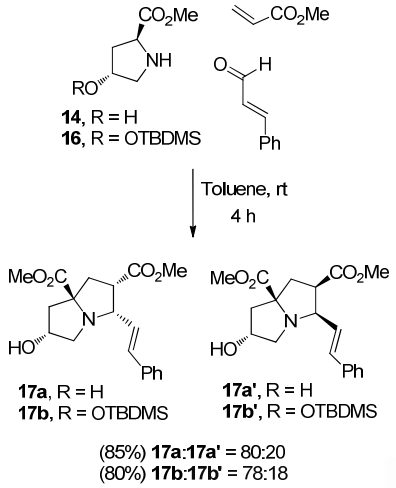

Scheme 2. Study of the selectivity induced by prolines **14** and **16**.

The study of the general scope and the increment of the diastereoselection moved us to test several dipolarophiles maintaining the aldehyde structure. Thus, the incorporation of *tert*-butyl acrylate instead of methyl acrylate produced an increment of the diastereoselection (95:5 *dr*) of the product **17c** (85% yield, Scheme 3). When (*E*)-3-(but-2-enoyl)oxazolidin-2-one was tested as dipolarophile the diastereoselection was even higher obtaining up to 95:5 *dr* for molecule **17d** (Scheme 3). In contrast, the *N*-methylmalimide gave the lowest diastereoselection of **17e** (75:25 *dr*).

The effect of Lewis acids such as $Ti(OPr^i)_4$, ZnCl, and AgOAc in the diastereoselection of the overall process was investigated. Only AgOAc was able to promote the reaction generating very clean reaction products **17**. So, a parallel study employing this silver salt was necessary. In all transformations the results of the cycloadditions run in the presence of silver acetate were compared with the analogous reactions performed without it. An improvement of the diastereomeric ratio was observed in the reaction where *tert*-butyl acrylate was the selected dipolarophile. In this example, compound **17c** was isolated in good chemical yileds (82%) and 98:2 *dr* (Scheme 3). Reactions involving *N*-alkenoyl oxazolidinone and NMM did not reveal any variation of disatereoselection when working in the presence of 5 mol% of silver acetate (Scheme 3). The role of this Lewis acid is not very clear but the acceleration of the iminium salt formation and a possible weak interaction with the negatively charged dipole area must not be discarded.

In both silver-catalyzed and non-catalyzed processes the crude reaction mixtures of diastereoisomers were very clean (^{1}H NMR spectroscopy) and their yields were excellent such as it was shown in (Schemes 2 and 3).

As we can observe the affinity of the α-attack of the intermediate 1,3-dipole is very elevated in all tested examples, the regioisomeric product derived from the corresponding γ-attack being not detected by ^{1}H NMR spectroscopy of the crude sample (Scheme 3).

The absolute configuration of compounds **17** was unambiguously established after X-ray diffraction analysis of molecule **17a**.[28] Comparative nOe, and bidimensional experiments and analysis of the corresponding coupling constants confirmed the proposed structure for pyrrolizidines **17'**.

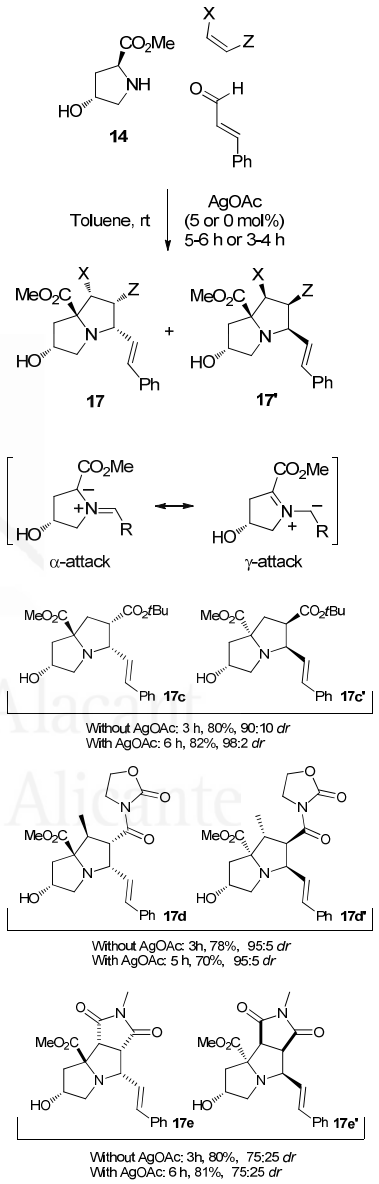

Scheme 3. Multicomponent cycloaddition of **14**, cinnamaldehyde and different dipolarophiles in the presence or in the absence of silver acetate.

A variation of the aldehyde structure was next evaluated. Benzaldehyde, hydroxyproline ester **14** and *tert*-butyl acrylate were allowed to react under optimized conditions affording diastereoisomer **18a** (>90:1 *dr*) as unique reaction product in good purified chemical yield (74%) (Scheme 4). Polysubstituted indolizidine **18b**, obtained through the same process but using 1,2-bis(phenylsulfonyl)ethylene (BPSE) as dipolarophile, was isolated in moderate yield (54%) but as only one stereoisomer as well (Scheme 4). Crude reaction product originated from *tert*-butyl acrylate was very pure (96% chemical yield, by ^{1}H NMR spectroscopy) unlike the crude product generated from BPSE, which was contaminated with unidentified side products. The effect of the addition of silver acetate was tested in the multicomponent cycloaddition involving the disulfone but any improvement was observed. Again, the prevalence of the α-attack (see Scheme 3) was the driving force of the generation of pure regioisomers **18**.

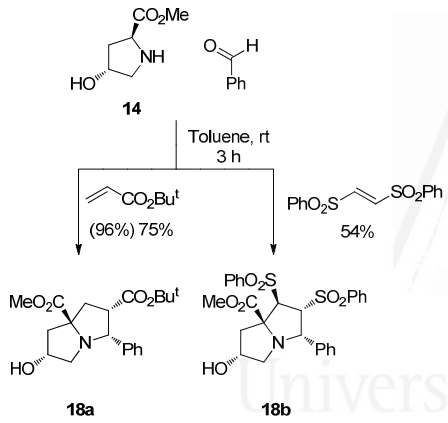

Scheme 4. Multicomponent cycloaddition of **14**, benzaldehyde and different dipolarophiles in the absence of silver acetate.

Attempts to introduce an aliphatic aldehyde such as isovaleraldehyde were unsuccessful. When **14**, isovaleraldehyde, and *tert*-butyl acrylate were mixed and allowed to react in toluene Michael-type addition adduct **19** (Figure 2) was diastereoselectively obtained (>99:1 *dr*) in good chemical yield (84%).

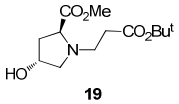

19

Figure 2. Michael-type adduct **19** isolated in the reaction performed with isovaleraldehyde.

1,3-DC using iminium salts derived from proline methyl ester 15a.

In this work, the synthesis of pyrrolizidines **20** was initially tested at room temperature employing an analogous multicomponent process as described in the previous section. In this case, (*S*)-proline methyl ester hydrochloride **15a** was allowed to react with cinnamaldehyde and methyl acrylate using triethylamine (1 equiv). Despite toluene afforded a slower reaction (5 h) with methyl acrylate (96% crude yield of pure **20aa** by ^{1}H NMR spectroscopy), it was selected as solvent again because a higher diastereoselection (99:1) was obtained in this example (Scheme 5). In this transformation the presence of the benzyl or methyl ester in the starting proline **15** was not very noticeable (compare **20aa** and **20ba**, Scheme 5). Other two acrylates such as allyl acrylate and (*E*)-3-(but-2-enoyl)oxazolidin-2-one resulted to be excellent dipolarophiles for this domino process giving pyrrolizidines **20ab**, and **20ac** as unique diastereoisomers in excellent chemical yields (Scheme 5). NMM was tested in the presence of both methyl and benzyl prolinates obtaining, after 2 h of reaction, similar *dr* but compounds **20ad** and **20ad'** gave a cleaner crude product (^{1}H NMR spectroscopy) than the reaction involving proline **15b** (Scheme 5). Dimethyl fumarate and β-nitrostyrene offered identical behavior in terms of diastereoselections and chemical yields. In both examples, mixtures of **20ae**:**20ae'** and **20af**:**20af'** were identified as clean crude samples (^{1}H NMR spectroscopy) and each isomer could be separated by flash chromatography (Scheme 5, and Table 2, entries 7, and 8). Phenyl vinyl sulfone furnished only one diastereoisomer **20ag** in 71% (Scheme 5), whilst BPSE gave a very complex crude reaction mixture of products, from which **20ah** and **20ah'** could be isolated in lower overall yield (69%) (Scheme 5). The presence of the silver acetate (5 mol%) made the reactions slower, and with the same efficiency in the examples reported with all dipolarophiles depicted on Scheme 5 except in the reaction run with BPSE. Here, both the diastereoselectivity and the conversion were noticeably higher in comparison with the non-catalyzed process.

In the case of the domino reaction involving nitroalkene, an important amount of the regioisomer **20af'** was observed due to the attack of the dipole by its γ-position (Scheme 5). For entries dealing with dimethyl fumarate or BPSE the assumption of a preferential attack could not be made.

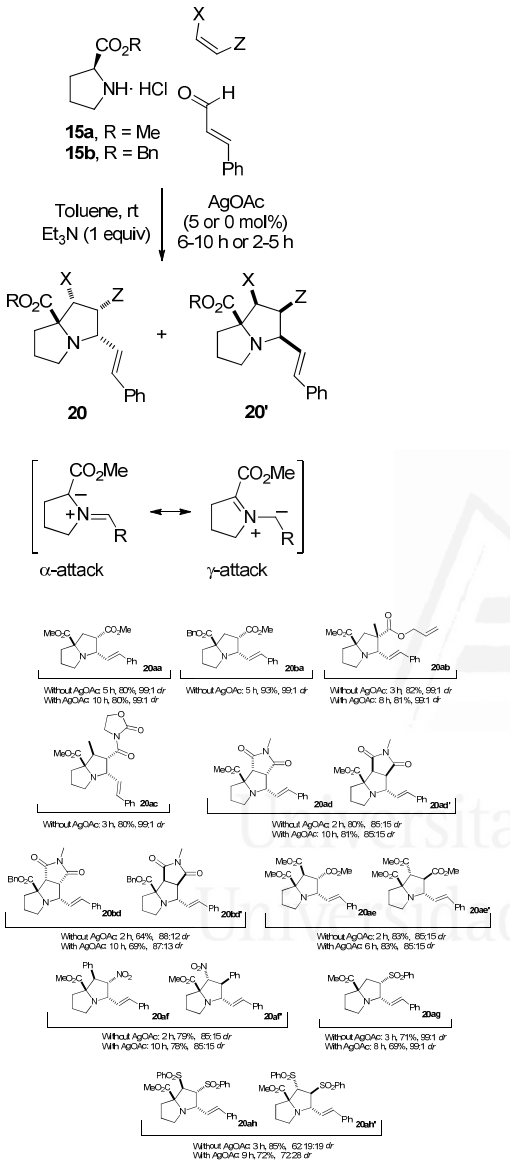

Scheme 5. Multicomponent cycloaddition of **15a** or **15b**, cinnamaldehyde and different dipolarophiles in the presence or in the absence of silver acetate.

The use of crotonaldehyde instead of cinnamaldehyde in the multicomponent reaction of **15a** together with acrylates under the same reaction conditions was evaluated. In general, the α-attack of the dipole was preferred. Methyl acrylate did not give as good diasteresoselections of **21aa** as in the same reaction using cinnamaldehyde, independently whether the process was catalyzed or not (Scheme 6). However, a very important difference was found when allyl methacrylate was essayed. The non-catalyzed process was discarded because AgOAc diastereoselectively (99:1) promoted the generation of pyrrolizidine **21ab** in high yield (85%) (Scheme 6).

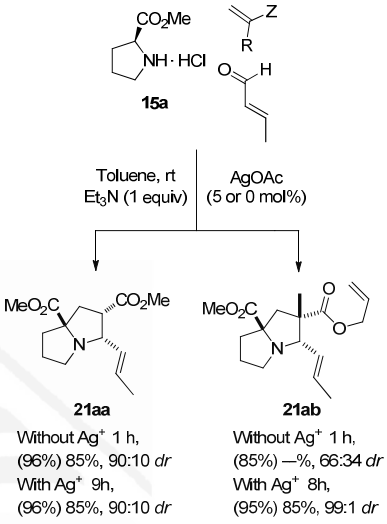

Scheme 6. Multicomponent cycloaddition of **15a**, crotonaldehyde and acrylates in the presence or in the absence of silver acetate.

Benzaldehyde induced the formation of the corresponding regioisomer through the γ-attack (anion placed at the benzylic position, Scheme 5) in both silver-catalyzed and non-catalyzed processes. In the first example the conversion and chemical yield of compounds **22** were higher with moderate 80:20 diastereomeric ratio (Scheme 7). By contrast, isovaleraldehyde did not favor the presence of the anion at the γ-position giving access to regioisomeric pyrrolizidine **23aa** as a 80:20 mixture of diastereoisomers (Scheme 7).

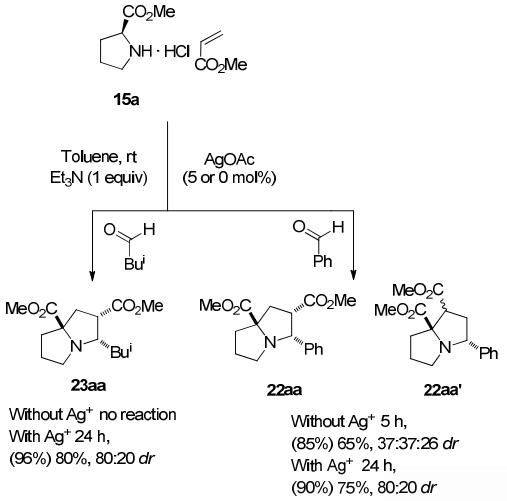

Scheme 7. Multicomponent cycloaddition of **15a**, methyl acrylate and benzaldehyde or isovaleraldehyde, in the presence or in the absence of silver acetate.

The utilization of α-functionalized aldehydes was very attractive from the synthetic point of view. Following with the experience acquired in this type of the freshly generated 1,3-dipoles by combining α-amino esters, dipolarophiles and ethyl glyoxylate[30,31] or 2,2'-dimethoxyacetaldehyde,[31] we design a new synthetic approach to the more funtionalized pyrrolizidines **24** and **25** (Scheme 8). The domino process exclusively took place by silver-promoted catalysis in 1 d at room temperature. The reactions involving methyl acrylate and dimethyl fumarate afforded compounds **24aa** and **24ac** as almost pure diastereoisomers in 59 and 82% yield, respectively (Scheme 8). Unexpectedly, allyl acrylate reacted with a very low diastereoselection furnishing heterocycles **24ab** and **24ab'** in 55% yield (Scheme 8). A very similar comment can be extracted from the result in the reaction with β-nitrostyrene which yielded products **25** with low diastereoselectivity.

Unlike the previous results described across the text, the formation of the dipole able to attack by its γ-position was much more favored due to the presence of the ethoxycarbonyl group and the inner-ring double bond (Scheme 8).

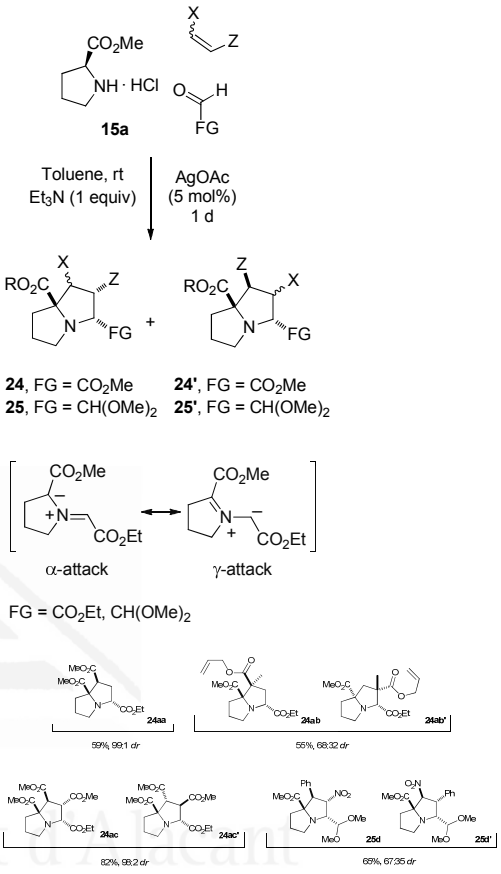

Scheme 8. Multicomponent cycloaddition of **15a** with several dipolarofiles and α-functionalized aldehydes in the presence of silver acetate.

The synthesis of indolizidines constitutes another important field of the general alkaloid's family.[32]Despite working under several silver-catalyzed or non-catalyzed conditions at 25 ºC, it was not possible to generate indolizidines starting from racemic pipecolic acid methyl ester hydrochloride **26**, cinnamaldehyde and methyl acrylate. However, a diastereoselective cycloaddition occurred in refluxing toluene with 1 equiv. of triethylamine. Indolizidine **27** was isolated in 78% yield with a 93:7 *dr* (Scheme 9) following a reactivity pattern identical to the already detailed for the reactions dealing with proline and cinnamaldehyde (Scheme 5).

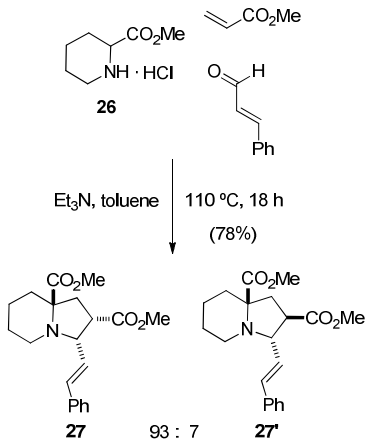

Scheme 9. Synthesis of indolizidine **27** through multicomponent cycloaddition of **19** with cinnamaldehyde and methyl acrylate.

Conclusions

In conclusion, a very efficient and mild multicomponent diastereoselective 1,3-DC of proline derivatives, aldehydes and dipolarophiles have been optimized for the final synthesis of polysubstituted pyrrolizidine alkaloids. In many examples the diastereoselection and chemical yields improved the results published in the literature.[23b,26] The analysis of the general scope of the reaction allowed to direct the attack of the *in situ* formed 1,3-dipole, that means, the α-attack is favored when conjugated, aromatic, and aliphatic aldehydes were used, whereas a favored γ-attack occurred whether ethyl glyoxylate was employed instead. In this last example the role of the silver salt was crucial, otherwise the reaction did not take place at all in its absence. With other aldehydes the presence of silver was not necessary except in the case of working with proline methyl ester and BPSE as dipolarophile and the reactions involving crotonaldehyde. Finally, the multicomponent diastereoselective synthesis of indolizidines only could be achieved using thermal conditions.

Experimental

See electronic Supplementary Information (ESI).

Acknowledgements
This work has been supported by the DGES of the Spanish Ministerio de Ciencia e Innovación (MICINN) (Consolider INGENIO 2010 CSD2007-00006, CTQ2010-20387), FEDER Generalitat Valenciana (PROMETEO/ 2009/039), and by the University of Alicante.

Notes and references

[a] *Department of Organic Chemistry and Institute of Organic Synthesis. Faculty of Sciences, University of Alicante, E-03080 Alicante, Spain.*

† Footnotes should appear here. These might include comments relevant to but not central to the matter under discussion, limited experimental and spectral data, and crystallographic data.

Electronic Supplementary Information (ESI) available: [details of any supplementary information available should be included here]. See DOI: 10.1039/b000000x/

1 As recent reviews concerning this topic, see: (a) D. Langel, D. Ober, P. B. Pelser, *Phytochem. Rev.* 2011, **10**, 3. (b) L. Joosten, J. A. van Veen, *Phytochem. Rev*. 2011, **10**, 127.

2 Glycosidase inhibition is a common general biological property of these pyrrolizidine alkaloids: A. A. Watson, G. W. J. Fleet, N. Asano, R. J. Molyneux, R. J. Nash, *Phytochemistry* 2001, 265.

3 For very recent examples, see: (a) L. Cramer, H.-M. Schiebel, L. Ernst, T. Beuerle, *J. Agric. Food Chem.* 2013, **61**, 11382. (b) E. Roeder, H. Wiedenfeld, *Pharmazie* 2013, **68**, 83.

4 (a) S. E. Denmark, A. Thorarensen, *J. Am. Chem. Soc.* 1997**, 119**, 125-137. (b) A. Silva Flores, A. M. Goulart de Azevedo Tozzi, J. R. Trigo, *Biochem. System. Ecol.* 2009, 37, 459. (b) K. Le Roux, A. A. Hussein, N. Lall, *J. Ethnopharm.* 2011, **138**, 748. (c) M. S. Rao, P. S. Rao, *Fitoterapia* 1999, **70**, 449.

5 D. T. T. Huong, M.-T. Martin, M. Litaudon, T. Sévenet, M. Païs, *J. Nat. Prod.* 1998, **61**, 1444.

6 R. J. Nash, P. I. Thomas, R. D. Waigh, W. J. George; G. W. J. Fleet, M. R. Wormald, P. M. de Q. Lilley, D. J. Watkin, *Tetrahedron Lett.* 1994, **35**, 7849.

7 C. Roche, P. Delair, A. E. Greene, *Org. Lett.* 2003, **5**, 1741.

8 M. Brambilla, S. G. Davies, A. M. Fletcher, P. M. Roberts, J. E. Thomson, *Tetrahedron* 2014, **70**, 204.

9 D. Koley, K. Srinivas, Y. Krishna, A. Gupta, *RCS Adv*. 2014, **4**, 3934.

10 K. K. S. Reddy, B. V. Rao, S. S. Raju, *Tetrahedron: Asymmetry* 2011, **22**, 662.

11 (a) T. J. Donohoe, R. E. Thomas, M. D. Cheeseman, C. L. Rigby, G. Bhalay, I. D. Linney, *Org. Lett.* 2008, **10**, 3615. (b) A. C. Breman, J. Dijkink, J. H. van Maarseveen, S. S. Kinderman, H. Hiemstra, *J. Org. Chem.* 2009, **74**, 6327. (c) T. Ponpandian, S. Muthusubramanian, *Tetrahedron* 2013, **69**, 527. (d) X. Garrabou, L. Gómez, J. Joglar, S. Gil, T. Parella, J. Bujons, P. Clapes, *Chem. Eur. J*. 2010, **16**, 10691. (e) I. Izquierdo, M. T. Plaza, J. A. Tamayo, F. Franco, F. Sanchez-Cantalejo, *Tetrahedron* 2010, **66**, 3788. (f) D. Muroni, M. Mucedda, A. Saba, *Tetrahedron Lett*. 2008, **49**, 2373. (g) A. Iza, L. Carrillo, J. L. Vicario, D. Badía, E. Reyes, J. L. Martínez, *Org. Biomol. Chem.* 2010, **8**, 2238.

12 E. A. Brock, S. G. Davies, J. A. Lee, P. M. Roberts, J. E. Thomson, *Org. Lett.* 2011, **13**, 1594.

13 P. V. Reddy, J. Smith, A. Kamath, H. Jamet, A. Veyron, P. Koos, C. Philouze, A. E. Greene, P. Delair, *J. Org. Chem.* 2013, **78**, 4840.

14 R. Lahiri, A. A. Ansanri, Y. D. Vankar, *Chem. Soc. Rev.* 2013, **42**, 5102.

15 For general reviews dealing with general 1,3-DC, see: (a) *Synthetic Applications of 1,3-Dipolar Cycloaddition Chemistry Towards Heterocycles and Natural Products*, A. Padwa, W. H. Pearson, Eds. John Wiley & Sons, New Jersey, 2003; (b) C. Nájera, J. M. Sansano,

Curr. Org. Chem. **2003**, *7*, 1105; (c) W. Eberbach, *Sci. Synth.* 2004, **27**, chp. 11, 441; (d) I. Coldham, R. Hufton, *Chem. Rev.* **2005**, *105*, 2765. (e) V. Nair, T. D. Suja, *Tetrahedron* 2007, **63**, 12247. (f) A. Padwa, S. K. Bur, *Tetrahedron* 2007, **63**, 5341.

16 For recent reviews of asymmetric 1,3-DC, see: (a) H. Pellissier, *Tetrahedron* 2007, **63**, 3235. (b) C. Nájera, J. M. Sansano in *Topics in Heterocyclic Chemistry*, *vol. 12* (Ed.: A. Hassner), Springer-Verlag: Berlin-Heidelberg, 2008, pp. 117; (c) L. M. Stanley, M. P. Sibi, *Chem. Rev.* 2008, **108**, 2887. (d) M. Álvarez-Corral, M. Muñoz-Dorado, I. Rodríguez-García, *Chem. Rev.* 2008, **108**, 3174. (e) M. Naodovic, H. Yamamoto, *Chem. Rev*. 2008, **108**, 3132. (f) C. Nájera, J. M. Sansano, M. Yus, *J. Braz. Chem. Soc.* 2010, **21**, 377. (g) M. Kissane, A. R. Maguire, *Chem. Soc. Rev*. 2010, **39**, 845. (h) J. Adrio, J. C. Carretero, *Chem. Commun*. 2011, **47**, 6784.

17 W. Zhang, *Chem. Lett.* 2013, **42**, 676.

18 (a) S. Stecko, M. Jurczak, Z. Urbanczyk-Lipkowska, J. Solecka, M. Chmielewski, *Carbohyd. Res.* 2008, **343**, 2215. (b) S. Cicchi, M. Marradi, P. Vogel, A. Goti, *J. Org. Chem.* 2006, **71**, 1614. (c) A. Brandi, F. Cardona, S. Cicchi, F. M. Cordero, A. Goti, *Chem. Eur. J.* 2009, **15**, 7808. (d) J.-S. Zhu, S. Nakagawa, W. Chen, I. Adachi, Y.-M. Jia, X.-G. Hu, G. W. J. Fleet, F. X. Wilson, T. Nitoda, G. Horne, R. van Well, A. Kato, C.-Y. Yu. *J. Org. Chem.* 2013, **78**, 10298. (e) C. Parmeggiani, F. Cardona, L. Giusti, H. U. Reissig, A. Goti, *Chem. Eur. J.* 2013, **19**, 10595.

19 R. G. Thorat , S. V. Pansare, *Eur. J. Org. Chem.* 2013, 7282.

20 E. Mironiuk-Puchalska, T. Rowicki, W. Sas, M. Koszytkowska-Stawinska, *Tetrahedron* 2013, **69**, 9826.

21 W.-Y. Xu, R. Iwaki, Y.-M. Jia, W. Zhang, A. Kato, C.-Y. Yu, *Org. Biomol. Chem.* 2013, **11**, 4622.

22 C. Bonaccini, M. Chioccioli, C. Parmeggiani, F. Cardona, D. Lo Re, G. Soldaini, P. Vogel, C. Bello, A. Goti, P. Gratteri, *Eur. J. Org. Chem.* 2010, 5574.

23 (a) R. Grigg, M. Jordan, J. F. Malone, *Tetrahedron Lett.* 1979, **20**, 3877. (b) N. G. Argyropoulos, V. C. Sarli, M. Gdaniec, *Eur. J. Org. Chem.* 2006, 3728. (c) L. Faraji, H. Arvinnezhad, N. Alikami, K. Jadidi, *Lett. Org. Chem.* 2010, **7**, 472. (d) R. M. Gorman, M. A. Little, J. A. Morris, V. Sridharan, *Chem. Commun*. 2012, **48**, 9537.

24 In some examples proline itself has been generated from a previous 1,3-DC. For selected examples of racemic and non-racemic processes, see: (a) P. Cui, L. Xu, Z. Shi, L. Gan, *J. Org. Chem.* 2011, **76**, 4210. (b) J. A. Codelli, A. L. A. Puchlopek, S. E. Reisman, *J. Am. Chem. Soc.* 2012, **134**, 1930. (c) Q. Lu, G. Song, J. P. Jasinski, A. C. Keeley, W. Zhang, *Green Chem.* 2012, **14**, 3010. (d) A. D. Lim, J. A. Codelli, S. E. Reisman, *Chem. Sci*. 2013, **4**, 650.

25 P. D. Barman, I. Sanyal, S. B. Mandal, A. K. Banerjee, *Synthesis* 2011, **21**, 3563.

26 F. Felluga, C. Forzato, P. Nitti, G. Pitacco, E. Valentin, E. Zangrando, *J. Heterocyclic Chem.* 2010, **47**, 664.

27 T.-R. Kang, Y. Cheng, L. He, J. Ye, Q.-Z. Liu, *Tetrahedron Lett.* 2012, **53**, 2552.

28 For preliminary results, see: J. Mancebo-Aracil, C. Nájera, J. M. Sansano, *Chem. Commun.* 2013, **49**, 11218.

29 T. Sengupta, S. Khamarui, S. Samanta, D. K. Maiti, *Chem. Commun.* 2013, **49**, 9962.

30 J. Mancebo-Aracil, C. Nájera, J. M. Sansano, *Org. Biomol. Chem.* 2013, **11**, 662.

31 J. Mancebo-Aracil, C. Nájera, J. M. Sansano, *Org. Chem. Front.* 2014, submitted.

32 (a) I.-S. Kim, Y. H. Jung, *Heterocycles* 2011, 83, 2489. (b) S. M. Bronner, G.-Y. J. Im, N. K. Garg, *Heterocycles in Natural Product Synthesis* 2011, 221. (c) P. Shapland, *Nature Chem.* 2012, **4**, 441.

CONCLUSIONES

VII.- CONCLUSIONES

El estudio cinético por DSC de la cicloadición 1,3-dipolar entre el fumarato de isobutilo y la imina formada por condensación del benzaldehído y el aminofenilalaninato de metilo aporta interesantes conclusiones. En primer lugar, la reacción tiene una cinética de orden fraccionario, mostrando un carácter autocatalítico, en la que el control de la velocidad lo proporciona la formación del dipolo. Así pues, la cinética de esta reacción es muy susceptible a cambios en la concentración del iminoéster de partida.

Por otro lado, pueden cuantificarse valores cinéticos de la reacción como la energía de activación o el orden de reacción con la metodología propuesta, así como termodinámicos como la entalpía de reacción. Queda demostrado pues, además del análisis concreto que se hace de esta reacción con estos componentes, que esta metodología puede extenderse y aplicarse a otras reacciones en síntesis orgánica que cumplan una serie de parámetros, pudiendo realizarse medidas de forma rápida y eficaz mediante calorimetría diferencial de barrido.

En esta memoria se describen además ejemplos concretos de la cicloadición 1,3-dipolar multicomponente con iluros de azometino. Desde esta perspectiva, enfocado a la síntesis de pirrolidinas se demuestra la versatilidad de esta reacción a la hora de sintetizar este tipo de moléculas con una metodología sencilla, en la que la economía de átomos queda optimizada, obteniéndose, en general, los productos deseados con buenos rendimientos y diasteroselectividades.

El estudio llevado a cabo en condiciones térmicas, mediante calentamiento convencional e irradiación por microondas mostró interesantes resultados especialmente para el segundo caso. Bajo calentamiento por microondas, los rendiemientos fueron buenos así como la diastereoselectividad, para el caso de dipolarófilos simétricos como el fumarato de dimetilo o las maleimidas *N*-sustituidas. Sin embargo, en el caso del acrilato de metilo, la reacción no tenía lugar bajo una regioquímica determinada, obteniéndose para los diferentes aminoésteres, mezclas de diasteroisomeros prácticamente en igual proporción. El aminoéster que ofreció mejores resultados fue el clorhidrato del éster etílico de fenilalanina, motivo por el cual fue elegido para optimizar la versión asimétrica de

esta reacción. Además se consiguió sintetizar un derivado de uno de los cicloaductos con estructura bicíclica que guarda una estrecha similitud con los ligandos colinérgicos receptores y moduladores de la acetilcolina (ver ref. 59).

El estudio realizado de esta reacción mediante catálisis con sales de plata(I) con glioxilato de etilo por un lado, y 2,2-dimetoxiactealdehído por otro, como precursores de iluros de azometino mostró buenos resultados especialmente en el caso del segundo aldehído. Mientras que la cicloadición 1,3-dipolar térmica con glioxilato de etilo y la catalizada por plata(I) mostraron resultados similares, en el caso del 2,2-dimetoxiacetaldehído, mediante catálisis con plata(I) se obtuvo un solo diastereoisómero en el ejemplo mostrado gracias a la formación del metalodipolo tipo W, favorecido por la interacción de este metal con el grupo NH, así como con ambos grupos metoxi, controlando además la regioquímica de la reacción obteniéndose los productos finales con configuración relativa 2,4,5-*all cis*.

El estudio pues, de la cicloadición 1,3-dipolar multicomponente asimétrica, catalizada por una sal de plata(I) y un ligando quiral fosforado "privilegiado" mostró excelentes resultados para el caso de la reacción entre glioxilato de etilo, fenilalaninato de etilo y maleimidas *N*-sustituidas como dipolarófilos, con rendiemientos casi cuantitativos en muchos casos y excesos enantioméricos de hasta un 92%. Lamentablemente, dicha reacción con otros dipolarófilos, o bien manteniendo las maleimidas y sustituyendo los α-aminoésteres mostraron baja o nula enantioselectividad pese a obtenerse los cicloaductos finales con buenos rendimientos.

Con la misma metodología, se sintetizaron pirrolizidinas con buenos rendimientos a través de la cicloadición 1,3-dipolar multicomponente usanto ésteres de prolina a través de una sal de iminio. Esta reacción pudo llevarse a cabo a temperatura ambiente sin necesidad de añadir ningún catalizador, para aldehídos α,β-insaturados como el cinamaldehído o el crotonaldehído, aromáticos como el benzaldehído, o con otro tipo de funcionalidad como el 2,2-dimetoxiacetaldehído, independientemente del dipolarófilo utilizado. Sin embargo para alguno de estos casos, la adición de una sal de plata(I) mejoró los rendimientos y la diastereoselectividades, y para el caso concreto del glioxilato de etilo, y del aldehído alifático isovaleraldehído solo con presencia de plata(I) podía darse esta reacción. El rol por tanto de este metal para dicha reacción no queda claro, probablemente actue como ácido de Lewis activando aquellos aldehídos algo menos reactivos. Se obtuvieron también, productos enantioméricamente

enriquecidos cuando se partía del clorhidrato del éster metílico de (2*S*,4*R*)-4-hidroxiprolina, efecto causado por el grupo alcohol en dicha posición. Por último, con el fin de consolidar la metodología descrita a otro tipo de estructuras se trató de sintetizar el esqueleto de indolizidina a partir del éster metílico del ácido pipecolínico. Esto no fue posible a temperatura ambiente, con y sin el uso de una sal de plata(I), pero sin embargo, si pudo obtenerse mediante reacción 1,3-dipolar térmica a reflujo de tolueno, con una buena relación además de diastereoisómeros (rto. de 78%, 93:7 *endo*:*exo*)

ABREVIACIONES

VIII.- ABREVIACIONES

B/D: Método de Borchardt & Daniels

Binap: 2,2,-bis(Difenilfosfanil)-1,1,-binaftilo

Boc: *N*-(*terc*-butoxicarbonilo)

Col. : colaboradores

DBU: 1,8-Diazabiciclo-[5,4,0]-7-undeceno

DCM: diclorometano

DIPEA: Diisopropiletilamina

DMF: dimetilformamida

DMSO: dimetilsulfóxido

***dr*:** relación de diasteroisómeros

DSC: Calorimetría diferencial de barrido (Differential Scanning Calorimetry)

DTA: análisis diferencial térmico

***ee*:** Exceso enantiomérico

equiv.: equivalentes

HOMO: orbital molecular ocupado de mayor energía

HPLC: Cromatografía líquida de alta eficacia

ICTAC: confederación internacional de análisis térmico y calorimetría

LDA: *N*,*N*-Diisopropilamiduro de litio

LUMO: orbital molecular vacío de menor energía

MCR: reacción multicomponente

MFK: metodología de análisis libre de modelo (Model Free Kinetics)

MLR: análisis de regresión multilineal (multiple linear regression)

MW: microondas

NAD^+/NADH: nicotinamida adenina dinucleótido (especie oxidada/reducida)

nOe: Efecto nuclear Overhauser

NOESY: Espectroscopía 2D por efecto nuclear Overhauser

OAc: acetato de

OBz: benzoato de

OFW: Método de Ozawa-Flynn-Wall

OTf: Triflato de

Quinap: 1-[2-(Difenilfosfanil)-1-naftil]isoquinolina

RMN: resonancia magnética nuclear

Rto.: Rendimiento

TA: análisis térmico

TAA: análisis termoacústico

TBS ó **TBDMS:** *terc*-butildimetilsilil

TEA: análisis termoeléctrico

TFA: Ácido trifluoroacético o trifluoroacetato de

TG: Termogravimetría

THF: Tetrahidrofurano

TMA: análisis termomecánico

TMEDA: *N*,*N*,*N*',*N*'-Tetrametiletilendiamina

TMS: tetrametilsilano o tetrametilsililo-

TOA: análisis termoóptico

TOF: Teoría de Orbitales Frontera

VHC: virus responsable de la hepatitis C

REFERENCIAS

IX.- REFERENCIAS

[1] Huisgen, R; *Angew. Chem., Int. Ed. Engl.* **1963**, *2*, 565.

[2] **a)** Nájera, C.; Sansano, J.M.; *Angew. Chem. Int. Ed.* **2005**, *44*, 6272. **b)** Husinec, S.; Savic, V.; *Tetrahedron: Asymmetry* **2005**, *16,* 2047. **c)** Coldham, I.; Hufton, R.; *Chem. Rev.* **2005**, *105*, 2765 **d)** Nájera, C.; Sansano, J.M.; *Curr. Org. Chem.* **2003**, *7*, 1105 **e)** *Synthetic Applications of 1,3-Dipolar Cycloaddition Chemistry Toward Heterocycles and Natural Products*, Eds: Padwa, A., Wiley: Nueva York, **2003 f)** Kanemasa, S.; *Synlett* **2002**, 1371. **g)** Gothelf, K.; *Cycloaddition Reactions in Organic Synthesis*, Eds: Kobayasi, S.; Jørgensen, K. A.; Wiley-VCH, Weinheim **2002**, 211 **h)** *Cycloaddition Reactions in Organic Synthesis*, Eds: Carruthers, W., Pergamon Press: Oxford **1990**, 269 **i)** Bonin, M; Chauveau, A.; Micouin, L.; *Synlett* **2006**, *15*, 2349 **j)** Pellissier, H.; *Tetrahedron* **2007**, *63*, 3235 **k)** Padwa, A.; Bur, S.; *Tetrahedron* **2007**, *63*, 5341 **l)** Nair, V.; Suja, T.; *Tetrahedron* **2007**, *63,* 12247 **m)** Nájera, C.; Sansano, J.M.; *Heterocycl. Chem*. **2008**, *12*, 117. **n)** Pellisier, H.; *Tetrahedron* **2007**, *63*, 3235. **ñ)** Pandey, G.; Banerjee, P.; Gadre, S. R.; *Chem. Rev.* **2006,** *106,* 4484 **o)** Pinho, T. M.; Melo, V. D. *Eur. J. Org. Chem.* **2006**, 2873. **p)** Nájera, C. ; Sansano, J.M.; Yus, M.; *J. Braz. Chem. Soc*. **2010**, *21*, 377.

[3]Domingo, L.R.; Emamian, S. R.; *Tetrahedron* **2014** DOI 10.1016/j.tet.2013.12.059

[4]**a)** Grigg, R.; Sridharan, V.; *Advances in Cycloaddition*, JAI Press Inc.: Greenwich, **1993**, *3*, 161 **b)** Grigg, R.*; Chem. Soc. Rev*. **1987**, *16*, 89. **c)** Grigg, R.; Kemp, J.; Malone, J.; Tangthongkum, A.; *J. Chem. Soc., Chem. Commun.* **1980**, 648 **d)** Tatsukawa, A.; Kawatake, K.; Kanemasa, S.; Rudzinski, J.; *J. Chem. Soc. Perkin Trans. 2* **1994**, 2525 **e)** Annunziata, R.; Benaglia, M.; Cinquini, M.; Raimondi, L.; *Tetrahedron* **1993**, *49*, 8629 **f)** Ayerbe, M.; Arrieta, A.; Cossío, F.; Linden, A.; *J. Org. Chem.* **1998**, *63*, 1795 **e)** Vivanco, S.; Lecea, B.; Arrieta, A.; Prieto, P.; Morao, I.; Linden, A.; Cossío, F.; *J. Am. Chem. Soc.* **2000**, *122*, 6078 **f)** Vivanco, S.; Tesis doctoral, Universidad del País Vasco, San Sebastián, **2002**

[5] **a)** *Frontier Orbitals and Organic Chemical Reactions*, Eds: Fleming I., Wiley: Chichester, **1976 b)** *Pericyclic Reaction*, Eds: Fleming, I., Oxford Science Publications, Oxford, **1994**.

[6] **a)** Grigg, R.; Donegan, G.; Gunaratne, H.; Kennedy, D.; Malone, J.; Sridharan, V.; Thianpatanagul, S.; *Tetrahedron* **1989**, *45*, 1723 **b)** Van Es, J.; Jaarsveld, K.; van der Gen, A.; *J. Org. Chem.* **1990**, *55*, 4063 **c)** Van Es, J.; Wolde, A.; van der Gen, A.; *J. Org. Chem.* **1990**, *55*, 4069 **d)** Grigg, R.; Jordan, M.; Malone, J.; Armstrong, P.; *Tetrahedron* **1985**, *41*, 3547 **e)** Grigg, R.; Kemp, J.; *Tetrahedron Lett.* **1980**, *21*, 2461 **f)** Tsuge, O.; Ueno, K.; Kanemasa, S.; Yorozu, K.; *Bull. Chem. Soc. Jpn.* **1986**, *59*, 1809.

[7] **a)** Casella, L.; Gulloti, M.; Pasini, A.; Pasaro, R.; *Synthesis* **1979**, 150 **b)** Grigg, R.; Sridharan, V.; Thianpatanagul, S.; *J. Chem. Soc., Perkin Trans.* **1986**, *1,* 1669. **c)** Casella, L.; Gulloti, M.; Melani, E.; *J. Chem. Soc., Perkin Trans.* **1982**, *1,* 1827 **d)** Tsuge, O.; Kanemasa, S.; Yoshioka, M.; *J. Org. Chem.* **1988**, *53*, 1384 **e)** Barr, D.; Grigg, R.; Gunaratne, H.; Kemp, J.; McMeekin, P.; Sridharan, V.; *Tetrahedron* **1988**, *44*, 557

[8]de Cózar, A.; Cossío, F.; *Phys. Chem. Chem. Phys.* **2011**, *13*, 10858.

[9] Grigg, R.; Montgomery, J.; Somasunderam, A.; *Tetrahedron* **1992**, *48*, 10431.

[10] Wright, M. R.; *An Introduction to Chemical Kinetics*, John Wiley & Sons, Chichester, **2004**.

[11] El láser abarca desde el rango de microondas hasta el infrarrojo (IR) visible, y desde el visible al ultravioleta (UV).

[12] Gallagher, P. K; *Handbook of Thermal Analysis and Calorimetry*. Ed. Vol. 1-5, Elsevier Science, Amsterdam, **2003-2007**.

[13] Suriñach, S.; Baro, M. D.; Bordas, S.; Clavaguera, N.; Clavaguera-Mora, M. T.; *Bol. Soc. Esp. Ceram. Vidr.* **1992**, *31*, 11.

[14] ASTM E2070-00, ASTM Int., West Conshohocken, US.

[15] Borchardt, H.J.; Daniels, F.; *J. Am. Chem. Soc.* **1956**, *79*, 41.

[16] Kissinger, H. E.; *Anal. Chem.* **1957**, *29*, 1702.

[17] **a)** Ozawa, T. J.; *Therm. Anal.* **1970**, 2, 301 **b)** Flynn, J. H.; Wall, L. A.; *J. Res. Nat. Bur. Stand* **1966**, *70A*, 487.

[18] Arrhenius, S.; *Z. Phys. Chem.* **1889**, *4*, 226.

[19] Roura, P.; Farjas, J.; *J. Mater. Res.* **2009**, *24*, 3095.

[20]Lee, J.W.; Kim, H.S.; Lee, J.Y.; Kang, J.K.; *Appl. Phys. Lett.* **2006**, *88*, 143126.

[21] **a)** Jona, E.; Simon, P.; Nemcekova, K.; Pavlik, V.; Rudinska, G.; Rudinska, E.; *J. Therm. Anal. Calorim.* **2006**, *84*, 673. **b)** Srivastava, A.P.; Srivastava, D.; Dey, G.K.; *J. Magn. Magn. Mater.* **2006**, *306*, 147.

[22] Ladbrook, B.D.; Chapman, D.; *Chem. Phys. Lipids* **1969**, *3*, 304.

[23] Budrugeac, P.; Segal, E.; *J. Therm. Anal. Calorim.* **2007**, *88*, 703.

[24] http://www.scientificsoftware-solutions.com

[25] Liu, S.H.; Hou, H.Y.; Shu, C.M.; *Proceedings of the 6th International Conference on Process Systems Engineering (PSE ASIA)* 25 - 27 June **2013**, Kuala Lumpur.

[26] Kappe, T.; Stadlbauer, W.; *Molecules*, **1996**, *1*, 255.

[27] Cammenga, H.K.; Epple, M.; *Angew. Chem. Int. Ed. Engl,.* **1995**, *34*, 1171.

[28] Belichmeier, J.A.; Cammenga, H.K.; Schneider, P.B.; Steer,A.G.; *Thermochimica Acta*, **1998**, *310*, 147.

[29] ΔH = 262.5 J/g.

[30] Mancebo-Aracil, J.; Nájera, C.; Sansano, J.; *Org. Biomol. Chem.* **2013**, *11*, 662.

[31] *Handbook of Thermal Analysis*, T. Hatakeyama, Z. Liu, Eds. John Wiley & Sons, New York, **1998**, cap. 4

[32] Mata-Pérez, F.; Pérez-Benito, J.; *J. Chem. Educ*. **1987**, *64*, 925.

[33] Apróximadamente, de unos $5 \cdot 10^{-3}$ mmol de imina **X** en el experimento de **DSC** a 2 mmol en el tubo de ensayo.

[34] Rodriguez-Ruiz, V.; Tesis Doctoral, Universidad Politécnica de Valencia, **2010**.

[35] Nicolau, K.C.; Edmonds, D.J.; Bulger, P.G.; *Angew. Chem. Int. Ed.* **2006**, *45*, 7134.

[36] **a)** Anastas, P.T.; Warner, J.C.; *Green Chemistry: Theory and Practice,* Oxford University Press, Oxford, **2000**; **b)** Matlack, A.S.; *Introduction to Green Chemistry*, Marcel Dekker, New York, **2001**.

[37] **a)** Tietze, L.F.; Brasche, G.; Gericke, K.; *Domino Reactions in Organic Synthesis*, Wiley-VCH, Weinheim, **2006**; **b)** Tietze, L.F.; Beifuss, U.; *Angew. Chem.* **1993**, *105*, 137; *Angew. Chem. Int. Ed. Engl.* **1993**, *32*, 131; **c)** Tietze, L.F.; *Chem. Rev.* **1996**, *96*, 115.

[38] Dömling, A.; Ugi, I.; *Angew. Chem. Int. Ed.* **2000**, *39*, 3168.

[39] Strecker, A.; Liebigs *Ann. Chem.* **1850**, *75*, 27.

[40] Laurent, A.; Gerhardt, C.F.; *Ann. Chimie Phys.***1838**, *66*, 181.

[41] Robinson, R.; *J. Chem. Soc. (London)* **1917**, *111*, 876.

[42] Hantzsch, A.; Liebigs *Ann. Chem.* **1882**, *215*, 1.

[43] **a)** Radziszewski, B.; *Ber. Dtsch. Chem. Ges.* **1882**, *15*, 1499; **b)** Radziszewski, B.; *Ber. Dtsch. Chem. Ges.* **1882**, *15*, 2706.

[44] Hantzsch, A.; *Ber. Dtsch. Chem. Ges.* **1890**, *23*, 1474.

[45] **a)** Biginelli, P.; *Ber. Dtsch. Chem. Ges.* **1891**, *24*, 1317, 2962; **b)** Biginelli, P.; *Ber. Dtsch. Chem. Ges.* **1882**, *26*, 447.

[46] Mannich, C.; Kröschl, W.; *Arch. Pharm.* **1912**, *250*, 647.

[47] Fédou, N.M.; Parsons, P.J.; Viseux, E.M.; Whittle, A.J.; *Org. Lett.* **2005**, *7*, 3179.

[48] Presset, M.; Mohanan, K.; Hamann, M.; Coquerel, Y.; Rodriguez, J.; *Org. Lett.* **2011**, *13*, 4124.

[49] van Es, J.; Jaarsveld, K.; van der Gen, A.; *J. Org. Chem.* **1990**, *55*, 4063.

[50] Khlebnikov, A.K.; Novikov, M.S.; Khlebnikov, V.A.; Kostikov, R.R.; *Russian Journal of Organic Chemistry* **2001***, 37*, 5073512.

[51] Cheng, Q.; Zhang, W.; Tagami, Y.; Oritani, T.; *J. Chem. Soc*., *Perkin Trans.* **2001**, *1*, 452.

[52] Cossío, F.; Díaz-Ortiz, A. y colaboradores; *J. Org. Chem.* **2007**, *72*, 4313.

[53] Lopes, S. y colaboradores; *Synthesis* **2009**, *14*, 2403.

[54] Liu, H.; Dou, G.; Shi, D.; *J. Comb. Chem.* **2010,** *12,* 633.

[55] Harwood, L.M.; Lilley, I.A.; *Tet. Assym.* **1995**, *6*, 1557.

[56] Wittland, C.; Flörke, U.; Risch, N.; *Synthesis*, **1997**, 1291.

[57]Chung, F.; Chauveau, A.; Seltki, M.; Bonin, M.; Micouin, L.; *Tetrahedron Letters* **2004,** 45, 3127.

[58]Argyropoulos, N.G.; Sarli, V.C.; Gdaniec, M.; *Eur. J. Org. Chem.* **2006**, 3738.

[59] Ver por ejemplo: Peters, D.; Redrobe, J.P.; Nielsen, E.O.; Pat., WO **2009** 109517, Apr. **2009**, CAN 2009:1107687.

[60] Huang, L.J.; Teng, D.W.; *Chin. Chem. Lett.* **2011**, *22*, 523.

[61] Frühauf, H.W.; *Chem. Rev.* **1997**, *97*, 523.

[62] Grigg, R.; Gunaratne, H.; *J. Chem. Soc., Chem. Commun.* **1982**, 384.

[63] **a)** Grigg, R.; Gunaratne, H. ; Sridharan, V.; *Tetrahedron* **1987**, *43*, 5887. **b)** Amornraksa, K.; Barr, D.; Donegan, G.; Grigg, R.; Ratananukul, P.; Sridharan, V.; *Tetrahedron* **1989**, *45*, 4649.

[64] Dondas, H.A.; Durust, Y.; Grigg, R.; Slater, M.J.; Sarker, M.; *Tetrahedron* **2005**, *61*, 10667.

[65] Grigg, R.; Sarker, M.; *Tetrahedron* **2006**, *62*, 10332.

[66] Subramaniyan, G.; Raghunathan, R. *Tetrahedron* **2001**, *57*, 2909.

[67] Subramaniyan, G.; Raghunathan, R.; Castro, A.; *Tetrahedron* **2003**, *59*, 335.

[68] Pandey, G.; Laha, J.K.; Lakshmaiah, G.; *Tetrahedron* **2002**, *58*, 3525.

[69] Martín, M.; Univesidad de Alicante, Tesis Doctoral, Alicante, **2012**.

[70] Allway, P.; Grigg, R.; *Tetrahedron Lett.* **1991**, *32*, 5817.

[71] Longmire, J.; Wang, B.; Zhang, X.; *J. Am. Chem. Soc.* **2002**, *124*, 13400.

[72] Pellissier, H.; *Adv. Synth. Catal*. **2012**, *354*, 237.

[73] Oderaotoshi, Y.; Cheng, W.; Fujitomi, S.; Kasano, Y.; Minakata, S.; Komatsu, M.; *Org. Lett.* **2003**, *5*, 5043.

[74] **a)** Chen, C.; Li, X.; Schreiber, S.; *J. Am. Chem. Soc.* **2003**, *125*, 10174; **b)** Knöpfel, T.; Aschwanden, P.; Ichikawa, T.; Watanabe, T.; Carreira, E.; *Angew. Chem. Int. Ed.* **2004**, *43*, 5971; **c)** Zheng, W.; Zhou, Y.; *Org. Lett.* **2005,** *7,* 5055; **d)** Stohler, R.; Wahl, F.; Pfaltz, A.; *Synthesis* **2005**, 1431.

[75] Zeng, W.; Zhou, Y.; *Tetrahedron Lett.* **2007**, *48*, 4619.

[76] **a)** Melhado, A.; Luparia, M.; Toste, D.; *J. Am. Chem. Soc.*, **2007**, *129* (42), 12638; **b)** Martín, M.; Nájera, C.; Sansano, J.; Wu, F.; *Tetrahedron: Asymmetry* **2010**, *21*, 1184.

[77] Carretero, J.; López, A.; Adrio, J.; *J. Am. Chem. Soc.* **2008**, *130*, 10085.

[78] Nájera, C.; Sansano, J.; *Org. Biomol. Chem.* **2009**, *7*, 4567.

[79] **a)** Nájera, C.; Martín, M.; Retamosa, M.; Sansano, J.; de Cózar, A.; Cossío, F.; *Eur. J. Org. Chem.*, **2009**, 5622. **b)** Nájera, C.; Retamosa, M.; Sansano, J.;. *Patente Española:P200800908,* Mayo **2008.**

[80]Moyano, A.; Rios, R; *Chem. Rev.* **2011**, *111*, 4703.

[81] Arai, S.; Takahashi, F.; Tsuji, R.; Nishida, A. *Heterocycles* **2006**, *67*, 495.

[82] Vicario, J.L.; Reboredo, S.; Badia, D.; Carrillo, L. *Angew. Chem., Int. Ed.* **2007**, *46*, 5168.

[83] Ibrahem, I.; Rios, R.; Vesely, J.; Córdova, A. *Tetrahedron Lett.* **2007**, *48*, 6252.

[84] Chen, X.-H.; Zhang, W.-Q.; Gong, L.-Z. *J. Am. Chem. Soc.* **2008**, *130*, 5652.

[85] **a)** Yu, J.; He, L.; Chen, X.-H.; Song, J.; Chen, W.-J.; Gong L.-Z. *Org. Lett.* **2009**, *11*, 4946. **b)** Iza, A.; Carrillo, L.; Vicario, J.L.; Badía, D.; Reyes, E.; Martínez, J.I.; *Org. Biomol. Chem.* **2010**, *8*, 2238. **c)** Shi,F.; Luo, S.; Tao, Z.-L.; He, L.; Yu, J.; Tu, S.T; Gong, L.-Z.; *Org. Lett.* **2011**, *13*, 4680. **d)** He, L.; Chen, H.X.; Wang, D.; Luo, S.; Zhang, W.Q.; Yu, J.; Ren, L.; Gong, L.-Z.; *J. Am. Chem. Soc.* **2011**, *133*, 13504. **e)** Liu, W.-J.; Chen, H.X.; Gong, L.-Z.; *Org. Lett.* **2008**, *10*, 5357. **f)** Chen, H.X.; Wei, Q.; Luo, S.W.; Xiao, H.; Gong, L.-Z.; *J. Am. Chem. Soc.* **2009**, *131*, 13819. **g)** Reboredo, S.; Reyes, E.; Vicario, J.L.; Badía, D.; Carrillo, L.; Cózar, A.; Cossío, F.; *Chem. Eur. J.* **2012**, *18*, 7179. **h)** Guo, C.; Song, J.; Gong, L.-Z.; *Org. Lett.* **2013**, *15*, 2676.

[86]**a)** Mancebo-Aracil,J.; Martín-Rodríguez,M.; Nájera, C.; Sansano, J.M.; Costa, P.; Crizanto, E.; Dias, A.; *Tet. Asymm.* **2012**, *23*, 1596 **b)** Martín, M.; Nájera, C. Sansano, J.M.; Costa, P.; Crizanto, E.; Dias, A.; *Synlett* **2010**, 0962.

[87] Precios Sigma-Aldrich en **2013** para: Ag_2CO_3 (3.70 €/g, 4.70 €/g Ag), AgTFA (5.60 €/g, 11.40 €/g Ag).

[88] Zhao, Y.; Zhang, Q.; Tu, G. ; Cheng, T.; *Tetrahedron* **2002**, 6795.

[89] Kam, T.; Sim, K.; *Phytochemistry*, **1997**, *47*, 145.

[90] Yamato, M.; Hashigaki, K.; Qais, N.; Ishikawa, S.; *Tetrahedron* **1990**, *46*, 5909.

[91] Tarí, S; Chinchilla, R; Nájera, C; *Tetrahedron: Asymmetry* **2009**, *20*, 2651

[92] Ammendola, S.; Mosca, L.; Bovicelli, P.; *Arkivoc* **2008**, *VIII*, 105.

[93] **a)** Burton, G.; Ku, T.; Carr, T.; Kiesov, T.; Sarisky, R. ; Lin-Goerke, J.; Hofmann, G.; Slater, M.; Haigh, D.; Dhanak, D.; Johnson, V.; Parry, N.; Thomes, P.; *Bioorg. Med. Chem. Lett.*, **2007**, *17*, 1930; **b)** Slater, M. y colaboradores; *J. Med. Chem*., **2007**, *50*, 897; **c)** Slater, M. y colaboradores; *J. Org. Chem.* **2008**, *73*, 3094.

[94] **a)** Nicolau, K. y colaboradores; *J. Am. Chem. Soc.* **1993**, *115,* 12550. **b)** Kuethe, J.; Davies, I.; Dormer, P.; Reamer, R.; Mathre, D.; Reider, P.; *Tetrahedron Lett.* **2002**, *43*, 29.

[95] Kang, T.R.; Cheng, Y.; He. L.; Ye, J.;Liu, Q.Z.; *Tet. Lett.* **2012**, *53*, 2552.

[96] Liddell, J.R.; *Nat. Prod. Rep.* **2002**, *19*, 773.

[97] Pyne, S.G.; Tang, M.Y.; *Curr. Org. Chem.* **2005**, *9*, 1393.

[98] Wang, G.-C.; Wang, Y.; Zhang, X.-Q.; Li, Y.-L.; Yao, X.-S.; Ye, W.-C.; *Chem. Pharm. Bull.* **2010**, *58*, 390.

[99]Tamayo, J.A; Franco, F.; Lo Re, D.; Sánchez, F.; *J. Org. Chem.* **2009**, *74*, 5679.

[100] Sinnot, M.L.; *Chem. Rev.* **1990**, *90*, 1171.

[101] Marco, J.A.; Química de los productos naturales, Ed. Síntesis S.A., **2006**.

[102] Brock, E. A.; Davies, S.G.; Lee, J.A.; Roberts, P.M.; Thomson,J. E.; *Org. Lett.* **2011**, *13*, 1594.

[103] Yip, K.T.; Yang, D.; *Org. Lett.* **2011**, *13*, 2134.

[104] Xing, D.; Yang, D.; *Org. Lett.* **2013**, *15*, 4370.

[105] Kato, A.; Yu, C.-Y. y colaboradores; *J. Org. Chem.* **2013**, *78*, 10298.

[106] Nakamura, I.; Yamamoto, Y.; *Chem. Rev.* **2004**, *104*, 207.

[107] **a)** Arredondo, V.M.; Tian, S.; McDonald, F.E.; Marks, T.J.; *J. Am. Chem. Soc.* **1999**, *121*, 3633; **b)** Tian, S.; Arredondo, V.M.; Stern, C.L.; Marks, T.J.; *Organometallics* **1999**, *18*, 2568.

[108] **a)** Li, Y.; Marks, T J.; *J. Am. Chem. Soc.* **1996**, *118*, 707; **b)** Li, Y.; Marks, T.J.; *J. Am. Chem. Soc.* **1998**, *120*, 1757.

[109] Hirner, J.J.; Roth, K.E.; Shi, Y.; Blum, S.A.; *Organometallics* **2012**, *31*, 6843.

[110] Sengupta, T.; Khamarui, S.; Samanta, S.; Maiti, D.K.; *Chem. Commun.* **2013**, *49*, 9962.

[111] Mancebo-Aracil, J.; Nájera, C.; Sansano, J.M.; *Chem. Commun.* **2013**, *49*, 11218.

[112] Lim, A.D.; Codelli, J.A.; Reisman, S.A.; Chem. Sci. **2013**, *4*, 650.

BIOGRAFÍA

X.- BIOGRAFÍA

Nací en Alicante el día 11 de agosto de 1984.

Realicé los estudios de primaria, E.S.O. y Bachiller en el colegio Jesús-Maria de Vistahermosa (Alicante).

Entre los cursos 2001-02 a 2006-07 realicé los estudios correspondientes al primer ciclo de la Licenciatura de Ciencias Químicas de la Facultad de Ciencias de la Universidad de Alicante, y de 2007-09 el segundo ciclo de la Licenciatura de Ciencias Químicas de la Facultad de Químicas de la Universidad de Valencia, donde trabajé en la síntesis de productos naturales con esqueleto de labdano que presentan actividad antimicótica y antitumoral, pudiendo aplicarse para fines médicos , bajo la supervisión del Dr González Cardenete.*****

En octubre de 2009 me incorporé al Departamento de Química Orgánica de la Facultad de Ciencias de la Universidad de Alicante, donde realicé un Máster de introducctión a la experimentación en Química, defendiendo el trabajo de fin de máster en septiembre de 2010 con título "Aplicaciones en Síntesis Orgánica de cicloadiciones 1,3-dipolares enantioselectivas".

Desde entonces hasta la actualidad he estado preparando mi Tesis Doctoral, cuyos resultados se recogen en la presente memoria.

***** *"Synthesis and biological evaluation of (+)-labdadienedial, derivatives and precursors from (+)-sclareolide"* Miguel A. González, Juan Mancebo-Aracil, Veronica Tangarife-Castaño, Lee Agudelo-Goméz, Bibiana Zapata, Ana Mesa-Arango, Liliana Betancur-Galvis; *European Jorunal of Medicinal Chemistry* **2010**, *45*, 4403.